LEVEL II

AD A109127

AFHRL-TP-80-41

STUDY AND DESIGN OF HIGH G AUGMENTATION DEVICES FOR FLIGHT SIMULATORS

Gerald J. Kron
Frank M. Cardullo
Link Div., The Singer Company
Binghamton, NY 13902

Laurence R. Young
Massachusetts Institute of Technology
Cambridge, MA 02139

12 548

DTIC
ELECTE
DEC 30 1981
D
H

Final Report
December 1981

APPROVED FOR PUBLIC RELEASE
DISTRIBUTION UNLIMITED

PREPARED FOR

U. S. AIR FORCE HUMAN RESOURCES LABORATORY

WRIGHT-PATTERSON AIR FORCE BASE, OHIO

DTIC FILE COPY

THIS DOCUMENT IS BEST QUALITY PRACTICABLE.
THE COPY FURNISHED TO DTIC CONTAINED A
SIGNIFICANT NUMBER OF PAGES WHICH DO NOT
REPRODUCE LEGIBLY.

393270

81 12 28 111

DISCLAIMER NOTICE

THIS DOCUMENT IS BEST QUALITY PRACTICABLE. THE COPY FURNISHED TO DTIC CONTAINED A SIGNIFICANT NUMBER OF PAGES WHICH DO NOT REPRODUCE LEGIBLY.

AFHRL-TP-80-41

STUDY AND DESIGN OF HIGH G AUGMENTATION DEVICES FOR FLIGHT SIMULATORS

Gerald J. Kron
Frank M. Cardullo
Link Div., The Singer Company
Binghamton, NY 13902

Laurence R. Young
Massachusetts Institute of Technology
Cambridge, MA 02139



Final Report
December 1981

APPROVED FOR PUBLIC RELEASE
DISTRIBUTION UNLIMITED

OPERATIONS TRAINING DIVISION
AIR FORCE HUMAN RESOURCES LABORATORY
WILLIAMS AIR FORCE BASE, ARIZONA 85224

UNCLASSIFIED
SECURITY CLASSIFICATION OF THIS PAGE (When Data Entered)

REPORT DOCUMENTATION PAGE	READ INSTRUCTIONS BEFORE COMPLETING FORM
1. REPORT NUMBER: AFHRL-TP-80-41	2. GOVT ACCESSION NO.: AD-A109127
	3. RECIPIENT'S CATALOG NUMBER:
4. TITLE (and Subtitle): STUDY AND DESIGN OF HIGH G AUGMENTATION DEVICES FOR FLIGHT SIMULATORS	5. TYPE OF REPORT & PERIOD COVERED: Final
	6. PERFORMING ORG. REPORT NUMBER:
7. AUTHOR(s): Gerald J. Kron; Frank M. Cardullo; Laurence R. Young - Massachusetts Institute of Tech	8. CONTRACT OR GRANT NUMBER(s): F33615-77-C-0055
9. PERFORMING ORGANIZATION NAME AND ADDRESS: Singer Company - Link Division, Binghamton, New York 13902	10. PROGRAM ELEMENT, PROJECT, TASK AREA & WORK UNIT NUMBERS: 62205F; 61141908
11. CONTROLLING OFFICE NAME AND ADDRESS: Hq. Air Force Human Resources Laboratory (AFSC), Brooks AFB, Texas 78235	12. REPORT DATE: December 1981
	13. NUMBER OF PAGES: 544
14. MONITORING AGENCY NAME & ADDRESS (if different from Controlling Office): Operations Training Division, Air Force Human Resources Laboratory, Williams Air Force Base, Arizona 85224	15. SECURITY CLASS. (of this report): Unclassified
	15a. DECLASSIFICATION/DOWNGRADING SCHEDULE:

16. DISTRIBUTION STATEMENT (of this Report)

Approved for Public Release Distribution Unlimited.

17. DISTRIBUTION STATEMENT (of the abstract entered in Block 20, if different from Report)

18. SUPPLEMENTARY NOTES

19. KEY WORDS (Continue on reverse side if necessary and identify by block number)

Simulation	Motion	G-Seat	Biomechanical
Flight Simulation	Acceleration	Stress	Labyrinthine
Somatic	G-Cuing	Cardiovascular	Auditory
Perception	Anti-G Suit	Protective Devices	Lacrimation

20. ABSTRACT (Continue on reverse side if necessary and identify by block number)

The physiological effects of accelerated flight are considered to contain perceptual information important to vehicle control and contribute to defining flight envelopes accessible to the pilot. As such, these effects, or acceptable surrogates thereof, must be considered for inclusion within ground-based devices designed to train pilots for their flight mission. This study investigates the physiological effects of accelerated flight within the cardiovascular musculoskeletal, visual, auditory, tactile, and respiratory systems. The study advances conceptual designs of research-oriented devices thought capable

DD FORM 1 JAN 73 1473 EDITION OF 1 NOV 65 IS OBSOLETE

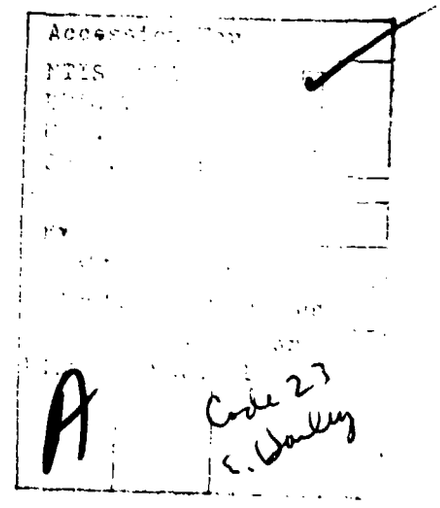
UNCLASSIFIED
SECURITY CLASSIFICATION OF THIS PAGE (When Data Entered)

19. Key Words (continued)

Extremities	Sustained Acceleration	Neck Forces
Shoulder Harness	Prolonged Acceleration	Oculometer
Visual Acuity	Human	Plethysmographic Goggles
Liquid Crystals	Pilots	Variable Transparency Visor
Cockpit Lighting	Acceleration Tolerance	
Muscle Loader	Thresholds	Acceleration Grayout
Pheripheral Light Loss	Physiological Effect	Acceleration Blackout
Hypoxia	Endurance	Central Light Loss
Skin Temperature	Positive G	Negative Pressure Breathing
M1 Maneuver	Vision	Retina Circulation
Valsalva	Respiration	Interocular Pressure
Helmet Loader	Manual Control	Lower Body Negative Pressure (LBNP)
Vestibular	Tactile	
Efference Copy	Environmental Force	Thermoelectric Module
Acceleration Physiology	Musculoskeletal	Oculogravic Illusion

20. Abstract (continued)

of inducing, in the unaccelerated state, the perception of accelerated flight physiological effects. The authors conclude that one of the most important effects impacting vehicle control and successful mission execution is loss of visual acuity under accelerated flight conditions and propose a dual effect matrixed liquid crystal variable transparency visor to replicate this effect. A math model to simulate the effect is also presented. The study contains a bibliography of 277 references pertinent to accelerated flight physiological effects and equivalent simulation device design. The study presents an appendix containing an annotated bibliography of 133 references.



ACKNOWLEDGEMENTS

The authors acknowledge the research contributions of Timothy Hale, Karen Wike and George Minnich as being essential to the conduct of the High G Augmentation Devices Study. In addition a debt of gratitude is owed to Margaret Conklin of the Link Library for her efforts concerned with the prodigious task of obtaining reference material necessary to the performance of this study.

TABLE OF CONTENTS

Section	Title	Page
1.	INTRODUCTION	1
1.1	Background	1
1.2	Approach	4
1.3	Study Objectives	7
2.	LITERATURE SEARCH	8
2.1	Sources	8
2.2	NTIS Interactive Search Key Words	9
2.3	DDC Search Key Words	10
2.4	Medlars II Search Key Words	10
2.5	Catalog and Review	11
2.6	Personal Contacts	13
3.	HIGH G PHYSIOLOGICAL EFFECTS	14
3.1	General	14
3.2	Physiological Systems Affected by Excessive G Levels	14
4.	MECHANIZATION	18
4.1	General	18
4.2	Lower Body Negative Pressure	19
4.2.1	Background	19
4.2.2	LBNP Research	20
4.2.3	LBNP Applications	24
4.2.4	Non-Invasive Cardiovascular Monitors	32
4.3	High G Visual Effects Generation	38
4.3.1	General	38
4.3.2	Oculometer	40
4.3.3	Simplified High G Visual Acuity Model	41
4.3.4	Ophthalmodynamometry: Plethysmographic Goggles	60
4.3.4.1	Introduction	60
4.3.4.2	Similarities Between Effects of Acceleration and of Plethysmographic Goggles	61
4.3.4.3	Hardware Considerations - Plethysmographic Goggles	66

4.3.5	Area of Interest Variable Transparency Visor	68
4.3.5.1	Visor Concept	70
4.3.5.1.1	Dual Optical Effects of Interest	71
4.3.5.1.2	Flat Plate Display Prototype	73
4.3.5.1.3	Matrix Addressing	75
4.3.5.1.4	Display Pattern of Specific Interest	76
4.3.5.1.5	Multiplexing, Drive Waveform, and Power	77
4.3.5.2	Visor Response	78
4.3.5.3	Visor Subsystem Structure and Developmental Approach	82
4.3.6	Diminution of Visual Acuity Simulation	84
4.3.6.1	Flight Instruments	84
4.3.6.2	Visual Displays	86
4.3.6.3	Visual System Drives	88
4.3.6.4	Cockpit Lighting Drives	91
4.4	Musculoskeletal Loaders	94
4.4.1	Head/Neck Loading	94
4.4.1.1	Helmet vs Head Motion	109
4.4.2	Upper/Lower Arm Loaders	111
4.4.2.1	Introduction	111
4.4.2.2	Concept	113
4.4.2.3	Drive Scheme	119
4.5	Tactile Devices	124
4.5.1	Shoulder Harness	124
4.5.2	Skin Temperature Driver	127
4.5.3	Face Mask Loader	137
4.5.4	Localized Firmness Cells	142
4.6	Respiratory Devices	146
4.6.1	Subatmospheric Face Mask	146
4.6.2	Hypoxia Induction	151
4.6.3	Respiration Rate Monitoring Devices	152
5.	SUGGESTED MECHANIZATION PLAN	154
6.	SUMMARY	159
7.	BIBLIOGRAPHY	167-202
	APPENDIX A	
A.	HIGH G PHYSIOLOGICAL EFFECTS	
A.1	General	

A.2	Cardiovascular Effects	A-4
A.2.1	Effects of Acceleration on the Cardiovascular System	A-17
A.2.2	Effects of Transverse Acceleration	A-27
A.2.3	Protective Devices	A-27
A.3	Visual System	A-40
A.3.1	Visual Effects of Vertical (G_z) Acceleration	A-43
A.3.2	Visual Effects of Transverse Acceleration	A-62
A.3.2.1	Lacrimation	A-62
A.3.3	Summary	A-68
A.4	Musculoskeletal	A-68
A.4.1	Extremities	A-68
A.4.2	Head/Neck	A-90
A.4.2.1	Helmet vs. Head Motion	A-99
A.5	Auditory Effects	A-103
A.5.1	Auditory Perception Under High G	A-103
A.5.2	Auditory Stimulus Composition Change	A-104
A.6	Tactile	A-105
A.6.1	Tactile Sensation in Ischial Tuberosity, Shoulder Harness and Face Mask Regions	A-105
A.6.2	Temperature/Pressure Relationships	A-108
A.7	Respiration	A-113
A.7.1	Respiration in the Unaccelerated Environment	A-114
A.7.1.1	Ventilation	A-114
A.7.1.2	Perfusion	A-119
A.7.1.3	Ventilation-Perfusion Ratio and Gas Exchange in the Lung at 1G	A-122
A.7.1.4	Control of Respiration and Work of Breathing	A-125
A.7.2	Respiration in the Accelerated Environment	A-126
A.7.2.1	Lung Mechanics Under Acceleration	A-127
A.7.2.2	Similarity of Negative Pressure Breathing to $+G_x$ Effects	A-129
A.7.2.3	Effects of Acceleration on Ventilation/Perfusion Ratio, Gas Exchange and Arterial Saturation	A-132
	APPENDIX B	
B.	ANNOTATED BIBLIOGRAPHY	B-1

LIST OF FIGURES

Figure	Title	Page
1.1-1	G levels experienced in a 1938 Heinkel 50 flight	1
1.1-2	Recorded G levels	2
1.1-3	F15 engagement capabilities	2
4.2.2-1	Comparison of the effects of 15 minutes LBNP at 20, 40, and 60 mm Hg	22
4.2.3-1	Vacuum/pressure chamber	26
4.2.3-2	Vacuum/pressure chamber control system diagram	29
4.2.3-3	Possible configuration of LBNP device	31
4.2.4-1	Automatic electrosphygmomanometer	33
4.3.4-1	Monocular visual field loss	65
4.3.4-2	Component parts of the plethysmographic goggle	67
4.3.4-3	Goggles seal	68
4.3.5-1	Helmet assembly without shroud	71
4.3.5-2	Flat plate visor display	75
4.3.5-3	Dual frequency addressing and one third voltage select method	80
4.3.6.1-1	Region of diminution of visual acuity	85
4.3.6.3-1	Selected spot dimming block diagram	89
4.3.6.3-2	Raster with selected spot dimming	90
4.3.6.4-1	Visual display/instrument panel blending of selected spot dimming	91
4.3.6.4-2	Cockpit interior selected spot dimming block diagram	92
4.3.6.4-3	Instrument panel light addressing	93
4.4.1-1	Heavy fluid cavity approach	96
4.4.1-2	Head/helmet apparent weight as a function of G_z	98
4.4.1-3	Helmet loader installed in DMS	100
4.4.1-4	Step response	101
4.4.1-5	Helmet loader control diagram	102
4.4.1-6	Helmet firmness bladder	104

4.4.1-7	Helmet firmness bladder control diagram	104
4.4.1-8	Cable/boom and drogue approach	106
4.4.1.1-1	Dual firmness bladder helmet	109
4.4.2-1	Arm loader arrangement	114
4.4.2-2	Lower arm loader motor detail	115
4.4.2-3	Upper arm loader windlass mechanism	117
4.5.1-1	Functional layout of shoulder harness tension system	126
4.5.1-2	Example shoulder harness loader	128
4.5.2-1	Typical thermoelectric module	129
4.5.2-2	Thermoelectric module cross-section	130
4.5.2-3	Typical thermoelectric assembly installation and heat flow capability	131
4.5.2-4	Thermoelectric assembly control loop	133
4.5.2-5	Ischial tuberosity heat flow diagram	134
4.5.2-6	Skin temperature change resulting from current doublet of various magnitudes	135
4.5.2-7	Thermoelectric module plate temperature	136
4.5.3-1	Face mask loader arrangement	138
4.5.3-2	Face mask loader motor	139
4.5.4-1	Helmet firmness cells	143
4.5.4-2	Arm undersurface firmness bladder	144
4.5.4-3	Boot innersole firmness bladder	144
4.5.4-4	Firmness cell control system	145
4.5.4-5	G-seat firmness cell response	145
4.6.1-1	Respiratory rate as a function of G_x	148
4.6.1-2	Respiration dynamics control system	148
4.6.1-3	Partial O_2 pressure	150
A.2-1	Simplified diagram of circulation through the heart	A-6
A.2-2	Blood pressure throughout the systemic circulation	A-8
A.2-3	Effect of hydrostatic pressure on the systemic pressure throughout the body	A-11
A.2-4	Dynamics of various arterial pressure control systems	A-13

A.2-5	Baroreceptor system	A-14
A.2-6	Baroreceptor response as a function of arterial pressure	A-15
A.2.1-1	Seated systolic blood pressure as a function of G_z	A-19
A.2.1-2	Mean arterial blood pressure as a function of G_z	A-21
A.2.1-3	G-Tolerance curve with various acceleration rates	A-22
A.2.1-4	Effects of +3.5 G_z stress on cardiovascular function	A-23
A.2.1-5	The effect of $+G_z$ upon cerebral arterial and jugular venous pressure	A-23
A.2.1-6	A typical response to +7 G_z in an unanesthetized miniature swine	A-25
A.2.3-1	Arterial Pressure (AP) and Heart Rate (HR) response to the valsalva maneuver	A-30
A.2.3-2	Psa response during PPB and during Ml maneuver at +8.0 G_z for 60s	A-31
A.2.3-3	Mean eye-level blood pressure changes during $+G_z$ while performing the Ml and Ll maneuvers	A-31
A.2.3-4	Comparison of Ml maneuver and positive pressure breathing	A-32
A.2.3-5	Direct paper chart recording during a rapid-onset (ROR) and slow-onset (SOR) $+G_z$ acceleration profile	A-33
A.2.3-6	Mean blood pressure for eight subjects during rapid onset run 0.2-0.3 G prior to the run in which peripheral light loss occurred	A-34
A.2.3-7	Increase in $+G_z$ tolerance afforded by a standard 5-bladder anti-G suit	A-36
A.2.3-8	Effects of $+G_z$ Acceleration with and without an anti-G suit	A-37
A.2.3-9	Decreased vertical heart-to-eye distances obtained by tilting backward	A-38
A.3-1	Right eye showing visual axis passing through center of lens to point of sharpest vision at fovea	A-41

A.3-2	Dimensions of the human eye	A-42
A.3.1-1	a, b, & c Degradation in the field of view at three levels of acceleration	A-44
A.3.1-1	d, e, & f Monocular visual field loss	A-45
A.3.1-2	Remaining upper half of three seat-back angles	A-46
A.3.1-3	Responses of subject operating visual field limit tracker during simulated ACM G stress at 65^{o}, 45^{o}, and 13^{o} seatback angles	A-47
A.3.1-4	Mathematical model of visual effects of acceleration	A-48
A.3.1-5	Decreased vertical heart-to-eye distances obtained by tilting backward	A-49
A.3.1-6	Heart-to-eye vertical distance as a function of seat-back angle	A-50
A.3.1-7	G-tolerance curve with various acceleration rates	A-52
A.3.1-8	Changes in P_{aO_2} associated with various levels of HSG	A-56
A.3.1-9	Visual acuity relative to the fovea at a function of eye-level blood pressure	A-57
A.3.1-10	Blood diagram of modification to visual effects model	A-58
A.3.1-11	Eye-level arterial pressure and blood flow responses during rapid onset run	A-59
A.3.1-12	Occurrence of retrograde flow in the temporal artery prior to peripheral light loss and subsequent blackout	A-60
A.3.2.1-1	Sagittal section through eyelid and eyeball	A-63
A.3.2.1-2	Frontal diagram of selected elements of the right eye	A-64
A.3.2.1-3	Primary afferent and efferent pathways affiliated with the lacrimal gland	A-65
A.4.1-1	Model for Golgi Tendon organ function	A-71
A.4.1-2	Muscle sensors	A-73
A.4.1-3	Qualitative discharge patterns of spindle primary and secondary afferents	A-74

A.4.1-4	Reaching error in $+G_z$ environment without hand/eye fixation	A-80
A.4.1-5	Direction and error of reaching moments in $+G_z$ environments	A-86
A.4.1-6	Maximal hand/arm forces in various $+G_z$ environments	A-88
A.4.2-1	Neck muscles used to control head motion	A-91
A.4.2-2	Head/muscle system	A-92
A.4.2-3	Lateral head/neck proprioceptor model	A-93
A.4.2-4	Inner ear labyrinth	A-94
A.4.2-5	Semicircular canal cupula	A-95
A.4.2-6	Sensing stratoconia of the utricle	A-96
A.4.2-7	Ormsby model of the vestibular system	A-97
A.4.2-8	Head rotations, all helmet loadings averaged	A-99
A.4.2-9	Linear depression of the left pupil	A-100
A.4.2.1-1	Helmet pitch relative to head pitch	A-101
A.4.2.1-2	Reticle depression in z direction with respect to left pupil	A-102
A.6.1-1	Pilot's face at +4.5 G_z	A-107
A.6.1-2	Pilot's face at +7.5 G_z	A-108
A.6.2-1	Changes in nerve impulse amplitude as a function of temperature	A-110
A.7-1	Effect of pleural pressure gradient on the volume distribution of gas within the lung	A-115
A.7-2	Regional subdivisions of lung volume in seated men	A-117
A.7-3	Effects of pulmonary arterial, alveolar and venous pressures on the topographical distribution of blood flow in the lung	A-120
A.7-4	Reduction of blood flow of the most dependent zone of the lung as a result of a raised interstitial pressure	A-121
A.7-5	The effect of positive acceleration on the variation in ventilation	A-123
A.7-6	Extremes of ventilation-perfusion ratio	A-123

A.7-7	The effect of forward acceleration on lung capacity	A-128
A.7-8	Effect of back angle on respiration in room air	A-129
A.7-9	Static relaxation pressure-volume curves	A-130
A.7-10	Mean values from all respiratory quantities investigated at $+G_z$ acceleration	A-133
A.7-11	Changes of the O_2 and CO_2 alveolar plateaus for increasing values of $+G_z$ acceleration	A-134
A.7-12	Time course of changes in arterial oxygen saturation induced by positive acceleration	A-135
A.7-13	Arterial oxygen saturations reported during exposure to varying levels and axes of acceleration	A-136
A.7-14a	Actual mean response and mean response predicted by initial synthetic transfer function to ACM G stress	A-139
A.7-14b	Predicted response to 6-G pulse	A-139
A.7-15	Effects of forward ($+G_z$) acceleration on intrathoracic pressures	A-141
A.7-16	Relative ventilation-perfusion ratios plotted against distance	A-142
A.7-17	Effect of exposing an anaesthetised dog to -7G on arterial oxygen saturation and venous pressure	A-144
A.7-18	Changes in arterial oxygen saturation during acceleration when breathing oxygen or air	A-144

LIST OF TABLES

Table	Title	Page
2-1	Bibliography topical distribution	11
4.2.2-1	Mean percent change in blood pressure by source and for various levels of LBNP	21
4.2.2-2	Mean physiological responses of men and women during -20, -40, and -60 mm Hg LBNP	23
4.2.3-1	Mean systolic pressure	28
4.3.4-1	Comparison of visual and plethysmographic goggle effects	62
4.4.1-1	Head and helmet weight as a function of G_z	95
4.6.1-1	Summary of high G effects on the respiratory system	147
5-1	High G augmentation devices development process	156-158
A-1	Axis system definition	A-3
A.3.1-2	$+G_z$ levels at which end points occurred along with visual symptoms at each end point and time at which they occurred	A-53
A.5.1-1	Light and sound reaction times as a function of G	A-103
A.7-1	Oxygen exchange under various conditions of acceleration	A-137

1. INTRODUCTION

1.1 Background

For tactical air superiority a pilot should know where in the flight envelope he enjoys slight advantage, attempt to structure the engagement to enter this region, and be willing to travel to the border of his flight envelope to capture the advantage. Unfortunately, in the very important case of maneuverability, for years the borders of the flight envelope have produced bodily acceleration levels which represent a physiologically hostile environment. The acceleration data plotted in Figure 1.1-1 is taken from a 1938 flight of a Heinkel He 50 biplane dive bomber (18) and demonstrates very significant acceleration onset rates to the 4g level and elevated G levels sustained for up to six seconds.

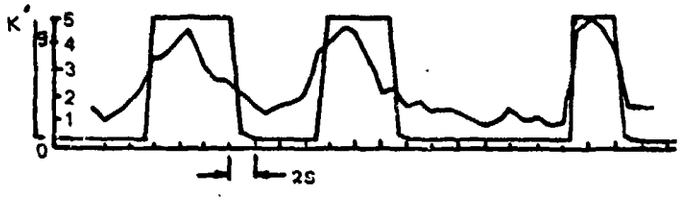


Figure 1.1-1 G levels experienced in a 1938 Heinkel 50 flight (from Von Beckh (18)) (courtesy of Aerospece Medical Association).

The evolution of tactical aircraft has intensified this hostile environment in terms of acceleration magnitude, duration, and frequency of occurrence as demonstrated in Figure 1.1-2 which illustrates G levels recorded during an actual F4E combat engagement (154). The newest domestic tactical aircraft designs have further intensified acceleration levels as depicted in Figure 1.1-3 demonstrating F15 engagement capabilities (86). We often think of such maneuvering as being the sole province of air combat maneuvering (ACM); however, close air support and other air to ground sorties can employ low level terrain avoidance flight strategically.

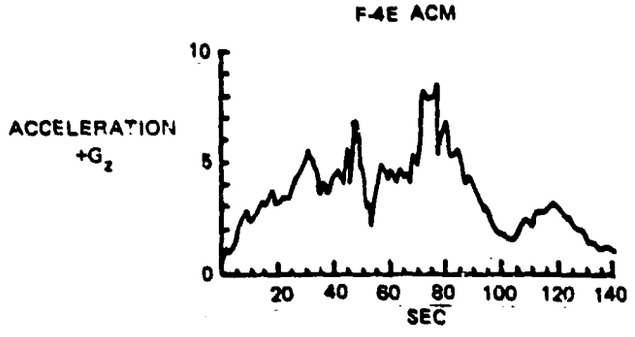


Figure 1.1-2 Recorded G levels (from Leverett & Burton (154)) (courtesy of Advisory Group for Aerospace Research and Development).

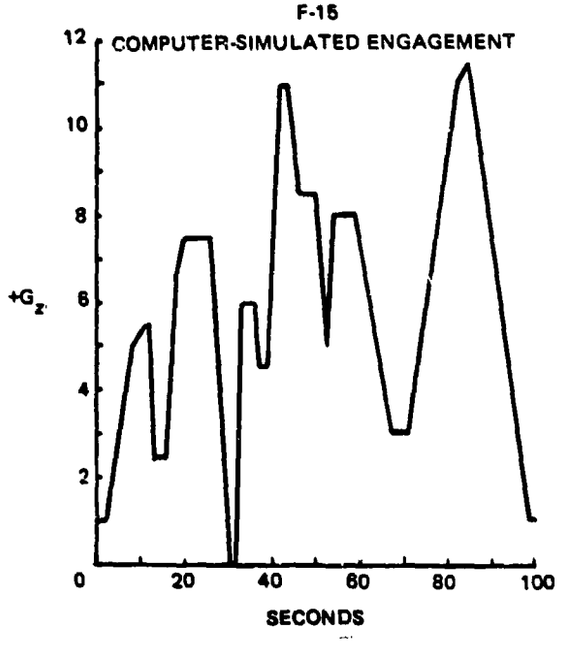


Figure 1.1-3 F15 engagement capabilities (from Gillingham & Krutz(86)).

Perdriel and Whiteside (170) report on significant acceleration induced visual degradation occurring in such flight. It is evident that the technology of aircraft design and mission strategy have produced increases in flight acceleration boundaries reaching the

threshold of that which can be withstood by pilots. Assuming such advantages have been provided friend and foe alike, the measure of advantage may more directly fall on the efficacy of protective devices a pilot is provided with to help increase his resistance to the adverse effects of elevated acceleration and how well trained the pilot is in functioning in this environment.

Entrance to and operation in the high G environment occurs for strategic reasons to gain advantage, and affects, depending on the severity of the acceleration levels encountered, pilot aircraft control (50, 98). Similarly, maneuvering tactics are structured to accommodate the physiological stresses of high G and attempt to minimize the more serious physiological abuse which could lead to catastrophic consequences. Thus, during World War II dive bomber pilots found it preferable to enter a dive with a roll over maneuver which would maintain "positive G's" rather than a push-over which would expose them to the whipsaw effect of "negative G's" during the dive with immediate reversal to positive G's during the subsequent dive pullout. In the latter case the cardiovascular system would complete its compensation for a negative G condition and leave the pilot very unfavorably prepared for the subsequent onslaught of positive G. Even in the more advantageous condition of maintenance of positive G's throughout the maneuver, unconsciousness with resulting involuntary relaxation of the stick was feared and aircraft were normally trimmed up nose-high such that, should syncope (brief loss of consciousness due to sudden lowering of blood pressure) occur, the aircraft might fly itself out of the dive (176).

Simulation for the purposes of pilot training, in the main, has not provided means to replicate the physiological effects of high G. Although centrifuges are invaluable for research, they are not practical for pilot training. Even the lower acceleration levels of normal maneuvering have been exceedingly difficult to

simulate satisfactorily through the use of large simulated cockpit motion systems.

The G-seat approach to somatic stimulation teaches that direct sensory stimulation can be acceptable, useful, and perhaps extended to produce some of the high G effects of importance for training. But what are the effects associated with high G? Which effects are important to pilot control of the aircraft? Which effects alter the structure of a mission? How might these effects be best generated in the 1g training environment? Do the physiological effects include lower acceleration range stimuli useful to the pilot in a broader range of maneuvering circumstances than just those found at high G levels? Are the inclusion of these effects within tactical aircraft simulation worth the cost and possible pilot encumbrance necessary to generate the effects?

These are questions without readily available answers. Yet the trend of aircraft technology indicates both a greater utilization of the high G regime and increased reliance on simulation for training. Therefore those responsible for tactical aircraft pilot training programs and equipment must be concerned with addressing these questions and initiating work leading to their answer.

1.2 Approach

The answers to these questions posed above are rooted in an understanding of the behavioral changes which occur as a function of acceleration induced physiological change. At least two possible approaches could be taken: experimentation within the actual task and attempt to monitor the relationship of individual physiological variables to behavior or, secondly, work within a totally simulated environment and sequentially add the simulation producing additional physiological stimuli while observing behavioral change.

The prognosis in using th' first approach to determine the importance of high G effects is unfavorable. Collyer, in a 1973 report (50) addressing psychomotor testing, addresses this point pessimistically.

"The studies reviewed in this report section indicate that only a few attempts have been made to measure, simultaneously, G-induced changes in both the behavioral and the physiologic variables. The results have generally been disappointing. Indeed, considerable doubt has been expresssed by some researchers that the combined physiologic-psychologic approach has a significant probability of success in the near future. The main reason for this doubt is the complexity, in all psychomotor tasks, which makes it difficult (if not impossible) to establish connection between behavioral integrity and the integrity of physiologic systems. Howard has stated that 'alterations in performance cannot, in general, be predicted from the physiological response to acceleration, because the ability to carry out a task always depends on the functioning of more than one system' (ref. 37; p. 652). Other authors, such as Chambers (14), have stressed that previous research has shown the difficulty of predicting the acceleration thresholds for a performance drop on the basis of those for physiologic changes. The commonly employed physiologic indices have not been reliable or sensitive correlates to the subtle changes in human psychomotor efficiency -- especially in comparatively complex tasks which approximate operational conditions.

Another reason for this difficulty, of formulating general principles for the prediction of behavioral change based on physiologic change, is that both physiology and behavior are affected by stress. As pointed out by Hartman (36) changes in a specific physiologic parameter may be evident as the G-level is gradually increased; but measurable behavioral

changes may not occur until a relatively high G-level has been reached -- at which time the performance decrement may be sudden and dramatic."

We have selected the second approach which advocates that the importance of an acceleration effect can be best evaluated through production of the effect itself within a simulation of the task in which the effect is normally experienced. The Air Force Human Resources Laboratory (HRL) has commissioned the study reported on herein as a step toward that end. We see the overall approach being executed in three phases. This study forms the first phase with an objective of identifying the physiological consequences of, and stimuli associated with, exposure to the high G regime. An engineering assessment of the high G physiological effects is employed with the objective of establishing concepts by which these effects might be introduced in lg laboratory simulation. We believe that a greater number of devices, thus a greater number of high G effects can be initially simulated and investigated in a laboratory environment in which the design of the device may make certain trespasses on environmental fidelity and pilot imposition which may not readily be accepted in line simulation.

The second phase would deal with the design, construction, installation, verification and use of the laboratory devices set forth in the study. This would be the critical phase in identifying the importance of acceleration induced physiological effects as it pertains to the pilot training effort and it is expected that the high G simulation augmentation device would be employed in an otherwise high fidelity task simulation to determine its effect on pilot performance and mode of control. Comparison of pilot simulator performance with and without the benefit of the high G effect would be made against the performance observed in the actual task. It is therefore anticipated that either instrumented aircraft flight or, where feasible, centrifuge simulation would be required to support the investigation. In comparisons of

this nature the more "favorable" simulation performance, and thus a measure of the importance and suitability of the physiological effect under examination, would be defined as that which more closely approximates pilot performance and behavior in the actual task, irrespective of the quality of the performance measured against any other standard.

The objective of the third phase would be to move those high G augmentation devices found to increase the fidelity of high G simulation from laboratory configuration to that configuration acceptable in line simulation. In some cases we would expect the laboratory configuration to be directly acceptable and little effort need be expended in the transfer. However there would likely be other device configurations in which design effort would be required in an attempt to find a configuration which would be acceptable to line pilots. It is unfortunate, but entirely possible, that some of the laboratory devices would demonstrate the importance of a high G effect but not lead to acceptable line simulation implementation.

1.3 Study Objectives

As mentioned above the study phase involves a review and search of acceleration induced physiological effects which are likely to alter pilot performance or mission structure as well as an engineering assessment of concepts which might be employed to introduce these effects within laboratory simulation. The authors' backgrounds represent a mix of expertise in physiological research and principles of simulation. Past experience has provided us with an awareness of the peculiarities of pilot acceptance of simulation techniques. Therefore the thrust of this study is not directed at adding to the body of knowledge pertaining to the physiological effects of high G but rather to cull this body of knowledge for effects we suspect are important and might be subject to a form of simulation.

This technical report is structured in three basic sections: (a) high G physiological effects, (b) mechanization concepts by which some of these effects can be introduced in laboratory simulation, and (c) an appendix containing a summary of information from the more pertinent references discovered during the literature search.

It is apparent that the human physiological processes can be substantially affected by the administration of various chemical substances. Likewise there are physiological effects, or control thereof, which might be most directly achieved via invasive techniques. Based on the potential hazards which exist in both of these areas, they have been excluded from consideration herein.

2. LITERATURE SEARCH

2.1 Sources

The literature search supporting this study was two phased. In the initial phase a search was conducted of the following data banks employing key words relevant to acceleration induced physiological effects:

A) National Technical Information Service

B) Defense Documentation Center

C) Medlars II

Abstract listings were obtained, reviewed, and pertinent reports ordered. These reports in turn referenced material not appearing in the initial search. In the second phase second generation references such as these were made available to us through the Link Library dealing primarily with DDC. Additional refer-

ences were obtained through the libraries of the Massachusetts Institute of Technology and the State University of New York.

2.2 NTIS Interactive Search Key Words

MIT facilities permitted an interactive search of the NTIS reference bank. The key words selected (and number of items found):

Group I

Sustained Acceleration (12)
Long Term Acceleration (1)
Prolonged Acceleration (21)
Long Acceleration (5)

Group II

Acceleration Physiology (562)

Group III

Human (15416)
Humans (2979)
Man (4076)
Astronauts (461)
Pilots (2271)

Grouping

Group II/and/Group III (33)
Group III/and/Group I (53)
Group III/and/Group I/and/Group II (20)

2.3 DDC Search Key Words

The DDC search was not conducted in an interactive mode and employed the following key words:

Group I

Acceleration
Acceleration Tolerance

Group II

Tolerances
Thresholds
Stress
Endurance
Acceleration Tolerance
Physiological Effect

Each item from Group II individually was logically "anded" with Group I to form the elements of the subset representing the product of the search-approximately 250 references.

2.4 Medlars II Search Key Words

The MEDLARS data bank contains references pertinent to the medical field. The key words employed in this search were:

Acceleration/and/Physiology

Approximately 170 references were cited under this key word combination.

2.5 Catalog and Review

All the abstracts obtained in the foregoing search were reviewed by each of the authors. The references which appeared to be useful enough to warrant acquisition were ordered and cataloged according to basic topical relevance. This selection process contributed to the 277 references listed in Section 7 which forms the bibliography of this study. Table 2-1 demonstrates the topical applicability of this bibliography.

Table 2-1 Bibliography topical distribution.

RANK	TOPIC	NUMBER OF REFERENCES SIGNIFICANTLY ADDRESSING LISTED TOPIC
1	Cardiovascular Effects	71
2	Visual Effects	47
3	Misc. (Includes Physiological monitoring devices, data useful to mechanization section herein, etc.	40
4	General Physiological	33
5	High G Protective Devices	25
6	Respiratory Effects	21
7	Lower Body Negative Pressure	21
8	Biomechanical (Static/sustained effects and general information	19
9	Biomechanical (Dynamic, Musculoskeletal Impedance, vibration reaction, impact reaction	16
10	General Review f High G Origin and Effects	10
11	Manual Control Effects	9
12	Simulation	7
13	Labryinthine	6
14	Tactile	6
15	Environmental Force Effects	5
16	Auditory Effects	5

Note: Documents with major applicability in more than one topic are included in total for each topic.

Each author reviewed all the references pertaining to his area of responsibility and as many of the other references as time would permit. Annotated bibliography data sheets (presented in Appendix B of this study) were employed to record particularly pertinent information from the references. In general, annotated bibliography sheets were not used in the review of lengthy works such as text books covering a broad range of physiological information.

By contract statement of work we were to be alert specifically to information relevant to acceleration induced physiological effects related to:

a) Head/helmet loading stimuli

b) Shoulder strap tactile stimuli

c) Extremity (arm) loading stimuli

d) Audition alteration

e) Visual alteration

Further, lower body negative pressure/upper body positive pressure was to be investigated for its simulation applicability. As can be seen in Table 2-1, only minor amounts of information were discovered in the biomechanical audition and wide field tactile areas where as the majority of information pertains to the cardiovascular and visual areas.

2.6 Personal Contacts

In addition to the formal literature search using computer data bases and conventional bibliographic tracing, some extremely valuable leads were generated by discussions with several outside specialists regarding work in progress or additional avenues for exploration. In particular, we received important leads from Dr. Thomas Duane in the area of plethysmographic goggles, Dr. Kent Gillingham in consideration of the relationship between G stress and visual field using quantitative models, Dr. Dana Rogers in the modeling of grayout, Dr. Ralph Goldman in the matter of localized skin heating and cooling, and Dr. Emilio Bizzi in the area of extremity loading.

3. HIGH G PHYSIOLOGICAL EFFECTS

3.1 General

This section briefly introduces the physiological effects we consider to have significance in pilot training. For an extensive examination of the physiological systems at work during sustained high G levels and the resulting effects of high G maneuvers upon these systems, refer to Appendix A.

3.2 Physiological Systems Affected by Excessive G Levels

THE CIRCULATORY SYSTEM

The circulatory system is severely disturbed by excessive inertial forces with the most noticeable and gross effects occurring under increasing positive G_z. As $+G_z$ increases, the blood vessels in the legs passively dilate in response to increasing hydrostatic pressure causing the blood from the upper part of the body to be drained toward the lower extremeties. As a result, the venous return decreases causing a decrease in cardiac output. The upper part of the body does not receive its required amount of nourishment. The pilot notices this deficiency by experiencing a diminution of vision, progressively approaching "blackout" and ultimately loss of consciousness.

It is believed that $-G_z$ causes blood from the lower part of the body to be drained towards the head producing a full feeling in the head and pain in the face and eyes. There exist a controversy as to whether or not this phenomenon causes the so called "redout" (Appendix A).

The circulatory system is not effected by transverse accelerations. However, visual disturbances have been reported above 12 G_x (71). Blurring of vision is not uncommonly experienced at rela-

tively high levels of G_x. Visual blurring has been attributed to lacrimation, the process of tears forming in the eyes disrupting the path of incoming light rays, and is also associated with $+G_z$ effects induced by other physiological phenomena. Thus, the visual effects of G_x can be generated indirectly by the approaches suggested for the simulation of the visual G_z effects.

EXTREMITIES

Subjected to conditions of $+2G_z$, a person can barely rise from his seat; $+3G_z$ makes it nearly impossible to raise the leg; $+6G_z$ restricts arm movement to head level; $+8G_z$ does not allow the forearm to be raised from a horizontal rest (120, 256). A study of the mechanization of limb proprioception under high G and of some physiological performance findings (Appendix A) suggests means to recreate these effects in the 1g environment. Based on this study, we conclude that actual skeletal segment external loading will be required to appropriately generate proprioceptive cuing of environmental acceleration magnitude and to place the proper constraints upon manual task performance.

HEAD/NECK

A review of the literature has indicated a significant amount of head and neck motion exist as a result of acceleration (74, 135, 142, 182). Perception and resistance of head movement are of primary interest to the purpose of this study. Perceptual information relating to head position and movement is supplied primarily by two, possibly three, sensory systems. Besides resisting the inertial reaction of the head, the head/neck musculature detects external displacement forces. The vestibular apparatus supplies information relating to head attitude. It is further believed that the joint receptors may add to the ability of perceiving head/neck motion.

AUDITORY EFFECTS

It has been found that there exist a diminution of auditory acuity at high G levels (42). The occurrence of this is so close to the point of unconsciousness that the two are treated as one and the same.

Since there exist no degradation in auditory acuity until unconsciousness is approached, it was of concern that possibly there might be a need to simulate acoustic characteristics peculiar to the acceleration forces on the airframe. However, no evidence of such specific acoustics existing has been found. Thus, it is the conclusion of this study that no useful training value can be derived in this area of physiological effects.

TACTILE

The most important tactile effects of the high G environment are results of touch and pressure sensations. We are concerned with mainly three tactile effects; perception and magnitude discrimination of large field flesh pressure, perception of light contact of the skin with foreign objects providing an appreciation of the magnitude of inertial load by estimation of body tissue deformation, and perception of the magnitude of skin tension and/or outright scrubbing induced in those areas restrained by or supporting a foreign body.

The literature search revealed a paucity of data concerning these physiological tactile effects occurring under G loading. However, the effects of tactile stimuli on the piloting task must be considered important until proven otherwise.

TEMPERATURE/PRESSURE

It has been found that there exists a sensory relationship

between pressure and temperature perceptions. Because of the difficulty of producing pressure stimuli in the 1g environment within safety limitations, temperature will be considered as a means to produce and/or strengthen pressure sensation.

RESPIRATION

The effects of acceleration upon respiration is most disturbing under the conditions of $+G_x$ and $+G_z$. As a result of pulmonary shunting associated with pooling of blood in the lower regions of the pulmonary circulation and filling of the upper parts of the lung with air under $+G_z$ conditions, there is a decrease in oxygen transport, inspiration becomes difficult, and there is a reported tendency for the breath to be held during inspiration. Under +5 and $+6G_x$ conditions, difficulty of breathing and chest tightness producing much pain are reported. As the G level increases approaching $+12G_x$, the breathing difficulty and chest pain become severe and gas exchange is inefficient to the point of producing hypoxia.

Negative pressure breathing appears to have nearly identical effects on lung mechanics as does forward acceleration, and consequently is considered as a high G augmentation concept. Another approach is to reduce the oxygen content of the inspired air on a breath by breath basis.

4. MECHANIZATION

4.1 General

During the literature search supporting the High G physiological effects discussion presented in Appendix A, the authors searched for information concerning the methods by which a desired physiological effect might be generated in a laboratory simulation environment. Careful attention was paid to investigating whether:

a) A suitable device or concept had been postulated by others and, if so, evaluating its applicability to this program.

b) A by product of an unrelated activity might form a means of generating a physiological response sought herein.

c) A direct address of the physiological system monitoring or sensing the high G effect would form the most favorable approach in view of encumbrances and side effects resident in the direct approach device.

Each of the above considerations has yielded concepts or devices included within the mechanization section. For instance the National Aeronautics and Space Administration has already developed a helmet loader which may be suitable for use in part of this program. Duane's (63) plethysmographic goggles may form a suitable surrogate system to initially evaluate the importance of visual peripheral and central light loss in the tactical aircraft training task. It may be economically preferable to employ the goggles first before committing to the final, and likely expensive, development of a light metering device which directly addresses the eye's photo sensors and is suitable for line simulation production of high G visual effects.

The organization of the mechanization section is closely patterned after the discussion of high G physiological effects. Approaches to stimuli production are advanced in the cardiovascular, musculoskeletal, visual, tactile and respiratory areas. Where possible, the authors have carried the conceptual development to sketch level and identified potential hardware component selection as information supporting the current state-of-the-art feasibility of constructing the device. In those areas where we have discovered that the method by which the device should be driven contains non-obvious elements, a development of the presently envisioned drive scheme is provided.

4.2 Lower Body Negative Pressure

4.2.1 Background

The application of reduced pressure to various parts of the human body has been the subject of investigation for quite some time. Early studies centered about reduced pressure applied to relatively small portions of the anatomy such as the calf, foot, hand, etc. Later interest has been focused on leg negative pressure (LNP), where the reduced pressure has been applied to the total leg, and lower body negative pressure (LBNP), where the area from the iliac crest to the bottoms of the feet are subjected to reduced pressure.

The first such experiments were conducted in 1841 by Junod as reported by Wolthuis (260). He recommended reduced pressure applied to small anatomical areas, to effect localized hyperemia, thereby drawing blood away from diseased organs or areas of the body. He further noted that the resultant pooling of blood in the extremities could induce syncope, which at the time was a satisfactory state for surgery.

In the 1960's LBNP and LNP were the subjects of investigation for two primary purposes, both related to cardiovascular deconditioning. Aerospace researchers connected with the manned space program were interested from the point of view of countering the effects of long periods of weightlessness on circulation. Medical researchers were also interested in the possible application of the technique to patients enduring long periods of bed rest.

The application of LBNP to flight simulation was first proposed by Howard (118) in 1976. He theorized that the visual effects of high G flight could be induced in a flight simulator by artifically reducing venous return from the legs by LBNP.

Another possible application of LBNP to the training of pilots of high performance aircraft is in the training of straining maneuvers such as Ml/Ll etc. This concept would address the concerns of Gillingham (82) with regard to potential blood pressure changes affiliated with practicing Ml or Ll under lg. LBNP could be employed to maintain the eye level blood pressure at safe levels.

4.2.2 LBNP Research

As was indicated above, the LBNP research that has been conducted has not been performed with the application to high G simulation as the intention. The research has been directed towards the previously mentioned applications, however, there is some indication from these data that, at least in terms of magnitude, the desired levels can be achieved. Table 4.2.2-1 reproduced from Wolthuis (260) shows the mean percent change in blood pressure for various levels of LBNP recorded by several researchers. These data are somewhat inconclusive. There are not enough cases at the various LBNP levels to demonstrate the gradient in blood pressure as a function of LBNP level. Some of the data were taken by direct arterial measurement (designated D in Table 4.2.2-1) and

Table 4.2.2-1 Mean percent change in blood pressure by source and for various levels of LBNP (from Wolthuis (260)).

Blood Pressure	Source	LBNP, mmHg		
		-40	-50	-60
Systolic				
D*	Stevens et al. (81)	- 7		
	Stevens and Lamb (80)	-10		- 9
	Murray et al. (57)	- 2	- 5	
I	Wolthuis et al. (90)	- 6		
	Hoffler et al. (43)	- 7	- 9	
	Wolthuis et al. (ms. in prep.)	- 4		
Diastolic				
D	Murray et al. (57)	+10	+14	
	Stevens et al. (81)	- 3		
I	Wolthuis et al. (90)	- 1		
	Hoffler et al. (43)	+ 6	+ 7	
	Wolthuis et al. (ms. in prep.)	+ 2		
Pulse				
D	Stevens and Lamb (80)	-17		-20
	Rowell et al. (73)		-40	
I	Hoffler et al. (43)	-23	-32	
	Wolthuis et al. (ms. in prep.)	-14		
Mean				
D	Dowell et al. (23)	- 6		
	Gilbert and Stevens (33)			- 4
	Murray et al. (57)	+ 4	+ 2	
	Rowell et al. (73)		-13	
	Abboud et al. (1)	- 1		-11
	Stevens et al. (81)	- 5		

* D = direct arterial measurements; I = indirect Korotkov.

some were taken by indirect, i.e., Korotkoff sounds (designated I in Table 4.2.2-1). The systolic pressure shows a general decrease with LBNP as expected. However, the diastolic pressure data produced some rather surprising results; these show either an increase or a very slight decrease.

These results were confirmed to some extent by Musgrave et al (180). Musgrave found that while systolic pressure dropped signi-

ficantly (up to 20 mm Hg) the diastolic pressure increased slightly with increase in LBNP (Figure 4.2.2-1).

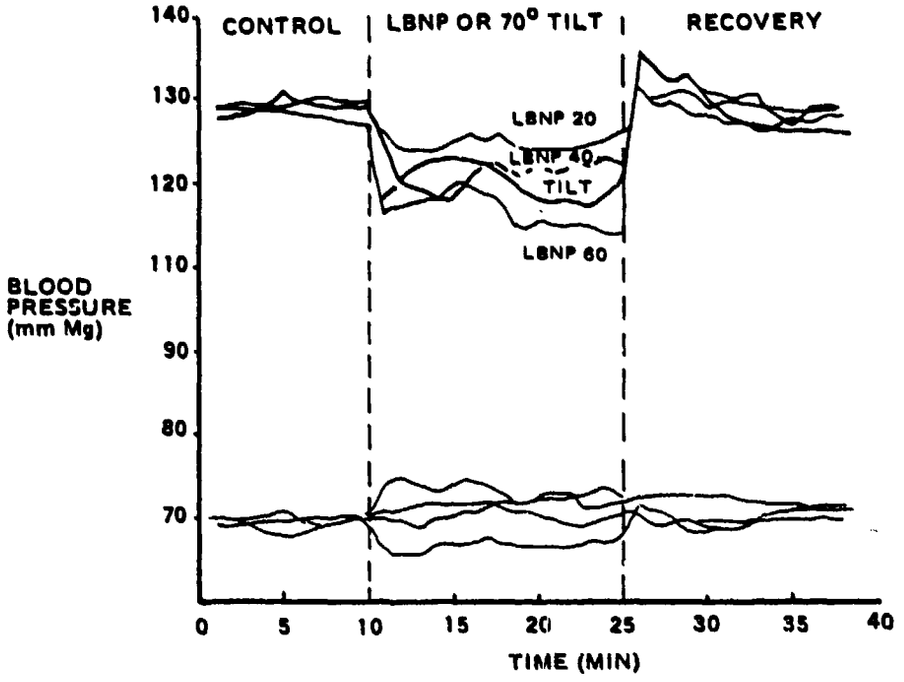


Figure 4.2.2-1 Comparison of the effects of 15 minutes of LBNP at 20, 40 and 60 mm Hg, and a tilt at 60° on blood pressure (from Musgrave (180)).

Wolthuis et al (260) also report a general reduction in pulse pressure with LBNP. The mean blood pressure data are influenced by the diastolic results and are therefore of questionable use here.

The fact that the diastolic pressure does not seem to follow the pattern of the systolic pressure is in itself an interesting question which was not resolved by this study. This is an area

where more data are necessary. Montgomery et al (153) add some interesting data to the controversy over diastolic pressure. They show a sex related difference; males produced similar results to the previously cited work, while females show a decreasing diastolic pressure with increasing LBNP (Table 4.2.2-2).

Table 4.2.2-2 Mean physiological responses ± S.E. of men and women during the recumbent control period and at peak stress during -20, -40, and -60 mm Hg LBNP (from Montgomery (177)).

	Men				Women			
Variable	Control	-20 mm Hg	-40 mm Hg	-60 mm Hg	Control	-20 mm Hg	-40 mm Hg	-60 mm Hg
Heart rate (b/m)	63.6 (3.1)	64.5 (3.1)	76.3 (4.2)+	95.3 (5.2)+	71.1 (2.4)*	81.4 (3.1)*+	105.6 (7.1)*+	118.7 (10.3)*
Systolic blood pressure (mm Hg)	113.3 (1.3)	111.3 (1.6)	107.6 (3.4)*	94.6 (3.7)*	111.3 (1.7)	105.7 (2.3)+	97.5 (2.7)+	63.5 (5.9)+
Diastolic blood pressure (mm Hg)	76.4 (2.6)	75.6 (2.4)	78.3 (2.8)	79.3 (3.4)*	74.4 (1.7)	74.3 (2.8)	71.9 (2.9)	55.0 (4.3)+
Pulse pressure (mm Hg)	37.4 (1.2)	35.6 (1.1)*	29.3 (1.4)+	25.3 (1.6)*+	36.9 (1.5)	31.7 (1.7)+	25.6 (1.9)+	10.3 (1.2)+

*Significant response difference between men and women.
+Significantly different from preceding LBNP stress level.

Other sex linked differences are noticeable such as; the systolic differential pressure is greater for women, also the heart rates are significantly higher for women. This aspect is not of substantial concern at the present time, but if women do become a significant portion of the pilot population, these differences would have to be accounted for if LBNP were employed in a simulator. Further indication that the required magnitude of blood pressure change is achievable with LBNP is that several authors including Wolthuis et al (260) and Shaw et al (220) report that syncope has been induced by LBNP.

However, the question that currently does not have an answer is; does LBNP provide sufficiently high rates of change of blood pressure to follow a 10g/sec or so aircraft profile? The presently available data does not provide an answer to this question.

Looking at the slopes of Figure 4.2.2-1 there is some hope that this may be accomplished.

Musgrave (180) et al raise an interesting point concerning the feasibility of using LBNP in a flight simulator to induce the cardiovascular effects of high G flight. They state that an increase in LBNP produces a sensation of head up tilt, while a decrease in LBNP produces a sensation of head down tilt because of altered blood flow to or from the head. This phenomenon, while understandable, could cause some interference with motion system cuing. Further, no research has been done concerning combinations of LBNP and upper body positive pressure (UBPP).

4.2.3 LBNP Applications

Because of the unanswered questions concerning the applicability of LBNP to the stimulation of the visual effects of high G flight in a flight simulator, it is the recommendation of this study that further research be conducted to verify the concept. The approach appears promising but the following points must be addressed:

- Will LBNP provide suitable cardiovascular time response?
- What is the cause and effect of the diastolic anomaly?
- Are the conditions reproducible?
- Can the safety of the pilot be ensured via non-invasive monitoring techniques?
- Can a suit be designed which permits sufficient mobility to the pilot?
- Is the use of Anti-G Suits and LBNP mutually exclusive?

- Are combinations of LBNP/UBPP and lower body positive pressure (LBPP) upper body negative pressure (UBNP) viable concepts?

- Do the orthostatic effects of LBNP give false cues of subject attitude and therefore interfere with other motion cuing devices?

While all these questions must be addressed prior to considering a device for implementation in a flight simulator there is an order which is felt should be followed. Also there is a manner in which the experiments should be run to extract the desired data.

It is suggested that the Air Force engage the services of a research organization that possesses sufficient physiological resources to conduct these experiments. Further it would be desirable to engage an organization skilled in taking centrifuge data and conducting acceleration research directed at determining visual endpoints. Organizations such as the USAF School of Aerospace Medicine or the centrifuge facility at the Naval Air Development Center are examples.

EXPERIMENTAL APPARATUS

It is felt that the cardiovascular dynamics under LBNP should first be established. These experiments should be conducted in a chamber which would enclose the subject's lower body from just above the iliac crest. The chamber should permit the subject to be seated as in an aircraft seat with his feet on simulated rudder pedals. Figure 4.2.3-1 illustrates a concept for a LBNP chamber. The chamber is designed in two modules; a lower body module (LBM) and a torso module (TM). These are designed such that they are pressure isolated from each other in order that the torso module may have positive pressure while the lower body module is experiencing negative pressure or vice versa. The two modules should be

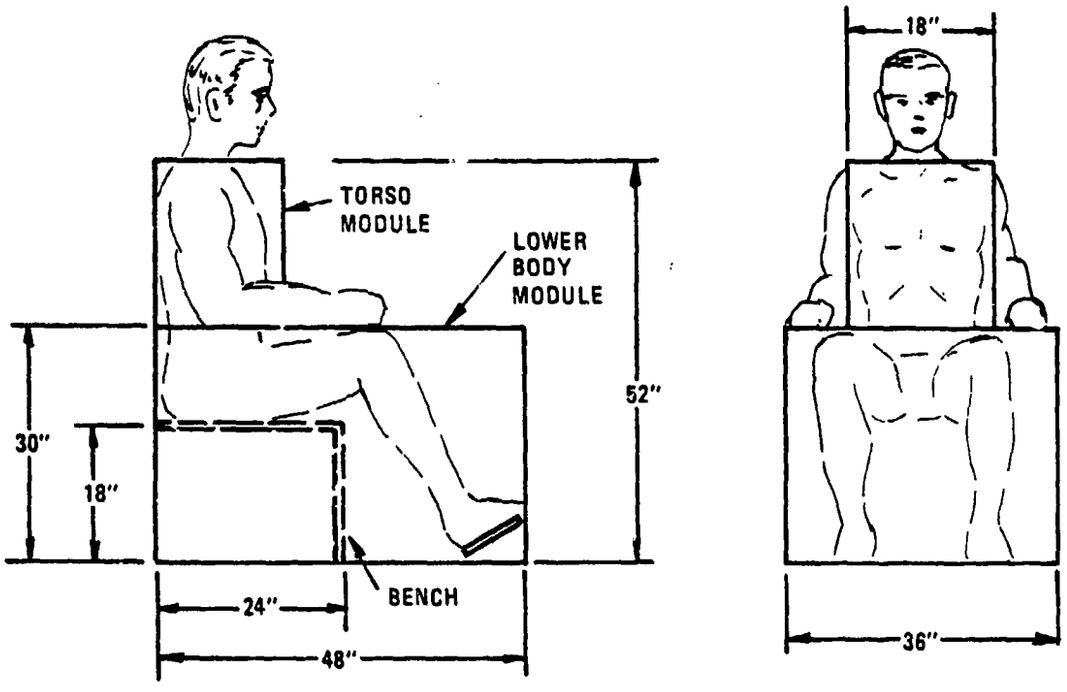


Figure 4.2.3-1 Vacuum/pressure chamber.

separable such that LBNP experiments can be executed without the encumberances on the subject of the torso module.

The openings in each of the modules which permit passage of body elements (head, arms, torso) must have an adjustable seal. Wolthuis (261) presents a design for an adjustable seal that was developed for NASA. This seal consists of a three panel iris type device constructed of 3/4" masonite which close around the body protruding from the chamber. The panels form the support for the rubber sheet that completes the actual air seal. This sheet is 11-13 mil thick dental dam material purchased from Hygenic Manufacturing Company, Akron, Ohio. Rubber sheets should be employed on either side of the panels to provide appropriate seals for both the positive and negative pressure cases.

The chamber itself should be constructed from 3/4" plywood which has been calculated to provide a safety factor of about nine in compression. The plywood should be glued and caulked on all joints to ensure a proper seal. Both torso and lower body modules should be designed to separate at the mid-point fore and aft. The sections should be held together with an adjustable snap lock and the joints should be edged with a compressible material such that when the snap lock is tightened an airtight seal will be formed.

The lower body module shall be constructed with an integral bench, including a fascia member, all constructed from 3/4 inch plywood. These joints should also be glued and caulked. A piece of 3/4" plywood should also be used for the simulated rudder pedal.

The lower body module should also be fitted with a simulated side arm control stick on the right side and a simulated throttle lever, on the left side. These are to provide hand grips and to permit the evaluation of the effects of muscle tension on the experiments.

The volume of the vacuum/pressure chamber is the sum of the torso module and the lower body module. The volume of the torso module is 3.4 cubic feet and the volume of the lower body module is 21 cubic feet. The maximum rate of change of acceleration in the airplane can be considered to be 10 g/sec. It must now be determined what flow capacity is required to control the pressure in the chamber.

Stevens and Lamb (233) state that -80 mm Hg is sufficient to induce symptoms of impending syncope. They also state that at a LBNP level of -80 mm Hg there is a 37% reduction in systolic pressure. Based on the fact that a nominal level for central light loss is 5g then one might assume that the pre-syncopal episode occurs at approximately the same blood pressure as central light

loss and therefore -80 mm Hg would produce about the same reduction in eye level blood pressure as 5g acceleration. The rate of change of pressure in the chamber would then be about -80 mm Hg in 0.5 sec or 160 mm Hg/sec which is approximately 3.2 psi/sec. These are then the pneumatic criteria for the design of the vacuum system.

Table 4.2.3-1 lists the mean systolic pressure for the subjects in the Stevens and Lamb (233) experiments.

Table 4.2.3-1 Mean systolic pressure (from Stevens (233)).

LBNP (mm Hg)	% Reduction
0	0
-25	12
-40	23
-60	32
-80	37

The control system required for the conduct of these experiments is shown in Figure 4.2.3-2. A compressor unit as well as a vacuum pumping station are required. The flow to the two modules is controlled by a flow control valve for each module. The flow control valves are driven by a microprocessor which can be programmed with various profiles simulating aircraft acceleration profiles. The microprocessor should also sequence the solenoid valves. Pressure feedback to the microprocessor is provided by a pressure transducer associated with each module. The pressure profile could be programmed either with a table lookup technique or with an analytic expression relating pressure as a function of time.

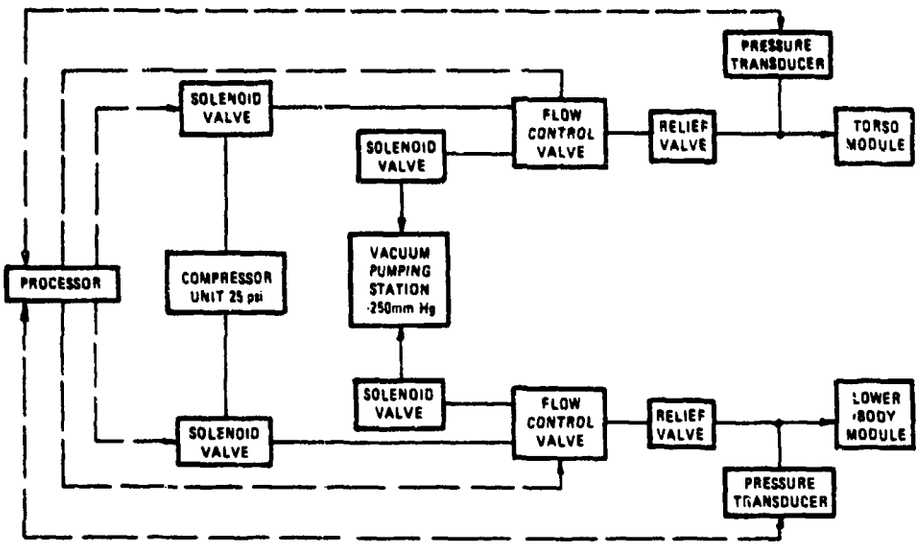


Figure 4.2.3-2 Vacuum/pressure chamber control system diagram.

A light bar similar to that used by Rositano et al (209) should be employed to investigate the visual effects induced by LBNP. The data that are required as results of these experiments are, in decreasing order of importance.

- Blood pressure as a function of LBNP level
- Time response of blood pressure
- Visual acuity as a function of LBNP level
- Visual acuity time response
- Determine the effects of anti-G suit and straining maneuvers
- Employ all modalities LBNP alone, LBNP and UBPP, UBNP and LBPP

Blood pressure and heart rate should be continuously monitored during these experiments. Non-invasive blood pressure monitoring devices are discussed in a following section (4.2.4). It may be useful to conduct these experiments with both invasive and non-invasive measuring devices in order to evaluate the effectiveness of the non-invasive devices.

PORTABLE LBNP DEVICE

If the results of the experiments are favorable, the next step would be to construct a LBNP device that could be worn in the simulator and employing an existing simulator in an attempt to ascertain

- If the motion and LBNP cues conflict
- If there are any artifacts due to LBNP
- If so, what are their effects?
- If the device is suitable for use in a simulator

A possible design of a portable LBNP device is shown in Figure 4.2.3-3. Four pressure vessels are required one enclosing each leg (leggings), one enclosing the lower torso (lower torso girdle) and one enclosing the upper torso (upper torso vest). The pressure vessels are to be of rigid or stiffened construction with articulated joints to provide mobility. These vessels must be able to support a pressure differential of at least 2 psi (there does not appear to be a differential difficulty of joint movement at high and low pressures with $\Delta P \simeq 2$ psi), the pilot must be able to fly the simulated aircraft while in this device and there should be consideration given to the possibility of heat generation inside the suit. Further, the system must not interfere with

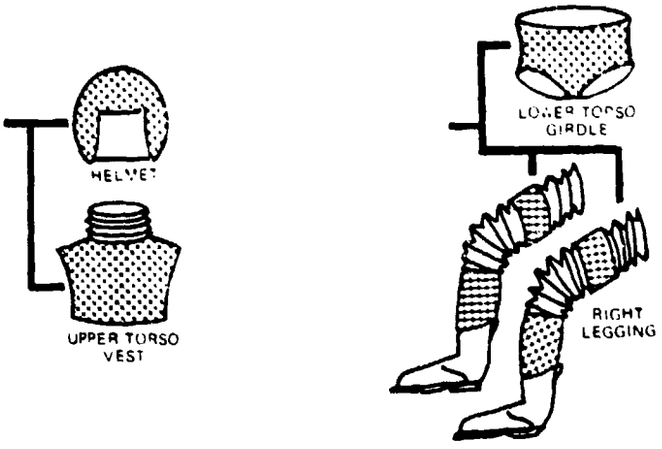


Figure 4.2.3-3 Possible configuration of LBNP device.

G-seat operation. Consideration must also be given to the visual and tactical environmental fidelity loss due to this device.

A possible vendor for the LBNP device is the David Clark Company of Worcester, Mass. They have experience in pressure suits and space suits. They also built a collapsible LBNP for Cooper and Ord (51) for their LBNP experiments.

USE OF LBNP FOR M1/L1 MANEUVER TRAINING

It is well known that the M1/L1 maneuvers provide significant relief from the effects of high sustained/rapid onset accelerations (section A.2 of this report). However there may be problems associated with practicing these maneuvers in a one G environment. Dr. Gillingham of USAF School of Aerospace Medicine (82) states that a properly performed M1/L1 maneuver will raise the eye level blood pressure by 100 to 150 mm Hg. This, Gillingham believes, is an unacceptable risk. As was indicated previously, a possible application of LBNP is suggested by these facts. As reported by

Stevens and Lamb (233), a better than 50 mm Hg drop in systolic pressure was observed with the application of -80 mm Hg LBNP. This would seem to alleviate most of the concern Gillingham has expressed if pilots were to train in an LBNP device for the M1/L1 maneuvers. This has an obvious cost advantage over training in the centrifuge. Also, one of these devices could be provided at each USAF base, thereby eliminating the need for travel to a centrifuge for this training. It is suggested that the feasibility of this approach be verified as part of the research recommended herein.

CONCLUSIONS

Since insufficient data on the time response of blood pressure to LBNP and since no data directly applying this technique to the problem addressed here is available, it is recommended that research be conducted to ascertain the viability of this approach. Hardware required was specified. A possible mechanization for line simulation use was also presented. Finally, an additional use of LBNP was suggested for the training of pilots in the proper execution of the M1/L1 maneuvers.

4.2.4 Non-Invasive Cardiovascular Monitors

During exposure to LBNP it is necessary to monitor the subjects cardiovascular condition (particularly blood pressure) continuously. There are two reasons for this; the first is to ensure subject safety and the second to provide feedback for the control of vacuum in the LBNP device. For the research phase, it would be possible to employ invasive techniques. However, in either application directed to training pilots, either in a flight simulator or in the M1/L1 training device, it would be extremely undesirable and indeed perhaps impossible in some instances to resort to invasive techniques. Therefore, it is relevant to this study that non-invasive techniques be investigated. A device must be found

to monitor automatically, continuously and non-invasively the blood pressure of the subjects in the LBNP research apparatus, in the simulator LBNP device, and the M1/L1 training device.

AUSCULATORY BLOOD PRESSURE TECHNIQUES

The most common method for measuring human blood pressure indirectly is the ausculatory method proposed by Korotkoff in 1905. This technique employs a sphygmomanometer and relies on the interpretation of the Korotkoff sounds and relating them to a pressure reading on a mercury manometer. The ausculatory method can be automated. Nolte (130) reports on a device designed by Martin Marietta Co., Denver, for use on the Skylab flights. Figure 4.2.4-1 illustrates the system. There are several of these devices available such as one reported on by Fernandez and Robinson (68) and another described by Cromwell et al (53) and manufactured by Narco Biosystems Inc., Houston. In general these systems all have automatic cuff inflators, pressure transducers and signal

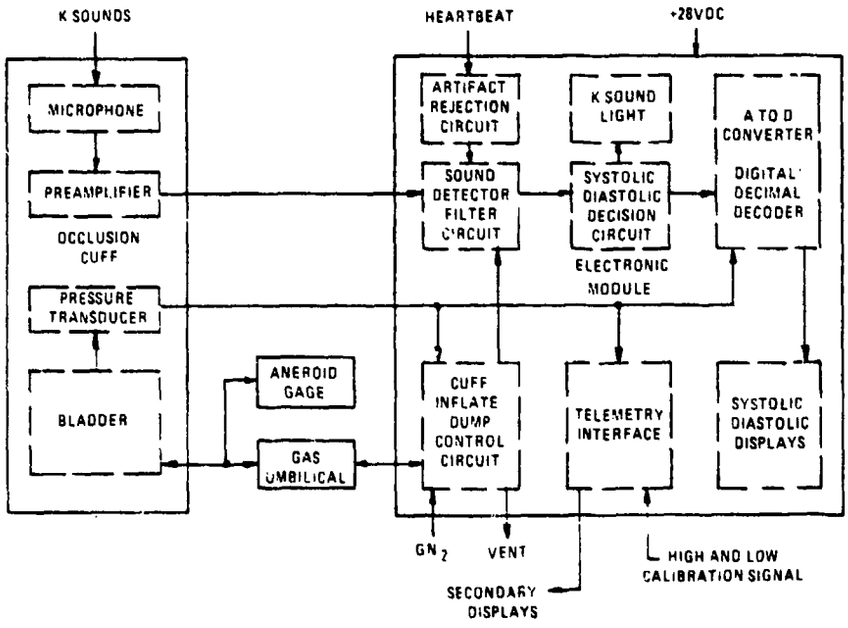


Figure 4.2.4-1 Automatic electrosphygmomanometer designed by Martin Mainetta of Denver for the kylab program (from Nolte(130)).

processing equipment to identify automatically the Korotkoff sounds and correlate a cuff pressure reading with it. The Narco unit does not have signal processing electronics.

While the ausculatory method has merit in that it provides reasonably accurate results, it has some drawbacks, the major drawback being that these devices are not truly continuous since they can be sampled only once every 30 seconds or so. The reason for this as stated by Geddes (76) is that the cuff deflation rate should be 2-3 mm Hg/sec to prevent venous conjestion in the distal bed.

Another disadvantage to the ausculatory technique is that the presence of an inflating/deflating cuff would be a distracting artifact to the pilot.

ULTRASONIC BLOOD PRESSURE MEASUREMENTS

One method of monitoring blood pressure ultrasonically is similar to the ausculatory method described above. However, the interpretation of Korotkoff sounds is replaced by the Doppler shift of the transmitted ultrasonic frequency. This shift is proportional to the arterial wall velocity which gives information to identify the instant that the vessel opens and closes. This method also employs a pneumatic cuff and is therefore subject to the same restrictions as the ausculatory. A device employing this technique is marketed by the Roche Medical Electronics Division of Hoffmann-La Roche Inc., Cranbury, N. J. It is marketed under the trademark Arteriosonde.

Another ultrasonic technique employed is the use of a ultrasonic signal to determine the velocity of blood flow in an artery. The Doppler shift of the signal reflected from the moving red cells is proportional to the velocity of the blood flowing in the artery. This method may also be used with a cuff and provides the

same information as the arteriosonde except the diastolic pressure may be more inaccurate and is subject to the same limitations. A device of this type is manufactured by Parks Electronics Lab., Beaverton, Oregon and is called an Ultrasonic Doppler Flow Detector, Model 811.

The Doppler flow velocity may possibly be used to directly determine blood pressure. If it can be assumed that the vascular resistance is constant for some small length of artery and for a given person then the relation

$$V = \frac{\Delta P}{R} \qquad \text{[Eq. 4.2.4-1]}$$

should hold; where $\dot{V}$ is blood velocity, R is vascular resistance, and ΔP is pressure change. Therefore blood pressure may be considered proportional to velocity. While this method is not very accurate, if each subject is calibrated it may be sufficient for monitoring purposes during LBNP in a training device. But, it would not be adequate if any quantitative measure is required.

PULSE WAVE VELOCITY

Pulse wave velocity is a measure of the velocity of the pulse wave as the pulsatile pressure wave of blood courses through the vascular system. The pulse wave is detected at two points, for example, the brachial artery and the radial artery, then knowing the distance between the points and the transit time of the pulse wave, the velocity may be computed. The proponents of this technique claim that blood pressure may be inferred from the velocity if the subject is calibrated. In 1976 Geddes (76) was skeptical of the claims of the proponents of pulse wave velocity primarily because, at that point in time, no reliable means for detecting the pulse wave had been developed. Today, however, it appears that the detection problem may have been solved. The Cyborg Corp.

of Boston, Mass. has developed a pulse wave velocity monitor which employs a displacement transducer applied over an artery close to the surface to detect the passage of the pulse wave. Cyborg claims a -0.913 to -0.98 linear correlation with blood pressure measured by cuff or cannula.

The disadvantage to this device is that it is highly subject to artifact due to movement. The processor has an artifact detection algorithm and suppresses the output at that time. Cyborg claims to be presently developing a system which will be less subject to artifact. It uses the output of a ECG sensor placed on the radial artery together with a displacement transducer located at another artery. This may have merit since the other sensor could be placed on the temporal artery and eye level blood pressure could be monitored. This sensor may be subject to artifact due to jaw movement such as talking.

EAR OXIMETRY

An ear oximeter is a photoelectric device for measuring the 0_2 saturation of the blood in the ear or the amount of blood in the vessels of the ear. The former uses red light at 64.0 mu and the latter infrared at 800 mu. Although this technique will not provide blood pressure directly, the amount of blood in the ear is a good indicator of cardiovascular performance and may be used as an indicator of LBNP effectiveness. Geddes and Baker discuss this technique at some length (77).

This may be the best technique which could be employed to monitor blood pressure in a flight simulator or M1/L1 training device during LBNP. The most difficult aspect may be to gain acceptance of pilots having the sensor attached to their ears.

PLETHYSMOGRAPHY

Plethysmography is the measurement of blood volume by measuring pressure changes in a pressurized chamber surrounding a limb of interest. The instrument, described by Cromwell et al (53) uses electrical sensors to measure changes in impedance as an indicator of volume changes. This technique is not very accurate in terms of absolute magnitude. However, it is quite good in terms of measuring changes in volume. This technique might be more acceptable to pilots than the pneumatic plethysmographs since it has fewer encumberances.

HEART RATE MONITORS

Monitoring heart rate indirectly is a much simpler problem to solve than that of monitoring blood pressure. Indeed, there are many devices on the market which serve quite nicely. Mennen Grealbatch Inc. of Clarence, New York, NARCO Bio-Systems Inc. of Houston, Texas and Cyborg Inc. of Boston, Mass, are three companies that manufacture devices that would be quite suitable for the intended application. The device would be used to monitor heart rate during LBNP episodes either in the flight simulator, the M1/L1 training device or the LBNP research device.

Some of these devices are stand-alone heart rate monitors; others are a by-product of other measuring devices such as ECG or pulse wave velocity.

CONCLUSIONS

As yet the state of the art has not advanced to the point of providing suitable unencumbering devices, free from artifact, as accurate as direct measurement techniques which provide continuous monitoring of blood pressure in a flight simulator or a M1/L1 training device. Among the most promising of these apparatus for

the aforementioned applications are ear oximetry, pulse wave velocity and impedance plethysmography, not necessarily in that order. It is worthwhile to note that Miller (173) provides a comprehensive survey and annotated bibliography of non-invasive physiologic measurement techniques.

4.3 High G Visual Effects Generation

4.3.1 General

In the high G environment the most often reported, the most thoroughly documented, the most exhaustively studied phenomenon is that of diminution of visual acuity. The physiological basis for these effects is discussed in section A.3 of this report. As is described in section A.2 of this report, the cardiovascular stress induced by high G flight is the primary source of all visual effects. The emphasis of this study is on the visual effects and their causes. The reason for this emphasis is because of the high degree of importance that this effect has on the pilot's performance. During air-to-air combat, with degraded peripheral vision a pilot may not see an attacking aircraft. Obviously, if the pilot blacks out (loss of central lights) during a high G maneuver, serious problems to his safety will occur. If these effects are not present in the simulator, the pilot will employ maneuvers which would not be possible in the actual aircraft.

The following subsections deal with means to implement these effects. Three general approaches are discussed. One employs the principles of ophthalmodynamometry to develop a set of plethysmographic goggles. These goggles would effectively artificially raise the intraocular pressure until it is greater than the eye level arterial pressure, thereby inducing the same effects as a lowering of the eye level arterial pressure below intraocular pressure as is the case in the aircraft under high $+G_z$.

A second approach uses liquid crystal technology to develop a helmet visor with the capability of selective variation of transmission of light. This technique would attempt to imitate the visual effects by altering the transmissibility of the visor by controlling the liquid crystal elements within the visor.

The third means of simulating the visual effects is to selectively attenuate the visual scene and the instruments' lighting to attempt to reproduce the effects of tunnel vision. All three of these techniques require an algorithm to provide the drive signals for each system consistent with the acceleration environment. In section A.3 a sophisticated model of the visual effects of high +Gz is postulated with some missing elements.

In this section a simplified algorithm is presented which provides for immediate implementation. The basic algorithm applies to all three systems.

In order to account for pilot eye movement, an oculometer is suggested to determine the pilot's line-of-sight thereby permitting a centering of the reduced acuity areas about the foveal view.

It is recommended that a set of plethysmographic goggles be evaluated along with an integrated system comprising an oculometer and visual system/instrument dimming all being controlled by the simplified algorithm. It is further recommended that this evaluation be conducted on the SAAC because of its wide field of view visual system, its six-degree-of-freedom motion system, its G-Seat, its Anti-G Suit simulation, its provision for air-to-air combat simulation and because contractor personnel are available to provide implementation.

The liquid crystal visor is recommended for phased development and evaluation.

4.3.2 Oculometer

As has been previously mentioned, the most important high G effect is the diminution of the cone of vision with increasing $+G_z$. In order to properly align the "tunnel", it is necessary to know in which direction the pilot is looking, i.e., his line of sight must be known. If the pilot's instantaneous line of sight is not known and the center of the cone of vision is chosen arbitrarily, say along X-body axis of the aircraft and if the pilot happens to be looking out along the T-body axis of the airplane, the tunnel will be 90° from the pilot's line of sight and will appear artificial.

To determine the pilot's line of sight an oculometer has been chosen. This device will provide the X and Y coordinates of the line of sight intersection with the plane of interest, such as the instrument panel or the display screen. The principles of operation of the oculometer are; a source of infrared light illuminates the eye, some of this light is reflected by the cornea and some passes through the pupil and is reflected by the retina and effectively backlights the pupil. This light is then sensed by a vidicon which passes a video signal to a signal processor which computes the relative displacement of the corneal reflection relative to the center of the pupil. The signal processor is a mini-computer with two specialized circuit boards.

Previously available oculometers have restricted head movement first in a one inch cube and then eventually to a one foot cube. The pilot of a simulator for a high performance aircraft requires unrestricted head movement thereby precluding the use of a device of this type. Middleton et al (171) describe the use and principles of operation of a state-of-the-art oculometer.

The Honeywell Company, Avionics Division located in Minneapolis is presently developing a helmet mounted oculometer which

should be available in 1979. An oculometer has been used in many different eye movement studies and has proved to be a useful device in locating the line of sight in space. The area that requires further study is the time lags inherent in the system. This data won't be available until a helmet mounted system is built and integrated into a flight simulator and tested.

If these lags are excessive when the pilot moves his head he would notice the "tunnel" disappear and then reappear at a new location. This would be a distracting artifact and could compromise the training value.

The oculometer could be used to determine the line-of-sight for selective dimming of the flight instruments and the visual scene. It can also be used in the variable transparency visor application described in section 4.3.5.

It is recommended that the helmet mounted oculometer presently under development by the Honeywell Corporation be purchased and tested on the SAAC as part of the system outlined in section 4.3.1. During this testing the time lag questions can be answered.

4.3.3 Simplified High G Visual Acuity Model

The high G literature assigns importance to, and dwells extensively on, G induced visual effects because of, we suspect, the overt noticability of the effects coupled with the fact that significant disruption or loss of vision effectively poses a bar preventing further positive pilot contribution to his required tasks. Vogl (246) points out that in flight simulation, it is important to teach a pilot those regions of the flight envelope not accessible to him physiologically. Vogl uses the discomfiture of the G-suit as an example of means to limit the pilot to physiologically accessible portions of the flight envelope. A parallel

argument can be made for the importance of including high G visual disruption within tactical aircraft simulation, for it's presence forces the pilot to recognize his physiological limitations and the impact these limitations pose on his mission performance vis-a-vis his control strategy and skill level.

In section A.3.1 of this study, the structure of a model defining visual perception degradation as a consequence of exposure to high G_z conditions is presented. The model parallels that suggested by Rogers and Quam (206) and employs G induced change in blood pressure as its primary drive parameter. At present the model lacks data specifying the very important relation between localized retinal hypoxia and acuity. It is expected that effort will continue to develop missing data in a context useful to this model and eventually the blood pressure model will form the basis for altering simulator visual effects in response to high G conditions. However in the interim, because of the apparent importance of the visual disruption, a simplified surrogate model is required for the purposes of developing visual disruption techniques as well as providing a basis for initial evaluation of the credibility and importance of the effect. This section presents a model the authors have developed to serve this purpose. It is presented in flow chart form and is directly suitable for implementation within digital computational simulation. A definition of symbols employed immediately follows the model flow chart.

As is the case in some of the other simulator models developed to approximate high G visual effects, the model developed herein is structured in the context of G magnitude as opposed to blood pressure change. Salient features which may be somewhat different however are:

1) Rather than strict sole dependance upon a threshold G level for producing the visual disruption, the model employs both G level and onset G rate as Stoll's data

(234) suggests in order to establish the dynamics of the ensuing visual disruption.

2) The G level above which visual disruption eventually will occur is permitted to vary as advocated by Rogers and Quam (206) based on G-suit operation and M1/L1 maneuver execution.

3) A reduction in foveal acuity is scheduled to occur at G levels below that producing peripheral dimming as suggested by Haines (107) and the data produced by White (258).

The model is structured to provide outputs to control simulator visual display systems. Cockpit instrument illumination, and/or an area of interest variable transparency visor is discussed elsewhere in Section 4 of this study. Inputs are accepted from these simulator subsystems as well as the flight dynamics model, the G-suit system, and an EMG device used to monitor the subject's execution of M1/L1 maneuvers.

Basically the model will command a reduction in either contrast ratio or, less preferably, illumination level, of low light level sources over the total expanse of the visual system and/or visor. This change will occur in linear relation to G_z acceleration when the G_z level ranges between 1.85 g's (derived from 258) and that level which will eventually produce peripheral light loss. Contrast ratio change is preferred because, although data demonstrates a reduction in acuity in these circumstances, it does not seem to be subjectively perceived as a light level dimming in the same sense as peripheral light loss. The contrast ratio of the cockpit scene, on the other hand, can be altered only by varying the illumination level of the low light level instruments.

Operation above that G_z level which eventually produces peripheral light loss (termed G_{CRIT} herein) triggers the sequential collapse of two terminators inward toward the center of the visual binocular FOV. The rate of collapse is established by the G_z onset rate extant below G_{CRIT} as modified by the current G_z margin above G_{CRIT} and has been derived from Stoll (234) data. The FOV dynamics produced by the derivation show good agreement with Rositano's experimentation (209) but less favorable agreement with McNaughten's 13° reclined seat centrifuge experience (87). The McNaughten run demonstrates an inexplicably high rate of FOV closure. The run also produced a rather precipitous entry to unconsciousness without passage through an identifiable blackout period and therefore may not form a reasonable comparison.

Both the Rositano (209) and Gillingham (87) work record FOV remaining and G level on x-t strip chart recordings which demonstrate a FOV closure profile with characteristics tending toward second order response. The model herein employs a two segment straight line approximation to the response. The first segment is used between the onset and completion of peripheral light loss and the second segment between complete peripheral light loss and completion of central light loss or total "blackout". A number of references comment on the comparative rapidity of FOV expansion upon return to lower G levels. Using the above mentioned strip chart recordings, a two second duration linear FOV expansion profile was selected for incorporation in the model.

The two terminators employed within this model form concentric circles in the binocular field of view and define a band between terminators. The inner terminator is called the "disturbance terminator" which defines, at any instant in time, an included circular area in which no visual disruption occurs due to G_z levels above the G_{CRIT} value. The outer terminator, called the "blackness terminator", describes an external area in which total light suppression is scheduled. Progressive contrast reduction

and subsequent illumination reduction occur radially within the annular area between terminators as described in Section 4.3.6. The width of the annular, or grayout, area is not defined in the literature reviewed and consequently is established within the model as a constant, K_{BAND}, subject to alteration. The model is responsible for maintaining a definition of the conical angles associated with both terminators and providing this information to the simulator visual, visor, and instrument subsystems where it can be merged with the oculometer data defining the direction of the subject's line of sight such that the appropriate visual effect can be properly positioned.

The terminators are both stored outside the binocular FOV, horizontally 95° (103), during 1g conditions. The terminators are held here until the G_z level surpasses the current value of G_{CRIT}, or that level which eventually would produce peripheral light loss, at which time the terminators are permitted to collapse inward. The rate of collapse will carry the blackness terminator to the position defined for complete peripheral light loss, nominally set herein at 8°, over a duration commensurate with the data. The disturbance terminator and grayout area precede the blackness terminator into the shrinking field of view and hold at the point of peripheral light loss while the blackness terminator "catches up" causing the grayout band to disappear, replaced by total light suppression. Once the blackness terminator reaches the peripheral light loss point, a new rate of closure is computed causing the remaining central FOV to collapse to total blackout over two seconds (234). The disturbance terminator and grayout band do not precede the blackness terminator in the central light loss phase.

The model will cause total light loss to remain until the G_z level is either lowered to the G_{CRIT} level or conversely the G_{CRIT} level is raised, by subject M1 maneuver execution, above the current G_z level. Both terminators rapidly expand outwards under

these conditions however the disturbance terminator delays long enough to reestablish the grayout band. Terminator direction reversal can occur at any point in the collapse or expansion sweep; consequently, a subject, by carefully controlling his G level and M1 execution, should be able to exercise some control over the penetration of the grayout band into his field of view.

The model advanced herein employs circular terminators. However, the binocular field of view is elliptical in shape (103). Gillingham (87) provides some interesting figures (see Figure A.3.1-2) depicting the shape of the field of view during collapse which suggests that this elliptical shape is at least preserved, and perhaps accentuated, during high G visual light loss. Once provided terminator positional definition in the context of circles, it is a fairly routine step to convert this information to elliptical form. However, this step must be undertaken by the using simulator subsystem in that the required conversion is a function of location along major and minor axes.

Although the flow chart of the model is liberally annotated to provide ease of understanding its mechanization, additional comment is worthwhile in some areas located by the numerical index provided to the left of the flow chart. At index #2 the critical G_Z level which will eventually produce peripheral light loss is computed. The critical level is considered to be the sum of a basic G level, the protection offered by inoperative and operative G-suit, and the further protection offered by execution of the M1/L1 maneuvers. The basic resistance level of a subject including involuntary cardiovascular compensation is taken as 3 g's and appears to be frequently cited in the literature and the data supporting this literature. The incremental protection of an inoperative and operative G-suit is drawn from Burton (34) and the full measure of incremental protection afforded by proper execution of the M1 maneuver is taken from Gillingham (86). Increased fidelity would be obtained by using a continuous rather than discrete func-

tion for the M1 protection. The modifiers converting discrete to continuous form can be derived from Rogers and Quam (206) and probably could take the form of passing the discrete signal through a first order lag network augmented with fixed decay.

Acuity reduction at levels below the G_{CRIT} value are computed for visual display system, instruments, and/or visor between index #6 and #18. The key expression used herein is found at index #8 where an effective target (foveal view) illumination level reduction, derived by cross plotting data provided by White (258), is implemented. The reduction in effective illumination level is employed, where possible, to alter contrast ratio where contrast ratio is defined as:

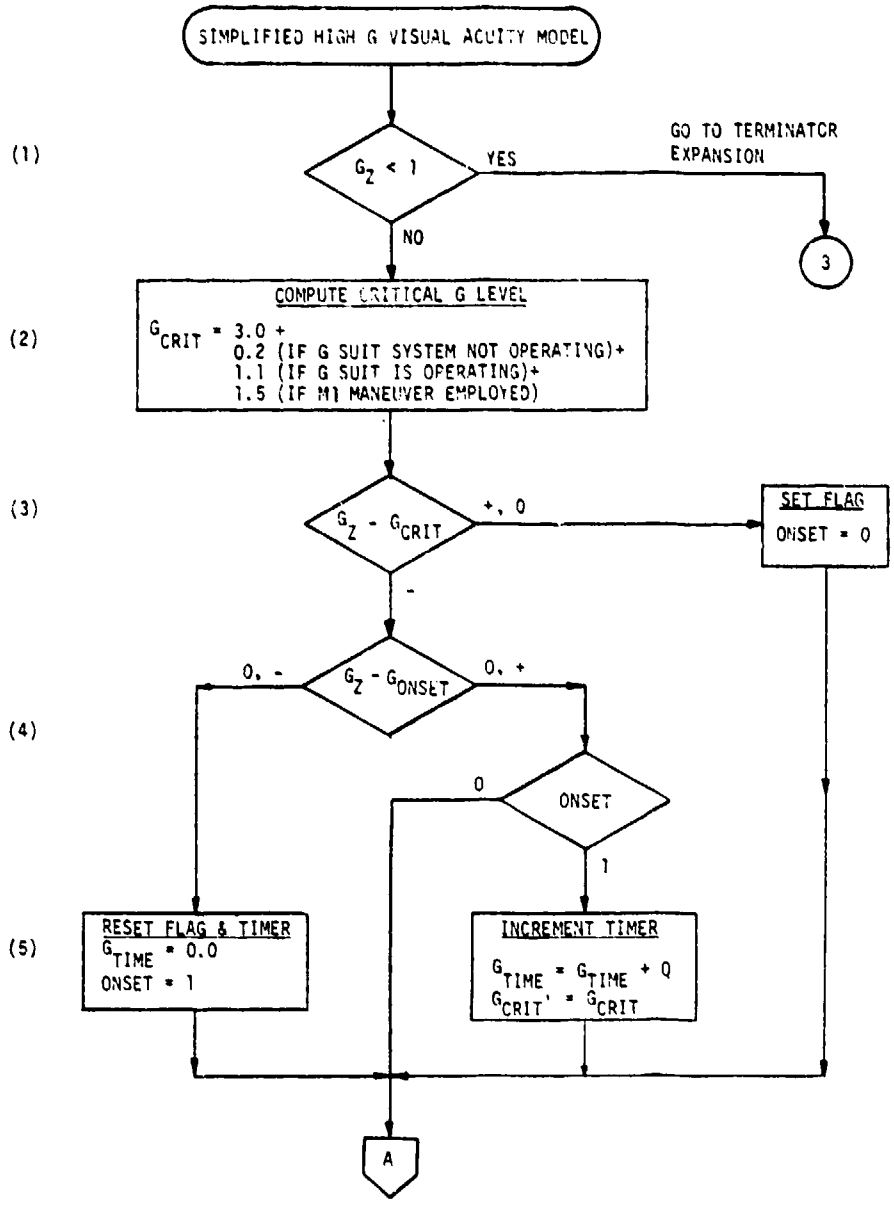
$$CR = \frac{\text{Target Illumination - Background Illumination}}{\text{Background Illumination}}$$

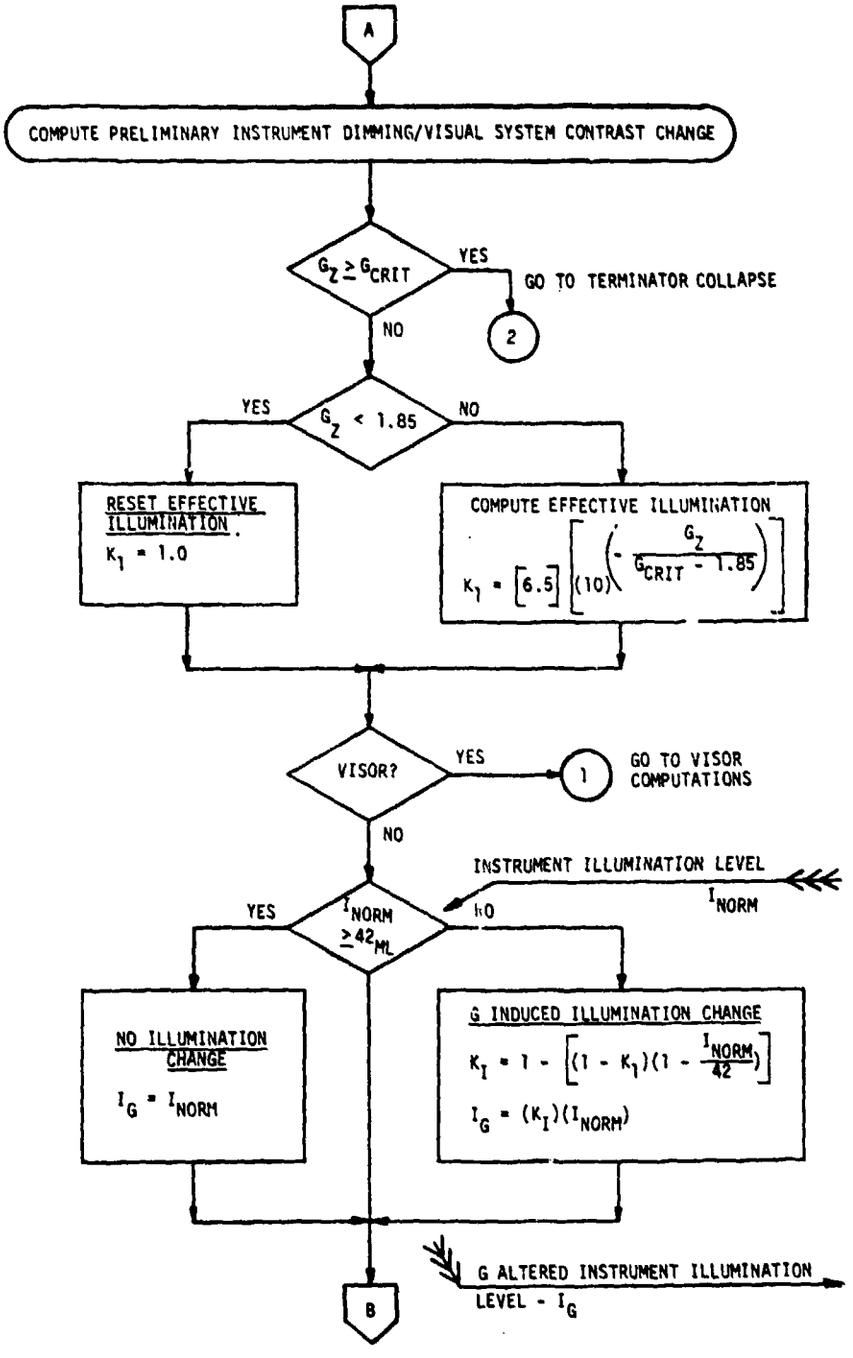
and the value of background illumination is considered to remain constant.

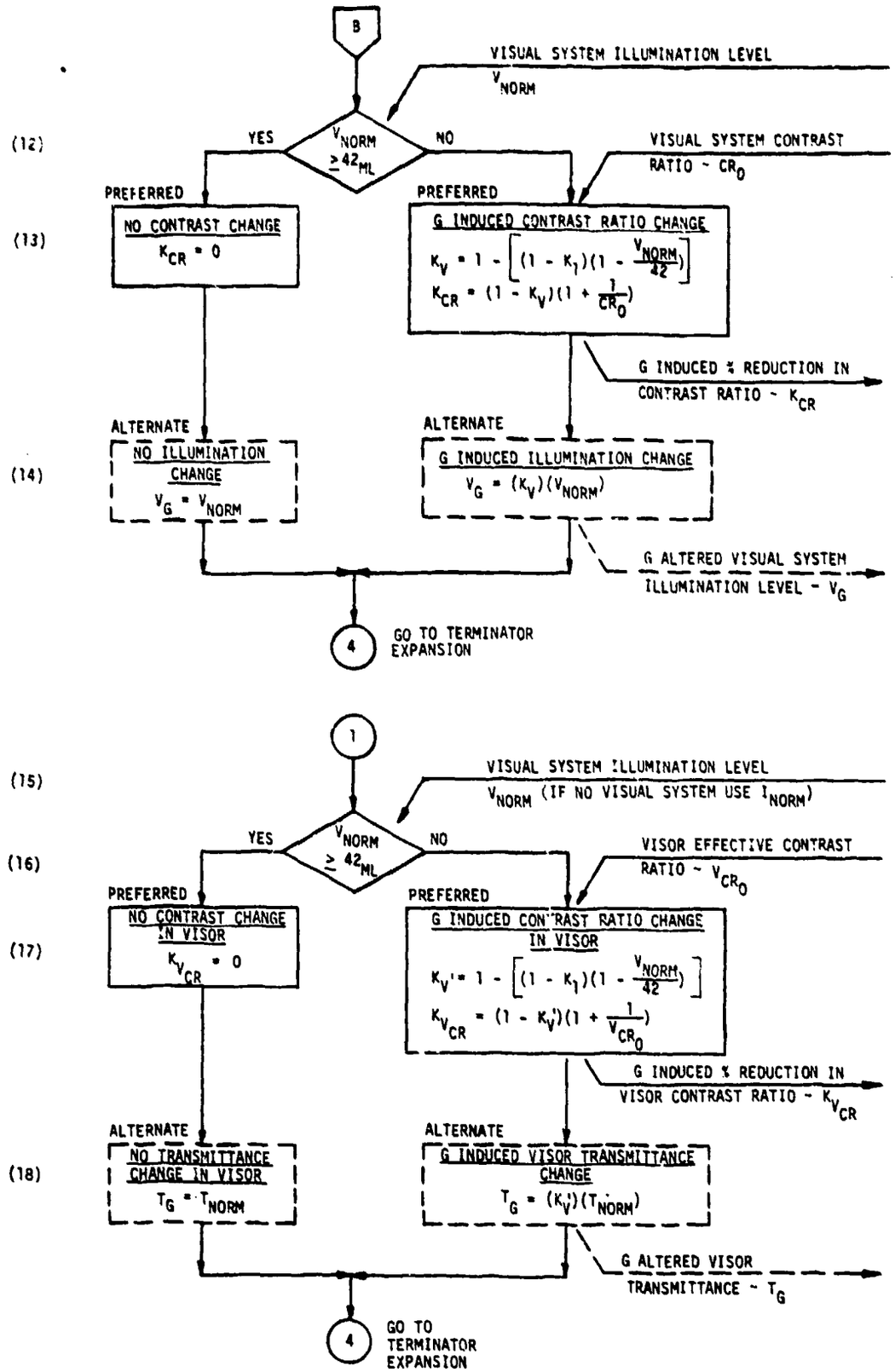
As pointed out by White (258), the significance of this effect tends to zero as the target illumination approaches the 42 mL level used in his dial reading experiments. Consequently, the model requires illumination level as an input and linearly reduces acuity degradation as a function of increasing illumination level. Most simulator visual display systems render daylight scenes at illumination levels below 42 mL. Consequently a philosophical decision must be made concerning whether the simulated visual scene illumination level should be applied as input to the model as opposed to the actual illumination level available from the visual display system. In the case of cockpit instruments, reference to U.S. Government and industry specifications governing instrument lighting (78, 172) indicates that instrument illumination in the 1-5 mL range is to be expected and therefore lies in the range of interest.

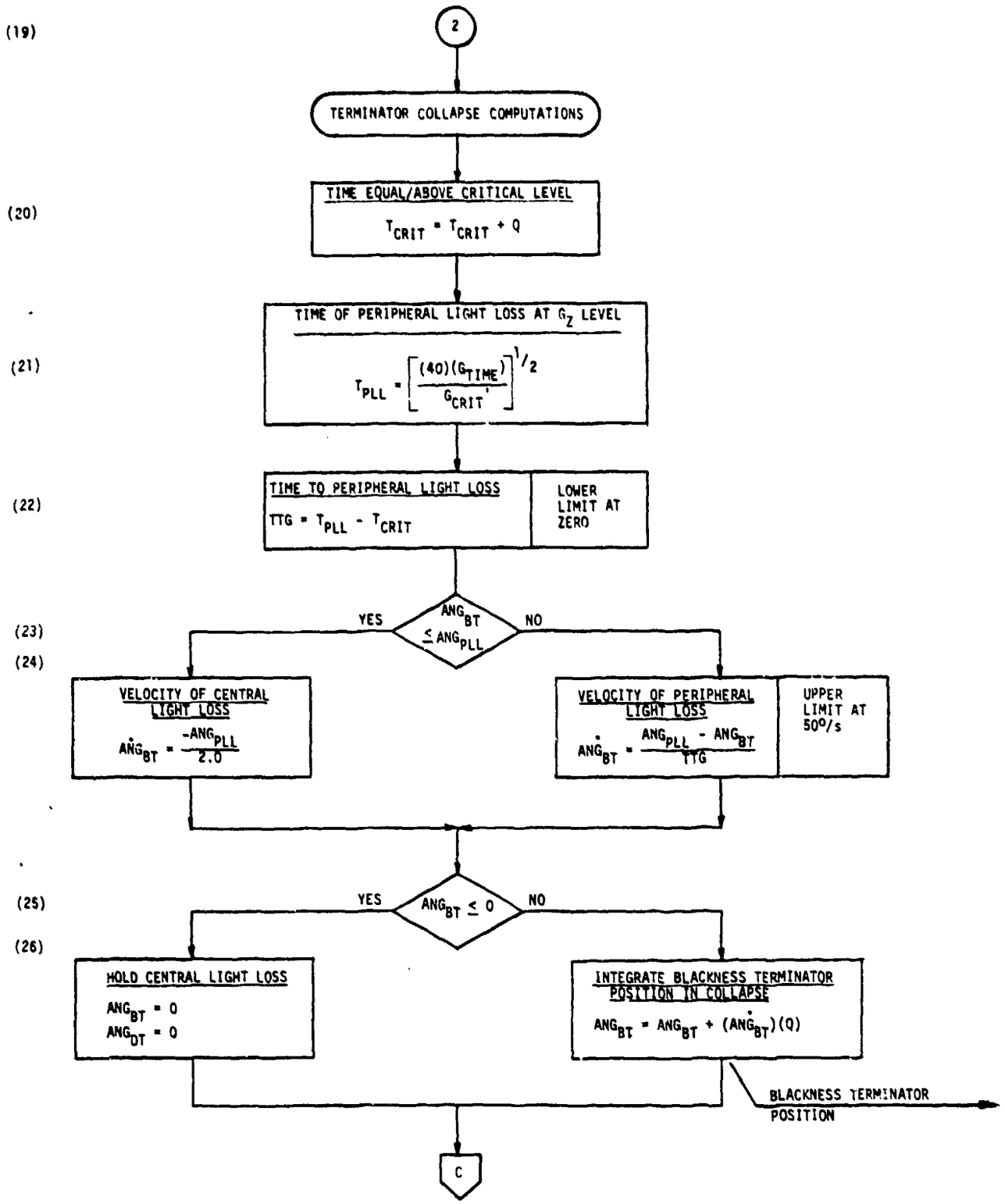
Index #21 and #22 establish the dynamics of the ensuing FOV collapse based on the average rate of application of G_z up to the G_{CRIT} level. The time of collapse is appropriately shortened for G_z levels above the G_{CRIT} level. The expression at index #21 is an approximation to the data provided by Stoll (234). By holding G_z slightly above G_{CRIT}, total peripheral light loss will eventually occur. If G_z falls slightly below G_{CRIT}, the inward bound terminators will reverse direction and enter expansion. Should G_z again rise above G_{CRIT} a new time for complete peripheral light loss is computed and the outward bound terminators will reverse and begin to collapse according to the newly computed duration for collapse.

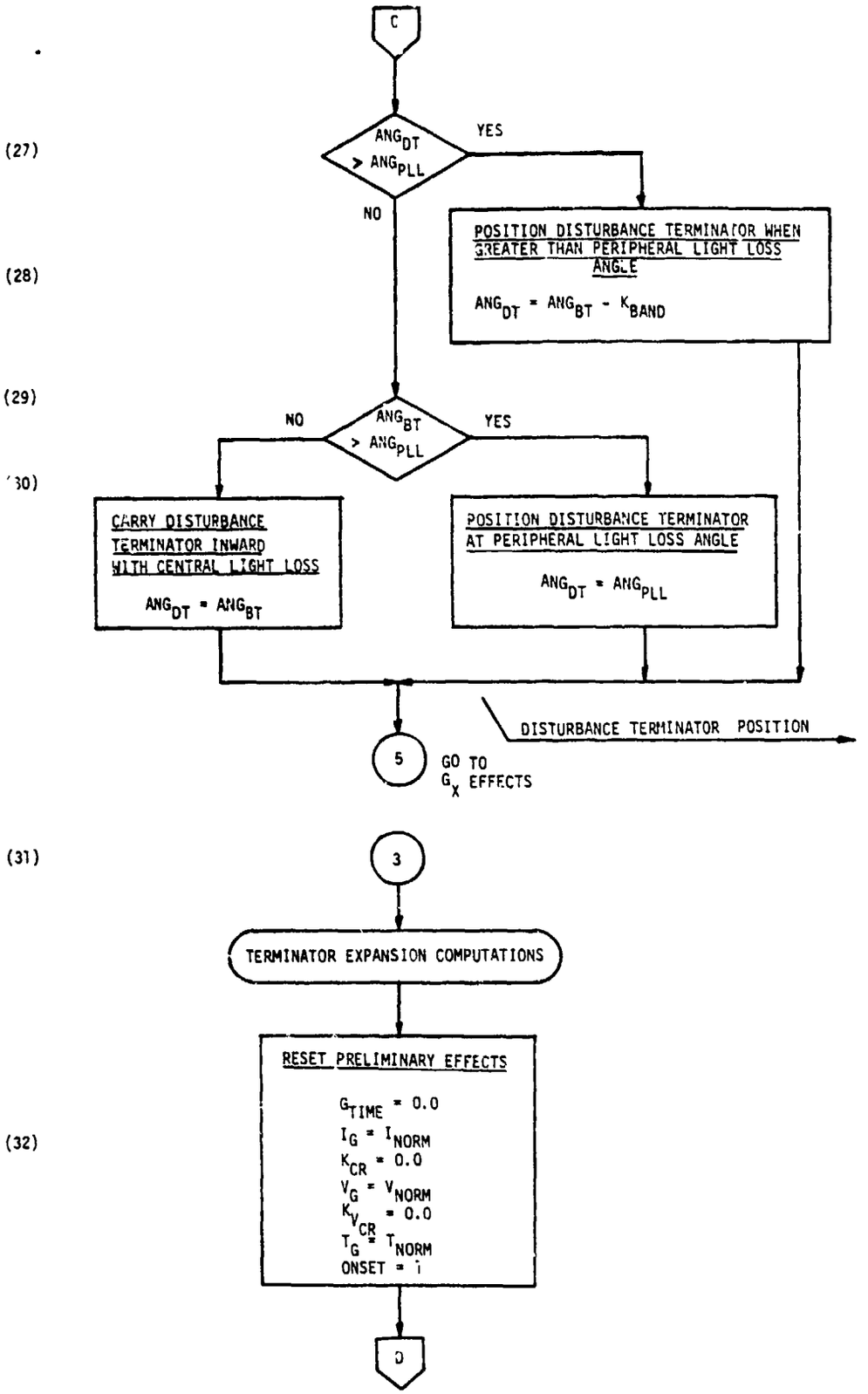
Terminator position, an arc measurement between line of sight and the specific terminator, is computed at index numbers 26, 28, 30, 36, and 38, and output to the user subsystems. The discussion in Section 4.3.6 treats the disturbance terminator position as R_1 and blackness terminator position as R_2.

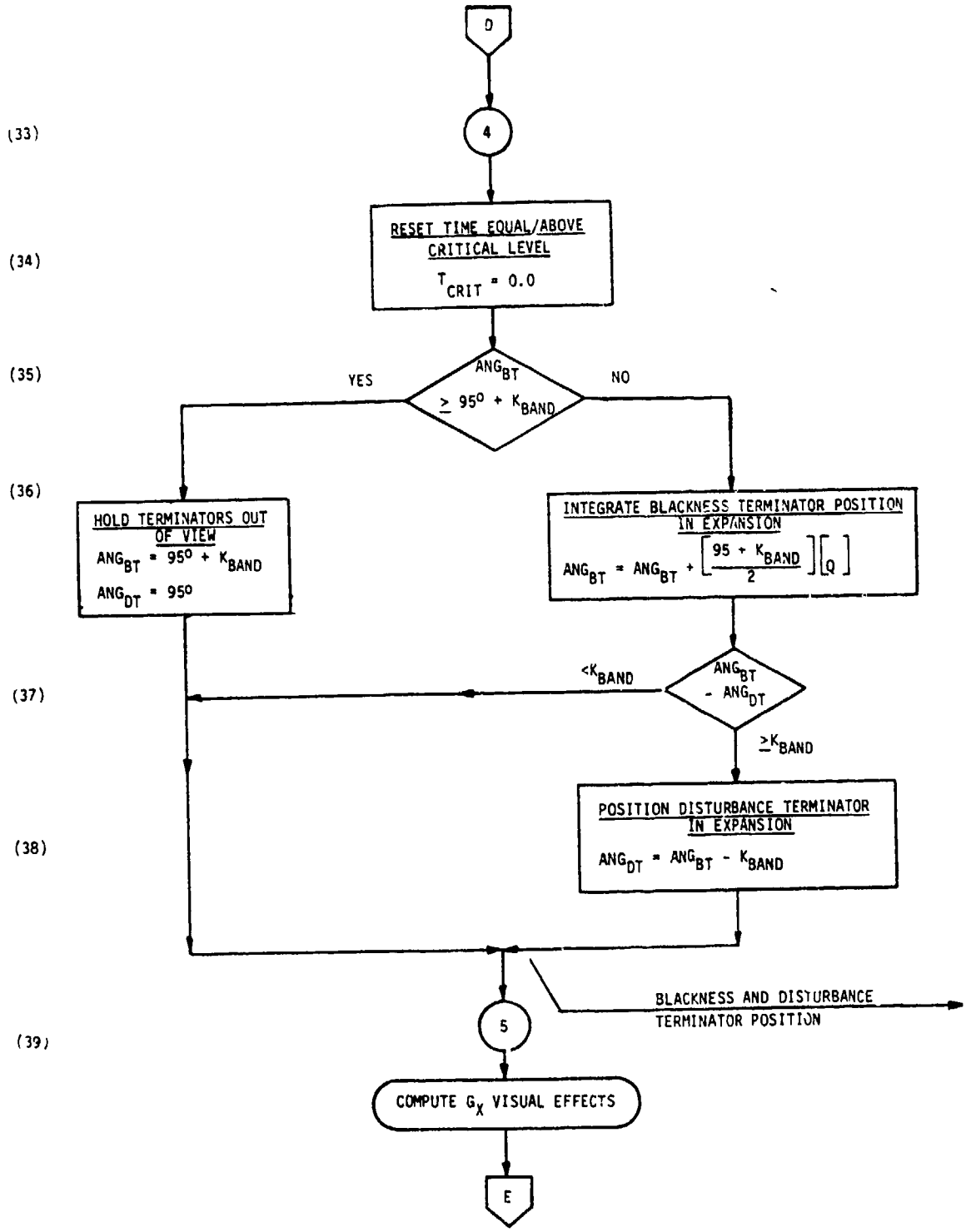

SIMPLIFIED HIGH G VISUAL ACUITY MODEL
(1)
$G_Z < 1$
YES
GO TO TERMINATOR EXPANSION
3
NO
(2)
COMPUTE CRITICAL G LEVEL
G_{CRIT} = 3.0 +
0.2 (IF G SUIT SYSTEM NOT OPERATING)+
1.1 (IF G SUIT IS OPERATING)+
1.5 (IF M1 MANEUVER EMPLOYED)
(3)
$G_Z - G_{CRIT}$
+, 0
SET FLAG
ONSET = 0
-
(4)
$G_Z - G_{ONSET}$
0, -
0, +
0
ONSET
1
(5)
RESET FLAG & TIMER
G_{TIME} = 0.0
ONSET = 1
INCREMENT TIMER
$G_{TIME} = G_{TIME} + Q$
$G_{CRIT'} = G_{CRIT}$
A

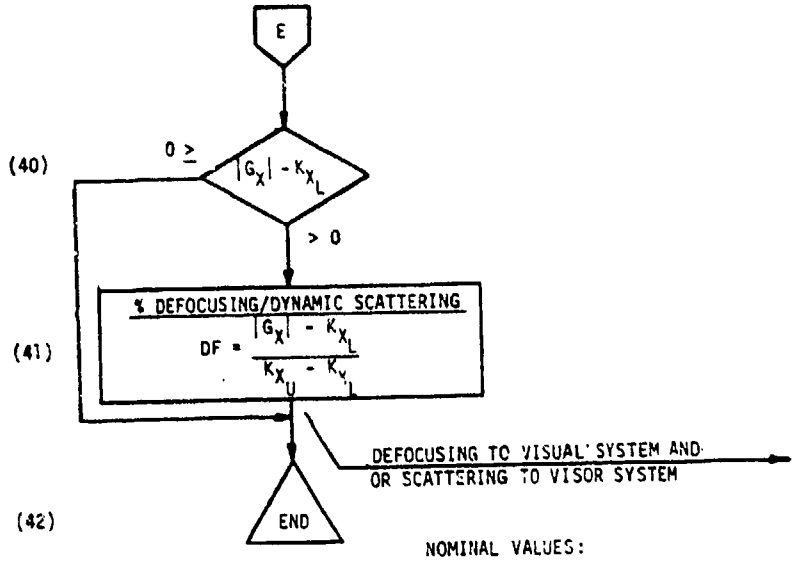

A
COMPUTE PRELIMINARY INSTRUMENT DIMMING/VISUAL SYSTEM CONTRAST CHANGE
(6)
$G_Z \geq G_{CRIT}$
YES
GO TO TERMINATOR COLLAPSE
2
NO
(7)
YES
$G_Z < 1.85$
NO
(8)
RESET EFFECTIVE ILLUMINATION
$K_1 = 1.0$
COMPUTE EFFECTIVE ILLUMINATION
$K_1 = [6.5][(10)^{(-\frac{G_Z}{G_{CRIT} - 1.85})}]$
(9)
VISOR?
YES
1
GO TO VISOR COMPUTATIONS
NO
INSTRUMENT ILLUMINATION LEVEL
I_{NORM}
(10)
YES
$I_{NORM} \geq 42_{ML}$
NO
(11)
NO ILLUMINATION CHANGE
$I_G = I_{NORM}$
G INDUCED ILLUMINATION CHANGE
$K_I = 1 - [(1 - K_1)(1 - \frac{I_{NORM}}{42})]$
$I_G = (K_I)(I_{NORM})$
G ALTERED INSTRUMENT ILLUMINATION LEVEL - I_G
B


B
VISUAL SYSTEM ILLUMINATION LEVEL
V_{NORM}
(12)
YES
$V_{NORM} \geq 42_{ML}$
NO
VISUAL SYSTEM CONTRAST RATIO ~ CR_0
PREFERRED
(13)
NO CONTRAST CHANGE
$K_{CR} = 0$
PREFERRED
G INDUCED CONTRAST RATIO CHANGE
$K_V = 1 - \left[(1 - K_1)(1 - \frac{V_{NORM}}{42})\right]$
$K_{CR} = (1 - K_V)(1 + \frac{1}{CR_0})$
G INDUCED % REDUCTION IN CONTRAST RATIO ~ K_{CR}
ALTERNATE
(14)
NO ILLUMINATION CHANGE
$V_G = V_{NORM}$
ALTERNATE
G INDUCED ILLUMINATION CHANGE
$V_G = (K_V)(V_{NORM})$
G ALTERED VISUAL SYSTEM ILLUMINATION LEVEL ~ V_G
4
GO TO TERMINATOR EXPANSION
1
(15)
VISUAL SYSTEM ILLUMINATION LEVEL
V_{NORM} (IF NO VISUAL SYSTEM USE I_{NORM})
YES
$V_{NORM} \geq 42_{ML}$
NO
(16)
VISOR EFFECTIVE CONTRAST RATIO ~ V_{CR_0}
PREFERRED
(17)
NO CONTRAST CHANGE IN VISOR
$K_{V_{CR}} = 0$
PREFERRED
G INDUCED CONTRAST RATIO CHANGE IN VISOR
$K_V' = 1 - \left[(1 - K_1)(1 - \frac{V_{NORM}}{42})\right]$
$K_{V_{CR}} = (1 - K_V')(1 + \frac{1}{V_{CR_0}})$
G INDUCED % REDUCTION IN VISOR CONTRAST RATIO ~ $K_{V_{CR}}$
ALTERNATE
(18)
NO TRANSMITTANCE CHANGE IN VISOR
$T_G = T_{NORM}$
ALTERNATE
G INDUCED VISOR TRANSMITTANCE CHANGE
$T_G = (K_V')(T_{NORM})$
G ALTERED VISOR TRANSMITTANCE ~ T_G
4
GO TO TERMINATOR EXPANSION


(19)
2
TERMINATOR COLLAPSE COMPUTATIONS
(20)
TIME EQUAL/ABOVE CRITICAL LEVEL
$T_{CRIT} = T_{CRIT} + Q$
TIME OF PERIPHERAL LIGHT LOSS AT G_Z LEVEL
(21)
$T_{PLL} = \left[\frac{(40)(G_{TIME})}{G_{CRIT}'}\right]^{1/2}$
(22)
TIME TO PERIPHERAL LIGHT LOSS
$TTG = T_{PLL} - T_{CRIT}$
LOWER LIMIT AT ZERO
(23)
YES
$ANG_{BT} \leq ANG_{PLL}$
NO
(24)
VELOCITY OF CENTRAL LIGHT LOSS
$\dot{ANG}_{BT} = \frac{-ANG_{PLL}}{2.0}$
VELOCITY OF PERIPHERAL LIGHT LOSS
$\dot{ANG}_{BT} = \frac{ANG_{PLL} - ANG_{BT}}{TTG}$
UPPER LIMIT AT 50°/s
(25)
YES
$ANG_{BT} \leq 0$
NO
(26)
HOLD CENTRAL LIGHT LOSS
$ANG_{BT} = 0$
$ANG_{DT} = 0$
INTEGRATE BLACKNESS TERMINATOR POSITION IN COLLAPSE
$ANG_{BT} = ANG_{BT} + (\dot{ANG}_{BT})(Q)$
BLACKNESS TERMINATOR POSITION
C


C
(27)
ANG_DT > ANG_PLL
YES
NO
(28)
POSITION DISTURBANCE TERMINATOR WHEN GREATER THAN PERIPHERAL LIGHT LOSS ANGLE
ANG_DT = ANG_BT - K_BAND
(29)
NO
ANG_BT > ANG_PLL
YES
(30)
CARRY DISTURBANCE TERMINATOR INWARD WITH CENTRAL LIGHT LOSS
ANG_DT = ANG_BT
POSITION DISTURBANCE TERMINATOR AT PERIPHERAL LIGHT LOSS ANGLE
ANG_DT = ANG_PLL
DISTURBANCE TERMINATOR POSITION
5
GO TO G_X EFFECTS
(31)
3
TERMINATOR EXPANSION COMPUTATIONS
RESET PRELIMINARY EFFECTS
(32)
G_TIME = 0.0
I_G = I_NORM
K_CR = 0.0
V_G = V_NORM
K_VCR = 0.0
T_G = T_NORM
ONSET = 1
D


D
4
(33)
RESET TIME EQUAL/ABOVE CRITICAL LEVEL
$T_{CRIT} = 0.0$
(34)
$ANG_{BT} \geq 95^{o} + K_{BAND}$
(35)
YES
NO
HOLD TERMINATORS OUT OF VIEW
$ANG_{BT} = 95^{o} + K_{BAND}$
$ANG_{DT} = 95^{o}$
(36)
INTEGRATE BLACKNESS TERMINATOR POSITION IN EXPANSION
$ANG_{BT} = ANG_{BT} + \left[\frac{95 + K_{BAND}}{2}\right][Q]$
$ANG_{BT} - ANG_{DT}$
$< K_{BAND}$
$\geq K_{BAND}$
(37)
POSITION DISTURBANCE TERMINATOR IN EXPANSION
$ANG_{DT} = ANG_{BT} - K_{BAND}$
(38)
BLACKNESS AND DISTURBANCE TERMINATOR POSITION
5
(39)
COMPUTE G_X VISUAL EFFECTS
E



NOMINAL VALUES:

$K_{X_L} = 6\ G_X$

$K_{X_U} = 12\ G_X$

SIMPLIFIED HIGH G VISUAL ACUITY MODEL

CONSTANTS	SYMBOL DEFINITION
ANG_{PLL}	Angular measure of field of view (measured from center of FOV) considered to exist at complete peripheral light loss (deg.). Nominal value = 8°.
G_{ONSET}	G_z level beyond which a significant acceleration onset is considered to be in process (g's). Nominal value = 1.25 g's.
K_{BAND}	Visual peripheral angle subtended between non-disrupted vision and complete light loss (deg.). Nominal value = 20°.
K_{X_L}	G_x acceleration level for the onset of lacrimal blurring (g's). Nominal value = 6.0 g's.
K_{X_U}	G_x acceleration level for full blurring effect (g's). Nominal value = 12.0 g's.
Q	Quadrature interval of the digital simulation. Reciprocal of software iteration rate (seconds). Nominal value = same as employed in flight equations of motion software but not less than 1/20 sec.
VISOR	Discrete flag = 1 when high G visor is to be employed for high G visual effects.

VARIABLES

$\dot{ANG}_{BT}$	Rate of collapse and expansion of visual FOV under high G_z conditions (Deg/S).
ANG_{BT}	Angular measure of FOV (measure from center of FOV) subtended by the leading edge of visual disturbance (deg.).
ANG_{DT}	Disturbance terminator.
DF	Percent defocusing (or dynamic scattering) uniformly applied across FOV for blurring effect (%).
G_{CRIT}	G_z acceleration plateau at/or above which eventual peripheral light loss will occur (g's).
G_{TIME}	Elapsed time between the onset of a significant G_z acceleration and occurrence of G_{CRIT} conditions (seconds).
G_X	Acceleration level measured along the X physiological axis (g's).
G_Z	Acceleration level measured along the Z physiological axis (g's).
I_G	Cockpit instrument illumination level altered for G_z effects below the G_{CRIT} level (mL).
I_{NORM}	Cockpit instrument illumination level discounting G_z effect alteration (mL).

K_{CR}	Reduction in visual display system contrast ratio due to G_z effects below the G_{CRIT} level (%).
K_I	Cockpit instrument illumination attenuation factor due to G_z effects below the G_{CRIT} level (non-dim).
K_V	Visual display system illumination attenuation factor due to G_z below the G_{CRIT} level (non-dim).
$K_{V'}$	Visor transmittance attenuation factor due to G_z effects below the G_{CRIT} level (non-dim).
$K_{V_{CR}}$	Reduction in visor contrast ratio due to G_z effects below the G_{CRIT} level (%).
K_1	Effective target illumination attenuation due to G_z effects below the G_{CRIT} level (non-dim).
T_{CRIT}	Elapsed time G_z above G_{CRIT} level (seconds).
T_G	Visor transmittance altered for G_z effects below the G_{CRIT} level (%).
T_{NORM}	Visor transmittance discounting G_z effect alteration (%).
T_{PLL}	Time between G_z broaching G_{CRIT} and eventual complete peripheral light loss (seconds).
TTG	Time to go to complete peripheral light loss (seconds).

V_G	Visual display system illumination level altered for G_z effects below the G_{CRIT} level (mL).
V_{NORM}	Visual display system illumination level discounting G_z effect alteration (mL).

4.3.4 Ophthalmodynamometry: Plethysmographic Goggles

4.3.4.1 Introduction

It has been well established, as reviewed in section A.3.1, that the visual effects of grayout and blackout associated with $+G_z$ acceleration are attributable to a drop in eye level arterial pressure. It has been further established that when pressure in the retinal arteries drops to below intraocular pressure (P_i) visual impairment results in a matter of a few seconds. It remained for a series of excellent experiments using ophthalmodynamometry, which artificially raised the intraocular pressure to reach or exceed that of the retinal artery, in order to demonstrate that the visual effects under both $+G_z$ and increased P_i were identical, and that each was attributable to the original collapse of the retinal circulation - first in the temporal retinal area and then the nasal retinal area, and finally in the last "island of vision" corresponding to a retinal location between the macula and the optic disc. The physiological explanation for the pattern of monocular visual field loss is believed to lie within the retina. Dividing the retina into two portions (temporal and nasal), fifty percent more retina lay temporal to the optic disc than nasal. Therefore, the temporal arterioles have considerably more distance and more tissue to nourish than the nasal arterioles. Also, there does not appear to be any increased vascular network temporally to compensate for nourishment in this larger area. Hence, monocular visual field loss would be experienced earliest in the temporal retina producing a nasal field loss (62), followed by nasal retinal ischemia producing a temporal field loss. Duane (62) points out this monocular effect may not be overly apparent because most studies are conducted using binocular vision. Likewise, we note that the visual disturbance associated with high G conditions is predominantly experienced under binocular conditions. The above disturbances originate both in the temporal and nasal sections of the retina external

to the macula (fixation or foveal area) and binocularly materialize as disruptions of the peripheral field of view.

As will be discussed below, all of the visual effects associated with $+G_z$ can be reproduced in a one G field using plethysmographic goggles - which artificially raise P_i by applying greater than ambient pressure air to the eye ball. Experiments with such goggles and centrifuge accelerations have been able to demonstrate conclusively the anatomical site of the visual phenomenon of grayout and blackout.

4.3.4.2 Similarities Between Effects of Acceleration and of Plethysmographic Goggles

Andina (81) is usually credited with the earliest explanation of acceleration grayout in terms of the effect of the hydrostatic pressure drop on the retinal circulation. Lambert, in a brief report in 1945, was the first to demonstrate directly that the physiological basis of acceleration blackout could be explained and mimicked by raising intraocular pressure through ophthalmodynamometry (151). He concluded that the visual effects of acceleration and of externally applied pressure depended only upon the difference between systemic blood pressure at eye level and any externally applied pressure, as through plethysmographic goggles. He termed this pressure difference "effective systolic arterial pressure" (ΔP) and found that the visual field would begin to show dimming for ΔP in the region of 30 to 49 mm Hg, that peripheral vision was lost in the region of ΔP = 20 to 32 mm Hg, and that blackout resulted when ΔP was 0 to 21 mm Hg. He further concluded that the latency and progress of the development of the visual effects was the same for use of external pressure as it was for development with $+G_z$ on a centrifuge. For a simplified example of the simulated effects of the plethysmographic goggles, see Table 4.3.4-1.

Table 4.3.4-1 Comparison of actual visual effects due to high acceleration with simulated effects induced by plethysmographic goggles.

Actual Acceleration Effects

Temporal Level Systemic Pressure	Intraocular Pressure	ΔP	Visual Effects	Temporal Artery Flow Direction
80 mm Hg	21 mm	+59	Normal Vision	Posigrade
70	21	+49	Dimming of	Posigrade
60	21	+39	visual field	
50	21	+29	Peripheral vision	Posigrade
40	21	+19	lost	
30	21	+09		Posigrade
20	21	-01	Blackout is	Retrograde
10	21	-11	experienced	
0	21	-21		Retrograde

Acceleration Effects Simulated With Plethysmographic Goggles

Temporal Level Systemic Pressure	Plethysmographic Goggles + Intraocular Pressure	ΔP	Visual Effects	Temporal Artery Flow Direction
80 mm Hg	0 + 21 = 21 mm	+59	Normal vision	Posigrade
80	10 + 21 = 31	+49	Dimming of	Posigrade
80	20 + 21 = 41	+39	visual field	
80	30 + 21 = 51	+29	Peripheral	Posigrade
80	40 + 21 = 61	+19	vision lost	
80	50 + 21 = 71	+09		Posigrade
80	60 + 21 = 81	-01	Blackout	Retrograde
80	70 + 21 = 91	-11		Retrograde
80	80 + 21 = 101	-21		Retrograde

The use of ophthalmodynamometry as a clinical tool for investigating the retinal circulation was, of course, an old matter, stemming from the work of Baillert in 1917. Although a number of clinical investigators used the springloaded dynamometer to press against the sclera and observe changes in the retinal circulation, it was not until a significant research program by members of the Ophthalmology Department of Jefferson Medical College in Philadelphia working with the Johnsville centrifuge began to attack problems in the 50s and 60s that a clear understanding of the scientific basis of ophthalmodynamography and the practical use of plethysmographic goggles became established. A comprehensive

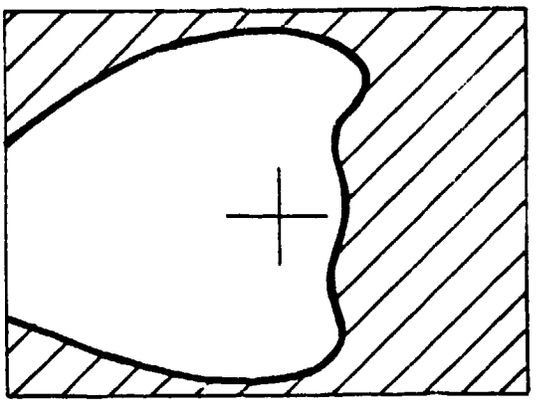
review of ophthalmodynamometry was prepared in 1963 by Wiegelin and Lobstein. An excellent summary of the vast number of experiments relating visual field changes during positive acceleration and those occurring with increased pressure over the orbit was the subject of the thesis by Duane, summarized in 1966 (63) and in a slightly shorter version in 1967 (62). Duane and his associates demonstrated clearly the quantitative similarities between the grayout and blackout associated with the use of plethysmographic goggles and that occurring on the centrifuge. They further showed that in both cases, the grayout of the visual field proceeded from temporal to nasal periphery and finally narrowed to the remaining island as the flow was cut off in the corresponding areas of the retinal circulation. The peripheral light loss or grayout, following $+G_z$ occurring at an average of 4.5g's, corresponds to the initial collapse of the retinal arterioles in the periphery. Similarly blackout corresponds to complete collapse of the retinal arteries, total arterial exsanguination. The delay between the objective changes and the visual sensation of dimming was approximately 5 seconds for grayout and 2-3 seconds for blackout. Both of these times are consistent with the durations associated with anoxia development after impairment of the blood supply.

Since the retinal circulation is an "end artery system", Duane and his associates assume that collapse would occur first in the smaller arterioles serving the peripheral branches, and only later in those associated with central vision. The same pattern of collapse is seen with pressure increase using the plethysmographic goggles. In addition to the dominant factor of interest for simulation, that of grayout and blackout, there are other related similarities of visual effects which are of some importance. Acceleration induced blackout and blackout caused by increased P_i, both abolish the pupillary response to light. However, as demonstrated by using monocular increase in P_i, consensual reflexes associated with illumination of the other eye remain. Eye move-

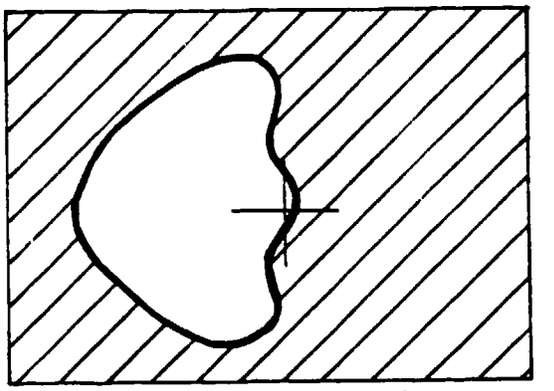
ments were inhibited during positive acceleration, and the hypothesis has been put forward that this "limitation of ocular mobility in response to acceleration (LOMA)" is associated with a central nervous dysfunction associated with hypoxia. This explanation, however, is not obviously consistent with the observation that negative pressure over the eyes, restoring circulation and vision to the retinas, returns not only the sensory feedback but also normal eye movements. The exact relationship between plethysmographic goggle pressure and LOMA remains to be investigated. Electroretinography (ERG), a very primitive measure of light processing by the retina, has light processing to continue unabated through blackout and up to and including unconsciousness for $+G_z$ and, apparently also for similar visual stages of ophthalmodynamometry. The explanation is that the rods and cones which are required to function for the electroretinogram, as well as the bipolar cells, are nourished chiefly by the choroid and not by the retinal circulation. The choroidal flow is not impeded significantly by stresses. Duane (62) discussed other less direct results on pupillary response, photic driving and the algorithm under acceleration and pressure stresses in his review. Finally, Anderson et al (5) reported that inhalation of 100% oxygen at high pressure produces "significant prolongation of visual function after occlusion of the retinal circulation by ophthalmodynametric pressure on the eye". Although their interests were solely in clinical applications of hyperbaric oxygen treatment, it is interesting to note that a similar increase in tolerance to grayout or blackout associated with $+G_z$ is observed when breathing 100% oxygen. (Obviously, none of the limiting benefits of 100% oxygen during $+G_z$ associated with altered ventilation and perfusion ratios are at work in this.)

The specific changes in visual field and visual acuity during ophthalmodynamometry using the pressure goggles have been published and are apparently identical to those observed with centrifugation yielding +Gz acceleration. The latter is demonstrated by

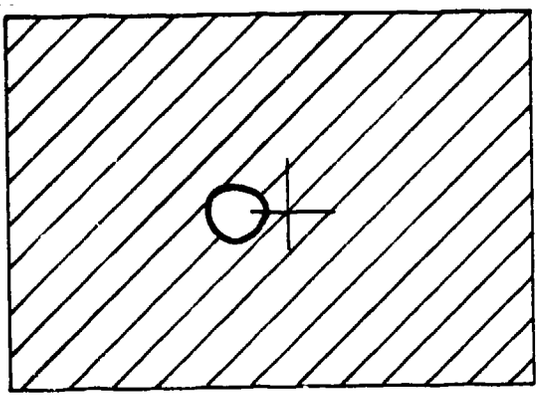
Jaeger et al in their paper "Visual Field Changes During Positive Acceleration" (127) and the former is shown in Jaeger et al "Parametric and Visual Acuity Changes During Ophthalmodynamometry" (128). Figure 4.3.4-1 shows the changes in the field at various stages of chamber pressure above retinal arterial diastolic pressure. The similarity to $+G_z$ grayouts and blackouts is to be noted.



Initial field loss is pronounced in the nasal field (left eye). Temporal field loss is minimal and limited to the periphery. These illustrations represent a composite field loss of the group tested.



Nasal field loss (left eye) approaches fixation and temporal peripheral field loss is more pronounced.



The subject is approaching blackout. Fixation has disappeared and the last remaining island of vision is located 5-10^0 peripheral to fixation.

Figure 4.3.4-1 Monocular visual field loss (from Jaeger et al. (127)). "Field" as used above refers to that field as seen by the left eye.

4.3.4.3 Hardware Considerations - Plethysmographic Goggles

The earliest ophthalmodynamometry equipment was basically an outgrowth of the tonometer, permitting the clinician to increase pressure in the eye by pressing against it and observing the changes in the fundus. Various clinical versions of this equipment were brought into use as reviewed in several sources (Ref. Goldstein, Lobstein A. and Nordmann, J. Modern Ophtalm, 1959). An instrument called the "Ophthalmic Artery Pulsensor" was available in the early sixties for clinical investigation (240). It did not permit the subject to see through the device. It remained for Weeks et al (255) of the aforementioned group in Philadelphia to develop the Plethysmographic goggle which would permit the subject wide peripheral field view as well as allowing the experimenter to observe the retina. They developed a device consisting of two individually inflatable chambers fit into a mask, and a tight fitting seal around the orbits. Straps were used to attach the goggle to the chamber and inflatable bladders placed between the headband and the occipital skull to produce a counterpressure for reduced discomfort and better fit. The components of their device are shown in Figure 4.3.4-2. These goggles could be pressurized to 200 mm Hg. It was found that grayout occurs at approximately 8 to 25 mm Hg above eye level diastolic pressure. This method, however, which used a rigid shell of necessity made the problem of the seal increasingly severe as pressure increase within the goggle tended to pull the shell away from the face. This problem was solved by a newer design published by Behrendt et al (19) in 1966, in which they use a soft and flexible material which folds under at the junction with the orbit so that increasing pressure in the chamber presses the seal tighter much in the manner of a tubeless tire. This goggle is shown schematically and in pictures in Figure 4.3.4-3. This system has a leak rate which is maximum between 50 and 80 mm Hg and decreases as pressure goes higher, up to 150 mm Hg. Tape is used to maintain the seal at low pressures. The authors reported that pressure decreased only by 1 mm Hg per min-

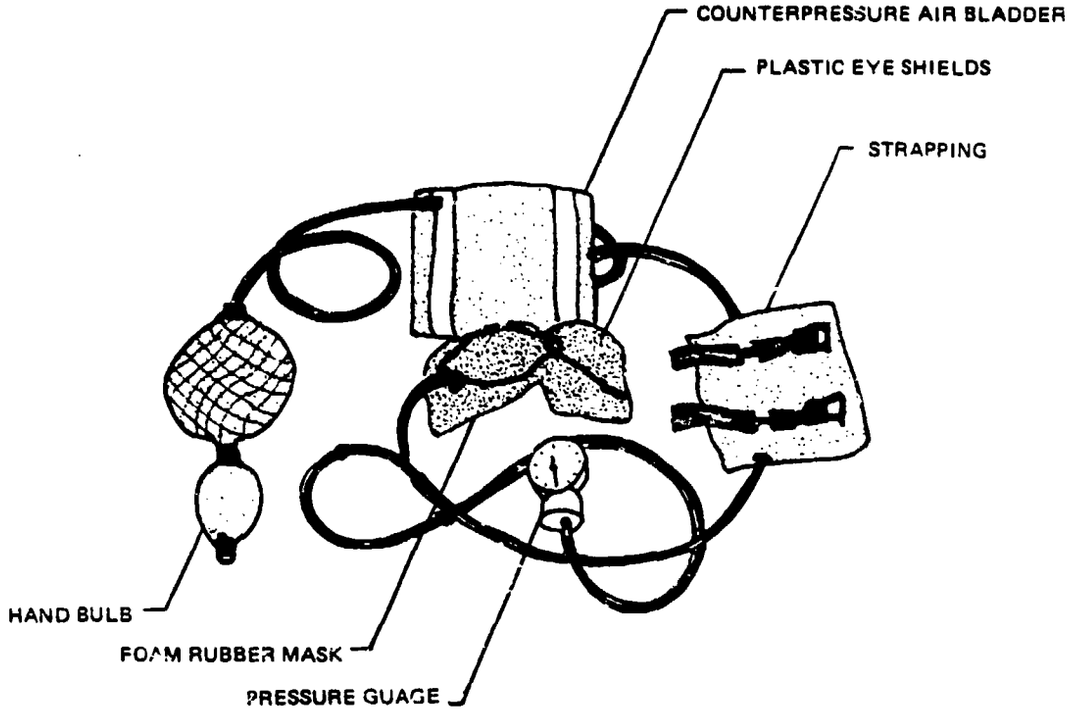
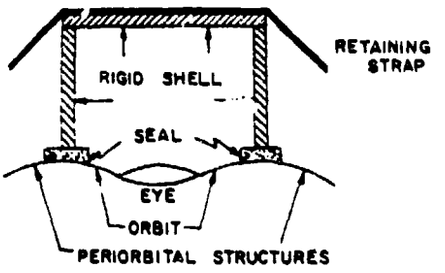


Figure 4.3.4-2 Component parts of the plethysmographic goggle: (1) hand bulb, (2) foam rubber mask, (3) plastic eye shields, (4) counter-pressure air bladder, (5) strapping, and (6) pressure gauge (from Weeks (255)) (courtesy of Official Journal of the American Academy of Neurology).

ute, which was easily replenished with a hand pump. The goggles were worn comfortably for one hour, and required on the order of thirty minutes to fit. This version of the goggle appears entirely consistent with the experimental device to be included within or as an adjunct to the pilot's flight helmet for investigation of the utility of ophthalmodynamometry in training.

Duane reports on some early attempts to increase P_i by a full face aviator's mask using a full pressure high altitude flying suit. They found that the retinal circulation could be occluded, but abandoned the technique as being too cumbersome and techni-



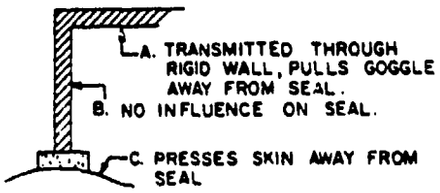


Abb. 2 a

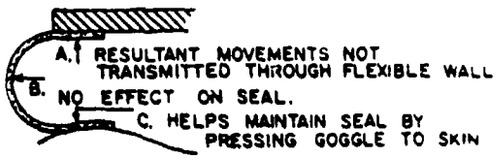


Abb. 2 b

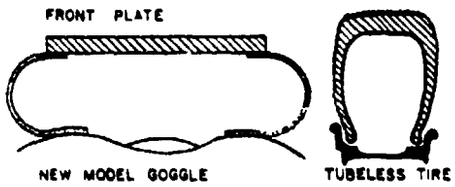


Figure 4.3.4 - 3 Goggles seal (from Behrendt(19)) (courtesy of Keinischi Monatsblatter Fur Augenheilkunde)

cally difficult. If the effects are deemed worth while, this could be further investigated.

4.3.5 Area of Interest Variable Transparency Visor

The pilots of most high performance tactical aircraft wear helmets equipped with visors which afford protection to the pilot's eyes and face, and, through the use of filters, improves vision by cutting glare in daylight operations. In searching for

means to alter the simulator pilot's visual environment to replicate the visual effects of high G conditions, the visor offers many merits as a potential site for such alteration.

1) In that the visor is employed in the actual task of piloting an aircraft, its presence and use in the simulator is natural and expected. There is no loss of environmental fidelity which is considered a very important benefit.

2) As described in prior sections, the pilot's instantaneous line of sight is required to appropriately position the high G visual effects and the use of a helmet mounted oculometer is a preferred method of generating this information. The helmet mounted oculometer is constructed with the visor forming an integral part of its operation; consequently, the requirement to provide and use a visor is already established.

3) By concentrating the visual alteration at the visor site, the more cumbersome computations and hardware alterations required to replicate the effects using simulator cockpit instrumentation lighting and visual displays as discussed in Section 4.3.6, could be eliminated. Further, a continuum of effect between cockpit interior and exterior scene is assured.

4) The visor site permits imposition of effect in those areas of the field of view in which luminescence is strictly a consequence of general ambient lighting and not subject to selective control. This would include areas such as cockpit panel faces, miscellaneous cockpit structures, or even portions of the pilot's own body.

5) The authors have noted in the literature discussing the subjective description of the appearance of high G peripheral light loss a consistent suggestion that the effect is often perceived as a visual description occurring external to the eye as if something intercedes between subject and scene. Vasil'yev and Kotovskaya (244) most directly address this where they characterize grayout as "a gray veil, fog, whitish fog.....like looking through rain or fog." Note the use of the word 'through'. The simulation of such effects can more faithfully be simulated by introducing the disruption within a medium through which the pilot must view this environmental scene rather than at the scene itself.

4.3.5.1 Visor Concept

The visor concept advocated herein is closely related to the challenging variable transmittance visor work accomplished by Rockwell International Corporation's J.P. Dobbins in 1973. Under AMRL contract F33615-71-C-1938, Dr. Dobbins developed and constructed helmet visors possessing the capability to vary automatically, and in continuous form, light transmittance such that under brilliant illumination conditions the light level reaching the pilot's eyes can be reduced so as to preserve perception of low light level tactical information displayed to the pilot via onboard avionic systems. Dobbins employed what currently has become generically known as liquid crystal techniques to vary the visor transmittance factor. One of these units is pictured in Figure 4.3.5-1.

Hoyt et. al. in Patent #3,942,270 held by The Singer Company applied liquid crystal visor construction concepts for the purpose of gradually dimming, from the periphery of the visor inwards, the pilot's view in order to replicate high G conditions. This concept held that the center of the visor expanse was the most likely



Figure 4.3.5 - 1 Helmet assembly without shroud (from Dobbins (58)).

position of the pilot's line of sight and that peripheral luminescence dimming was the effect sought. Visor design established the center of the visor expanse to be the last area of dimming; consequently, if the pilot shifted his line of sight without moving the visor itself, the clear central field of view would not move with the line of sight. The visor concept discussed herein extends the liquid crystal approach far beyond that suggested in this patent and draws on high speed liquid crystal display techniques which are currently in the developmental phase.

4.3.5.1.1 Dual Optical Effects of Interest

Fundamentally liquid crystals are mesomorphic substances whose optical activity is alterable based on applied voltage. Sandwiched between two transparent conductors a thin layer of

liquid crystal can be exposed to both dielectric and conduction forces which, depending on the type of liquid crystal material selected, can produce various optical alterations in the light passing through the liquid crystal layer. The optical alteration occurs in the region of the conductors and reveals the otherwise nonapparent pattern selected for the conductors. A popular pattern found today is the seven individually addressable bars or segments which comprise the display of a digit employed in liquid crystal numerical displays. The optical change occurs as a voltage, higher than some threshold voltage, and is applied to the transparent conductor surfaces. The severity of the optical disturbance is related to the magnitude of the impressed voltage potential. The gain of optical change-to-voltage change is quite high making only a few intermediate states of optical disturbance realizable in practice.

Two basic types of liquid crystal electro-optic phenomena exist: field effects caused by dielectric forces only and conduction phenomena induced by a combination of dielectric and conduction forces. Induced birefringence, twisted nematic, guest-host interaction, and cholestric-nematic transitions are found within the field effects category wherein optical disruption occurs as the liquid crystal deforms due to the presence of a dielectric field. These phenomena can be employed to block the passage of light passing through the liquid crystal display and consequently vary illumination levels of external light viewed through the display. The twisted nematic used with a polarizing film is a popular configuration for battery operated watch digital displays because of its low power requirements. Here light passes from the front of the display to a reflecting surface behind the display and back out the front. When the liquid crystal, taken together with polarizer, is commanded to a light blocking mode, the shape of the segment becomes apparent by silhouette.

Dynamic scattering and storage effects, on the other hand, produce a different optical appearance and are part of the conduction phenomena. Conduction induced fluid flow occurs in nematic materials with negative dielectric anistropy and the wide angle forward scattering phenomena known as "dynamic scattering" is the most important by-product of the turbulence associated with electrohydrodynamic flow. In this case the view through the display in its non-scattering mode is clear and as the display is caused to increase in dynamic scattering, it takes on the appearance of increasingly apparent ground glass. Because we are interested in causing the visor to replicate not only the high G visual effect of light level dimming but also the loss of contrast associated with grayout, both field effect and dynamic scattering light crystal phenomena are pertinent to our application. Some vendors of liquid crystal technology, when briefed on our potential application, felt that it might be possible to chemically bond together nematics from the above two categories such that one film of liquid crystal medium could be made to perform both the task of scattering and light level reduction as a progressive effect. Should this not be possible, it is apparent the two unique films, one from each category, could be sandwiched to produce the varied optical effect sought.

4.3.5.1.2 Flat Plate Display Prototype

Developing a visor as a liquid crystal display requires that the visor be constructed of transparent inner and outer shells which are separated slightly to permit the insertion of a thin film of nematic material. The inner and outer shells actually form a vessel containing the nematic. The inner surface of the vessel is coated with a thin film of conducting material such that the nematic can be exposed to dielectric and conducting forces. In the case where two different and separately contained nematics are to be employed the vessel must be constructed with three walls providing two cavities and four conductor films may be employed.

One of the most serious problems facing Dobbins (58) was the vessel forming process which would yield not only visors of the correct contour but, more importantly, would provide dimensional uniformity in the thickness of the internal cavity. He ultimately recommended the use of thermosetting castings of allyldiglycol carbonates (ADC) glazing resins. Nevertheless, of importance is the fact that generating a curved surface "display" presented difficulties. Liquid crystal vendors we have contacted seem to express the same concerns. The concepts suggested herein border the state-of-the-art in flat plate liquid crystal display technology without considering curved surface fabrication. None would say that the principles required to achieve the desired flat plate display are violated or nonapplicable in curved surface displays, but most seem to adopt a serial approach to the problem: first develop and evaluate a suitable flat plate display, then approach the curved surface fabrication problem. Therefore the balance of this section will consider the visor display as a flat plate prototype.

Figure 4.3.5-2 depicts a planform of the flat plate visor measuring four by eight inches. It would be constructed in either two or three wall construction depending on the suitability of chemically bonding or maintaining as separate the field effect and conduction nematics. Either way, provision is made for both dynamic scattering and light dimming optical effects. If a twisted nematic is employed for light dimming a set of polarizing films must cover the display expanse. The addition of a pleochroic dye mixed with the nematic and operating under guest-host interaction could reduce the polarization requirement to a single film. Selection of a cholesteric-nematic mixture could remove the requirements for polarization altogether (200) which would be advantageous since polarizer films are susceptible to temperature and moisture degradation (225). Dobbins avoided the use of "liquid crystals", per se, and employed a formulation of electrodichroic crystals in liquid suspension in order to eliminate the need for

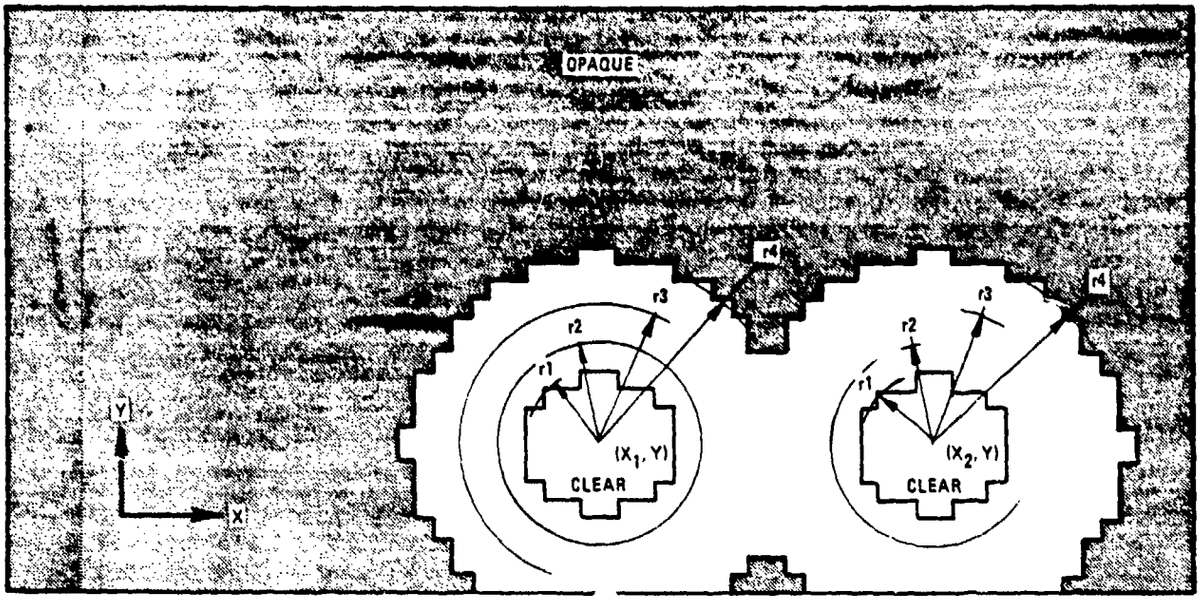


Figure 4.3.5 - 2 Flat plate visor display.

polarizers and to obtain a lower optical effect-to-voltage drive gain (58). The latter permits more precise control over the degree of transmittance attenuation than that afforded by the twisted nematic. As we shall see, our configuration may not require such precise control.

4.3.5.1.3 Matrix Addressing

The transparent conductor films used in the four by eight inch flat plate display are deposited on the inner surface of the vessel so as to form a 40 x 80 matrix of 0.1 x 0.1 inch elements. That is, on one side of the liquid crystal are located rows of conductors 0.1 inch wide and on the other side of the liquid crystal film are located columns of conductor 0.1 inch wide. Thus by matrix addressing, wherein a specific row and column are subjected to an electric potential, the optical effect can be commanded to occur at selective positions within the expanse of the

flat plate visor. Likewise it is possible to "paint" an optical pattern and cause it to move about the expanse of the flat plate.

4.3.5.1.4 Display Pattern of Specific Interest

The specific pattern of interest to us is illustrated in Figure 4.3.5-2 wherein the paired monocular rendition of high G grayout and peripheral light loss is painted centered on the location of the pilot's current visual line of sight as made known by the oculometer. Cerebral assimilation of the monocular views produces a uniform binocular effect. The origin of the radius vectors are permitted to move according to that detected by the oculometer. The magnitude of the radius vectors shorten during the onset of high G visual impairment and expand during recovery and are driven by an algorithm such as that presented in Section 4.3.3. The radius r_1, corresponds to the "disturbance terminator" and r_4 corresponds to the "blackness terminator" as introduced in section 4.3.3. Within the area of r_1, dynamic scattering and transmission attenuation would not be scheduled. Between r_1 and r_2, r_2 and r_3, and r_3 and r_4 sequentially more intense scattering and/or a greater density of elements commanded in dynamic scattering would be scheduled to replicate grayout conditions. Commencing to draw on the second major optical effect of the visor, between r_3 and r_4 transmission attenuation might be scheduled by activating a sparse population of light blocking elements. At r_4 a greater density of light blocking elements would be activated to higher levels of attenuation and at some radius beyond r_4 the display would become completely opaque to simulate complete light loss. As can be deduced from the preceding description, the matrix approach, when employed to cause visual disruption, lessens dependence upon driving all elements in intensity variations. The same net effect can be achieved with less control of the intensity of a given element's optical effect supplanted by control over the density of the effect considered from an area-wise standpoint. This phenomena is somewhat analogous to that employed in printing photo-

graphs by half-tone methods. For this reason high gain twisted nematics may be entirely suitable for use in the visor.

4.3.5.1.5 Multiplexing, Drive Waveform, and Power

The optical patterns we wish to construct in the visor are complex enough to require a modified form of signal multiplexing. In order to preclude the perception of flicker in the display, each element should be updated at least 25-30 times a second (225). Ideally each element could be individually addressed to the exclusion of simultaneously addressing all other elements in the display. This would involve incorporating multiplexers on both the X and Y axes. The multiplexers could be mounted on the helmet itself and would reduce the wires servicing the helmet to the X and Y data chain, X and Y address enables, and multiplexer power. The luxury of such independent non-simultaneous addressing reduces individual address duration in our 3200 element display to approximately 10 microseconds which may be inordinantly short to successfully stimulate the element within a reasonable response time.

A more classical form of liquid crystal multiplexing is to multiplex on but one axis while providing individual and simultaneous access to all elements on the other axis. Dividing our display into two 40 x 40 element sections with the intent of simultaneously scanning each section and further stipulating that a set of 40 individual address lines will be provided to each of the two sets of 40 Y axis columns will significantly increase element connect duration. In this case the 40 X axis rows are multiplexed such that the display is swept, 40 columns at a time, row by row along the Y axis. Connect time increases from 10 microseconds to nearly a millisecond.

The life of liquid crystal displays are sometimes quoted as high as 50,000 hours. However, in order to achieve this type of

life, it is necessary to drive the display with an AC waveform and keep residual DC levels below a minimum. Residual DC levels tend to slowly degrade the optical effect by permitting the accumulation of an insulating film at the anode (200,225). Liquid crystals respond to the RMS voltage potential to which they are exposed; consequently a pulse chain with polarity systematically reversed is a preferred means to excite the display elements (225). Threshold voltages depend upon the material but can be found in the 1-2 Vrms region. Saturation voltages also vary but may be found in the 10-20 volt region. Typical power requirements run in the 10-20 micro-amp/cm^2 region.

Liquid crystals are sensitive to the frequency employed in generating the dielectric field. Critical frequencies exist, peculiar to the material employed, above which activation thresholds are increased and delay times decreased. This phenomena is used to advantage in generating displays by employing a high frequency component to alter response characteristics while simultaneously employing a low frequency component to activate the intensity of the electro-optical effect. Dual frequency addressing will be further discussed in the next section.

4.3.5.2 Visor Response

Many of the problems encountered in developing a liquid crystal display center not so much on generating a display but on developing a highly responsive display. Because the visor display must reposition the high G visual impairment pattern according to the movement of the pilot's line of sight, pattern movement must occur during visual saccades. Although precise data on acceptable time decays is missing, it would be appropriate to assume that pattern repositioning should occur within 100 milliseconds and this requirement in itself would qualify the visor as a high response display.

The rise times at 20°C of the majority of field effect materials seems to fall in the 100 millisecond region and approximately 150-200 milliseconds for dynamic scattering materials. Decay times range from 200-400 milliseconds for field effect and 100 milliseconds for dynamic scattering materials. Some twisted nematics, however, display rise times as short as 10 milliseconds. Multiplexing the matrix as earlier discussed aggravates the situation by reducing the connect time to each element and promoting conditions where increased potentials are sought to establish higher RMS values of applied potential. Higher RMS potentials indeed reduce optical response time but can contribute to cross talk between matrixed elements. As of the early part of this decade displays employing 50 x 50 and 100 x 100 elements with a scan time of 1 second and a 260 x 260 element array with a 10-20 second scan time were reported. A 120 x 120 array operating at television update rates was functional but displayed some defects (200). Smith concludes in his 1978 article on multiplexing of liquid crystal displays (225) that improved liquid crystal materials currently under development will make multiplexing easier and permit the development of large dot-matrix arrays for video games and data display terminals. Techniques have been developed to improve the responsiveness of liquid crystal displays. Some of these techniques must be considered in the design of the visor in concert with the selected array size. The aforementioned twin 40 x 40 matrix of 0.1 inch square elements must be treated only as a point of departure and should be reconsidered in a resolution vs. response analysis.

The pulse chain generated in the multiplexing process aids response time in one aspect in that it permits establishing a steady state RMS potential just shy of the crystal threshold voltage; therefore, the element is "set" to activate without delay (225). Secondly, rather than establishing the "activate" dielectric potential at the intersection of a row and column by placing half the activate potential at one polarity on the row and the

same magnitude but opposite polarity on the column which results in the unselected elements "seeing" one-half the activate polarity, a one-third voltage select scheme is employed as illustrated in Figure 4.3.5-3. Note that the unselected elements are exposed to only one third of the activate voltage. Conversely, if the voltage residing at the unselected elements is maintained at just below the threshold level, it is apparent the one-third scheme permits the "activate" voltage to be of larger magnitude than that permitted in the former "one-half" scheme. Increasing the activate potential reduces response time.

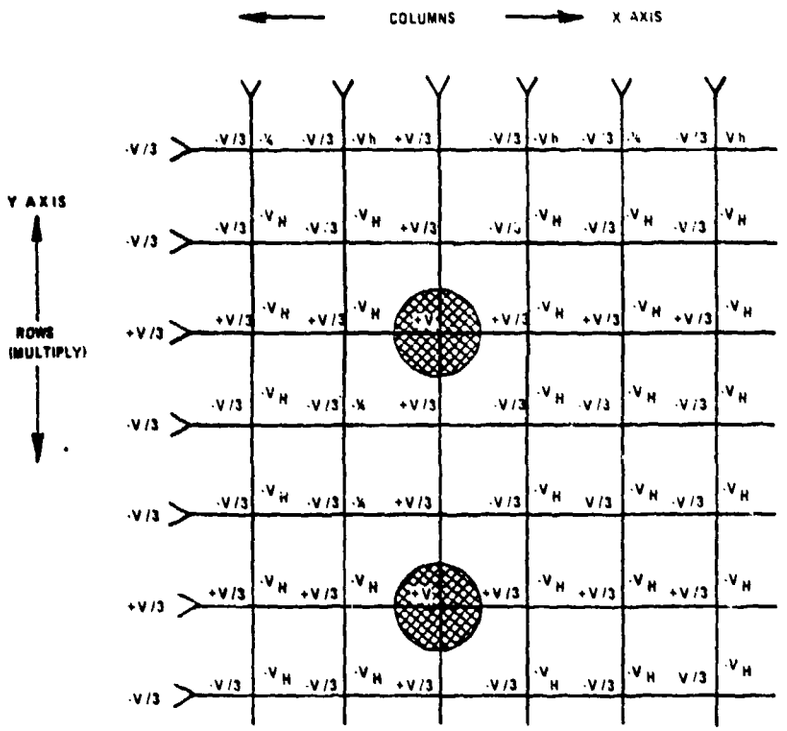


Figure 4.3.5 - 3 Dual Frequency Addressing and One Third Voltage Select Method (after Priestly (200))

Another method of further increasing the abovementioned activate potential is to capitalize on the impact high frequency potentials impose on crystal threshold potentials. Dual frequency addressing selectively employs both a low frequency activate poten-

tial and a higher frequency signal, above the nematic's cr[illegible] frequency, to raise the threshold potential of unselected elements. This is demonstrated in Figure 4.5.3-3 by the symbol V_H. By raising the threshold potential of unselected elements, it is possible to increase the activate potential which shortens response time. Viewed conversely, higher activate potentials inducing quicker response can be employed without encountering cross talk, or the condition when neighboring unselected elements become inadvertently active.

Dual frequency addressing displays an additional benefit in that the high frequency component has the effect of shortening the decay time of both field effect and dynamic scattering nematics. In the case of dynamic scattering nematics, for instance, the high frequency component adds a dielectric orienting field to the element which tends to suppress hydrodynamic flow. In the visor application the response associated with eliminating an optical effect is equally as important as the response associated with initiating the effect. Fortunately the application of high frequency potentials to shorten decay time is a discretionary action because slow natural decay makes possible multiplex scanning of arrayed liquid crystal displays. In fact in some cases it is desirable to prolong the decay.

Multiplex scanning subjects each element in the array to a pulse chain. When an element is to be activated, the amplitude of the pulse is increased such that the RMS potential is raised above threshold levels. During multiplex scanning an element is exposed to pulses separated by intervals of zero potential. As the number of array elements to be scanned per unit time increases these intervals become longer and the pulse width smaller. The dielectric field is increased during the pulse and permitted to decay according to its dielectric relaxation time during the interval of zero potential. Thus even though the pulse width may be small, if decay is small or can be retarded, the field will persist long

enough to activate the desired optical effect. Consequently, the selection of the nematic material must, in part, be made based on its natural decay characteristics compared against the temporal constraints formed by the multiplexed scan pattern selected.

One of the methods to further retard decay is through the addition of cholesteric material to the nematic which, it will be recalled, is also suggested as a method of eliminating light polarization requirements. A second method to retard decay is to electrically isolate each element from its common connection to other array elements in the row or column, thereby reducing dielectric relaxation via external paths. Polycrystalline thin-film transistors have been used for this purpose; however, their applicability to the visor application requires additional investigation.

This section has concentrated on the question of response because of its obvious importance in the visor application and also because it forms a very complex problem involving interrelationships between the selection of nematic materials, selection of array size and scan patterns, the characteristics of the potential used in addressing an array element, and the address strategy itself. Other factors must also be considered in the design of the display such as temperature and humidity effects, liquid crystal layer thickness effects, and variation in optical effects as a function of viewing angle; however, we do not foresee major difficulties arising from these considerations.

4.3.5.3 Visor Subsystem Structure and Developmental Approach

The preceding sections have been directed primarily at discussing the primary element of the subsystem: the visor display apparatus. We envision the total subsystem to include the visor display, helmet mounted oculometer, and a microprocessor or minicomputer containing its own I/O structure to interface the oculo-

meter and visor together and further to interface these two items to the host computational system serving the simulator.

A small dedicated computational capability operating at fast cycle rates is required to:

1) Minimize delays between the generation and use of oculometer produced line of sight information.

2) Generate the pulse chains required to activate the display according to the structure of multiplex scanning selected.

3) Handle the high speed digital to analog conversion required by the display.

The visor computer is responsible for converting the patterns and location of the patterns sought in the display to appropriate array element commands and then sequencing these commands according to the scan process employed. It is responsible for controlling the analog scan process as well as the techniques for response enhancement. The high G visual impairment model presented in Section 4.3.3 could be located in either the simulator host computer if experimenter control over model behavior is emphasized or in the visor computer if a minimum of model adjustment is anticipated. The latter configuration significantly decreases the interface between host and visor computers.

As earlier indicated, we believe the appropriate approach to developing the visor subsystem is two phased involving the development and evaluation of a flat plate display and then, assuming the evaluation confirms the worth of the concept, developing a similar display in the curved shape of the visor. Because of the highly specialized technology associated with fabricating liquid crystal displays and, in particular, addressing matrixed liquid

crystal displays, the development of the visor computer, I/O, and flat plate display should be maintained as a single effort and the liquid crystal display vendor selected should demonstrate expertise in the development of specialized displays as well as computer systems to drive the displays. In the second phase, where the flat plate system is converted to a curved surface display it may be beneficial to attempt to involve Dr. Dobbins or other individuals key to the earlier AMRL visor contract in order to benefit by their experiences in fabricating liquid crystal displays in the form of a visor.

4.3.6 Diminution of Visual Acuity Simulation

4.3.6.1 Flight Instruments

As mentioned in Section 3, the pilot experiences a diminution of visual acuity during $+G_z$. This dimming process begins with an interruption of vision in the far most periphery proceeded by a gradual degradation of vision moving inwards towards the foveal. As the radii of the field of view gradually collapse, a complete loss of vision is experienced.

Two concentric circles define the regions of diminution of visual acuity from the simplified algorithm (Section 4.3.3) (see Figure 4.3.6.1-1).

The instrument axis system has it's origin located in the lower left corner with the positive abscissa extending horizontally out to the right and the positive ordinate extending vertically upwards from the origin.

In Figure 4.3.6.1-1, R_1 is the radius of the inner circle and R_2 is the radius of the outer circle. R_I defines the radius to the point of interest (I) from the fixation point (F). "I" is the

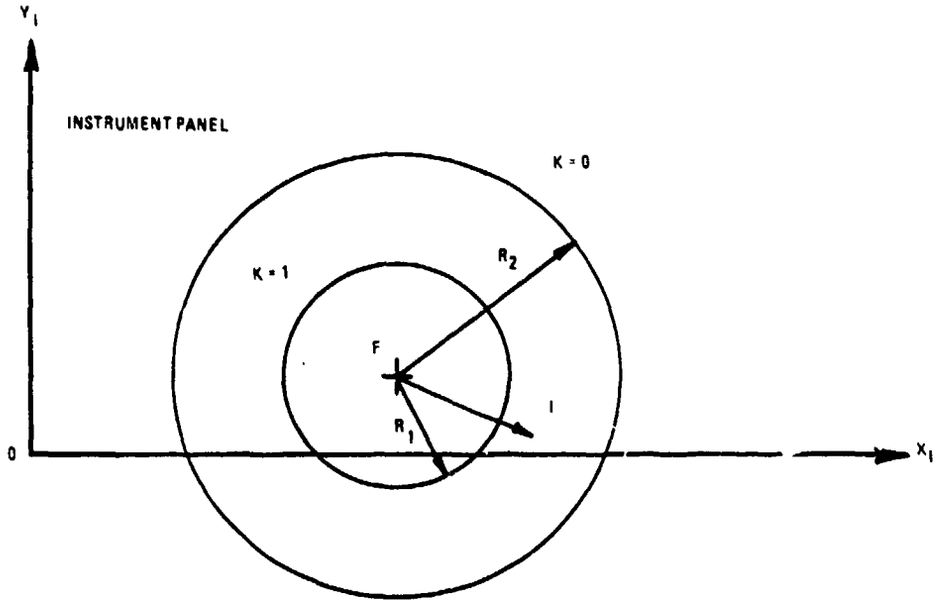


Figure 4.3.6.1-1 Region of diminution of visual acuity.

point of interest which, in this case, is an instrument located on the instrument panel.

When $R_I \leq R_1$, visual acuity is normal (K = 1)

$R_I \geq R_2$, there is a total loss of vision (K = 0)

$R_1 < R_I < R_2$, visual acuity varies linearly ($0 < K < 1$)

The center of these circles is at the fixation point (F) which is the intersection of the LOS (line of sight) with the instrument panel. The coordinates of F are provided by the oculometer system and are represented by (X_{los}, Y_{los}). The coordinates of each instrument are fixed relative to the instrument axis system and are represented by (X_I, Y_I) for each instrument. R_1 and

R_2 are provided by the dimming algorithm. Thus, the locations of the fixation point and the instrument are known along with the radii of the two concentric circles with center F. The objective is to determine the level of attenuation (K) of a particular instrument in relation to it's location relative to R_1 and R_2.

$$R_I = [(X_I - X_{los})^2 + (Y_I - Y_{los})^2]^{1/2} \quad \text{[Eq. 4.3.6.1-1]}$$

For $R_I \leq R_1$, K = 1 (there is no dimming effect)

$R_I \geq R_2$, K = 0 (total loss of vision)

$R_1 < R_I < R_2$, $0 < K < 1$ (visual acuity will vary linearly) such that

$$K = 1 - \frac{R_I - R_1}{R_2 - R_1} \quad \text{[Eq. 4.3.6.1-2]}$$

for any given instrument.

4.3.6.2 Visual Displays

The foregoing has been a discussion on determining the level of attenuation of a particular instrument. It is also of importance to know the level of attenuation of a particular part of the visual display in order to obtain the proper dimming effect.

The display axis system is similar to the instrument axis system with it's origin located in the lower left corner from which the positive abscissa is directed to the right (X_D) and the positive ordinate is directed upwards (Y_D).

Considering a CRT display system, the display consists of 1,000 raster scan lines. If the elements along a horizontal scan line are designated H_D and if each scan line has a vertical desig-

nation V_D relative to the display axis system, then H_D and V_D can both be thought of as counters where H_D gives the number of picture elements along a particular raster scan line and V_D gives the number of raster scan lines. Thus, the fixation point (F) can be defined in terms of (H_{los}, V_{los}) such that,

$$H_{los} = \frac{H_{max}\ (X_{los_D})}{X_D} \qquad \text{[Eq. 4.3.6.2-1]}$$

$$V_{los} = \frac{V_{max}\ (Y_{los_D})}{Y_D} \qquad \text{[Eq. 4.3.6.2-2]}$$

Where

H_{max} = The maximum number of elements along a horizontal scan line

V_{max} = The maximum number of scan lines

X_D = The X_D coordinate of the point of interest on the display

Y_D = The Y_D coordinate of the point of interest on the display

Since the coordinates of the fixation point (F, and the point of interest (I) have been established, it is now possible to define R_D (the radius from F to I) and thus, the attenuator on the image intensity (K).

The following computations must be performed by analog circuitry because they are required to be done at video frequency.

$$R_D = [(H_D - H_{los})^2 + (V_D - V_{los})^2]^{1/2} \qquad \text{[Eq. 4.3.6.2-3]}$$

For

$R_D \leq R_1$, K = 1 (Normal image intensity)

$R_D \geq R_2$, K = 0 (Complete blackness)

$$R_1 < R_D < R_2, \quad K = 1 - \frac{R_D - R_1}{R_2 - R_1} \qquad \text{[Eq. 4.3.6.2-4]}$$

For any point of interest on the visual display.

The above development for the CRT display can also pertain to the dome display because a light valve maps from a flat plane to a spherical surface optically, and is a raster scan projector.

4.3.6.3 Visual System Drives

Since both a CRT display and a light valve projector require raster generation and visual signal processing the technique which is related herein will be applicable to both schemes.

Consider the hardware described in Figure 4.3.6.3-1. The hardware described assumes a sweep generating method utilizing a crystal feeding down counter to determine the timing for the horizontal and vertical sweep generation. These signals would be compared against those generated by the visual acuity computer to locate in the raster the center of foveal view and the corresponding lengths along the raster line as well as the intensity of visual signal at that point. This information would then be fed to an in-line video multiplying D/A to properly attenuate the video prior to going to the CRT or light valve projector.

The visual acuity computer (VAC) will determine, from the algorithm, the center of diminution and the radii of peripheral dimming and connect them by appropriate transformations to horizontal and vertical locations within the raster. Further the VAC will

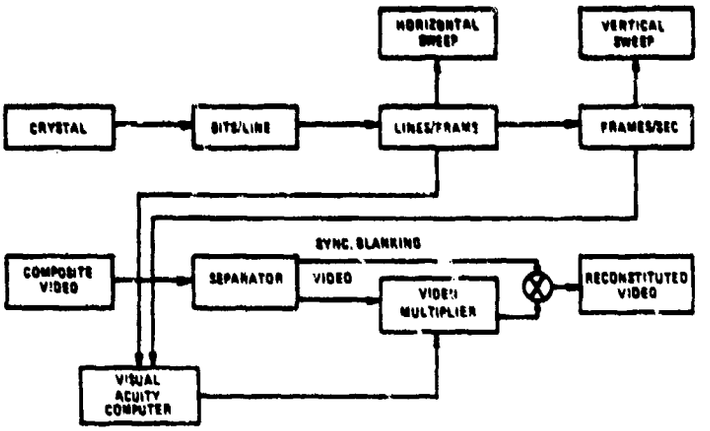


Figure 4.3.6.3-1 Selected spot dimming block diagram.

compute the appropriate level of acuity for each picture element which will serve as the video modulation level fed to the video multiplier.

Figure 4.3.6.3-2 serves as a further aid to explanation of the type of signal computation considered. The center of diminution is 75% along line 11 in the hypothetical raster. Four levels of acuity are assumed. Proceeding from left-to-right the effect of the visual acuity signal from the VAC, after having been transformed and referenced to the raster, is shown for lines 4, 5 and 11. The dotted portions of the raster depict the retrace lines which are blanked during normal operation.

The main element outside the VAC is the multiplying video D/A. In terms of this hardware description the amplifier of the D/A will be capable of handling the standard video frequencies consistent with the resolution and scanning frequencies of the visual device. Depending on the number of levels of acuity chosen between complete blackout and clear vision, the settling time of

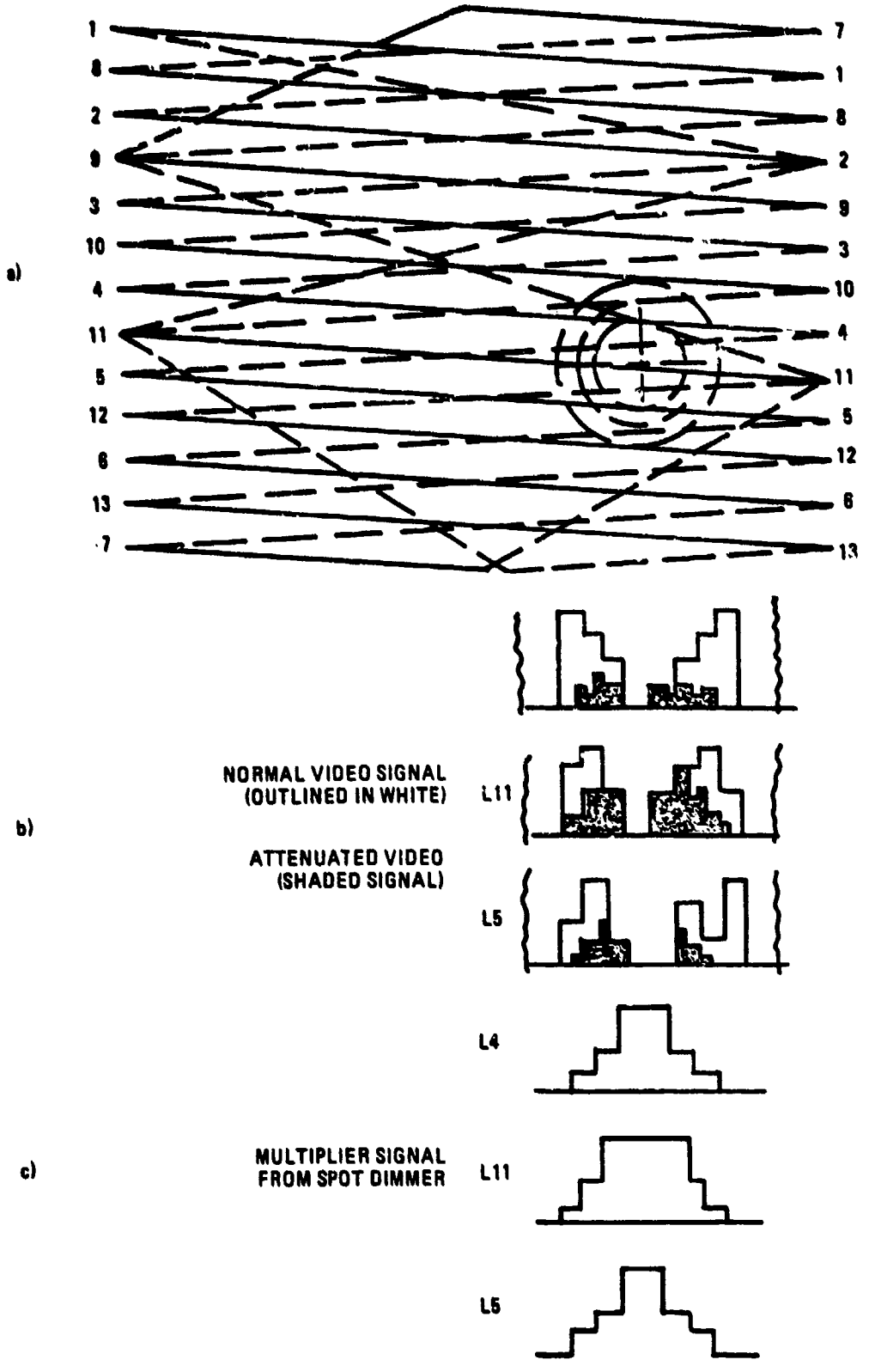


Figure 4.3.6.3-2 Raster with selected spot dimming.

the DAC will be determined. Consistent with state-of-the-art the settling times would probably be about 50n-sec. This translates to a bandwidth of 7 mhz which may cause some loss of resolution along the scan line at a point where acuity levels are changing. Because of the nature of the simulation this may cause some blurring at changes in acuity level. This is not considered to be a serious problem at this time but would be a consideration in a future hardware study.

4.3.6.4 Cockpit Lighting Drives

In a situation where the field of view covers the visual display and the cockpit instrument panel, (Figure 4.3.6.4-1) the visual display would be covered by the hardware described in section 4.3.6.3. Even though the center of foveal view is off the display

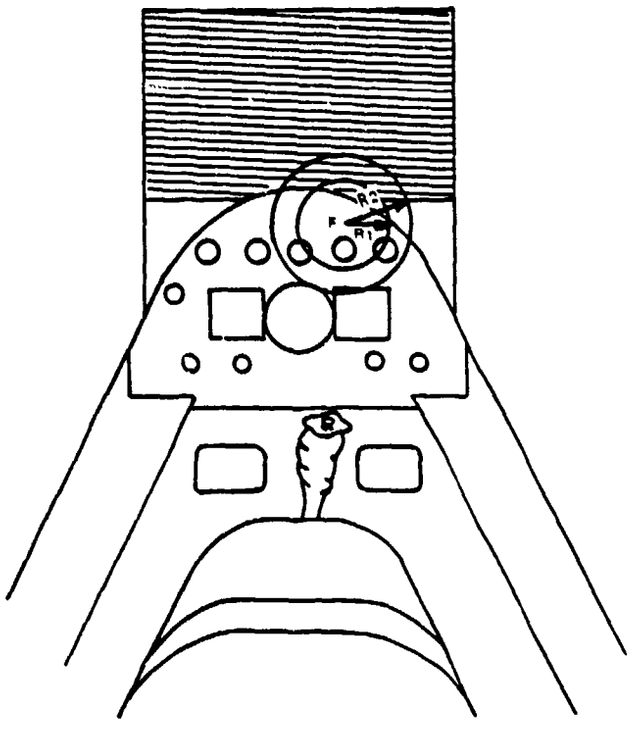


Figure 4.3.6.4-1 Visual display/instrument panel blending of selected spot dimming.

screen the radii of diminution will cause the appropriate dimming in the required area. To simulate the loss of acuity in the cockpit interior scene, it has been decided that this loss would be simulated by dimming the instrument lighting (Figure 4.3.6.4-2). The following is a description of the simulation hardware.

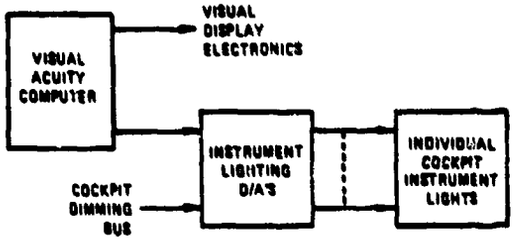


Figure 4.3.6.4-2 Cockpit interior selected spot dimming block diagram.

The visual acuity computer (VAC) will predict the center of foveal vision and the radii of diminution based on the G's being experienced according to the prescribed algorithm. Since the instrument lighting is based on a fixed reference system each light will have a fixed address in X and Y (Figure 4.3.6.4-3). The addresses will be continually compared to the values generated by the VAC. When the VAC determines that a given instrument light falls within the field of diminution the signal to that light will be attenuated according to the algorithm. Normal cockpit lighting, switching and dimming will also be accomplished through the instrument lighting D/A's.

Side panel lighting and auxiliary cockpit lighting could be handled in the same manner as front panel lighting. The amount of hardware and its complexity could be reduced considerably if this lighting were considered to be in the area of complete vision loss

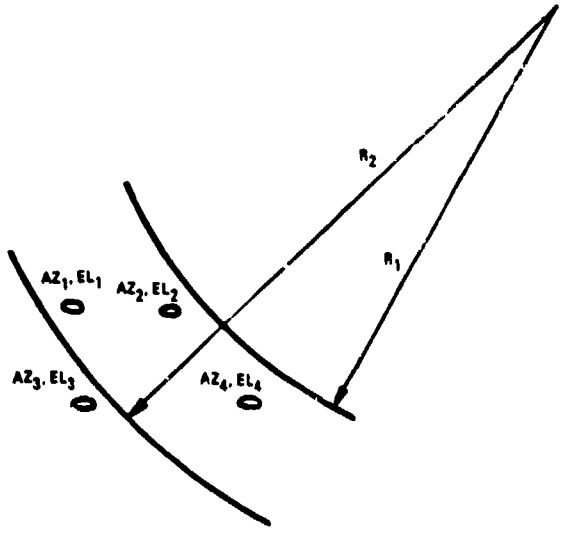


Figure 4.3.6.4-3 Instrument panel light addressing.

and be driven in normal simulator fashion. This possibility could be investigated prior to any hardware implementation.

The D/A utilized in controlling the instrument lighting will require a current buffer on a standard D/A to handle the current requirements of the various bulbs used in aircraft instrument lighting. Again the D/A will be the multiplying type which allows a variable reference voltage to be used. Since only a single variable is required the most stringent requirements will be 1) multiplying capability, 2) current drive capability, and 3) number of bits required to perform the dimming requirements of the algorithm.

4.4 Musculoskeletal Loaders

4.4.1 Head/Neck Loading

In the environment of high acceleration flight, the forces on the pilot's head represent a significant obstacle to the pilot moving his head. Pilots have been quoted as saying their shirt collar size has increased substantially during their tour of flying high performance aircraft. This is a result of the neck musculature resisting the inertial effects on the head. Because of the fact that the neck muscles resist both head and helmet inertial effects, it is logical to assume that if these effects are reproduced in the simulator the combined inertia of head and helmet must be considered.

Since it was found that there was significant movement of the helmet with respect to the head as well as the resistive effects on the neck, it was decided that these two areas should be treated separately. Therefore, the effects of the head and helmet together stimulating the neck muscles is considered in this section. Subsequently, the helmet motion relative to the head will be treated.

In section A.4.2 it is shown that the head responds with both pitch and vertical motion to $+G_z$ stimuli. The data is lacking in other degrees of freedom as indicated in section A.4.2. However the other degrees of freedom could be investigated with some of the hardware suggested in the following sections. This head motion stimulates three sets of physiological receptors, the muscle sensors, vestibular sensors and visual perspective. In addition, the flesh pressure sensors in the head may also be stimulated by the apparent increase in helmet weight.

Several approaches have been considered in attempting to provide the stimulation indicated above and in section A.4.2.

- o Heavy fluid/helmet cavity
- o Cable torque motor
- o Skull pressure firmness bladders
- o Cable/boom and drogue
- o Magnetic field effects

HEAVY FLUID/HELMET CAVITY

The heavy fluid/helmet cavity approach was first introduced during the study proposal. The concept employed is to fill cavities in the pilot's protective helmet with a fluid of sufficient density to stimulate the physiological sensors consistent with an increase in apparent mass of the head and helmet due to an increase in vertical acceleration. As the acceleration increases the cavities are filled and as it decreases the cavities are emptied. In order to develop the design parameters of this system the quantity of fluid required must be determined. Table 4.4.1-1 lists the apparent increase in head and helmet weight as a function of +Gz. Also presented in this table are the volumes of mercury and a 20% lead slurry required to achieve those apparent head and helmet weights.

Table 4.4.1-1 Head and helmet weight as a function of G_z.

$+G_z$	Head Weight(kg)	Helmet Weight(kg)	Total Weight(kg)	Volume Hg(cm^3)	Volume Pb/oil(cm^3)
1.0	4.6	1.1	5.7	0	0
2.0	9.2	2.2	11.4	422.2	1900
3.0	13.8	3.3	17.1	844.4	3800
4.0	18.4	4.4	22.8	1266.6	5700
5.0	23.0	5.5	28.5	1688.8	7600
6.0	27.6	6.6	34.2	2111.0	9500
7.0	32.2	7.7	39.9	2533.2	11400
8.0	36.8	8.8	45.6	2955.4	13300
9.0	41.4	9.9	51.3	3377.6	15200
10.0	46.0	11.0	57.0	3799.8	17100

The number of heavy fluids available which do not require special handling are very few. Mercury, because of its toxicity causes special problems. It is also an expensive fluid. It was eliminated from consideration here because of the safety considerations. The 20% lead/oil slurry would be safe, however the quantities required are very high to effect a 1:1 correspondence to the actual acceleration. At 5g and 10g, 5.7 and 17.1 liters respectively would be required. The standard USAF helmet modified with several chambers as shown in Figure 4.4.1-1 would hold approximately one liter. Rare earth colloidal solutions or slurries, such as depleted uranium may be an alternative with higher densities but they would be cost prohibitive.

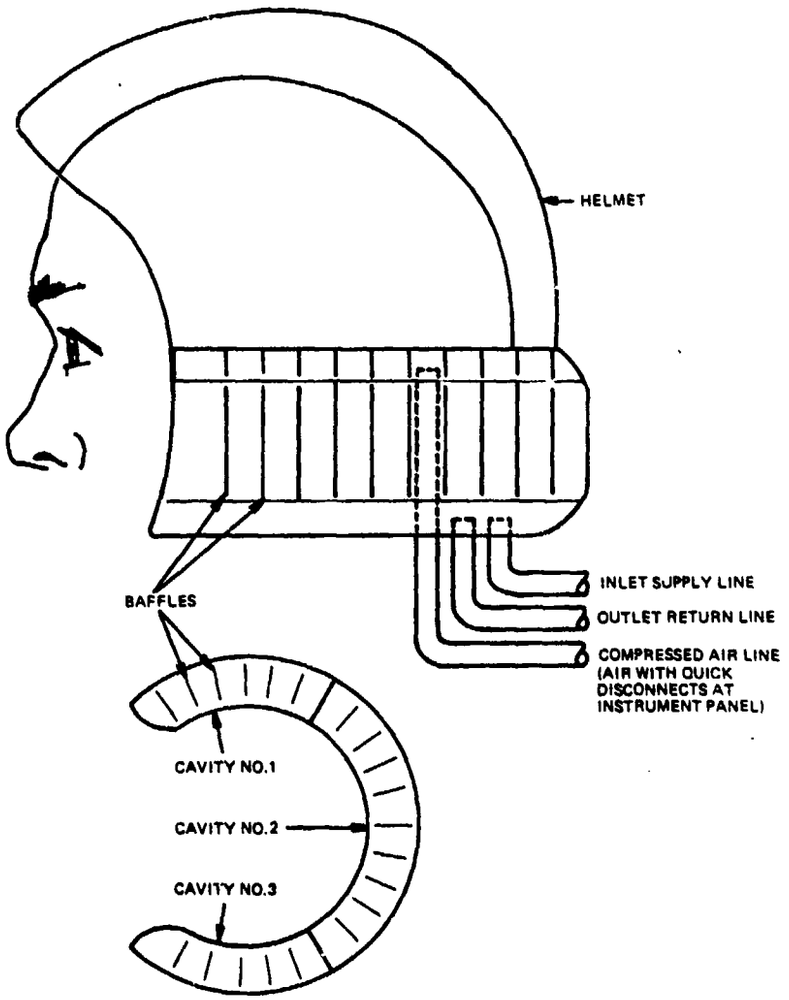


Figure 4.4.1-1 Heavy fluid cavity approach.

In order to scale the system to 10g, which seems to be a minimum requirement for the present generation of high performance fighter aircraft, the apparent weight of the head/helmet would have to be reduced to about 6% for the lead slurry and to about 26% for the mercury which would give the scaled weights in Figure 4.4.1-2. This figure illustrates that at 10g the scaled increase in apparent weight is only 3.1 kg or 6.8# for the lead slurry and 13.3 kg or 29.3# for mercury while in fact the increase is 51.3 kg or 112.9#.

These results raised several questions; first, would the generation of the full forces as indicated above impose a safety hazzard to the pilot? Second, what is the value of reduced amplitude cuing? Third, what is the effect of applying the full gravitational load to the helmet and thereby transmitting the force to the head and neck when in reality those forces are distributed between the head and helmet in a ratio of their weights?

The safety question is one of considerable concern. While it can be stated that these loads are the same as what could be expected in flight, it is a fundamental concept of flight simulation that these devices actually be safer than the aircraft. Therefore the imposition of in excess of 50 kg to a pilot's head should be done with a great deal of care if at all. One major problem here is that the attitude of the head and neck relative to the spine cannot easily be determined and therefore the application of this force could cause injury if the head is not in an optimum position for transmitting the forces. A further point to be considered is that the heavy fluid cavity approach does not have the inherent characteristics to make the system totally fail-safe.

Assuming then that it is undesirable to replicate the forces exactly, but rather to employ a scaled version of the loads, the concept of reduced amplitude cuing should be considered. This

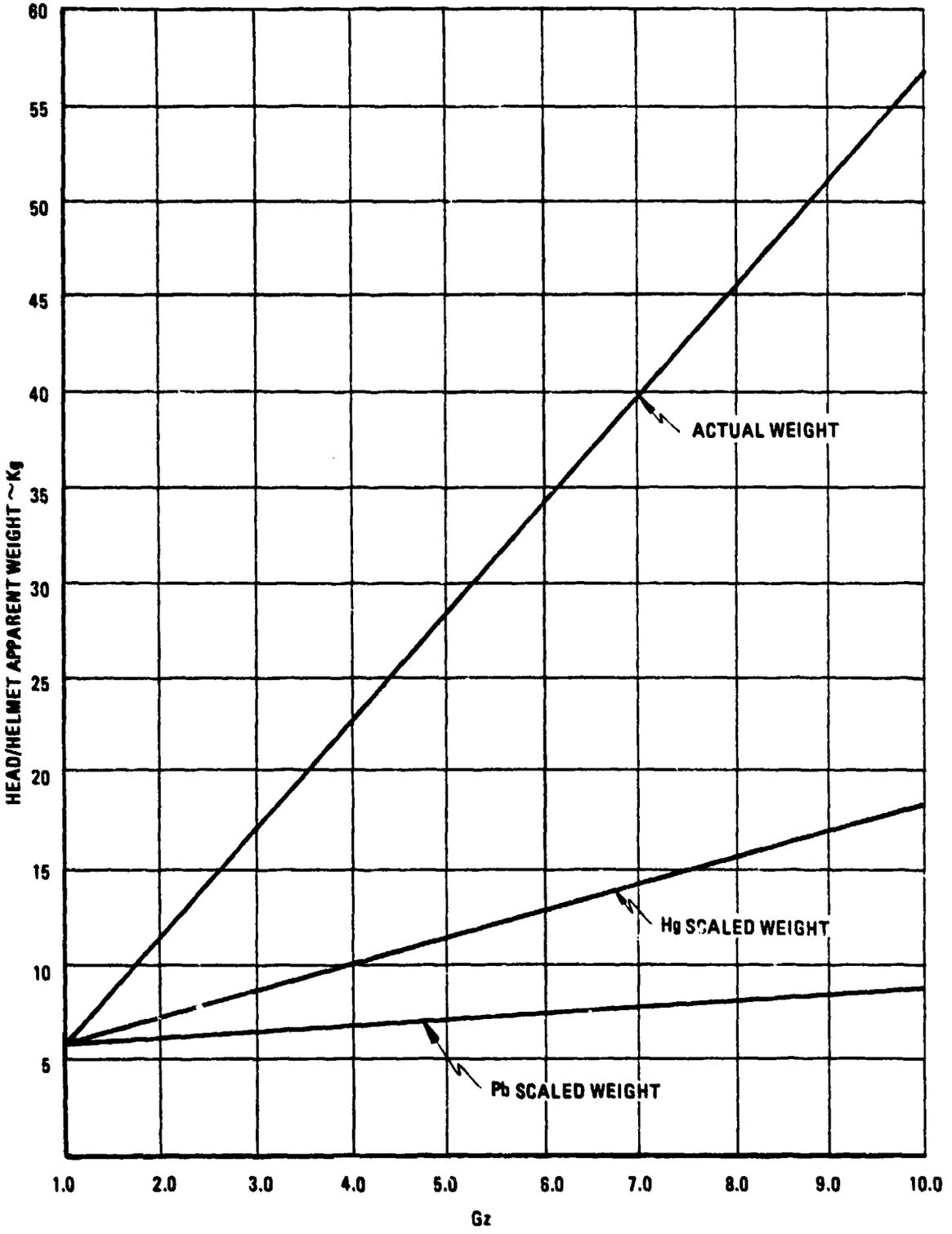


Figure 4.4.1-2 Head/helmet apparent weight as a function of G_z (actual and scaled).

concept has been employed successfully in other areas of simulation. However the concept is not without controversy. Therefore, to determine the applicability or the value of a reduced amplitude cue training value, experiments must be undertaken.

The third question concerning the application of the total head/helmet forces through the helmet is one that requires further study. It is unrealistic to impose the forces totally through the helmet since the flesh pressure sensors in the head would indicate that all the force is applied through the helmet. Perhaps this effect could be countered by the use of firmness bladders in the helmet liner. These devices would be inflated during this period to distribute the load over a larger area and thereby reduce the stimulation of the flesh pressure sensors. This drive philosophy would be in opposition to that of using the firmness bladders to enhance the helmet loading cues.

Of course the fallacy in this approach is that to some extent some of the load will be absorbed by the compressibility of the air in the firmness bladder. Again this concept can only be verified empirically.

The high flow requirements indicated in Table 4.4.1-1 for a 10 g/sec acceleration rate are on the order of 4 liters/sec. Since this would impose significant constraints on the design of a pumping station, it does not seem feasible to use this system (heavy fluid cavity) to conduct the experiments to determine the training value of reduced amplitude cuing. Coupling this fact with the safety aspect and the fact that this would be an expensive system indicates that another approach be used to develop a laboratory device to evaluate the concept. This device has already been developed, the NASA Langley Helmet Loader.

CABLE TORQUE MOTOR

The cable torque motor approach would employ a system of cables attached to the helmet through which tension could be adjusted by a torque motor. As was stated above, a device of this type has been developed, built and tested by NASA Langley. This device, referred to as a helmet loader is described by Ashworth and McKissick (8).

The system employs two small strings attached to the helmet and routed through pulleys on the shoulder harness to a torque motor and employing a force transducer in the control loop. The force feedback is utilized in order to follow the pilot's movements while maintaining the appropriate helmet forces. Figure 4.4.1-3 shows the installation of the NASA helmet loader in the DMS at Langley.

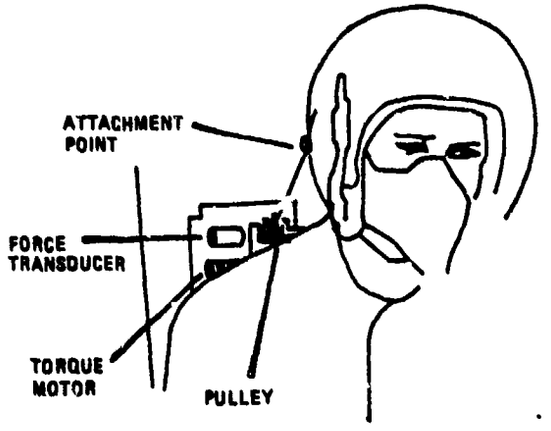


Figure 4.4.1-3 Helmet loader installed in DMS (from Ashworth and McKissick (8)). (reprinted with permission from the American Institute of Aeronautics and Astronautics, AIAA Paper No. 78-1573, Figure 1).

The two small pulleys attached to the pilot's shoulder harness provide a loosening of the straps as force is exerted down-

ward on the helmet for positive G. Unrestricted head movement is permitted by the amount of cable wound on the reel of the torque motor.

The helmet loader system is described by its developers as a 0.4 damped second order system with a 20 msec steady state time delay. Figure 4.4.1-4 illustrates the response to a 50% step. It can be seen from this figure that the 0-90% rise time is approximately 50 msec. The system response as stated in the technical requirements for this study specify, as a response to a step input, a 50 msec initial response and a 30 msec rise time (10%-90% of final value). The NASA helmet loader displays less transport delay but a slightly longer rise time with the total time lag being less in the case of the helmet loader.

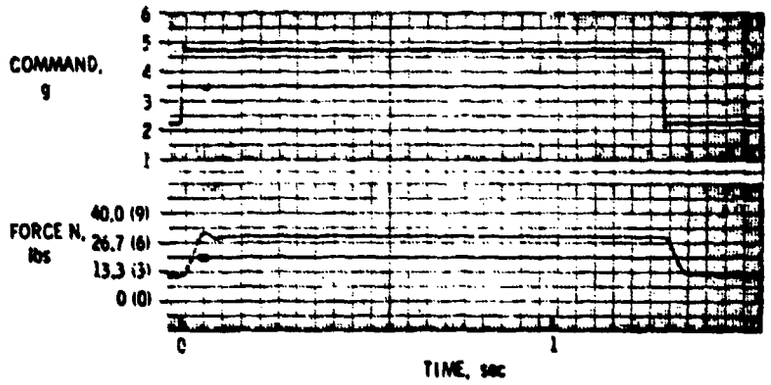


Figure 4.4.1-4 Step response (from Ashworth and McKissick (8)).

This device is scaled to produce 2/3 of the inflight helmet loads up to a maximum of 6g where the total force exerted is 9 pounds. The developers state that their studies on the DMS have shown that the "helmet loader has a measurable effect on the pilot/simulator system". They further state that "subjective data indicates that the cue provided through the use of the helmet loader is realistic, and there is no noticeable time delay in the

presentation of the cue. However, the pilots had mixed opinions about the effect of the helmet on their performance."

The device is designed with pilot safety as a consideration and thereby uses breakaway snaps on the helmet, current and voltage limiting and small torque motors to ensure that the pilot does not experience excess forces.

The system is driven with a force command from the drive algorithm. This algorithm is very straight forward where the commanded force is proportional to the aircraft z-body axis acceleration.

$$F_H = 1.8\ (G_S - 1.0)\ ;\ C \leq F_H \leq 9 \qquad \text{[Eq. 4.4.1-1]}$$

where F_H is the helmet commanded force and G_S can be computed from the expression

$$G_S = -K_S \frac{AZA}{32.2} \qquad \text{[Eq. 4.4.1-2]}$$

where K_S is the scaling coefficient and is set at 0.667 by Ashworth and McKissick. The negative sign is in recognition of the fact the positive G_z is produced by a negative AZA. Figure 4.4.1-5 illustrates the system control loop.

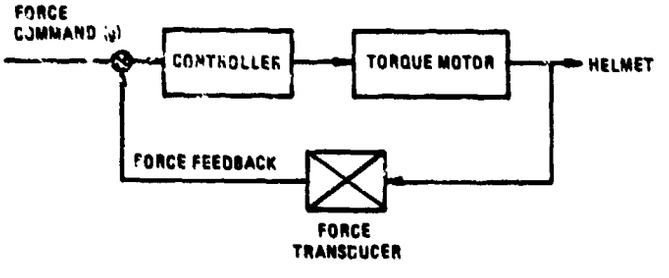


Figure 4.4.1-5 Helmet loader control diagram.

One disadvantage to this system is that it does not lend itself to inducing head pitch down resulting from $+G_z$ as is described in section A.4.2. However with the addition of one torque motor and a helmet attach point at the base of the helmet, pitch up could be achieved as would be expected in $+G_x$ maneuvers. Although the data does not necessarily support this modality, it appears that there should be head motion in this degree of freedom. It might be worthwhile at a later date to expand the capability of this system to accomplish the pitch up capability. Also, the addition of one torque motor and isolating the two strings in the current design on separate torque motors to permit differential drive as a function of roll acceleration might be beneficial. These would be relatively straightforward modifications to the existing design and could yield useful subjective data.

SKULL PRESSURE FIRMNESS BLADDER

As the aircraft accelerates in a $+G_z$ direction the apparent weight of the helmet increases according to the data of Table 4.4.1-1. This increase in apparent helmet weight manifests itself in one way as increased skull pressure. This increase in skull pressure is sensed by the flesh pressure sensors in the area over the skull.

It has been postulated that these sensors can be stimulated by the use of so-called firmness bladders. These devices, when deflated, cause an apparent increase in pressure on the flesh pressure sensors much the same as is currently employed in the ALCOGS G-Seat (143). In that device, the firmness bladders are deflated to cause an apparent increase in pressure on the buttocks consistent with an increase in $+G_z$. To enhance this cue, the helmet would be designed with an exaggeration of the support members in the helmet such that the localized pressure sensation would be increased. Figure 4.4.1-6 illustrates the firmness bladder as employed here for increase in skull pressure to increase in $+G_z$.

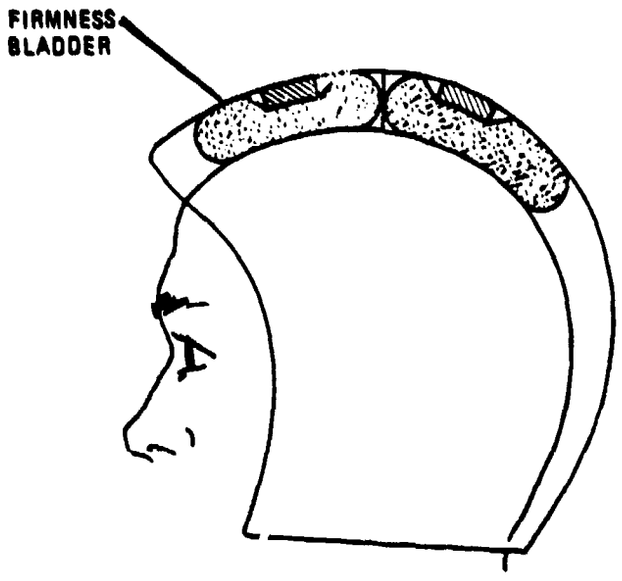


Figure 4.4.1-6 Helmet firmness bladder. Bladder is illustrated in cross hatched area.

The device would be pressure controlled with the loop closed on pressure. Figure 4.4.1-7 illustrates the control system required to appropriately control the pressure in the firmness bladder. The firmness bladder should be 6.5 inches front to back and 5 inches side to side and a maximum thickness of 0.75 inches. The maximum pressure required is 2 psi and the maximum required flow rate for the bladder should be 1 SCFM. If a hydraulic servo control flow control valve is employed, scavenge air is required at about 3 SCFM so that the total flow required to the system is 4 SCFM. Also a vacuum at -5 psi is required in order to provide appropriate response at the low pressures used here.

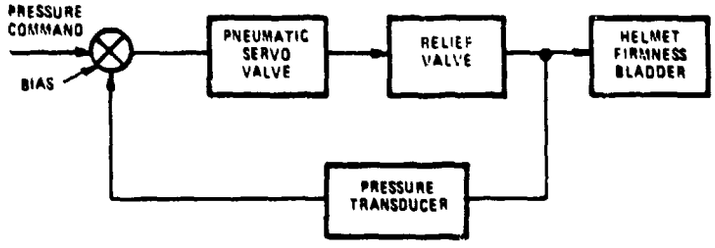


Figure 4.4.1-7 Helmet firmness bladder control diagram.

The firmness bladder would be driven with a pressure command such that the pressure in the bladder would be a function of $+G_z$. The algorithm would be of the form

$$P_B = +0.009 \frac{A2A}{32.2} + 0.071 - BIAS \qquad \text{[Eq. 4.4.1-3]}$$

A modification of this system would be to employ a loaded helmet say 10 pounds equally distributed over the helmet and employing an elevated pressure in the firmness bladder to redistribute the loading on the skull. This would, when deflated, increase the loading on the skull and give a cue of a higher acceleration. (With the firmness bladder described herein the required pressure at 1g would be about 0.4 psi.)

The firmness bladder approach is safe, relatively inexpensive, and allows for a significant variation in research protocols. It should therefore be given a relatively high priority in the hierarchy of further investigation.

CABLE/BOOM AND DROGUE

The cable boom and drogue (CBD) approach is an outgrowth of a rather simple three cable system which would pull down from either side and the rear of the helmet. The cables would be driven by helmet mounted torque motors and would be attached to seat back and harness strapping. Continued assessment of this approach with particular attention to improving visual environmental fidelity, led to modifications which evolved into the CBD approach. The approach is briefly introduced here, but not recommended for design because of its comparative mechanical complexity. The CBD approach is depicted in Figure 4.4.1-8.

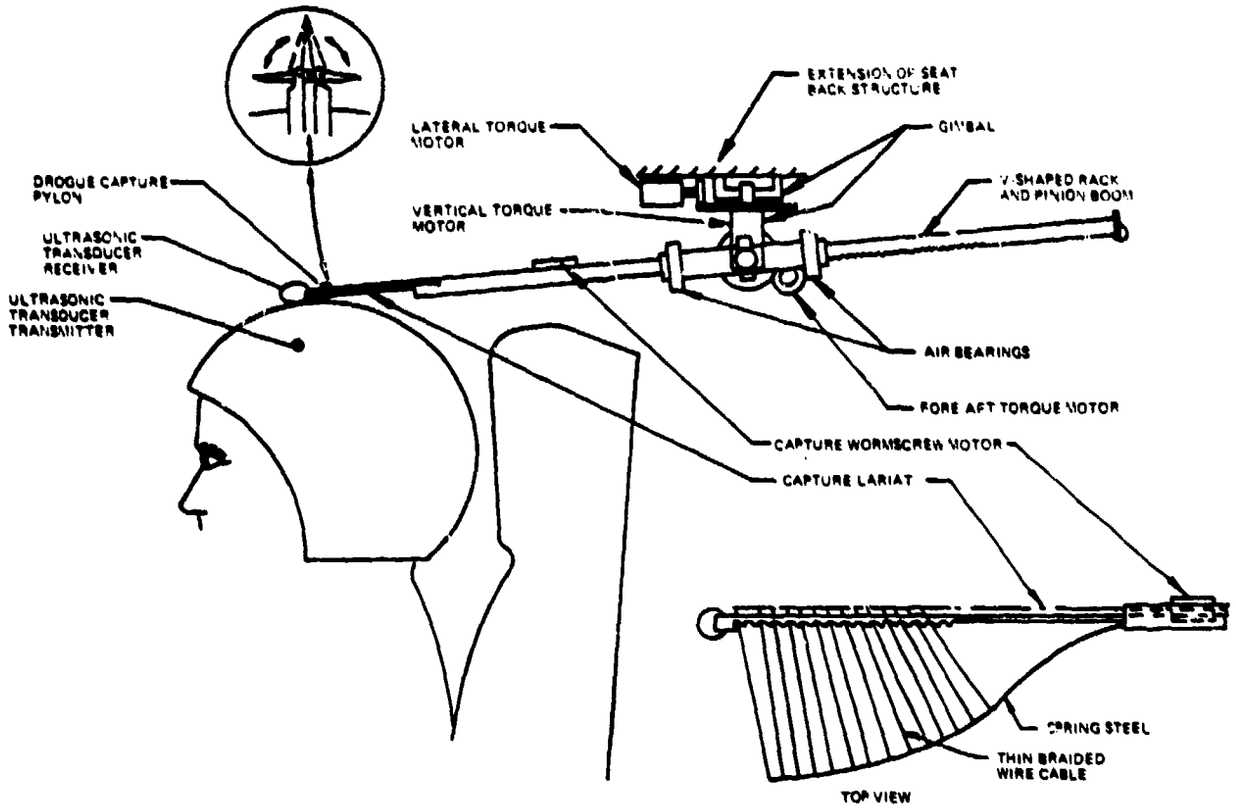


Figure 4.4.1-8 Cable/boom and drogue approach.

The CBD approach employs three main active elements: a helmet with active drogue pylon and ultrasonic transducer transmitters, a lariat for capturing the drogue and securing the boom to the helmet, and an air-bearing-mounted drive boom capable of passive or driven extension and passive or driven pitch and yaw degrees of freedom about the boom mounting point. Once attached to the helmet, torque motors at the boom gimbal system would apply forces through the boom to the helmet in direct proportion to the stall torque at commanded current. Pilot head activity is permitted at force levels exceeding commanded force. The commanded forces can produce all the desired head/helmet goals and would be controlled so that maximum force available from the system occurred at maximum anticipated simulated acceleration.

The helmet would appear very similar to flight issue and could be donned before or after entering the cockpit. The boom would be stowed in the full aft up position with the lariat drive open and the drogue pylon leaves deenergized and in the up position. Plugging the helmet headset into the instrument panel would activate the ultrasonic transducer helmet transmitters and boom receivers and cause the boom to extend within the pilot's "blind spot" and home on the pylon. Excessive pylon/boom relative motion would cause a pause in the homing. The boom would be driven lightly down to the helmet, and upon contact, the drogue capture pylon leaves would be energized to their horizontal position, trapping the lariat wires between helmet and pylon leaves. The capture wormscrew would retract the lariat cable, trapping the pylon between boom and lariat spring steel spreader. The system would then exit the capture mode and begin to display computer-generated (commanded) helmet forces.

Safety would be assured by designing the pylon leaves to raise if the boom is lifted with a force greater than the maximum desired lifting force. This would permit the drogue to slip from the lariat's grasp. Pylon leaf raising and boom up motion would automatically occur under simulator off conditions or canopy opening.

MAGNETIC FIELD EFFECTS

The magnetic field effects employ the use of magnetic fields to impose forces on the pilot consistent with the forces of the high G environment of the simulated aircraft. This approach has had, for a long time, a certain degree of enchantment because it does not require any apparatus to be imposed directly on the pilot thereby maintaining the visual environment fidelity of the simulated cockpit.

One of the long time concerns for this approach has been that of safety. This does not seem to be of great concern currently because of the short duration of the exposure. However, the intense magnetic field required could adversely affect other simulator systems. This approach was not pursued to any great extent in favor of concentrating resources on the more readily adaptable approaches such as previously described. The approach should not be totally abandoned however. Perhaps some future work could be done to further explore magnetic field effects.

SUMMARY

It was found that the heavy helmet fluid cavity had significant drawbacks in attempting to implement the concept into hardware which would meet the operating criteria in the high performance aircraft environment. The cable, boom and drogue approach and the magnetic field effects approach were discussed and discarded on the basis of complexity. The localized firmness bladder was determined to provide cues of a somewhat reduced amplitude but the device is considered worthy of being implemented and subjected to further experimentation. A major drawback is that it only stimulates the flesh pressure sensors and does not provide any stimulation of the neck muscle receptors. Its main value may be in providing an enhancement of some other method such as being used in conjunction with the NASA helmet loader to counter the ambiguity which arises from applying head and helmet apparent weight through the helmet.

It appears that the most viable approach to providing head/neck loading cues is the NASA Langley helmet loader. Primarily because this device has been built and tested and can be modified fairly readily to achieve higher loadings and additional degrees of freedom. Also, when combined with localized firmness bladders, it will provide a useful research device.

4.4.1.1 Helmet vs. Head Motion

It is shown in section A.4.2.1 that there exists a significant amount of relative motion between head and helmet up to four degrees at 6g mean for all data. Also demonstrated is a 15 mm vertical depression of the helmet which is probably just the vertical component of the pitch since this data was taken from a reticle attached to the front of the helmet.

The approach that is recommended here to achieve this movement is via localized firmness bladders in the helmet. Two bladders could be employed and driven differentially to produce helmet pitch and in unison to provide vertical helmet motion. Figure 4.4.1.1-1 illustrates the configuration. The two firmness bladders have the same total area as the one in section 4.4.1. Considering two bladders of equal size, 3.25 inches front to back and 5 inches side to side, the required stroke would be a half inch. This is within the capability of the 3/4 inch bladder designed in section 4.4.1. The total flow parameters are the same as for the single bladder. Two equivalent HSC valves of the same (each half

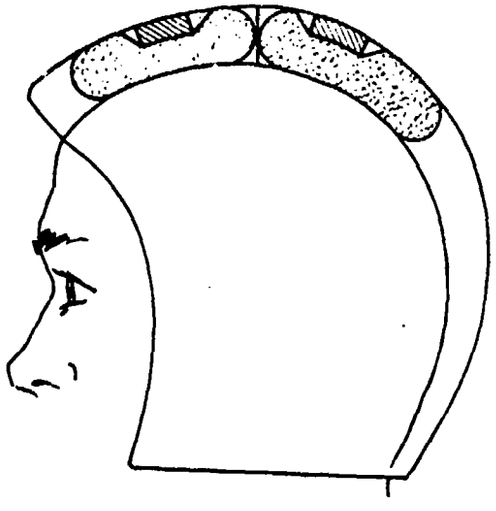


Figure 4.4.1.1-1 Dual firmness bladder helmet.

the capacity of the one in section 4.4.1) could be employed. Each firmness bladder will then be 3.25 inches, front to back by 5 inches, side to side.

The algorithm to drive the two bladders would be given as follows. The helmet angle is given by

$$\theta_H = 0 \text{ for } G_Z \leq 2.0 \qquad \text{[Eq. 4.4.1.1-1]}$$

$$\theta_H = -G_Z + 2.0 \text{ for } G_Z > 2.0 \qquad \text{[Eq. 4.4.1.1-2]}$$

The differential vertical excursion of the two bladders is given by

$$\Delta Z_H = K_H(3.25 \text{ Tan } \theta_H) \qquad \text{[Eq. 4.4.1.1-3]}$$

where K_H is a gain constant to permit reduced amplitude scaling. Then the forward bladder excursion would be

$$Z_{H_F} = \frac{\Delta Z_H}{2} \qquad \text{[Eq. 4.4.1.1-4]}$$

The aft bladder excursion is given by

$$Z_{H_A} = \frac{-\Delta Z_H}{2} \qquad \text{[Eq. 4.4.1.1-5]}$$

The pressure for each cell is proportional to the excursion

$$P_{B_F} = K_p Z_{H_F} \;\&\; P_{B_A} = K_p Z_{H_A} \qquad \text{[Eq. 4.4.1.1-6]}$$

These pressures are about a biased pressure, as employed in section 4.4.1. The control diagram (Figure 4.4.1-7) for the single bladder is applicable to the dual bladder approach duplicated for each bladder.

This approach is recommended since it can fulfill the requirements of section 4.4.1 as well as this section.

4.4.2 Upper/Lower Arm Loaders

4.4.2.1 Introduction

The reader will recall that the discussion of Section 3.2 strongly suggested that, in order to obtain useful G induced extremity loading stimuli, it will be necessary to actually physically load the extremity in question. It is shown in Section A.4.1 that acceleration effects operating on the upper arm are indeed significant and lead to cross loading error wherein, in horizontal plane reaching movements in the presence of $+G_z$ conditions, the hand falls short of its intended target. With this in mind the mechanization of arm loading stimuli production requires equipment configured to exert force or load on the arm itself and the mechanization must allow load to be individually placed on upper and lower arms. The following conceptual development will be limited to the acceleration loading of primary consequence: $+G_z$.

Obviously the inherent high degree of arm mobility and the requirements to exercise this mobility, in the course of piloting and operating the onboard systems of a tactical aircraft, severely constrain the arm loading concepts. It is not satisfactory to require that the arm be confined to a specific attitude or location in order to permit loading, rather the loader must "follow" arm motion operating when appropriate. Nominally we would expect to find the upper arm in the neutral position which causes it to be approximately parallel to the spinal column. In reaching forward toward cockpit instruments or controls, shoulder flexion (elbow directed forward) up to 90° can be expected and occasionally may be accompanied by some adduction (elbow directed transversely across the body) or abduction (elbow directed transversely away from the body). Shoulder joint forward elevation (elbo

directed upwards above the horizontal plane) is much less likely to occur in tactical aircraft due to the absence of controls above shoulder height.

Under high G conditions the mass of the upper arm, when in the neutral state, increases the load required to be supported by the shoulder joint and when in flexion, with or without adduction or abduction, increases not only load but the torque operating at the shoulder joint. The load is supported by the skeletal frame and torso muscular system governing this frame and is likely less noticeable than the torque which affects the shoulder joint muscular system alone. Under worst case conditions wherein the arm is horizontally outstretched (zero degrees elbow flexion, 90° shoulder flexion) and assuming a 5 pound upper arm mass operating 5.5 inches from the shoulder joint and a 5 pound lower arm mass operating 17.5 inches from the shoulder joint (108), the G_z induced shoulder torque amounts to approximately 9.5 ft-lb/g. As the upper arm is rotated downwards toward the neutral position, the effective mass moment arm becomes less and the torque diminishes.

Under nominal cockpit conditions, we would expect to find the lower arm in near 90° flexion (parallel to the horizontal plane when the upper arm is in the neutral position) and may be rotated internally (transversely across the body) or in minor amounts externally (transversely away from the body). Maintaining lower arm at 90° flexion and raising the upper arm from the neutral point to 90° flexion causes the lower arm to be vertically oriented. This position as well as lower arm internal and external rotation from this position produce arm attitudes of a special nature which impose constraints affecting the design approach and will be addressed later.

A typical reaching maneuver requires the upper arm to move in flexion various amounts from the neutral point toward 90° flexion while relaxing the lower arm a commensurate amount from 90° flex-

ion toward zero degrees (arm horizontally extended forward from the shoulder). The lower arm is generally maintained somewhat parallel to the horizontal plane at the varied amounts of upper arm flexion. Under these conditions high G effects on the lower arm increase the load and torque. Considering the lower arm weight to be 5 pounds operating 6.5 inches from the elbow, 2.7 ft-lb/g of torque is experienced.

Initially the authors felt that a suitable mechanization would employ thin long pneumatic bellows to drive an elbow hinge embedded within the flight suit and thus torque the lower arm with respect to the upper arm. This approach was abandoned due to the problems which arise in accounting for bellows spring rate force which is positionally dependent and would interact with subject movement of elbow flexion angle and unduly complicate the drive model. The characteristics of a torque motor in which torque or force, independent of position, is obtained is a much more suitable drive device. The recent introduction of samarium cobalt motors which display up to five times the torque of similarly sized Alnico motors makes a torque motor approach feasible. Suitable force can be generated by devices which are small enough to be contained on one's person.

4.4.2.2 Concept

The approach selected is illustrated in Figure 4.4.2-1. Lower arm torque is provided by a pancake torque motor embedded within a flight suit modified with additional zippers to permit ease of entry. The torque motor transmits torque to the arms via an arrangement of plastic stays and struts sewn between the cloth layers of the flight suit. The weight of the assembly is estimated to be 2.75 to 3.0 pounds. Upper arm loading is provided by a torque motor driven tether line shown here embedded within the flight suit slightly above waist line. This unit will serve to create shoulder torque, load the upper arm, and retard forward

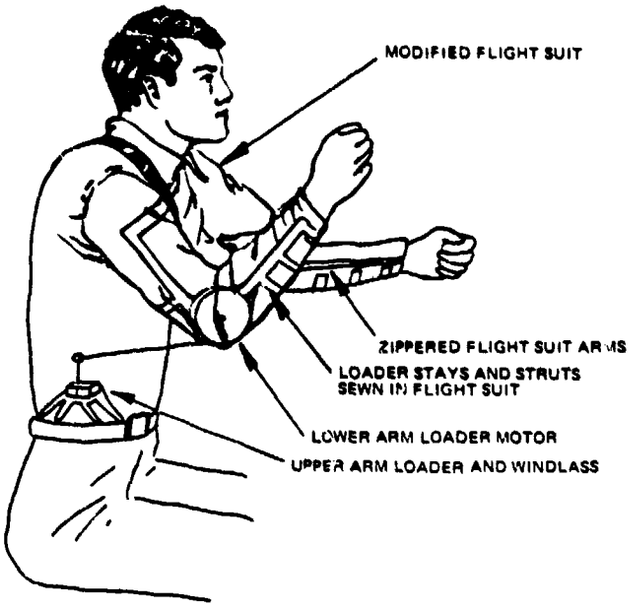


Figure 4.4.2-1 Arm loader arrangement.

movement of the elbow. The unit is shown situated in the flight suit where no special action is required to hook tether to arm; however the unit could be seat frame mounted and tether secured after the pilot enters the cockpit. The former approach is preferable in that one less unnatural pilot action is required. In any event, a DC electrical connection to the flight suit will be required and if undue duty cycles are encountered it may be necessary to provide cooling medium to the torque motors and this will represent an additional flight suit connection. The tether loader weight is estimated to be 1.0 pound.

Figure 4.4.2-2 is a detail of the lower arm loader. An Inland Motor samarium cobalt stator and rotor assembly is supported in a housing designed specifically for this application. The rotor transmits torque to the outer housing and lower arm strut and stays through a servo loop torque load cell which serves as an internal motor shaft. A Lebow 25 foot-pound torque load

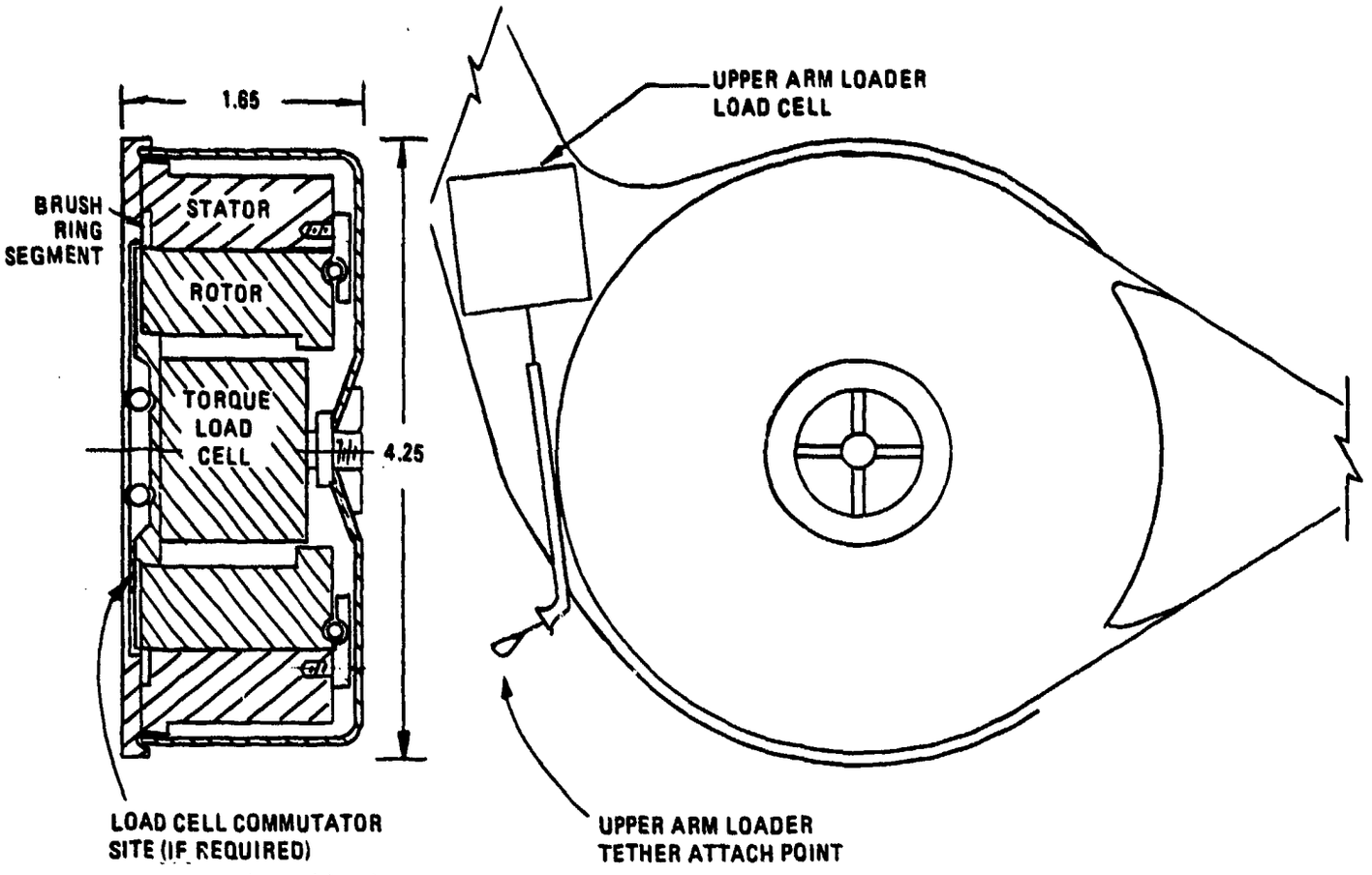


Figure 4.4.2-2 Lower arm loader motor detail.

cell dimensionally fits this application and is used to close the lower arm loader servo loop. Since it is necessary to position the torque load cell between rotor and lower arm strut, it must rotate through the lower arm flexion range of 0-145 degrees. Thus it may be necessary to commutate the torque load cell leads.

Although not shown, it is possible to insert motor stops to prevent torquing the elbow into the hyperextension. A device for rotor/stator angular displacement can also be accommodated and would take the form of a wire wound or carbon filament element situated either close to the above mentioned commutator or around

the outside of the stator. The wiper arm would be either rotor mounted in the first instance or mounted to the inside of the outer housing in the latter case.

Under +8 G_z loading conditions, it is barely possible to raise the arm off its support area (24). Using this value as the maximum, elbow torque can approach 21.6 foot-pounds. The lower arm torque motor is capable of 4.5 foot-pounds of peak torque thereby providing a simulation system loading scale factor of 20%. Maximum subject induced elbow velocity is taken as 3.9 rad/sec (175) whereas the maximum no-load motor velocity is more than sufficient at 139 rad/sec. Likewise motor no-load acceleration of over 10,000 rad/sec^2 is much higher than peak 16.0 rad/sec^2 elbow flexion acceleration (175).

In that the motor is used as a force producer with very little positional displacement, temperature rise is of some concern, however, this is difficult to predict unless realistic duty cycles are available. Simulation of the 100 second acceleration profile given in Figure 1.1-3, assuming the lower arm is maintained near horizontal and peak available torque is to be applied at the peaks of the acceleration profile, would result in a 50°C motor temperature rise. This indicates that, as a minimum, thermal overrides and thermal insulation along the subject side of the motor housing will be required. Whether an auxiliary cooling medium is required cannot be ascertained at this time.

The side view of the lower arm loader shows the position of the upper arm loader load cell. A Schaevitz tensile load cell is attached to the upper arm strut and connected via cable-in-guide-tube to a bail protruding from the back of the flight suit elbow some 14 inches from the shoulder. The load cell is used to close the upper arm tether force servo loop. The monofilament tether extends from an eyelet in the side of the flight suit approximately 14 inches below the shoulder joint and is attached to the

above bail. Figure 4.4.2-3 is an illustration of the upper arm loader which is to be situated within the sides of the flight suit and to which the tether is attached. The assembly is a torque motor driven geared windlass which retracts the tether and applies force to the lower arm loader assembly. A small amount of bias torque is always present in order to keep the tether taut and avoid fouling.

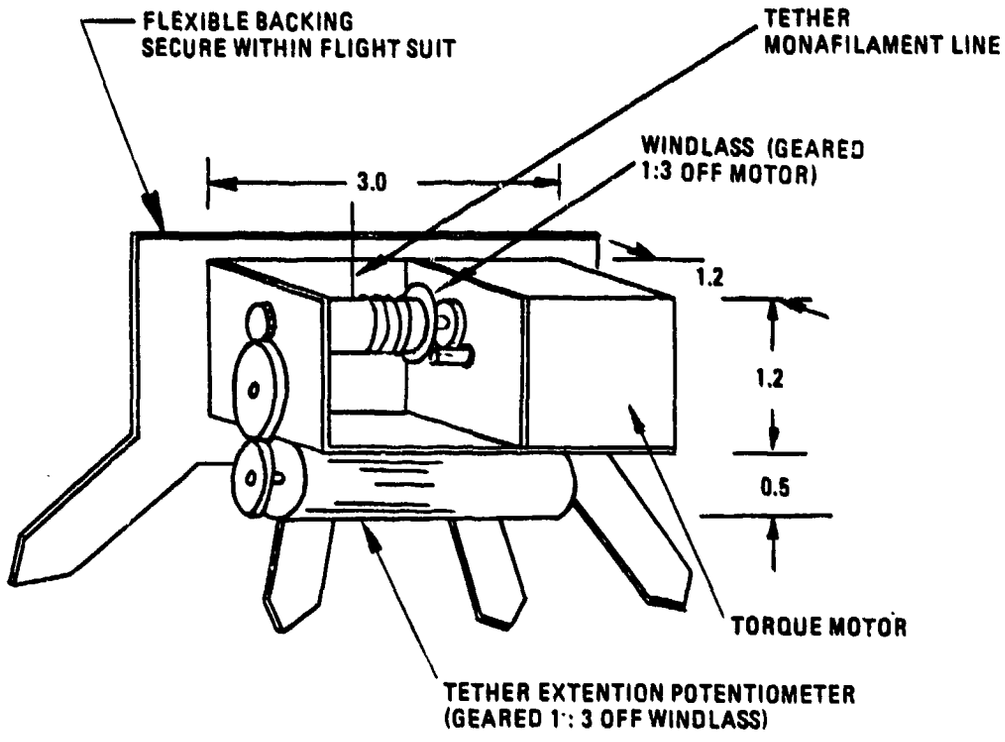


Figure 4.4.2-3 Upper arm loader windlass mechanism.

A ten turn CEC followup potentiometer is further geared off the windlass to provide a measure of tether line extention which in turn permits computation of upper arm flexion or abduction angles. Two principle parameters are employed in sizing this torque assembly. First, under +8 G_z conditions when the upper and lower

arm is horizontally extended, the torque at the shoulder is 76.6 foot-lbs. Maintaining the simulation device consistently scaled at 20% for both upper and lower arm torquers reduces the 76.6 ft-lb. maximum torque to 15.32 ft-lbs. which requires a peak tether line force of 18.5 pounds. Assuming a maximum upper arm forward elevation of 25° (above horizontal) 23 inches of tether line is required and adopting a design goal of limiting windlass turns to 20 or less yields a windlass diameter of 0.366 inches and a maximum windlass torque of 54.3 oz-in.

The second parameter of importance is to select a gearing reduction factor which will satisfactorily relax motor torque requirements to reduce undue thermal effects yet provide a windlass rotational retract velocity which accommodates peak shoulder joint velocities. The peak shoulder joint velocity is taken as 175°/sec (175) which can produce a maximum tether line velocity of approximately 42 inches/second. Selecting a gearing ratio of 3.1 (motor to windlass) reduces the peak motor torque requirement to 18.1 oz. in. and establishes a peak motor velocity requirement of 688 rad/second. The selected Inland Motor samarium cobalt motor is very compact and displays a peak stall torque of 30 oz-in and a maximum rotational velocity of 730 rad/second. The latter figure implies a maximum tether line velocity of 44 inches/second which is greater than that required by only a small margin. The configuration allows a theoretical no-load acceleration capability of 6535 in/sec^2 at the tether line which is well above the 183 in/sec^2 anticipated as resulting from peak shoulder joint acceleration of 750°/sec^2 (175).

Even though a large gearing ratio was selected to suppress peak motor torque requirements, and the selected motor has a high motor constant yet modest thermal constant, heating can pose a problem. As is the case with the lower arm torquer, heating is directly affected by duty cycle. Employing the same acceleration profile of Figure 1.1-3 used to evaluate the lower arm loader

thermal increase yields an upper arm loader temperature increase of 55°C for the 100 second profile. Thermal overrides will definately be required and, similar to the lower arm loader, external cooling may also be required.

4.4.2.3 Drive Scheme

As was mentioned in Section 4.4.2.1, $+G_z$ load induced torque experienced at the shoulder and elbow joints is most pronounced when the arm segment in question is maintained in the horizontal plane where in the effective mass moment arm is largest. A knowledge of the attitude of these arm segments is therefore useful in increasing the fidelity of the drive signals provided by the torque motors. It should also be apparent that there exists an interrelationship between lower and upper arm loaders in addition to the obvious fact that the upper arm loader must account for the load imposed by the lower arm on the upper arm. In lower arm attitudes, where the lower arm torquer is activated, it is necessary to commensurately increase the tension in the upper arm loader tether line to appropriately represent the lower arm mass moment-arm effect upon the shoulder joint.

The following discussion assumes the attitude of lower arm with respect to upper arm is made available by an angular follow-up device included within the lower arm loader. The output of this device, elbow flexion angle S, is measured from the 90° elbow flexion angle (0° at 90° elbow flexion) and increases positively as elbow flexion reduces from 90°. Secondly, shoulder flexion and/or abduction angle is a function of the amount of tether line extended, X measured in feet, and is made available by the upper arm loader windlass potentiometer.

The drive equation for the lower arm torque motor is derived as:

$$T_E = \text{Cos}(2\text{Sin}^{-1}(\frac{X}{2L})-S)(2.7)(K)$$

$$(G_Z^{-1})(\text{S.F.})\ \text{ft-lbs.}$$

[Eq. 4.4.2.3-1]

where:

a) G_z is limited or scaled not to exceed 8 G_z input.

b) L is shoulder joint to tether line elbow attach point distance taken herein as 1.1666 feet.

c) K is a potential attenuation factor to be discussed later.

d) S.F. is the previously introduced simulation scale factor of 0.2.

The expression demonstrates that when the upper arm is left in the neutral position ($X \simeq 0$) and elbow flexion is 90° ($S = 0$), conditions wherein the lower arm lies in the horizontal plane, elbow torque is 2.7 ft-lbs/g and employing the simulation scale factor of 0.2 the torque motor will be driven at 0.54 ft-lbs/g. As the upper arm is raised to 90° flexion ($X = 1.65$ feet) while holding the elbow crooked at 90° flexion ($S = 0$), the commanded torque relaxes appropriately following the cosine function. As the lower arm is allowed to fall forward from this position ($S \rightarrow 90°$) as if in reaching, the lower arm is no longer perpendicular to the horizontal plane and a commensurate increase in elbow torque is experienced.

The drive equation for tether line force accounts for the force application angle formed by the upper arm and tether and is derived as:

$$F_T = \left[\frac{(6.875)(X)(S.F.)}{L^2} + \frac{T_E}{L(1-\frac{X^2}{4L^2})^{\frac{1}{2}}} \right] \left[G_Z - 1 \right] + C \text{ lbs.}$$

[Eq. 4.4.2.3-2]

where C is the residual tether anti-fouling force and the other terms are as defined above.

The expression demonstrates that when holding the arm extended forward at shoulder level (90° shoulder flexion or X = 1.65 feet, 0° elbow flexion) where elbow torque T_E is 0.54 ft-lbs/g, the tether force is 2.32 lbs/g. This force applied at a 45° angle to the upper arm L feet from the shoulder joint produces a shoulder torque of 1.91 ft-lbs/g or 20% (simulation scale factor) of the 9.57 ft-lbs/g expected for this case. Raising the lower arm to the vertical state (90° flexion) while holding the upper arm raised at 90° flexion drives T_E to zero and reduces F_T to 1.66 lbs producing a shoulder torque of 1.375 ft-lbs/g or 20% (simulation scale factor) of the 6.875 ft-lbs/g expected of this case.

Holding the lower arm perpendicular to the upper arm (90° elbow flexion) as above while allowing the upper arm to sag from 90° flexion to 45° flexion should cause torque to build in the elbow which is reflected as an increased torque at the shoulder joint. Simultaneously the contribution of shoulder joint torque made by the upper arm should decrease as the upper arm mass moment

arm decreases to .707 of its former value due to the upper arm flexion angle of 45 degrees. In this movement S remains at zero degrees while X reduces to 0.892 feet. T_E increases to 0.38 ft-lbs/g and F_T reduces to 1.25 lbs/g which due to the new angle the tether makes with the upper arm (67.5°) yields a shoulder joint torque of 1.34 ft-lbs/g. Both elbow and shoulder joint torque values, 0.38 and 1.34 ft-lbs/g, are 20% (simulation scale factor) of their expected "real world" values for this arm position.

In Section 4.4.2.1 it was noted that an arm attitude in which the upper arm is directed forward (90° shoulder joint flexion) and the lower arm is directed upwards with respect to the upper arm (90° elbow flexion) presents special problems. If the lower arm is angled forward from this position (decrease in elbow flexion) the lower arm loader torque, T_E, will appropriately increase under $+G_z$ conditions. However should the lower arm be rotated internally from the upright position the plane of elbow flexion moves from the vertical plane toward the horizontal plane. Lower arm loader torque under these conditions will produce forces on the lower arm with significant horizontal components which are, of course, inappropriate under $+G_z$ conditions. The higher the elbow is held (large upper arm flexion angles), the larger are the unwanted horizontal components.

This problem could be eliminated if a convenient method of monitoring elbow rotation (not flexion) could be designed into the apparatus. We have not found the type of monitoring device we seek: one which, with minimum encumberance, provides a progressive measure of lower arm internal rotation. However a useful discrete measure might be available through the use of mercury switches strategically located along the torso side of the arm loader plastic stays. When these switches (gravity vector detectors) detect that the plane of elbow flexion is no longer substantially vertical, the drive to the lower arm loader, T_E, could be set to

zero. It would be appropriate, in the software, to employ this discrete sensor in a ramp network to avoid step discontinuities in T_E. The output of the ramp circuit would control the value of the attenuator, K, found in the expression for T_E. The suitability of this approach can only be determined through experimentation.

A second simpler, but less desirable, approach to this problem is based on the recognition that the severity of the problem is related to the magnitude of upper arm flexion or abduction which, as already described, is known by monitoring X, tether line extension. Under this approach the attenuation factor, K, would be computed based on the magnitude of X such that further increases above some predetermined upper arm flexion/abuction angle results in a proportionate attentuation in elbow torque. This latter approach suffers, of course, from its arbitrary nature and can reduce lower arm loading in arm reaching conditions when the plane of elbow flexion is maintained vertical and lower arm load reduction is unwanted.

One of the merits of the arm loader embodiment wherein the loaders are fully contained within the flight suit and powered through the personal leads block is that no additional impediments to cockpit ingress/egress are posed by the device. The direction of upper arm force application should not create safety problems and if appropriate lower arm torque motor stops are employed, hypertension conditions can be avoided. The peak torque employed are low enough that, under maximum drive but in the lg environment, the subject can readily overpower the loaders. To avoid safety problems which might arise in a loader system inadvertently entering instability it may be advisable to construct a network which can monitor polarity changes and rate of change of positional followup with a trigger to cause the system to be decoupled from power in the event of frequency or amplitudes judged dangerous.

4.5 Tactile Devices

4.5.1 Shoulder Harness

Tactile stimuli are likely experienced in the shoulder harness area of a pilot subjected to certain high G conditions and are caused by inertial loading on the upper torso. Present simulation techniques employing the G-Seat provide a part of these shoulder harness cues by causing bodily movement within the harness. These cues could be made more pronounced by adjusting the tension of the shoulder straps themselves. The design of most current shoulder harness assemblies employ an inertia reel which, when the pilot places his harness in the "automatic" mode, allows relatively unimpeded harness extension/contraction at the pilot's discretion up to the 1.5 - 3.0g region at which time the harness automatically locks securing the pilot from additional movement. A "locked" mode is also available to the pilot which simply removes the automatic feature and, when selected by the pilot, secures the shoulder harness against extension/contraction.

By the nature of the inertia reel device operating features, when in the automatic mode the inertia reel will automatically lock when subjected to a range of 1.5 - 3g inertia load. Within the simulation this would be the actuation point for the automatic mode harness force application. In order to insure proper operation of the shoulder harness device, the inertia reel must have a software-controlled electrically operated positive lock feature which will lock at the threshold in the automatic mode or can be manually overridden to the locked state by the conventional means the pilot uses to lock his harness. This locking action permits force to be applied to the shoulders.

The harness belt mechanism would consist of the inertia reel device in a locked mode during high G periods, a cable extending from the inertia reel to the end of the shoulder strap, pulleys to

guide the cable, servo actuator to drive the belt during high G conditions and a shear pin safety device. If possible the shear pin assembly should be located at the forward ends of the shoulder harness (end employed by the pilot in strapping himself into the cockpit) for accessibility reasons.

The shoulder straps would be driven individually or in unison so that either equal force or differential forces may be applied as demanded by the situation. Preliminary inspection of commonly employed ejection seats indicates adequate room exists on the back outboard vertical surface of the seat backrest to mount the necessary components. Initially the authors felt that a capability to move the straps laterally on the pilots' shoulders might be valuable. We have found nothing which counters this position however the overall lack of information concerning the pertinence of shoulder harness tactical stimuli suggests that the system initially should not be overly complex with additional capability.

As earlier mentioned shoulder strap forces simulated as a consequence of accelerated flight are permitted to occur only when the inertia reel is locked either by pilot manual intervention or by the G level. During unlocked periods shoulder strap forces are permitted to vary based on pilot movement within the seat. On the other hand, once locked, the simulation would call for impressing a strap force in a direct relationship to G level. The potential for strap force discontinuities in moving from the variable force (unlocked) to the simulated force (locked) state is minimized and the simulation made simpler by employing a servo loop closed on position rather than force. During unlocked conditions the strap tension actuator would be held in the midpoint of its travel and the strap permitted to move over this point according to pilot movement and inertial reel tension. Upon inertial reel locking the strap tension actuator would be driven, bidirectionally, according to G conditions providing smooth force build up or relaxation from those levels extant at the point when the inertia reel

is locked. The position servo loop approach also circumvents problems arising from intersubject strap tension variations and right and left shoulder strap force variation observed within a subject as reported by M. C. Champion (37). The position servo loop approach also permits subject induced force variation to occur naturally.

Figure 4.5.1-1 illustrates the functional arrangement of the shoulder harness system as located on the aft side of the backrest. A typical shoulder strap system has an inertia reel which allows 18 inches of strap movement in an automatic mode. This

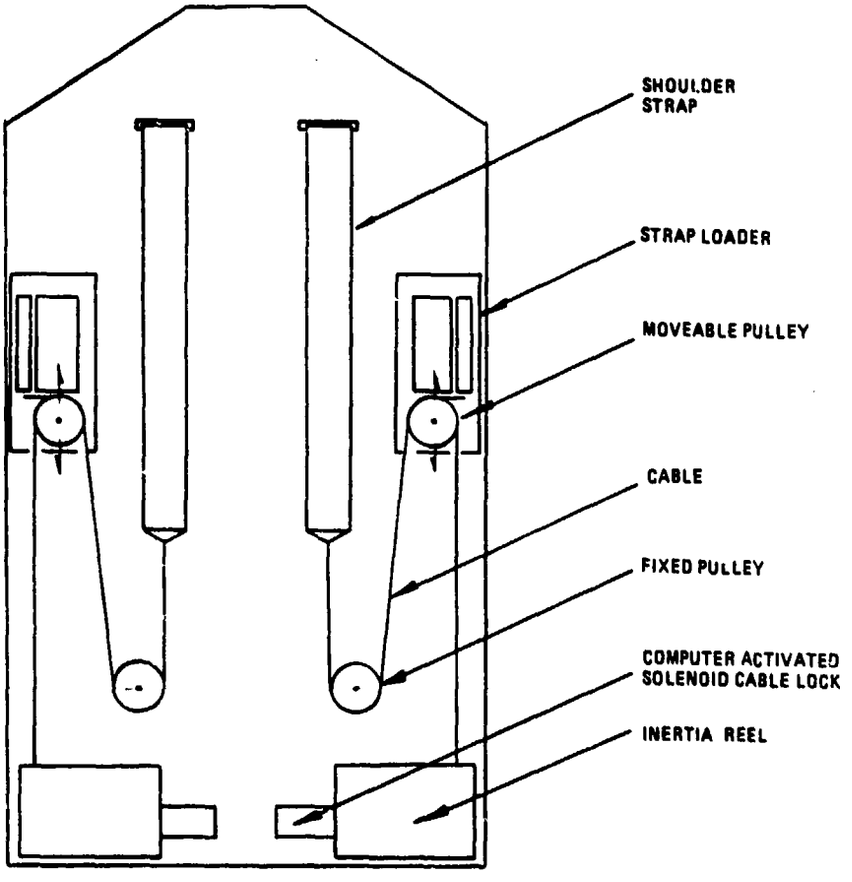


Figure 4.5.1-1 Functional layout of shoulder harness tension system.

inertia reel will lock up between 1.5 and 3g inertia load. However, this lockup feature, in automatic mode, will reset when the inertia load is relaxed. To avoid inadvertent release of this lock, there must be solenoid lock energized as part of the inertia reel during high G activity. Duplicate driven belt systems are required.

A cable is attached from the inertia reel output to the shoulder strap. The cable first passes over a fixed-position pulley and then over a movable pulley which is part of the servo actuator assembly. With the strap in the locked position, the servo actuator package will provide the necessary belt tightening forces by displacing the pulley, thus pulling on the cable. Relaxation of the straps is also possible by extension of the actuator.

The strap driver illustrated in Figure 4.5.1-2 is provided as an example of a modification to an existing position servo actuator design which could be employed to vary strap tension by altering the position of the movable pulley. Two inches of strap movement would be provided by this design. Strap tension would be increased for $-G_x$ and $-G_z$ conditions and assuming a worst case condition of $-1G_x$ operating on the pilots upper torso. Under inertia reel locked conditions, a maximum strap tension of 50 pounds must be developed. The example design employs a hydraulic actuator to meet these force requirements and provide rapid response.

4.5.2 Skin Temperature Driver

In section A.6.2, a case for the existence of pressure/temperature relationships is advanced and it is suggested that mild temperature stimulation could enhance the sensation of pressure. Further it is noted that conflicting evidence exists concerning whether elevated or depressed temperature levels intensify the

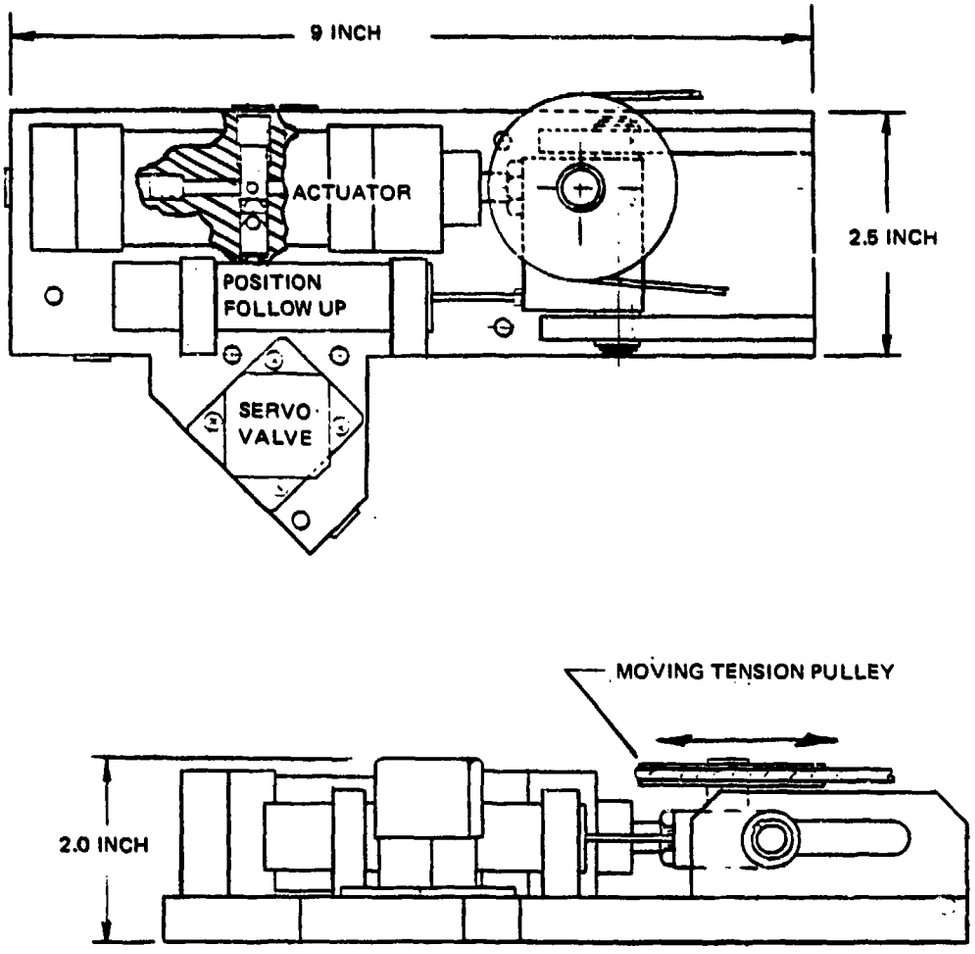


Figure 4.5.1-2 Example shoulder harness loader.

perception of pressure which increases the importance in advancing a bidirectionally driven mechanization concept. The approach put forth herein involves embedding bidirectional thermoelectric modules in the [illegible] tion of the cockpit seat such that the ischial tuberosity region of a seated subject's buttocks are brought in close proximity to the thermoelectric modules. The ischial tuberosity region is selected based on the presumption that this bony region re[illegible]ds with the most intense pressure sensation under high G loading.

The thermoelectric modules suggested for use are thin wafers nominally measuring approximately 0.2 inch thick by 1.0 inch square. A typical module is illustrated in Figure 4.5.2-1.

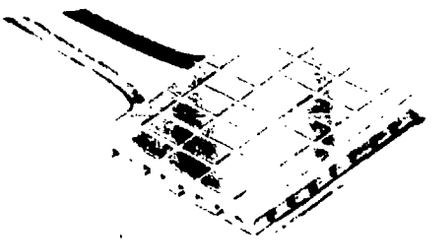


Figure 4.5.2-1 Typical thermoelectric module.

These solid state devices are miniature heat pumps which operate on the principle of the Peltier effect. Jean C. A. Peltier in 1834 found that the passage of an electrical current through the junction of two dissimilar conductors in a certain direction produced a cooling effect and when in the opposite direction, a heating effect. In a thermoelectric cooler, semiconductor materials with dissimilar characteristics are connected electrically in series and thermally in parallel so that two junctions, a couple, are formed. The semi-conductor materials are N- and P-type. Heat absorbed at the "cold" junction is pumped to the "hot" junction at a rate proportional to carrier current passing through the circuit from a D.C. source.

Couples are added serially to increase heat transport capability as shown in the module cross section of Figure 4.5.2-2. Current reversal causes the device to be usable as either a heat pump for heating an object or a heat pipe for cooling that same object by reversing heat flow.

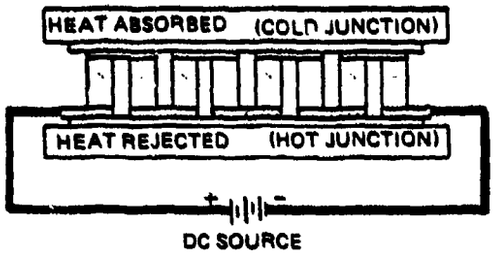


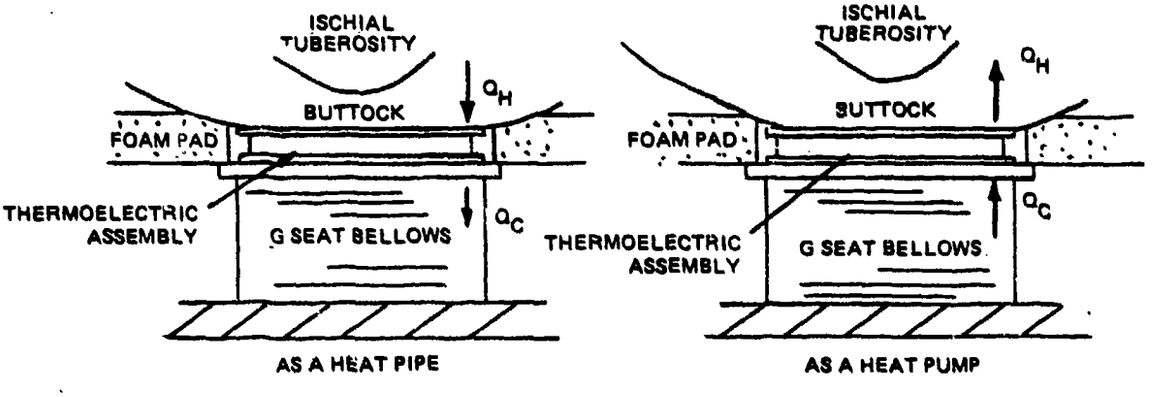
Figure 4.5.2-2 Thermoelectric module cross-section.

A plurality of modules may be arranged in mosaic form to increase area of coverage or stacked vertically to increase thermal range. Our application will require but one level however a 3 x 3 mosaic composed of nine modules is suggested to form a 3.75 inch square, 0.2 inch thick heating/cooling assembly. Two assemblies, one per tuberosity, would be employed in the seat pan. This size assembly is compatible with the pneumatic bellows G-seat in that a 3.75 inch square thermal assembly can be rigidly affixed to the top of the 3.88 inch square bellows top plate stationed beneath each of the tuberosities. To reduce thermal resistivity, the closed foam pad normally over-lying the bellows would be cut out and eliminated in the area of the tuberosity bellows. The thermoelectric assemblies will ride on the bellows in this cutout area. The air driven metal bellows will form a good heat sink for heat rejected from the system.

The approach is also compatible with the USAF Human Resources Laboratory Advanced G Cuing System G-Seat. In this implementation the thermoelectric assembly would be rigidly affixed to the metal seat pan moving plane in the region of the tuberosities. The moving plane will form a heat sink/source for the device. Firmness bladder employed in this type of G-seat design would overlay the thermoelectric assemblies and due to the firmness bladder drive philosophy which calls for deflation under simulated G load, would

not pose appreciable additional thermoresistivity between thermoelectric assembly and buttocks.

Figure 4.5.2-3 depicts a typical installation, the bidirectional mode of the device, and the heat flow capability of a typical thermoelectric assembly applied to our case. Data presented in this figure and the preliminary time response analysis presented in this section is based on a number of assumptions which will be introduced as needed. The initial assumption pertains to buttocks and seat nominal temperature. It is assumed that the seat (thermoelectric device mounting surface) heat sink/source is maintained at approximately 20°C (68°F). The nominal temperature of the buttocks is taken from Parker (194) as 34.6°C (94.4°F). The heat flow capabilities tabulatd in Figure 4.5.2-3 demonstrate asymmetry between heating and cooling. Energy is expended in creating the heat flow condition and this energy, Joule effect, is transported in the direction of the heat sink. In the heat pump mode the buttock forms the heat sink however, in the cooling mode, the seat assembly is the heat sink.



CURRENT (A).

Q_H BTU/HR	0-4 VDC	Q_H BTU/HR
285	2	162
440	4	450
540	6	790
600	8	1180
612	10	1700

Figure 4.5.2-3 Typical thermoelectric assembly installation and heat flow capability.

Two aspects of safety have been considered. First, it is apparent that required amperage levels are quite high even though voltage is maintained in a low region of 0-4 volts. Concern for shock hazard should be tempered by the fact that, although the thermoelectric device itself is electrically insulated from its environment (top and bottom plates are thermoconductors, not electrical conductors), an additional measure of insulation is provided by the seat upholstery and subject clothing. Further the power source is direct current. One might accord the thermoelectric device power the same respect shown in handling an automobile battery.

A second safety consideration involves acceptable levels of heat input/extraction from the surface of the body. Woodcock (266) in reporting on experimentation involving the application of heat to localized sections of the body advocates, in general, that heat flow be maintained at not greater than 51 BTU/hr.-ft^2 or approximately 5 BTU/hr for the area of the applicator suggested herein. We suspect that this limit is oriented more toward possible wide field application of heat rather than the small 3.75 inch square area under consideration herein. In one of Woodcock's experiments a similar sized applicator (10 cm x 10 cm) was used without adverse effects to provide 22 BTU/hr to the buttocks over 10-20 minute periods. In that our application would involve heat flow periods of much shorter duration we suggest the larger figure (22 BTU/hr) is acceptable.

In a related aspect, Woodcock notes that the subjective assessment of "hot" was associated with a buttock skin temperature of 41.1°C or 6.8°C above that which we have assumed to be normal. Further, subjects reported "slightly warm" at 37.9°C in the back area. In that we wish to subtly employ temperature to attempt to augment pressure sensation but not forcefully ellicit perceptions of warmth and cold, even the latter temperature of 37.9°C, or 3.3°C above normal, is probably much larger than that sought in

this application. Parker (194) indicates that sensations of warmth and cold occur with skin temperature changes of 0.008°C and .004°C, respectively, with a latency of 3 seconds. Mueller (178) suggest a comparable figure of 0.1°C. However, neither Parker nor Mueller indicate the magnitude of surface area over which these thresholds are applicable. Based on the preceding, we will assume that the maximum skin temperature change sought over the area of our applicator is $\pm$1.0°C.

Although it might be possible to instrument subjects in the laboratory environment such that skin temperature is known and can be employed in the thermoelectric assembly control loop, this would be unacceptable in the line simulation environment. The next best control, admittedly less precise due to subject variability, is to control thermoelectric assembly plate temperature according to profiles which nominally produce desired skin temperature. The laboratory version should employ this approach as well to validate not only the usefulness of temperature as an augmentation of pressure but also the acceptability of this type of temperature control when dealing with a variety of subjects. The control loop suggested is diagrammed in Figure 4.5.2-4 and simply represents a temperature controller closed on plate temperature.

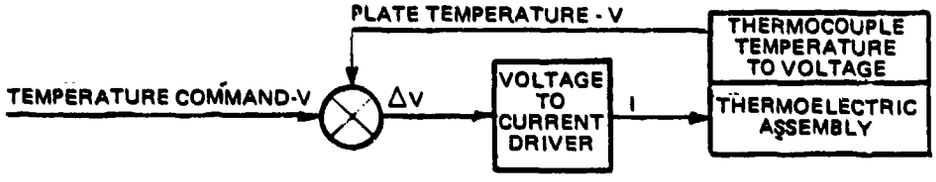


Figure 4.5.2-4 Thermoelectric assembly control loop.

A preliminary analysis of skin thermal response to the thermoelectric assembly has been conducted based on the model depicted in Figure 4.5.2-5. The analysis is based on employing a thermo-

electric assembly composed of nine Cambion® 3958-01 thermoelectric modules each containing 31 couples.

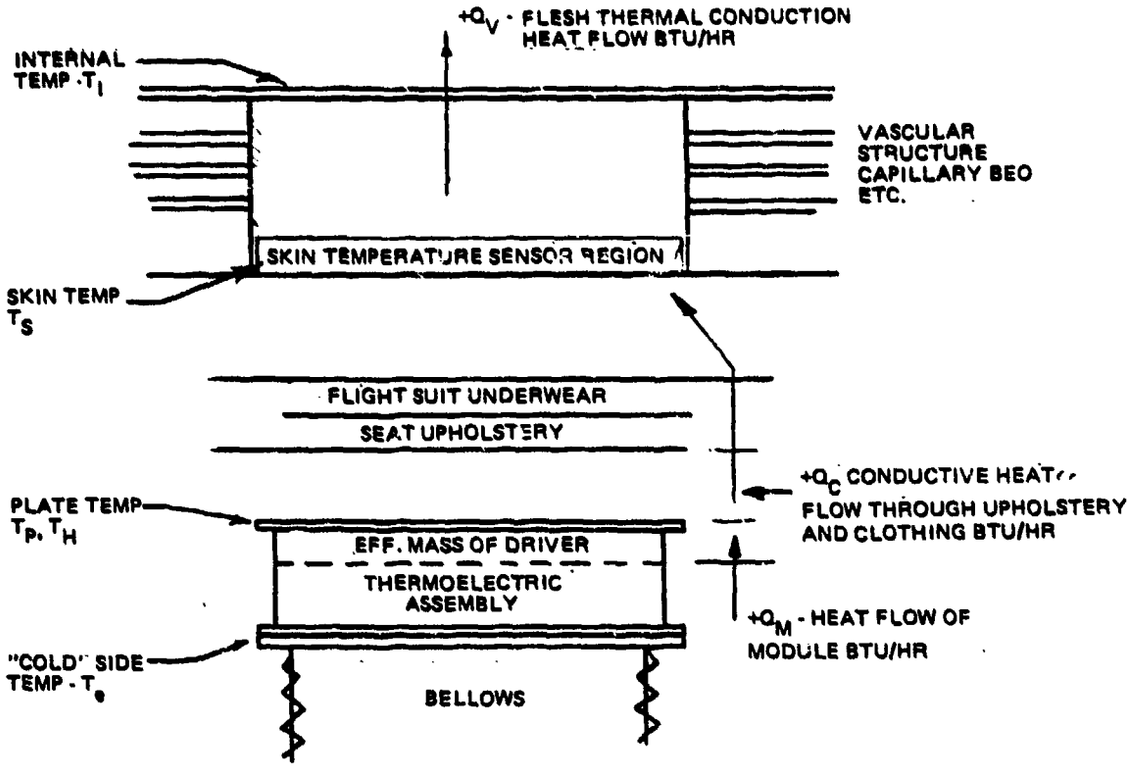


Figure 4.5.2-5 Ischial tuberosity heat flow diagram.

The assumptions and constants employed in this analysis are as follows:

a) Bellow source/sink temperature = 20°C constant

b) Buttocks vascular bed temperature = 34.6°C constant

c) Median thermoelectric module temperature = 30°C constant

d) (Mass)(Specific Heat of Thermal Electric Module) = (9.486×10^{-4}) $(0.00527 \times T_p + 2.427)$ BTU/°C

e) Flight Suit & Underwear Clo Factor = 0.7

f) Seat Upholstery Clo Factor = 0.8

Thermal Conductivity of e) & f) = K/L = 1.364 BTU/Hr-ft^2-°C

g) Skin Thickness = 0.2 inch (from 194)
Skin Specific Gravity = 1.1 (from 194)
Skin Mass = 0.111 lbs.

h) Flesh Thermal Conductance = 7.37 BTU/ft^2-Hr-°C
Thickness = 2 cm @ mean vasoconstriction (from 194)

A 100 second doublet profile was used for current at various magnitudes. Figure 4.5.2-6 illustrates the theoretical change in skin temperature as a function of time for various thermoelectric current magnitudes. As anticipated, the usefulness of the skin temperature driver in augmenting short term transient G loading

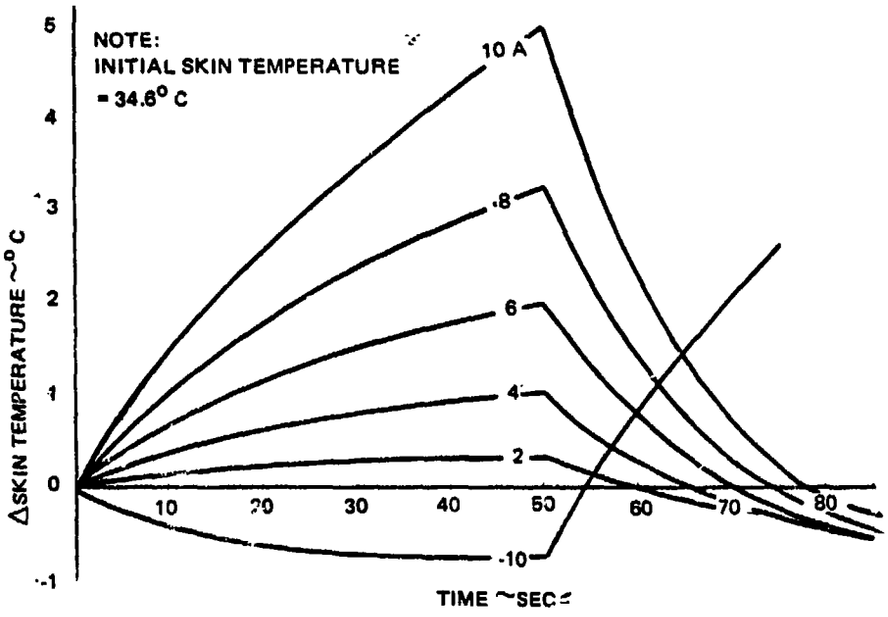


Figure 4.5.2-6 Skin temperature change resulting from current doublet of various magnitudes.

pressure sensation appears questionable. However, the response appears suitable for use as a low pass component in the long term G loading shown in Figures 1.1-1, 2 and 3. The thermal operating bounds of the thermoelectric assembly have been taken as ±125°C and Figure 4.5.2-7 demonstrates that, in the heat pump mode, the higher current levels can be maintained only briefly to hasten temperature change with low levels used thereafter to maintain temperature levels.

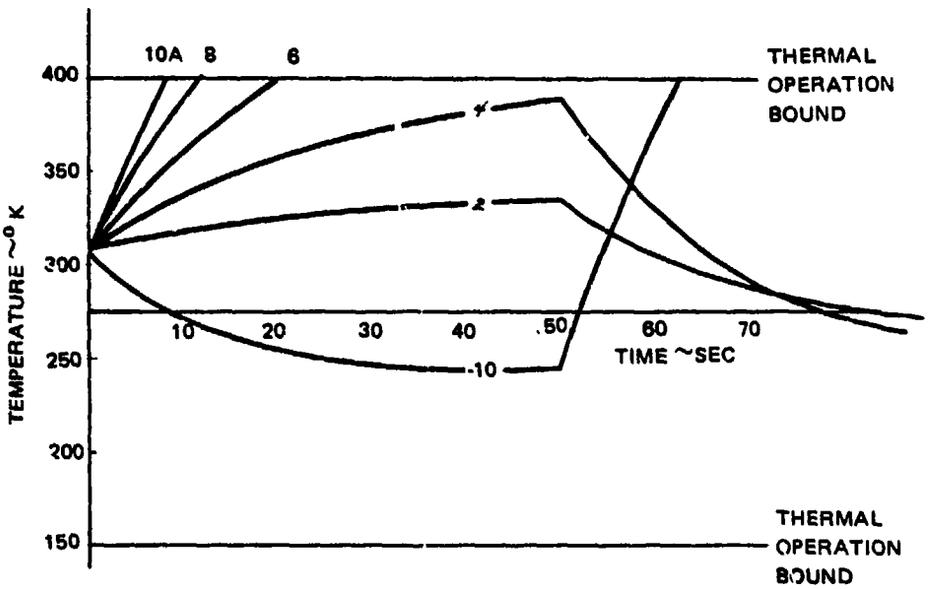


Figure 4.5.2-7 Thermoelectric module plate temperature (under current doublet).

Heat flow resistivity of seat upholstery and flight suit form a major system constraint. Response and range of skin temperature change will obviously decrease if heavier clothing is worn by the subject. On the other hand the thermal conductivity factors used in this analysis demonstrate that heat uptake is limited to 10 BTU/hr at Δ skin temperature of 1°C, our maximum range of interest. In contrast to the upholstery and clothing heat flow resistivity, the thermal conductance of flesh is relatively high de-

pressing the range in which skin temperature may be driven. A value of tissue thermal conductance for mean conditions of vasoconstriction was employed herein. For full vasoconstriction the amplitude of the curves in Figure 4.5.2-6 would be doubled and for full vasodilation the amplitude would be halved.

The drive scheme to be employed will obviously relate temperature change to G load. However, as earlier mentioned, there is question concerning the sign sense of appropriate drive. Additional unknown factors involve the import of temperature threshold, the magnitude by which this threshold may beneficially be exceeded, and the role of temperature adaptation and the latitude this effect may permit in obtaining temperature augmented pressure sensation. We would suggest that a simple linear relationship between G load and temperature command form the initial drive scheme with alteration to occur as a function of experimental results.

4.5.3 Face Mask Loader

The photographs of face mask slippage presented in Figures A.6.1-1 and A.6.1-2 lead us to believe that tactical stimuli, probably predominantly experienced as skin tension variation, occur under high G conditions due to inertial loading of the face mask worn by the pilot. The facial area is noted for low thresholds of tactile perception (178). The mechanism suggested herein provides a means to artifically load the face mask assembly in concert with simulated G loading.

The approach selected involves placing a downward force on the face mask by means of a miniature torque motor and windlass housed in a G-suit modified for such purpose. The concept is illustrated in Figure 4.5.3-1. In this arrangement the torque motor drives the windlass around which is wound a monofilament tension line which leads upwards along the pilot's gig line to the face mask. The upper end of the tension line is terminated in a clip

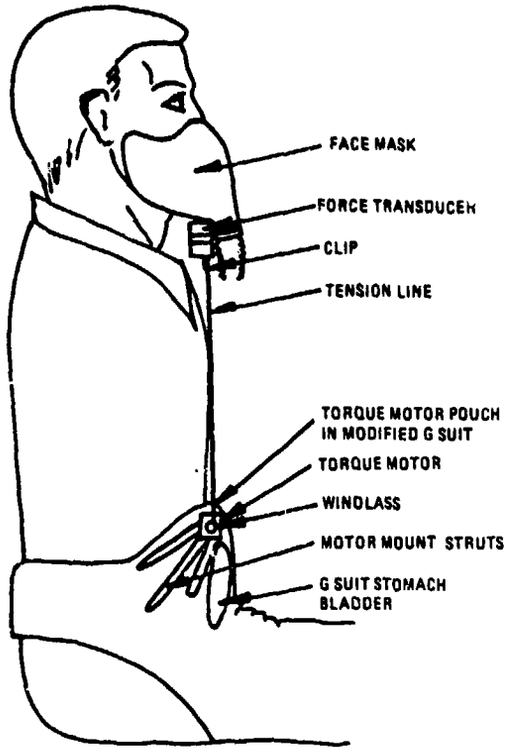


Figure 4.5.3-1 Face mask loader arrangement.

which must be snapped over a bail on the lower end of a force transducer which is secured to the lower surface of the face mask. The subject, after seating himself and securing the face mask to the helmet, must withdraw the clip from the G-suit pouch and snap it over the force transducer bail. Obviously this act is a departure from real world flight preparation procedure and therefore may compromise line-simulation utilization of this concept. The magnitude of this discrepancy is small enough to pose no problems in a laboratory environment. Considerable thought was given to other embodiments which might eliminate or disguise any unnatural act however none was found more favorable.

The servo loop advanced herein is closed on tension line force by a force transducer mounted on the underside of the face mask. Although it should be possible to operate the system in

open loop form and simply drive the torque motor with a scaled version of $+G_z$ loading, the closed loop form will allow more uniform force application in the presence of pilot head movements. The force transducer site is selected based on simplicity, unobtrusiveness, and that the electrical leads may be routed along with the face mask leads and therefore require no unnatural act in preparing the system for operation. Likewise the location of the tension line is unobtrusive and minimizes probability of fouling.

The torque motor/windlass assembly illustrated in Figure 4.5.3-2 measures approximately 1 x 1 x 2 inches and could be concealed within and secured to the subject's flight suit. This location is unfavorable since, depending on the manner in which the G-suit is worn, the torque motor might become trapped between stomach bladder and the body which, at best, would be noticeable and at worst, painful. Locating the torque motor assembly within

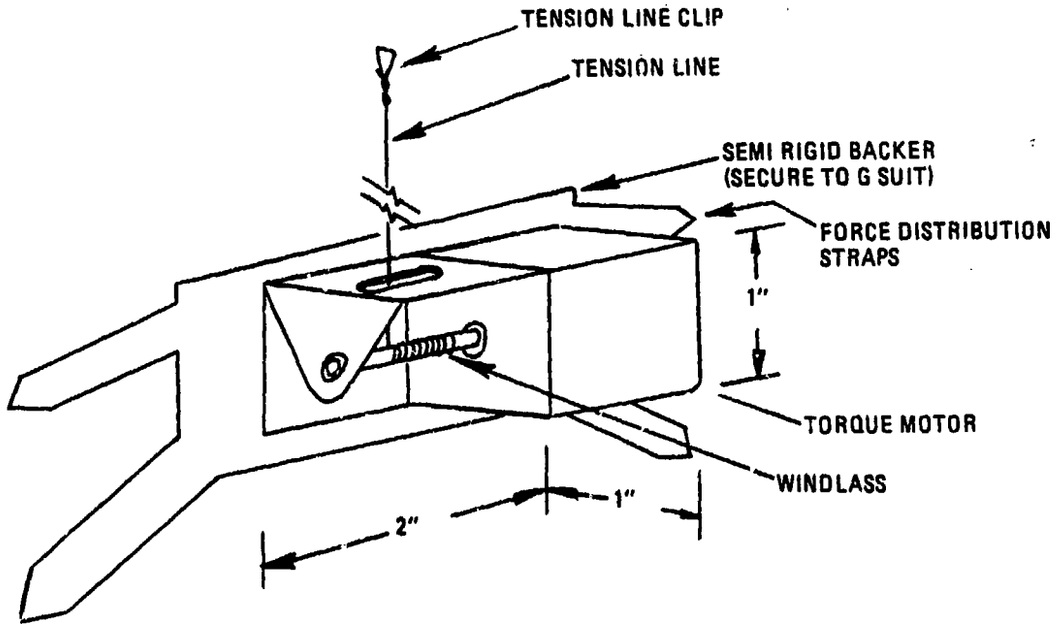


Figure 4.5.3-2 Face mask loader motor.

a modified G-suit eliminates this problem and has the following additional attributes:

a) Reactive forces due to torque motor activity operating on the suit are masked by the natural activity of G-suit bladder inflation affiliated with $+G_z$ loading conditions.

b) A source of air is naturally made available in close proximity to the torque motor should cooling be required.

c) The torque motor power leads may be dressed inside the G-suit pneumatic supply hose and terminated in such a way as to be automatically made by the subject during G-suit hookup at preflight.

In preliminarily sizing the torque motor, the authors assumed that the pilot could induce peak vertical motion of the face mask over a maximum distance of 5 inches at peak velocity of 5 inches/sec and acceleration of 10 inches/second^2. Although military specifications were searched, face mask weights were not found and two pounds is assumed as a representative weight. We further assumed that in order to keep the tension line from fouling, the torque motor should maintain a minimum 0.25 pounds tension in the line at all times.

Figure 1.1-3 shows $+G_z$ acceleration peaks of 11g's which would imply an inertial face mask load of approximately 22 pounds. It is seldom necessary to use full scale replication to impart a realistic kinesthetic cue within simulation and in this case we tend to believe that full scale force may displace the face mask more than that experienced in the actual case. Under $+G_z$ loading, the head and helmet as well as the face mask are subject to increased loading. The helmet (and face mask support) lowers on the

head, the head lowers and pivots slightly forward (142) and tend to bring the face mask closer to the chest which, in turn, offers support to the face mask reducing additional slippage. In the absence of a helmet loading system, the above helmet and head allied movement will not occur and full scale face mask load is not warranted. However, to permit experimentation in imparting loads to the helmet and head through the face mask we have selected a scale factor larger than the 20% used in the extremity loaders. With this in mind we have assumed a 1/2 scale factor or approximately 11 pounds of tension line force to be the maximum desired.

An Inland Motor samarium cobalt motor displaying 11 oz.-in. of peak stall torque direct driving a windlass shaft of 0.1 inch diameter would appear to meet our requirements. This implementation would permit a peak line tension of approximately 13 pounds and a maximum no-load line velocity of approximately 38 inches/second. Temperature increase to maintain the 0.25 pound minimum tension line force would be acceptable at approximately 1°C. Temperature rise to simulate the $+G_z$ profile of Figure 1.1-3 is estimated to be approximately 40°C in the absence of special cooling provisions and would be acceptable. However a 100% duty cycle composed of such profiles would produce unacceptable temperatures and therefore either special cooling provisions and/or a thermal override should be incorporated in the design.

The control system must be further protected with an interlock which indicates that the tension line has been secured to the force transducer such that the force transducer is mechanically included within the servo loop. This interlock could be an implied interlock wherein the torque motor drive would be limited to 0.25 pound until such time the force transducer registered this tension. Transient force relaxation registered by the force transducer due to pilot induced movement would be eliminated by a low pass filter in the interlock network.

4.5.4 Localized Firmness Cells

In locations where normal body load causes flesh pressure conditions, the ability to successfully vary the pressure perception through the use of firmness cells has been well demonstrated in the Air Force Human Resources Laboratory Advanced G Cuing System. Firmness cells, thin pneumatic bladders, are located between the body and supporting structure and slightly inflated so as to support the body under near-uniform distribution of tissue pressure in close proximity to the supporting structure. Deflation of the cell transfers support from the compliant cell to the comparatively non-compliant support structure and in doing so, alters load distribution causing localized flesh pressure increase.

This technique has been successfully employed to vary buttock flesh pressure and probably could be extended to other regions of the body where G load induced pressure sensation is pronounced. As mentioned in Section A.6.1 we suspect other candidate areas to include the under-surface of forearms when resting against a support object, sole area of the feet, and scalp supporting the weight of the helmet. Although our literature search revealed no data assigning import to tactile cues, we could advocate the firmness cell approach be employed in tactile cuing experimentation involving the above-mentioned sites.

In the case of scalp tactile cues the firmness cell(s) would be located between scalp and helmet as depicted in Figure 4.5.4-1. As G load increases, firmness cell pressure would be decreased allowing the helmet load to be concentrated at specific areas of the scalp. The firmness cells also permit motion of the helmet with respect to the skull which, visually, may provide it's own set of cues. It is not clear at the present time that both visual and pressure cues can appropriately be simultaneously delivered using the firmness cell approach. As is evident in Section 4.4.1.1 we tentatively are assigning higher priority to helmet/

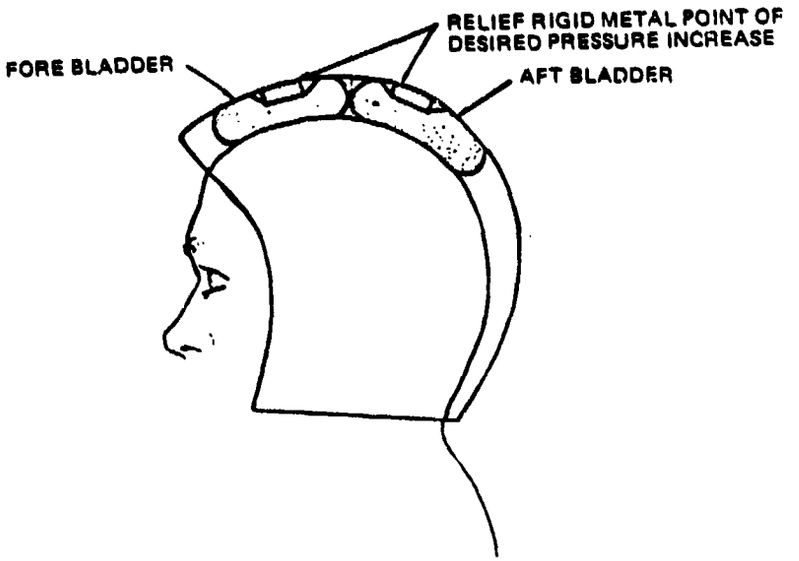


Figure 4.5.4-1 Helmet firmness cells.

skull motion and believe the helmet firmness cells should be employed to replicate this effect.

Figures 4.5.4-2 and 4.5.4-3 illustrate the same concept as applied to the forearm and foot area. The arm under-surface firmness bladder would be a thin bladder sandwiched between the inner and outer layer of the flight suit in the under surface area of the lower arm. During negative or 1g simulated flight, the bladder would be slightly inflated. Upon entering positive G conditions the bladder would be progressively deflated regardless of the position of the arm. If the arm is not resting on a supporting surface nothing is lost; however, should the arm be in contact with a supporting surface, strengthened pressure stimuli will occur as a result of bladder deflation.

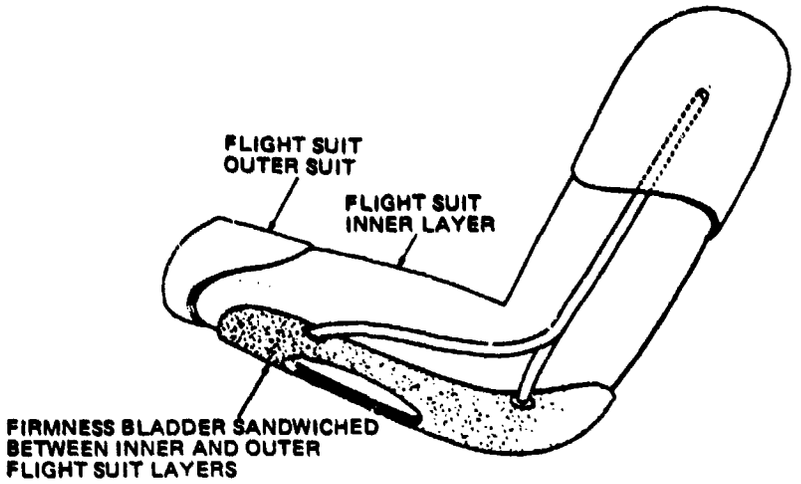


Figure 4.5.4-2 Arm undersurface firmness bladder.

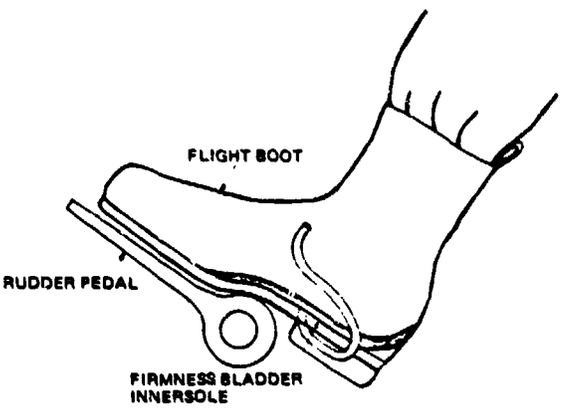


Figure 4.5.4-3 Boot innersole firmness bladder.

The firmness cell control system illustrated in Figure 4.5.4-4 has previously been employed with pneumatic flow boosting relays to successfully drive fairly large volume G-seat firmness cells. Response characteristics depicted in Figure 4.5.4-5 are rapid with a system bandpass of approximately 6 hz (143). In

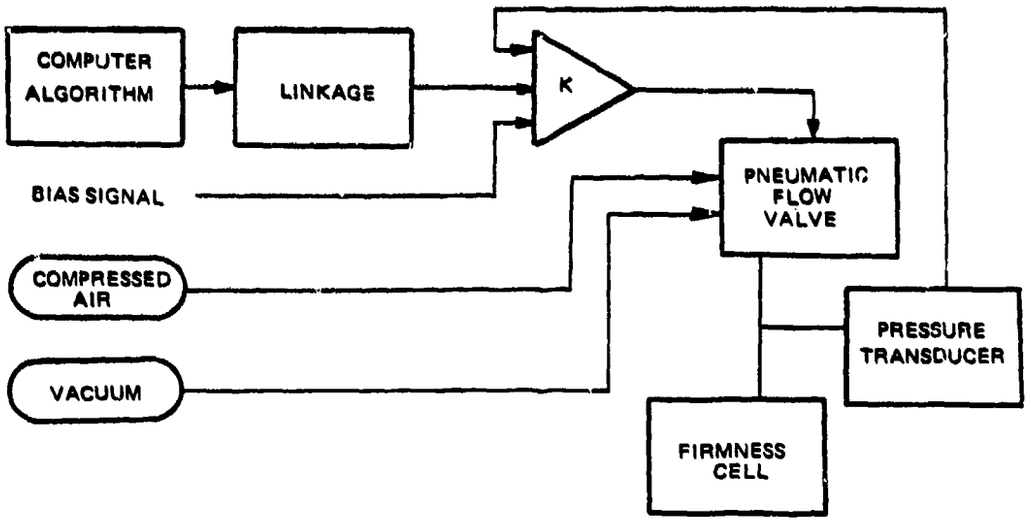
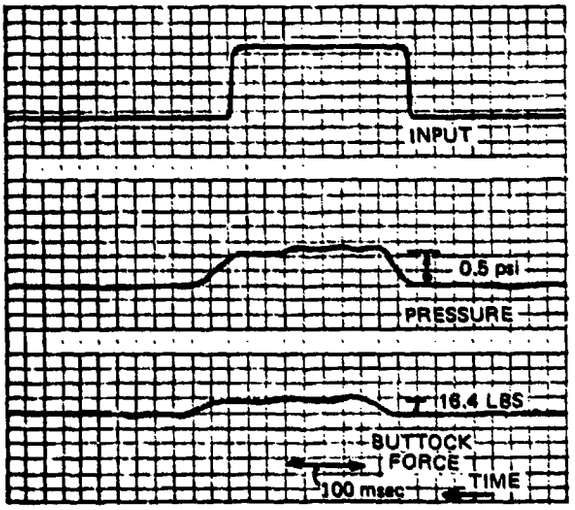


Figure 4.5.4-4 Firmness cell control system.



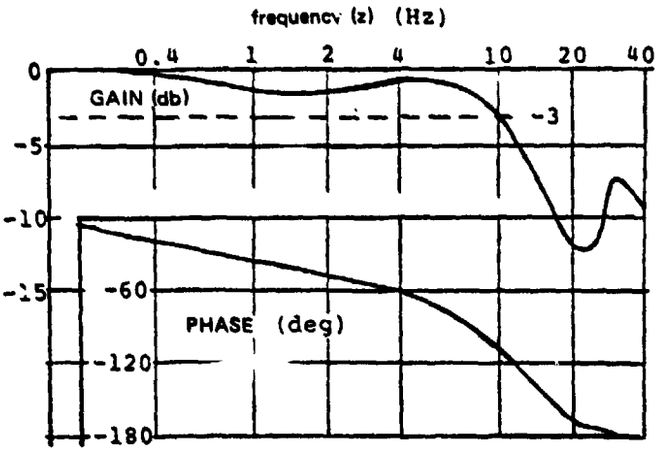


Figure 4.5.4-5 G-seat firmness cell response (from Kron and Kleinwaks (143)).

that the volume of the firmness cells suggested herein is considerably smaller (except for the helmet firmness cell) than that employed in G-seats there should be no need for flow boosters, however, the vacuum assist would still be required in order to preserve response at the low pressures utilized in driving the firmness cells. Flow booster capability is received for the helmet firmness cell.

4.6 Respiratory Devices

4.6.1 Subatmospheric Face Mask

In section A.7 it is stated that the respiratory effects of $+G_z$ are much less dramatic than the cardiovascular ones. Nonetheless they exist and entail an increase in the work of breathing and decreased oxygen transport. Respiratory reactions are most noticeable for forward acceleration ($+G_x$) where breathing difficulties come into play long before any cardiovascular problems become evident. These difficulties are manifested as shallow breathing in reaction to the difficulty of expanding the chest against the inertial load and combines with a significant increase in the effective dead space of breathing and a major mismatch between ventilation and perfusion in the lung region to make gas exchange inefficient and produce hypoxia even with inspired pure 0_2. Table 4.6.1-1 lists the acceleration effects on the respiratory system that are discussed in section A.7. These effects may provide useful cues to the pilot of a flight simulator operating in the high G environment.

An approach for providing these cues could be implemented via the "subatmospheric face mask." This implementation would simply reduce the pressure of air in the face mask causing the pilot to breathe more rapidly in order to satisfy his oxygen deficit. In section A.7.2.2, the similarity of negative pressure breathing to the G_x effects is discussed and forms the physiological basis for

Table 4.6.1-1 Summary of high G effects on the respiratory system.

G_z	G_x
o Increased work of breathing	o Shallow breathing
	o Chest tightness & pain
	o Increase respiration rate
o Decreased O_2 transport	o Inefficient gas exchange producing hypoxia

the subatmospheric face mask. Figure 4.6.1-1, which is also presented in section A.7, illustrates the effect of G_x on respiration rate. The subatmospheric face mask would provide breathing air to the pilot at pressures below atmospheric. This can be accomplished by employing a system as shown in Figure 4.6.1-2. For accelerations less than or equal to 1.0g, the mask is supplied air at 0.05 psi and for accelerations in excess of 1.0g, the pressure is reduced .096 psi/g. This will cause the breathing rate to increase probably producing some chest tightness and pain.

For the normal 1g condition, the compressor is providing air to the mask through the dryer and filter (.08 micron). The pressure is then regulated by a fixed regulator to .05 psi. When the effective acceleration component perpendicular to the pilot's chest (G_p) is greater than 1g, the solenoid is switched exposing the mask to a partial vacuum. The pressure transducer corrects the current to the flow control valve permitting the pressure at the mask to be that which has been commanded by the computer according to the algorithm above (-0.096 psi/g). The respiration rate is monitored simultaneously and fed back to the computer whereupon it is compared to the computed value and adjustments to

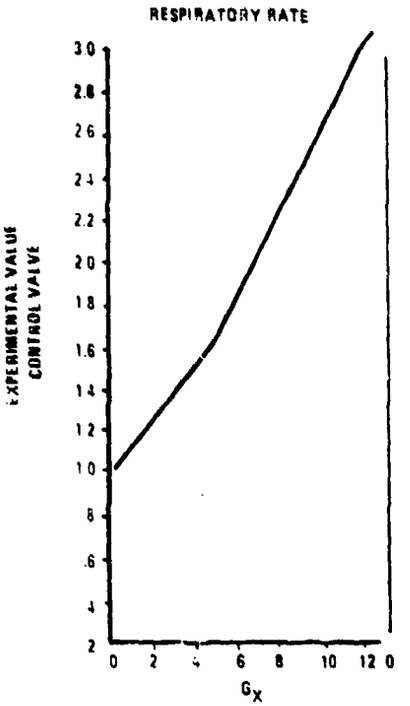


Figure 4.6.1-1 Respiratory rate as a function of G_x (modified from Fraser (71)).

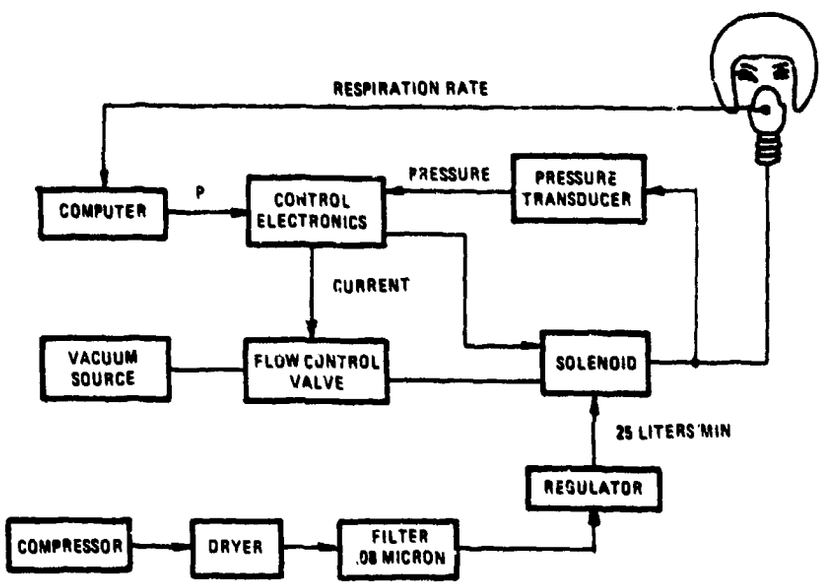


Figure 4.6.1-2 Respiration dynamics control system.

pressure are made appropriately. The effective perpendicular acceleration is given by

$$G_p = G_Z \sin SBA + G_x \cos SBA \qquad \text{[Eq. 4.6.1-1]}$$

where SBA is the aircraft seat-back angle measured from the vertical i.e., a zero seat-back angle is one in which the seat-back is vertical. SBA increases for inclinations backward. The respiration rate is computed from

$$RR = (0.1818\ G_p + 0.8182)\ RR_{NORM} \qquad \text{[Eq. 4.6.1-2]}$$

where RR_{NORM} is the normal respiration rate taken as that value measured at simulator initialization.

SYSTEM SAFETY

The safety of the system can be assured by the respiration rate being fed simultaneously into the control electronics whereupon the solenoid is shifted to the pressure breathing side if the respiration rate falls below some threshold such as 2 breaths/minute.

In addition the face mask can be easily removed by the pilot if he feels distressed.

REDUCED PARTIAL PRESSURE OF O_2

Another approach to produce the same effects is to reduce the partial pressure of oxygen in the breathing air. At sea level the

approximate partial pressure distribution of the gases in breathing air are

O_2	158	mm Hg
CO_2	0.3	mm Hg
N_2	596	mm Hg
H_2O	5.7	mm Hg
	760.0	mm Hg

Since the contribution of carbon dioxide and water vapor combined is less than 1%, they can be ignored and air considered as composed solely of oxygen and nitrogen. The sea level partial pressure distribution will then become 159.26 mm Hg for O_2 and 600.74 mm Hg for N_2. The alternate system would then employ a control system such as depicted in Figure 4.6.1-3.

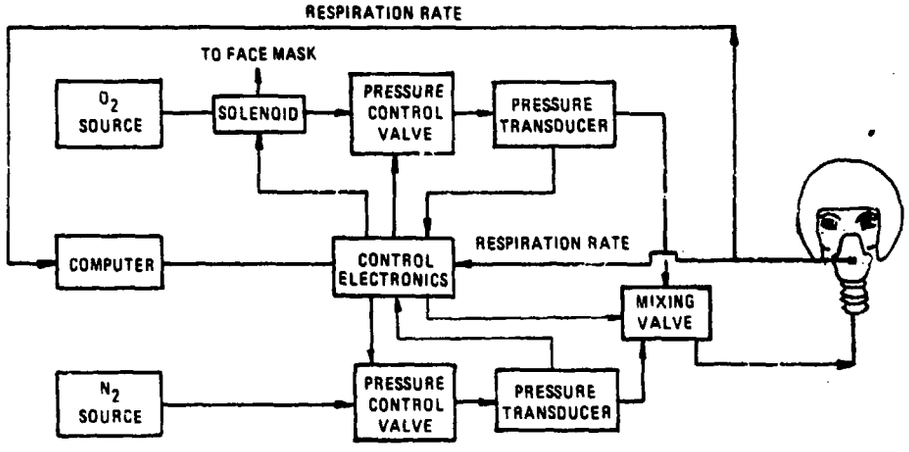


Figure 4.6.1-3 Partial O_2 pressure.

An oxygen and nitrogen source are provided. The pressure of each gas is controlled by the computer via the pressure control valves. The established base pressures are those from above. The partial pressure of O_2 is then reduced by 5 mm Hg/g and the respiration rate monitor will continually adjust the O_2 partial

pressure until the desired respiration rate is achieved. The partial pressure of N_2 is increased by the amount that the partial pressure of 0_2 is decreased. The algorithm to implement this concept is given by

$$P_{0_2} = 159.26 - 5\ G_p - K\ (RR_M - RR) \qquad \text{[Eq. 4.6.1-3]}$$

where RR_M is the measured respiration rate, and P_{0_2} is the partial pressure of oxygen

$$P_{N_2} = 600.74 + (159.26 - P_{0_2}) \qquad \text{[Eq. 4.6.1-4]}$$

where P_{N_2} is the partial pressure of nitrogen.

The same safety capability can be provided for this system as for the subatmospheric face mask by placing a solenoid between the 0_2 source and the pressure valve. If the respiration rate falls dangerously low, the solenoid would shunt pure oxygen directly to the face mask.

SUMMARY

Both systems would probably produce satisfactory results. However the subatmosperic face mask has more substantial theoretical basis and is therefore recommended as the device to be used for laboratory testing for the purpose of determining the cue value of the device.

4.6.2 Hypoxia Induction

Hypoxia induction is postulated as a technique for causing the visual effects of high G_z. As was discussed in section 3.2, as G_z increases, the cardiovascular effects cause a reduction in blood supply to the retina. The reduction in oxygenated blood to the retina effectively causes localized hypoxia which in turn

causes a reduction in visual acuity. The technique described herein is an attempt to reproduce this effect by reducing the oxygen available to the pilot. This can be accomplished in two ways; one is to reduce the partial pressure of oxygen in the breathing mixture, the other is to reduce the flow rate or pressure of the gas mixture.

Both of these techniques would reduce the tidal volume (see section A.7) and thereby induce hypoxia. Unfortunately the desired effects will not be realized. If any of the above mentioned techniques for hypoxia induction are induced via the respiratory system the following will occur. After an initial decrease in tidal volume, the respiration rate will increase to compensate such that the volume of air integrated over a period of time would be the same as that inhaled under normal 1g conditions. In addition, the pulmonary effects would mimic those of longitudinal acceleration (G_x) rather than vertical (G_z), such as chest pain and tightness as well as the increased respiration rate referred to above. This would present to the pilot an ambiguity for him to resolve which is in fact an unrealistic cue.

Further inducing retinal hypoxia in this way would be a second order effect, i.e., the reduction of oxygen at the retina is a secondary effect brought about by reduction of blood supply. This reduction of oxygen available in the lungs which in turn reduces the oxygen in the blood which finally causes hypoxia at the retina has a longer delay than that which exists in the real world. This delay is an additional objection to this approach. It is for these reasons that no further investigation of this technique be pursued at present.

4.6.3 Respiration Rate Monitoring Devices

In section 4.6.1 a requirement for monitoring respiration rate was established. There are several devices marketed for this

purpose. They consist of impedance pneumographs, chest band pneumographs, thermistor transducers, and flow measurement devices.

Impedance pneumographs are devices which measure impedance between two electrodes applied to the thorax. Voltage changes reflecting impedance changes due to tissue volume and conductivity are sensed and interpreted to reflect respiration rate. This measurement can be made from EKG chest leads without a need for additional leads. These devices are available from several sources; among them are Narco Biosystems, Houston, Texas and Mennen-Greatbatch Electronics Inc., Clarence, New York. The major disadvantage of this device is the requirement for electrodes attached to the pilot's chest.

Chest band pneumographs are devices which measure the expansion and contraction of the chest. They are of several types; a mercury chestband consisting of a column of mercury, within a small bore rubber tube. When the chest expands the resistance of the mercury column increases. Honeywell Biomedical Denver, Colorado is a source for this device. Narco Biosystems produces a Bellows Pneumograph employing a photoelectric transducer in a flexible neoprene bellows. A third type of chest band pneumograph is one in which a potentiometer measures a mechanical displacement as the chest expands and contracts. Chestband pneumographs are not suitable for this application because of the encumberances and artifact introduced by their use.

Thermistor transducers appear to be the most applicable respiration rate monitoring device for the flight simulation environment. This device employs a small lead thermistor to measure the temperature of the breathing air during inspiration and expiration. The heating of the thermistor during expiration and cooling during inspiration can be interpreted to provide respiration rate. Devices of this type are available from Honeywell Biomedical and

Narco Biosystems. It is recommended that a thermistor transducer be used in the implementation of section 4.6.1 because it can be conveniently concealed in the breathing mask and will introduce no artifact.

Flow measurement devices are also employed as respiration rate monitors. These are basically of two types; one is called a spirometer which measures the amount of gas inhaled and exhaled. Another flow device measures flow as a function of pressure drop in a small tube. Honeywell Biomedical produces the latter device and refers to it as a pneumotachometer. The pneumotachometer would be the second most acceptable respiration rate monitor. It's main drawback is that it presents more of a packaging problem than the thermistor. However, it may provide a higher response capability.

5. SUGGESTED MECHANIZATION PLAN

As earlier stated, the inclusion of high G augmentation devices within tactical aircraft simulation is warranted only if the effect produced by these devices causes pilot behavior to more closely match that which occurs in actual flight and the resultant improvement in the fidelity of behavior alters the training task. The assessment of behavior change can best be accomplished within a laboratory simulation environment which we will consider to be the "short term" mechanization goal. In some cases, additional development will be required prior to arriving at a high G augmentation device design suitable for use in line simulation which is the long term goal. Alternately, two or more devices may produce nearly the same effect and, based on their respective merits, a decision made as to which to employ within line simulation.

Although the short term goal is the actual experimentation with a device, developmental work to produce a laboratory-acceptable version of the device and its drive algorithms is part of

the short term effort. In some cases the potential success of the short term form of a device may rest heavily on the acceptability of a concept or component. In these cases it would be appropriate to "breadboard test" the concept or component prior to committing resources for development of the device or concept in laboratory-acceptable form.

The following table (5-1) offers a plan for each of the devices or techniques introduced herein in terms of progression to fully developed device. It should be noted that rightward progression through the table is predicated only on positive findings in the preceding phase. Because of the preoccupation with visual effects demonstrated by the high G literature we would recommend resource allocation emphasis be provided the plethysmographic goggles, oculometer, visor, instrument and display alteration, and the simplified visual acuity model.

Table 5-1. High G Augmentation Devices Development Process

Device or Technique	Subsystem or Component Test	Short Term (If component test results justify)	Long Term (If laboratory simulation results justify)
Lower body negative pressure (LBNP)	None	Employ research facility to determine response & usefulness to L1/M1.	Possible design of part task trainer for L1/M1.
Non invasive pressure monitors	None	Pulse wave velocity monitor may be useful in LBNP research.	Potential use in L1/M1 PTT.
Plethysmographic goggles	Purchase existing design & test usefulness.	Potential immediate laboratory simulation use to determine G induced visual acuity effect on training task.	No probable line-simulation applicability.
Helmet mounted oculometer	Purchase Honeywell unit & test. Use with flat plate liquid crystal visor tests.	Use with prototype curved visor and/or instrument & visual system drives for laboratory simulation.	Use with curved visor and/or instrument & visual system drives for line-simulation of G induced visual effects.
Visor	Purchase flat plate system plus mini-computer control from liquid crystal manufacturer. Bench test with oculometer drive.	Develop curved vessel visor useing North American Rockwell Technology coupled with flat plate display technology developed in component test. Use in laboratory simulation employing simplified visual acuity algorithm.	Develop production visor for use in line simulation if visor technique is more attractive than instrument and visual display alteration. Specify such systems on future tactical A/C simulators.
Instrument & visual display alteration	None	Develop hardware for altering instrument & visual displays for the specific simulation system employed as the laboratory simulation test bed.	If instrument and visual display alteration is more attractive than visor or visor is non standard A/C equipment specify instrument & visual system alteration on simulator procurement.
Simplified visual acuity model	None	Program for laboratory simulatory use. Make available for line simulation use if satisfactory.	Compare against complete visual acuity model. Specify the more attractive model for line-simulation use.

Table 5-1. High G Augmentation Devices Development Process

(Con't)

Device or Technique	Subsystem or Component Test	Short Term (If component test results justify)	Long Term (If laboratory simulation results justify)
Complete visual acuity model	None	None	If visual effects found important to training and devices to produce these effects are satisfactory enter into research program to develop complete visual acuity model and its mechanization.
Helmet loader	None	Employ NASA Langley design.	Develop device acceptable in line-simulation.
Helmet/ skull motion	Verify bladders control helmet motion. Initial assessment of tactile stimuli.	Develop prototype helmet/skull motion hardware. Employ in laboratory simulation.	Specify in procurement of high performance tactical A/C simulators.
Extremity loaders & face mask loader	Purchase & test samarium cobalt torque motors servo loops, & drivers. Response & thermal characteristics of particular interest.	Develop prototype loader systems - program for laboratory simulation use.	Develop production systems for line-simulation use.
Shoulder harness loader	None	Develop prototype harness loader for laboratory simulation use.	Specify in tactical simulation procurement.
Localized firmness cells	Test forearm undersurface bladder for initial assessment of tactile stimuli.	Develop prototype bladder system/servo for use in laboratory simulation.	Specify in procurement of high performance tactical A/C simulators.
Skin temperature driver	Construct breadboard test unit/servo system & measure skin thermal response.	Augment G seat with skin temperature driver test unit for use in laboratory simulation.	Specify in procurement of high performance tactical A/C simulators.
Subatmospheric face mask	Develop & test pressure control servo loop of appropriate flow sizing. Develop & test safety device.	Modify mask air system with air supply servo loop system developed in component test-use for laboratory simulation.	Specify in procurement of high performance tactical A/C simulators.

Table 5-1. High G Augmentation Devices Development Process

(Con't)

Device or Technique	Subsystem or Component Test	Short Term (If component test results justify)	Long Term (If laboratory simulation results justify)
Respiration rate monitors	Purchase and test Honeywell Accudata 137 to support sub-atmospheric face mask test.	Use device purchased in component test to support laboratory simulation experimentation.	Employ in line-simulation if fundamental to sub-atmospheric face mask servo system or safety device.

6. SUMMARY

The trend of aircraft technology indicates increased utilization of the high G regime and increased dependence upon simulation for pilot training. The study presented herein discusses the physiological effects of high G exposure and postulates means by which the more obvious effects might be induced within laboratory simulation structured to experimentally determine the importance of these effects in the pilot training task. The type of G loading most often encountered in piloting present day aircraft is $+G_z$ referred to colloquially as "eyeballs down" and arises in dive pullouts and inside turns, common piloting maneuvers. Patterning the high occurrence of $+G_z$, the majority of literature discussing the physiological effects of high G deals principally with $+G_z$ physiological effects. The introduction of the reclined seat increases the importance of $+G_x$ physiological effects and, in the limited instances where $+G_x$ effects are documented, the authors have included them within this study.

By far, the physiological system most sensitive to high G conditions is the cardiovascular system. However, the pilot is less likely to notice cardiovascular changes themselves as he is to notice the affiliated visual effects of peripheral and central light loss induced by the cardiovascular changes. Under elevated levels of $+G_z$ the blood is inertially forced toward the lower torso and legs causing a commensurate reduction in blood pressure and flow rate at the temporal level which, if unchecked, ultimately may produce unconsciousness due to cerebral hypoxia. Pilots wear G-suits which proportionally squeeze the lower torso and extremities under $+G_z$ conditions to retard blood mass shift, prolong useful visual capability, and avoid unconciousness. Further, pilots are taught to perform a compressive respiratory maneuver known, based on its variations, as a M1 or L1 maneuver to aid the G-suit in forestalling blood mass shift. The cardiovascular system itself enters a compensatory condition and employs increas-

ed heart rate and vasodilation and constriction in an attempt to maintain normal cerebral blood flow. Negative G_z loading, much less often experienced in aircraft maneuvering, can produce the opposite conditions (blood engorgement of the upper torso and cerebral areas).

Exposing the lower portion of the body to a negative pressure differential has been shown in the Salut and Skylab space missions as well as earth bound experimentation to be capable of replicating a measure of the blood shift experienced under G load. The technique, termed lower body negative pressure (LBNP), requires that the lower torso and/or lower extremities be placed in a container capable of supporting subatmospheric conditions. Unfortunately, there does not exist sufficient application-related data to determine the feasibility of using LBNP in flight simulators for inducing cardiovascular symptoms of high G flight. The lack of data is primarily in the response area for it is not known whether the technique can produce a cardiovascular reaction as rapidly as experienced under varying aircraft G load. Other unanswered questions include identification of artifact production, potential interference with the G-suit, adverse interaction with motion cuing devices, loss of environment fidelity, and potential safety problems. Blood pressure would form the likely parameter upon which to close the LBNP control loop and a non-invasive technique considered near mandatory. Non-invasive devices presently available fall into the categories of ausculatory devices, ultrasonic devices, pulse wave velocity monitors, oximeter and plethysmographs. Of these, the ear oximeter, pulse wave monitor, and impedance plethysmographs are the most promising however, artifact production is also a problem here and accuracy, although probably not overly severe in the LBNP application, is suspect. We have concluded that significant additional clinical research must be conducted in this area before LBNP can be considered a candidate system for the laboratory form of high G augmentation devices. Further, the very severe imposition on environmental fidelity will

likely exclude the LBNP technique from line simulators employed as full- or near full-mission simulators. However, it has been pointed out that LBNP may be a very useful and acceptable technique to employ in a part-task trainer to teach pilots to appropriately perform the important L1/M1 maneuvers. Such training is currently available only in the more expensive environments of the centrifuge and actual aircraft flight.

Respiratory effects of high G conditions are normally considered in importance second to the cardiovascular system effects. As in the case of the cardiovascular system itself, this importance stems not from the system itself but because of visual liabilities arising from system performance degradation induced by high G. The cardiovascular system is responsible for delivering oxygenated blood to the cerebral and retinal areas. If G loading interferes with the delivery system, adverse conditions ensue. The respiratory system is responsible for oxygenation of the blood in the first instance and should this process be degraded by G loading, similar adverse conditions arise. For $+G_z$, respiratory effects are much less dramatic than the cardiovascular ones, and entail an increase in the work of breathing and decreased oxygen transport as a result of pulmonary shunting associated with pooling of blood in the lower regions of the pulmonary circulation and filling of the upper parts of the lung with air. The respiratory reactions are most noticeable for forward acceleration, $+G_x$, where breathing difficulties come into play long before any cardiovascular problems become evident and may be characterized as increased difficulty in breathing, chest pain, and increased respiration rate. Positive pressure and 100% oxygen breathing techniques are sometimes used to offset the impact of these effects.

This study investigates two methods to replicate the aforementioned respiratory effects. Negative pressure breathing employing a subatmospheric face mask and possible minor reductions in the partial pressure of oxygen is suggested as a means to

induce increased breathing difficulty, chest pain, and increased breathing rate. A second approach, advocating major changes in the partial pressure of oxygen in order to induce hypoxia and its related visual disruption, was ruled out due to excessively long temporal response as well as the obvious safety hazard inherent to the approach.

The servo loop controlling the subatmospheric face mask should employ respiration rate as one of its loop closure parameters. Respiration rate monitors which were investigated included impedance pneumographs, thermistor bead pneumographs, bellows pneumographs, mercury chestband pneumographs, and pressure transducer augmented flow rate pneumographs. The Honeywell Accudata 137 appears to be well suited to the task in that it includes its own signal processor and provides versatality by employing thermistor bead, mercury chestband, and flow rate pneumographic detectors.

The high G effect most often reported, surprisingly to the exclusion of musculoskeletal and tactile effects which quite obviously are also present, is the dramatic visual disruption induced by cardiovascular and respiratory system degradation as well as inertial loading of the visual apparatus itself. Under $+G_z$ conditions, peripheral and eventual central light loss, sometimes referred to as "tunnel vision", progressively occur as the retinal area enters, from its outer boundaries inward, a condition of hypoxia. Large magnitude G_x produces a blurring of vision possibly related to the production of an excessive tear film across the cornea area. The lacrimal process was investigated to determine if a replication of blurring could be satisfactorily induced on command through the use of eye irritants. This approach was abandoned due primarily to the sensation of pain which is allied with eye irritants but apparently missing in the high $+G_x$ experience and, secondly, to the fact that apparatus inducing the $+G_z$ peri-

pheral and central light loss can be developed to also produce blurring in $+G_x$.

The study advances the structure of a model defining visual acuity as a function of $+G_z$ conditions and where data is available defines relationships employed in this model. The completion of this model awaits key information relating acuity or minimum discrimination angle as a function of retinal blood pressure. In the interim, a simplified model is advanced as a substitute until the more sophisticated model can be completed. The simplified model treats the $+G_z$ visual effect as an aberration symetric about the foveal view. Twc concentric terminators respectively defining the onset of visual disruption and the loss of all light sensation are permitted to collapse inward toward the foveal view or expand outwards in the opposite direction based on $+G_z$ level and onset rate. The area between the terminators is subject to radially progressive light ray disruption, misting or graying, and intensity attenuation.

Because of the importance attached to high G visual disruption, considerable emphasis within the study is devoted to means by which these effects may be generated within laboratory simulation. A very simple device, plethysmographic goggles, is suggested as a means to quickly permit experimentation to begin without waiting for the development of other light alteration devices. Plethysmographic goggles have already been used to successfully induce progressive peripheral and central light loss. The goggles operate on a principle which dictates that as eyeball ambient pressure is increased above atmospheric pressure, a commensurate increase in intraocular pressure is experienced. As intraocular pressure approaches the level of retinal blood pressure, retinal oxygen perfusion decreases with concomitant loss of light sensitivity very nearly identical to that occurring under $+G_z$.

Although the goggles may be satisfactory for laboratory experimentation, other visual disruption techniques must be developed for use in line simulation. The study advances methods by which present day simulator cockpit instrument lighting systems and surround visual display systems may be driven to provide a rendition of the high G physiological visual disruption. Alternately the study discloses a method by which the visor worn by tactical aircraft pilots may be constructed as a vessel containing liquid crystal medium(s) capable of being selectively driven to produce either or both misting and light transmission attenuation. The disruption location may be commanded to occur anywhere within the visor expanse as dictated by the computer program controlling the visor. In terms of environmental fidelity, the visor approach holds much promise.

Simulator instrument lighting alteration, visual display system alteration, and the visor effects all are generated about the foveal view as is experienced in actual high G conditions. Therefore a definition of the foveal vector orientation is required and can be provided by a helmet mounted oculometer. Link Division is currently employing a helmet mounted oculometer approach as an integral part of an Air Force visual display program. Therefore the technology, in its developed state, should be directly transferable to the high G application.

The author's review of the literature dealing with musculoskeletal response to the high G environment causes us to conclude, particularly in the case of the upper extremities, that simulation devices intended to provide appropriate musculoskeletal cues must actually load the body. Artificial means to induce the kinesthetic perceptions of such loading, if available, will likely not suffice. Although the whole body is subject to increased inertial loading, the pilot is probably most aware of head/neck loading and its affect on visual perspective, and upper extremity loading as noticeably reflected in disruption of reaching and hand control

movements. Experimental data demonstrates a very significant rearward force component present when the arm is outstretched under $+G_z$. Consequently the arm loading mechanism suggested for use in high G simulation involves not only moment production at the elbow but also a separate prime mover to force the elbow rearward toward the torso. High power miniature samarium cobalt torque motors embedded within the flight suit form the preferred method for inducing a proportionate level of arm loading to that which exists under actual $+G_z$ conditions.

A number of approaches were investigated pertaining to head/neck loading devices. However for the short term, until a more accurate assessment of the importance of head/neck loading is experimentally determined, the torque motor driven helmet loader constructed by NASA Langley appears to be the most cost effective approach to this simulation and the acquisition of this type of device is recommended. If experimentation with this type of device tends to confirm preliminary findings that head/neck loading is indeed important to the pilot training task, additional expenditure to develop an approach displaying more acceptable environmental fidelity will be justified. A somewhat surprising development related to head/neck loading is the larger than expected G load induced movement of helmet with respect to skull. In that both tactile and visual cues may be induced by this movement, a simple approach, involving the inflation/deflation of pneumatic bladders located in the helmet liner area, is suggested as a means to replicate helmet movement within the simulation.

Quite obviously G induced body load should produce many changes in tactile stimulation. However there appears to be unusually small comment concerning tactile perceptions in the experimentation involving high G conditions. Although the tactile sensory system does not impose a physiological endpoint in high G exposure, the tactile perceptions are certainly likely candidates of importance for providing a perception of existing G load. The

authors advance four concepts for generating or enhancing the simulation of high G tactile perceptions. Shoulder harness tension and face mask loader devices employ force production to produce the desired tactile perceptions. The utilization of small thin bladders, localized firmness cells, in areas of the torso normally supported by external structures, can be employed to vary body load distribution and thereby vary tissue pressure with concomitant production of tactile stimuli. There appears to be basis for believing that flesh temperature change can augment and heighten the sensation of flesh pressure. A means for altering skin temperature through the use of solid state devices is presented.

Audition under high G conditions was investigated to determine whether either the physiological effects or the composition of environmental sounds offer cues related to G level. The only aural effect found is a loss of hearing that occurs so close to G load-related unconciousness it's occurrence does not provide a useful cue. Some indication of increased reaction time to aural stimuli was found, however, the literature offers no indication as to whether this was due to loss of aural perception or a disturbance of motor response. A review of aircraft cockpit sound recordings under high G maneuvering produced no identification of G level peculiar sounds. Thus we believe that aural cuing does not offer stimuli useful to the subject for G load assessment and further resources should not be expended in this area.

The study concludes with a set of recommendations covering, in the authors' opinion, the appropriate path toward the development of devices which will be useful as high G augmentation devices.

7. BIBLIOGRAPHY

1. Adler, F.H., "Physiology of the Eye," C.V. Mosby Company, (1965).

2. Aeromed Memo #MCREXD4-695-74D, "Venous Pressure in the Head Under Negative Acceleration," Aero Medical Laboratory, January, (1948).

3. AGARD, "Principles of Biodynamics-Applicable to Manned Aerospace Flight Prolonged Linear and Radial Acceleration," AGARD-AG-150, (1971).

4. Allan, J.R., Crossley, R.J., "Effect of Controlled Elevation of Body Temperature on Human Tolerance to $+G_z$ Acceleration," Journal of Applied Physiology, Vol. 33, No. 4:418-420, Oct., (1972).

5. Anderson, B., Saltzman, H.A., and Heyman, A., "The Effects of Hyperbaric Oxygenation on Retinal Arterial Occlusion," Archives of Ophthalmology, Vol. 73, March (1965).

6. Anonymous, "Basic Results of the Medical Research Conducted During the Flight of Two Crews on the Salyut-5 Orbital Station," National Aeronautics and Space Administration, Washington, D.C., Dec. (1977).

7. Ashutosh, K., "Impedance Pneumograph & Magnetometer Methods for Monitoring Tidal Volume," Journal of Applied Physiology, Vol. 37, No. 6, Dec. (1974).

8. Ashworth, B.R., McKissick, B.T., "The Effect of Helmet Loader G-Cuing on Pilot's Simulator Performance," The

American Institute of Aeronautics and Astronautics, AIAA Paper No. 78-1573.

9. Banister, J., Torrence, R.W., "The Effects of the Trached Pressure Upon Flow: Pressure Relations in the Vascular Bed of Isolated Lungs," Q.Jl. Exp. Physid. 45:352-367, (1960).

10. Barcsay, J., Anatomy for the Artist, Octopus Books, London Wl, (1973).

11. Barer, A.S., Golov, G.A., Zubavin, V.B., Murakhovskiy, K.I., Rodin, S.A., Sokorina, Ye.I., and Tikhomirov, Ye.P., "Physiological Reactions of the Human Body to Transverse Acceleration and Some Means of Increasing the Organism's Resistance to These Effects," Aerospace Med., Feb. (1966).

12. Barer, A.S., Golov, G.A., Zubavin, V.B., Murakhovskiy, K.I., Rodin, S.A., Sokorina, Ye.I., and Tikhomirov, Ye.P., "Physiological Reactions of the Human Organism to Transverse Accelerations and Means of Raising the Resistance to Such Forces," National Aeronautics and Space Administration, Sept. (1964).

13. Barnes, G.R., "A Theoretical Model of the Utricular Otolith and its Response to Angular Motion with Respect to an Acceleration in Shear," Flying Personnel Research Committee, London, England, April (1972).

14. Barnes, G.R., Rance, B.H., "Transmission of Angular Acceleration to the Head in the Seated Human Subject," Aerospace Medicine, April (1974).

15. Bartok, S.J., Carlson, L.D., and Walters, R.F., "Cardiovascular Changes During Tilt and Leg Negative Pressure Tests," Aerospace Medicine, Nov. (1968).

16. Beaumont Van, Greenleaf, J.E., Young, H.L., and Juhos, L., "Plasma Volume and Blood Constituent Shifts During $+G_z$ Acceleration After Bedrest with Exercise Conditioning," Aerospace Medicine, 45(4):425-430, (1974).

17. Beaupert, J.E., "Subjective Reaction to Dual Frequency Vibration," The Boeing Company, Wichita Division, Dec. (1967).

18. Beckh Von, H.J., "Positioning of Aircrews - Ultima Ratio of G Protection?" Aerospace Medicine, July (1972).

19. Behrendt, T., Sever, R.J., and Duane, T.D., "Ein Pneumatisches Ophthalmomodynamometer Fur Den Laborgebrauch", Keinischi Monatsblatter Fur Augenheilkunde, 149:550-556, (1966).

20. Benson, A.J., Reason, J.T., and Diaz, E., Flying Personnel Research Committee - "Testing Predictions Derived from a Model of Progressive Adaptation to Coriolis Accelerations," Ministry of Defense (Air Force Department) July (1971).

21. Blake, J., Transactions of the Opthalmological Societies of the U.K. - "Ocular Effects of High Speed Flight," Vol. XCI, Session (1971).

22. Borah, J., "Sensory Mechanism Modeling," Air Force Human Resources Laboratory, AFHRL TR 77-70, October (1977).

23. Brown, E., Goei, J.S., Greenfield, A.D.M., and Plassaras, G.C., "Circulatory Responses to Simulated Gravitational Shifts of Blood in Man Induced by Exposure of the Body Below the Iliac Crests to Sub-Atmospheric Pressure," Journal of Applied Physiology, 183, pp. 607-627, (1966).

24. Brown, J.H.V., "Physiology of Man in Space," Academic Press, New York/London, (1963).

25. Bryan, A.C., Milic-Emili, J., and Penselly, D., "Effect of Gravity on the Distribution of Pulmonary Ventilation," Journal of Applied Physiology, 21:778-784, (1966).

26. Buchdahl, H.A., "Optical Aberration Coefficients," An Introduction to Hamiltonian Optics, London, Oxford University Press, (1954).

27. Bulpitt, C.J., Dollery, C.T., "Estimation of Retinal Blood Flow by Measurement of the Mean Circulation Time," Cardiovascular Research, 5:406-412, (1971).

28. Burns, J.W., "Re-Evaluation of a Tilt-Back Seat as a Means of Increasing Acceleration Tolerance," Aviation, Space, and Environment, 46(1):55-63, (1975).

29. Burstein, A.H., "Human Musculoskeletal Tolerance Limits to Ejection and Related High Mechanical Stress Environments," Air Force Office of Scientific Research, Contract Number AFOSR-75-2820, July (1977).

30. Burton, R.R., "Positive ($+G_z$) Acceleration Tolerances of the Minature Swine: Application as a Human Analog," Aerospace Medicine, 44(3):294-298, (1973).

31. Burton, R.R., Iampietro, P.F., and Leverett, S.D., "Physiologic Effects of Seatback Angles 45° (from the Vertical) Relative to G," Aviation, Space, and Environmental Medicine, 46(7):887-897, (1975).

32. Burton, R.R., Krutz, R.W., "G-Tolerance and Protection with Anti-G Suit Concepts," Aviation, Space, and Environmental Medicine, 46(2):119-124, (1975).

33. Burton, R.R., Leverett, S.D., and Michaelson, E.D., "Man at High Sustained $+G_z$ Acceleration: A Review," Aerospace Medicine, 45(10):1115-1136, (1974).

34. Burton, R.R., Parkhurst, M.J., and Leverett, S.D., "G_z Protection Afforded by Standard and Preacceleration Inflations of the Bladder and Capstan Type G-Suits," Aerospace Medicine, 44(5):488-494, (1973).

35. Canfield, A.A., "The Influence of Increased Positive g on Reaching Movements," The Journal of Applied Physiology, Vol. 37, 230-235, (1953).

36. Canfield, A.A., Comrey, A.L., and Wilson, R.C., "A Study of Reaction Time to Light and Sound as Related to Increased Positive Radial Acceleration," Aviation Medicine, Vol. 20, 350-355, (1949).

37. Champion, M.C., Port, W.G.A., "Head and Neck Mobility of Pilots Measured at the Eye," Aeronautical Research Council Reports and Memoranda, (1977).

38. Chandler, R.F., Trout, E.M., "Child Restraint Systems for Civil Aircraft," Civil Aeromedical Institute Federal Aviation Administration, Oklahoma City, Oklahoma (1978).

39. Cheek, R.J., et.al., "New Cine Recording Ophthalmoscope with Television Monitoring Capability for Use in Aerospace Research," Aerospace Medicine, Dec. (1969).

40. Clark, D.C., et. al., "Exploratory Investigation of the Man Amplifier Concept," Defense Documentation Center, Aug. (1962).

41. Clarke, N.P., "The Pathophysiology of High Sustained $+G_z$ Acceleration Limitation to Air Combat Maneuvering and the Use of Centrifuges in Performance Training," AGARD-CP-189, April (1976).

42. Coburn, K.R., "Physiological Endpoints in Acceleration Research," Aerospace Medicine, 41(1):5-11, (1970).

43. Coerman, R.R., "The Mechanical Impedance of the Human Body in Sitting and Standing Position at Low Frequencies," Human Factors, V. 4, pp. 227-253, (1962).

44. Coerman, R.R., "The Passive Dynamic Mechanical Properties of the Human Thorax-Abdomen System and of the Whole Body System," Aerospace Medicine, 31(6):443-455, (1960).

45. Cohen, G.H., Brown, W.K., "Changes in ECG Contour During Prolonged $+G_z$ Acceleration," Aerospace Medicine, 40(8):874-879, (1969).

46. Cohen, L.A., "Analysis of Position Sense in Human Shoulder," Neurophysiology, v. 21, pp. 550-562, (1958).

47. Cohen, M.M., "Disorienting Effects of Aircraft Catapult Launchings," Aerospace Medicine, 44(1):37-39, (1973).

48. Cohen, M.M., "Hand-Eye Coordination in Altered Gravitational Fields," Aerospace Medicine, 41(6):647-649, (1970).

49. Cohen, M.M., "Sensory-Motor Adaptation and After-Effects of Exposure to Increased Gravitational Forces," Aerospace Medicine, 41(3):318-322, (1970).

50. Collyer, S.C., "Testing Psychomotor Performance During Sustained Acceleration," School of Aerospace Medicine, Dec., (1973).

51. Cooper, K.H., Ord, J.W., "Physical Effects of Seated and Supine Exercise With and Without Subatmospheric Pressure Applied to the Lower body," Aerospace Medicine, May, (1968).

52. Crago, P.E., Houke, J.C., and Hasan, Z., "Regulatory Actions of the Human Stretch Reflex," The John Hopkins University School of Medicine, Sept. (1976).

53. Cromwell, L., Weibell, F.J., Pfeiffer, E.A., and Usselman, L.B., "Biomedical Instrumentation and Measurements", Prentice-Hall Inc., Englewood Cliffs, N.J., (1973).

54. Crosbie, R.J., "A Cardiovascular Dynamic Response Index," Bureau of Medicine and Surgery Work Unit No. MF12.524.005-7001 Report No. 13, June (1970).

55. DDC Bibliography Acceleration Tolerance, Vol. 1 of II Volumes DDC-TAS-68-81 February (1969).

56. De Roetth, A., "Lacrimation in Normal Eyes," A.M.A. Archieves of Ophthalmology, pp. 185-189.

57. Diringshofen Von, H., Kissel, G., and Osypka, P., "Thresholds for the Perception of Linearly Increasing Angular Accelerations," Aerospace Medicine, August (1964).

58. Dobbins, J.P., "Variable-Transmittance Visor for Helmet-Mounted Display," Aerospace Medical Research Laboratory, October, (1973).

59. Dowell, A.R., Schaal S.F., Spielvogel, R., and Pohl, S.A., "Effect of Lower Body Negative Pressure Upon Pulmonary Ventilation and Perfusion as Measured Using Xenon-133," Aerospace Medicine, 40(6):651-654, (1969).

60. Dowell, A.R., Schmid, P.G., Nutter, D.O., and Sullivan, K.N., "Ventilation, Lung Volumes, and Gas Exchange During Lower Body Negative Pressure," Journal of Applied Physiology, Vol. 26, No. 3, pp. 352-359, March, (1969).

61. Dowell, A.R., Shropshire, S., and McCally, M.D., "Ventilation and Pulmonary Gas Exchange During Headward ($+G_z$) Gradient Acceleration," Aerospace Medicine, Sept. (1968).

62. Duane, T.D., "Experimental Blackout and the Visual System," Aerospace Medicine, Sept. (1967).

63. Duane, T.D., "Experimental Blackout and the Visual System," Transactions of the American Ophthalmology Society, 64:488-342, (1966).

64. Erickson, H.H., Ritzman, J.R., "Instrumentation for the Rhesus Monkey as a Cardiovascular Analog for Man During Air-Combat Maneuvering Acceleration," Aviation, Space, and Environmental Medicine, Nov. (1976).

65. Erickson, H.H., Sandler, H., and Stone, H.L., "Cardiovascular Function During Sustained $+G_z$ Stress," Aviation, Space, and Environmental Medicine, July (1976).

66. Erlebacher, J., Gilbert, R., and Auchincloss, J.H., "An Impedance Pneumograph Utilizing an Actively Regulated Constant-Current Source," Journal of Applied Physiology, Vol. 37, No. 6:961-963, Dec. (1974).

67. Ewing, C.L., Thomas, D.J., and Beeler, G.W., "Dynamic Response of the Head and Neck of the Living Human to $-G_x$ Impact Acceleration," U.S. Army Aeromedical Research Laboratory Naval Aerospace Medical Institute, March (1969).

68. Fernandez, H., Robinson, R., "An Automatic Device for Recording Blood Pressure," Aerospace Medicine, 42(2): 209-210, (1971).

69. Fessenden, E., "Acceleration Effects on the Ability to Activate Emergency Devices in F-4 Aircraft," Report No. NADC-77105-40, July (1977).

70. Forlini, F.J., "Indirect Measurement of Systolic Blood Pressure during $+G_z$ Acceleration," Journal of Applied Physiology, Vol. 37 No. 4:584-586, Oct. (1974).

71. Fraser, T.M., "Human Response to Sustained Acceleration," National Aeronautics and Space Administration, SP-103, (1966).

72. Frazier, J.W., Whitney, R.U., and Ashare, A.B., "Performance of the Anti-G Valve When Subjected to Varying Lateral Forces," Aerospace Medical Research Laboratory, Feb. (1973).

73. Frazier, J.W., Whitney, R.U., Ashare, A.B., Rogers, D.B., and Skrowronski, V.D., "G Suit Filling Pressures Determined by Seat Back Angle," Aerospace Medicine, 45(7):755-757, (1974).

74. Frisch, G.D., D'Aulerio, L., and O'Rourke, J., "Mechanism of Head and Neck Response to $-G_x$ Impact Acceleration: A Math Modeling Approach," Aviation, Space, and Environmental Medicine, 48(3):223-230, (1977).

75. Gauer, A., "The Physiological Effects of Prolonged Acceleration," German Aviation Medicine, World War II, Vol. I, U.S. Government Printing Office (1950).

76. Geddes, L.A., "The Direct and Indirect Measurement of Blood Pressure," Year Book Medical Publishers Inc., Chicago, (1970).

77. Geddes, L.A., Baker, L.E., "Principles of Applied Biomedical Instrumentation," 2nd Edition, John Wiley & Sons, New York, (1975).

78. General Dynamics, F16 Instrument Lighting Specification Nos. 16ZF031 16ZF032.

79. Gibson, J.J., The Senses Considered as Perceptual Systems, Prentice-Hall Inc., New Jersey (1965).

80. Gilbert, R., Auchincloss, J.H., Brodsky, J., and Boden, W., "Changes in Tidal Volume, Frequency, and Ventilation Induced by Their Measurement," Journal of Applied Physiology, 33(2):252-254, (1972).

81. Gillies, J.A., A Textbook of Aviation Physiology, Pergamon Press, (1965).

82. Gillingham, K.K., Authors private discussions with Dr. Gillingham, (1979).

83. Gillingham, K.K., "Eye Level Blood Flow Transfer Function," Correspondence from K.K. Gillingham, June (1978).

84. Gillingham, K.K., Burton, R.R., "Transfer Functions for Arterial Oxygen Saturation During $+G_z$ Stress," Aviation, Space, and Environmental Medicine, 46(11):1329-1335, (1975).

85. Gillingham, K.K., Freeman, J.J., and McNee, R.C., "Transfer Functions for Eye-Level Blood Pressure During $+G_z$ Stress," Aviation, Space, and Environmental Medicine, November, (1977).

86. Gillingham, K.K., Krutz, R.W., "Aeromedical Review: Effects of the Abnormal Acceleratory Environment of Flight," USAF School of Aerospace Medicine, Dec. (1974).

87. Gillingham, K.K., McNaughton, G.G., "Visual Field Contraction During G Stress at 13°, 45°, and 65° Seat-Back Angles," Aviation, Space, and Environmental Medicine, 48(2):91-96, (1977).

88. Glaister, D.H., "Distribution of Pulmonary Blood Flow and Ventilation During Forward ($+G_x$) Acceleration", Journal of Applied Physiology, 29(4):432-439, Oct. (1970).

89. Glaister, D.H., "Regional Ventilation and Perfusion in the Lung During Positive Acceleration Measured with Xe-133," Journal of Applied Physiology, (Lond) 177: 73-74, (1965).

90. Glaister, D.H., "The Effects of Gravity and Acceleration on the Lung," AGARDograph #133, Technovision Services, Nov. (1970).

91. Goldstein, J.A., Peczon, J.D., and Cogan, D.G., "Intraocular Pressure and Ophthalmodynamometry," Archives of Ophthalmology, 74:175-176, (1965).

92. Goodhart, G.L., "A Review of Experimental Data on the Cardiovascular Response to Acceleration," Aerospace Medical Research Dept., Dec. (1970).

93. Goodwin, G.M., McCloskey, D.I., and Matthews, P.B.C., "The Contribution of Muscle Afferents to Kinesthesia Shown by Vibration Induced Illusions of Movement and by the Effects of Paralyzing Joint Afferents," Brain, 95, 705-748, (1972).

94. Graboys, T.B., Michaelson, E.D., "Systolic Time Intervals During $+G_z$ Acceleration," Journal of Applied Physiology, 41(1):52-56, July (1976).

95. Gray, S., Shaver, J.A., Kroetz, F.W., and Leonard, J.J., "Acute and Prolonged Effects of G Suit Inflation on Cardiovascular Dynamics," Aerospace Medicine, 40(1): 40-43, (1969).

96. Green, J.F., Miller, N.C., "A Model Describing the Response of the Circulatory System to Acceleration Stress," Annals of Biomedical Engineering, 1,455-467, (1973).

97. Greenleaf, J.E., Haines, R.F., Bernauer, E.M., Morse, J.T., Sandler, H., Armbruster, R., Sagan, L., and Van Beaument, W., "$+G_z$ Tolerance in Man After 14-Day Bedrest

Periods with Isometric and Isotonic Exercise Conditioning," Aviation, Space, and Environmental Medicine, 46(5):671-678, (1975).

98. Grether, W.F., "Acceleration and Human Performance," Aerospace Medicine, 42(11):1157-1166, (1971).

99. Grigg, P., "Mechanical Factors Influencing Response of Joint Afferent Neurons from Cat Knee," Journal of Neurophysiolcgy, April, (1975).

100. Gum, D.R., "Modeling of the Human Force and Motion-Sensing Mechanisms," AFHRL-TR-72-54, (1973).

101. Gurovsky, N.N., "Medical Investigations During the Flights of Soyuz-12, Soyuz-13, Soyuz-14, and the Salyut-3 Orbiting Space Station," A Reproduced copy of N75-25516, Aug. (1965).

102. Guyton, A.C., Textbook of Medical Physiology, 5th Edition, W.B. Sanders Co., (1976).

103. Haines, R.F., "A Review of Peripheral Vision Capabilities for Display Layout Designers," Proceedings of the S.I.D., Vol. 16/4, Fourth Quarter, (1975).

104. Haines, R.F., "Effect of Passive 70° Head-Up Tilt on Peripheral Visual Response Time," Journal of Applied Physiology, Vol. 34, No. 3, March, (1973).

105. Haines, R.F., "Effect of Prolonged Bedrest and $+G_z$ Acceleration on Peripheral Visual Response Time," NASA TN D-7161, (1973).

106. Haines, R.F., "Effect of Prolonged Bedrest and $+G_z$ Acceleration Upon Peripheral Visual Response Time," Aerospace Medicine, 44(4):425-432, (1973).

107. Haines, R.F., Rositano, S.A., and Greenleaf, J.E., "Effect of Gradual Onset $+G_z$ Acceleration on Rate of Change of Visual Field Collapse and Intraocular Pressure," Life Sciences Directorate Ames Research Center, Moffett Field, CA, (1978).

108. Hanson, R., Cornog, D., and Hertzberg, H.T.E., "Annotated Bioliography of Applied Physical Anthropology in Human Engineering," WADC TR 56-30, May (1958).

109. Henzel, J.H., "The Human Spinal Column and Upward Ejection Acceleration: An Appraisal of Biodynamic Implications," Aerospace Medical Research Laboratories, Aerospace Medical Division, Air Force Systems Command, Wright-Patterson Air Force Base, Ohio, Sept. (1967).

110. Hirsch, C., "Biomechanics in Motor Skeletal Structures," Aerospace Medical Research Laboratories, Aerospace Medical Division Air Force Systems Command, Wright-Patterson Air Force Base, Ohio, Dec. (1971).

111. Hitchcock, L., Chambers, R.M., "Effects of Acceleration on Pilot Performance," Aviation Medical Acceleration Laboratory HADC-MA-6219, March (1963).

112. Holden, F.M., et.al, "Evaluation of Arterial Oxygen Concentration in Humans Exposed to G_z G_x Acceleration Forces," Aerospace Medical Research Laboratory, Wright-Patterson Air Force Base, Ohio, November (1973).

113. HONEYWELL Radiation Center, "Helmet Mounted Oculometer," Forbes Road, Lexington, Mass., Oct. (1977).

114. Houk, J.C., "The Phylogeny of Muscular Control Configurations", Biocybernetics IV: 125-144, VEB Gustav Fischer, Verlag, (1972).

115. Houk, J.C., Singer, J.J., and Goldman, M.R., "An Evaluation of Length and Force Feedback to Soleus Muscles of Decerebrate Cats", J. Neurophysiology, 33:784-811, (1970).

116. Howard, I.P., Templeton, W.B., Human Spatial Orientation, John Wiley & Sons, (1966).

117. Howard, J.C., "A G-Load Display for Remotely Piloted Vehicles and Other Aircraft that are Subject to Maneuvering Constraints," National Aeronautics and Space Administration, Washington, D.C., Sept. (1975).

118. Howard, J.C., "Feasibility of Using Lower Body Negative Pressure (LBNP) to Simulate Transient and Sustained Acceleration Forces," NASA-AMES LTI:239-3 Moffett Field, CA, March (1976).

119. Howard, J.C., "Precautions Taken to Ensure the Safety of Subjects During LBNP Experimentation," NASA-AMES memorandum, March (1976).

120. Howard, P., "The Effects of High Speed Flight on the Human Body," Triangle, Volume 7 Number 8 (1968).

121. Hutton, G.B., "Vertical Cockpit Accelerations Measured on an Operational Jet Transport Aircraft," Aeronautical Research Council Current Papers, Oct., (1969).

122. Hyde, A.S., Raab, H.W., "Summary of Human Tolerance to Prolonged Acceleration," Biophysics Laboratory, Aerospace Medical Research Laboratories, Aerospace Medical Division, Air Force Systems Command, Wright-Patterson Air Force Base, Ohio, Feb. (1965).

123. Inman, D.R., Peruzzi, P., "The Effects of Temperature on the Responses of Pacinian Corpuscles," J. Physiol. (1961), 155, PP. 280-301.

124. Ishiko, N., Loewenstein, W.R., "Effects of Temperature on the Generator and Action Potentials of a Sense Organ," The Journal of General Physiology, Vol. 45: 105-123, (1961).

125. Jacobs, D.H., "Fundamentals of Optical Engineering," New York and London McGraw Book Co., Inc., (1943).

126. Jacobson, L.B., Hyatt, K.H., and Sandler, H., "Effects of Simulated Weightlessness on Responses of Untrained Men to $+G_z$ Acceleration," Journal of Applied Physiology, 36(6):745-752, (1974).

127. Jaeger, E.A., Severs, R.J., Weeks, S.D., and Duane, T.D., "Visual Field Changes During Positive Acceleration," Aerospace Medicine, pp. 969-1072, Oct. (1964).

128. Jaeger, E.A., Weeks, S.D., and Duane, T.D., "Perimetric and Visual Acuity Changes During Ophthalmodynamometry," Archives of Ophthalmology 71: 484-488, (1964).

129 Jasper, H., Cipriani, A., and Lotspeich, E., "Physiological Studies on the Effect of Positive Acceleration in Cats and Monkeys," DCC Report Bibliography, Search Control No. 062819 (1942).

130. Johnston, R.S., Dietlein, L.F., "Biomedical Results from Skylab," National Aeronautics & Space Administration, (1977).

131. Jones, G.M., "Interactions Between Optokinetic and Vestibulo-Ocular Responses During Head Rotation in Various Planes," Aerospace Medicine, Feb. (1966).

132. Kazamias, T.M., Gander, M.P., Franklin, D.L., and Ross, J., "Blood Pressure Measurement with Doppler Ultrasonic Flowmeter," Journal of Applied Physiology, 30(4):585588, (1971).

133. Keatinge, W.R., Howard, P., "Effect of Local Cooling of the Legs on Tolerance to Positive Acceleration," Journal of Applied Physiology, 31(6):819-822, (1971).

134. Kennealy, J.A., Kirkland, J.S., and Sneider, R.E., "Bradycardia Induced by Negative Acceleration," Aviation, Space, and Environmental Medicine 47(5): 483-383, (1976).

135 Kennedy, K.W., Kroemer, K.H.E., "Excursions of Head, Helmet and Helmet-Attached Reticle Under $+G_z$ Forces, AMRL-TR- 72-127, May (1973).

136. Kirkland, V.E., "A Technique for Photographing Human Retinal Circulation During Blackout on the USAFSAM Human Centrifuge," USAF School of Aerospace Medicine, Aerospace Medical Division (AFSC), Brooks Air Force Base, Texas, March (1968).

137. Klein, K.E., Bruner, H., Jovy, D., Vogt, L. and Wegmann, H.M., "Influence of Stature and Physical Fitness on

Tilt-Table and Acceleration Tolerance," Aerospace Medicine, 40(3):293-297, March (1969).

138. Knapp, C.F., "Response of the Cardiovascular System to Vibration and Combined Stresses," Interim Scientific Report, Sept.-Aug. 1975.

139. Kotovskaya, A.R., "Certain Problems Resulting from Effects of Acceleration During Space Flight (Effects of Cumulation and Adaptation)", National Aeronautics and Space Administration, Washington, November (1966).

140. Kroemer, K.H.E., "Effects of High G on Pilot Muscle Strength Available for Aircraft Control Operation," Aerospace Medical Research Laboratory, Aerospace Medical Division, AFSC, Wright-Patterson AFB, Ohio, AMRL-TR-73-22, July (1976).

141. Kroemer, K.H.E., "Human Force Capabilities for Operating Aircraft Controls at 1, 3, and 5 G_z." Aerospace Medical Research Laboratory, Aerospace Medical Division, Air Force Systems Command Wright-Patterson Air Force Base, Ohio, February (1975).

142. Kroemer, K.H.E., Kennedy, K.W., "Involuntary Head Movements and Helmet Motions During Centrifuge Runs with up to +6 G_z," Aerospace Medicine, 44(6):639-644, June (1973).

143. Kron, G.J., Kleinwaks, J.M., "Development of the Advanced G Cuing System," Compendium of AIAA Flight Simulation Conference Papers: 1-14, (1978).

144. Krutz, R.W., Rositano, S.A., and Mancini, R.E., "Comparison of Techniques for Measuring $+G_z$ Tolerance in Man," Journal of Applied Physiology, 38(6):1143-1145, (1975).

145. Krutz, R.W., Rositano, S.A., and Mancini, R.W., "Correlation of Eye-Level Blood Flow Velocity and Blood Pressure During $+G_z$ Acceleration," USAF School of Aerospace Medicine, Aerospace Medical Division (AFSC), Brooks Air Force Base, Texas, November (1973).

146. Kydd, G.H., Ashley, A., "Physiologic Responses to Short Duration G_z," Department of the Navy, Aerospace Medical Research Department, NADC-MR-7012, August (1970).

147. Labarthe, D.R., Hawkins, C.M., and Remington, R.D., "Evaluation of Selected Devices for Measuring Blood Pressure," American Journal of Cardiology, 32(9):546-553, (1973).

148. Lackner, J.R., Graybiel, A., "Some Influences of Touch and Pressure Cues on Human Spatial Orientation," Aviation, Space and Environmental Medicine, 49(6):798-804, (1978).

149. Lamb, L.E., Stevens, P.M., "Influence of Lower Body Negative Pressure on the Level of Hydration During Bedrest," Aerospace Med., Dec. (1965).

150. Lambert, E.H., "Comparison of the Protective Value of an Antiblackout Suit on Subjects in an Airplane and on the Mayo Centrifuge," Aviation Medicine, V 21: 28-37, (1950).

151. Lambert, E.H., "The Physiologic Basis of Blackout as it Occurs in Aviators", Fed. Proc., 4:43, (1945).

152. Largerwerff, J.M., Luce, R.S., "Artifact Suppression in Indirect Blood Pressure Measurements," Aerospace Medicine, 41(10):1157-1161, (1970).

153. Lavnikov, A.A., "Principles of Aviation and Space Medicine," National Aeronautics and Space Administration, March (1977).

154. Leverett, S.D., Jr., Burton, R.R., "The Use of a Fixed Base Simulator as a Training Device for High Sustained or ACM (Air Combat Maneuvering) $+G_z$ Stress," AGARDograph 189:A8-1 to A8-8, April (1976).

155. Leverett, S.D., Jr., Cooper, K.H., "Physical Conditioning Versus $+G_z$ Tolerance," Aerospace Medicine, May (1966).

156. Leverett, S.D. Jr., Gillingham, K.K., Unpublished Notes, Viewgraphs and Pilot Comments Relative to High G Training (1978).

157. Levison, W.H., "Biomechanical Response and Manual Tracking Performance in Sinusoidal, Sum-of-Sines, and Random Vibration Environments," Aerospace Medical Research Laboratory, Aerospace Medical Division, Air Force Systems Command, Wright-Patterson Air Force Base, Ohio, April (1976).

158. Lipman, R.L., Ulvedal, F., Brown, W.K., Leverett, S.D., Lecocq, R., and Schnure, J.J., "Metabolic Response to Acceleration in Man," Aerospace Medicine, 41(8):905-908, August (1970).

159. Little, L.J., "The Design and Analysis of a Human Body Motion Measurement System," National Technical Infor-

mation Service, U.S. Department of Commerce, Sept. (1972).

160. Little, V.Z., Hartman, B.O., Leverett, S.D., "Effects of Acceleration on Human Performance and Physiology with Special Reference to Transverse G," USAF School of Aerospace Medicine, Aerospace Medical Division (AFSC), Brooks Air Force Base, Texas, June (1966).

161. Little, V.Z., Sidney, M.A., Leverett, S.D., and Hartman, B.O., "Psychomotor and Physiologic Changes During Accelerations of 5, 7, and 9 $+G_x$," Aerospace Medicine, November (1968).

162. Liu, Y.K., Cowin, S.C., Rosenberg, D.U.V., and Adams, K.A., "A Continuum Model of the Primate Body Response to Impact," Aerospace Medical Research Laboratory, Jan. (1972).

163. Loewenstein, W.R., "Mechano-Electric Transduction in the Pacinian Corpuscle. Initiation of Sensory Impulses in Mechanoreceptors," Handbook of Sensory Physiology Vol. I Principles of Receptor Physiology (1971).

164. Lohrbauer, L.A., Wiley, R.L., Shubrooks, S.J., and McCally, M., "Effect of Sustained Muscular Contraction on Tolerance to $+G_z$ Acceleration," Journal of Applied Physiology, 32(2):203-209, (1972).

165. London, S.B., London, R.E., "Critique of Indirect Diastolic End Point," Archives of Internal Medicine, 119:39-49, (1967).

166. MacKenzie, W.F., Burton, R.R., "Heart Pathology Associated with Exposure to High Sustained $+G_z$," Aviation,

Space and Environmental Medicine, 46(10):1251-1253, (1975).

167. McGuire, T.F., "The Normal Human EKG and its Common Variations in Experimental Situations," Aero Medical Laboratory, June (1956).

168. Meier, G.E., Sackman, J.G., and Grabmaier, Application of Liquid Crystals, Springer Verlag, (1975).

169. Mercier, A., "Visual Problems in Aviation Medicine"

170. Mercier, A., Perdriel, G., and Whiteside, T.C.D., "Problems of Vision in Low Level Flight," North Atlantic Treaty Organization, (1967).

171. Middleton, D.B., Hurt, G.J. Jr., Wise, M.A., and Holt, J.D., "Description and Flight Tests of an Oculometer," National Aeronautics and Space Administration, Washington, D.C., June (1977).

172. Military Specification Lighting, Instrument, Integral, White and Red; MIL-L-27160C (USAF) and MIL-L-25467D, May (1964).

173. Miller, N.D., "Evaluation of Non-Invasive Physiologic Measurement Techniques," Technology, Incorporated, San Antonio, Texas, Dec. (1976).

174. Miller, P.B., Leverett, S.D., "Tolerance to Transverse ($+G_x$) and Headward ($+G_z$) Acceleration After Prolonged Bed Rest," Aerospace Medicine, (1):13-15, (1965).

175. Mizen, N.J., "Design and Test of a Full-Scale Wearable Exoskeletal Structure," Interim Technical Report Con-

tract No. NONR-3830(00) CAL Report No. VO-1692-V-3, March (1964).

176. Mohler, S.R., "G Effects on the Pilot During Aerobatics," Federal Aviation Administration, Washington, D.C., July (1972).

177. Montgomery, L.D., Kirk, P.J., Payne, P.A., Gerber, R.L., Newton, S.D., and Williams, B.A., "Cardiovascular Responses of Men and Women to Lower Body Negative Pressure," Aviation, Space Environmental Medicine, 48(2): 138-145, (1977).

178. Mueller, G.G., Sensory Psychology, Prentice-Hall Inc., New Jersey, (1965).

179. Murray, R.H., Krog[illegible]J., Carlson, L.D., and Bowers, J.A., "Cumulative Effects of Venesection and Lower body Negative Pressure," Aerospace Medicine, March (1967).

180. Musgrave, F.S., Zechman, F.W., and Mains, R.C., "Comparison of the Effects of 70° Tilt and Several Levels of Lower Body Negative Pressure on Heart Rate and Blood Pressure in Man," Aerospace Medicine, 42(10):1065-1069, (1971).

181. Mutch, J.R., "The Lacrimation Reflex," The British Journal of Ophthalmology, July (1944).

182. Muzzy, W.H. III, Lustick, L., "Comparison of Kinematic Parameters Between Hybrid II Head and Neck System with Human Volunteers for $-G_x$ Acceleration Profiles," Naval Aerospace Medical Research Laboratory Detachment, June (1977).

183. Nagasaka, T., Mori, S., Takagi, S. and Mitarai, G., "Changes in Cerebral Blood Flow and Brain Temperature Induced by Lower Body Negative Pressure," The Japanese Journal of Physiology, v. 19, pp. 260-271, (1969).

184. Nieding Von, G., Krekeler, H., "Effect of Acceleration on Distribution of Lung Perfusion and on Respiratory Gas Exchange," Plugers Arch, 342, 159-176 (1973).

185. Niven, J.I., Whiteside, T.C.D., and Graybiel, A., "The Elevator Illusion: Apparent Motion of a Visual Target During Vertical Acceleration," Bureau of Medicine and Surgery, Project MR005. 13-6001, October (1963).

186. Nunneley, S.A., Shindell, D.S., "Cardiopulmonary Effects of Combined Exercise and $+G_z$ Acceleration," Aviation, Space, and Environmental Medicine, 46(7):878-882, (1975).

187. Nutter, D.O., Hurst, V.W., and Murray, R.H., "Ventricular Performance During Graded Hypovolemia Induced by Lower Body Negative Pressure," Aerospace Medical Research Laboratories, Wright-Patterson Air Force Base, Ohio, January (1969).

188. O'Briant, C.R., Ohlbaum, K., "Visual Acuity Decrements Associated with Whole Body $\pm G_z$ Vibration Stress," Aerospace Medicine, 41(1): 79-92 (1970).

189. O'Brien, J.A., Sloan, G.H., and Thorpe, R.W., "Annual Report in Support of Joint Army Navy Air Crew Impact Prevention Program," QEI Inc. Bldg., 6 Third Avenue, Burlington, Mass., Nov. (1972).

190. Olson, R.M., "Human Carotid Artery Wall Thickness, Diameter, and Blood Flow by a Noninvasive Technique," Applied Physiology Branch, Environmental Sciences Division, USAF School of Aerospace Medicine, Brooks Air Force Base, Texas, Dec. (1974).

191. Ormsby, C.C., "Model of Human Dynamic Orientation," PHD Thesis MIT, NASA CR-132537 N75-12585 Jan. (1976).

192. O'Rourke, J., "Measurement of Human Head Resultant Acceleration During Impact," Naval Air Development Center Warminster, Penn., November (1974).

193. Parin, V.V., "Evaluation of Soviet Reprint: Response of the Circulation System to the Effects of Accelerations and Weightlessness," Aerospace Medical Division, Deputy for Foreign Technology, Feb. (1966).

194. Parker, J.F., "Bioastronautics Data Book," Bio Technology, Inc. (1973).

195. Parkhurst, M.J., Leverett, S.D., and Shubrooks, S.J., "Human Tolerance to High, Sustained $+G_z$ Acceleration," Aerospace Medicine, 43(7):708-712, (1972).

196. Permutt, S., Bromberger-Barnea, B., and Bane, H.N., "Alveoler Pressure Pulmonary Venous Pressure and the Vascular Waterfall," Med. Thorac. 19: 239-260, (1962).

197. Peterson, D.F., Bishop, V.S., and Erickson, H.H., "AntiG Suit Effect on Cardiovascular Dynamic Changes Due to $+G_z$ Stress," Department of Pharmacology, The University of Texas Health Science Center at San Antonio, and US Air Force School of Aerospace Med. April (1977).

198. Potanin, C., Morehead, S., Neblett, W.W., and Sinclair-Smith, B.C., "Respiratory Mechanics with Lower Body Negative Pressure (LBNP) A Simulation of the Erect Posture," Aerospace Medicine, 40(10): 1101-1104, (1969).

199. Prasad, P., Mital, N., King, A.I., and Patrick, L.M., "Dynamic Response of the Spine During $+G_x$ Acceleration," Wayne State University, ONR N00014-75-C-1015.

200. Priestly, E.B., Introduction to Liquid Crystals, Plenum Press, New York, (1975).

201. Putzulu, D.A., Rota, P., "Ricerche Sperimentali Circa Gli Effetti Della Manovra Di Muller Sulla Resistenza Alle Accelerazioni-G_z," Riv. Med. Aeron, e Sp., XIX, (1966).

202. Rance, B.H., Barnes, G.R., "Head Movement Induced by Angular Oscillation of the Body in the Pitch and Roll Axes," Aviation, Space, and Environmental Medicine, 46(8):987-993, (1975).

203. Reading, V.M., "Analysis of Eye Movement Responses and Dynamic Visual Acuity," Magers Arch, 333: 27-34, (1972).

204. Roberts, L.G., "The Lincoln Wand," Lincoln Laboratory, Massachusetts Institute of Technology, Lexington, Mass.

205. Rodbard, S., Robbins, A.S., "The Components of the Korotkoff Sounds," American Heart Journal, 74(2): 278-282, (1967).

206. Rogers, D., Quam, D., "Myoelectric Feedback Control of Acceleration Induced Visual Scene Dimming in Aircraft Training Simulators," Published in the 1978 NTEC Conference, NAVTRAEQUIPCEN IH-306, Orlando, Fla.

207. Rogge, J.D., "Relation of Signal Light Intensity to Physiologic End Points During $+G_z$ Acceleration," USAF School of Aerospace Medicine, Aerospace Medical Division, (AFSC) Brooks Air Force Base, Texas, May (1968).

208. Rogge, J.D., Meyer, J.F., and Brown, W.K., "Comparison of the Incidence of Cardiac Arrhythmias During $+G_x$ Acceleration, Treadmill Exercise and Tilt Table Testing," Aerospace Medicine, 40(1):1-5, (1969).

209. Rositano, S.A., Gillingham, K.K., Sandler, H., and Skrettingland, K.R., "Correlation of Eye Level Blood Flow Velocity and Peripheral Light Loss During $+G_z$ Stress," Aerospace Medical Association, (1975).

210. Ross, B.M., Chambers, R.M., "Effects of Transverse G-Stress on Running Memory," Perceptual and Motor Skills, 24, 423-435, (1967).

211. Rothe, W.E., "Research on the Human Physiologic Response to Prolonged Rotation and Angular Acceleration," USAF School of Aerospace Medicine Aerospace Medical Division (AFSC) Brooks Air Force Base, Texas, September (1967).

212. Rothstein, J.D., Hanson, P.G., "Cardiac Rate Changes in Humans After Abrupt Deceleration," Journal of Applied Physiology, 22(4):645-647, (1967).

213. Ruskin, S.L., "Control of Tearing by Blocking the Nasal Ganglion," Reprinted from Archives of Ophthalmology, V. 4:208-211, (1930).

214. Ryan, E.A., Kerr, W.K., and Franks, W.R., "Some Physiological Findings on Normal Men Subjected to Negative G.," Aviation Medicine, June (1950).

215. Sackner, M.A., Wanner, A., "Detection and Prevention of G-Induced Regional Atelectasis, Edema, and Hypoperfusion," Division of Pulmonary Diseases of Mt. Sinai Medical Center, Miami Beach, Florida, Oct. (1973).

216. Sackner, M.A., Wanner, A., "Effects of G-Induced Stress on Pulmonary Circulation," Division of Pulmonary Diseases of Mt. Sinai Medical Center, Miami Beach, Florida, May (1975).

217. Schneider, L.W., Bowman, B.M., Snyder, R.G., and Peck, L.S., "A Prediction of Response of the Head and Neck of the U.S. Adult Military Population to Dynamic Impact Acceleration from Selected Dynamic Test Subjects," Highway Safety Research Institute/University of Michigan, May (1976).

218. Sears, W.J., Meehan, J.P., "Effects of LBNP on Central Venous Pressure, Venous Tone and Heart Rate," Reprinted from Federation of American Societies for Experimental Biology. Proceedings, V. 25, PP. 393, (1966).

219. Sergeylev, A.A., "Physiological Mechanisms of the Action of Accelerations," U.S. Department of Commerce Clearinghouse for Federal Scientific and Technical Information, November (1967).

220. Shaw, D.B., Cinkotai, F., and Thomson, M.L., "Syncope Induced by Application of Negative Pressure to the Lower Body and its Effect on Lung CO Diffusing Capacity," Aerospace Medicine, pp. 154-157, February (1966).

221. Shubrooks, S.J., "Changes in Cardiac Rhythm During Sustained High Levels of Positive ($+G_z$) Acceleration," Aerospace Medicine, 43(11): 1200-1206, (1972).

222. Shubrooks, S.J., "Positive Pressure Breathing as a Protective Technique During $+G_z$ Acceleration", Journal of Applied Physiology, 35(2):2940297, (1973).

223. Shubrooks, S.J., Epstein, M., and Duncan, D.C., "Effects of an Anti-G Suit on the Hemodynamic and Renal Responses to Positive ($+G_z$) Acceleration," Journal of Applied Physiology, Vol. 36, No. 3 March (1974).

224. Shubrooks, S.J., Leverett, S.D., "Effect of the Valsalva Maneuver on Tolerance to $+G_z$ Acceleration," Journal of Applied Physiology, Vol. 34, No. 4, April (1973).

225. Smith, P., "Multiplexing Liquid-Crystal Displays", Electronics, May (1978).

226. Sorokina, Y.I., "Certain Aspects Concerning Oxygen Metabolism of the Body Exposed to Prolonged Accelerations," National Aeronautics and Space Administration, Washington, D.C., August (1967).

227. Southall, J.P., "Introduction to Physiological Optics," New York, Dover (1937).

228. "Space Biology and Aerospace Medicine," No. 5, (1977).

229. Stauffer, F.R., "The Effect of High Acceleration Forces Upon Certain Physiological Factors of Human Subjects Placed in a Modified Supine Position: SDC Project 9-U-37a: Position 3," U.S. Naval School of Aviation Medicine and Research, October (1949).

230. Stein, P.D., Blick, E.F., "Arterial Tonometry for the Atraumatic Measurement of Arterial Blood Pressure," Journal of Applied Physiology, 30(4):593-596, (1971).

231. Steiner, S.H., Mueller, G.C.E., "Pulmonary Arterial Shunting in Man During Forward Acceleration," Journal of Applied Physiology, 16:1081-1086 (1961).

232. Steiner, S.H., Mueller, G.C.E., and Cherniack, N.S., "Pulmonary Gas Transport as Influenced by a Hypergravitational Environment," Journal of Applied Physiology, 16:641, (1961).

233. Stevens, P.M., Lamb, L.E., "Effects of Lower Body Negative Pressure on the Cardiovascular System," The American Journal of Cardiology," V. 16, pp. 506-515, October (1965).

234. Stoll, A.M., "Human Tolerance to Positive G as Determined by the Physiological End Points," Aviation Medicine, pp. 356-366, (1956).

235. Stone, H.L., Alexander, W.C., "Abdominal Blood Flow Changes During Acceleration Stress in Anesthetized Dogs," Aerospace Medicine, February (1968).

236. Stone, H.L., Erickson, H.H., and Sandler, H., "Changes in Mesenteric, Renal, and Aortic Flows with $+G_x$ Acceleration," Aerospace Medicine, 45(5):498-504, (1974).

237. Swearingen, J.J., "Protection of Shipboard Personnel Against the Effects of Severe Short-Lived Upward Forces Resulting from Underwater Explosions," Civil Aeromedical Institute Oklahoma City, January (1960).

238. Tabusse, L., Pingannaud, P.M., "The Physiopathological Effects of Acceleration on Astronauts", NASA TT F-15, 384, February (1974).

239. Tennyson, S.A., Mital, N.K., and King, A.I., "Electromyographic Signals of the Spinal Musculature During $+G_z$ Impact Acceleration," Orthopedic Clinics of North America - Vol. 8, No. 1, January (1977).

240. Thorner, M., "The Ophthalmic Artery Pulsensor," Transactions of the American Neurology Association 86:161-164, (1961).

241. Trumbull, R., "Environment Modification for Human Performance," Office of Naval Research, Sept. (1965).

242. Urschel, C.W., "Pulsus Paradoxus Effect of Gravity and Acceleration in its Production," The American Journal of Cardiology, Vol. 19, pp. 360-364, March (1967).

243. Urschel, C.W., Hood, W.B., "Cardiovascular Effects of Rotation in the Z Axis," Aerospace Medicine, pp. 254, March, (1966).

244. Vasil'yev, P.V., Kotovskaya, A.R., "Prolonged Linear and Radial Accelerations," Moscow Acadamy of Sciences, USSR, (1973).

245. Verghese, C.A., Nair, C.S., "New Criteria in Indirect Blood Pressure Recording," Aerospace Medicine, 40(12): 1377-1380, (1969).

246. Vogl, E., "Differences Between Simulation and Real World at the IABG Air to Air Combat Simulator with a Wide Angle Visual System", AGARD-CP-249, (1978).

247. Vogt, L.H., Coermann, R.R., and Fust, H.D., "Mechanical Impedance of the Sitting Human Under Sustained Acceleration," Aerospace Medicine, July (1968).

248. Vogt, L.H., Krause, H.E., Hohlweck, and Devlr, E.M., "Mechanical Impedance of Supine Humans Under Sustained Acceleration," Aerospace Medicine, 44(2):123-128, (1973).

249. Vykukal, H.C., "Dynamic Response of the Human Body to Vibration When Combined with Various Magnitudes of Linear Acceleration," Aerospace Medicine, November (1968).

250. Walters, R.F., "Systems Analysis of Physiological Performance Related to Stresses Such as those Experienced in High Performance Aircraft," University of California, AFOSR, Bolling AFB, Washington, D.C., Dec. (1976).

251. Warrick, M.J., Lund, D.W., "Effect of Moderate Positive Acceleration (G) on Ability to Read Aircraft-Type Instrument Dials," U.S. Air Force Air Material Command Wright-Patterson Air Force Base, November, (1946).

252. Watson, J.F., Cherniack, N.S., "Effects of Positive Pressure Breathing on the Respiratory Mechanics and Tol-

erance to Forward Acceleration," Aerospace Medicine, 33:583, (1962).

253. Watson, J.F., Cherniack, N.S. and Zechman, F.W., "Respiratory Mechanics During Forward Acceleration," J.Clin. Inves., 39:1737, (1960).

254. Weaver, J., Rubinstein, M., Clark, C.C., Gray, R.F., "Encapsulation of Humans in Rigid Polyurethane Foam for Use as a Restraint System in High Acceleration Environments," Aviation Medical Acceleration Laboratory, May (1962).

255. Weeks, S.D., Jaeger, E.A., and Duane, T.D., "Plethysmographic Goggles: a New Type of Ophthalmodynamometer," Official Journal of The American Academy of Neurology, Vol. 14 - No. 3, March (1964).

256. Weissler, A.M., "Non-Invasive Methods for Assessing Left Ventricular Performance in Man," American Journal of Cardiology, 34(7):111-114, (1974).

257. West, J.B., "Regional Differences in Gas Exchanged in the Lung of Erect Man," Journal of Applied Physiology, 17:893-898, (1962).

258. White, W.J., Riley, M.B., "The Effect of Positive Acceleration (G) on the Relation Between Illumination and Dial Reading," Reprinted from Symposium on Air Force Human Engineering, Personnel and Training Research NAC-NRC Publication 455, National Academy of Sciences, Washington, D.C., (1956).

259. Wilburn, D.L., Kurzenberger, J.L., "Kinematic Analysis of a Six Degree of Freedom Vibration Table," Aerospace Medical Research Laboratory, September (1970).

260. Wolthuis, R.A., Bergmen, S.A., and Nicogossian, A.E., "Physiological Effects of Locally Applied Reduced Pressure in Man," Physiological Reviews, Vol. 54, No. 3, July (1974).

261. Wolthuis, R.A., Hoffler, G.W., and Baker, J.T., "Improved Waist Seal Design for Use with Lower Body Negative Pressure (LBNP) Devices," Aerospace Medicine, 42(4):461-462 (1971).

262. Wolthuis, R.A., Hoffler, G.W., and Johnson, R.L., "Lower Body Negative Pressure as an Assay Technique for Orthostatic Tolerance: 1. The Individual Response to a Constant Level (-40 mm. Hg) of LBNP," Aerospace Medicine, 41(1):29-35, (1970).

263. Wolthuis, R.A., Hoffler, G.W., and Johnson, R.L., "Lower Body Negative Pressure as an Assay Technique for Orthostatic Tolerance: Part II. A Comparison of the Individual Response to Incremental vs Constant Levels of LBNP," Aerospace Medicine, 41(4):419-424, (1970).

264. Wolthuis, R.A., Hoffler, G.W., and Johnson, R.L., "Lower Body Negative Pressure as an Assay Technique for Orthostatic Tolerance: III. A Comparison of the Individual Response to Incremental Leg Negative Pressure vs. Incremental Lower Body Negative Pressure," Aerospace Medicine, 41(12):1354-1357, (1970).

265. Wood, E.H., "Some Effects of Gravitational and Inertial Forces on the Cardiopulmonary System," Aerospace Medicine, March (1967).

266. Woodcock, A., "Bodily Acceptance of Locally Applied Heat," Quatermaster Climatic Research Laboratory Final Report Contract DA44-109-qri-1289.

267. Woodson, W.E., Conover, D.W., Human Engineering Guide for Equipment Designers, University of California Press, (1966).

268. Young, L., Unpublished Correspondence, Massachusetts Institute of Technology, February (1978).

269. Young, L., Unpublished Correspondence, National Aeronautics and Space Administration, June (1978).

270. Young, L., Unpublished Notes of Meeting with Dana Rogers, (1978).

271. Young, L.R., Kupfer, C., "A Systems Analysis View of Intraocular Pressure Regulation," Digest of the 6th International Conference on Medical Electronics and Biological Engineering, (1965).

272. Young, L.R., Sheena, D., "Methods and Designs - Survey of Eye Movement Recording Methods," Behavior Research Methods & Instrumentation, Vol. 7(5), 397-429, (1975).

273. Zarriello, J.J., Norsworthy, M.E., and Bower, H.R., "A Study of Early Greyout Threshold as an Indicator of Human Tolerance to Positive Radial Acceleratory Force," Bureau of Medicine and Surgery Research Project NM 11 02 11 Subtask 1 Report No. 1, July (1958).

274. Zechman, F.W., Cherniack, N.S., and Hyde, A.S., "Ventilation Response to Forward Acceleration," Journal of Applied Physiology, 15:907, (1960).

275. Zechman, F.W., Mueller, G., "Effect of Forward Acceleration and Negative Pressure Breathing on Pulmonary Function," Journal of Applied Physiology, 17:909, (1962).

276. Zechman, F.W., Musgrave, F.S., Mains, R.C., and Cohn, J.E., "Respiratory Mechanics and Pulmonary Diffusing Capacity with Lower Body Negative Pressure," Journal of Applied Psychology, v. 22, pp. 247-250, (1967).

277. Zotterman, Y., Sensory Functions of the Skin in Primates, Pergamon Press, New York, (1976).

APPENDIX A

HIGH G PHYSIOLOGICAL EFFECTS

A.1 General

A very significant portion of this study has been devoted to searching the body of literature pertaining to human physiological response to elevated acceleration levels in order to determine the nature and method of manifestation of those effects which are likely to be most noticeable, employed in pilot assessment of flight dynamics, and/or have impact in aircraft control and mission performance. Only by identifying the effects and understanding their functional relationship to bodily acceleration magnitude will it be possible to intelligently propose means by which such effects can be laboratory-simulated and, if found to be important to the training task, introduced within operational flight simulators. The sponsor of the study suggested that the following physiological systems be investigated; cardiovascular, visual, aural, and selected portions of the musculoskeletal and tactile systems. To this list we added the respiratory system.

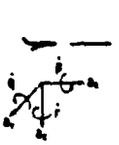
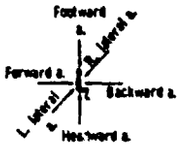
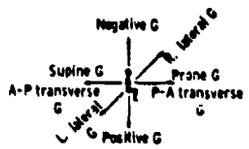
This section introduces and examines not only physiological effects we consider to be significant and very likely of importance in pilot training but also reports on physiological systems which do not appear to be affected by high G conditions to an extent worthy of immediate simulation consideration. Secondly, in preparing this section, the authors have investigated the normal operation of the physiological systems in an attempt to determine methods by which these systems might be artificially stimulated to respond in a manner similar to that encountered under high G conditions.

One of the more troublesome problems experienced in this search can be characterized as a "too little or too much data" syndrome. As will be seen, very little data was found in the area of

large field tactile response to high G conditions or, alternately, the importance of tactile response in flight dynamics assessment and aircraft control. Conversely, a plethora of information exists in the cardiovascular area, which is the physiological system most dramatically affected by acceleration often encountered in aircraft maneuvering and produces direct effects on other physiological systems, especially visual. Not unexpectedly, the wealth of cardiovascular information leads to apparent contradictions requiring close scrutiny to extract that information which seems most directly applicable to physiological effects likely to occur in routine tactical aircraft high G maneuvering. Our general approach to this problem has been, where only marginal amounts of data have been found, to present the complete findings. Where an abundance of data exists we have presented a synopsis of those findings which tend to be common within the literature.

Two axis systems are employed within this study for the purpose of defining the directional characteristics of acceleration. The first is the conventional aircraft body axis system commonly employed to describe aircraft translational and rotational flight dynamics. The second is an anatomical axis constructed within the pilot and reflects the <u>inertial</u> acceleration forces acting on the pilot's body. These two axis systems are defined in Table A-1 taken from Fraser (71, after Gell). The table reflects that, for a conventionally seated pilot, a thrusting maneuver is described as a $+a_x$ aircraft acceleration producing a $+G_x$ chest-to-back inertial acceleration reaction on the pilot's body. Likewise a flat right turn involving $+a_y$ produces a leftward $+G_y$ inertial acceleration reaction, and an increase in aircraft lift or aircraft nose up rotation involves $-a_z$ aircraft acceleration producing a $+G_z$ head-to-feet inertial reaction. The orientation of

Table A-1 Axis system definition (from Fraser (71)) after Gell).

Direction of motion	Table A Direction of acceleration		Table B Inertial resultant of body acceleration		
	Aircraft computer standard (System 1)	Acceleration descriptive (System 2)	Physiological descriptive [a] (System 3)	Physiological computer standard (System 4)	Vernacular descriptive
	 System 1	 System 2	 System 3	 System 4	
Linear					
Forward	$+a_x$	Forward accel.	[b] Transverse A–P G Supine G Chest-to-back G	$+G_x$	Eyeballs in
Backward	$-a_x$	Backward accel.	[c] Transverse P–A G Prone G Back-to-chest G	$-G_x$	Eyeballs out
Upward	$-a_z$	Headward accel.	Positive G	$+G_z$	Eyeballs down
Downward	$+a_z$	Footward accel.	Negative G	$-G_z$	Eyeballs up
To right	$+a_y$	R. lateral accel.	Left lateral G	$+G_y$	Eyeballs left
To left	$-a_y$	L. lateral accel.	Right lateral G	$-G_y$	Eyeballs right
Angular					
Roll right	$+\dot{p}$		Roll	$-\dot{R}_x$	
Roll left	$-\dot{p}$			$+\dot{R}_x$	
Pitch up	$+\dot{q}$		Pitch	$-\dot{R}_y$	
Pitch down	$-\dot{q}$			$+\dot{R}_y$	
Yaw right	$+\dot{r}$		Yaw	$+\dot{R}_z$	
Yaw left	$-\dot{r}$			$-\dot{R}_z$	

[a] The capital letter G is used as a unit to express inertial resultant to whole-body acceleration in multiples of the magnitude of the acceleration due to gravity. Acceleration due to gravity g. is 980.665 cm/sec² or 32.1739 ft/sec².

[b] A–P refers to anterior-posterior.

[c] P–A refers to posterior-anterior.

the anatomical axis system will be maintained throughout this study even though the pilot's body may assume a different orientation in the aircraft. Thus, when considering the reclined attitude the pilot assumes in an F16 aircraft, the study will reflect that increased aircraft lift, for instance, yields anatomical axis inertial reaction components of $+G_X$ and $+G_Z$.

A.2 Cardiovascular Effects

The cardiovascular system is the principle part of the body that is affected by excessive G_Z during aircraft maneuvers (3) Tolerance to acceleration depends largely upon the response of the cardiovascular system. It was recognized in the early days of acceleration research that the circulation is more profoundly affected by positive G_Z than any other system (81). These cardiovascular effects, while they are not serious in and of themselves (i.e., they do not in general cause any chronic effects on the cardiovascular system), are responsible for the progressive deterioration of vision and ultimately loss of consciousness.

It is important to understand these effects in order to properly synthesize, evaluate and control the various methods for either simulating or stimulating these effects.

Since the results of this study are not directed towards the acceleration physiologist but rather the flight simulation community, it seems appropriate, at the risk of appearing pedantic, to provide some basic background in the cardiovascular physiology. The reader who is familiar with this information may choose to skip this section and proceed to the subsequent sections which deal with the direct effects of acceleration on the cardiovascular system.

PHYSIOLOGY OF THE HEART AND CIRCULATORY SYSTEM

To begin a discussion of the heart and circulation it seems appropriate to introduce the anatomy of the heart and its function as a pump. Subsequently the vascular system and the physics of blood flow will be reviewed and finally the cardiovascular control system will be treated briefly. The objective here is not intended to provide an extensive treatment characteristic of a textbook of medical physiology but rather an overview for the flight simulation researcher and designer.

The heart is a pulsatile, four chamber pump divided into a right half which supplies the pulmonary circulation and a left half which supplies the systemic (peripheral) circulation. Each half contains an atrium which is an ante-chamber to the ventricle (Figure A.2-1). The ventricles are the main pumps which supply the force to propel the blood through the pulmonary and peripheral systems. The atria and ventricles are separated by valves to prevent reverse flow.

Blood returns to the heart from the systemic circulation(s) via the superior vena cava (1) (upper circulation) and inferior vena cava (2) (lower circulation) and fills the right atrium (3) from where it is pumped into the right ventricle (4). The blood is then pumped to the pulmonary circulation at a systolic pressure of approximately 22 mm Hg through the pulmonary artery (5).

Oxygenated blood returning to the heart from the pulmonary circulation (P) via the pulmonary veins (6), enters the left atrium (7) and is pumped to fill the left ventricle (8). Contraction of the left ventricle pumps the blood through the aorta

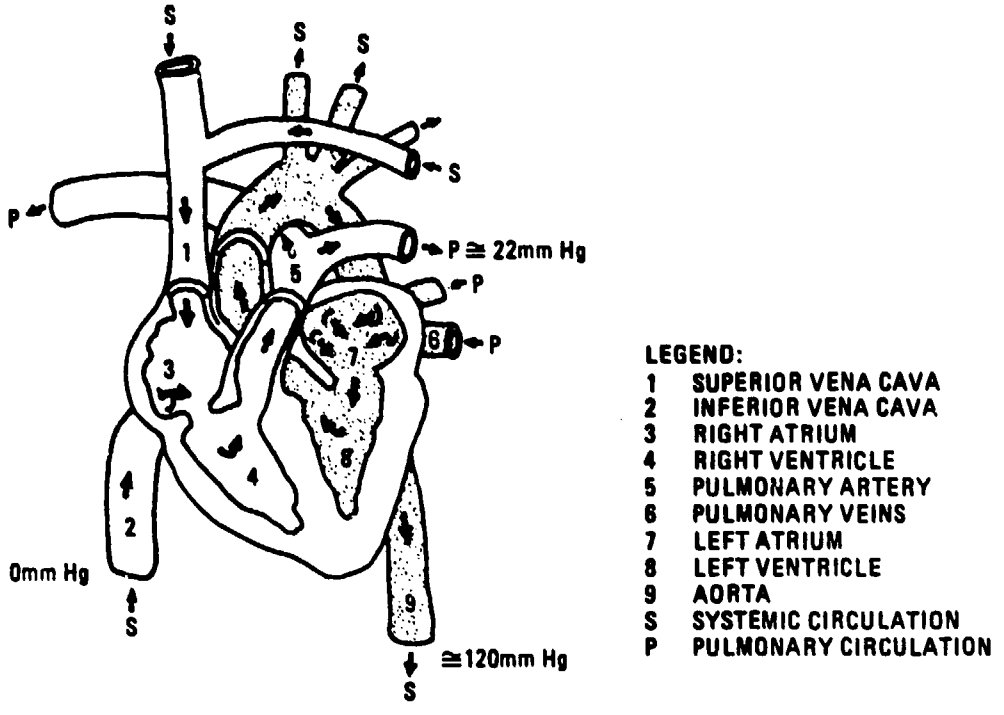


Figure A.2-1 Simplified diagram of circulation through the heart.

(9) to the systemic circulation (S) at a pressure of approximately 120 mm Hg. This process is repeated each cardiac cycle.

THE SYSTEMIC CIRCULATION

As was mentioned previously the circulation is divided into two components systemic and pulmonary. The pulmonary circulation supplies the lungs with blood. The systemic, also often referred to as the peripheral circulation, serves for the remainder of the body. The purpose of this section is to discuss the aspects of the systemic circulation which are important in the understanding of the "high G" cardiovascular effects.

The systemic circulation comprises <u>arteries</u> which carry blood from the aorta to smaller distribution vessels called <u>arterioles</u>

which in turn distribute blood to the capillaries where the nutrients are passed to the interstitial spaces. Blood is then collected from these interstitial spaces by venules. These vessels then aggregate into larger veins. The veins then return the blood to the right atrium to be re-oxygenated by the lungs and subsequently redistributed by the peripheral circulation.

Of the total circulation 64% of the blood volume is normally contained in the systemic veins and 15% in the systemic arteries (102). It follows then that the most significant orthostatic (effects due to blood pooling) effects of acceleration would be on the peripheral venous circulation since the volume of the veins is three to four times the volume of the arteries.

The heart, as mentioned previously, pumps blood into the aorta at a pressure of 120 mm Hg. This pressure being the maximum of the cardiac cycle or the systole is referred to as the systolic pressure. At the low pressure end of the cardiac cycle, diastole, the pressure in the aorta is nominally 80 mm Hg. This pressure ultimately reaches zero by the time it courses through the systemic circulation and reaches the right atrium.

Blood flows with almost no resistance in the larger vessels of the circulation. However, considerable resistance to flow is manifested in the arterioles and the capillaries (102). Since the decrease in arterial pressure in each part of the systemic circulation is directly proportional to the vascular resistance, a plot of mean systemic pressure throughout the circulation would appear as in Figure A.2-2.

The pulsatile nature of blood pressure in the arteries is illustrated also in Figure A.2-2. Note that by the time the flow has passed through the arterioles, the pulsatile aspects of the pressure have dissipated.

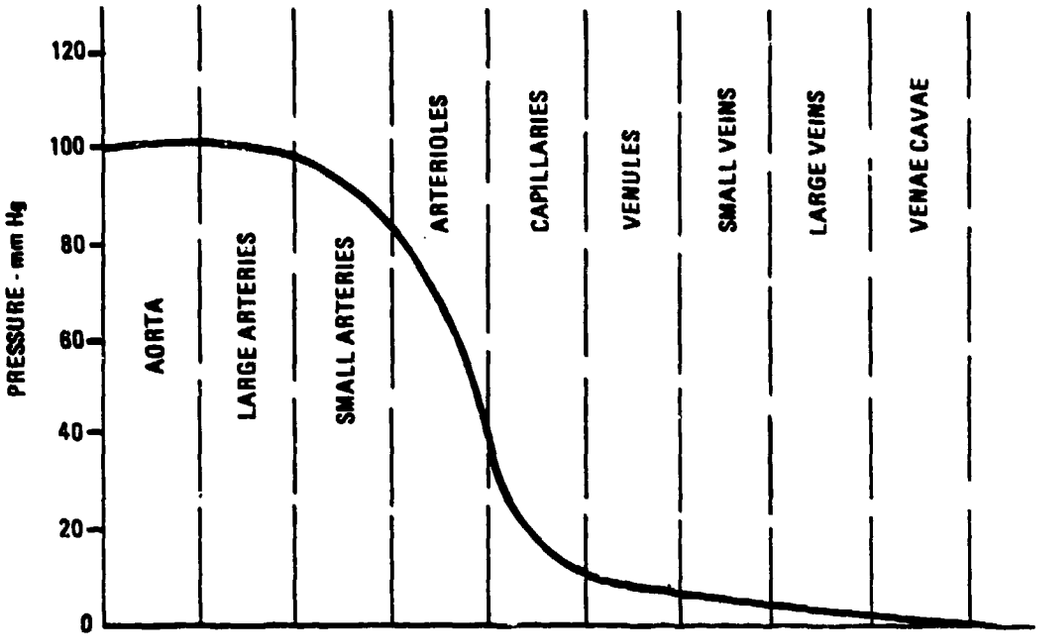


Figure A.2-2 Blood pressure throughout the systemic circulation (after Guyton (102)).

HEMODYNAMICS

The two factors determining the flow of blood through a blood vessel are pressure drop and vascular resistance. This concept can be stated mathematically as:

$$Q = \frac{\Delta P}{R} \qquad \text{[Eq. A.2-1]}$$

where Q is the volume rate of flow (ml/sec), P is the pressure drop (mm Hg), and R is the vascular resistance (dyne sec/cm^5). The normal adult at rest has a volume rate of approximately 83 ml/sec. Because this is the amount of blood that is pumped through the systemic and pulmonary circulation, this quantity is also referred to as cardiac output.

In the large vessels such as the aorta and the pulmonary artery, blood flow tends to be turbulent because of the high Reynolds' number, and the pulsatile nature of the flow.

The reasons for high Reynolds' number are the high velocity close to the ventricles and the sudden increase in vessel diameter. The effects of these parameters may be more easily understood by examining the following relationship for Reynolds' number;

$$R_e = \frac{vd}{\eta_e} \qquad \text{[Eq. A.2-2]}$$

where v is the flow velocity, d vascular diameter, and (η/e) viscosity/density ratio.

Hemodynamics is a complicated area of fluid dynamics. It is such because blood is basically a non-homogeneous (mixture of cells and plasma in varying configurations) non-Newtonian (the relationship between stress and strain tensors is nonlinear) fluid. It is further complicated by the fact that the vessels are distensible, the flow is pulsatile and the characteristics of the various vessels varies greatly (arteries, arterioles, capillaries, veins). For these reasons and since a detailed discussion of the physics of blood flow is not required for this study, none will be entered here. If the reader is interested in exploring this area deeper, several good textbooks exist on the subject. However, there are still a few more points which should be mentioned. One of these is the critical closing pressure of a blood vessel. This effect is a result of the distensibility of the vessels. Increasing the transmural pressure (excess of blood pressure in the vessel over pressure in the fluid surrounding the vessel) causes the blood vessel to dilate and decreasing the pressure causes the vessel to constrict. At a transmural pressure of approximately 20 mm Hg the arterioles do not permit the passage of any blood. If plas-

ma only is flowing through the vessels, the critical closing pressure is 5-10 mm Hg (102). This fact is important in understanding the blackout/grayout phenomena of the $+G_z$ environment.

The critical closing pressure may be affected considerably by sympathetic nervous system inhibition and stimulation. Sympathetic inhibition allows far more blood to flow through a tissue for a given pressure gradient. Sympathetic stimulation vastly decreases the blood flow. Sympathetic inhibition, therefore, decreases the critical closing pressure to as low as 5 mm Hg., while sympathetic stimulation can increase the critical closing pressure to as much as 100 mm Hg (102).

Vascular distensibility has a considerable effect on hemodynamics. Because of the anatomical differences between arteries and veins, the veins are 6 to 10 times as distensible as the arteries (102). Therefore a given pressure will permit 6 to 10 times the accumulation of blood as in arteries of a comparable size. A related factor which contributes to the accumulation of blood in vessels is compliance or capacitance. The compliance is equal to the product of volume and distensibility. Therefore, the compliance of a vein is on the order of 24 times its corresponding artery, since they differ in distensibility by a factor of 8 and volume by a factor of 3 (102). Venous compliance accounts for venous pooling under $+G_z$ conditions.

Figure A.2-3 illustrates the effect of hydrostatic pressure (pressure due to the column of blood above) on the systemic pressure throughout the body of a standing adult. The hydrostatic pressure is simply a function of the distance above and below the heart and the weight of the blood in the vessels. Note that the venous pressure in the dural sinus of the head is negative. This is a consequence of the fact that the veins in the skull are in a non-collapsable chamber and because of the hydrostatic suction between the top of the skull and the base of the skull (102). Of

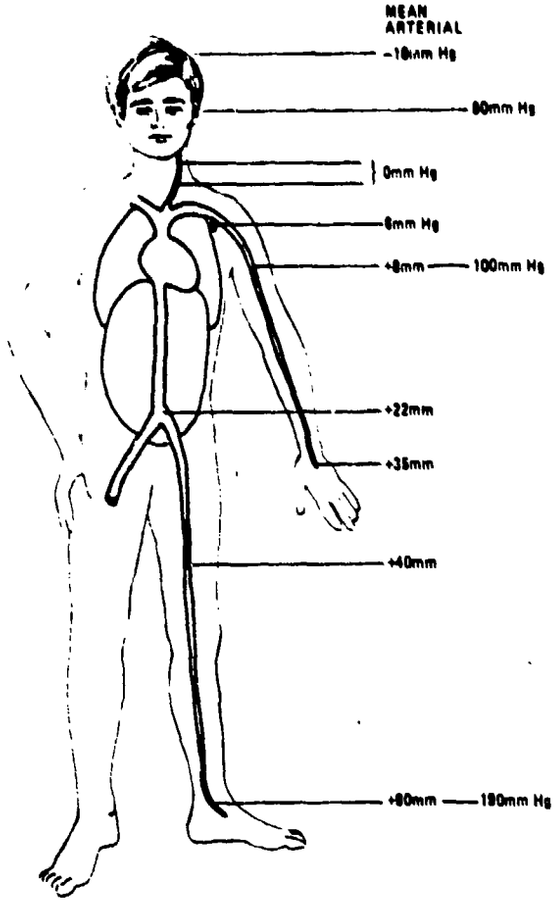


Figure A.2-3 Effect of hydrostatic pressure on the systemic pressure throughout the body (modified from Guyton (102)).

course, the transmural pressure will still be positive to keep these veins from collapsing.

As is shown in Figure A.2-3 the venous pressure in the feet is approximately 90 mm Hg. This pressure is somewhat lessened by virtue of the valves in the veins. The tensing of muscles in the leg tend to propel the blood in the veins. The valves allow the passage of blood towards the heart but do not permit retrograde flow. This function, referred to as the venous pump, reduces the venous pressure at the feet in an exercising adult to less than 25 mm Hg.

In the case of a perfectly still individual, or one in which some external force has produced the same hydrostatic effect, the pressure can rise to the full 90 mm Hg in about 30 seconds (102). This causes leakage from the circulatory system into the tissue spaces causing leg swelling and a diminution of blood volume. The ultimate result is a reduction of venous return to the heart.

CIRCULATORY REGULATION

The previous sections have dealt with discussing the heart as the pump for the circulatory system and the basic functions of the circulatory system as a conduit for distribution of blood throughout the body. This section deals with the regulation of the cardiovascular system.

Control of the circulatory system can be considered in terms of local control or systemic control. Local control deals primarily with the microcirculation and is concerned with the demand by tissues for oxygen, glucose, amino acids and other nutrients. These demands simply alter the flow of blood to specific tissues.

The systemic control system has a more widespread effect. It can be divided into the rapidly acting and the long term regulatory systems. The rapidly acting systemic control system is of most concern to this study. Figure A.2-4 illustrates the dynamics of the various arterial pressure control systems.

The rapidly acting pressure control systems operate through nervous or hormonal control of the circulation. In the neural control system, receptors in the arterial system detect pressure reductions and transmit a signal to the nervous system which in turn signals the heart to increase its output by altering its strength and rate of contraction. Also the vascular system is signaled to constrict the arterioles and veins. All these effects

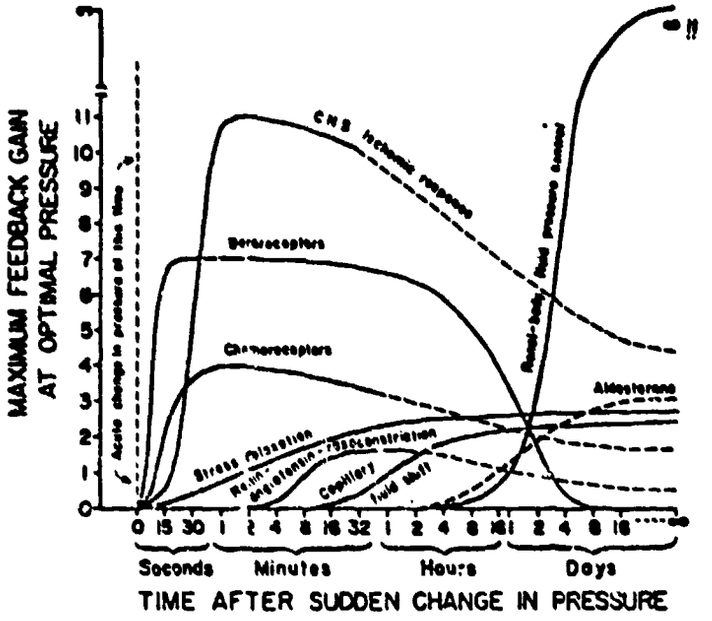


Figure A.2-4 Dynamics of various arterial pressure control systems. (after Guyton (102)) (courtesy of Saunders Co.).

are combined with a resulting increase in arterial pressure within seconds.

The hormonal control system operates through chemoreceptors which signal hormonal secretion principally angiotension to rapidly return pressure to normal.

The best known and most rapidly acting system for arterial pressure control is the baroreceptor reflex. The reflex, a high pressure control, is initiated by pressure receptors located in the walls of the large systemic arteries. These pressure receptors, called either baroreceptors or pressoreceptors, are spray type nerve endings in the walls of almost every large artery of the thoracic and neck region. These receptors are extremely abundant in the aortic arch and the carotid sinuses.

The mechanism is such that a rise in pressure in one of these vessels stretches the walls and stimulates a baroreceptor which in turn transmits a signal to the central nervous system (CNS) via one of the paths shown in Figure A.2-5 signaling the circulation to reduce the pressure. The baroreceptors are more sensitive to rising pressure than to stationary and are even less sensitive to falling pressure. They are not stimulated at all for pressures less than 60 mm Hg and the slope is greatest for pressures between 90 and 110 mm Hg (102). This is illustrated in Figure A.2-6.

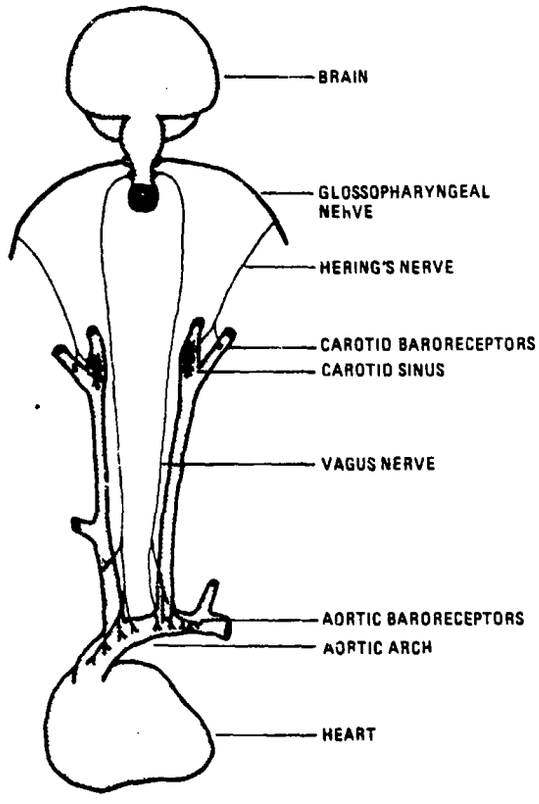


Figure A.2-5 Baroreceptor system.

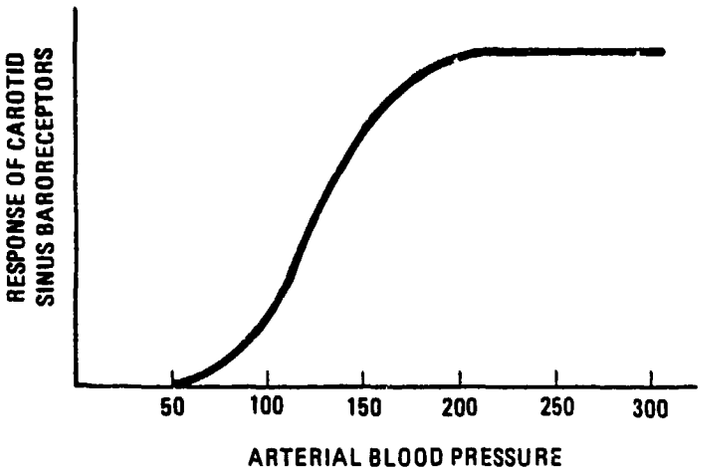


Figure A.2-6 Baroreceptor response as a function of arterial pressure (modified from Guyton (102)) .

The result of the baroreceptor reflex impulses is to inhibit the vasoconstrictor center thereby producing vasodilation, decreased cardiac rate and stroke volume. There is an analogous reflex system which operates to raise the arterial pressure when it has been somehow lowered. There are similar stretch receptors to the baroreceptors which provide the analogous function. These receptors are called low pressure receptors and are located in the walls of both the atria and pulmonary artery.

A familiar situation is that of a person lying down who suddenly arises causing the arterial pressure in the head to immediately drop. If this pressure is not quickly corrected, snycope may ensue. However, the baroreceptors elicit an immediate reflex and the resulting pressure drop in the head and upper body is reduced.

It should be noted that in general arterial pressures cited are mean arterial pressures. This pressure is defined as the mean of the cardiac cycle and not simply the average of the systolic and diastolic pressures. In fact the mean arterial pressure tends

to be closer to the diastolic pressure, since systole is relatively brief.

Another reflex arterial pressure regulating mechanism is the central nervous system (CNS) ischemic response. With a reduction in arterial pressure, the blood flow to the brain is insufficient to maintain normal function of the brain tissue. Under these conditions the brain is said to be ischemic. In response, the vasomotor system signals the vasoconstrictor system cutting flow to the less vital parts of the body and the systemic arterial pressure rises very rapidly. The buildup of carbon dioxide in the vasomotor system is thought to be responsible for this response (102). Figure A.2-4 shows the potential power of the CNS ischemic response.

The third major arterial reflex system is the chemoreceptor reflex system whose sensors are located in the bifurcations of the carotid arteries and in the aortal arch. These sensors are sensitive to lack of oxygen. They generate signals which pass along Hering's nerves and the vagus nerves into the vasomotor center (Figure A.2-5), whereupon the reaction is similar to baroreceptor reflex response.

Up to this point the discussion of circulatory control has dealt mainly with the arteries. The veins participate in the same reflex pressure regulating mechanisms as the arteries. The impulses to the vein are carried by sympathetic vasoconstrictor fibers which cause the veins to constrict by an increase in venous tone in response to even weaker sympathetic stimuli than the arteries.

The major venous effect is not in vascular resistance but rather in capacitance and according to the Frank-Starling Law of the Heart, the major factor in determining cardiac output is the

rate of venous return. This law states in essence, that the heart works hard enough to pump out all the blood that returns to it.

Skeletal muscles and skeletal nerves also have a role in circulatory control. When the sympathetic vasoconstrictor system is stimulated, the abdominal compression reflex aids in displacing blood out of the abdominal veins towards the heart. Exercise contracts skeletal muscles thereby compressing the vessels resulting in an increase of systemic filling pressure from 7 mm Hg to as high as 20 to 30 mm Hg (102).

A.2.1 Effects of Acceleration on the Cardiovascular System

High performance aircraft are capable of significant accelerations in all of the vehicle's six degrees-of-freedom. These accelerations impose unique physiological effects on the pilot. Along some axes the effects are direction dependent. For example, positive and negative accelerations along the Z axis produce substantially different physiological effects.

The most often experienced inertial force in high performance aircraft is in a head-to-foot direction ($+G_z$). In modern low wing loading, highly maneuverable aircraft levels of 12 G_z are quite possible. Negative "G's" ($-G_z$) are much less often experienced in the flight envelope and are restricted to about -3 G_z, both because of aircraft limitations and pilot tolerances. Longitudinal acceleration $\pm G_x$ are confined to the range of ± 2.5 G_x but are usually in the range of $\pm$ 1 G_x unless aircraft carrier operations, of catapult launch and arresting, are considered. In the lateral direction ± 1.5 G_y is generally the maximum capability while the usual environment is on the order of 1/4 G_y.

For good reason the literature abounds in treatment of the +Z axis accelerations, -Z axis is less thoroughly treated and $\pm$X axis even less. Treatment of the Y axis accelerations is very limited

(studies in this area are presently being implemented). This discussion will essentially follow that pattern.

POSITIVE G_z

Positive G_z produces the most profound effects on the cardiovascular system and therefore will be provided the most extensive discussion. Since the early days of acceleration research, it was observed that symptoms such as peripheral light loss, to blackout, to loss of consciousness could only be explained by a decrease in blood flow to the head. Subsequently, some researchers believed that mechanical factors made a contribution (210), but it became evident that the cardiovascular system was the primary source of difficulty.

The circulation, supported by elastic blood vessels and depending on well defined pressures and volumes, is grossly disturbed by excessive gravitational forces (3).

A simplistic view of the cardiovascular phenomena associated with G_z shows that as G_z increases, the hydrostatic pressure in the legs increases, the vessels passively dilate, and a major portion of the blood from the upper part of the body is displaced to the lower vessels. Since the venous return decreases, the cardiac output decreases thereby further causing a decrease in pressure at the aorta and above the heart. A more rigorous explanation involves a discussion of initial inertial effects, hydrostatic effects, orthostatic effects and the reflex activity of the cardiovascular and central nervous system.

To begin with, consider Figure A.2.1-1 which illustrates the hydrostatic effects of the column of blood on systolic blood pressure at the heart, eye level, and at the feet, as a function of acceleration along the longitudinal (z) axis of the body. These data represent a short duration acceleration and do not consider

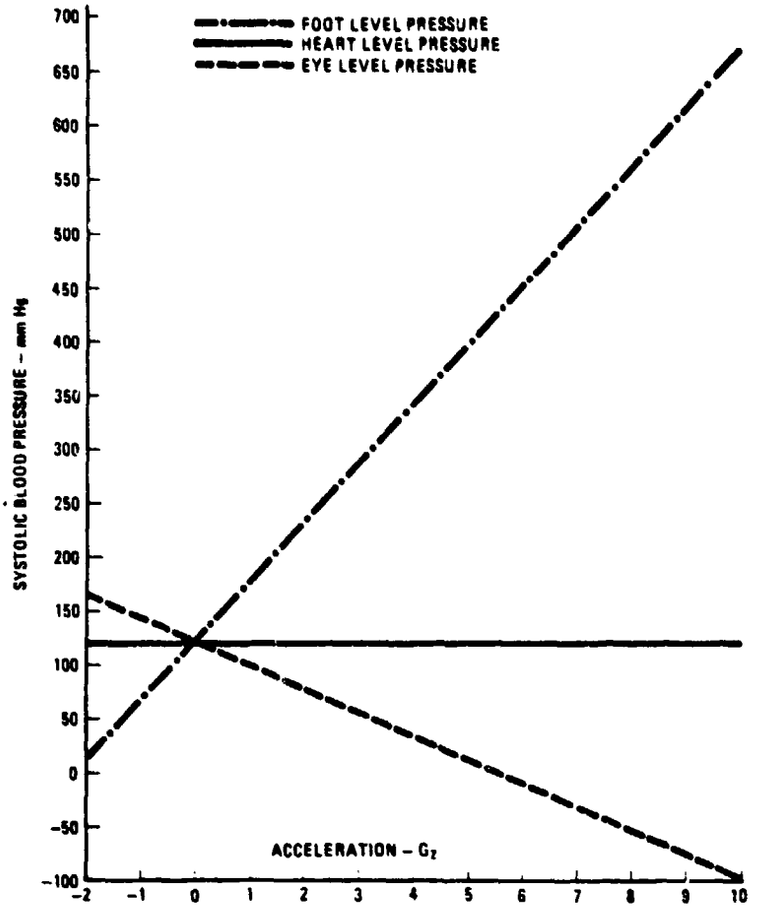


Figure A.2.1-1 Seated systolic blood pressure as a function of Gz.

the compensatory cardiovascular adjustments. It is also assumed that there is no change in heart level systolic pressure.

Using a model of a seated human with a heart to eye distance of 30 cm and a heart to foot distance of 75 cm, a 120 mm Hg systolic arterial pressure at the heart yields a 98 mm Hg eye level pressure and a 175 mm Hg pressure at the feet (86). The remainder of the data can be computed using the concepts of fluid statics. Green and Miller (96) postulate an equation for the computation of

blood pressure as a function of acceleration referenced to any point in the body.

$$P_S = P_H \pm gh \qquad \text{[Eq. A.2.1-1]}$$

where P_H is the heart level blood pressure and h is the vertical distance between the heart and point of interest. Burton (30) empirically derives a similar linear relationship. The foregoing assumes that the heart level pressure is maintained at a constant which in fact is not the case.

A more realistic model considers the distensibility of the vascular system thereby causing a "ballooning" of the vessels below the heart, primarily the veins, reducing venous return, and causing the heart output to decrease, therefore the heart level blood pressure is reduced almost instantly (30, 65, 81, 139). Figure A.2.1-2 illustrates the drop in heart level mean arterial blood pressure as a function of acceleration. A slight displacement of the heart may affect prediction of hydrostatic effects.

However, cerebral or retinal perfusion, which affect unconsciousness and blackout respectively, cannot be predicted on the basis of this model because it neglects cardiovascular compensatory adjustments which occur in the six to ten seconds after acceleration onset. Also, because the concurrent drop in venous pressure within the skull tends to keep the arterial-venous pressure differences constant thus "sucking" blood through the circulation as discussed below. Howard (81) states that the rate of onset of acceleration has an effect on the predictability of the simplified model, to the extent that if the onset rate exceeds the rate at which the lower vascular system distends the simplified model provides reasonable results.

The compensatory cardiovascular systems discussed in Section A.2 provides the reflex stimulation of the sympathetic nervous

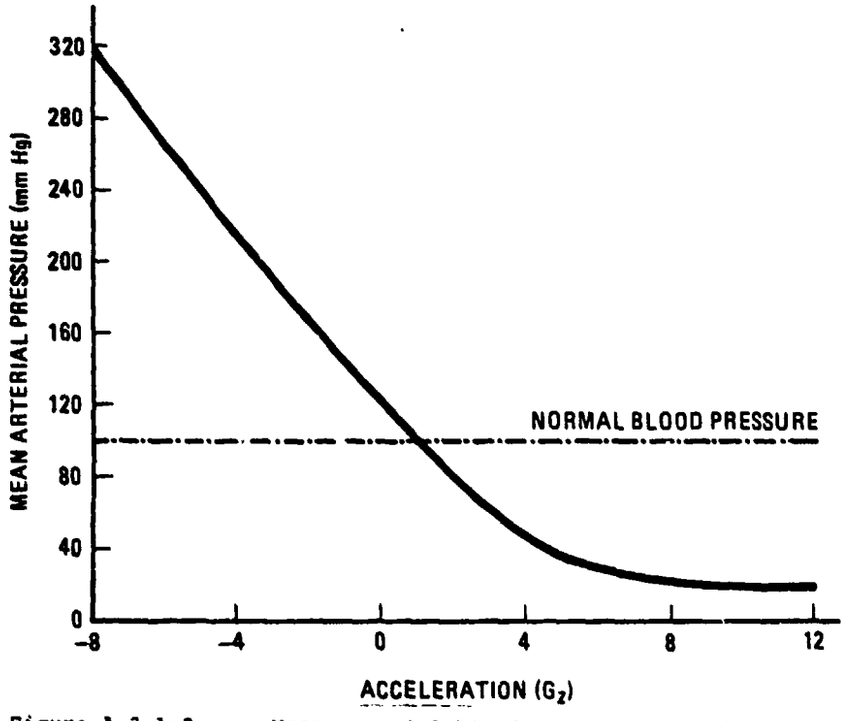


Figure A.2.1-2 Mean arterial blood pressure as a function of Gz (after Guyton (102)).

system which serves to readjust the systemic blood pressure. As was stated, this is accomplished by adjusting cardiac output and by vasoconstriction. These adjustments occur within 6 to 10 seconds of the onset of acceleration (86). This factor provides a rationale for the effects of rate of onset on blackout as well as duration (Figure A.2.1-3) (234).

The cardiovascular scenario in response to rapid onset acceleration is as follows. There is an immediate increase in hydrostatic pressure drop resulting from the acceleration. Momentarily the heart continues with its preacceleration output so the heart level pressure does not instantly drop but may actually increase slightly (154) then begin to drop as venous return to the heart is

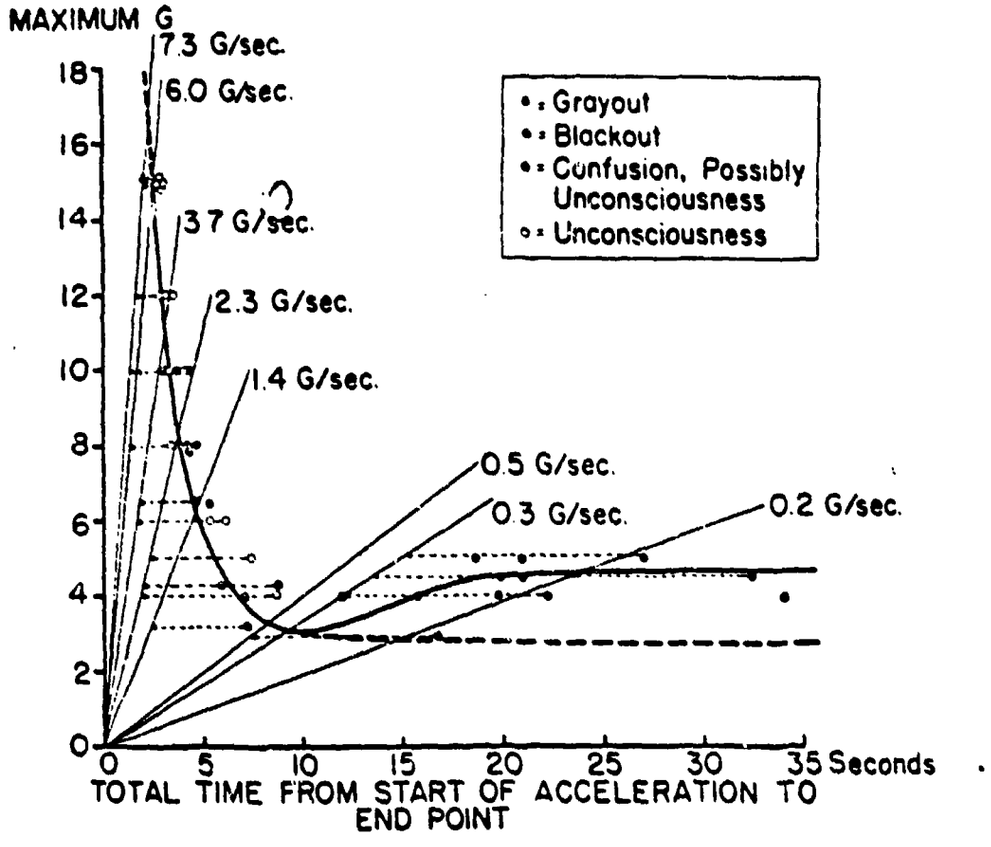


Figure A.2.1-3 G-Tolerance curve with various acceleration rates (after Stoll (234)) (courtesy of Journal of Aviation Medicine).

reduced by the pooling effects in the lower vasculature. The reduced venous return causes a reduced cardiac output. The baroreceptors in the aortic arch and carotid sinus respond causing an increased cardiac output and vasoconstriction both serving to increase the systemic blood pressure, thereby increasing the supply to the head. Figure A.2.1-4 (65) illustrates this cardiovascular response to 3.5 G_z on a dog.

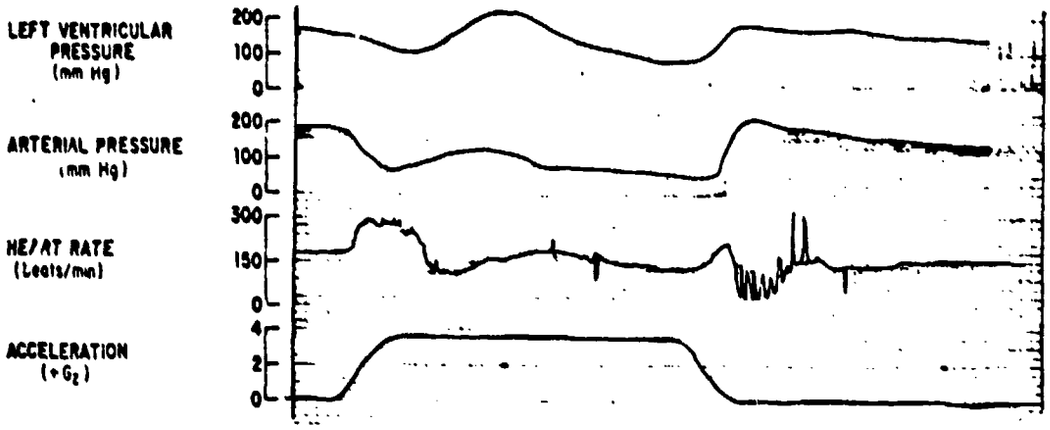


Figure A.2.1-4 Effects of +3.5 Gz stress on cardiovascular function (after Erickson (65)) (courtesy of Aviation Space Environmental Medicine).

The cerebral circulation is further protected by a fall in jugular venous pressure which helps maintain arteriovenous pressure differential and a decrease in cerebrospinal fluid pressure which reduces intracranial resistance to blood flow (Figure A.2.1-5) (86). Venous and cerebral spinal fluid actually become subatmospheric, at 4g on the order of -30 mm Hg (3). While at this point the arterial pressure at brain level may be close to

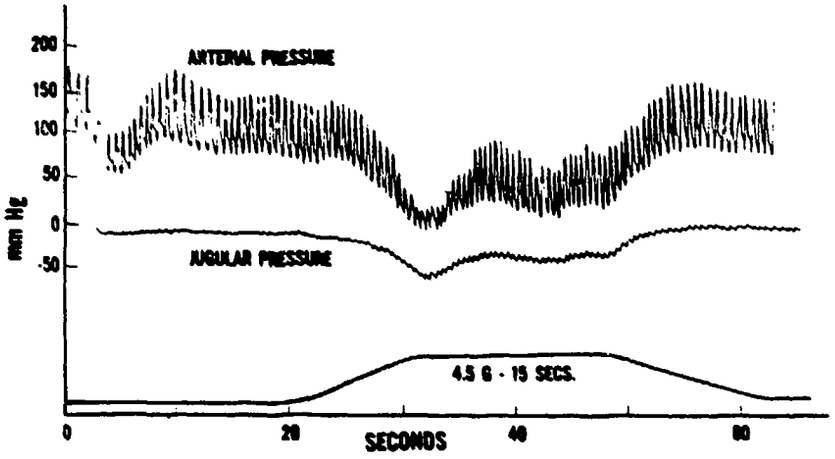


Figure A.2.1-5 The effect of +Gz upon cerebral arterial and jugular venous pressure. Note that a high arteriovenous pressure gradient is maintained because of a marked fall in jugular venous pressure during acceleration (from Gillingham (86)).

zero, the pressure gradient between the cerebral arteries and veins is adequate for blood flow. This effect is sometimes referred to as the "jugular suction effect" (3).

An analogous hemodynamic situation exists in the retinal circulation. However, retinal perfusion requires an eye level arterial pressure in excess of approximately 20 mm Hg, independent of reduced venous pressure, to overcome intraocular pressure and keep the arteries and veins from collapsing. If the eye level blood pressure falls below this, diminution of vision and eventual blackout will occur. Loss of vision precedes unconsciousness because cerebral flow is still adequate.

Visual failure is a continuum from loss of peripheral vision (grayout) to total loss of vision (blackout). One artery enters the retina at the optic disc, and arterioles and capillaries extend to the periphery. The details of the visual phenomena are presented in Section A.3 but are mentioned here because their genesis is cardiovascular.

The electrocardiogram shows some changes from the normal heartbeat pattern during $+G_z$. These consist of decreased amplitude and occasional inverted T waves (3) and altered systolic intervals (94). Cohen and Brown (45) also report an increased P wave. None of these anomalies are regarded as permanent or dangerous nor do they have much value in this study, other than to monitor any cardiovascular stimulation which may be attempted such as LBNP.

Tachycardia (fast heart rate) has been reported as a $+G_z$ effect. One interesting aspect is that the increased heart rate seems to start at the onset of acceleration (Figure A.2.1-6) (154). The increased heart rate precedes any reflex stimulus response. The data are for a miniature swine therefore preknowledge

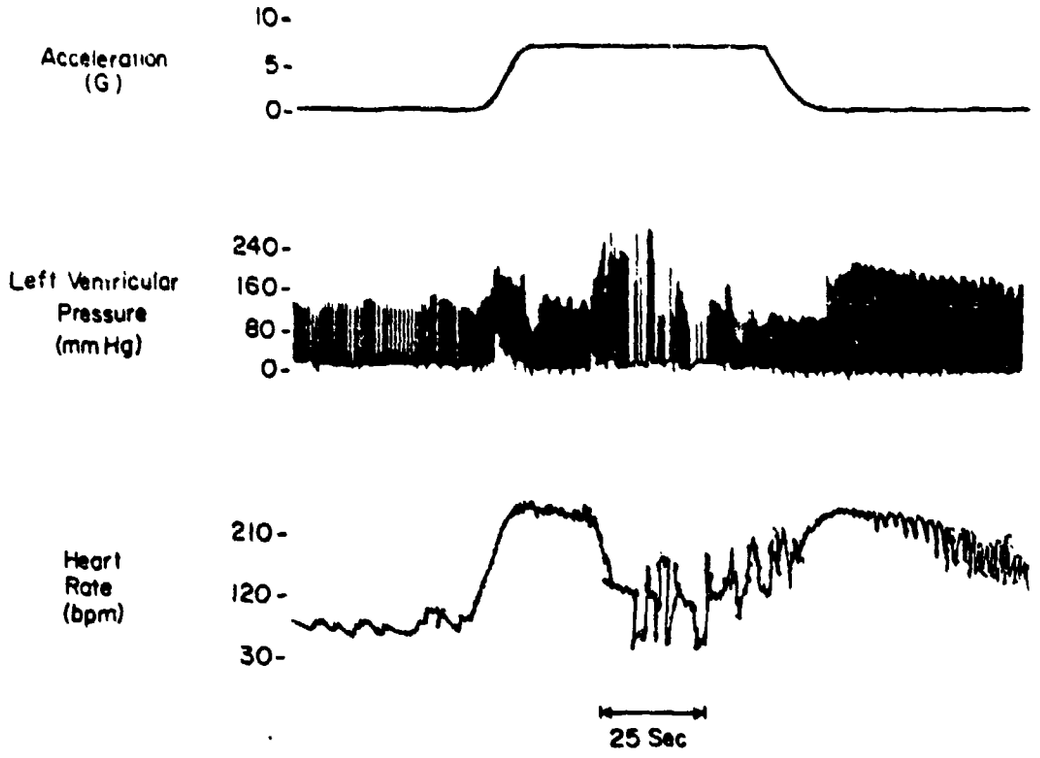


Figure A.2.1-6 A typical response to +7Gz in an unanesthetized miniature swine. Note the heart rate response to the acceleration profile (from Leverett and Burton (154)) (courtesy of Advisory Group for Aerospace Research and Development).

of centrifugation cannot be the reason. Perhaps general anxiety due to unfamiliar surroundings is the explanation.

NEGATIVE G_z

While $+G_z$ accelerations are the most often encountered and produce the most profound cardiovascular effects, $-G_z$ accelerations produce some significant cardiovascular effects. Negative G_z is an acceleration which produces a foot-to-head inertial force. Blood pressure above the heart rises immediately, including venous pressure. However, the intracranial venous pressure is counterbalanced by a rise in intracranial cerebro spinal fluid pressure, therefore the chance of intracranial hemorrhage is

slight. However, small hemorrhages surrounding the eyes cause significant problems.

After a few seconds of $-G_z$ acceleration the carotid sinus reflex and the high pressure receptors cause the arterial blood pressure to drop due to a slowing of the heart and a dilation of the arterioles. Asystole (missing a contraction) may occur and heart block may become imminent (3). Guyton (102) states that negative G_z produces such a strong baroreceptor reflex that severe vagal slowing of the heart occurs even to the extent of stopping the heart for 5 or 10 seconds.

The effects are the opposite of what occurs in $+G_z$. Blood from the lower part of the body drains towards the head causing the soft tissue of the face and neck to become engorged with blood.

This engorgement may cause petechial hemorrhages over the conjunctiva. This phenomenon may or may not cause the so called "redout". This $-G_z$ effect is controversial and is discussed in the visual section of this study. The blood engorgement produces a full feeling in the head and pain in the face and eyes.

Kennealy, et at (134) reported that all four subjects in their centrifuge study reported discomfort, but none lost consciousness or vision. All exhibited sinus bradycardia as well. These authors also state that -5 G_z was achieved by a national aerobatics champion, while Gillingham & Krutz (86) state that -3 G_z is considered the upper limit of human tolerance for "sudden" acceleration.

It is postulated by Howard (81) that negative G_z can produce unconsciousness even though the conditions have never been defined nor have they been produced in the laboratory. He further states that it is possible that unconsciousness may result from exposure

to accelerations greater than -4 or -5g, but the exact level depends on the duration, and that a minimum of 5 seconds of exposure is required for unconsciousness.

The major ECG changes are asystole, bradycardia (slowing of the heart), extra-systoles, alterations of the P wave and shifts of the pacemaker (firing pattern in the cardiac muscle) (81).

Gillingham & Krutz (86) do not consider negative G_z to be much of a problem in military flying because aircraft are not stressed for high $-G_z$ loads and hence pilots avoid it in their maneuvers whenever possible.

A.2.2 Effects of Transverse Acceleration

Transverse accelerations produce virtually no cardiovascular effects in the range of G_x that is part of a high performance jet aircraft operating envelope i.e., $\pm$2.5g for very short periods of time. Unless the accelerations reach 4 to 8g for 10 seconds or 2g for 20 minutes, the cardiovascular problems are minimal (81). These performance characteristics are outside of the operational envelope of today's fighter aircraft even for aircraft carrier launch and recovery operations.

A.2.3 Protective Devices

Protective devices are implements and techniques used by pilots of high performance aircraft to increase their tolerance to high acceleration. The implements commonly used are anti-G suits and tilt-back seats. The techniques employed are the M1 maneuver, the L1 maneuver (modified Valsalva), positive pressure breathing and various other forms of muscular/skeletal straining. The Muller maneuver is employed as a protective device for negative G's and is found to be effective in that environment.

The anti-G Suit (currently standard for United States military pilots) is a five bladder device, two calf bladders and two thigh bladders designed to reduce the venous pooling in the legs and an abdominal bladder which is designed to keep upward pressure on the diaphragm, both to reduce pooling and to limit the downward travel of the heart under G_z conditions, thereby maintaining the eye to heart distance.

Tilt-back seats are A/C seats wherein the standard seat back angle of 13° back from the vertical is increased in order to reduce the heart to eye distance along the Z-axis for G_z maneuvers.

BREATHING/STRAINING MANEUVERS

The M1 maneuver (straining maneuver number 1) is accomplished by repeated forceful exhalations against a partially closed glottis combined with generalized muscular straining. In addition the head is pulled down between the shoulders in an attempt to further reduce the eye/aorta distance. The M1 maneuver is generally repeated every four to five seconds during long duration exposures. The exhalation phase of this maneuver results in an intrathoracic pressure of 50 to 100 mm Hg. This raises the arterial pressure at head level and thereby increases $+G_z$ tolerance at least 1.5g (86). The inspiratory phase is generally a fast gasp followed immediately by the exhalation phase. It is important that the exhalation phase follows immediately since during inhalation the mean eye level blood pressure falls close to 0 mm Hg and could thereby cause loss of vision and possibly unconsciousness. The M1 maneuver is often referred to by pilots as a grunt maneuver. It is interesting to note that Burton (30) found in his experiments with miniature swine that this animal instinctively performs straining maneuvers not unlike the M1 maneuver which produces similar arterial blood pressure response to that reported for man.

In training for a properly performed M1 maneuver, subject safety is of considerable concern. Dr. Gillingham (82) reports that the properly performed M1 maneuver will raise the blood pressure at eye level by 100 to 150 mm Hg. He further states that he believes this to be an unacceptable risk in ground training and recommends against training for the M1 maneuver in a 1g environment. Gillingham (86) reports that the M1 maneuver contributes significantly to a raising of the heart rate. He asserts that a person performing a maximum M1 maneuver at 1g would have the same heart rate as those found during exposures to +6g.

Some persons report an irritation in the throat resulting from the M1 maneuver (33) which has led to a wider acceptance of the modified Valsalva (L1) maneuver. The modified Valsalva involves a protocol similar to the M1 maneuver with the exception that the exhalation is performed against the fully closed glottis. The difference between the Valsalva and the modified Valsalva or L1 maneuver is that the former is performed without the use of muscular contraction or straining. This has been found to not be an effective device for raising the tolerance to positive G's but indeed has the opposite effect. Therefore the original Valsalva maneuver is never used as a protective device in the high G environment.

Figure A.2.3-1 illustrates the effect of a Valsalva maneuver for a 3.7g profile. The left illustration is at 3.7g with and without the performance of the L1 maneuver while the right illustration is with the L1 maneuver and the vision remains clear up to 4.5g, whereas peripheral light loss occurred at 3.7g without the exercise maneuver. Figure A.2.3-2 illustrates the effect of an M1 maneuver for an 8 G_z profile. Notice that the blood pressure at eye level is kept elevated with this maneuver except for the inspiratory phase where it drops close to 0 mm Hg. Figure A.2.3-3 illustrates the effects of both an M1 and L1 maneuver to a 5.7g exposure. The comparison shows that the eye level blood pressure

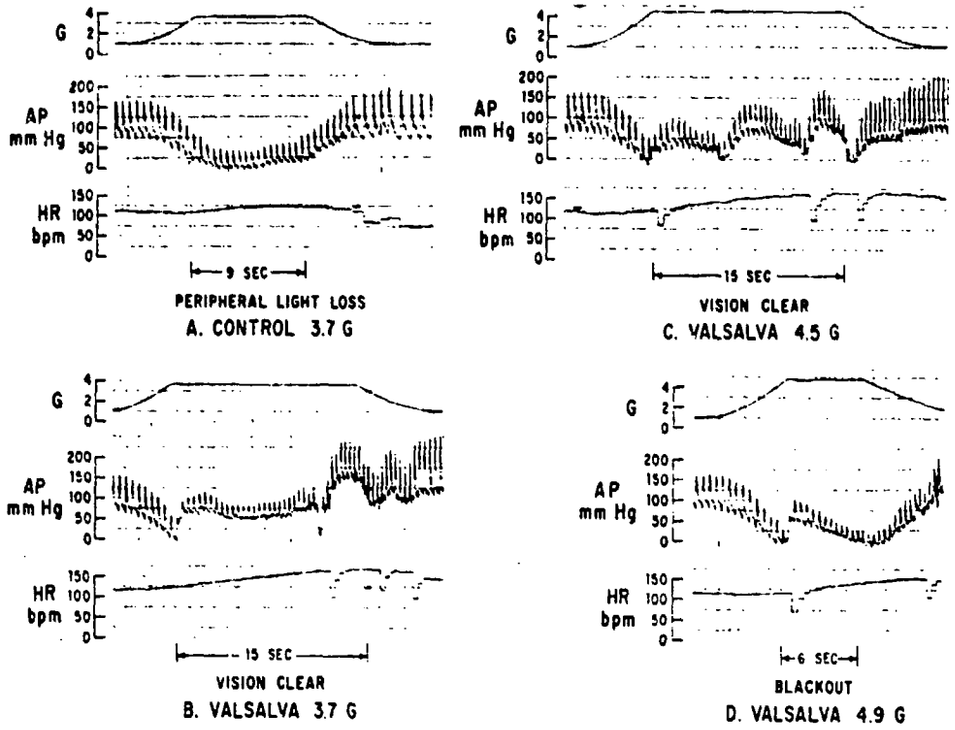


Figure A.2.3-1 Arterial Pressure (AP) and Heart Rate (HR) response to the valsalva maneuver with voluntary muscular straining without use of the anti-G Suit (subj. F). All arterial pressures are referred to eye level. Inhalations between repeated valsalva maneuvers in this and all other figures are indicated by the sudden drop in AP. Beat-by-beat HR was recorded from the ECG using a brush instruments cardiotachometer; occasional sharp drops in HR seen in this figure are artifacts occuring when baseline shift of the ECG prevented triggering of the cardiotachometer (from Shubrooks & Leverett (224)) (courtesy of Journal of Applied Physiology).

is elevated to essentially the same level by either maneuver and falls close to 0 mm Hg, also for either maneuver.

Both the M1 and L1 maneuvers have as their major drawback the fact that they are extremely fatiguing maneuvers and during prolonged air-to-air combat engagements may become ineffective because of the pilots unwillingness to continue to perform them. It has been reported by Shubrooks (222) that continuous positive pressure breathing provides the same level of protection as the M1 or

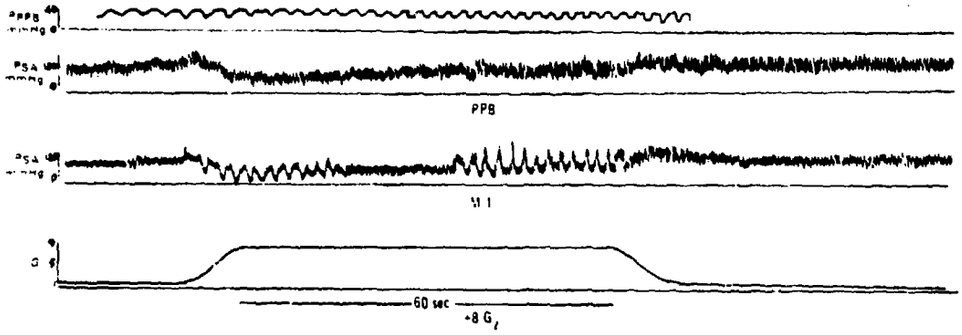


Figure A.2.3-2 Psa response during PPB and during M-1 maneuver at +8.0 Gz for 60s (subj. P). Acceleration profile, the same for both runs, is indicated in the lower tracing. Eye-level Psa for both maneuvers, performed 1 week apart, is shown along with breathing pressure (Pppb) for PPB (upper tracing.) (from Shubrooks & Leverett (224)) (courtesy of Journal of Applied Physiology).

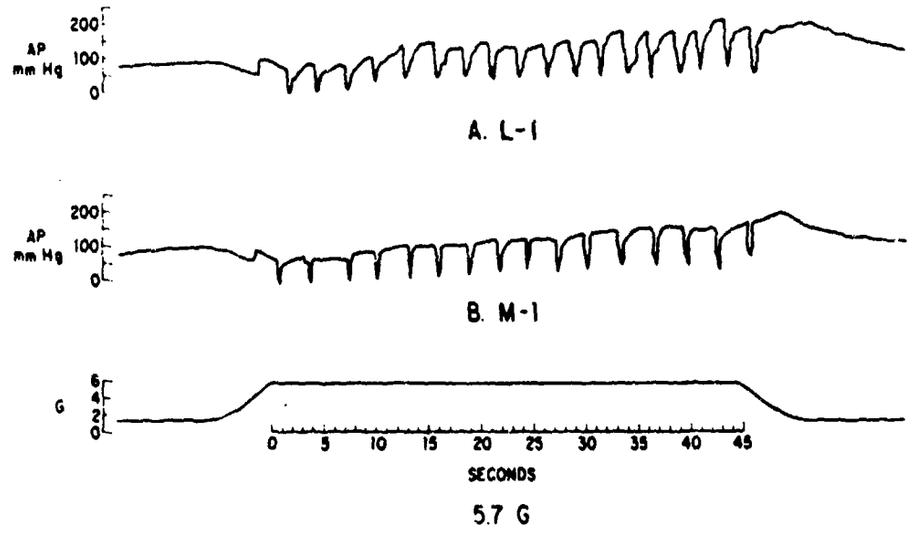


Figure A.2.3-3 Mean eye-level blood-pressure changes during +Gz while performing the M-1 and L-1 maneuvers. Mean blood pressure falls to zero during the inspiratory phase of either maneuver. (from Gillingham & Krutz (86)).

Ll maneuvers without the penalty of severe fatigue. Continuous positive pressure breathing has received the same endorsement from Gillingham (86). Figure A.2.3-4 compares the relative effectiveness of the Ml maneuver and positive pressure breathing. The esophageal pressure is presented for both maneuvers as an indicator of the amount of muscular straining required in the performance of both maneuvers. It is clear that much less straining is required for positive pressure breathing than for the Ml maneuver.

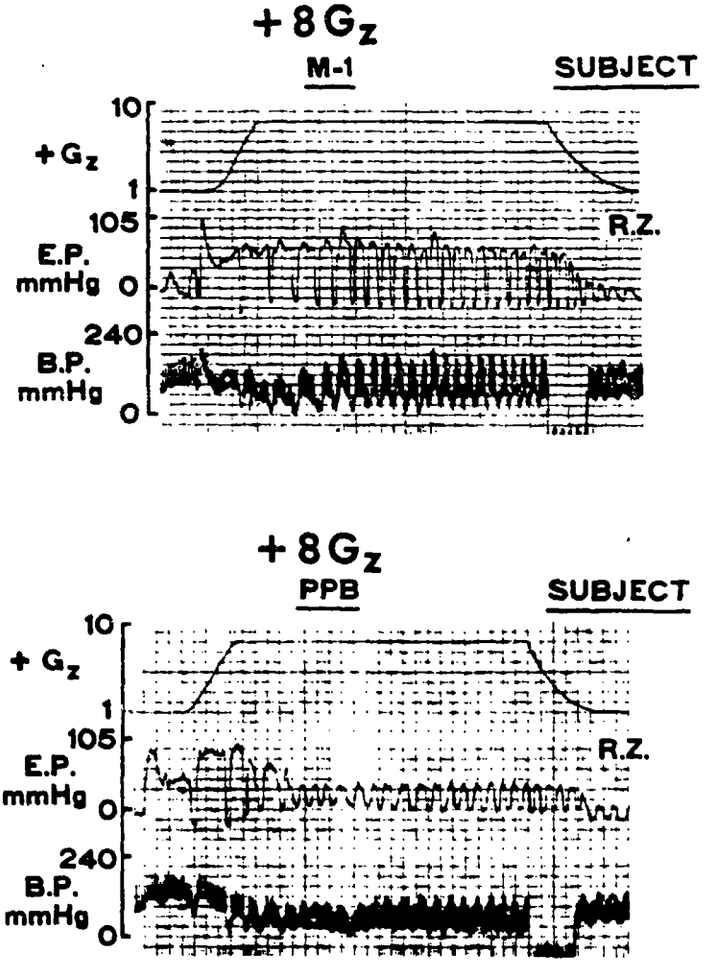


Figure A.2.3-4 Comparison of M-1 maneuver and positive pressure breathing (from Gillingham & Krutz (86)).

Another technique which has been shown to have varying degrees of effectiveness as a protective device is that of sustained static (isometric) muscular contraction. Lohrbauer (164) reports a linear rise in arterial blood pressure as long as the contraction is maintained. He states that mean arteriole pressure increases of 40 to 50 mm Hg at the point of fatigue are not uncommon during static exercise with a simple hand grip which utilizes forearm flexor muscles. Figure A.2.3-5 illustrates the effect of this maneuver for both rapid onset and slow onset positive G_z acceleration profiles. Varying degrees of muscular contraction can be used in the same manner to achieve some level of protection for example, increase tension in the leg muscles pressing on the rudder pedals, forearm upper arm contractions, back muscles and

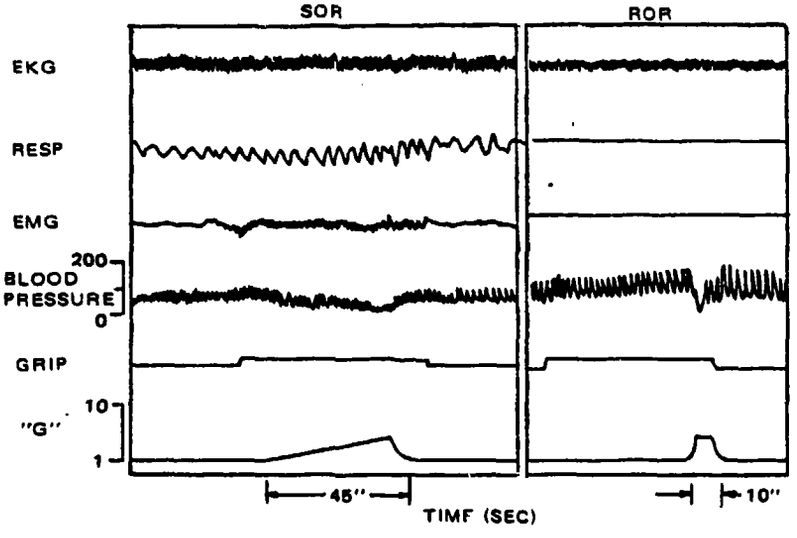


Figure A.2.3-5 Direct paper chart recording during a rapid-onset (ROR) and slow-onset (SOR) +Gz acceleration profile (from Lohrbauer et al (164))(courtesy of Journal of Applied Physiology).

neck muscles, contractions. Figure A.2.3-6 offers a comparison among four conditions, a control which employs no protective measures, a subject wearing G-suit alone, a subject employing the grip technique and a subject employing a grip technique and wearing a G-suit. Notice in all cases at rest the arterial blood pressure is approximately at 80 mm Hg. For the cases of both the G-suit and grip, and the grip case, the mean eye level blood pressure rises to about 100 mm Hg by the time the acceleration has reached its maximum, while the unprotected eye level blood pressure drops close to 0 mm Hg, the grip and the grip G-suit case remains at approximately 20 mm Hg or approximately the intraocular pressure thereby maintaining vision.

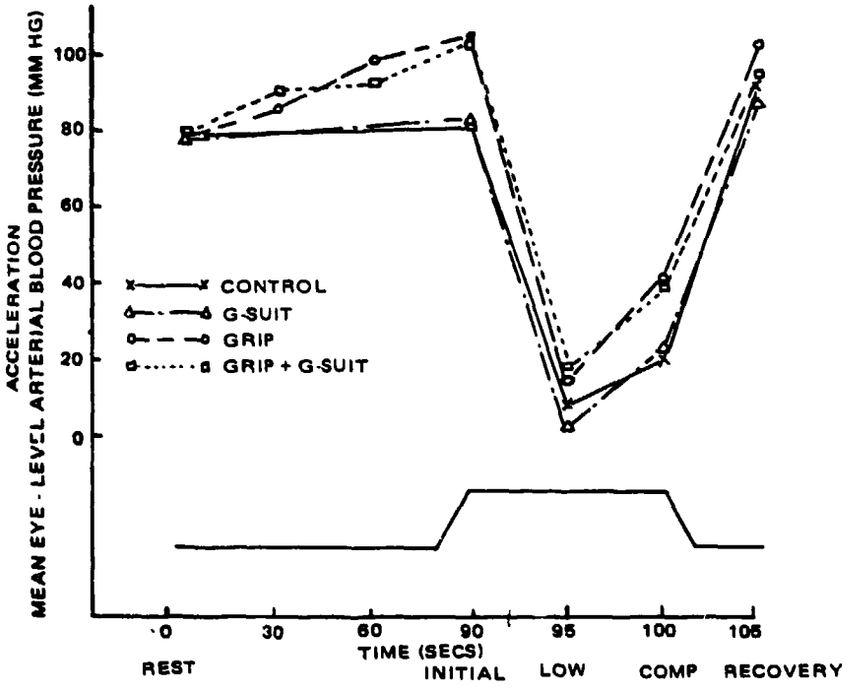


Figure A.2.3-6 Mean blood pressure for eight subjects during rapid onset run 0.2 - 0.3 G prior to the run in which peripheral light loss occurred (from Lohrbauer et al (164))(courtesy of Journal of Applied Physiology).

As was shown above, all of these techniques provide significant protection to the pilot and it is therefore important that pilots of high performance aircraft be instructed properly in the use of these maneuvers however, as Gillingham (82) has cautioned it may be dangerous to perform these maneuvers in a 1g environment. He offers as a solution training for pilots be accomplished in one of the Air Force's human centrifuge facilities. Another alternative will be discussed in the lower body negative pressure portion of this report.

The anti-G suit is perhaps the most well-known and most widely used device for providing high G protection. The basic description of the anti-G suit was provided above. The valve which controls the pressurization of the anti-G suit is activated at +2 G_z and thereafter increases suit pressure at the rate of 1.5 psi/g to a maximum of 10.5 psi. The anti-G suit gives about 1.5g increased tolerance above normal relaxed values (86). Burns (28) has suggested a relationship between acceleration tolerance (relaxed) and retinal/aorta vertical distance as;

$$G_T = \frac{180.3}{h} - 2.1 \qquad \text{[Eq. A.2.3-1]}$$

where G_T is G tolerance based on the end point of 100% PLL (peripheral light loss) with peripheral lights subtending a 50° angle, and h is the retinal/aorta distance in cm. Burton et al (34) have postulated the following relationships:

a) With an uninflated G-suit worn

$$G_T = 1.2\ G_C - 0.41 \qquad \text{[Eq. A.2.3-2]}$$

b) And for an inflated G-suit

$$G_T = 1.2\ G_C + 0.78 \qquad \text{[Eq. A.2.3-3]}$$

where G_C is G tolerance (PLL) without G-suit. G_T here was defined as 50% CLL (central light loss) or central light dimming (CLD).

Figure A.2.3-7 demonstrates the effect of the anti-G suit on the delay of peripheral light loss (PLL). The subject in question suffered peripheral light loss at 3.3g in the absence of a G-suit. However, with the anti-G suit he was able to withstand 4.6g before peripheral light loss. Figure A.2.3-8 illustrates in the first panel the effects of 3 G_z without anti-G suit, panel B the effects of + 3 G_z with anti-G suit and panel C the effects of +6 G_z with the protection of an anti-G suit. There remains no question as to the efficacy of an anti-G suit. Also, in recent years, it has been demonstrated that the anti G-suit can be well simulated and provide useful cues in a ground based flight simulator. The thrust of the research in this study, towards the anti-G suit, is to determine the magnitude of the cardiovascular effect such that any additional stimulation or simulation that occurs in the presence of this garment can have the appropriate compensation for the device's effect.

TILT BACK SEATS

Another device which has been well studied is the effect of a tilt back seat on a pilot's tolerance to high acceleration. While extensive investigation has been carried out in this area, it is only with the introduction of the F-16 aircraft that the implementation of tilt-back seats has been provided. Spacecraft have used

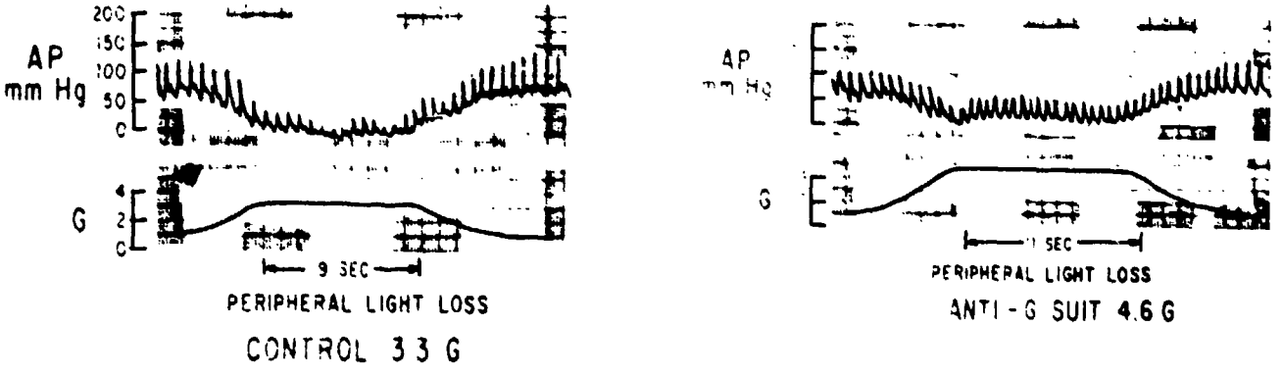


Figure A.2.3-7 Increase in +Gz tolerance afforded by a standard 5-bladder Anti-G suit (relaxed subject) (from Gillingham & Krutz (86)).

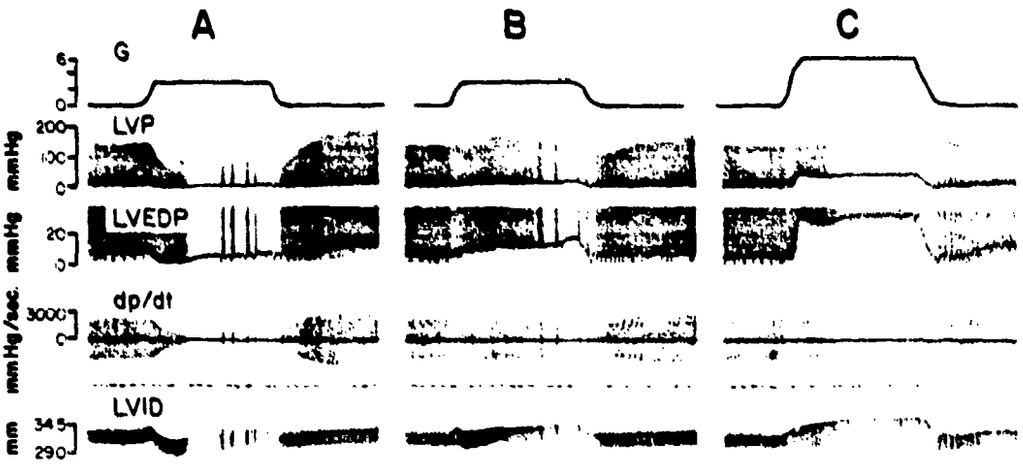


Figure A.2.3-8 Effects of +Gz acceleration with and without an Anti-G suit. Responses to +3Gz without Anti-G suit are illustrated in Panel A. Responses with suit inflating at 2.2 G are illustrated in Panel B (+3Gz) and Panel C (+6Gz). In each panel, top trace represents the G profile; LVP = left ventricular pressure; LVEDP = left ventricular end-diastolic pressure; dp/dt = first derivative of LVP; LVID = left ventricular internal diameter. Bottom trace is time in seconds. (from Peterson et al (197)) (courtesy of Journal of Applied Physiology).

body postural attitude as a protective device since the beginning of the manned space program. As was previously stated, the purpose of a tilt-back seat is to reduce the vertical heart-to-eye distance. Figure A.2.3-9 illustrates the effect in vertical heart-to-eye distance at various angles of the seat-back orientation. It is interesting to note that the vertical heart-to-eye distance actually increases before it begins to decrease proceding from 0° from the vertical to larger angles and it isn't until 30° where the heart-to-eye distance is the same as it was at 0° (28 cm). This is due to the fact that the eye is actually forward of the vertical plane through the heart. These geometric data explain the lack of significant difference in relaxed tolerance between the 13° back angle and the 30° back angle as mentioned by Burns

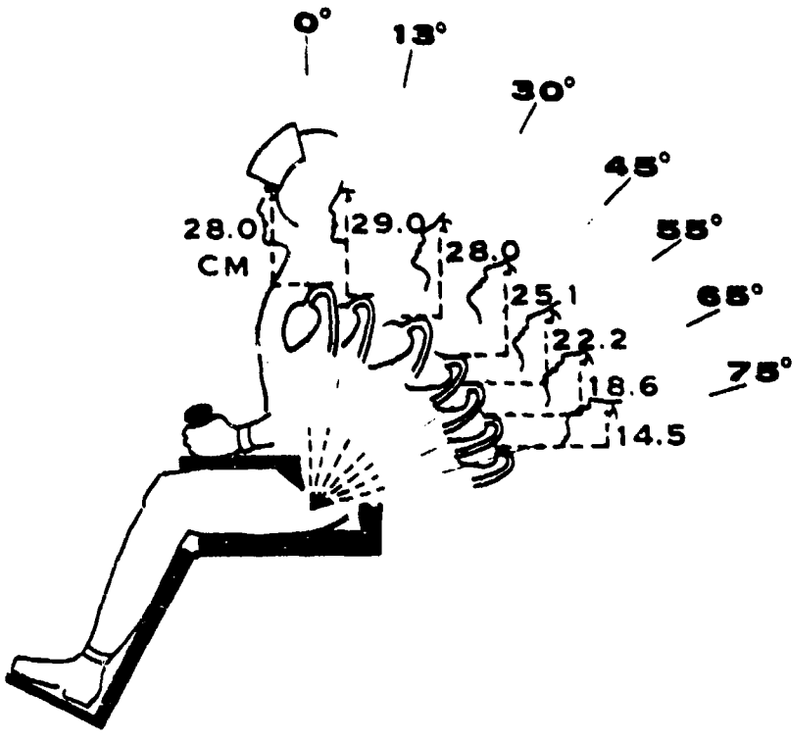


Figure A.2.3-9 Decreased vertical heart-to-eye distances obtained by tilting backward (from Burns (28)) (courtesy of Aviation Space and Environmental Medicine).

(28). According to Gillingham (86) significant tolerance increase is not achieved until a 45° tilt from the vertical is obtained. Accurate simulation models must take into account both the effects of an anti-G suit and the effects of the seat back angle in order to provide appropriate training. Burns (28) has also postulated a relationship for heart rate as a function of carotid sinus/aorta vertical distance in cm.

$$HR = 3.4\ h_c + 53 \qquad \text{[Eq. A.2.3-4]}$$

All the aforementioned devices or implements are used primarily for increasing G_z tolerance in the positive direction. However, with modern aircraft flying at high angles of attack and

with seat back angles such as the F-16, 30° from vertical tilt, accelerations in the aircraft X axis can produce substantial components along the physiological Z-axis and vice versa. This factor furthermore, must be taken into account in any simulation which includes these devices.

NEGATIVE G PROTECTION

Information on techniques for increasing the tolerance to negative G_z acceleration is somewhat less plentiful than for positive G_z. In fact, in the literature search only two papers were uncovered dealing with this subject. Both papers refer to the Muller maneuver. This maneuver is essentially the opposite of the M1 or L1 maneuver. The glottis is closed and the subject attempts inspiration. According to Putzulu (201), this maneuver was first proposed in 1838 by Muller specifically for the purpose of demonstrating the effects of respiration on blood circulation and determining the effect of negative intrapulmanory pressure on a reduction of venous pressure.

A U.S. Air Force Aero Medical Laboratory memorandum of January 1948 (2) discusses the subject of venous pressure in the head under negative acceleration and the authors point out that the Muller experiment causes a decrease in intrathoracic pressure and results in a marked relief of discomfort during exposure to negative acceleration. However, this maneuver was performed in an intermittent fashion since it was found to cause alarming symptoms when sustained under negative G. Since this maneuver is not well documented in the current literature it seems that no further consideration should be given presently, however, it could be a subject of future research in this area.

Another technique which has apparently not received extensive research is the effect of cooling local areas to increase the tolerances to positive acceleration. It has been shown that local

cooling of the legs, particularly (133), has increased the tolerance to positive acceleration, by local thermally induced vaso-constriction, on the order of 0.3 g. This device has received so little attention and is apparently not used in the active services and therefore, it also bears no further attention at this point in time.

PROTECTIVE DEVICES SUMMARY

This section has attempted to set forth a description of the effects of the various protective devices such that any simulation or stimulation techniques suggested in the mechanization portion of this study would have the benefit of a proper physiological basis for these protective devices. The implementation of any simulation devices should not interfere with the effect of standard pilot procedures under high G environment. In fact the intent will be to incorporate those effects into the software drive model such that any delays of achieving various thresholds due to protective devices will be taken into account.

A.3 Visual System

Loss of visual acuity is one of the most profound effects of high acceleration flight maneuvers. The fact that a pilot "blacks out" under certain high "G" conditions limits his capabilities in the air-to-air combat arena. The advent of modern fighter aircraft, with low wing loading and high thrust, has caused the pilot and not the airplane to be the limiting factor.

The visual effects are perhaps the most heavily researched area of high acceleration physiological reactions. However, much of the data that have resulted from this research are not easily correlated due to an absence of standard definitions and techniques. The genesis of virtually all visual effects is cardiovascular. In the Z-axis, the major problem is either not enough

blood at the retina ($+G_z$) or too much blood ($-G_z$). For accelerations along the aircraft longitudinal axis the visual effects are minimal and have cardiovascular, mechanical and respiratory origins. The vast majority of research in the high "G" environment has been conducted for positive G_z. This is motivated by the fact that fighter aircraft have the greatest capability in that direction.

At this point a brief anatomical description of the eye is appropriate to provide background for the ensuing discussion. Figure A.3-1 is an illustration of the right eye viewed from the outer side showing the visual axis passing through the center of the lens to the point of sharpest vision at the fovea, where cones are concentrated. The distribution of the central retinal artery explains the changes in the ability of the eye to function in an excessive-G environment. Each of the retinal arteries' branches is an end artery without anastomotic connections (interconnection of arteries and veins). After the main artery enters the eyeball at the optic disc, it divides, then subdivides into

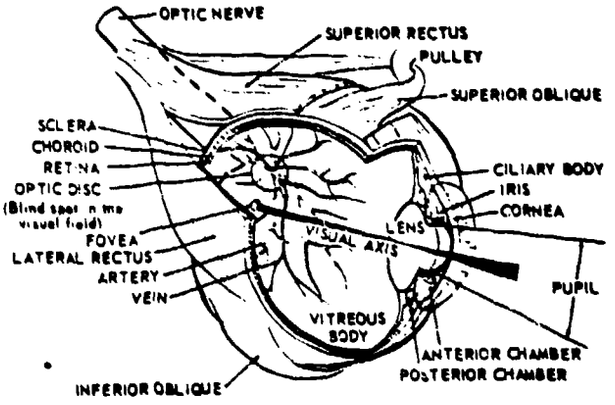


Figure A.3-1 Right eye, viewed from outer side, showing visual axis passing through center of lens to point of sharpest vision at fovea, where cones are concentrated (from Taylor (194)).

increasingly fine vessels as they approach the periphery of the retina, resulting in a blood pressure reduction as the vessels decrease in size.

If the blood supply is reduced, it is not unreasonable to assume that the reduction in vision would proceed inward from the periphery in a somewhat concentric manner. There is some asymmetry, however, due to the fact that the retinal artery does not enter at the center of the retina (Figure A.3-2). The pattern of the visual field collapse will be discussed later.

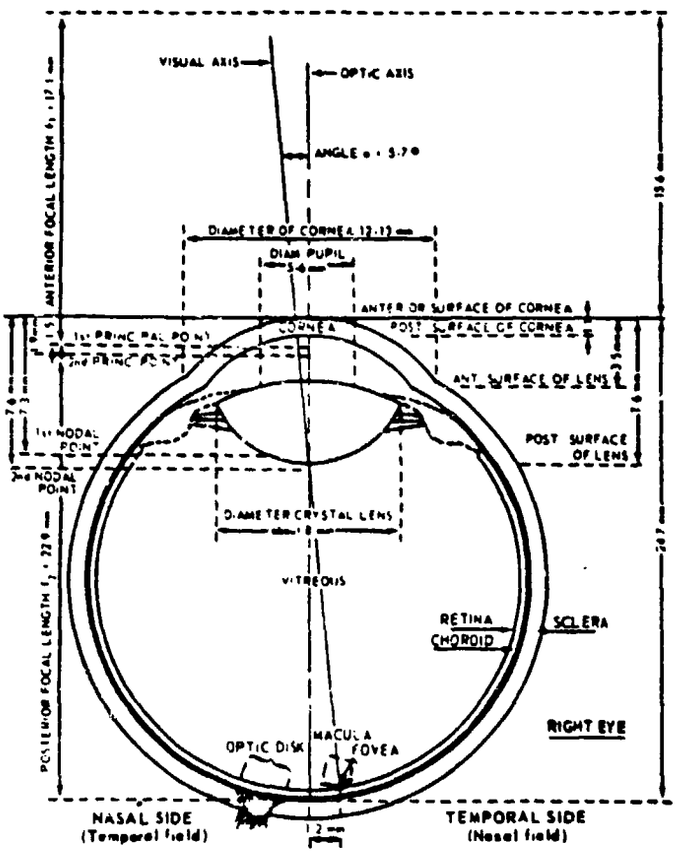


Figure A.3-2 Dimensions of the human eye (from Taylor (194)).

Since there is no direct blood supply to the fovea it is reasonable to assume a degradation in visual acuity prior to the blackout. This may explain reports of "veiling", or "dimming" of vision.

A.3.1 Visual Effects of Vertical (G_z) Acceleration

As was stated previously this regime of acceleration is the most well researched area of acceleration visual effects. It is also the most important (especially positive G_z) vector to be considered since it is the most often encountered and it produces the most significant effects.

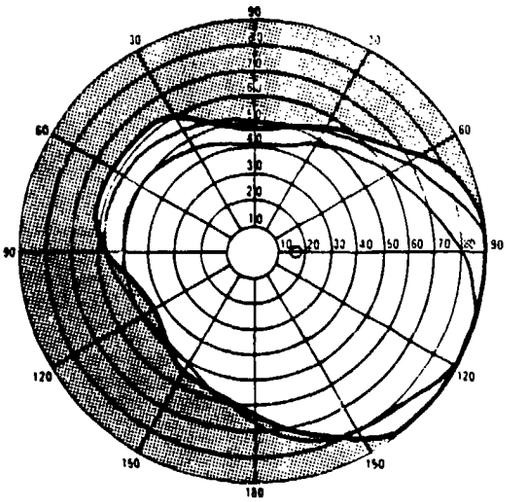
VISUAL ENDPOINTS

Grayout and blackout are the most often employed endpoints used in acceleration research. However, the lack of a clear definition of these two terms is a handicap in attempting to apply the results of various research uniformly. It is generally accepted that grayout is the loss of peripheral lights (PLL) and that blackout is the loss of central light (CLL). But, there does not exist a uniformly employed standard for peripheral lights or central lights in terms of angular reference from the fixation point, or some other convenient point. Also, intensities of the lights employed are not necessarily standardized. Unconsciousness is an often used endpoint, which is sometimes confused as "blackout". Parkhurst, et al. (195) echo this sentiment and support it with data from several sources that state different thresholds:

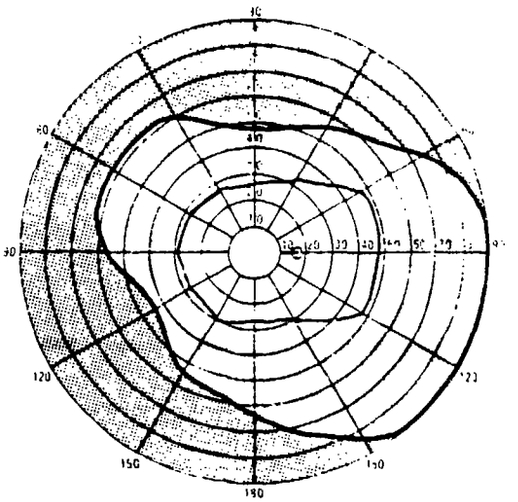
Researcher	PLL	CLL	UNC
Howard	4g	5g	5.5-6.0g
Cochran	4.1g	4.7g	5.4g
Gauer	3.0-3.5g	----	4.5-5.0g

Other variables which affect the results are the onset rates employed, duration, the size of the centrifuge arm and the variations in the population.

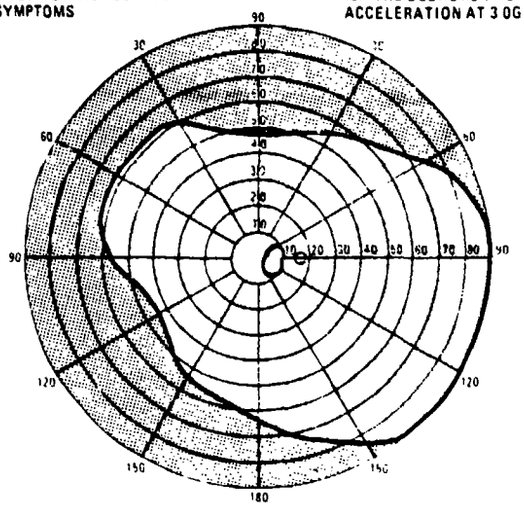
The geometry of visual field collapse has not been widely researched. Gillies et. al (81) (Figure A.3.1-1a, b, & c) and Jaeger (57) (Figure A.3.1-1d, e, & f) have provided some insight



(A) THE DECREMENT OF THE VISUAL FIELD DURING POSITIVE ACCELERATION AT 2.8G – NO VISUAL SYMPTOMS



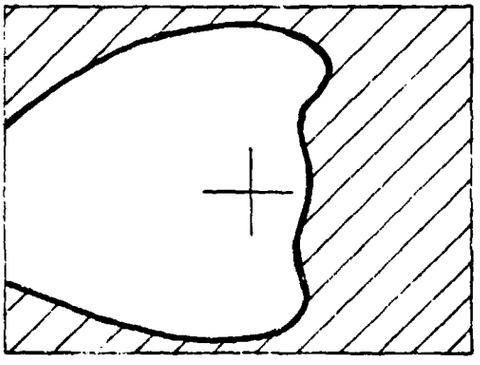
(B) THE DECREMENT OF THE VISUAL FIELD DURING POSITIVE ACCELERATION AT 3.0G – "GREYOUT" AND LOSS OF PERIPHERAL VISION



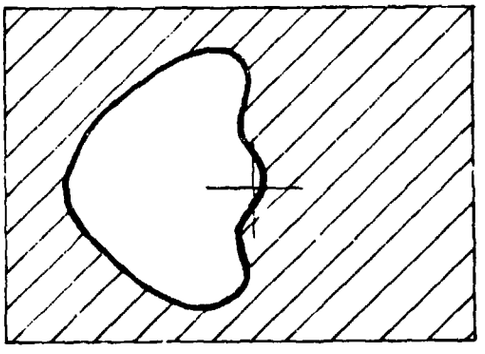
(C) THE LOCATION OF THE LAST REMAINING AREA OF VISION AS BLACK-OUT IS APPROACHED

Figure A.3.1-1 a,b, &c Degradation in the field of view at three levels of acceleration (from Howard, Gillies et al (81)).

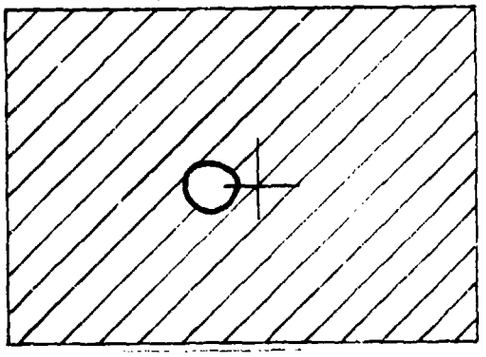
into this aspect of the problem. Howard's plots illustrate the degradation in the field of view at three levels of acceleration: 2.6g (a), 3.0g (b) and the last remaining area of vision as blackout is approached. The elliptical area to the right of the fixation point is the "blind spot" at the optic disc. Note that the last remaining island of vision is between the fixation point and the blind spot.



Initial field loss is pronounced in the nasal field (left eye). Temporal field loss is minimal and limited to the periphery. These illustrations represent a composite field loss of the group tested.



Nasal field loss (left eye) approaches fixation and temporal peripheral field loss is more pronounced.



The subject is approaching blackout. Fixation has disappeared and the last remaining island of vision is located 5-10^0 peripheral to fixation.

Figure A.3.1-1 d, e, & f Monocular visual field loss (from Jaeger et al (127)). "Field" as used above refers to that field as seen by the left eye.

Jaeger's data was taken by use of plethysmographic goggles and verified by centrifuge runs. The two data sets illustrate basically the same results with slightly different geometry. However, the details of Howard's experiments are not known; therefore correlation is difficult.

Experiments by Gillingham & McNaughton (87) seem to have produced some of the best information on visual field collapse. Figure A.3.1-2 illustrates the remaining upper half of the three different seat-back angles.

The rate at which the visual field collapses is also not thoroughly researched. Haines (107) provides the results of his work with gradual onset rates (GOR) of acceleration which are not applicable to the fighter aircraft environment. Kydd (146) presents data on time to PLL for haversine input profiles which probably fairly closely resemble aircraft acceleration profiles. However, PLL is only one point, albeit not a uniformly defined one.

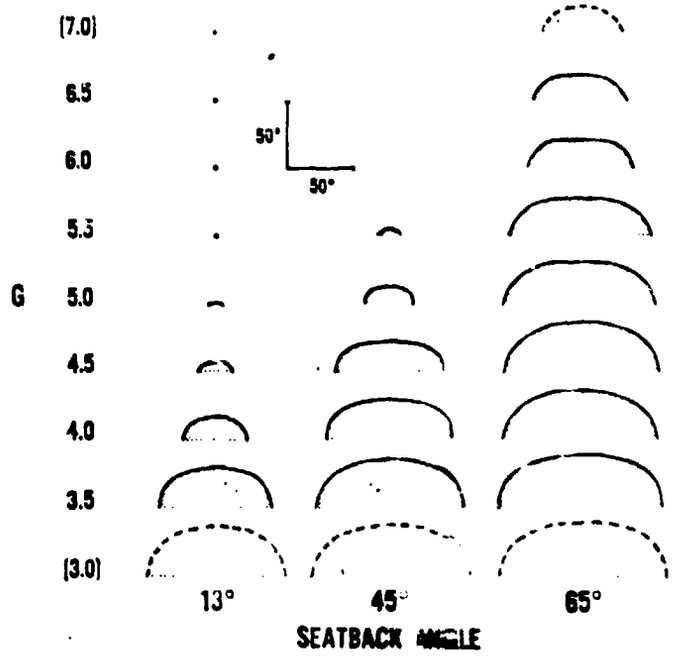


Figure A.3.1-2 Remaining upper half of three seat-back angles from Gillingham & McNaughton (87 [courtesy of Aviation Space and Environmental Medicine).

Gillingham & McNaughton (87) have provided some useful data in this area as well. Figure A.3.1-3 illustrates some of these data; however, the effects of onset rate and duration are not easily separated.

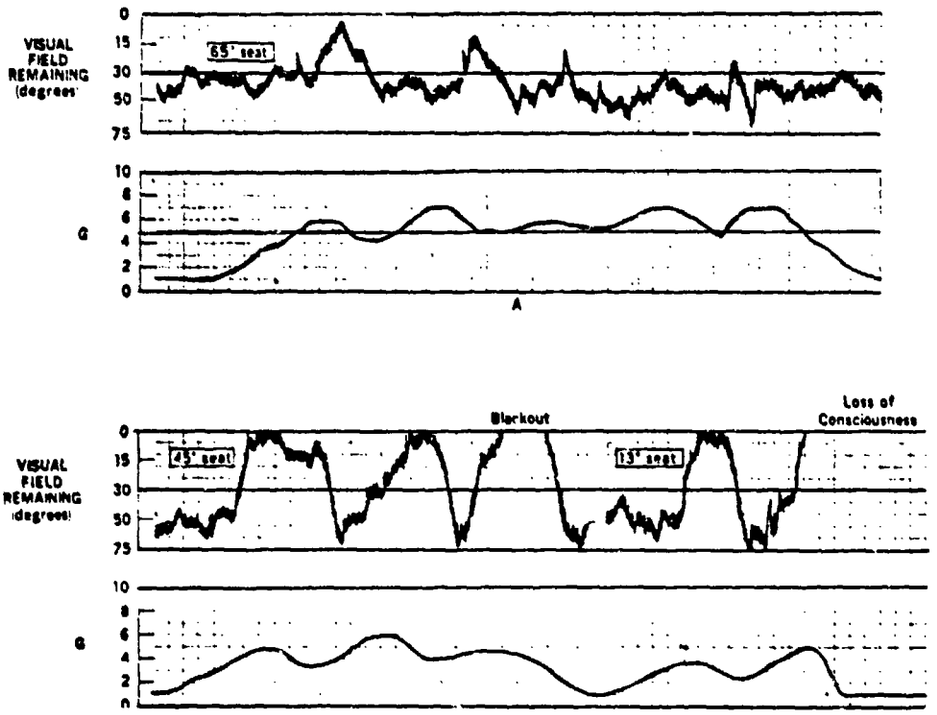


Figure A.3.1-3 Responses of subject G. M. operating visual field limit tracker in vertical mode during simulated ACM G stress at 65°, 45°, and 13° seatback angles. At 65°, subject tolerated 7-G peaks with little visual loss; at 45°, he blacked out after a 6-G peak; at 13°, he lost consciousness during a 5-G peak. (from Gillingham & McNaughton (87)) (courtesy of Aviation Space and Environmental Medicine).

MATHEMATICAL MODEL OF VISUAL SYSTEM

The manner in which the physiological effects of vertical acceleration are discussed is to employ a mathematical model of the system. Figure A.3.1-4 presents this mathematical model.

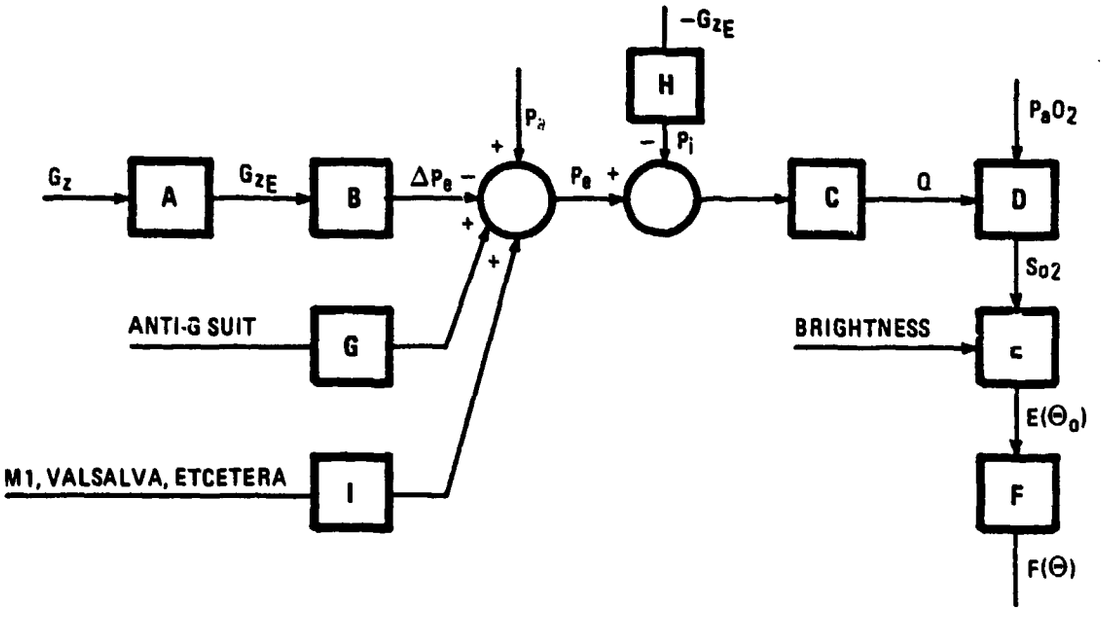


Figure A.3.1-4 Mathematical model of visual effects of acceleration.

Block A represents the relationship of heart-to-eye distance as a function of aircraft seatback angle. This reflects the altered hydrostatic pressure requirements due to different seatback configurations. The normal heart-to-eye vertical distance measured in an erect seated position is approximately 28 cm. The manner in which the distance changes is illustrated in Figure A.3.1-5.

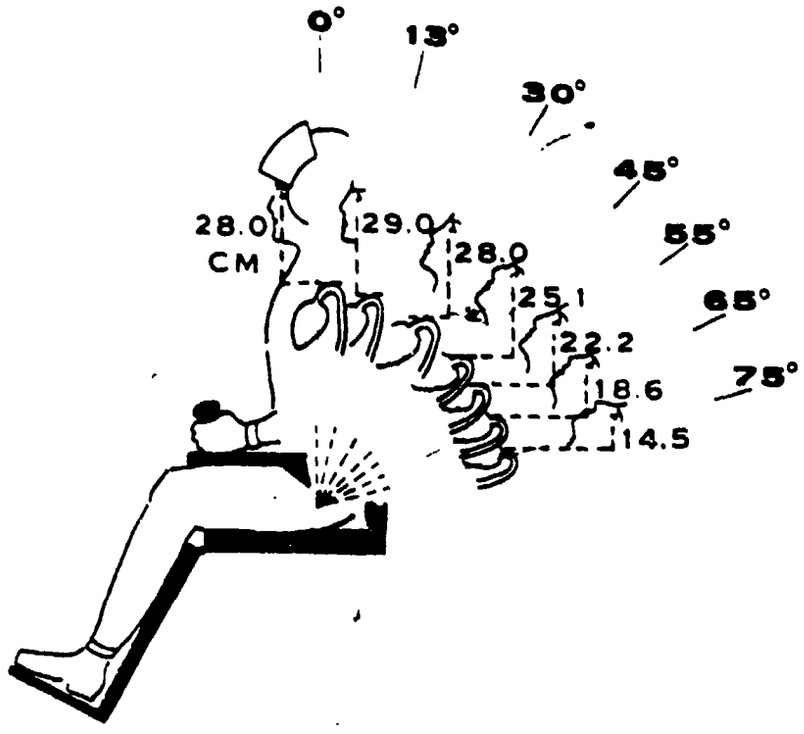


Figure A.3.1-5 Decreased vertical heart-to-eye distances obtained by tilting backward (from Burns (28)) (courtesy of Aviation Space and Environmental Medicine).

As can be seen there is no significant decrease until a seat back angle of 45° is attained. Current aircraft seat back angles do not exceed 30°. Assuming 28 cm distance, a pressure of 25 mm Hg is required to overcome the force of gravity in order to raise the blood from heart to eye level. With an acceleration of +4 G_z (4g turn), the pressure required would be about 100 mm Hg. Assuming the subject's systolic arterial pressure at the heart level is 120 mm Hg, the systolic pressure of blood at the head level during exposure to a force of 4g would be 120 minus 100 mm Hg. Assuming that the normal intraocular pressure is approximately 20 mm Hg, it is evident that the blood flow to the eye will cease under these conditions (1).

The effects of acceleration on vision can be compared to the impairment produced by applying pressure to the eyeballs with a tonometer. As the intraocular pressure is increased above eye level arterial pressure, the vascular wall collapses, thus reducing retinal blood flow and causing progressive impairment of vision. Andina (81) found that complete loss of vision was produced when effective blood pressure in the central retinal artery was reduced to 21 mm Hg (82). With the normal intraocular tension being about 20 mm Hg, he concluded that there existed no blood flow into the eyes.

SEAT BACK ANGLE EFFECTS

The relationship for Block A can be given as:

$$G_{ze} = \frac{G_z \, D_{H/E} \, (SA)}{28} \qquad \text{[Eq. A.3.1-1]}$$

Where G_{ze} is the effective acceleration, $D_{H/E}$ is the approximate heart to eye distance in centimeters, from Figure A.3.1-6, as a function of seat back angle. The function given as Figure A.3.1-6

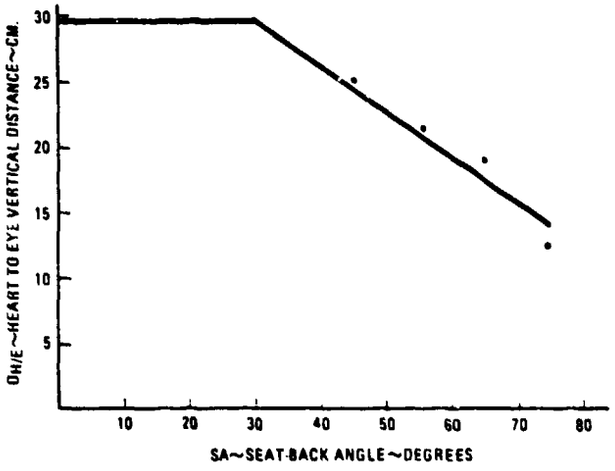


Figure A.3.1-6 Heart-to-eye vertical distance as a function of seat-back angle.

is approximated from the data of Figure A.3.1-5. Since the model is largely a series of approximations, a linear approximation here does not cause a reduction of rigor and is quite adequate.

EYE LEVEL BLOOD PRESSURE

Next a relationship between effective acceleration and a change in eye-level blood pressure must be provided. This is represented as Block B in Figure A.3.1-4. The change in eye level blood pressure due to acceleration is not a simple function of acceleration. Howard (81) feels that the time dependencies are of a vascular origin, i.e., capillary vessels within the eye hold blood pressure until the main artery is in total retrograde flow. Early work in this area suggest that high G visual disturbances are dependent on onset rate. Stoll (234) experimentally developed the relationship among rate of onset, symptoms, and elapsed time from onset to symptoms as shown in Figure A.3.1-7. More recently, Gillingham et al. (85) developed a G to mean eye level blood pressure transfer function, H(s), of the form:

$$H(s) = \frac{A(s) + B(s)\ D(s)}{1 + B(s)\ C(s)} \qquad \text{[Eq. A.3.1-2]}$$

where A(s) represents the direct effects of the hydrostatic load on the blood and body, B(s) represents the various neural, hormonal, and mechanical effectors that translate control signals into blood pressure (primarily via changes in the heart rate, venous compliance, and arterial resistance), and C(s) represents the dynamics of the several baroreceptor feedback mechanisms. The effects of the vestibulo-cerebellar inputs to the cardiovascular control system are included in D(s) (85). Figure A.3.1-7 presents the comparison of the empirical results with the actual response. The results of Gillingham's (85) work produced the following transfer function:

$$H(s) = -18.1 \frac{1 + 7.66s}{1 + 4.46s + 7.63s^2} e^{0.464s} \quad \text{[Eq. A.3.1-3]}$$

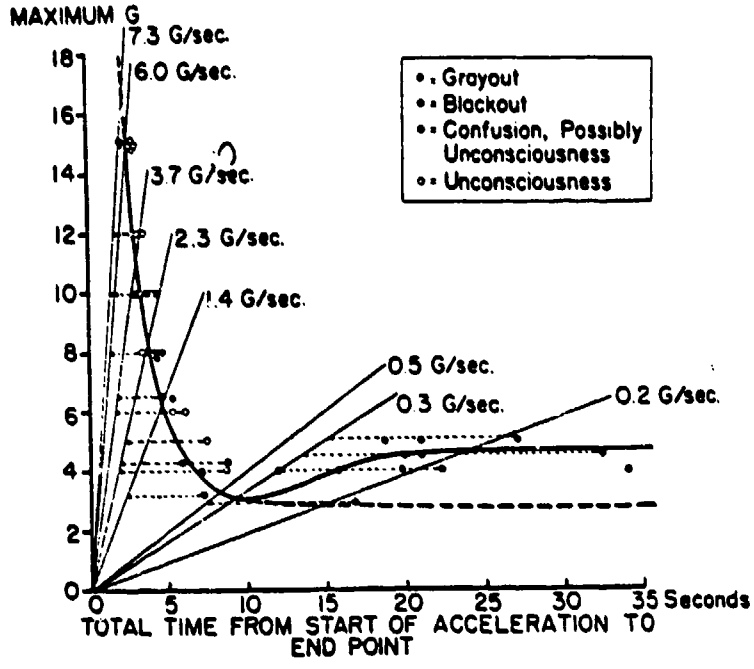


Figure A.3.1-7 G-tolerance curve with various acceleration rates (from Stoll (234)) (courtesy of Journal of Aviation Medicine).

EFFECTS OF PROTECTIVE DEVICES

To this point in the discussion, all considerations were with a relaxed pilot with no protective devices. This is not normally the case, as high performance fighter pilots wear anti-G suits and employ straining maneuvers such as the Valsalva, M-1, or positive pressure breathing.

Table A.3.1-2 illustrates the effects the anti-G suit and Valsalva maneuver have on the PLL end point.

The data from Shubrooks & Leverett (224) given in Section A.2.3 of this report indicate an elevation of the eye level blood

pressure of 50-80 mm Hg for the Valsalva maneuver. Gillingham and Krutz (86) show approximately 60 mm Hg increase. Therefore it seems reasonable to employ a relationship such as;

$$P_{es} = 60 \text{ mm Hg} \qquad \text{[Eq. A.3.1-4]}$$

for any of the straining maneuvers. A detailed explanation of the maneuvers is given in Section A.2.3 of this report.

Table A.3.1-2 +Gz levels at which end points occurred during 15-s exposures along with visual symptoms at each end point and time at which they occurred.

Subj	Control	Valsalva w/o suit	Suit Alone	Suit + Valsalva
A	3.1 PLL-9s	4.0 PLL-10s[a]	4.5 PLL-5s	5.2 PLVD-11s[e]
B	3.9 PLVD-7s	5.2 PLL-7s	6.1 NVS-15s[d]	6.3 NVS-15s[d]
C	4.4 PLL-14s	5.1 PLL-14s[b]	5.4 PLL-15s	7.0 NVS-15s[f]
D	3.3 PLL-9s	3.9 PLL-6s	4.6 PLL-11s	6.2 PLL-7s[g]
E	4.3 PLL-6s	5.0 NVS[c]	5.3 PLL-4s	6.8 NVS-15s[h]
F	3.7 PLL-9s	4.9 BO-6s	5.2 PLD-15s	6.7 PLD-6s[i]

Abbreviations: PLL = peripheral light loss; PLVD = peripheral light dim; BO = black out; NVS = no visual symptoms. [a]PLL during long inhalation; Psa 60/27 just before centrifuge stopped. [b]PLL at end of single valsalva held for 14s. [c]Psa did not fall below 86/65 except during the one inhalation when peripheral lights dimmed slightly. [d]With suit alone at 6.1 G and with suit + valsalva at 6.3G, peripheral lights were approximately 50% dimmed early in run only, followed by complete clearing of vision; Psa was at most times higher during the valsalva run. Valsalva maneuver was not well performed. [e]PLVD during prolonged inhalation at 11s; full run was completed and Psa had increased to 65/40 just before centrifuge stopped at 15s. [f]Psa never less than 60/45 and was 120/80 at end of run. No further runs were performed because of fatigue. [g]PLL during prolonged inhalation at 7s; Psa had increased to 75/25 just before centrifuge stopped. [h]Psa at no point lower than 75/55 and had reached 182/120 during third valsalva just before end of run. No furtner runs performed because of fatigue. Peripheral and central lights approximately 50% dimmed during inhalations; Psa was 115/50 just before the inhalation. All above arterial pressures are referenced to eye level. (from Shubrooks & Leverett (224)).

A relationship for change in eye level blood pressure due to the use of an anti-G suit (ΔP_{egs}) is derived from the following considerations. Burton et al. (34) have postulated the following relationships for an increase in G tolerance due to wearing and inflating an anti-G suit. These relationships were defined in Section A.2.3.

If it is assumed that the increase in eye level blood pressure is 25 mm Hg for each G unit of increased tolerance the equation for ΔP_{egs} in mm Hg is given by

$$\Delta P_{egs} = 25\ (G_T - G_C) \qquad \text{[Eq. A.3.1-5]}$$

The algebraic sum of all the pressure changes is taken with heart level arterial pressure (P_a) which then yields the resulting eye level blood pressure (P_e).

INTRAOCULAR PRESSURE

The block H represents a transfer function which relates intraocular pressure to G_z. Intraocular pressure is normally relatively constant, being maintained by a complex pressure regulation system. Young & Supfer (271) propose the model

$$\Delta P_i(t) = \Delta V_{(t)}\ KP_o e^{-KP_o Ct} \qquad \text{[Eq. A.3.1-6]}$$

to relate change in intraocular pressure (ΔP_i) to change in external volume. In the above equations K represents scleral rigidity, P_o the nominal intraocular pressure, and C the flow conductivity. This relationship holds for a non-acceleratory environment. A relationship between ΔV_T and acceleration must be determined. To date none has been found.

Another approach might be possible, however, based on the fact that in a $-G_z$ acceleration environment venous return flow is

stopped. An acceleration of -3 G_z results in venous pressures on the order of 100 mm Hg (86):

"As the pressure in the vessels of the neck increases during $-G_z$, the carotid sinus reflex and reflexes initiated by low-pressure system volume receptors cause a slowing of the heart and a dilation of the arterioles. The reduced heart rate and the decreased total peripheral resistance cause the arterial pressure to approach the venous pressure. As the pressure gradient across the capillaries declines, cerebral blood flow decreases. This may result in cerebral stagnant hypoxia if the acceleration is prolonged" (86). Within the ocular circulation system, elevation of the intraocular pressure results in the dilation of the distensible blood vessels, chiefly the choriocapillars. When all the blood vessels dilate ad maximum, the intraocular pressure prevents the access of blood to the eye (1). The restricted blood flow produces ocular hypoxia and the general "grayout" and eventual loss of vision.

The relationship for intraocular pressure in this case is given by

$$P_i = 33\ (-G_z) \oplus + 20 \qquad \text{[Eq. A.3.1-7]}$$

where the symbol $\oplus$ implies that If $(-G_z) \leq 0$; $P_i = 20$
If $(-G_z) > 0$; $P_i = 33\ (-G_z)+20$.
However, this only admits to changes in P_i due to negative G_z. No support for the position that there is any change from + G_z has been found.

RETINAL CIRCULATION FLOW RATE

Block "C" represents the integration of the difference in eye level blood pressure and the intraocular pressure. The integration over the vessel area would yield the flow rate or velocity of

blood into the retina circulatory system. Of prime interest is the mass flow rate of oxygen to the retina. As flow rate slows, the peripheral retina may have insufficient oxygen to perform properly. Block "C" appears as

$$Q = \int \frac{(P_e - P_i)}{A} \, dt \qquad \text{[Eq. A.3.1-8]}$$

This term may be treated as a parametric control system, in which the resistance (A) is a positive monotonic function of $(P_e - P_i)$, going to ∞ with $P_e \geq P_i$, representing vessel collapse. Now combining the flow rate in the retinal circulatory system and the partial pressure of oxygen in the inspired air, the oxygen saturation at a particular point θ from the fovea could be computed if a relationship were available. However, none has been found to date. Another approach is to compute oxygen saturation ($S\text{-}O_2$) from a function derived from the data of Figure A.3.1-8, which relates P_aO_2 to G_z.

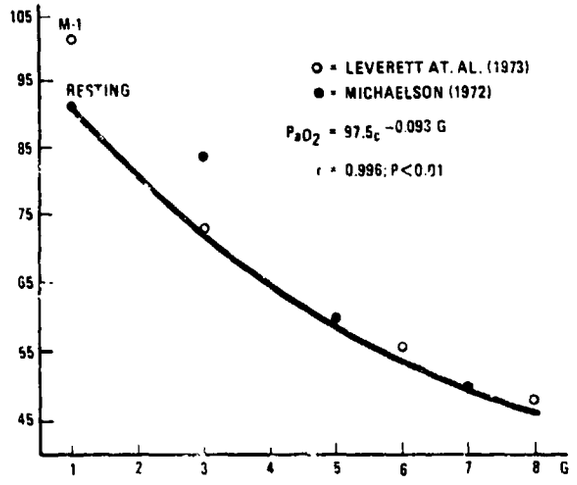


Figure A.3.1-8 Changes in P_{aO_2} associated with various levels HSG (from Burton, Leverett, and Michaelson) .

This relationship would appear in Block D. Another approach would be to relate blood pressure to visual effects with a delay and neglect O_2 tension. Further, if this approach were employed it would be advisable to consider the visual effects as a function of the product of acceleration and time in a "leaky" integral.

If a suitable relationship were available, the model would continue as Block E relates the level of oxygen saturation ($S\text{-}O_2$) at some angle θ. The output of Block E is then the dynamic response of that portion of the retina based on predicted $S\text{-}O_2$ levels. Block F represents the spatial relation of acuity of θ_o to the full acuity. The output is $D(\theta)$ and would follow a relationship of the form illustrated in Figure A.3.1-9.

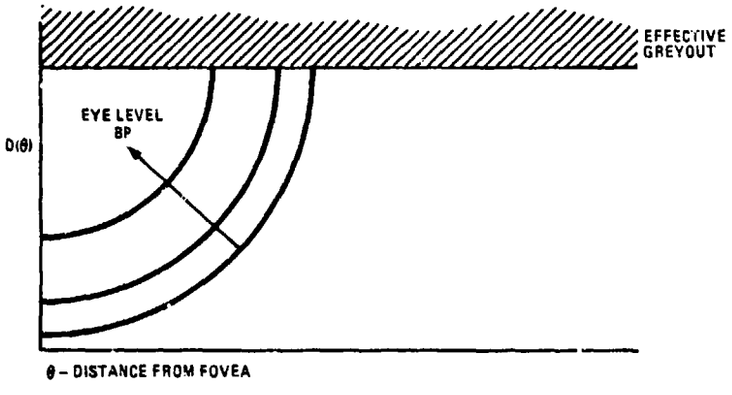


Figure A.3.1-9 Visual acuity relative to the fovea at a function of eye-level blood pressure.

The intersection of D_o, θ_o, and predicted eye level blood pressure yield the minimum discrimination angle visible at any particular point in the pilot's field of view.

Blocks D, E & F are not defined in current literature. Therefore a modified model appears in Figure A.3.1-10. Here Block C is a simplified model of C, D, and E. The representation maintains the model in blood pressure. The block contains a gain as a function of G to represent the change in P_aO_2, hence a change in $S\text{-}O_2$ of arterial blood and a first order lag that simulates the time dependency of depletion of oxygen in the retinal peripheral vessels.

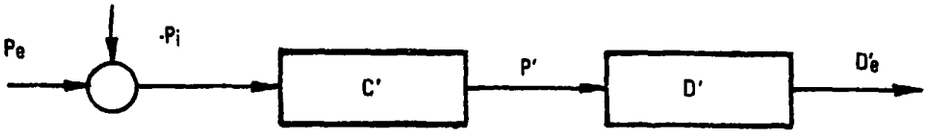


Figure A.3.1-10 Blood diagram of modification to visual effects model eliminating requirement of functional relationships among blood pressure, flow rate and 0_2 saturation.

Block C' would contain the relationship,

$$\frac{P_e - P_i}{P'} = \frac{K(G)}{Ts+1} \qquad \text{[Eq. A.3.1-9]}$$

where P' is the predicted blood pressure.

D' (θ) is then the relation of minimum discrimination angle as a function of predicted blood pressure in the eye and angular measure from the fovea. A relationship for D' (P', θ) is not available in the literature other than to be derived from relationships of acuity as a function of G_z and blood pressure (P') also as a function of G_z.

It is known that as positive acceleration lowers the central arterial pressure, blood flow stops in the small peripheral vessels. Haines (105) suggests there is a critical closing pressure

(pressure within a blood vessel) which is reached in the extreme peripheral area of the retina. The onset of the closing was evident in vision for greater than 70° from the line of sight (104). Krutz et al. (145) correlated the blood flow in the superficial temporal artery and direct eye level blood pressure to subjective visual symptoms during $+G_z$ accelerations. When blackout was approached (2.7 to 4.6 g's), eye level arterial blood pressure began to fall concomitant with the occurrence of retrograde flow in the temporal artery (Figure A.3.1-11 and Figure A.3.1-12). Zero forward temporal flow (Q_{TA}) was determined with both graphic and audio recordings 6 seconds (4 to 9 range) prior to blackout. Eye level mean arterial pressure (P_a) decreased to 20 $\pm$1 mm Hg when zero forward Q_{TA} was initially recorded (144). Based on arterial distribution, increasing acceleration should, by progressively cutting off the blood supply to the peripheral parts of the

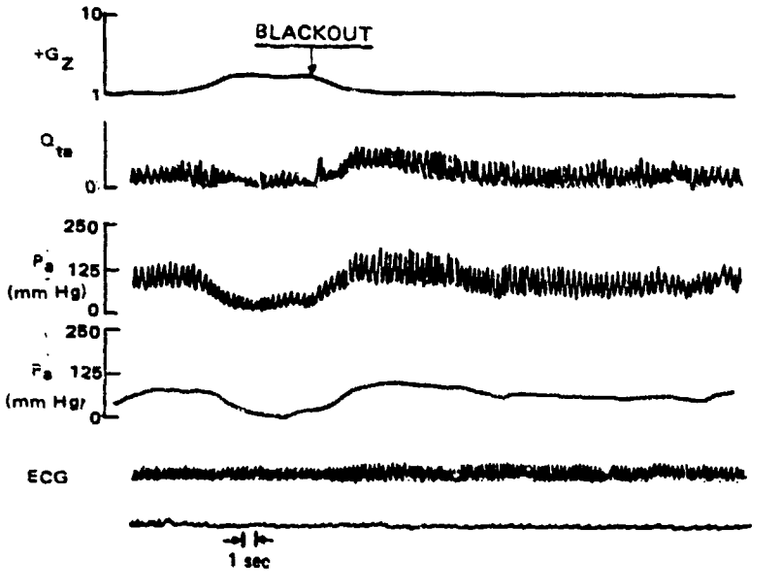


Figure A.3.1-11 Eye-level arterial pressure and blood flow responses during rapid onset run (ROR, 1 G/S). Qta = nondirectional temporal artery blood flow velocity; Pa = eye-level arterial blood pressure; $\bar{P}a$ = mean eye-level blood pressure. (from Krutz et al (144)) (courtesy of Journal of Applied Physiology).

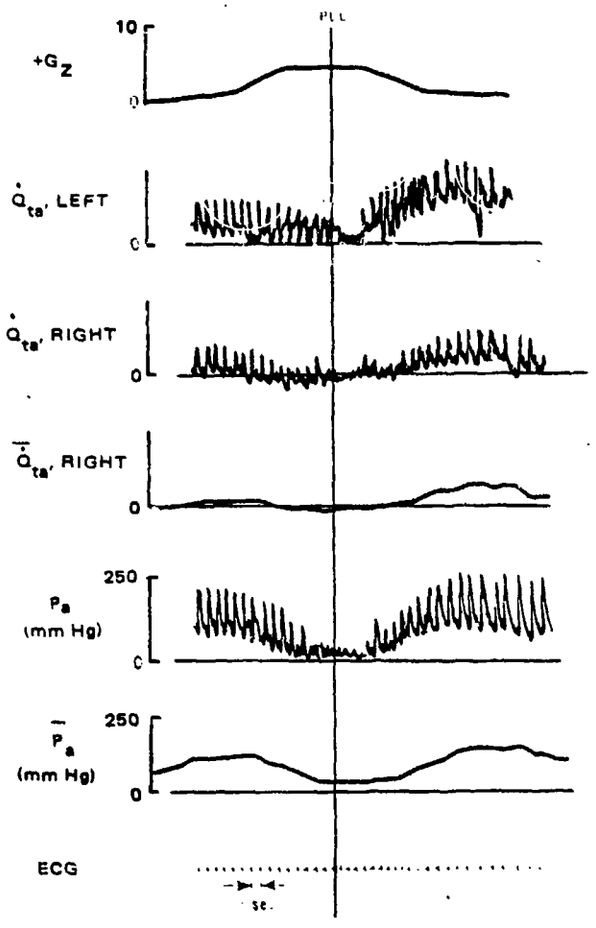


Figure A.3.1-12 Occurrence of retrograde flow in the temporal artery prior to peripheral light loss (PLL) and subsequent blackout. A nondirectional signal processor was used with the transducer on the left temporal artery; a directional signal processor was used with the transducer on the right temporal artery. (from Krutz et al (144)) (courtesy of Journal of Applied Physiology).

retina, produce an almost concentric narrowing of the field of vision. Since there is no direct arterial supply to the fovea, visual acuity degenerates well before perception of light is lost (81) (Figure A.3.1-1).

The derivation of this model has neglected any changes in color perception as a function of $+G_z$. There is no fir

indicate that color changes occur during high sustained $+G_z$. Brightness has also been neglected. Only at very low light levels (less than 0.2 ft-L) is visual perception a function of luminance and $+G_z$ (98).

A simplified model relating G_z to visual field remaining appears in Section 4.3.3. This model can currently be used in any mechanizations while the more sophisticated model must await further research.

NEGATIVE G EFFECTS

Some further notes on negative G_z are appropriate at this point. In general a small percentage of aircraft maneuvering is accomplished in the negative G environment. This is a result of two factors: 1) aircraft are not stressed to accommodate this environment and 2) pilots are uncomfortable in this environment and therefore avoid it. The most controversial area of negative G_z is that associated with the "redout" phenomenon. This phenomenon has had a great mystique associated with it. Some report that it has never been reproduced experimentally (86), some report it has occurred in flight (81 & 176), and one author has reported its occurrence in the centrifuge (Ryan (214)).

The mechanism which causes redout is also controversial. Some postulate petechical hemorrhages proliferated by lacrimal fluid; others conjecture that the engorged conjunctiva are pulled over in the eyes. Even the reports of it in flight are sporadic, causing the phenomenon to remain somewhat enigmatic. Also reported by Howard (81) is an occurrence of halos surrounding bright objects. While grayout dimming has not been reported (134), Ryan (214) reports "Visual symptoms during the negative G tests were frequent and diverse in character. Blurring of the vision was the most common complaint. A few subjects noted some graying of vision, while others, particularly during the -2.5 and $-3G_z$ runs,

experienced a reddening of vision, involving either the whole visual field or only its periphery".

Another interesting visual phenomenon, the "elevator effect", (43) is described in Section A.4.1 of this report.

A.3.2 Visual Effects of Transverse Acceleration

The visual effects of transverse G are minimal. According to Gillingham & Krutz (86), subjects have withstood up to 15 G_x without blackout. Some visual disturbances have been noted above 12 G_x. These disturbances have been in the form of blurring and excess lacrimation. The authors conjecture that the visual aberration may be caused by distortion of the eyeball due to the large force acting on the eye.

Duane (62) reports similar findings. Graying, he states, may be due to retinal ischemia, but he further states that no way to measure this is available. Duane noted that in myopic subjects, posterior shortening of the globe may occur.

Very little research has been accomplished in regard to lateral acceleration. Some petechiae have been reported in the right orbit at -5 G_y; also a scleral hemorrhage occurred at +4 G_y. Blurred vision was reported by one subject at +4 G_y. These effects are reported in Fraser (71); however, the likelihood of exposure to accelerations of this magnitude along the Y-axis of the body is virtually nonexistent.

A.3.2.1 Lacrimation

Blurring of vision at relatively high levels of prone and supine G acceleration effects (G_x) is not uncommon and has been attributed to lacrimation, the process of tears forming in the eyes, disrupting the path of incoming light rays. In most cases,

the symptom does not occur until G levels exceed the 6g range and is still evidenced in the 12 to 14g region (50, 86). Although the lacrimal event does not appear to be sensitive to the direction of G_x the authors note the use of adjectives "abundant" and "excessive" used to describe tearing under $-G_x$ (50, 244), whereas those accounts describing similar experiences under larger magnitude plus G_x conditions simply note the occurrence of lacrimation (86, 160). It is possible that more than one mechanism is at work in acceleration induced lacrimation.

The literature offers little insight into the causes of acceleration induced lacrimation. Secretions to lubricate and protect the eyes fall into three categories (1). Normal lacrimation lubricates and protects the conjunctiva/cornea interface and is issued in small quantities by accessory lacrimal glands of Wolfring and Krause located in the superior and inferior fornix, a sac beneath upper and lower eyelids (Figure A.3.2.1-1). Secondly, an oily secretion is exuded to the edge of the upper and lower eyelids to the cheek. The third category of secretion is the pro-

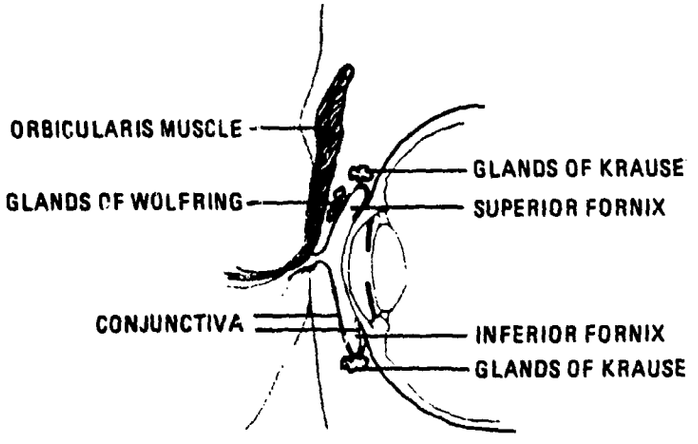


Figure A.3.2.1-1 Sagittal section through eyelid and eyeball (after Whitnall (1)).

duct of the lacrimal gland located in the upper temporal quadrant of the orbital area of the eye (Figure A.3.2.1-2). Whereas the accessory lacrimal glands produce only enough lacrimal fluid to keep the cornea/conjunctiva moist and much of this is lost to evaporation (181), the lacrimal gland can produce sufficient quantities of fluid to produce significant tearing and flush the eye of irritants.

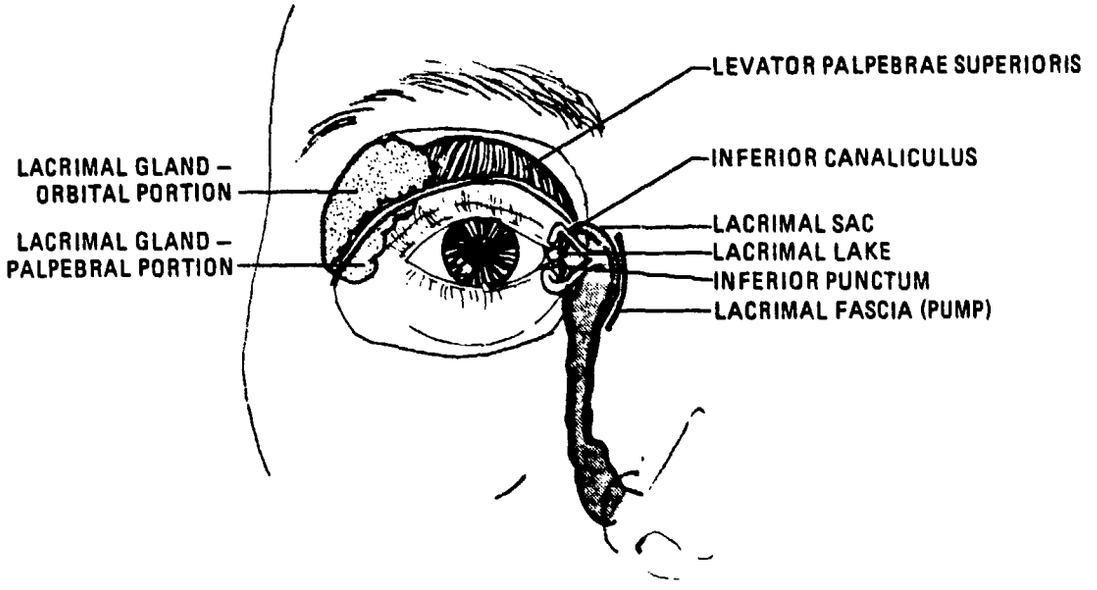


Figure A.3.2.1-2 Frontal diagram of selected elements of the right eye (modified after Adler (1)).

Lacrimal fluid generally enters temporally and is moved in a nasal direction under the "squeeze" action of orbicularis muscle to collect the lacrimal lake at the inner canthus. Upper and lower punctum form drains permitting fluid collecting in the lacrimal lake to enter the lacrimal sac through the tube-like canaliculi. Dissections of the lacrimal sac reveal a pumplike diaphragm which moves in a direction parallel to the horizontal plane. Tears form when lacrimal fluid flow from the lacrimal gland and the accessory

lacrimal glands exceed the capabilities of the lacrimal sac pump, canaliculi, and punctum to drain the lacrimal lake.

The literature suggests three types of lacrimation, but the innervation of each is not precisely and definitely known. Normal lacrimation from the accessory glands is governed in part by the cervical sympathetics (1), and it is also noted that parasympathetic and sympathetic fibers join the efferent nerve path leading toward the lacrimal gland (see Figure A.3.2.1-3), suggesting that normal secretion from the accessory lacrimal glands might be augmented at times by the lacrimal gland. The second type of lacrimation is psychic, the product of emotion, and its stimulus arises centrally and appears on the 7th cranial nerve path serving as the efferent nerve path leading to the lacrimal gland, which suggests lacrimal fluid issued during psychic weeping is primarily the product of the lacrimal gland. The third type of lacrimation is also a product of the lacrimal gland, wherein large quantities of fluid are required to flush the eye, and is known as reflex lacrimation.

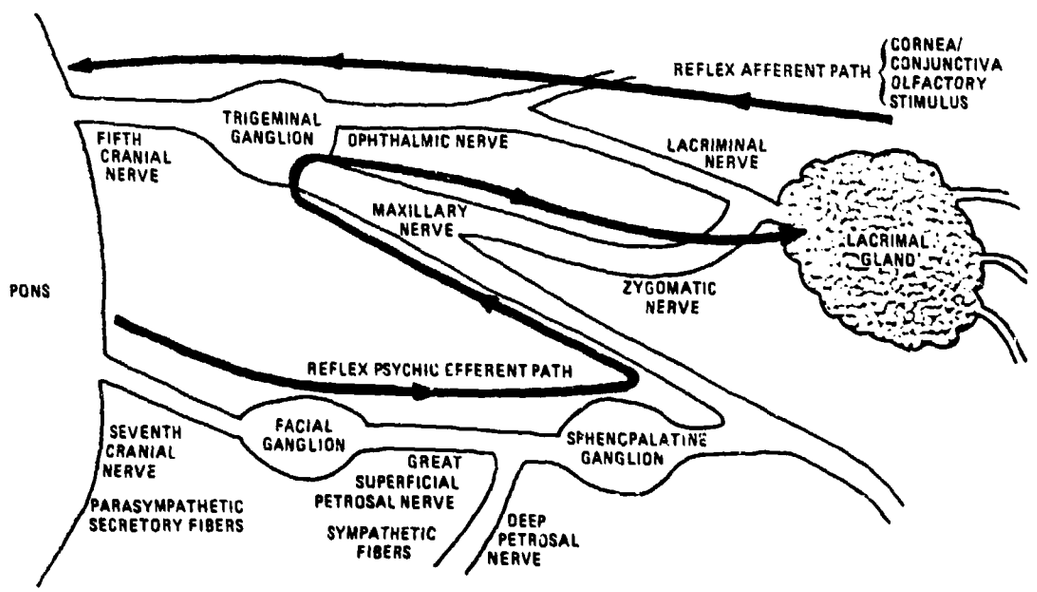


Figure A.3.2.1-3 Primary afferent and efferent pathways affiliated with the lacrimal gland (after Adler and Mutch (1)).

Afferent reflex stimuli issued when the conjunctiva or the olfactory sensors become irritated, travel inward along the lacrimal nerve, a branch of the ophthalmic division of the 5th cranial nerve. The reflex arc is completed by the appearance of reflex induced stimuli appearing at the 7th cranial nerve and traveling the efferent path to the lacrimal gland.

It does not seem reasonable to attribute acceleration induced lacrimation to psychic weeping because the emotional stress of $+G_z$ seems likely to be of the same or larger magnitude as that accompanying G_x yet lacrimation is not documented as a $+G_z$ symptom. A similar but less convincing argument might be made for reflex lacrimation. Superficially, it would seem that both G_x and G_z might cause conjunctiva/olfactory stimulation; however, without a detailed examination of the dynamics of these sensors as affected by the inertial effects of both x and z acceleration, the argument must be held in abeyance. It would be most interesting to subject individuals known to be capable of psychic weeping but possessing a dysfunction of the reflex afferent path to a G_x centrifuge experience in order to determine if lacrimation occurs. The absence of the symptom would build a case for acceleration induced reflex lacrimation. The presence of lacrimation in G_x but not G_z would tend to indicate that a mechanical rather than neurological condition is responsible for acceleration induced lacrimation.

A clue, possibly implicating mechanical rather than neurological lacrimal cause, is provided by Duane (62), who recounts a NASA experiment in $-G_x$ centrifuge runs wherein a graying of the visual field was observed at the 6 to 8g region. Cinephotography of the eyes captured the appearance of a tear film forming in the upper temporal quadrant of the eye and spreading across the cornea. The film issued from the region of the lacrimal gland and not the accessory lacrimal glands, suggesting that possibly this gland, caught between the forward inertial force of the eyeball and the unyielding boney structure forming the temporal portion of

the eyeball socket, may have been mechanically squeezed, inducing issuance of lacrimal fluid. The fact that the tear film spread across the cornea can obviously be attributed, in part, to inertial effects operating on the fluid as well as surface tension. It would also indicate the lacrimal issuance was in sufficient quantity to justifiably be considered the product of the lacrimal gland.

As earlier stated, the authors found lacrimation documented as occurring in both plus and minus G_x with less definitive statements associated with + G_x occurrence. Likewise, lacrimal gland compression in $+G_x$ does not seem so plausible. If we are to accept lacrimation, and unless there exists a major disruption in the accessory lacrimal glands significantly increasing their production capability, it would seem that the lacrimal gland must also somehow be involved in $+G_x$ lacrimation. A possible exception to this might exist if the lacrimal sac were found, under inertial compression, to permit already drained lacrimal fluid to reverse flow through the canaliculi into the lacrimal lake.

G CUING POTENTIAL

In the absence of considering the possible effects of drug usage, the only path to reliably induce lacrimation in the unaccelerated state appears to be through reflex arc stimulation. Initially, the authors felt that exposing the eye to a gaseous irritant would likely produce lacrimation on command. It does, but common irritants also produce detectable pain in the conjunctiva, which is not acceptable. Fumes of ammonia, onions, smoke and phenylbromo-aceto-nitrate (tear gas) administered without exposure to the olfactory apparatus all produce tears in varying quantities, but also the undesirable side effect of pain. Very significant reflex stimulation is possible by employing the olfactory sensors; however, the ingested irritant must be perceptibly odorless and, to be acceptable as a cuing mechanism, indisputably

harmless. Finding such a substance may be more difficult than it is worth when it is noted that the end products of lacrimation, visual blurring and fogging, are also associated with $+G_z$ effects and induced by other physiological phenomena. As such, the visual effects of G_x could most economically be generated by the G_z production. This approach is further warranted based on the infrequent occurrences in which a lacrimal acceleration environment exists in the high performance atmospheric aircraft flight envelope.

A.3.3 Summary

The visual effects resulting from high G flight have been presented in this section. A structure of a mathematical model of these physiological effects was postulated. Some functional relationships await further research to complete the model. However, a simplified model is presented in Section (4.3.3).

A.4 Musculoskeletal

A.4.1 Extremities

Extremity loading would seem to be an important part of the high G environment when considered as either proprioceptive cuing of environmental acceleration magnitude or as the introduction of constraints upon manual task performance. Under conditions of $+2\ G_z$ it is reported that a subject can barely rise from his seat, under $+3\ G_z$ it is nearly impossible to raise the leg, under $+6\ G_z$ the arms cannot be raised above the head, and under $+8\ G_z$ the forearm cannot be raised from a horizontal rest (120, 256). Surely with effects as noticeable as these one would expect considerable research to have been conducted in the area of extremity performance and proprioception under high G conditions. Such is not the case.

The authors share Kroemer's (140) surprise to find little systematic research regarding extremity muscular force capability under high G conditions. Grether (98) encountered the same absence of research concerning manual control capability under acceleration and drily observed that "perhaps the effects appeared so obvious to research workers that they felt research was unnecessary". Our search has revealed very little additional data, certainly none which directly assesses the importance of limb proprioception and control in the context of aircraft piloting and mission performance. Nevertheless, sufficient data does exist to provide a reasonable departure point for discussing a portion of the mechanization of limb proprioception under high G and some physiological performance findings will suggest means to recreate these conditions in the 1g environment. Our investigation herein will be limited to the arms.

Consider the human arm to be composed of two segments: the forearm and hand, hinged with respect to the upper arm at the elbow joint, and the upper arm hinged with respect to the upper torso at the shoulder joint. In a 160 pound male the weight of each of these two segments can be taken as five pounds (108). Joint freedom and muscular support permits both of these segments to be positioned such that, under inertial acceleration effects, moments about the supporting joint arise. These inertial acceleration moments are either:

a) Totally resisted by change in muscular tone such that segment position remains unchanged.

b) Partially resisted by muscle tonal change permitting some alteration in segment position.

c) Not resisted at all by muscle tonal change with consequent movement of the segments constrained only by the

dynamics of the acceleration event, the degrees of freedom permitted by the joints, and space [illegible].

Inertially induced segment movement and/or muscle tonal change can occur in the arm held static as well as the arm directed to movement.

PROPRIOCEPTION

The obvious sensory mechanisms for proprioceptive detection of inertially induced arm loading are those sensors which register muscular tension, muscle outflow, segment position, and tactile pressure. Under the predominant acceleration vector of concern, $\pm G_z$, and based on the positions the arm may normally assume within a tactical aircraft cockpit, the main muscular systems employed by the seated subject in resisting or compensating for $\pm G_z$ are the biceps/triceps governing the forearm/hand segment and the deltoid/lattissimus dorsi governing the upper arm segment. The shoulder joint and elbow joint play roles in perceiving segment position.

MUSCULAR TENSION REGISTRATION

Although controversy surrounds the method by which segment relative placement or skeletal spatial position and attitude is perceived, there seems relatively firm and consistent agreement that the Golgi tendon organ, Figure A.4.1-2, is the principal mechanism for measuring muscular tension. The rate of discharge of the tendon receptor tends to follow muscular strain such that as the contraction and tension of a set of muscular fibers becomes more severe, a greater number of tendon receptors contribute to the total discharge (116,178). Borah et al. (22) advocate a Golgi tendon organ response such as that shown in Figure A.4.1-1, which depicts a discharge output profile of very rapid rise time bordering on the characteristics of a discrete step with subsequent adaptation decay.

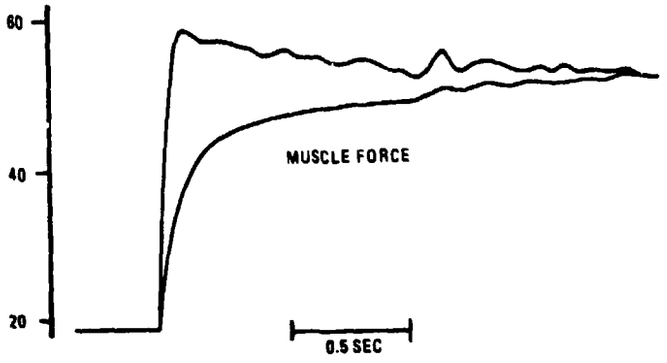


Figure A.4.1-1 Model for Golgi Tendon organ function and experimental result of increasing muscle tension (from Houk and Henneman, Borah et al (22)).

The above points, taken individually, do not specifically define how variable muscular tension is monitored in continuous form. Taken together they seem to suggest that if a uniform tension threshold applies for all tendon receptors in the set of muscular fibers, as an additional muscular support is desired, a greater number of muscular fibers and their tendon organs are "brought on-line" discretely. Alternately variable thresholds might be uniquely assigned the tendon receptors such that as tension increases, a greater number of tendon receptors enter their accelerated discharge state. The behavior of the discharge suggests the Golgi tendon organ to be positioned in series with the muscle fiber and this is supported by anatomical evidence (116). The afferent path from the Golgi tendon organ is stimulated by muscle fiber contraction. However, artificially placing the receptor under tension by invasive means does not produce a perception of increased load (93). There has been some success in artificially, in non-invasive form, stimulating the afferent paths of the overall set of receptors employed within the muscle fiber through the use of externally applied vibration (93, 99).

Although tendon organ afferents were somewhat stimulated by vibration, Goodwin et al. (93) believe the primary effect was experienced by the primary spindle receptors as opposed to the secondary spindle and tendon receptors. This conclusion was based on the fact that the vibratory stimulus primarily introduced an illusion of segment movement, or velocity, which materialized as an error in assessment of segment spatial position and was similarily experienced regardless of muscle tension levels. Therefore a vibratory stimulus of this nature does not seem to hold promise for usefully stimulating the Golgi tendon organ receptors for the purpose of forming an impression of muscle tension in the absence of actual muscle tension. Further the vibratory stimulus would introduce a set of related tactile perceptions which would detract from the desired perception.

SKELETAL SPATIAL POSITION PERCEPTION

Additional information concerning the magnitude of external load can be derived by assessing, in conjunction with the measure of muscular tension, the positional change of a skeletal segment subjected to the load. The acknowledgment of zero positional change is informative in itself. Perception of spatial position and attitude of upper and lower arm segments in this case is derived from joint receptors located in the shoulder and elbow joints as well as the estimate of the length, or stretch, of muscles controlling upper and lower arm.

As recently as 1966 the idea that muscle length registration is used in the perception of skeletal joint angles was met with skepticism (79, 178). Rather, the burden of this perception was ascribed, in the main, to joint receptor afferents. Only in the last few years have the muscle stretch receptors, muscle spindles, been assigned a more significant role in joint angle perception (93). The shift in emphasis is not so much a result of dramatic

findings concerning the stretch receptors as it is in a greater acceptance of a fundamental ambiguity of the joint receptor, whose afferent impulses are altered by tension in the muscular system driving the joint (99). This is not a new finding; in 1956 Skoglund observed this phenomenon within the knee joint of a cat (116). Muscle length registration would form a basis of compensation for joint receptor ambiguity.

The muscle spindle, Figure A.4.1-2, is interspersed throughout the fibers of the muscle. The spindle is innervated by γ (efferent) fibers in cross network form such that a single γ fiber

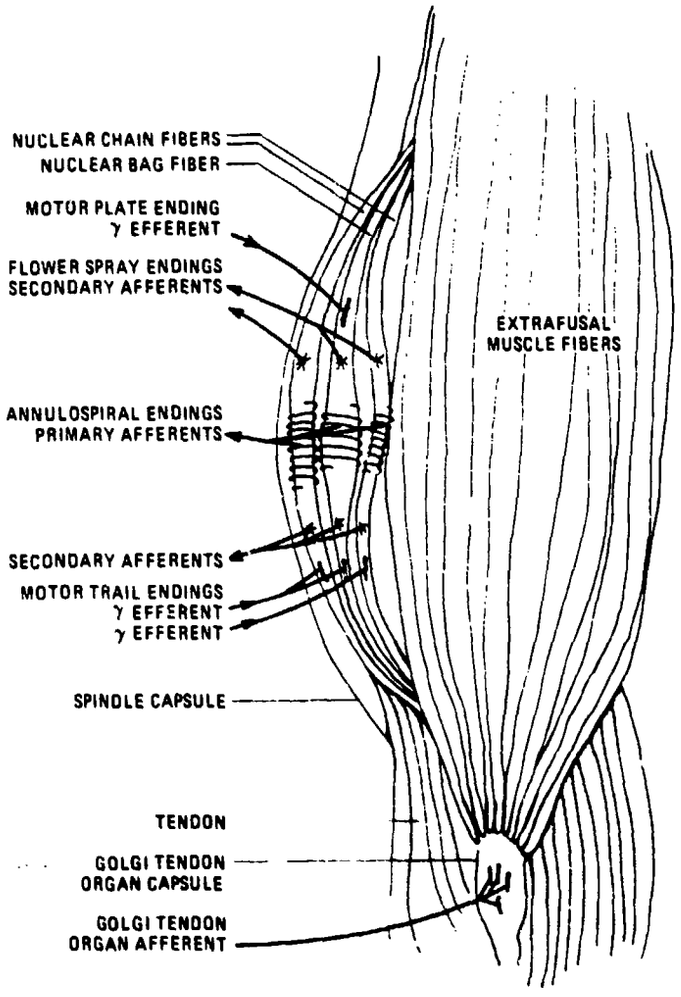


Figure A.4.1-2 Muscle sensors (modified from Borah (22) & Howard (116)).

services many spindles. The spindle contains a contractile element, intrafusal fibers, which is innervated by efferents leading to the motor plate and trail endings (22). Intrafusal fiber contraction maintains an appropriate amount of tension on the spindle so as to maintain its sensory endings at threshold levels in the presence of main muscle, extrafusal fiber, contraction and stretching. The spindle sensory endings are of two types: primary and secondary. The primary ending is characterized as an annulospiral structure located in the equatorial section of the spindle bounded at each polar region by the flower spray structure secondary endings. The discharge pattern of the afferents leading from the primary and secondary endings show marked differences in dynamic response as depicted in Figure A.4.1-3.

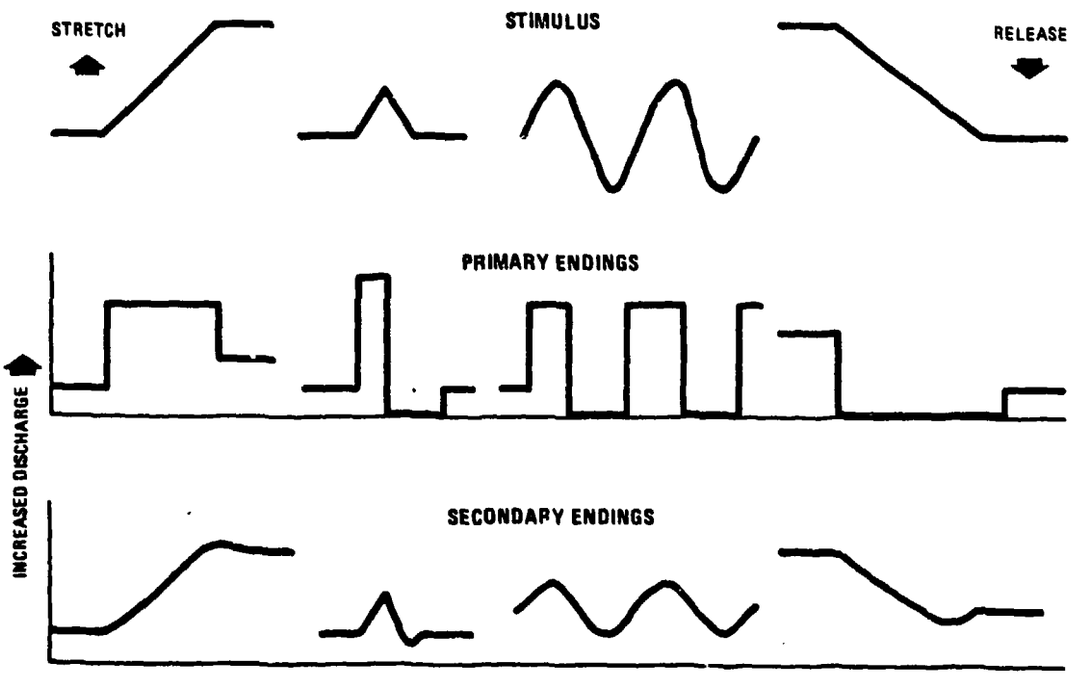


Figure A.4.1-3 Qualitative discharge patterns of spindle primary and secondary afferents (modified from Howard (116)).

The primary ending output is fast conducting and of low threshold. Although the discharge frequency increases with muscle stretch (tonic response) it is particularly sensitive to the rate of stretch (phasic response). This suggests a "differentiation" capability located in the nuclear-bag containing the primary endings. Velocity information such as this might be employed as rate feedback damping in the overall reflex arc governing muscular activity. An additional peculiarity of the primary ending discharge pattern is its "quiet periods." During extrafusal fiber contraction, the primary ending output falls silent as it is unloaded to less than the threshold stretch. Primary afferent signals do not reappear until, under γ efferent stimulation, the intrafusal fibers pick up the slack in the spindle and reestablish threshold conditions.

The secondary ending discharge intensity follows the amount of stretch with little or no rate sensitivity or silent periods. The primary endings, therefore, form a measure of both muscle length (or stretch) and rate of change of length, whereas the secondary endings provide simply a measure of position or muscle length (116). The spindle could be likened to the error detection circuit of a servo wherein it dutifully monitors stretch mismatch with the extrafusal fibers, responds with afferent signals which, through the reflex arc, results in γ efferents causing the extrafusal fibers to contract or expand toward elimination of misalignment.

This treats the spindle too simply and overlooks the importance of γ efferent effects on the spindle. Under voluntary muscular tonal change, when one wills a muscle to lengthen or contract, it is thought that the initiating stimulus arrives at the muscle via efference to both the intrafusal and extrafusal fibers and is termed α - γ co-activation. The principle feed forward control is by direct descending pathway command to the α motor neurons. In parallel, the system "sets" the spindle desired response and al-

lows the fine control of the spindle feedback to compensate for muscle and load variations. The delay associated with the spindle reflex arc is considered to be in the range of 60-140 ms. As measured between the onset of an impact or step inertial load applied to a muscle system, and the time of maximum α efferent activity resisting the impact is registered (239).

The spindle reflex normally acts to resist limb disturbance when the muscles being regulated are active. Only the voluntary decision to relax the musculature can inhibit the reflex. Consequently it is not possible to impress steady state information on the spindle afferents for the purposes of proprioceptive cuing without eliciting a reflex arc efferent causing muscle tonal change. In the absence of external loading, the skeletal segment controlled by the muscle would involuntarily enter unwanted motion. Within the literature reviewed by the authors, only the unacceptable approach of sectioning is mentioned as a means to inhibit the α efferent. However, as mentioned earlier, the external application of a vibratory stimulus does seem to bias the spindle afferents in a manner causing a perceived change of skeletal spatial attitude and position. The precise relationship between the vibration stimulus and the perceived limb movement is still under investigation (99).

Historically the joint receptors have been described as the main source of the information concerning skeletal spatial position and attitude. The joint receptor ambiguity mentioned earlier gives rise to the distinct possibility that the joint receptor is but one of several sensory mechanisms contributing to kinesthesis. The resulting accuracy of perception is really quite remarkable; Cohen (46) found that in arm outstretched pointing exercises, without the aid of visual fixation, subjects were able to point to a target, allow the arm to drop to the normal hanging position and return to within a mean value of 3.3 cm of the target point. He reasons that since two understandings or assessments are involved

herein the accuracy of the shoulder joint positional sense must be within 1.5 degrees. Cohen also notes that Goldscheider determined the positional movement threshold of the shoulder to be 0.04 degrees. Both of these findings suggest that arm movement induced by inertial loading can be precisely measured.

Joint receptor sensory ends are composed of Ruffini flower spray and Golgi type structures interspersed throughout the joint connective tissue. Some joint receptors seem active at all joint angles and others active through fairly large angular ranges. Still others form the functionally expected case wherein their discharge is confined to a unique joint angle such that as this joint angle is approached, discharge level becomes intense reducing again as the joint angle is passed. The discharge pattern demonstrates adaptation; should the joint angle pause, the discharge from the receptors attuned to this particular joint angle is at first intense with subsequent decay.

The joint receptors are considered to provide rate as well as positional information. Joint receptor discharge displays a profile containing overshoot the magnitude of which some references indicate is a function of joint rate (102, 178). Our review of the literature has not revealed means to noninvasively selectively stimulate the joint receptors in the absence of joint rotation, although overall activity can be increased by co-contraction of muscles.

MOTOR OUTFLOW

Within the spindle discussion, the concept of α-γ co-activation was introduced as a theory of motor control wherein the spindle afferents are employed in corrective feedback form. Howard speculates that a direct α route is used for rapid ballistic movement, without dependence upon the spindle afferent system. α direct or ballistic movements are exemplified by the pianist's

extremities/hands and fingers. Chernikoff and Taylor note that this type of activity is so rapid as to preclude the use of kinesthetic feedback and tends to substantiate an α direct type concept (116). We would add as examples of rapid, well-practiced movements that of typing, moving the foot between an automobile's accelerator and brake pedals, and many arm/hand movements employed in operating the controls of an aircraft and its subsystems.

If rapid ballistic type movements do not depend on kinesthetic feedback why include them within a discussion pertaining to extremity proprioception under inertial acceleration effects? First, as will be seen, there are very striking similarities between the effects of arm movement within a centrifuge and that which occurs under α direct type movements in the presence of varying external load. This leads us to believe ballistic movements may be selected often in the tasks which are to be performed within the cockpit. We suspect the initial phase of arm movement to be ballistic with visual fixation or tactile monitoring applied in the final phase to provide any necessary correction. Secondly, there appears to be a type of proprioception affiliated with α direct style movements and is characterized as a sense of "motor outflow". Should motor outflow be the primary means of monitoring muscular activity in the unaccelerated environment, only to become notably undependable in the accelerated environment, then it must be discussed within the context of high G physiological effects.

Motor outflow refers to a copy of how much α efferent is required to contract a muscle and hence move the skeletal element the muscle controls. The storage is called efference copy and forms a pattern against which α efference is compared. In some tasks such as learning where a control is located or how much a control must be moved to produce a desired result, efference copy is probably initially generated by movements heavily dependent upon α-γ co-activation. After practice, however, we speculate that α direct movements are selected with motor outflow providing

control. On the other hand other tasks, such as developing competency in dart throwing, may always employ α direct movement in a trial and error form so as to modify efference copy to that pattern producing acceptable dart accuracy.

Howard (116) points out that motor outflow is quite reliable in the absence of varying external loads and recounts an experiment performed by Lashley in 1917 which is of interest to us. Lashley discovered and worked with a subject suffering a bullet wound to the spinal cord which anaesthetized most of the leg afferents but left intact leg efferents. The subject was able to duplicate a given leg amplitude of movement as well as a normal subject so long as the leg was not loaded. Lashley attached spring loads to the subject's leg and noted the subject could not compensate for the various loads although the subject was under the impression he had indeed so compensated. (Recent experimentation with trained monkeys shows that afferent removal by dorsal root section does not interfere with the accuracy of ballistic movements.)

Compare Lashley's observation to that of Cohen's (49) centrifuge subjects who, when directed to point to a target in the presence of inertial acceleration effects, initially demonstrated a condition of underreach (see Figure A.4.1-4). They would appear to have been using ballistic α direct motor outflow controlled movements <u>without</u> a prior assessment of inertial load proprioceptive feedback and planned compensation. The conditions of inertial acceleration loading were available to the centrifuge subjects but they either were unaware of the stimuli or, if aware of them, either chose to neglect them or could not make use of the stimuli since an α direct movement ensued. Granted Lashley's subject never successfully compensated while the centrifuge subjects commenced compensation immediately after the first trial. This suggests the centrifuge subjects, on subsequent trials, fell back to greater dependence upon α-γ co-activation movements with close

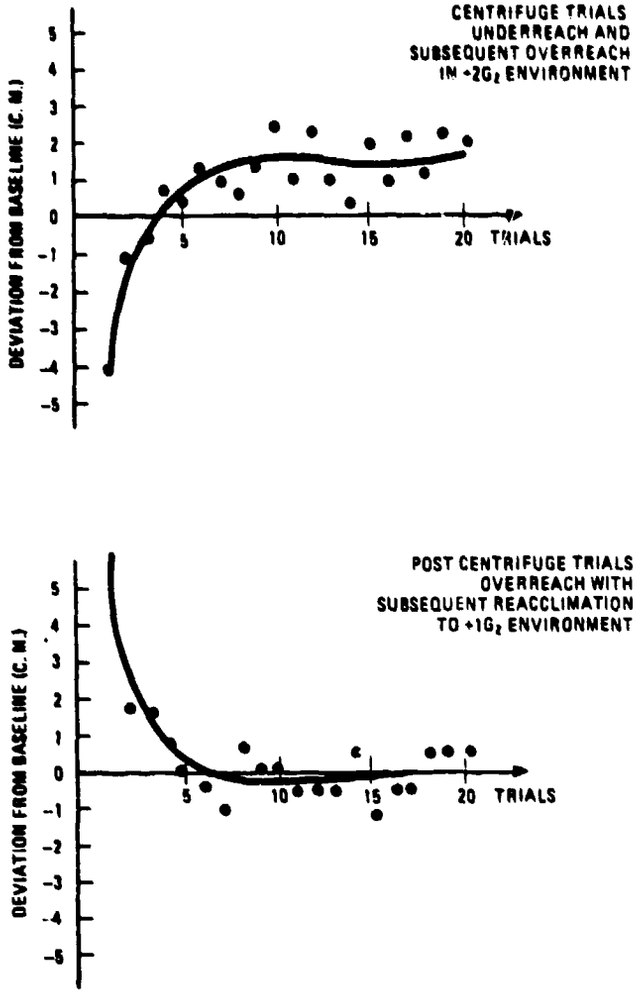


Figure A.4.1-4 Reaching error in +Gz environment without hand/eye fixation (from Cohen (49)).

proprioceptive control until apparent underreach disappeared and it was felt successful compensation was established. Evidently the experience of active motion in the altered environment is needed for adaptation. It is also likely that during this period of adaptation new measures of "desired" motor outflow were being stored away and utilized on subsequent trials with an immediate desire to move, as quickly as success would permit, away from close proprioceptive control back to direct movements.

Proof of this seems to lie in the fact that at the conclusion of the centrifuge run, the subjects overreached in the 1g environment indicating that proprioceptive compensation occurred quickly and the subjects were again practicing $\propto$ direct movements with a motor outflow control pattern incorrect for the current load environment. Further proof of the use of proprioceptive feedback simply for the purposes of establishing a repatterning of the primary control, motor outflow, is found by noting that although the trials under acceleration involved unilateral reaching, a central compensation occurred with subsequent bilateral overreaching when the subjects were returned to the 1g environment (Figure A.4.1-4).

The primary control of an aircraft, the stick, is not subject to movement which can be characterized as a reaching movement as previously discussed. A predominant form of stick movement practiced by experienced tactical aircraft pilots is a sharp, crisp input to stick position producing a desired aircraft response. These inputs often appear as steps, pulses, and pulse doublets with frequency increasing and amplitude decreasing as the tracking task becomes more demanding. No doubt force as well as length feedback is in effect at a given stick position since stick loading is an important feedback parameter. However, the movement to the desired position appears to have the abrupt characteristic of an $\propto$ direct movement.

The authors believe the Lashley and Cohen observations to be significant to the issue of high G physiological effects and their impact on piloting performance because of the apparent importance of motor outflow control, the dependence on $\propto$ direct type movement, and the somewhat secondary role kinesthesis seems to play in this activity except during compensation. We are lead to the suspicion that even if the proprioceptive sensors of the arm were somehow responding with multi-G loading information, if the physics of the event did not produce a requirement for motor outflow

change, the appreciation of the high G environment may be significantly eroded and the compensatory task, which is sought to be taught within high G simulation, missing. We are not suggesting that the proprioception of increased load is unimportant; only that, if an α direct ballistic type movement is going to be the likely maneuver and will be controlled by a stored pattern established in the 1g environment, it may be absolutely necessary to actually place the upper arm and forearm under external load in order to provide cause for motor outflow alteration.

To summarize our findings in the proprioceptive area as they pertain to simulation, it appears improbable that the Golgi tendon receptors can be appropriately stimulated in the absence of actual muscle tonal change. Unless the external load were varied, such muscle tonal change would produce segment movement exactly opposite to that which might be associated with the aircraft acceleration. Steady state stimulation of the spindle afferents will produce an α efferent with similar unwanted segment motion unless an external load were present. We have found no precedent suggesting the joint receptor afferents can be artificially stimulated in a useful manner. Admittedly, spindle receptors can be non-invasively stimulated by vibratory means to give a false impression of skeletal segment position; however, the relationship between stimulus and pseudo-motion impression is not clear and a vibratory stimulus would produce unwanted tactile perception. Motor outflow is likely the prevalent means of control but this appears to require actual changes in skeletal segment loading in order to force alteration. Based on this examination of each of the receptor mechanisms we conclude that actual skeletal segment external loading will be required to ellicit the desired proprioceptive effects imposed by inertial acceleration loading.

EXTREMITY PERFORMANCE UNDER HIGH G

Inertial acceleration loading is experienced as a proprioceptive input; it also introduces constraints within the control of a tactical aircraft. Little, et. al. (161) found that a 10-15% degradation in tracking tasks occurs as acceleration levels approach the 5-9 G_x range. They noted that the degradation was not progressive as a function of duration under acceleration and hypothesized that degradation occurred as a consequence of an adaptation process which is independent of duration under acceleration. Hence, once having executed adaptation, no further degradation was experienced. It is interesting to note that the adaptation did not appear to permit the elimination of the basic degradation in tracking. Only infrequently would we expect to find tactical aircraft acceleration levels in the 5-9 G_x region. Our primary concern is $\pm G_z$ and its effect on active arm movements and force capability.

We have already introduced some of Cohen's work (48, 49) in the discussion pertaining to motor outflow. It is one of two studies referenced herein regarding the effects of arm reaching under $+ G_z$. In the absence of visual fixation of the moving arm, Cohen's subjects initially reach low as expected but, on subsequent trials, ultimately end up overreaching their target. Cohen attributes this to a phenomenon termed "elevator effect" which manifests itself as the illusion that targets in the field of view appear to rise under increased $+ G_z$ and consequently appear to be higher than their true position.

The illusion of elevator effect was investigated at length by Niven, et. al., (185) who, interestingly enough did a portion of their experimentation within the elevator cars of the Empire State Building in New York City and the Waterman Building in Mobile, Alabama. Elevator cars were selected to provide translatory acceleration free of radial effects. Both subjects possessing

normal vestibular apparatus and those suffering vestibular dysfunction (labyrinthine defective) were exposed to $\pm G_z$ acceleration. Normal subjects experienced upward movement of viewed targets under $+ G_z$ and downward movement of same under $- G_z$. The apparent motion of retinal afterimages, reflecting the eye movement, was reversed. The labyrinthine defective subjects saw no illusion of movement of targets in their field of view and although they reported some afterimage movement, there was no clear-cut direction associated with a afterimage movement. The normal subject's eyes tended to rotate in a compensatory manner, down briefly under $+ G_z$ and up in $- G_z$. This did not occur in the labyrinthine defective subjects. The authors concluded that elevator effect is a transient portion of the oculogravic illusion and otolithic in origin.

Because the utricular otolith is oriented in a pitched up attitude relative to the normal anatomical axis of a human, an increase in $+G_z$ produces the same otolithic stimulus as an increase in body pitch attitude. The illusion of pitch up is the predominant sensation associated with the oculogravic illusion and it would appear that its onset phase, that of increasing pitch, reflexly induces the eyes to lower giving rise to the illusion that targets in a settling field of view are moving upwards. Although the sensations of increased pitch may be long lasting, Niven (185) believes that rapid adaptation to the effect is due to reestablishment of eye fixation and would occur within approximately 200 ms. Cohen's subjects demonstrate an ongoing condition of overreach which might be due to the fact that visual fixation on the moving hand was not permitted. Cohen did include some trials wherein visual fixation was permitted but does not comment whether the same type of overreach under inertial load occurred therein. Results of other work available to us do not allude to this type of overreach; however once at a given acceleration level, repetitive trials were not employed. Therefore we cannot be certain of the overall arm disturbance profile sought within the simulation. We

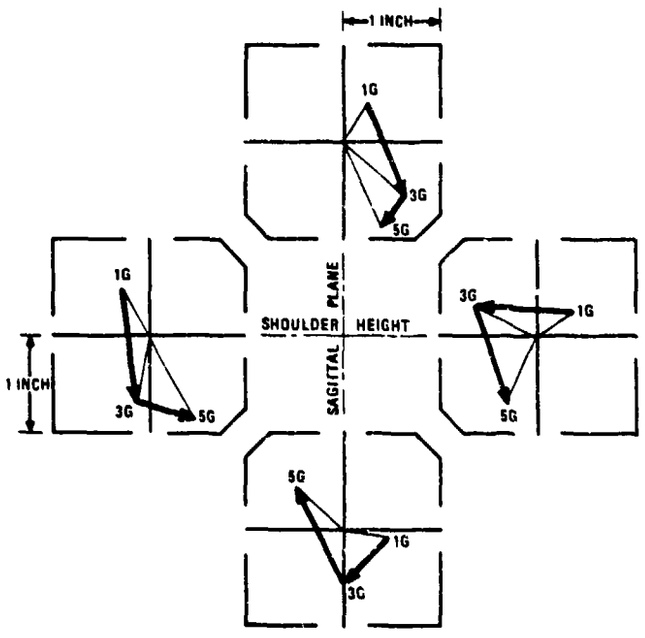
must keep in mind the possibility that eventual overreach purposely introduced at steady state acceleration levels may be desirable to mimic the results of elevator effect.

The results of a study by Canfield, et. al., (35) are quite helpful in understanding the constraints imposed upon arm reaching activity under inertial acceleration load and demonstrates that fore/aft as well as vertical arm forces are disturbed by G_z acceleration. Forty-eight centrifuge subjects were exposed to acceleration levels of +3 and +5 G_z and were requested to point to each of four targets located in front of the subjects and arranged in quadrant form approximately 30° above and below shoulder height and to the right and left of the midsaggital plane. The subjects were instructed to make rapid ballistic reaches to the targets under 1, 3, and 5 G_z conditions and attempt to be as precise as possible without dependence upon visual fixation for minor final corrections. Event timers monitored various phases of each reach.

Accuracy degrades as accleration level increases, which Canfield attributes to an inadequacy of normal kinesthetic cues under increased acceleration. Reaction time, that time necessary to start the reach upon command, increased and was attributed to an increased "cogitation period" required by subjects to consider changes necessary to preserve accuracy. Movement time, time to reach, increased and was attributed to a failure of the subjects to throw the arm with sufficient force to compensate for its "increased" weight. We would not fault the latter two explanations but would add that both could also be explained if presumably the subjects experienced the need for some type of required compensation and shifted to greater dependence on slower proprioceptive controlled movements rather than α direct execution.

Perhaps the most interesting findings are those pertaining to magnitude and direction of error which we have illustrated in Fig-

ure A.4.1-5. The four targets are shown each containing four quadrants. The radial distance from the center of each target is the mean error at the tested acceleration levels. The denoted position within each quadrant of a target is not necessarily a point struck by the subjects; rather it reflects a propensity to hit a given quadrant. The method selected to graphically illustrate this propensity is described in the caption accompanying the figure. The figure illustrates that two effects are operating simultaneously. First, there exists the expected downward shift, termed "error of downward tendency" by Canfield. Secondly, the strikes show a trend of moving inwards toward the center of the four targets taken collectively. Canfield attributes this shift to "negative inertia error" as termed by Brown et. al. (23) however we prefer to call it "cross loading error".



NOTE: POSITION WITHIN A QUADRANT IS ESTABLISHED BY MEASURING OUT A DISTANCE EQUIVALENT TO THE ERROR ALONG A SPECIFIC VECTOR. THE ORIENTATION OF THE VECTOR IS GIVEN AS TAN^{-1} (NET NUMBER ORDINANT STRIKES/NET NUMBER ABSCISSA STRIKES).

Figure A.4.1-5 Direction and error of reaching moments in +Gz environments (from Canfield et al (35)).

Cross loading error reflects the type of error which occurs when the hand falls short of its intended target because insufficient force was applied. Because the arm segments rotate about elbow and shoulder joint, an increase in inertial weight of the segments requires a complementary increase in force to extend the arm. Shortages in force will result in shorter hand travel. Canfield notes that both the error of downward tendency and cross loading error reinforce one another in the top target, act normal to one another in the side targets and oppose one another, with cross loading error predominant, in the bottom target. This finding suggests that a $+G_z$ inertial acceleration load is manifested in a significant force disruption not only along the Z axis but also the fore-aft X axis and is supported by recent force capability profiles developed by Kroemer, et. al., (140, 141). The logic of the X axis force disruption is apparent if one considers the arm, as we earlier suggested, as two serial mass segments. In the partially or completely outstretched position $+G_z$ loads acting on both masses will cause a moment to be experienced at the shoulder joint with potential downward droop of the cantilevered arm. The downward rotation of the upper mass tends to foreshorten the reach and reduce forward force capability. The likely ensuing upward rotation of the forearm segment, executed in attempt to keep the hand elevated, decreases the angle subtended by upper and lower segments and further aggravates the situation.

In a 1975 study (141), Kroemer shows the effects of maximum manual force capability under inertial acceleration load as a function of hand position with respect to the body. The perturbing acceleration was $+ G_z$ and effects on lateral force capability were minimal. The more relevant X and Z axis force capability effects have been replotted in Figure A.4.1-6.

The dotted line incorporated within the profiles is provided only for clarity and definition of the asymmetry associated with

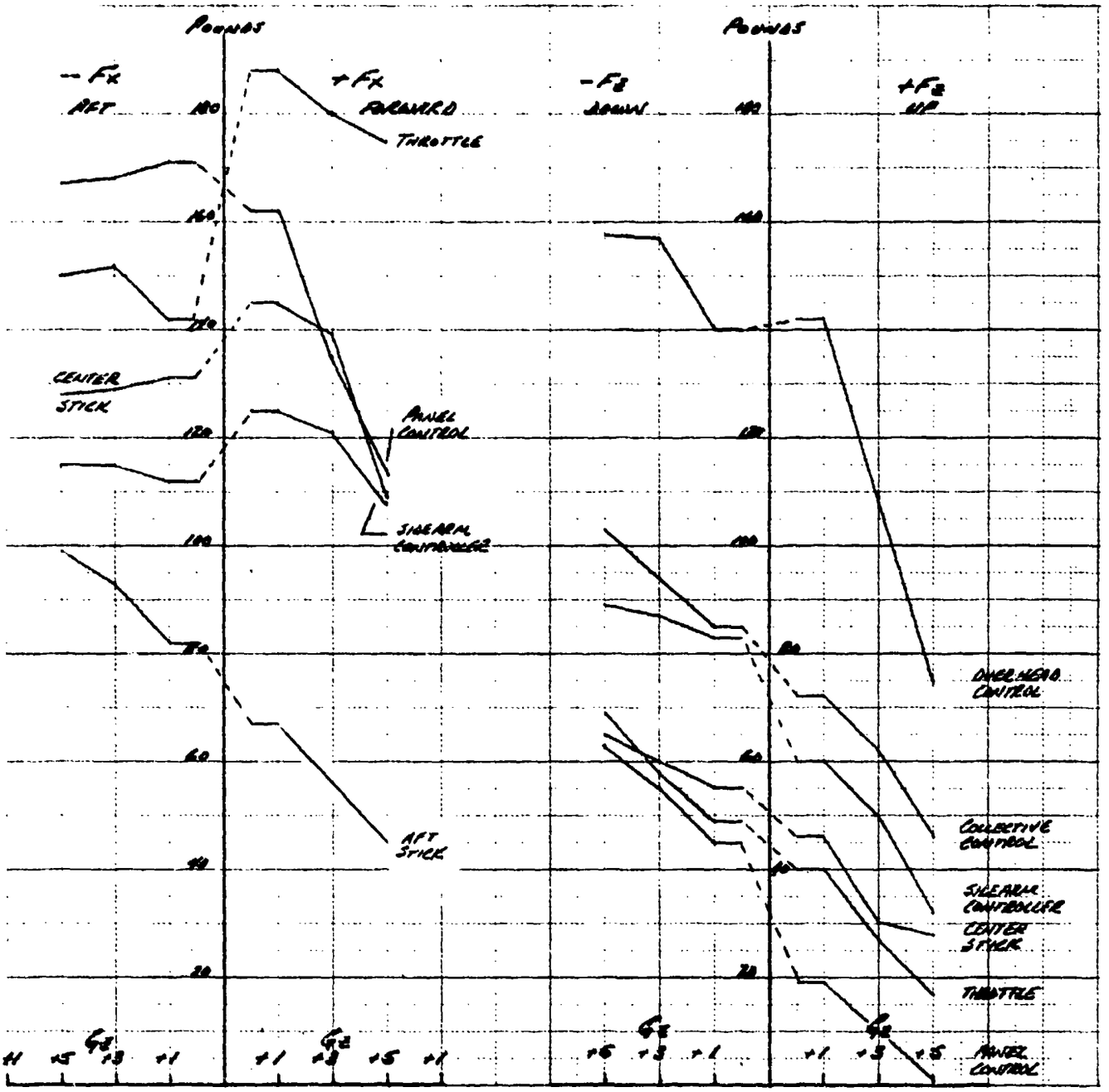


Figure A.4.1-6 Maximal hand/arm forces in various +Gz environments (from Kroemer (141)).

directional force capabilities in the 1g environment. Note that + G_z produces definite effects on forward force capability but markedly less significant effects on aft force capability.

This same symptom is borne out in the Z axis force capability associated with an overhead control wherein the same inertially induced force, which works to the disadvantage of upwards force, does not seem to be converted uniformly to an advantage in downwards force capability under like acceleration conditions. We would advance the tentative explanation that in changing applied force directions the subjects tend to alter the position of the upper arm mass segment with respect to the shoulder joint such that when pressing forward or pushing up, the upper mass segment is located further forward of the shoulder joint than when pulling down or backwards. Consequently its inertial load would more adversely affect hand force capability. The slopes established between maximum and minimum Z axis forces for the panel control, center stick, and overhead control locations compare favorably with that which would be predicted for two articulated mass segments, each weighing five pounds, and each of equal length. Unfortunately, the aft force capability as applied to an aft stick location does not seem predictable and therefore caution must be exercised in attempting to apply a simplified analogy to various arm positions.

The earlier discussion pertaining to extremity proprioception concluded with a strong suspicion that externally applied arm loads would be required to appropriately simulate inertial loading. The studies of Canfield and Kroemer concerning the constraints resulting from inertial loading tend to support a load application which would be deduced from kinematic analysis. The studies also emphasize the importance of ensuring that the scope of load imposition includes loading the upper arm as well as the forearm. Error of downward tendency can indeed be established by torque application at the elbow joint; cross loading error, reduc-

tion in throw rate, and X axis force disruption must be aided by loading the upper arm. Cohen's overreaching findings, if found prevalent, suggests the possibility of employing some type of transient loading profile but since this effect is introduced due to a phenomenon external to extremity loading, and secondly, based on the rapidity of load adaptation, we are unsure that significant ongoing overreaching could be induced through transient arm loading. The point may warrant further experimentation. Although the literature concentrates primarily on G_z effects, the fact that kinematic analysis tends to be supported by experimental findings in the case of + G_z suggests that, in the absence of G_x and G_y data, prediction via kinematic analysis is a reasonable first approximation.

A.4.2 Head/Neck

The literature indicates significant head and neck motion as a result of acceleration (74, 135, 142, 182). There are two aspects of head motion which are important to this study; the perception of motion of the head and resistance of head motion. The inertial reaction of the head is resisted by the head/neck musculature. These muscles not only resist motion caused by external forces but they also possess the sensors which detect external displacement forces. The manner in which these muscle sensors function was described in Section A.4.1 of this report.

MUSCULAR CONSIDERATIONS

The muscles of primary interest here are illustrated in Figure A.4.2-1. The sternocleidomastoideus (1) is attached to the skull in the mastoid area, runs down the neck and divides with the larger portion attaching to the clavical and the smaller portion to the sternum. This muscular structure exists as a right and left hand pair which operate antagonistically to cause the head to rotate about the longitudinal, i.e., the posterioranterior axis of

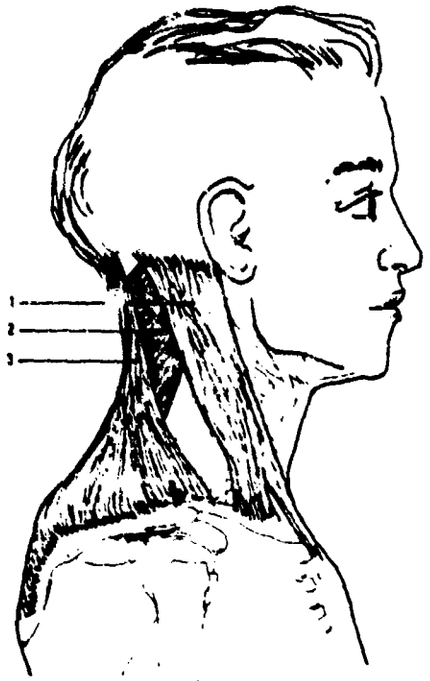


Figure A.4.2-1 Neck muscles used to control head motion (modified from Barcsay (10)).

the head. In addition, they act in conjunction to cause the head to rotate forward.

The splenius capitis (2) and the trapezius (3) are located at the rear of the neck with the trapezius superior and attaching to the shoulder. These two muscles are employed to pull the head backward.

Both Gum (100) and Borah et al (22) have modeled the head as an inverted pendulum. They have both modeled only the rotation about the longitudinal axis; however, the rotation about the lateral axis may be modeled in the same way with different physical parameters. The geometry of the system used in Gum's analysis is shown in Figure A.4.2-2.

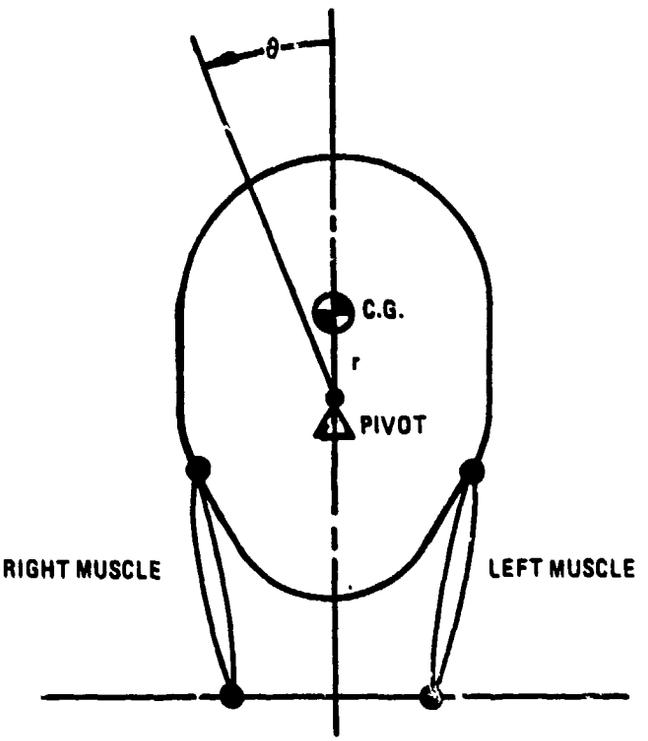


Figure A.4.2-2 Head/muscle system (from Gum (100)).

Gum's work was modified by Borah et al and resulted in the following model (Figure A.4.2-3).

Where:

I_h is the moment of inertia of the head about the neck pivot = 0.034 kgm^2

M_h is the mass of the head = 4.6 kg

r is the distance from the pivot to the center mass = 0.0498

g is the acceleration due to gravity

θ is the displacement angle

ξ is the damping ratio = 0.64

d is the muscle lever arm = 0.075 m

ω_n = 7.81 rad/sec

sf_{zhd} is the specific force parallel to body axis

sf_{yhd} is the lateral specific force

AFR is the muscle spindle afferent firing rate

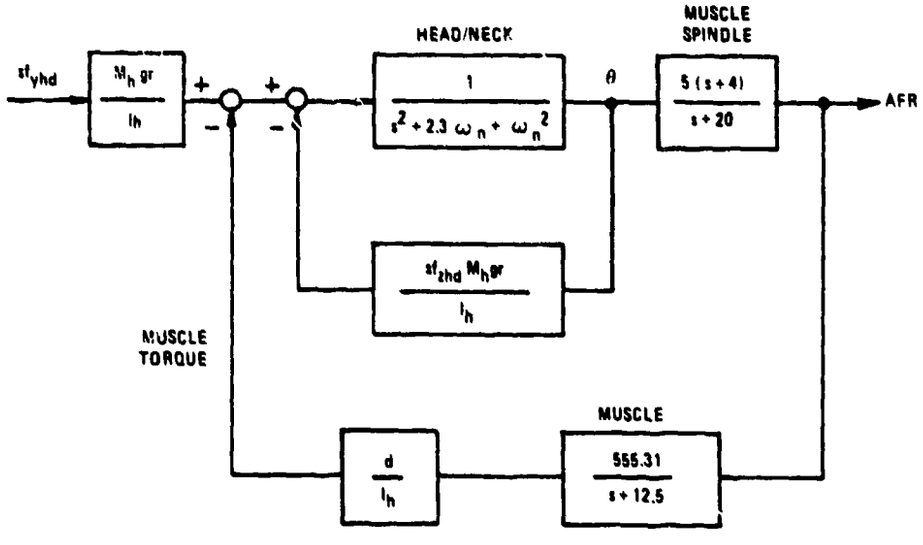


Figure A.4.2-3 Lateral head/neck proprioceptor model (from Borah et al (22)).

VESTIBULAR CONSIDERATIONS

In addition to the muscular sensors, information about head attitude is provided by the vestibular apparatus. Detailed discussions of the vestibular system are presented in other references (86, 100, 102, 116, 191), therefore only a summary will be included here. The human labyrinth (inner ear) comprises the non-auditory labyrinth or vestibular system and the cochlea. There is one labyrinth located in the temporal bone within each ear. The cochlea, is a part of the auditory system and will not be discussed further, herein. A non-auditory labyrinth is located in the vestibule of each inner ear and hence the name vestibular system. Within the vestibule there are two sets of motion sensors, one linear (the otoliths), and one angular (the semi-circular canals). Figure A.4.2-4 is an illustration of the inner ear labyrinth.

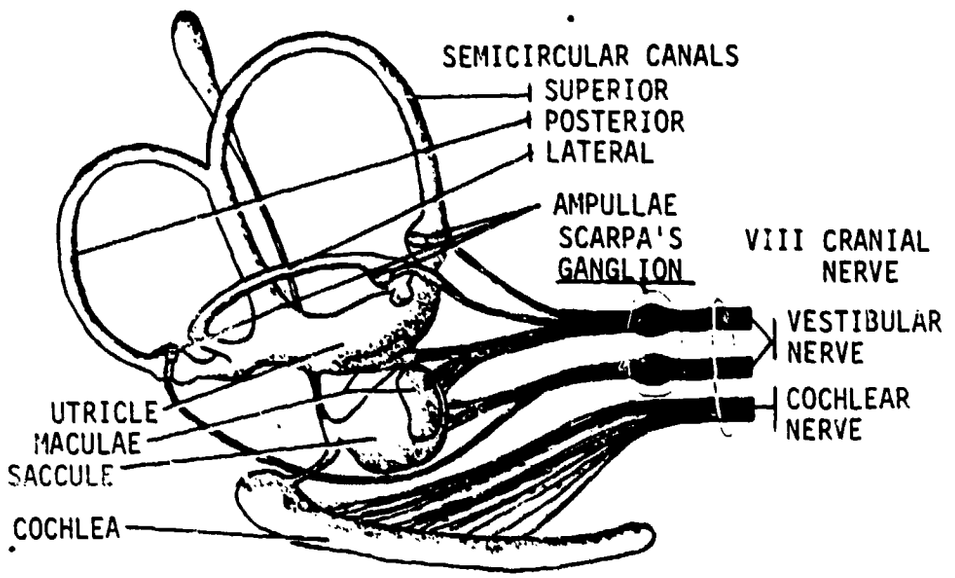


Figure A.4.2-4 Inner ear labyrinth (from Gillies (81)).

The semicircular canals occur as approximately orthogonal triads such that each canal senses rotation about each of the three axes of the head. These axes are essentially parallel to the vehicle body axis system when a crewman is seated erect and facing forward. The sensing mechanism within the semicircular canals is the cupula (Figure A.4.2-5), a valve-like protrusion in the ampulla of each canal. The fluid of the semicircular canal, endolymph, flows through the canal in response to movement of the head, and deflects the cupula. The deflection of the cupula is proportional to the velocity of the fluid flowing past it. Therefore, the semicircular canals sense rotational velocity.

Otolithic membranes exist in both the utricle and the saccule (Figure A.4.2-4). These maculae are somewhat orthogonal which give rise to the hypothesis that they work together to provide linear motion cues in the same manner as the semicircular canals. Another hypothesis is that the saccule has a dual function, the otolith bearing part responding to linear accelerations in the

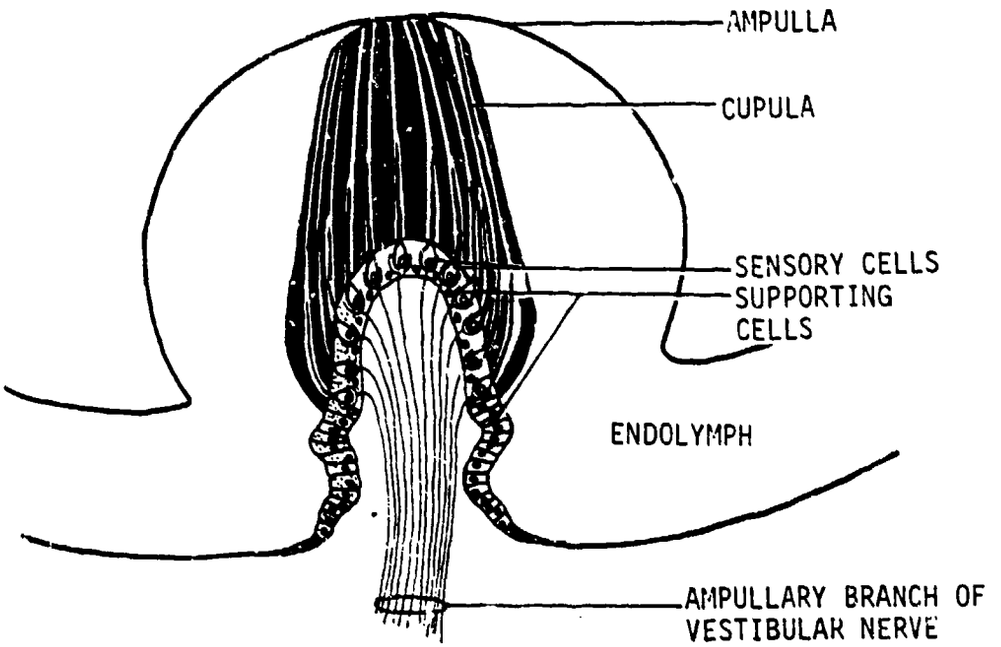


Figure A.4.2-5 Semicircular canal cupula (from Gillies (81)).

same manner as the utricular otolith, while that part which is not invested with stratoconia (Figure A.4.2-6) is thought to be stimulated by vibrations in a frequency of less than 10 Hz to 120 Hz. The function of the saccule is assumed to not contribute to the perception of linear motion and in fact the organ is considered vestigial by some. Therefore linear motion is thought by some to be sensed solely by the otolith of the utricle (100) which is stimulated by linear acceleration. The acceleration deforms the stratoconia thereby stimulating the sensory cells. Several authors (22, 102, 191) take different views however and subscribe to the theory that the otoliths of both the utricle and saccule contribute to resolving the orientation ambiguity. Ormsby (191), in his doctoral thesis, presents a model of the vestibular system which is shown in Figure A.4.2-7. This model reflects some of the latest thinking in this area and was employed by Borah, Young and Curry (22) in their work.

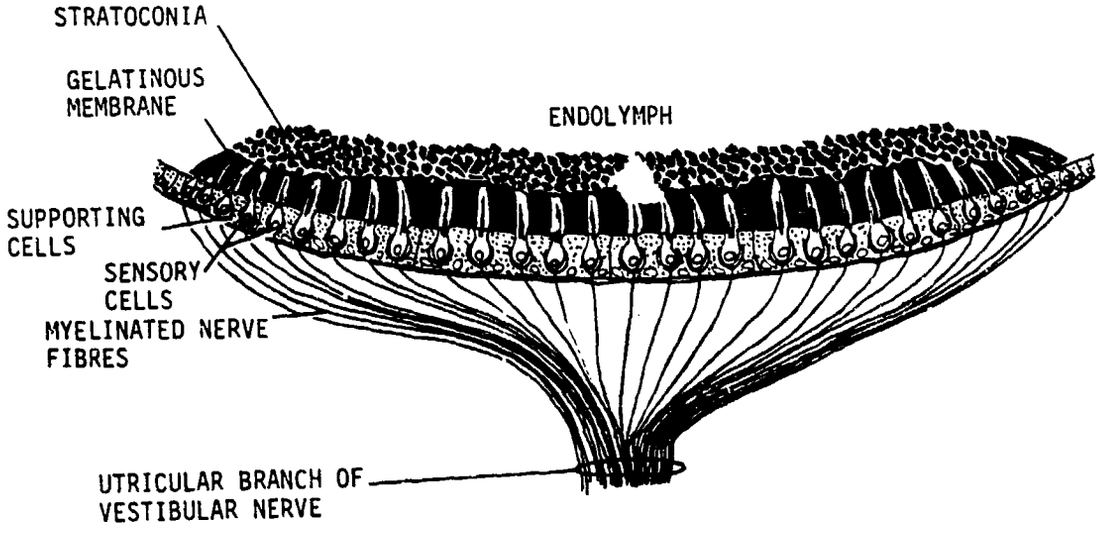


Figure A.4.2-6 Sensing stratoconia of the utricle (from Gillies (81)).

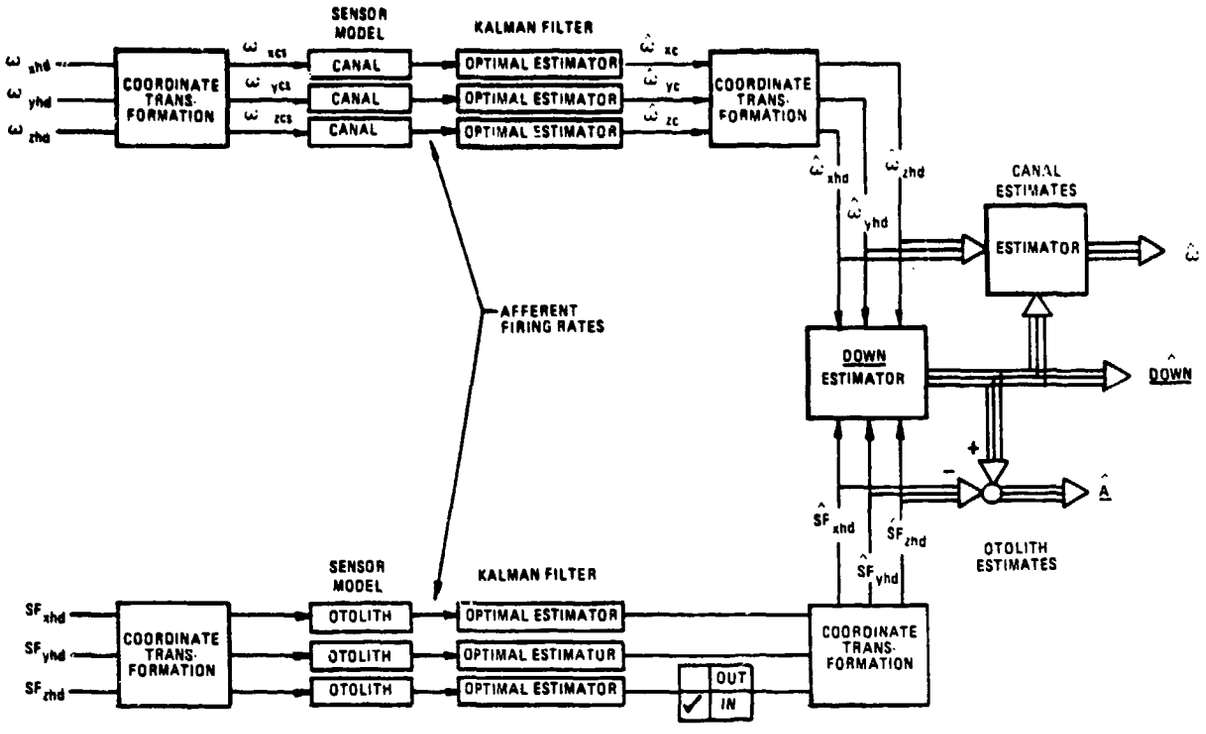


Figure A.4.2-7 Ormsby model of the vestibular system (from Borah et al (22)).

JOINT RECEPTORS

Joint receptors are another set of sensors which may add to the ability to perceive head/neck motion. (The possible contribution of the joint receptors to the perception of motion was discussed in Section A.4.1.)

HEAD/NECK MOTION

Data have been found for head/neck motion in response to G_z acceleration (135, 142) and G_x (74). Kroemer and Kennedy (135, 142) report on head motion in three degrees-of-freedom (pitch, roll, and yaw). Pitch seems to be the most significant in terms of excursion. The data show a considerable variability in head pitch among the various subjects. There is a trend illustrated

for head pitch to overshoot the 1g position upon return. Head movement seems to be independent of helmet weight. The data show that there is no significant rolling or yawing of the head due to G_z but an average 2° pitch down of the head at 6 G_z. This motion is shown to be linear from 1.0 to 6.0 G_z. It was found by Kroemer and Kennedy that the eye point was depressed 50 mm under 6 G_z; 1/6 of this was due to head pitch, the remainder neck/torso compression. This motion was also found to be linear from 1.0 to 6.0 G_z.

It is interesting to note that these data support the position proportional to acceleration concept employed in some G-seats as well as the excursion range of these devices. The 40 oz variation in helmet weight has no effect on neck/torso compression. Figure A.4.2-8 presents the head rotations for all helmet loadings averaged and Figure A.4.2-9 shows the linear depression of the left pupil.

Work done by Frisch et al (74) for $-G_x$ impact accelerations up to approximately 20 G_x show substantial head rotation. The value of these data is somewhat doubtful in this application since the range of accelerations is far beyond what can be expected in a maneuvering aircraft and secondly, because the data is a result of impact. These data show virtually no head movement up to 10 G_x.

SUMMARY

It has been shown that head motion is resisted by, and effected by the neck musculature. In addition, head orientation is sensed by the muscle receptors, the vestibular system, and possibly the joint receptors. Data has been presented to illustrate the amount of head motion associated with accelerations up to 6 G_z.

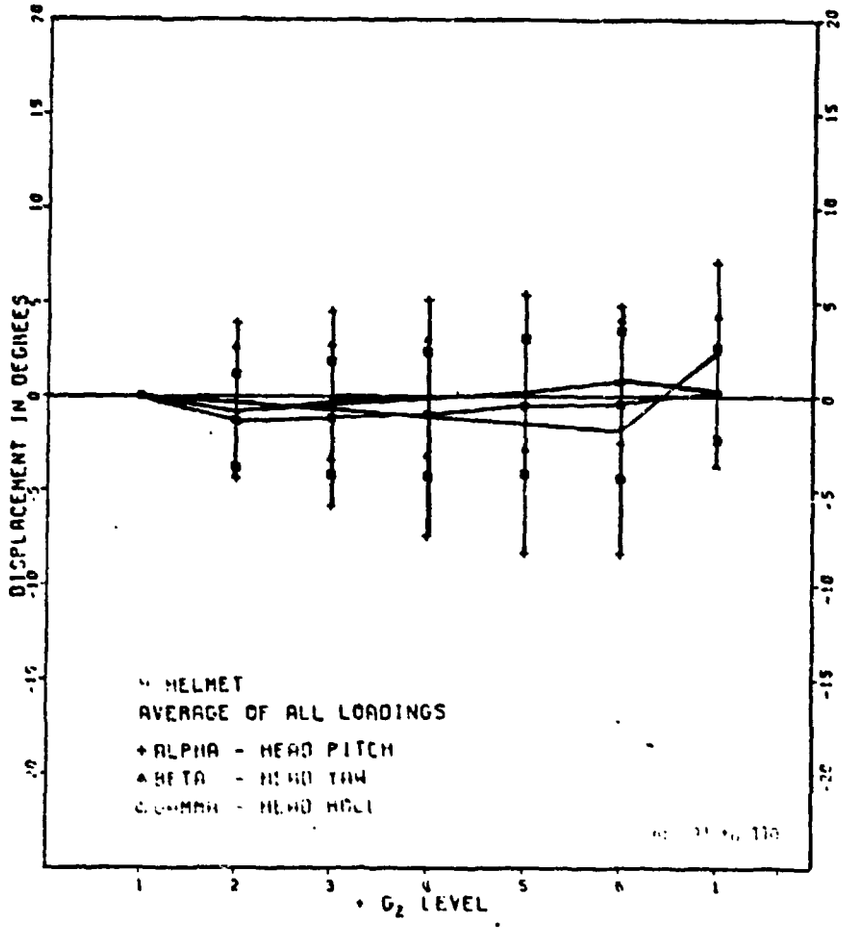


Figure A.4.2-8 Head rotations, all helmet loadings averaged (from Kroemer & Kennedy (142)).

A.4.2.1 Helmet vs. Head Motion

Kroemer and Kennedy (135, 142) present data which illustrates a significant amount of relative motion between the helmet and head can be expected under $\pm G_z$ conditions. Figure A.4.2.1-1 presents the relative pitch between head and helmet as a function of G_z and Figure A.4.2.1-2 presents the linear displacement vertically of the helmet relative to the left pupil.

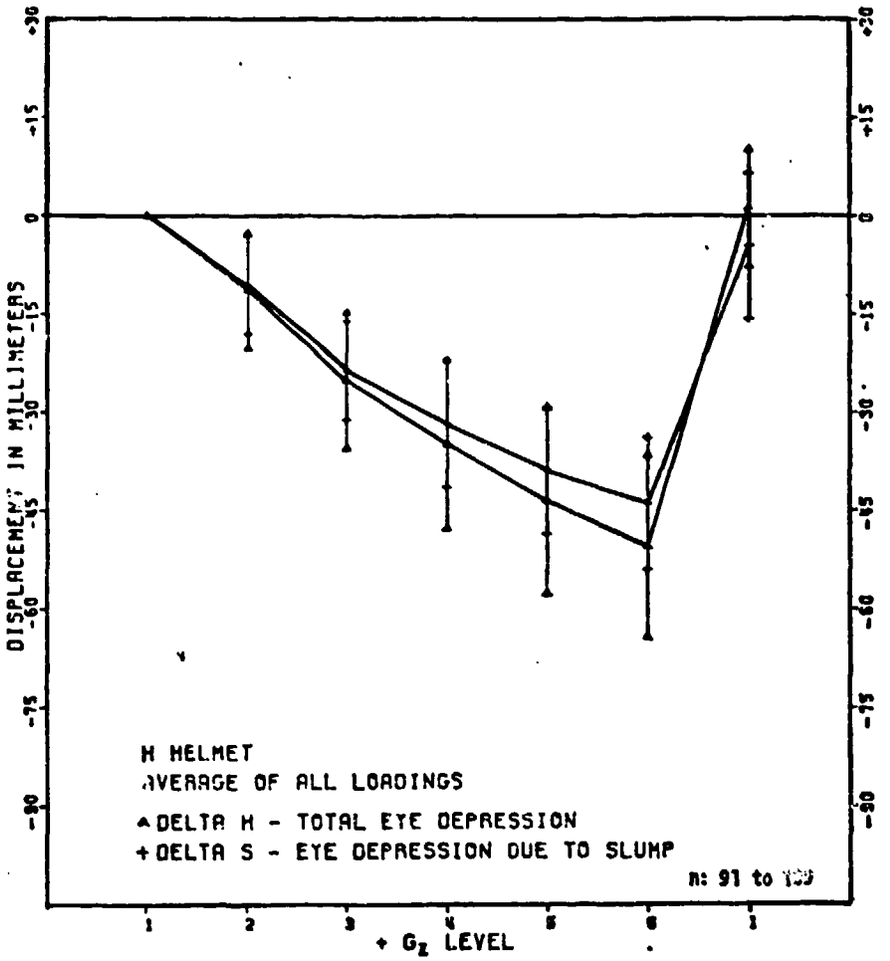


Figure A.4.2-9 Linear depression of the left pupil (from Kroemer & Kennedy (142)).

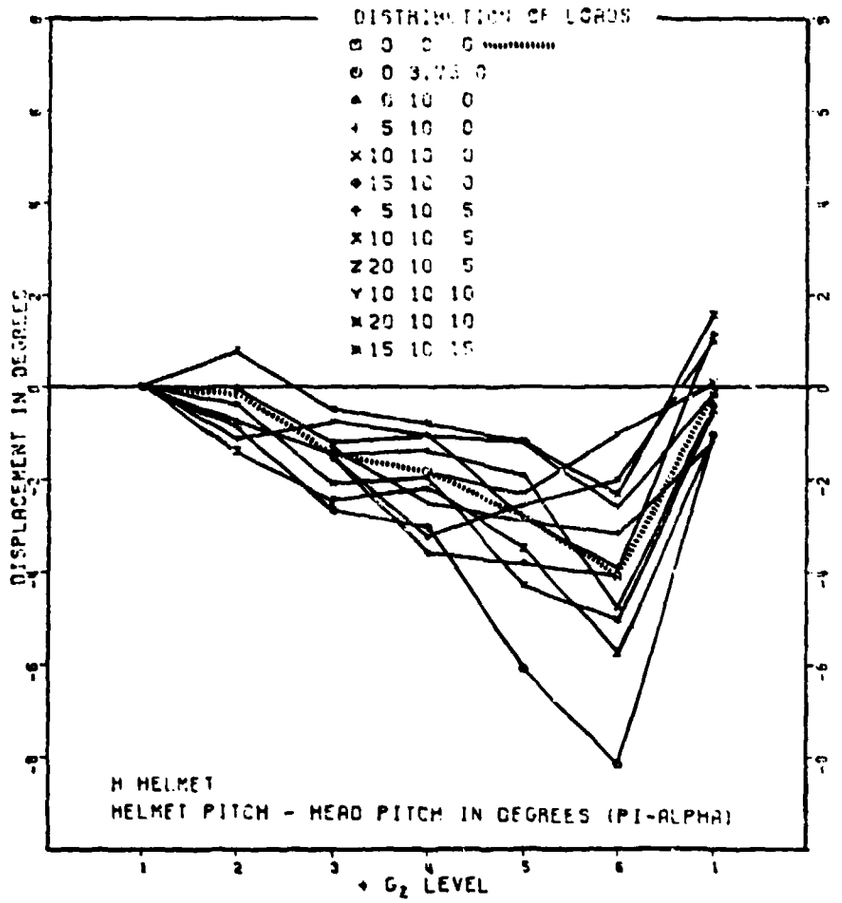


Figure A.4.2.1-1 Helmet pitch relative to head pitch (from Kroemer & Kennedy (142)).

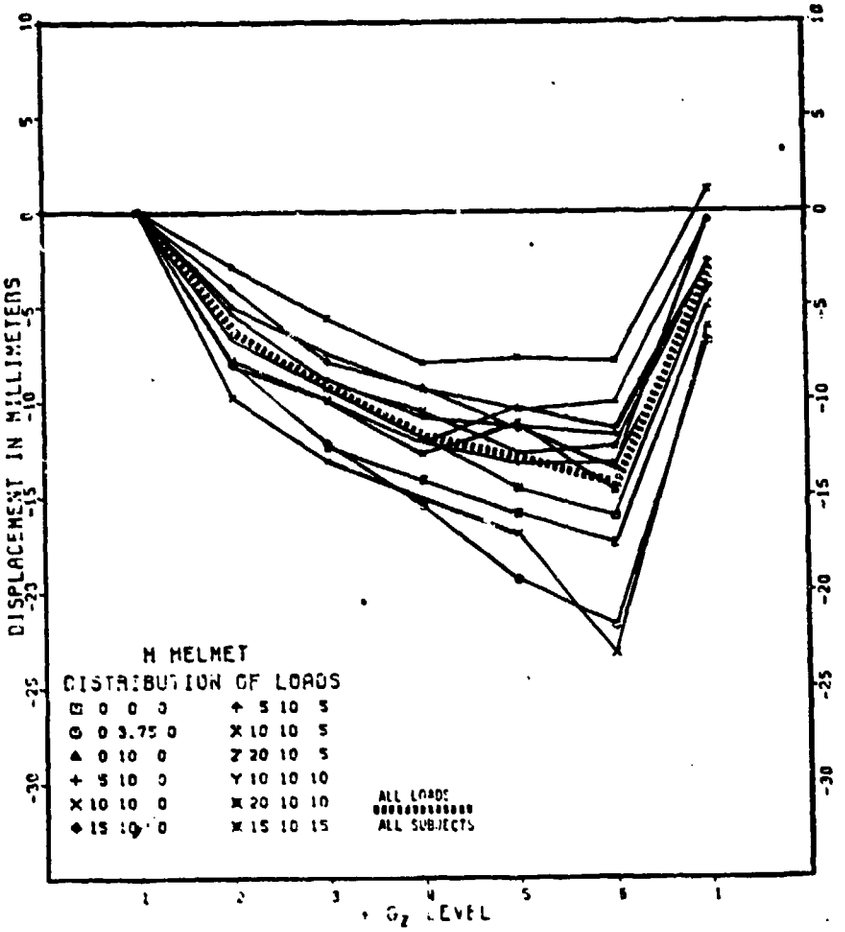


Figure A.4.2.1-2 Reticle depression in z direction with respect to left pupil (from Kroemer & Kennedy (142)).

A.5 Auditory Effects

A.5.1 Auditory Perception Under High G

The literature is rather limited in its treatment of auditory perception under high G. There seem to be two auditory characteristics of high G flight which have been addressed. Coburn (42) states that there is some evidence of diminution of auditory acuity at high $+G_z$ levels. However, the level at which this occurs is so close to the level at which consciousness is lost that the two points are nearly identical and are treated as such. Gillingham and Krutz (86), while not commenting on Coburn's observation of diminished acuity, concur in that hearing is the last available sensory modality, but since it occurs so close to loss of consciousness they do not recommend it as an end point.

The second auditory characteristic discussed in the literature stems from the work of Canfield et. al. (36) in 1949. Canfield reports that reaction times to both sound and light were increased under conditions of increased positive acceleration. He further concludes that "the difference in reaction to light and sound serve to substantiate the well established conclusion that reactions to sound are more rapid than those to light in the mid to high range of intensity." Table A.5.1-1 illustrates their findings.

Table A.5.1-1 Light and sound reaction times as a function of G.

G	Light	Sound
1	0.2458 sec	0.2012 sec
3	0.2578 sec	0.2122 sec
5	0.2654 sec	0.2262 sec

According to Canfield, these increases in time may be due to either reduced sensory efficiency or a decreased central nervous system efficiency or both. Little et al (160) have produced the same results, as Canfield, in reaction time. However, they state that there exists no change in auditory function per se and that the increased reaction time may be due, at least in part, to reduced motor performance. Fraser (71) in reviewing this topic points out that Franks et al in 1945 deny the findings of Canfield relative to increase in reaction time to auditory stimuli. Duane (62) also comments on the auditory phenomena. He states that a subject who has blacked out can't see ambient light but can cerebrate and respond to auditory, tactile and other sensory stimuli.

A.5.2 Auditory Stimulus Composition Change

It was considered that perhaps high performance aircraft might exhibit acoustic signatures characteristic of the accelera-tory forces on the airframe. Pilots were questioned on this point and there did not appear to be agreement. During the UPT/IFS program, audio recordings were made on-board a T38 aircraft during high G maneuvers. During the course of this study these tapes were analyzed and no evidence was found to support the aforementioned hypothesis. Further, no data was found in the literature which even alluded to this phenomenon. Since there is no quantitative evidence of maneuver specific auditory cues to support the structural noise hypothesis, it is the conclusion of this study that no useful training value can be derived in this area and therefore, further investigation of this type is not warranted.

A.6 Tactile

A.6.1 Tactile Sensation in Ischial Tuberosity, Shoulder Harness and Face Mask Regions

The sense of touch and pressure is extremely sensitive and is accorded high priority in the perceptual process. In discussing tactile effects under the inertial load of a multi-G acceleration environment we are concerned with assessing the importance of three effects which can be generated by the six types of uniquely identified touch/pressure receptors:

a) Perception and magnitude discrimination of large field flesh pressure, such as that which would occur in the buttock region under $+G_z$ or the lap belt/shoulder harness region under $-G_z$.

b) Perception of light contact of the skin with foreign objects providing an appreciation of the magnitude of inertial load by estimation of body tissue deformation in those areas restrained by the foreign objects. This proximity type perception yields an estimation of the area of flesh/foreign body contact and varies as a function of flesh deformation. An example of this would be a perception of "sinking" into a seat.

c) Whereas the above two effects are generated by forces normal to the flesh, the third is a perception of the magnitude of skin tension and/or outright scrubbing induced in those areas restrained by, or supporting, a foreign body and is generated by force components lying in the plane of the flesh at the point of foreign body contact. An example of this would be a sensation of tension and scrubbing in the spinal area caused by "sinking" in the seat as experienced under high G maneuvers.

Guyton (102) offers an informative concise description of the receptors employed in these somatic sensations and Borah et. al. (22) has compiled data anatomically describing the receptors, introducing sensitivity levels, and continuing the modeling work pertaining to a) above started by Gum (100). Very little information is available concerning the mechanization of the skin tension or scrubbing sensation. A recently published symposium proceedings (277) summarizes a good deal of the quantitative data concerning the neurophysiological and perceptual thresholds, sensitivity, and dynamic response for each of the types of velocity/displacement/pressure sense organs in the skin.

Except for the temperature/pressure relationship investigated in Section A.6.2 we have directed our investigation toward information pertaining to the inertial acceleration induced composite perceptions represented by a, b and c above rather than at the receptor level. G-seat simulation systems already approach artificial variation of the above perceptions in the primary areas of pilot/seat inertial coupling. Therefore we planned to confine our primary interest to regions of the body not specifically actively addressed by the G-seat such as tactile stimuli arising in the areas of the face mask, undersurface of the forearms, shoulder harness and soles of the feet.

Such restrictiveness proved to be unnecessary for the literature search produced very little data pertaining to inertial acceleration induced tactile stimulation in <u>any</u> region of the body. Within the articles reporting on acceleration induced physiological effects reviewed by the authors, none involved studies or centrifuge experiments aimed specifically at wide field tactile perception, although some of the basic research did trace out the spatial receptive fields of the senses over a few centimeters (277). Nor did we find many informative comments, in similar studies investigating other physiological systems, that could be related to the tactile system. One exception is shown in the

photographs of Figures A.6.1-1 and A.6.1-2 picturing the effects of high G_z on a pilots face, helmet and face mask. The significant amount of face mask slippage evident at 7.5 G_z would suggest strong tactile stimuli at those points where the face mask contacts the facial skin.

We suspect the paucity of data in the area probably stems from a feeling of obviousness: tactile sensations become more intense and encompassing as acceleration levels increase but, in themselves, do not form a physiological endpoint of resistance to acceleration effects and are therefore not of major interest to researchers of acceleration stress. Unfortunately this adversly impacts the availability of data pertaining to the importance of tactile stimuli in the piloting task. Consequently it would seem that if tactile stimulation is to be provided in areas not directly addressed by the G-seat, it must be justified on the assumption that such stimuli are important until proved otherwise.

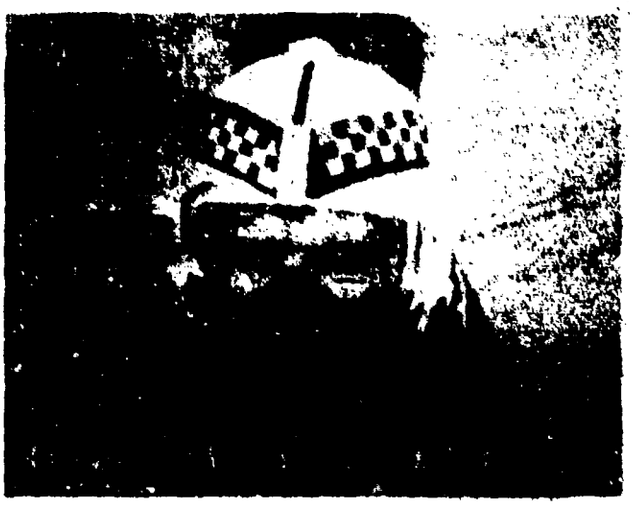


Figure A.6.1-1 Pilot's face at +4.5 Gz. Very slight facial distortion (from Leverett & Burton (184)) (courtesy of Advisory Group for Aerospace Research and Development).



Figure A.6.1-2 Pilot's face at +7.5 Gz. Severe facial distortion and oxygen mask slippage (from Leverett & Burton (184)) (courtesy of Advisory Group for Aerospace Research and Development).

A.6.2 Temperature/Pressure Relationships

Personal experience indicates that a sensory relationship may exist between pressure and temperature perceptions. Obviously, that is not to say one is entirely mistaken for the other. Rather it seems to suggest a type of allied perception that, when a perception of deep tissue pressure is clearly present, a vague sensation of elevated temperature is not unexpected. Because serious constraints and limitations exist in generating credible pressure stimuli in the unaccelerated 1g environment, sensory system characteristics which might be exploited to reinforce and enhance the pressure sensation should be pursued.

Before proceeding, the obvious should be noted. The mere physical act of applying a large surface area stimulus to the flesh is likely to alter the skin temperature. The temperature of the pressure source and the adjacent skin will tend toward equi-

librium and eventually, the pressure source may act as an insulator. Ordinarily, the largest magnitude bodily heat loss is by conduction/convection to the clothes and then by radiation to the environment. The proximity of the insulator would then reflect this radiation back to the body thereby depriving the area of heat loss with resultant temperature build-up toward internal body temperature levels. Thus, initial concurrent perception of pressure and temperature sensations could be explained by the thermodynamics of the physical configuration. However, we suspect an ongoing pressure/temperature relationship active beyond this initial transient period such that further changes in pressure are accompanied by either variations in the intensity of perceived temperature or variations in perceived temperature level.

Our approach has been to assume that if a temperature/pressure sensory relationship exists, an investigation of the skin thermoreceptors and their innervation might reveal parallel or causal interdependancies when compared to the pressure receptors and their innervation. We have examined two possibilities.

RECEPTOR CONFUSION

Like the pressure receptors, thermoreceptors are distributed throughout the skin in puntate form intermixed with the pressure receptors. Thermoreceptors are innervated by small size fibers as are the pressure receptors serving the coarser sensations of outright, non-specifically localized pressure. Loewenstein (163) indicates that the Pacinian corpuscle employed in deep tissue pressure perception is indeed sensitive to temperature as well as pressure changes which is supported by the data in Figure A.6.2-1 from Inman and Peruzzi (123). Mueller (178) states "there are fibers of small diameter that are known to respond to either touch or temperature". These fibers are of the A (δ) class and extend to different locations of the central nervous system. Woodson, et. al. (267) indicate that any strong stimulus applied to a speci-

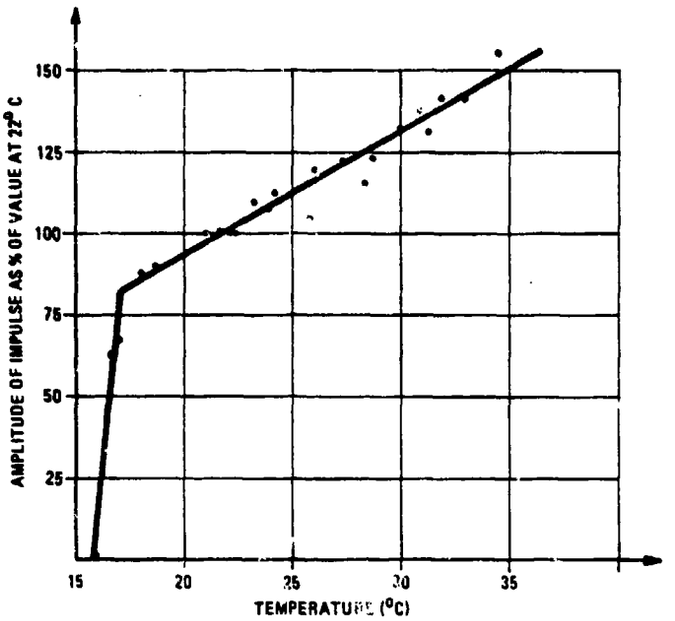


Figure A.6.2-1 Changes in nerve impulse amplitude as a function of temperature (from Inman & Peruzzi (123)).

fic receptor will excite that receptor and if the area stimulation is large enough may arouse sensations other than that characterized by the nature of the stimulus. At this point we could conclude that, although it may not be a prime order effect, there is basis to believe that temperature change could be perceived as augmenting an existing pressure change, an important consideration in high G simulation. The reverse condition of pressure influencing temperature sensation does not readily follow; it depends on the destination of the A (δ) fiber activity. Although the data of Inman and Peruzzi tend to suggest a direct correspondence between pressure sensation and temperature, Zotterman (277) presents some evidence suggesting the inverse relationship that cold stimulation may heighten pressure sensation. The polarity of the relationship obviously warrants further experimentation.

The neurological paths of both the small fiber pressure receptors and the thermoreceptors follow similar routes in entering the dorsal column. Here they split and rise on separate paths of

the spinothalamic track and terminate at different points within the thalamus (102). This type of separation would suggest that neurological intermixing of afferents in the path to the brain is unlikely. If both pressure and thermoreceptor fibers are active under common stimulus, it would seem to occur at the receptor rather than in transport.

Excision demonstrates that thermoreceptor and pressure receptor afferents project to different locations in a common portion of the cerebral cortex. Specific and unique modality of sensations are associated with these locations and appear to be independent of the nature of the stimulus exciting activity within the fiber servicing the location. Therefore an electrical stimulus exciting a fiber leading to a location responsible for touch sensation produces the perception of touch. Likewise it is assumed that should a fiber leading to a temperature sensation area be excited by pressure as Mueller and Woodson suggest is possible, then a temperature perception would ensue.

VASOCONSTRICTION AND DILATION

Proceeding on the premise that stimuli producing like bodily reactions might be interpreted as associative or affiliated, the process of vascular constriction and dilation was examined in the context of response to pressure and temperature stimuli. The body's internal temperature regulatory mechanism makes use of the blood circulatory system as a heat transport and radiator system. Vasoconstriction in the circulatory system occurs to conserve internal body heat and vasodilation to dissipate this heat. Constriction and dilation can occur on a local level based on the thermoreceptor cordal reflex arc wherein thermoreceptor afferents travel to the spinal cord and then immediately back to the initiating area with blood flow alteration commands (102). At a higher central nervous system level, similar thermoreceptor afferents travel to the hypothalamus to be compared with the "hypothalamic

set point" governing internal body temperature. The arc is completed by hypothalamus/vasomotor communication and peripheral sympathetic fibers which innervate the arteries and arterioles. Efferents initiated by the vasomotor pathways alter the vasoconstrictor tone and arterioles throughout the body and magnify the signals in the region of cordal reflex activity.

Pressure applied to the flesh can also cause localized vasodilation should the pressure tend to constrict or temporarily collapse the capillary beds preventing adequate blood flow through the area. However, on a localized level, there appears to be no afferent path for signals requesting dilation. The capillary beds are sensitive to the oxygen level present. The tone of precapillary sphincters controlling blood flow through the beds is also sensitive to oxygen levels (102) and should locally applied pressure restrict oxygenation, the sphincters will automatically dilate.

It is unlikely that the pressure application will cause a systematic blood pressure change of sufficient magnitude to affect the reflex arc through the baroreceptors and peripheral sympathetic nerves controlling arteriole vasoconstrictor tone. Thus it would appear that although temperature induced constriction or dilation employs a neurological reflex arc, such is not the case in locally applied skin pressure induced dilation. Further it seems two separate classes of elements are employed in the constriction/dilation process. Pressure induced dilation is apparently dependent upon the precapillary sphincter whereas temperature induced constriction/dilation affects the arterioles.

In summary, although a form of vasoconstriction/dilation occurs due to both locally applied temperature and pressure stimuli, parallelism sufficient to support a premise of allied sensation does not appear to exist. There seems to be basis at the receptor level for pressure/temperature sensory affiliation. Perhaps more

important for the formulation of high G cuing devices is the apparent justification for considering temperature as a means to enhance or strengthen pressure sensation.

A.7 Respiration

When considering the effects of acceleration on human physiological systems, the respiratory influences are normally ranked as second in importance only to the cardiovascular responses and their associated visual phenomena. In fact, the division of the cardiopulmonary effects into two groups, though traditional, is somewhat arbitrary, since the failure to supply a continuous flow of fully oxygenated blood to the brain, if not to the retina, depends upon both systems. There have been several excellent extensive reviews of the effects of acceleration upon respiration. Gillies (81) and Fraser (71) both deal extensively with acceleration influence upon breathing and gas exchange in the broader context of acceleration physiology. Glaister's 1970 AGARDograph on the effects of acceleration on the lung is perhaps the most complete recent review of the entire field and includes contributions by several other experts (90). The reader is referred to these reviews for a more comprehensive treatment of the subject than can be accomplished in these pages.

The principle effects of acceleration on respiration are quickly summarized, although an appreciation for their basis requires some understanding of lung mechanics. For $+G_z$ the results are much less dramatic than the cardiovascular ones, and entail an increase in the work of breathing and decreased oxygen transport as a result of pulmonary shunting associated with pooling of blood in the lower regions of the pulmonary circulation and filling of the upper parts of the lung with air. The respiratory reactions are most noticeable for forward acceleration ($+G_x$) where breathing difficulties come into play long before any cardiovascular problems become evident. The difficulty of expanding the

chest against the inertial load is reflected in shallow breathing and combines with a significant increase in the effective dead space of breathing and a major mismatch between ventilation and perfusion in the lung regions to make gas exchange inefficient and to produce hypoxia even with inspired pure O_2. With the trend toward use of cockpit seats with significant tilt back angles and airplanes capable of high G maneuvers, consideration of the respiratory effects of $+G_x$ stress is timely and investigation of cuing techniques for the simulator is appropriate.

A.7.1 Respiration in the Unaccelerated Environment

Respiration in the unaccelerated environment entails the exchange of gas between air in the lungs and blood in the pulmonary circulation. Before proceeding to a discussion of the effects of acceleration on respiration, we will review some of the basic aspects of the mechanics of breathing and lung perfusion in a 1g field. Each of these has an influence on the oxygenation of blood and the elimination of carbon dioxide.

A.7.1.1 Ventilation

The basic mechanisms of inspiration and expiration of air are, of course, the result of muscular effort to lower the diaphragm and expand the thorax forward, thereby creating negative pressures in the intrapleural space between chest and the lungs. This causes air at ambient pressure to be sucked down the airways and inflate the lungs. The pleural pressure is not constant, but increases with depth, following a similar hydrostatic pressure drop to that discussed in the cardiovascular section. For a seated man in a 1g field, for example, there is a pressure gradient from the apex toward the basalar end of 7.5 centimeters of water related to the weight of the lung. This pressure difference is of the order of 7.5 centimeters H_2O as illustrated in Figure A.7-1 where the average pleural pressure at the beginning

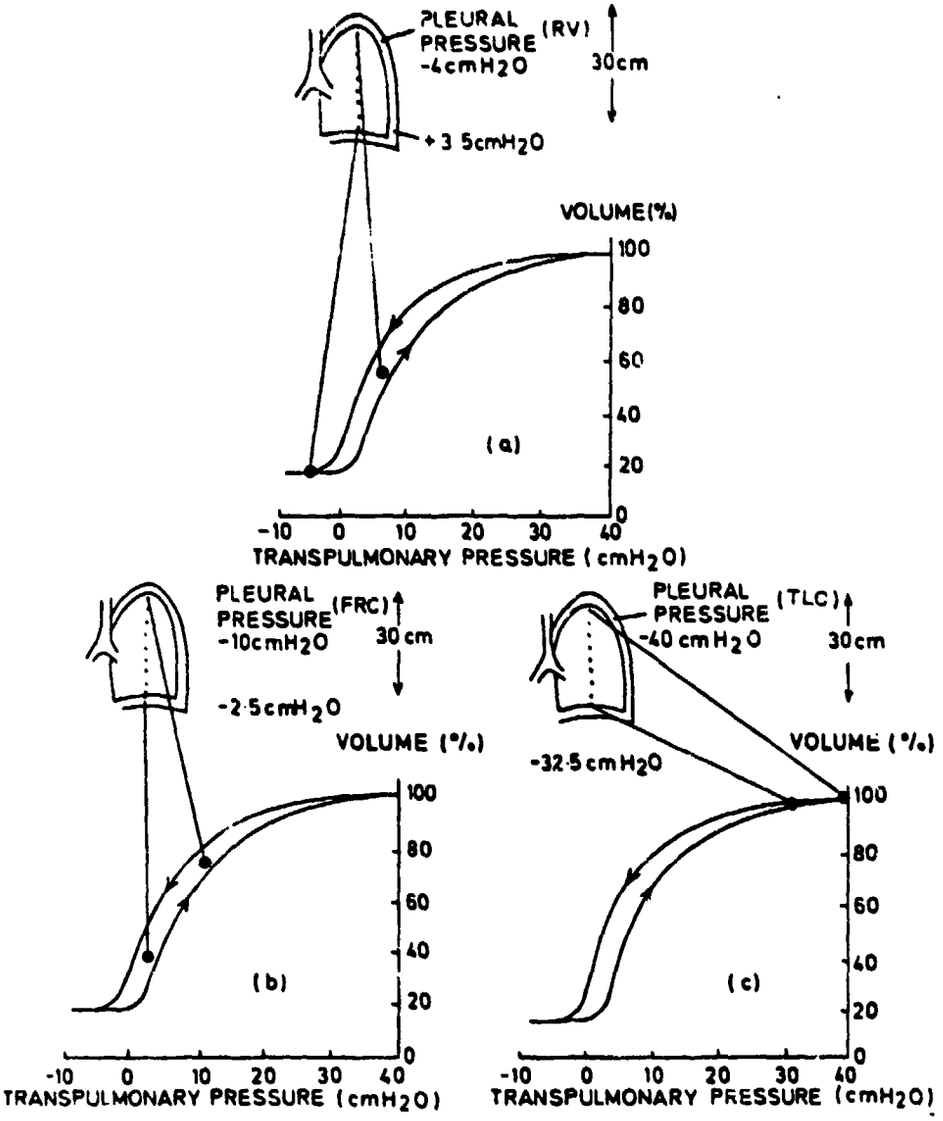


Figure A.7-1 Effect of pleural pressure gradient on the volume distribution of gas within the lung. The pressure is assumed to increase at a constant rate of 0.25 cm water/cm vertical distance. The elastic properties, as shown by the S-shaped static volume-pressure curves in the lower part of each panel, are assumed to be uniform throughout the lung. Values of pleural pressure at the apex and base existing at three lung volumes (RV, FRC, and TLC) are shown in the upper part of each panel. In C, at full inspiration (TLC), all lung regions are expanded virtually uniformly, in spite of the pleural pressure differences down the lung. On the contrary at RV and FRC (A and B, respectively), the pleural pressure gradient causes the upper lung regions to have a greater volume than the lower zones. from Glaister (90)) (courtesy of Advisory Group for Aerospace Research and Development).

of inspiration is approximately that of the ambient air. Because of the gradient in pleural pressure, as well as the elastic properties of the lung, as the chest is expanded and the diaphragm lowered during inspiration the lungs fill unequally, with the apex tending to fill toward its maximum volume before the base, rising along the lower line of the pressure-volume loop.

At full inspiration, with transpulmonary pressure on the order of 40 centimeters of water, all of the lung is nearly uniformly expanded reflecting the relatively flat pressure-volume curve near full inspiration to assure equal filling and reduce regional differences. For less than full inspiration, as will be discussed further under gravitational effects, it is seen that the dependent (lower) areas of the lung are significantly less filled on inspiration. Figure A.7-1 also illustrates schematically the major elastic and resistance elements affecting ventilation impedance. The S-shaped curves representing lung elasticity are assumed to be representative of all regions of the lung. The difference between the pressure at constant volume for inspiration and expiration represents primarily airway resistance.

At the end of each maximum inspiration, of course, not all of the inspired air comes into contact with the blood in the alveoli for gas exchange, nor is all air expired from the lung during exhalation. The essential definitions of respiratory mechanics which are important in the consideration of gravitational effects on respiration are illustrated in Figure A.7-2 along with the regional subdivisions of lung volumes for seated men in a 1g field. Total lung capacity (TLC) refers to the total amount of air contained in the lung following a maximal inhalation. For the later discussion of acceleration effects, it will be important to refer to the various subdivisions or regions of the lung. The data of the figure shows the various subvolumes within each lung region as a percentage of the total lung capac-

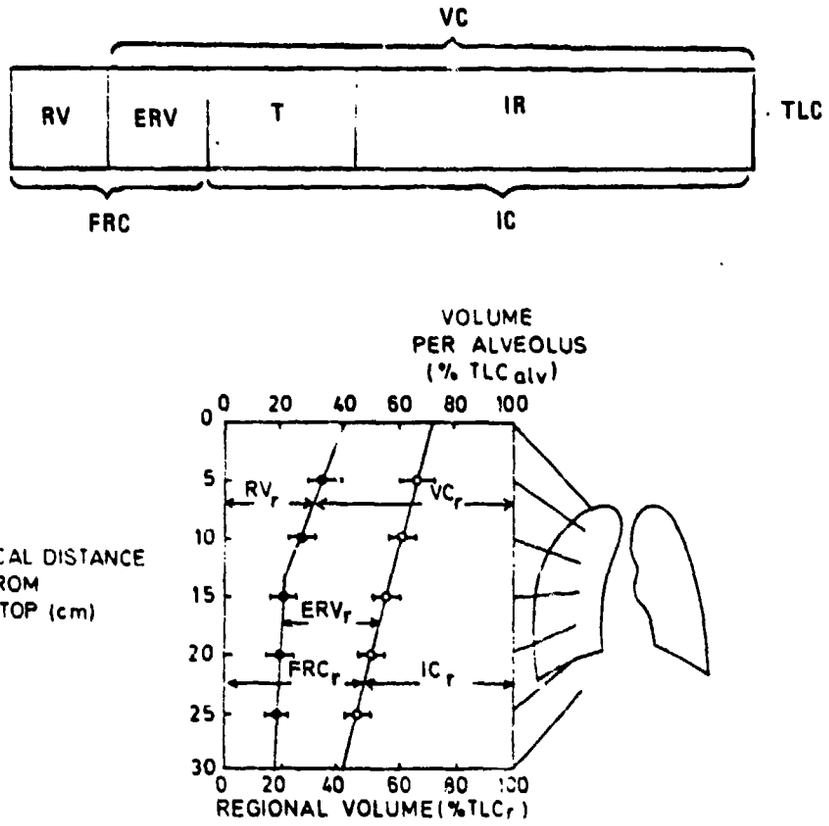


Figure A.7-2 Regional subdivisions of lung volume in seated men. Filled and open circles represent average results obtained on eight healthy young subjects at RV and FRC, respectively. Bars indicate 2 SE. RV = regional residual volume; IC = regional inspiratory capacity; ERV = regional expiratory reserve volume; VC_r = regional vital capacity (from Glaister (90)) (courtesy of Advisory Group for Aerospace Research and Development).

ity in that region (TLC). Beginning the definitions with a fully deflated lung region (never found normally), the first volume is the residual volume of that region (RV_r) and represents the air remaining in the lung region following a maximal forced exhalation. This represents a condition wherein pleural pressure is above airway pressure, so that the local airways collapse, trapping this amount of air behind. Notice that, for the seated man, RV_r is nearly constant for the lower half of the lung, indicating that the lower lung is at minimal volume at the end of exhalation. For the upper half of the lung, however, where pleural pressures are less because of hydrostatic effects discussed ear-

lier, the airways are not closed and the lung region is not driven all the way to its minimum at the end of a normal, maximum exhalation. The next subdivision is the expiratory reserve volume (ERV), which is the volume between RV_r and the lung volume at the end of a normal, relaxed exhalation. As the name implies, ERV is the reserve volume that can be forced out by a forced exhalation beyond the normal expiratory end point. The sum of ERV and RV_r is the volume of air remaining in the lung at the end of normal exhalation, and is referred to as the functional reserve capacity, (FRC). Notice that FRC is much less for the dependent (lower) regions than for the upper parts.

The next volume defined is the tidal volume (T), which is the volume of air normally inhaled and exhaled during each breath. When the lungs are maximally expanded by a deep breath, reaching TLC, the additional air inhaled beyond the tidal volume is the inspiratory reserve (IR). The sum of T and IR, representing the total volume of air that can be inspired beginning at the end of a normal exhalation, ERV, is referred as the inspiratory capacity (IC), and also increased with distance from the apex. Finally, the sum of IC and ERV is known as the vital capacity (VC) and is the volume of air that can be drawn in during a maximum inhalation following a maximum forced exhalation. Not all of the air that is inhaled on each breath takes part in gas exchange, however, since some never reaches the alveoli. This volume is the anatomical dead-space, and is also acceleration dependent. It is interesting to note that in a normal lg field, ventilation of the lung is greater in the dependent (lower) zones, independent of breathing depth or rate. Thus the normal regional distribution of ventilation is matched to the regional perfusion of blood in the pulmonary circulation which, as will be discussed below, also is greatest in the dependent part of the lung. Consequently, in a lg field the air and blood distributions are arranged to make gas exchange more efficient than it would be if the lung were uniformly ventilated. This matching,

reflected in the ventilation/perfusion ratio, will be shown to be significantly disturbed by linear acceleration. The minute volume is the amount of air inspired per minute, and is the product of respiration rate and average tidal volume. Finally, we will be concerned with the mechanical parameters of respiration, especially lung compliance and airway resistance.

A.7.1.2 Perfusion

A simple picture of pulmonary circulation is that it carries venous blood from the right ventricle to the capillaries in the lung, where it exchanges gas with air in the alveolar sacs and returns in the pulmonary veins to the left atrium, carrying oxygen in the form of oxyhemoglobin and having been purged of most CO_2. In fact, even in the normal upright lung at 1g, the local distribution of blood throughout the lung (regional perfusion) is nothing like uniform but increases markedly from top to bottom. This distribution of perfusion has led to lung perfusion models entailing originally 3 separate zones (Permutt et. al. (196), Banister and Torrance (9) and more recently 4 zones (West (257)) divided functionally according to the pressure relationships among pulmonary arterial, alveolar air, and pulmonary venous pressures. The three zone model is illustrated in Figure A.7-3. At the upper position of the lung for the upright man, where the air pressure in the alveolus (P_A) exceeds the pulmonary arterial pressure (P_a), the collapsible blood vessels are squeezed closed, with no blood and only a few trapped blood cells. Further down the lung the arterial and venous blood pressures drop relative to the air pressure in the alveoli because of the hydrostatic pressure head on the blood column, and the top of zone 2 is determined where P_a exceeds P_A. In this region the resistance to blood flow is controlled indirectly by alveolar pressure on the limp vessel, but the dominant factor is the P_a-P_v pressure drop along the vessel which accelerates blood through into the veins in what is known as the "vascular waterfall". As the perfusing

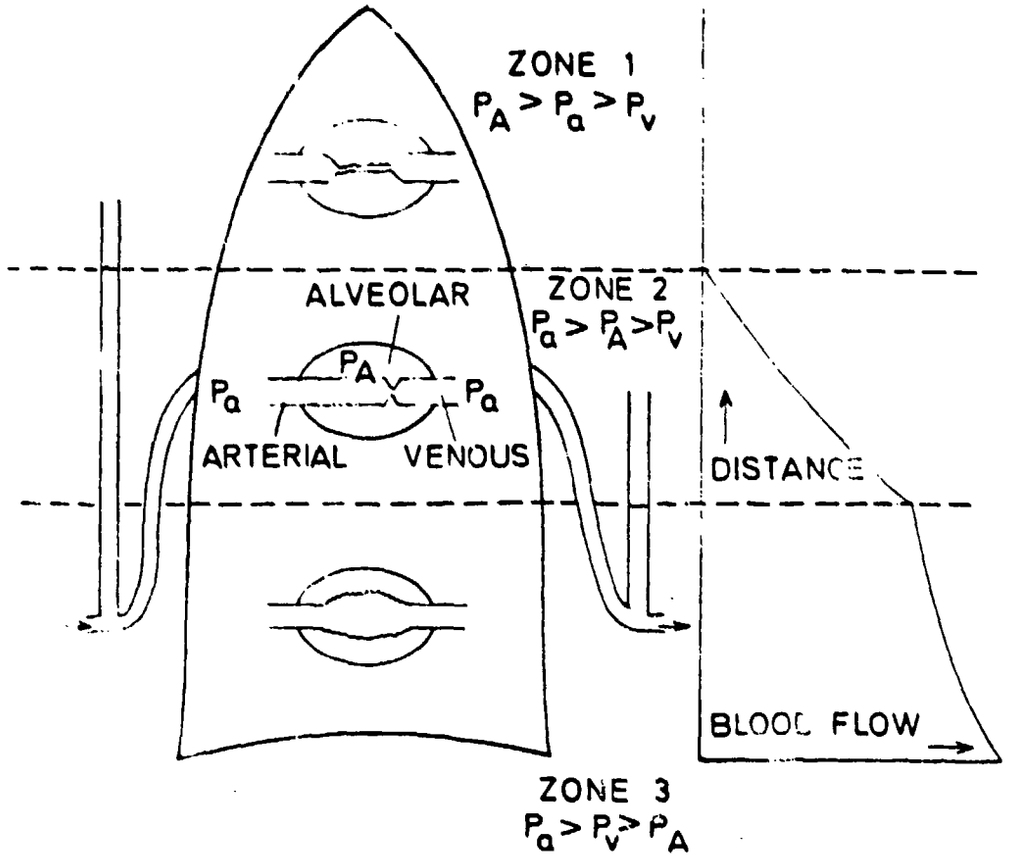


Figure A.7-3

Diagram to show the effects of pulmonary arterial, alveolar and venous pressures on the topographical distribution of blood flow in the lung. The lung is divided into three zones by the relative magnitudes of the three pressures. In zone 1, arterial pressure is less than alveolar pressure and there is no flow, presumably because collapsible vessels are directly exposed to alveolar pressure. In zone 2, arterial pressure exceeds alveolar, but alveolar pressure exceeds venous pressure. Here the vessels behave like Starling resistors and flow is proportional to the difference between arterial pressure (which is increasing down the lung) and alveolar pressure (which is constant). In zone 3, venous pressure exceeds alveolar pressure and flow is determined by the arteriovenous difference. Flow increases down this zone because the transmural pressure of the vessels increases so that the vessels have a larger calibre. (from Glaister (90)) (courtesy of Advisory Group for Aerospace Research and Development).

pressure (P_a) is increased in zone 2, the vascular resistance is decreased, both by dilating the vessels already open, and by opening up of additional parallel channels.

Proceeding further down the lung to region 3, where both the arterial and venous pressure exceeds the alveolar pressure, the vessels remain fully expanded, with a large cross-section, and

the flow is determined only by the arterial-venous pressure drop. This is the major highly perfused dependent region of the lung, and matches the increase in ventilation toward the base referred to earlier. Finally, toward the very bottom of the lung there has been identified yet a fourth region termed the zone of interstitial pressure by West (257), in which blood flow and vessel size are once again reduced. The explanation for this reduction in flow, despite the increase in hydrostatic pressure, is that the failure of the lung to fully expand in the furthest dependent zones leaves the elastic forces in the extra-alveolar vessels, and the muscle around these vessels free to partially constrict the vessels except at maximum lung filling. This fourth zone and the distribution of blood flow from apex to base for the erect lg case is shown in Figure A.7-4.

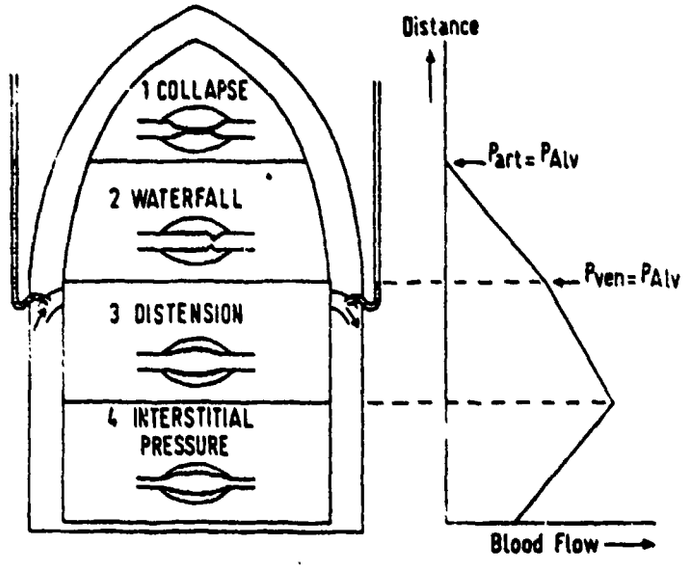


Figure A.7-4 How the three zone diagram of figure 3.7-3 can be modified to take account of the reduction of blood flow of the most dependent zone of the lung as a result of a raised interstitial pressure. The first three zones correspond to those featured in Figure 3.7-3, and to these has been added a fourth zone where the vascular resistance of the extra-alveolar vessels becomes significant because of a rise in interstitial pressure. This occurs in the normal lung at volumes below total lung capacity because of the relatively poor expansion of lung parenchyma in dependent zones. (from Glaister(90)) (courtesy of Advisory Group for Aerospace Research and Development).

A.7.1.3 Ventilation-Perfusion Ratio and Gas Exchange in the Lung at 1G

The preceding sections indicated that both the regional distribution of ventilation and that of blood perfusion to the lung were gravity dependent. In a 1g field they are reasonably matched, so that a greater blood flow appears in the dependent portion of the lung where the ventilation is greatest and the opportunities for gas exchange are maximized. The parameter used to describe the role of gas and blood flow in a region is the "ventilation-perfusion ratio". For a total lung in a 1g field, this might have an absolute ratio of approximately 0.85, corresponding to alveolar ventilation of 5.1 liters per minute and pulmonary blood flow of 6 liters per minute (Glaister 90). The regional ventilation-perfusion ratios are given in terms of their value relative to the total lung ratio (V_A/Q). For an ideal lung with optimal gas exchange, the regional ventilation-perfusion ratio should be approximately 1 throughout the lung so that the air in every alveolus has the opportunity to participate in gas exchange with blood flowing around it. Even in the 1g field this situation is not meant precisely, since at the apex of the lung there is insufficient blood supply to participate in gas exchange.

The distribution of regional relative ventilation-perfusion ratios with distance down the lung for a subject erect in a 1g field and at 2 and 3 G_z is shown in Figure A.7-5 where it is seen that ratios of approximately 1 exist only in the lower 15 centimeters of the lung even at 1g. The result of wide variations in this ratio is a disruption of the gas exchange process by either of two mechanisms as illustrated in Figure A.7-6. As seen on the left, when the ventilation-perfusion ratio goes to infinity, there is no gas exchange despite ample ventilation of the alveolus by air or even 100% oxygen. This situation is likely to occur principally because of acceleration effects on the pulmonary circulation, pooling blood in the lower portions of the lung.

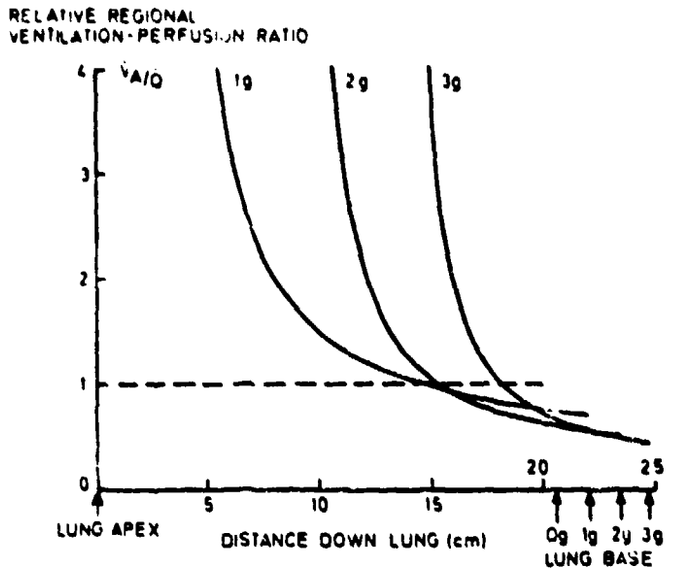


Figure A.7-5 The effect of positive acceleration on the variation in ventilation - perfusion ratio (V_A/Q) down the lung. The +1 to +3 G values were obtained by radioisotope scanning after inhalation and intrevenous injection of ^{133}Xe and the zero G values by extrapolation of this data. Values given are relative, the V_A/Q of the whole lung being taken as 1.0 (from Glaister (90)) (courtesy of Advisory Group for Aerospace Research and Development).

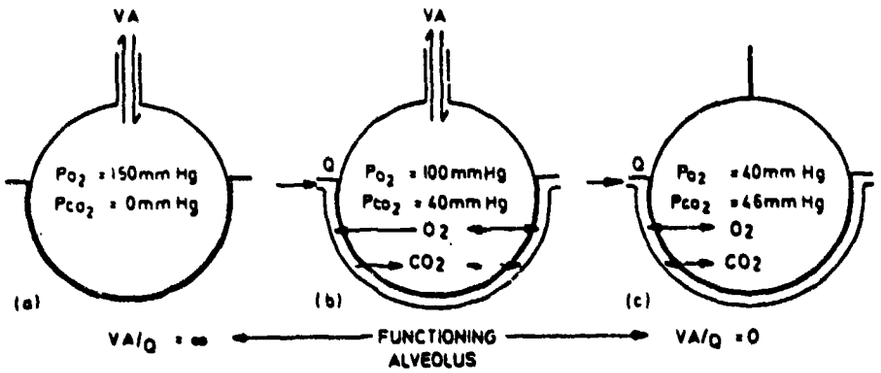


Figure A.7-6 Extremes of ventilation-perfusion ratio (V_A/Q) inequality as exhibited by a ventilated but unperfused alveolus (a) and by a perfused but unventilated alveolus (c), compared with an alveolus having normal ventilation and perfusion (b). Directions in which gas exchange takes place, and the alveolar gas contents which result, are indicated for each situation. (from Glaister (90)) (courtesy of Advisory Group for Aerospace Research and Development).

The other extreme, seen at the right side of Figure A.7-6, is where the ventilation-perfusion ratio is reduced to zero either because of trapped air in the airways which cannot be exchanged on each breath due to insufficient pressure to open the airways, or to actual collapse of the alveolar sacs, a condition known as atelectasis. For the former condition, of trapped gas, the breathing of 100 percent oxygen slows the decrease in arterial blood saturation and gas exchange continues to take place from the trapped oxygen in the alveoli. Carbon dioxide level continues to rise. For the latter condition, of atelectasis, surface tension tends to keep the sacs closed once they have been relaxed, until they are forced open by maximum inspiration or cough. It is easily seen that the functioning lung requires an adequate total blood supply which is properly distributed to match the regional ventilation. As might be expected, important effects of interference with respiration because of acceleration are seen in ability of the lungs to oxygenate blood.

The regions of the lung with very high ventilation-perfusion ratios effectively detract from the total useful lung area. However, because of the characteristics of the oxyhemoglobin dissociation curve, close to 100% oxygen saturation of blood can be maintained even though the partial pressure of oxygen in the blood drops considerably. This effect is largely compensated for unless the interference is massive or the inspired air has insufficient oxygen. At the other extreme, of zero ventilation-perfusion ratio, the effect is much more serious, since blood now passes directly from the arterial to the venous side of the pulmonary circulation without changing its gas content, and therefore drops the overall oxygen saturation of arterial blood with resulting hypoxia. There are of course other well known ways of producing hypoxia by manipulating the total air pressure or partial pressure of oxygen in the inspired air and these will be discussed under simulation mechanisms below.

A.7.1.4 Control of Respiration and Work of Breathing

The two obvious parameters under control of respiration, for delivery of the required minute volume of air, are tidal volume and respiration rate. Since the muscular activity involved in breathing itself entails additional oxygen need, it is obvious then for any total minute volume required, there is an optimum combination of respiration rate and depth. For example, whereas the resting human might have a breathing frequency of 15 to 20 per minute and an alveolar ventilation of 10 liters per minute, when subject exercises sufficient to raise the ventilation rate to 25 liters per minute, the optimum breathing rate increases by a factor of 2 and with it the total work of breathing goes up by approximately 40%. Most of this work of breathing is involved in expanding the chest during inspiration, with the assumption that exhalation is a passive relaxation process. As will be discussed below, the additional work of breathing entailed by the need to counter opposing forces on the chest at higher accelerations plays a considerable role in additional oxygen costs which further increase the required minute volume.

The neural signals involved in control of respiration rate and depth comes from several sources. The primary chemoreceptor sensors detect the carbon dioxide levels in the blood (rather than oxygen levels) and call for increased respiration depth and frequency when the CO_2 levels increase above their setpoints for arterial blood. However, arterial hypoxemia does have an effect in increasing minute volume as does any drop in arterial pressure as detected by baroreceptors. Respiration is inhibited by stimulation of the vagal nerve from any of a number of sources including overstretching of the lung, and acts against the maintenance of deep breathing. The role of each of these factors on acceleration effects on respiration rates will be discussed below.

The influence of partial pressure of oxygen in the ambient

air on the ability of the lungs to oxygenate blood in a normal 1g field is well known from altitude studies. Because of the efficient transport of oxygen by oxyhemoglobin, the partial pressure of oxygen in the inspired air can be dropped from its normal one atmosphere level of approximately 150 mm of mercury to much lower values before any significant reduction in arterial oxygen saturation appears. However, with inspired air partial pressures down to approximately 70 mm of mercury (corresponding to an altitude of 18000 ft), the oxygen saturation has fallen to 75% and definite signs of hypoxia appear (81). It must be remembered that the critical element is the partial pressure of oxygen. Total pressure of the inspired gas is of importance in this context only as it affects the "work of breathing" with positive pressure breathing assisting ventilation but requiring forced exhalation, and negative pressure breathing entailing considerably more work to expand the lungs.

A.7.2 Respiration in the Accelerated Environment

From the point of view of the pilot undergoing acceleration, the effects on the respiratory system are chiefly seen in $+G_x$ acceleration. Nonetheless for $+G_z$ acceleration he also finds that inspiration becomes difficult and there is a reported tendency for the breath to be held during inspiration. Oxygen saturation drops and the work of breathing increases, but these effects are all minor compared to the cardiovascular and resulting visual tunneling effects during $+G_z$. However, for forward acceleration, $+G_x$, the respiratory effects are of major concern. Chest tightness and pain along with difficulty of breathing are reported in the +5 to +6 G_x region and increased with further G levels until, by +12 G_x breathing difficulty and chest pain are severe. Various G protective devices, including the use of an anti-G suit and positive pressure breathing influence respiratory mechanics. The former unfortunately further reduces lung volume, making breathing and gas exchange more difficult. The principal mechanisms

underlying the observed effects of acceleration on respiration are considered below in terms of the models for respiration in the 1g environment developed in the preceding section.

A.7.2.1 Lung Mechanics Under Acceleration

The effects of acceleration are seen not so much directly on lung as on its ventilation and perfusion and on the work required to move its supporting structure. Under $+G_z$ acceleration, the weight of the abdominal viscera actually pulls the diaphragm down, thereby increasing vital capacity by up to 500 cc. Despite this, however, for reasons to be discussed below, the net effect of $+G_z$ acceleration exceeding 3g's is to reduce the oxygen transfer to the blood. Acceleration in the $+G_z$ direction, as well as in the $+G_x$ direction does little to change the residual volume of the lung, which seems to be an inherent characteristic of lung rather than of supporting structure. Vital capacity changes, but modestly under increasing $+G_z$ loads, reducing from approximately 5.5 liters to about 4.5 liters over the range from +3 G_z to +6 G_z. There is some increased oxygen uptake under $+G_z$ associated with the increased work of breathing, and breathing rate may increase although the results are highly variable. The variability may be understood when one realizes the two opposite influences on breathing are at play. Vagal inhibition from stretch receptors in the lung would tend to reduce breathing rate whereas the effects of hypotension from the cardiovascular effects of $+G_z$ and the arterial hypoxemia, to be discussed below, both would tend to increase breathing rate.

The matter of acceleration effects on lung mechanics in the supine position is quite another story, however. Inspiration then becomes a matter of raising the chest wall directly against the increased inertial force, and breathing becomes severely disrupted. Although the effective weight of the chest wall plays a small factor in $+G_z$ acceleration, it is a major factor in affect-

ing lung mechanics under $+G_x$ acceleration. Furthermore, since the abdomen is forced up against the diaphragm under forward acceleration, descent of the diaphragm is also made more difficult. This pressing up on the diaphragm under $+G_x$ acceleration reduces the expiratory reserve volume. Vital capacity and inspiratory capacity as well as total volume are severely reduced under $+G_x$ acceleration as seen in Figure A.7-7. Vital capacity decreases until it is nearly that of the tidal volume at +12 G_x, with no reserve for greater ventilation. As breathing capacity goes down, tolerance times approach those of breath holding. Respiratory rate, meanwhile, climbs rapidly and almost linearly with forward acceleration up to triple the resting level at + 12 G_x. Since tidal volume is falling, or at most peaks slightly at low acceleration levels, the minute volume does not continue to grow as indicated in Figure A.7-8. The marked increase in respiratory rate is probably primarily attributable to the hypoxia associated with inadequate ventilation/perfusion ratios, but also to some extent, responses to the chest compression.

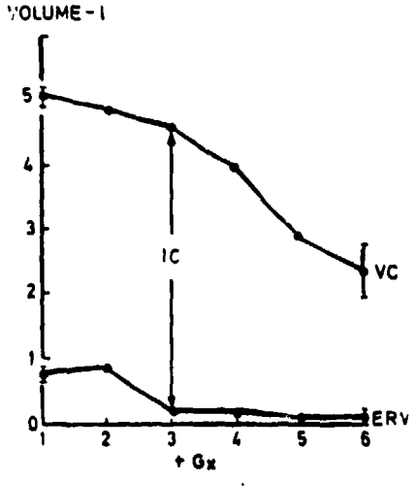


Figure A.7-7 The effect of forward acceleration on vital capacity (VC), inspiratory capacity (IC), and expiratory reserve volume (ERV). Plus and minus one standard deviation of the +1 and +6 Gz values are indicated by barred vertical lines (from Glaister (90)) (Courtesy of Advisory Group for Aerospace Research and Development).

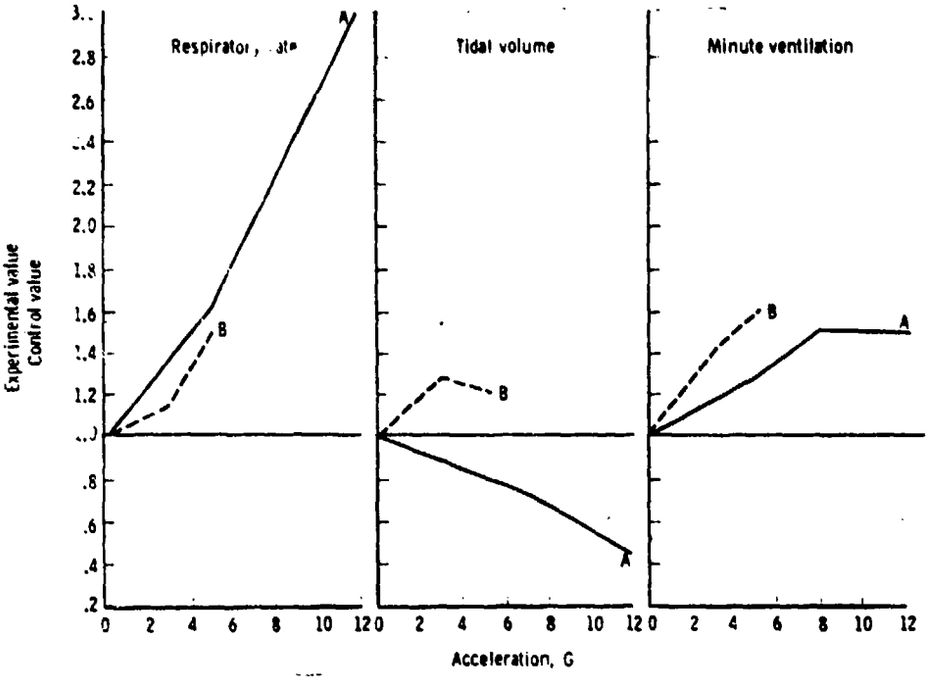


Figure A.7-8 Effect of back angle on respiration in room air. Curves labeled A represent measurements made on net seat with a 12° back angle, at 5, 8, and 12 G. The B curves represent measurements made on a rigid support with a 0° back angle, at 3 and 5 G. (from Fraser (71)).

A.7.2.2 Similarity of Negative Pressure Breathing to $+G_x$ Effects

The increased work of breathing and difficulty of expanding the chest wall under $+G_x$ has been previously noted as bearing some similarity to the similar forces associated with negative pressure breathing, when the inspired air pressure is below ambient. This is of course just the case found when breathing through a snorkel underwater, and sets the effective limit on depth to which one can descend using snorkel breathing. Watson and his colleagues (253) investigated in detail the relative effect of negative pressure breathing and forward acceleration on lung mechanics, and pointed out the very great quantitative similarity. For both increasing negative pressure and increasing $+G_x$, the lung volumes decrease and interpulmonic pressure at a given lung volume increases, shifting the pressure volume curves for the lung towards higher interpulmonary pressures by about 4

mm Hg/g. Lung compliance becomes smaller and the total work of breathing increases, approximately doubling from 1 to 4g's or for the equivalent negative pressure increase. For both cases, this additional work results in increased oxygen consumption. Frequency of breathing increases for negative pressure breathing in a manner similar to that for $+G_x$. Although the details of regional perfusion and ventilation of course would not be expected to be mimicked by negative pressure breathing, in all other respects negative pressure breathing appears to have nearly identical effects on lung mechanics as does forward acceleration, and consequently will be considered in more detail as a high G augmentation concept. The equivalence of negative pressure breathing of 5 mm Hg/g on lung volume is shown in Figure A.7-9.

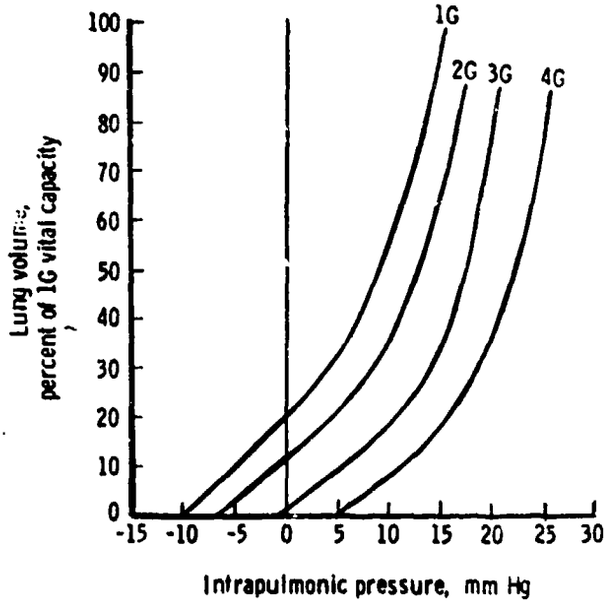


Figure A.7-9 Static relaxation pressure-volume curves during control (1G) and 2, 3, and 4 G forward acceleration. All lung volumes were obtained at 1G (from Fraser (71)).

Zechman and Mueller (275), in a similar study comparing effects of forward acceleration and negative pressure at a single comparison point (+ 4 G_x and -15 mm Hg) showed generally similar results but with some detailed differences in terms of lung mechanics and gas exchange. They reported that the ventilation response under negative pressure breathing was more by an increase in tidal volume than by the increase in breathing rate seen under acceleration. They fail to show the increase in oxygen uptake under acceleration reported by many others, and seen with negative pressure breathing. As a corollary, positive pressure breathing has been used to counter the effects of forward acceleration by making inspiration easier and overcoming the downward forces on the chest wall. Although the theoretical values of 5 mm Hg/1g increment would call for applied pressures up to 35 mm Hg at 8 g's, this was found to be excessive by nearly a factor of 2. Positive pressure breathing with oxygen did indeed increase tolerable exposure durations significantly at levels up to 10 G_x (253).

Zechman and Mueller (275) found one other interesting difference between negative pressure breathing and forward acceleration. Using a carbon monoxide diffusion technique they measured changes in lung diffusion capacity under both negative pressure breathing and under acceleration and found a change only for the latter, dropping from 21 to 12 ml/min/mm Hg. Whether this reflects detailed changes in alveolar capacity, pulmonary edema or some other factor is yet undetermined according to Fraser (71). The significance of this difference in terms of the major similarities between negative pressure breathing and forward acceleration effects on respiration is not clear.

The increased muscular activity associated with expanding the chest wall against a forward acceleration force is reflected in an additional metabolic load of approximately 141 ml/min at 6 g's according to Steiner et al (232). The additional oxygen load makes even worse the problems of oxygen delivery resulting from

mismatch of regional ventilation/perfusion ratios discussed below.

A.7.2.3 Effects of Acceleration on Ventilation/Perfusion Ratio, Gas Exchange and Arterial Saturation

EFFECTS OF + G_z ACCELERATION

In addition to the dominant cardiovascular effects, even moderate levels of prolonged headward acceleration can cause noticable symptoms because of reduced oxygen transport. Von Nieding et al (184) show a case of respiratory gas exchange alteration after six minutes of acceleration at only +2 G_z, leading to blackout at 10 minutes.

The increased work of breathing at +G_z acceleration is one factor, but clearly not the dominant one in the respiratory effects. Changes in the regional perfusion and ventilation of the lung with increasing acceleration has been clearly demonstrated to be the overriding factors of importance. As linear acceleration increases, the blood in the pulmonary circulation pools more and more toward the base of the lung, leaving the apical portion largely unperfused. Consequently, the upper portion of the lung does not contribute to gas exchange, which takes place only in the mid-portion. At the bottom of the lung, where much of the pulmonary circulation then takes place, ventilation is excluded as discussed earlier, with air trapped or atelectasis taking place. Pulmonary shunting takes place, with pure venous blood being mixed in with the oxygenated blood going back to the left heart, and thereby reducing total blood oxygen saturation. This hypothesis, discussed many years ago by Gauer (75) has since been confirmed both by x-ray studies of the lung (Bryan et al (25)) and by lung scanning using a number of techniques (Glaister, 89; Von Nieding et al, 184). The drop in arterial oxygen saturation is approximately linear with acceleration,

having a sensitivity of approximately 10 mm Hg per G. Simultaneous measurements of arterial oxygen (P_{aO_2}) and carbon dioxide (P_{aP_2}) partial pressures, arterial pH (pH_a), alveolar (end expiratory) gas partial pressures ($P_{A_{O_2}}$, $P_{A_{CO_2}}$), breathing frequency (f) and the arterial-alveolar oxygen and partial pressure gradients were measured by Von Nieding et al (184) on centrifuge runs. Their average values, shown in Figure A.7-10, show clearly this linear decrease in $P_{a_{O_2}}$, which is reflected in increases in both the alveolar oxygen level with increasing G and a consequent increase in the arterial-alveolar pressure gradient (A-a P_{O_2}). Although arterial carbon dioxide level remains relatively unaffected, probably because of the hyperventilation shown in the increase in breathing rate, the alveolar carbon dioxide level drops significantly with increasing acceleration levels. Breathing rate increases by about 15% per G. The drop

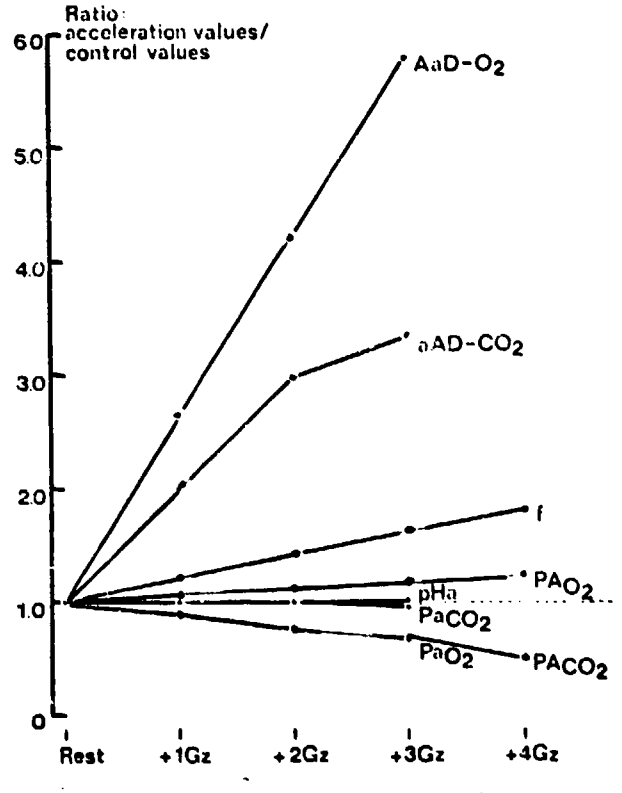


Figure A.7-10 Mean values from all respiratory quantities investigated at +Gz acceleration, relative to the value at rest (from Von Nieding (184)) (courtesy of Springer Verlag).

in end expiratory P_{O_2} begins immediately with the onset of acceleration and reaches its plateau level in about one minute.

The relationship between the change in gas exchange efficiency and the capillary perfusion of the different regions of the lung is shown clearly in Figure A.7-11. Note that even at +2 G_z the upper section of the lung is completely unperfused, and at +4 G_z fully 93% of the perfusion is in the lowest portion of the lung. The drop in arterial oxygen saturation is, of course, delayed some second after the decrease in gas exchange both because of some storage of O_2 and because of the hemoglobin saturation characteristics which permit $P_{a_{O_2}}$ to drop before a noticeable change in oxygen saturation is developed. The time course of arterial oxygen saturation for +G_z maneuvers of durations and

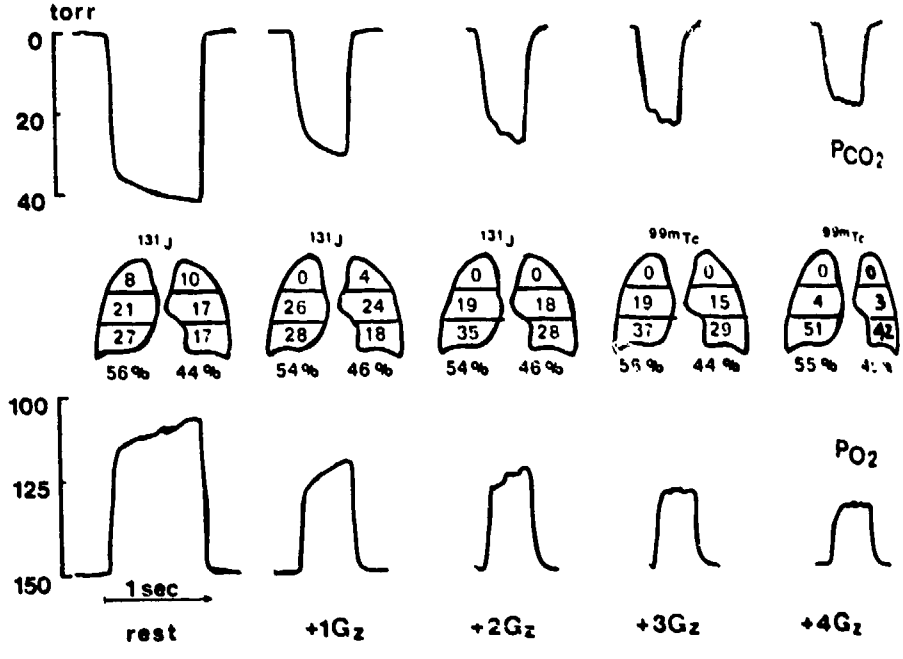


Figure A.7-11 Changes of the 0_2 and $C0_2$ alveolar plateaus for increasing values of +Gz acceleration. In the middle section percent distribution of the marked microspheres representing capillary perfusion (scintiscans during gravity, +2 and +4 Gz and all partial pressure curves originate from subject HK, the scintiscans during +1Gz and +3Gz are from subject KK) (from Von Nieding et al (184)) (courtesy of Springer Verlag).

magnitudes resembling those associated with ACM are indicated in Figure A.7-12. Note that the time course of the arterial oxygen saturation drop outlasts the acceleration. Measurements of O_2 saturation have also been taken during $+G_z$ accelerations intended to simulate an ACM G stress by Gillingham and Burton (84) and are used for modeling the relationship between G level and arterial saturation as will be discussed below. The steady state arterial oxygen saturation begins to drop significantly from its control levels at accelerations above +4 G_z, as indicated in the summary diagram of Figure A.7-13. Oxygen uptake and oxygen consumption similarly increase with increased acceleration, making the decreased gas exchange problem even more serious. A summary of the oxygen exchange parameters of interest for +3 G_z and +8 G_x, as well as the control values is given in Table A.7-1 from Glaister (90).

There have been numerous attempts to develop mathematical descriptions of the relationship between gravitational stress and

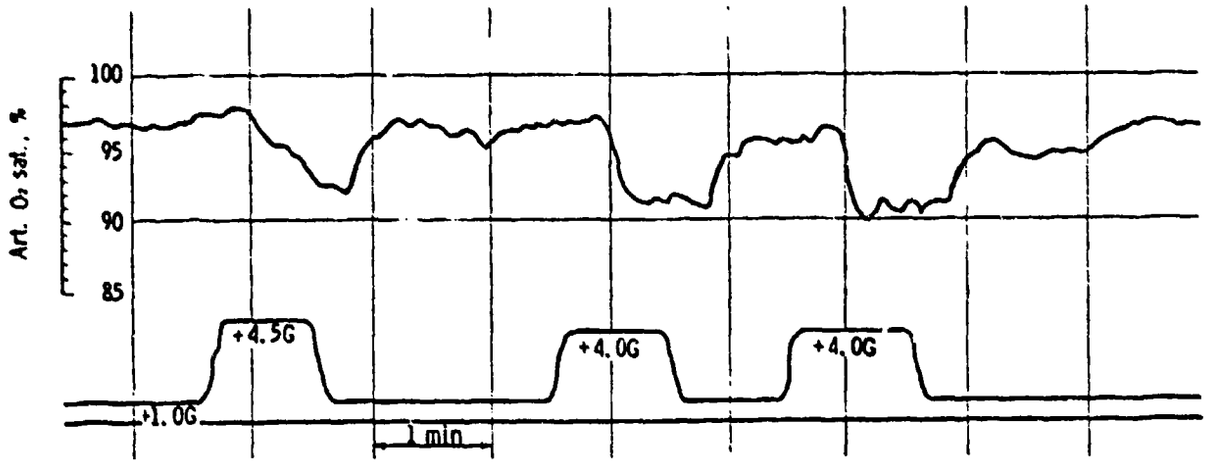


Figure A.7-12 Time course of changes in arterial oxygen saturation induced by consecutive exposures to positive acceleration (4.5, 4.0 and 4.0 G) in subject 20 years old, height 179 cm, weight 68 Kg, breathing air and wearing automatically inflated Anti-G suit. Note increasing rate and degree of unsaturation in consecutive runs; also impairment of resaturation in the postrun periods (from Fraser (71)).

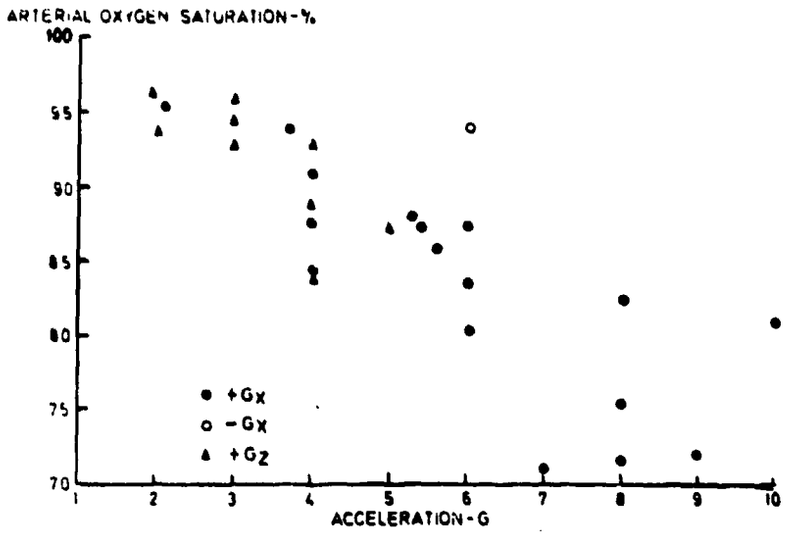


Figure A.7-13 Arterial oxygen saturations reported in man during exposure to varying levels and axes of acceleration. Each point represents the average of at least three, and up to 31 determinations made during exposures lasting from 50 seconds to six minutes with subjects breathing air (from Glaister (90)) (courtesy of Advisory Group for Aerospace Research and Development).

arterial saturation, since this is of such extreme practical importance in predicting the tolerance to various maneuvers. Gillingham and Burton have pursued this question the furthest in recent work, emphasizing the dynamic response to ACM type maneuvers as well as standard test pulses of acceleration. Burton, in earlier work, modeled the arterial oxygen tension and saturation as an exponential function of G as follows:

$$P_{a_{O_2}} = 97.5\ e^{-0.093G}, \text{ and}$$

$$S_{a_{O_2}} = 99 - 1.59G. \qquad \text{[Eq. A.7-1]}$$

Table A.7-1 Oxygen exchange under various conditions of acceleration (from Glaister (90)) (courtesy of Advisory Group of Aerospace Research and Development).

	$+1G_{x \text{ and } x}$ (78)	$+3G_z$	$+8G_x$
Arterial blood			
oxygen content (vol.%)	20.3	19.9	16.1
oxygen saturation (%)	97.1	95.1 (228, 273)	77.0
oxygen tension (mm Hg)	95	80	42
Mixed venous blood			
oxygen content (vol.%)	15.5	12.9	10.0
oxygen saturation (%)	75.0	61.8	47.8 (12)
oxygen tension (mm Hg)	40	32	26
Mean tissue capillary blood			
oxygen tension (mm Hg)	58	48	31
Oxygen uptake (ml/min)	275	265 (95)	205 (249)
Oxygen consumption (ml/min)	275	320	430
Oxygen stores (ml)	905 (80)	545	595
Oxygen debt (ml)	0	495	745
Cardiac output (l/min)	5.7	4.6 (228, 273)	6.8 (273)

Note: Oxygen uptake and oxygen consumption values are averaged over 3 minute acceleration exposures; all other values apply to the end of such exposures. Where values are taken from the literature, appropriate references are given in brackets.

They attempted to match measured oxygen saturation during an ACM type maneuver and a 6 G_z 60 second pulse with several models, including a synthetic transfer function given below.

$$S_{a_{O_2}} = 0, \quad t < 1.17$$

$$= 100, \quad 1.17 \leq t \leq 1.95$$

$$= 0, \quad 1.95 \leq t \leq 4.69$$

$$= -19.5e^{\frac{-t-4.69}{37.5}} \quad t \geq 4.69 \qquad \text{[Eq. A.7-2]}$$

The results of that simulated response to both the ACM G stress and the pulse are given in Figure A.7-14. Gillingham (82) has recently indicated in a personal communication, that he feels that a better approximation would be given by the following linear transfer function, relating $S_{a_{O_2}}$ as the output to $+G_z$ as the input:

$$H(s) = -3.87 \frac{1 + 7.20s}{1 + 48.2s} e^{-8.46\ s.} \qquad \text{[Eq. A.7-3]}$$

The initial peak that comes from such a lead lag transfer function is presumed to be related in some way to anticipatory breathing prior to the onset of G level, a phenomenon that has been noted by several authors. The implied delay of 3 seconds includes several seconds delay until the circulating blood reaches the ear where the oximetry measurement was taken.

AFFECTS OF 100% OXYGEN

Breathing of 100% oxygen does have a slight effect on reducing the drop in oxygen saturation with positive acceleration. However, if oxygen is prebreathed by 15 minutes or so prior to the onset of the G stress, there is an increasing occurrence of atelectasis, independent of the composition of the inspired gas at the time of the G stress. Consequently, alveolar collapse takes place, further interfering with gas exchange at $+G_z$. Following the cessation of acceleration, when 100% oxygen has been breathed, the return of oxygen saturation is slowed, further indicating the likelihood that atelectasis was responsible for the drop in gas exchange.

Although no direct data has been found which relates the effects of breathing of gas mixtures with lower than atmospheric oxygen content to G levels, it is quite clear that similar reductions in arterial saturation levels, both of magnitude and time,

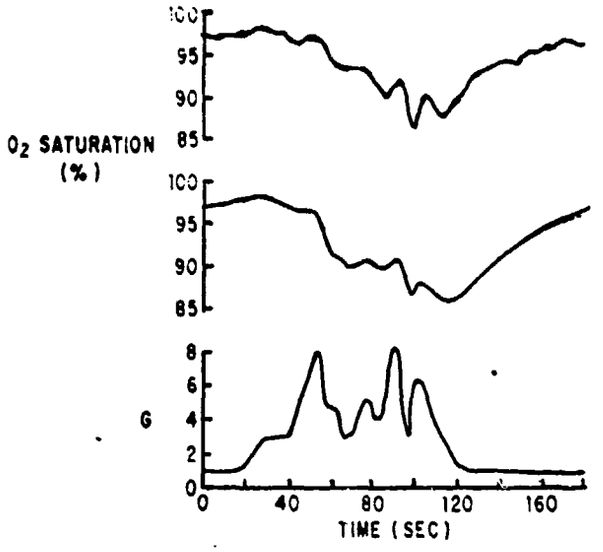


Figure A.7-14 a Actual mean response (above) and mean response predicted by initial synthetic transfer function (middle) to ACM G stress. (from Gillingham & Burton (84)) (courtesy of Aviation Space and Environmental Medicine).

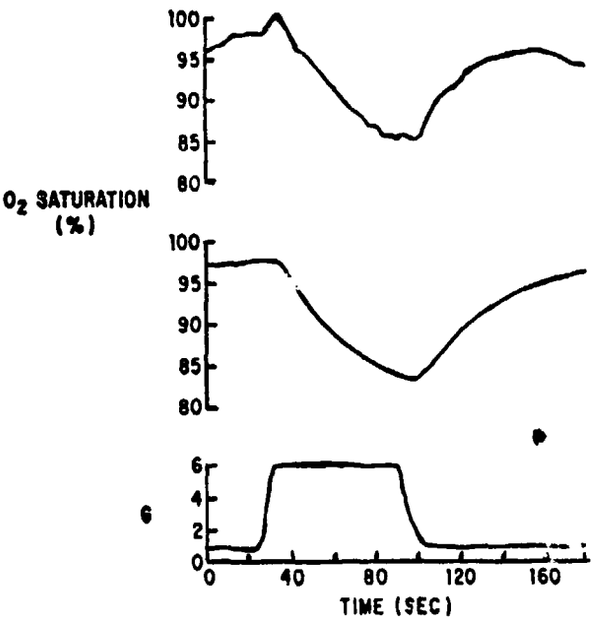


Figure A.7-14 b Predicted response to 6-G pulse based on four-subject, 12 run, average transfer function (above) and predicted response based on revised synthetic transfer function (middle) (from Gillingham & Burton (84)) (courtesy of Aviation Space and Environmental Medicine).

can be approached by reducing oxygen content of the inspired air on a breath by breath basis. The relationship including inspired air oxygen tension and arterial S_{aO_2} is well documented.

The question of inspired air content as well as that of positive or negative pressure breathing will be discussed further below under + G_x, Forward Acceleration.

ANTI-G SUIT

When the anti-G suit is inflated in response to acceleration, it presses up on the abdomen and diaphragm reducing end-tidal lung volume and vital capacity. As a result of both the reduction in lung volume and the fact that the increased pressure in the basilar part of the lung will close off even more alveoli, inflation of the anti-G suit increases the arterial desaturation which develops during $+G_z$ exposure.

EFFECTS OF FORWARD ACCELERATION ($+G_x$) ON GAS EXCHANGE

Although the mechanisms involved in the acceleration effects on respiration are similar for $+G_x$ to those already discussed for $+G_z$, the magnitude of the effect is much more severe. Combined with the observation that tilt back seats are used to increase acceleration tolerance associated with hydrostatic pressure drops to the cardiovascular system, the expected longer duration $+G_x$ stresses are of particular importance in consideration of their respiratory effects.

The increased work of breathing associated with elevating the chest wall during forward acceleration calls for an increased oxygen uptake with increasing G_x. The additional oxygen corresponds to an increment of about 15% at 5 g's and over 100% at 10 G_x (Zechman et al 274). If the oxygen cannot be supplied by respiration, an oxygen debt is accumulated which is repaid following

acceleration. In discussing somewhat conflicting results, Fraser concludes that there is generally a decrease in actual oxygen uptake during acceleration followed by an increase to make up for the accumulated debt after the acceleratory period (71).

Nearly all investigators are agreed that the major influence of forward acceleration on gas exchange is in a severe alteration of the regional ventilation perfusion ratios, whereby the ventral or forward part of the lung receives no perfusion and maximum ventilation with very large alveolar sacs, whereas the dorsal or back portion is maximally perfused but, because of the high pressure, has the airways blocked off or collapsed. This is shown clearly in Figure A.7-15, where the increase in pulmonary pressure from 30 mm Hg arterial at 1g to 70 mm Hg at 5g's, combined with the change in intrapleural pressure from -2 mm Hg to +18 mm Hg collapses the alveoli. This same information is shown quantitatively in Figure A.7-16 where the relative ventilation perfusion ratios at 1g and G_x are shown. For the 5 G_x case, it is only the limited region of the lung with the relative ventilation perfusion ratio close to 1 that is affected in gas exchange. As

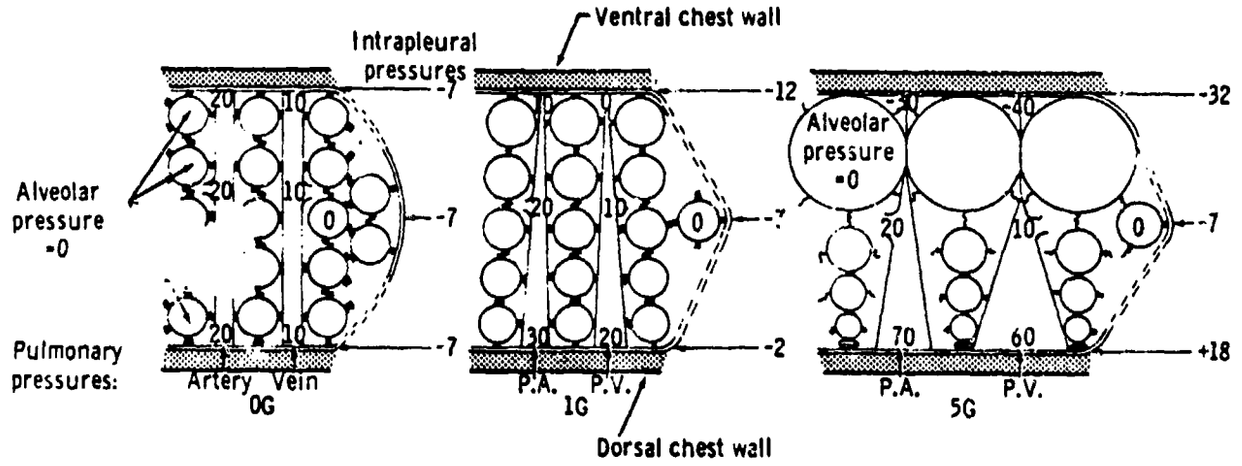


Figure A.7-15 Diagram of effects of forward (+Gx) acceleration on intrathoracic pressures (dorsal-ventral dimension of lung is 20 cm). Numerals indicate pressures as cm H_2O, and zero reference level is atmospheric pressure at midthoracic coronal plane (from Fraser (71)).

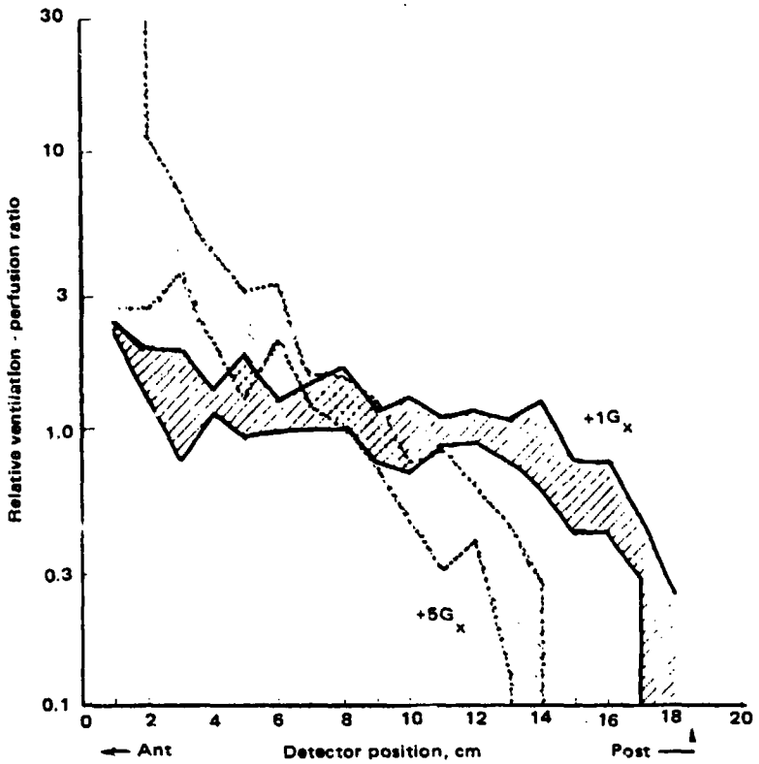


Figure A.7-16 Relative ventilation-perfusion ratios plotted against distance along anteroposterior axis of the lung at +1 and +5 Gx. Shaded areas cover values obtained from 3 subjects. Exposure to acceleration increases range of values and creates a considerable region of zero ventilation-perfusion ratio at the back of the lung (from Glaister (88)) (courtesy of Journal of Applied Physiology).

discussed previously, the development of arterial venous pulmonary shunts at the back portion of the lung reduces the oxygen saturation significantly. Even breathing 100% oxygen only delays its development and reduces its magnitude somewhat because, of course, where no gas is coming in contact with the blood, no exchange can take place. The data of Steiner and Mueller (231) shows an effective shunt of 40% at 6g's and 60% at 8g's in air, with the latter reduced to 40% at 8g's for breathing pure oxygen.

The time course of changing arterial oxygen saturation during forward acceleration is similar to that for headward acceleration, although of course the magnitudes of the desaturation are much greater. Figure A.7-17 and A.7-18 show the "step response" to rapid onset and rapid offset of forward accelerations at three different levels, and indicate the dominant time constant to be of the order of 30 to 60 seconds. Breathing 100% oxygen would appear to reduce the arterial oxygen saturation decrement on the order of 3 to 5%.

Several quantitative models came to our attention which were worked out specifically for the dynamics of arterial saturation in response to G_x acceleration. Holden (112), however, makes the case that it is in fact principally the magnitude of the imposed acceleration and not its direction which is of importance in determining arterial saturation, and, dealing with a wide variety of data for both G_x and G_z, he proposes a simple model based on this function and on physical principles. He argues that steady state arterial oxygen concentrations can be approximated as polynomials in the magnitude of each G vector, and that the rate of change to a step change in acceleration is an exponential decay. By curve fitting he comes up with the step response as follows:

$$P_{a_{O_2}}(t) = (0.5\ g - 0.4\ g^2)\ (1-e^{-0.05(t-8)}) + 98 \quad \text{[Eq. A.7-4]}$$

The 8 second time delay associated with the delay between onset of a step of acceleration and beginning of a change in arterial concentration is similar to that obtained for G_z as discussed in the model of Gillingham and Burton. In the steady state, of course, the exponential term dies out and the steady arterial saturation level in response to any G stress are given by

$$P_{a_{O_2}} = 98 + 0.5g - 0.4g^2. \quad \text{[Eq. A.7-5]}$$

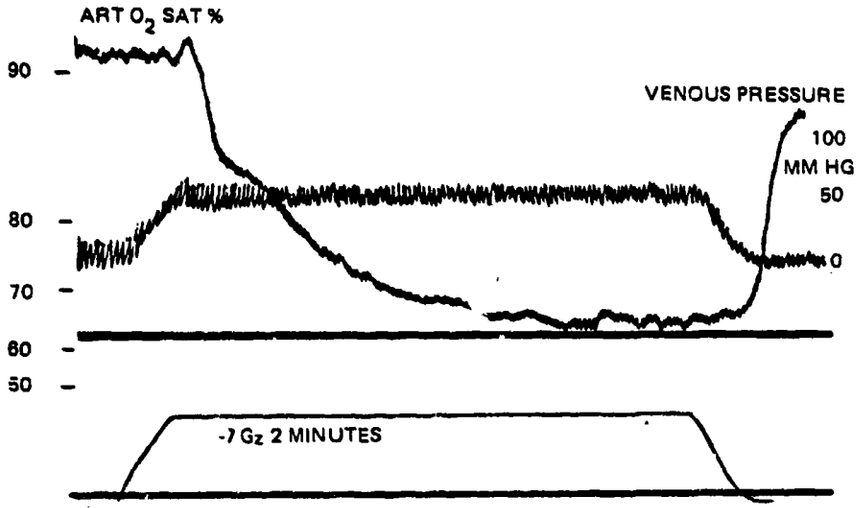


Figure A.7-17 Effect of exposing an anaesthetised dog to an acceleration of -7G for two minutes, on arterial oxygen saturation and venous pressure. Note the fall in saturation during the period of acceleration (from Glaister).

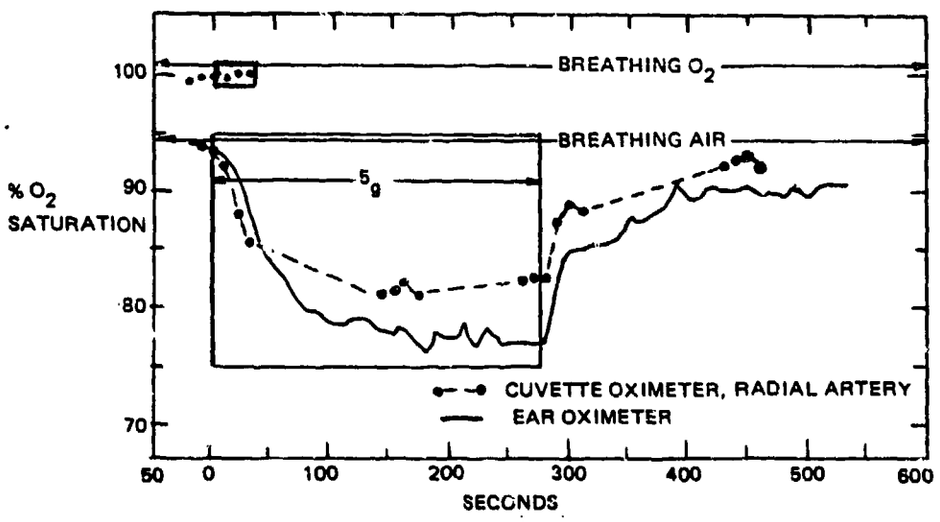


Figure A.7-18 Changes in arterial oxygen saturation during acceleration when breathing oxygen (30 seconds exposure to $+5G_x$) or air (4.5 minute exposure to $+5G_x$). The lack of response when the subject breathed 99.6% oxygen was presumably due to the run being terminated after only 30 seconds, at which time oxygen trapped in unventilated alveoli was still available for diffusion (from Glaister).

As a simple starting point for software to drive a model this would seem to be reasonable, although further experimental verification is obviously necessary.

PRESSURE BREATHING

Positive pressure breathing can reduce the work of breathing under forward acceleration, since the higher pressure in the inspired air tends to make it easier to expand the chest wall. In addition, of course, the positive pressure inspired gas tends to keep the dorsal portion of the lung ventilated and reduce the pulmonary shunting. Watson and Cherniak (252) found considerable increase in tolerance to positive accelerations of +6g and +8g with positive pressure breathing of 12 and 20 mm Hg respectively. Positive pressure breathing with pure oxygen increases the danger of atelectasis however. For the purposes of this study, it is reasonable to consider once again the effects of negative pressure breathing, not only on making the work of breathing and breathing mechanics resemble that of forward acceleration for the simulator case, but also in terms of creating an altered ventilation perfusion ratio which would result in reduced arterial saturation in the fixed base simulator.

APPENDIX B
ANNOTATED BIBLIOGRAPHY

"Reference Number To HG Reference And Appendix Page Index"

Reference Number	HG Number	Appendix Page Number
1	62	B-60
2	195	B-157
3	14	B-13
5	250	B-180
11	18	B-17
14	15	B-14
15	183	B-148
19	247	B-177
20	9	B-10
21	6	B-6
27	170	B-134
28	55	B-48
29	157	B-125
30	83	B-84
31	44	B-39
32	20	B-21
33	7	B-16
34	82	B-83
35	190	B-152
36	189	B-150
37	174	B-139
40	158	B-126
42	52	B-47
45	36	B-34
46	122	B-113
48	23	B-28
49	121	B-112
50	133	B-116
51	182	B-147
52	258	B-184
56	94	B-92
58	98	B-96
62	67	B-65
63	252	B-181
64	40	B-36
65	81	B-82
68	242	B-172
69	156	B-123
71	229	B-167
74	41	B-37
78	175	B-141
82	88	B-85&86
84	42	B-38
85	4	B-2
86	5	B-4
87	65	B-61
90	246	B-176
91	249	B-179
94	80	B-81
96	59	B-54
98	22	B-25
104	7	B-7
106	21	B-23
107	124	B-114
111	211	B-161
114	256	B-182
115	257	B-183
118	109	B-109
119	110	B-110
120	16	B-15
127	69	B-67
130	97	B-93,94,95
132	160	B-130
134	49	B-45
136	107	B-107
140	128	B-115

Reference Number	HG Number	Appendix Page Number
141	91	B-90
142	13	B-11&12
144	19	B-19
145	92	B-91
147	243	B-174
150	171	B-135
152	241	B-171
154	102	B-98
160	90	B-89
161	60	B-55
164	77	B-75
165	239	B-169
166	58	B-53
167	108	B-108
168	73	B-68
171	103	B-100
172	173	B-137
174	37	B-35
175	106	B-103
176	191	B-155
177	194	B-156
180	176	B-142
181	105	B-102
185	223	B-165
190	166	B-133
194	89	B-87&88
195	47	B-43
202	57	B-51
205	238	B-168
207	150	B-120
208	51	B-46
209	205	B-159
211	2	B-1
212	29	B-29
213	104	B-101
218	184	B-149
220	219	B-164
221	46	B-42
222	33	B-30
223	34	B-33
224	78	B-77
229	202	B-158
230	159	B-128
236	61	B-57
239	226	B-166
240	248	B-178
241	144	B-119
242	76	B-74
244	172	B-136
245	240	B-170
247	75	B-72
248	45	B-41
250	137	B-118
251	164	B-132
256	244	B-175
258	152	B-121
261	177	B-143
262	178	B-144
263	179	B-145
264	180	B-146
268	111	B-111
273	8	B-9

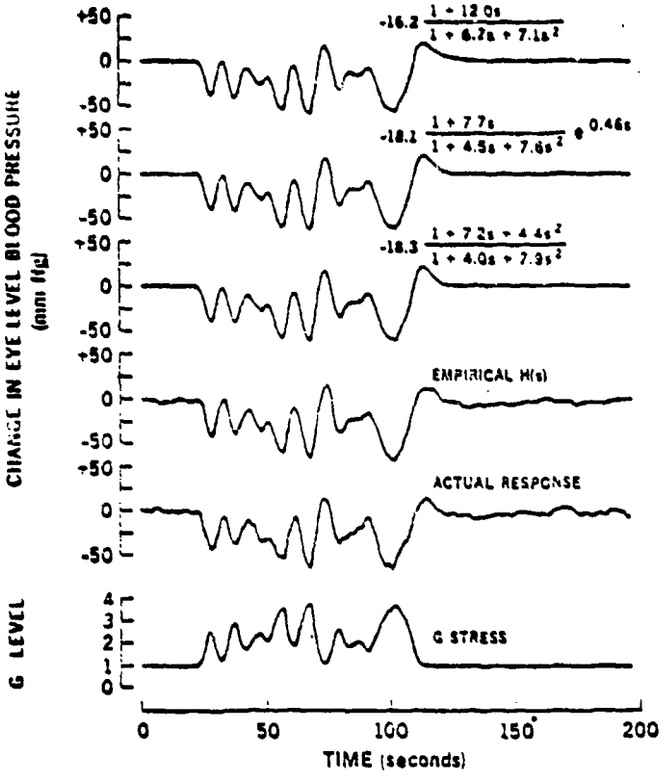


Fig. 11. Predicted and mean actual eye-level blood-pressure responses to #8 SACM G stress. Sequence as in Fig. 8. To avoid contaminating prediction with actual response data, data from each subject's #8 SACM run were subtracted from empirical transfer function prior to making prediction.

TITLE: Aeromedical Review; Effects of the Abnormal Accelerative Environment of Flight

REF.# 86

HG- 5

DATE:

LEAD AUTHOR: Gillingham, K. K.

HUMANS - X
ANIMALS -

ABSTRACT

Not available at this time

. . . . . .

RELEVANCE

An excellent brief review of the acceleration mechanics and major physiological effects, especially of Gz. Particularly good overview of spatial disorientation in flight. Summary of countermeasure affectiveness.

SALIENT DATA

(1) Blackout tolerance curves - duration vs Gz level as a function of rate at onset Fig. 9, p.31

(2) Ps 41 - "..., M-1 contributes significantly to the high heart rate; eg., the heart rates for persons performing a maximum M-1 @ +1Gz are the same as those found during exposures to +6 Gz."

(3) Positive Pressure Breathing (PPB) "PPB was found to be as effective as the M-1 maneuver regarding tolerable time at +6 and +8 Gz. The majority of the subjects preferred PPB to the M-1 because of less fatigue associated with PPB." Fig. 23 shows esophageal pressures which indicate changes in intrathoracic pressure and straining effort expended.

(4) Note: "... that current pressure demand oxygen regulators can only deliver 100% in the pressure settings, and the probability of an increased incidence of atelectasis associated w/ 100% oxygen presently prevents the use of PPB as an operational Anti-G method."

(5) Note rapid response to blood pressure change vs. G (p. 26 & 27). Note rapid change in F4 G level (p.7). Wonder if LBNP concepts can cause blood pressure changes rapid enough.

(6) Bottom p.28 - peripheral vision lost first because retina supplied as end artery item with vessels of decreasing size extending from retinal center toward periphery. Blood pressure drops ∴ first effects periphery.

PHYSIOLOGICAL CATEGORY
- X AUDITORY
- X BIOMECHNL
- X CARDIOVSCL
- FORCE
- X GENERAL
- X LABYRINTH
- MAN.CNTRL
- X PROTECTIVE
- X REVIEW
- X RESPIRAT'N
- X SIMULATION
- X VISUAL
- OTHER

AUGMENTATION DEVICES
- HELMET
- STRAPS
- X AURAL
- EXTREMITY
- X LBNP
- X VISUAL
- X RESPIRATORY
- X LACRIMATION
- TEMPERATURE
- MASK

SHEET 1 OF 2

AUTHOR Gillingham, K. K. REF # 86

(7) Bottom p.32 - audition - last to go before unconsciousness - not a good end point.

(8) Again note rapid response of blood pressure to G & M1 maneuver on p37.

(9) Tidal Respiration - p.39 - would a decrease in CO_2 in breathing air dilate the peripheral blood vessels with resultant drop in blood pressure ∴ helping LBNP? See also p42 & 43.

(10) Performance degrades inversely with G to 6 Gz and rapidly thereafter (p50).

(11) Red out not experimentally encountered (p53)

(12) Lacrimation noted above +12 Gx - outside our regime of consideration (P54).

(13) Elevator Effect p64 & p76.

SHEET 2 OF 2

TITLE: Ocular Effects of High Speed Flight

REF. # 21

IIG- 6

DATE:

LEAD AUTHOR: Blake, J.

HUMANS - X
ANIMALS -

ABSTRACT

Not available at this time

RELEVANCE

SALIENT DATA

PHYSIOLOGICAL CATEGORY
- AUDITORY
- BIOMECHNL
- CARDIOVSCL
- FORCE
- GENERAL
- LABYRINTH
- MAN.CNTRL
- PROTECTIVE
- REVIEW
- RESPIRAT'N
- SIMULATION
- VISUAL
- OTHER

AUGMENTATION DEVICES
- HELMET
- STRAPS
- AURAL
- EXTREMITY
- [illegible]NP
- VISUAL
- RESPIRATORY
- LACRIMATION
- TEMPERATURE
- MASK

SHEET 1
OF 1

TITLE: Effect of Passive 70° Head-up Tilt on Peripheral Visual Response Time

REF. # 104

HG- 7

DATE:

LEAD AUTHOR: Haines, R.

HUMANS - X
ANIMALS -

ABSTRACT

Peripheral visual response time was measured continuously in seven young men during a 30-min, 70° head-up tilt before and after 14 days of bed rest. Small test lights were flashed on at unexpected times and locations along the subjects' horizontal retinal meridian to determine what effect tilt would have on peripheral visual sensitivity and to better understand the physiological mechanisms that underlie peripheral visual sensitivity. Blood pressure was also measured every other minute throughout this period. The results indicated that response time lengthens significantly to stimuli imaged beyond about 70° from the line of sight for both the pre-and post-bed-rest periods during tilt.

PHYSIOLOGICAL CATEGORY
- AUDITORY
- BIOMECHNL
- X CARDIOVSCL
- FORCE
- X GENERAL
- LABYRINTH
- MAN.CNTRL
- PROTECTIVE
- REVIEW
- RESPIRAT'N
- SIMULATION
- VISUAL
- OTHER

RELEVANCE

Cardiovascular effects on vision

AUGMENTATION DEVICES
- HELMET
- STRAPS
- AURAL
- EXTREMITY
- LBNP
- VISUAL
- RESPIRATORY
- LACRIMATION
- TEMPERATURE
- MASK

SALIENT DATA

(1) With a small (<4mm HG) of mean systolic blood pressure, the author suggests that the critical closing pressure (Pc) (pressure within a blood vessel) - is reached in the extreme peripheral area of retinal - causing an increase in reaction time for a stimulus at 70° or greater from the line of sight.

SHEET 1 OF 2

Table IV

Maximum Objective Symptom Unconsciousness - Relaxed Subjects (All runs 10 Seconds or Less)

Groups	Number Subjects	Mean G Level: 80° Light Loss Objective	Mean G Level: Unconscious	80° Light Loss To Blackout Time (Sec.)	Blackout To Unconscious (Seconds)	80° Light Loss To Unconscious (Seconds)	Duration To Unconsciousness (Seconds)
Total Subjects	115	4.24					
Student Pilots	10	4.42	5.45	1.47	1.32	2.79	17.53
Others	7	3.92	4.46	1.42	1.37	3.69	10.11
Acceleration Personnel	6	4.2	5.26	2.68	2.17	4.85	12.4
Average	23	4.22	5.1 (± 0.8)	1.77	1.83	3.60	13.93

TITLE: A Study of Early Greyout as an Indicator of Human Tolerance to Positive Radial Accelerating Force

REF. # 273

HG- 8

DATE:

LEAD AUTHOR: Zarriello, J. J.

HUMANS - X
ANIMALS -

ABSTRACT

Not available at this time

. . . . . .

RELEVANCE

Data useful for peripheral dimming display drive

SALIENT DATA

(1) Loss of vision of lights at 80^{o} in the periphery occurs at 4.2 g's (Gz) (σ = 0.7), compared to 4.5g's (σ = .8) for lights at 23^{o} and 5.3 g's (σ = .8) for center light loss. A clear run had an average of 3.8 g's.

(2) The time between 80^{o} light loss and blackout had a mode of only 0.5 sec - but a mean of 2.7 sec.

(3) Normative data were obtained regardigg the 80^{o} LL and its relationship to 23^{o} LL, blackout, and unconsciousness.

(4) Subjects were relaxed.

PHYSIOLOGICAL CATEGORY
- AUDITORY
- BIOMECHNL
- CARDIOVSCL
- FORCE
- GENERAL
- LABYRINTH
- MAN.CNTRL
- PROTECTIVE
- REVIEW
- RESPIRAT'N
- SIMULATION
- X VISUAL
- OTHER

AUGMENTATION DEVICES
- HELMET
- STRAPS
- AURAL
- EXTREMITY
- LBNP
- X VISUAL
- RESPIRATORY
- LACRIMATION
- TEMPERATURE
- MASK

SHEET 1 OF 1

TITLE: Testing Predictions Derived from a Model of Progressive Adaptation to Coriolis Acceleration

REF. # 20

HG- 9

DATE:

LEAD AUTHOR: Benson, A. J.

HUMANS -X
ANIMALS -

ABSTRACT

A theoretical model for progressive adaptation to Coriolis accelerations is described. Thirteen subjects were tested under procedures identical to those using fixed velocity increments described in previous studies, but in this instance diminishing velocity increments, with an initial step of 3 rev/min were used. The findings provide positive but as yet, limited support for the theoretical model described.

RELEVANCE

Adaption of Labyrinth System to Coriolis acceleration in a centrifuge - not directly applicable.

PHYSIOLOGICAL CATEGORY
- AUDITORY
- BIOMECHNL
- CARDIOVSCL
- FORCE
- GENERAL
- LABYRINTH
- MAN.CNTRL
- PROTECTIVE
- REVIEW
- RESPIRAT'N
- SIMULATION
- VISUAL
- OTHER

AUGMENTATION DEVICES
- HELMET
- STRAPS
- AURAL
- EXTREMITY
- LBNP
- VISUAL
- RESPIRATORY
- LACRIMATION
- TEMPERATURE
- MASK

SALIENT DATA

SHEET 1 OF 1

TITLE: Involuntary Head Movements & Helmet Motions During Centrifuge Runs With Up to +6G_z

REF.# 142

HG- 13

DATE:

LEAD AUTHOR: Kroemer, K. H.

HUMANS - X
ANIMALS -

ABSTRACT

Open-loop centrifuge runs reaching +6G_z were performed with 13 subjects wearing the foam-padded standard HGU-2A/P helmet. Weights up to 20 oz were attached at top and sides. During the centrifuge runs, each subject attempted to maintain his gaze at a target directly in front of him. Hence, no voluntary motion of the head should have occurred. Position of the head, of the helmet, and of a helmet-attached reticle were recorded photographically at each G-level. From the photographs, data on actual displacements of head, helmet, and reticle were extracted and subjected to a computer-aided analysis.

Involuntary angular head movements, as well as rotational displacements of the helmet on the head, are discussed in this paper in terms of pitch, roll and yaw. Also described are linear changes in the vertical height of the subjects' eyes and of the reticle. Yaw and roll were found to be small and unstructured. Fore-and-down head and helmet pitch, and depression of eye and reticle were about proportional to the amount of +G_z stress.

. . . . . .

RELEVANCE

Paper presents data on head, helmet, eye and reticle displacements as a function of +Gz accelerations up to 6 Gz. These are measured (head & helmet) in three rotational degrees of freedom (pitch, roll & yaw).

SALIENT DATA

(1) Pitch seems to be the most significant degree of freedom in terms of excursion. There is a considerable variability in head pitch among the various subjects (13).

(2) The most significant motion is helmet pitch. There is a trend for head pitch to overshoot the 1G position upon return. Eye depression is relatively linear from 0 @ 1g to ≃ 45 mm at + 6G_z.

PHYSIOLOGICAL CATEGORY
- AUDITORY
- X BIOMECHNL
- CARDIOVSCL
- FORCE
- GENERAL
- LABYRINTH
- MAN.CNTRL
- PROTECTIVE
- REVIEW
- RESPIRAT'N
- SIMULATION
- VISUAL
- OTHER

AUGMENTATION DEVICES
- X HELMET
- STRAPS
- AURAL
- EXTREMITY
- LBNP
- VISUAL
- RESPIRATORY
- LACRIMATION
- TEMPERATURE
- MASK

SHEET 1 OF 1

TITLE: Involuntary Head Movements & Helmet Motions During Centrifuge Runs Up to $+6G_z$

REF.# 142

HG- 13

DATE:

LEAD AUTHOR: Kroemer, K. H.

HUMANS -X
ANIMALS -

ABSTRACT

Open-loop centrifuge runs reaching $+6G_z$ were performed with 13 subjects wearing the foam-padded standard HGU-2A/P helmet. Weights up to 20 oz were attached at top and sides. During the centrifuge runs, each subject attempted to maintain his gaze at a target directly in front of him. Hence, no voluntary motion of the head should have occurred. Position of the head, of the helmet, and of a helmet-attached reticle were recorded photographically at each G-level. From the photographs, data on actual displacements of head, helmet, and reticle were extracted and subjected to a computer-aided analysis.

Involuntary angular head movements, as well as rotational displacements of the helmet on the head, are discussed in this paper in terms of pitch, roll and yaw. Also described are linear changes in the vertical height of the subjects' eyes and of the reticle. Yaw and roll were found to be small and unstructured. Fore-and-down head and helmet pitch, and depression of eye and reticle were about proportional to the amount of $+G_z$ stress.

. . . . . .

RELEVANCE

Pertinant information for helmet movement on head (firmness bladder) & head/helmet movement (fluid cavity) & shoulder harness tightening (torso movement) & G seat utilization.

SALIENT DATA

(1) Helmet, head, & helmet vs head movement appears to be independnet of helmet weight.

(2) $\ddot{Z}$ induces no significant helmet/head rolling or yawing.

(3) $\ddot{Z}$ induces head pitch down (Ave 4^o @ 6G) and helmet pitch down WRT head (Ave 4^o @ 6G) the former linear between 1→6g; the: latter showing little movement between 1→ 2g then linear 2→6g.

4) Z axis compression of torso neck under $6G_z$ mounts to 50 mmΔin eye point (1/6 of which is due to head pitch) is very linear 1→6g substantiates position - action G seat concept and general excursion range of G seat 40 oz variation in helmet weight has "no" effect on said compression.

PHYSIOLOGICAL CATEGORY
- AUDITORY
- X BIOMECHNL
- CARDIOVSCL
- FORCE
- GENERAL
- LABYRINTH
- MAN.CNTRL
- PROTECTIVE
- REVIEW
- RESPIRAT'N
- X SIMULATION
- X VISUAL
- OTHER

AUGMENTATION DEVICES
- X HELMET
- X STRAPS
- AURAL
- EXTREMITY
- LBNP
- VISUAL
- RESPIRATORY
- LACRIMATION
- TEMPERATURE
- MASK

SHEET 1 OF 1

TITLE:

Principles of Biodynamics

REF. # 3

HG- 14

DATE:

LEAD AUTHOR:

HUMANS - X
ANIMALS -

ABSTRACT

Principles of Biodynamics is a manual prepared at the request of the AGARD Aerospace Medical Panel in order to give an updating of present knowledge about the medical implications of linear and radial acceleration for man in air and space vehicles. The aim of this book is to give the basic principles which have been accumulated in this field over many years of aero-medical research. It may also help research workers.

RELEVANCE

Summary, in outline form of the principle G-acceleration effects and effectiveness of protective measures. Data summary on G-tolerance levels with various protection. A good first look at effects, no physiological background needed. References good-included annotated bibliography.

SALIENT DATA

1. Table of axes and terminology (pp 5, 6)
2. Summary of effects (pp 14-19)
3. Good annotated bibliography.
4. Compilation of data on acceleration devices in US and Europe.

PHYSIOLOGICAL CATEGORY
- AUDITORY
- BIOMECHNL
- CARDIOVSCL
- FORCE
- X GENERAL
- LABYRINTH
- MAN.CNTRL
- PROTECTIVE
- X REVIEW
- RESPIRAT'N
- SIMULATION
- VISUAL
- OTHER

AUGMENTATION DEVICES
- HELMET
- STRAPS
- AURAL
- EXTREMITY
- LBNP
- VISUAL
- RESPIRATORY
- LACRIMATION
- TEMPERATURE
- MASK

SHEET 1 OF 1

TITLE: Transmission of Angular Acceleration to the Head in the Seated Human Subject.

REF. # 14

HG- 15

DATE:

LEAD AUTHOR: Barnes, G. R.

HUMANS - X
ANIMALS -

ABSTRACT

Sinusoidal angular oscillation in yaw of seated human subjects, both restrained and unrestrained, has demonstrated that responses of significant amplitude may be elicited in all three head axes. In the unrestrained condition, the torso appeared to absorb the input accelerator, the response of the head in the yaw axis exhibiting very rapid attenuation (5 log units/decade) and large phase lags at frequencies above 4 Hz. In the restrained condition, the transmission to the yaw axis of the head was much less severely alternated (1 log unit/degrade) with similar phase lags above 4 Hz. The yaw responses in the unrestrained condition exhibited a resonant peak at 2 Hz, probably attributable to the large mass of the shoulders and torso. In both experimental conditions there was a significant response in both the roll and pitch axes of the head. The response in pitch exhibited significant second harmonic components which were manifested as a frequency doubling effect between 1 and 6 Hz.

PHYSIOLOGICAL CATEGORY
- AUDITORY
- X BIOMECHNL
- CARDIOVSCL
- FORCE
- GENERAL
- LABYRINTH
- MAN.CNTRL
- PROTECTIVE
- REVIEW
- RESPIRAT'N
- X SIMULATION
- VISUAL
- OTHER

RELEVANCE

Helmet drive system only generally relevant. Shoulder straps - accept some of the torsional movement.

AUGMENTATION DEVICES
- X HELMET
- X STRAPS
- AURAL
- EXTREMITY
- LBNP
- VISUAL
- RESPIRATORY
- LACRIMATION
- TEMPERATURE
- MASK

SALIENT DATA

1. Stimulus was pure yaw about GG of Torso (unrestrained) and 4 Hz (restrained) of head due to mass of torso (unrestrained) and head (restrained). Rapid roll off. Authors conclude spring mass damper analogy does not represent this system & point to utilization of wave theory in bodies.

2. Important side note: Under vibratory regime vestibular conpensation occurs to help subject visually fixate but this must be suppressed when object of fixation is vibrating too (cockpit inst.). Seat shakers won't teach such suppression.

SHEET 1 OF 1

TITLE: The Effects of High Speed Flight on the Human Body.

REF. # 120

HG- 16

DATE:

LEAD AUTHOR: Howard, I. P.

HUMANS - X
ANIMALS -

ABSTRACT

No abstract is available at this time.

RELEVANCE

Largely irrelevant to our task. An elementary and unreferred review of the high G problem for laymen.

SALIENT DATA

1. Fig 6, p 298 shows eye level arterial pressure dropping before a 4g acceleration

2. Fig 5 gives tolerance levels in 3 directions

Motor Capability

2 g - "Just possible to rise from Seat"
3 g - "legs almost too heavy to lift"
6 g - "arms cannot be raised above the head", "fine movements of the fingers & hands can be made, but only if the rest of the arm is well supported"

Visual Effects

3 g - "Brightness & contrast diminish" also "veiling"
5-6g - "blackout"; 6-7g "Endangered cerebral circulation & loss of consciousness."

PHYSIOLOGICAL CATEGORY
- AUDITORY
- BIOMECHNL
- CARDIOVSCL
- FORCE
- GENERAL
- LABYRINTH
- MAN.CNTRL
- PROTECTIVE
- X REVIEW
- RESPIRAT'N
- SIMULATION
- VISUAL
- OTHER

AUGMENTATION DEVICES
- HELMET
- STRAPS
- AURAL
- XEXTREMITY
- L3NP
- VISUAL
- RESPIRATORY
- LACRIMATION
- TEMPERATURE
- MASK

SHEET 1 OF 1

TITLE:

Men at High Sustained $+G_z$ Acceleration, A Review.

REF.# 33

HG- 17

DATE:

LEAD AUTHOR: Burton, R. R.

HUMANS - X
ANIMALS -

ABSTRACT

No abstract is available at this time

Through review of high sustained $+G_z$ research at breaks emphasizing cardiovascular and respiratory responses, and manual performance to a lesser extent. Consideration of the physiological basis of the various countermeasures. Good background.

RELEVANCE

SALIENT DATA

1. Many relevant tables concerning arterial CO_2 and PO_2 as well as heart rate and blood pressure measures under $+G_z$ with various countermeasures.

PHYSIOLOGICAL CATEGORY
- AUDITORY
- BIOMECHNL
- CARDIOVSCL
- FORCE
- X GENERAL
- LABYRINTH
- MAN.CNTRL
- PROTECTIVE
- REVIEW
- RESPIRAT'N
- SIMULATION
- VISUAL
- OTHER

AUGMENTATION DEVICES
- HELMET
- STRAPS
- AURAL
- EXTREMITY
- LBNP
- VISUAL
- RESPIRATORY
- LACRIMATION
- TEMPERATURE
- MASK

SHEET 1 OF 1

TITLE: Physiological Reactions of the Human Body to Transverse Accelerations and some Means of Increasing the Organism's Resistance to these Effects.

REF. # 11

HG- 18

DATE:

LEAD AUTHOR: Barer, A. S.

HUMANS - X
ANIMALS -

ABSTRACT

Flight in a space vehicle is accompanied by the effects of exposure of the subject to different accelerations. Prolonged acceleration appears during the start and at the re-entry of the space vehicle into the earth's atmosphere. It also can occur during maneuvers while in flight. Three general groups of experiments are described herein. The first group considers the limits of human tolerance to prolonged forward acceleration at an angle of 65° to the longitudinal axis of the body. The second group of experiments include tests of different methods whereby human tolerance to transverse acceleration might be increased. The third group of experiments contain investigations in which the tolerance to acceleration was determined in time under selected optimal conditions. Detailed records and data were obtained during each experiment on certain physiological functions of the human body. Complete analysis of these data are discussed. Although estimates were made in this study of methods for increasing resistance of the human being to prolonged acceleration stress and limits of tolerance to this stress were established, unanswered questions still remain regarding the reaction of the organism to stress. Detailed analyses of the questions raised are considered in the paper. Physiological responses of the human being to these stresses are considered in light of the experimental data contained in the manuscript.

PHYSIOLOGICAL CATEGORY
- AUDITORY
- BIOMECHNL
- X CARDIOVSCL
- FORCE
- X GENERAL
- LABYRINTH
- MAN.CNTRL
- PROTECTIVE
- REVIEW
- X RESPIRAT'N
- SIMULATION
- X VISUAL
- OTHER

AUGMENTATION DEVICES
- HELMET
- STRAPS
- AURAL
- EXTREMITY
- X LBNP
- X VISUAL
- X RESPIRATORY
- LACRIMATION
- TEMPERATURE
- MASK

RELEVANCE

SALIENT DATA

1. Centrifuge data from USSR up to 22 g at angles of 65° & 80° to the longitudinal axis of the body. Data is mostly cardiovascular & pulmonary but also visual and CMS. Good data on respiratory rate and volume.

2. Reviewed Soviet centrifuge work on G_x. Emphasis on CV changes, but with good data on respiratory effects (frequency, volume, etc.) at 2-22 g exposures. Also some EEG changes and visual limits. Discussion of emotional factors in level of meat of "reciprocal reactions" of organisms.

SHEET 1 OF 2

AUTHOR Barer, A. S. REF # 11

1. The paper presents X-Ray data on changes in intra-thoracic volume due to increase in acceleration stress. Much data (qualitative) presented on ECG & EMG. Blood pressure increases of systolic 220 mm Hg & diastolic 170 mm Hg at 8 g_x and angle of 65° were reported.

2. Depth of respiratory increased only to 6g. Respiratory rate increased linearly in the range 4-12 g_x @ 65° and at greater (angle = 80°) remained constant at 25-27 breaths/min. At 65° blackout occurred at 10-12 g at 80° not until 16g.

3. Also there is acuity data presented (pg. 132).

4. Greater stress noted generally during momentum phase Question: is this due to experiment anxiety or centrifuge dynamics?

5. The index of breathing was measured with a pneumotachygraph. Should find out more about it.

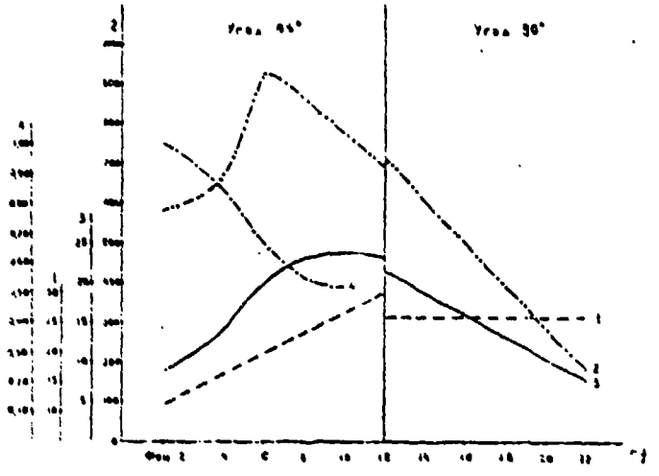


Fig. 4. Average values of the chief indices of external breathing in the studied range of accelerations: 1—frequency of breathing; 2—the volume of respiration; 3—the minute volume of respiration; 4—the vital capacity of the lungs (at the acceleration of 2-12g at an angle of 65°, at the acceleration of 12-22g at an angle of 80°).

SHEET 2 OF 2

TITLE: Comparison of Techniques for Measuring $+G_z$ Tolerance in Man.

REF. # 144

HG- 19

DATE:

LEAD AUTHOR: Krutz, R. B.

HUMANS - X
ANIMALS -

ABSTRACT

Two objective methods and one subjective method for measuring $+G_z$ tolerance (inertial vector in a head-to-foot direction) were compared on the human centrifuge. Direct eye-level blood pressure (PA), blood flow velocity in the superficial temporal artery (Qta), and subjective visual symptoms were used to determine tolerance to rapid onset acceleration (1 G/s) on the USAFSAM human centrifuge. Seven relaxed subjects with extensive centrifuge experience were exposed to gradually increasing $+G_z$ plateaus until the subjects reported 100% loss of peripheral centrifuge gondola lights (PLL) and 50% loss of central light (CI.D); viz, blackout. Zero forward Qta occurred 6 s (range 4-9 s) before subjective blackout and when mean eye-level blood pressure had reached 20 ±1 mm Hg (SE). The results of this study indicate that flow changes in the superficial temporal artery reflect flow changes in the retinal circulation during $+G_z$ stress.

RELEVANCE

The correlation of blood flow in the superficial temporal artery and direct eye level blood pressure (intra-ocular) to subjective visual symptoms during $+G_z$ accelerations.

SALIENT DATA

1. "When blackout was approached (2.7 to 4.6 Gs) eye level arterial blood pressure began to fall concomitant with the occurrence of retrograde flow in the temporal artery (F163)"

2. Retrograde flow (Fig 4). " Zero forward temporal flow (Qta) was determined both graphic and audio recordings 6s (4 to 9 range) prior to blackout Eye level mean arterial pressure (Pa) decreased to 20 ±1 mm Hg when zero forward Qta was initially recorded".

PHYSIOLOGICAL CATEGORY
- AUDITORY
- BIOMECHNL
- CARDIOVSCL
- FORCE
- GENERAL
- LABYRINTH
- MAN.CNTRL
- PROTECTIVE
- REVIEW
- RESPIRAT'N
- SIMULATION
- X VISUAL
- OTHER

AUGMENTATION DEVICES
- HELMET
- STRAPS
- AURAL
- EXTREMITY
- LBNP
- XVISUAL
- RESPIRATORY
- LACRIMATION
- TEMPERATURE
- MASK

SHEET 1 OF 2

AUTHOR Krutz, R. B.

REF # 144

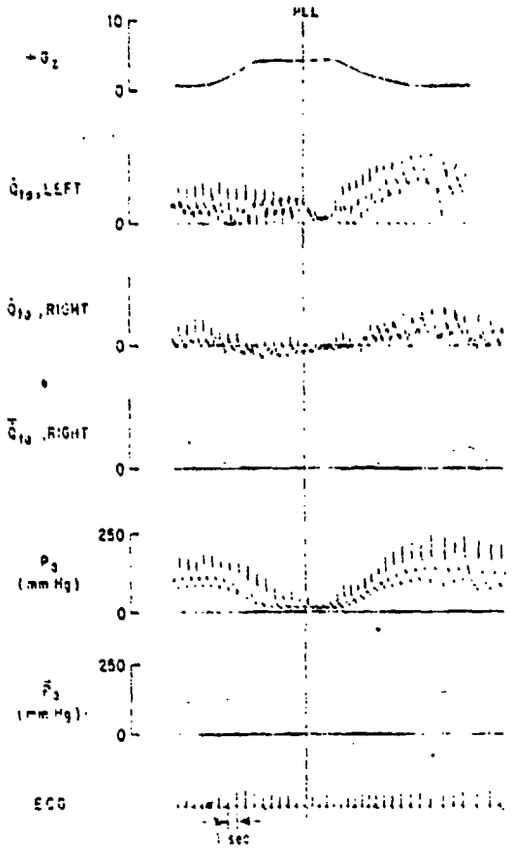


FIG. 4. Occurrence of retrograde flow in the temporal artery prior to peripheral light loss (PLL) and subsequent blackout. A nondirectional signal processor was used with the transducer on the left temporal artery; a directional signal processor was used with the transducer on the right temporal artery.

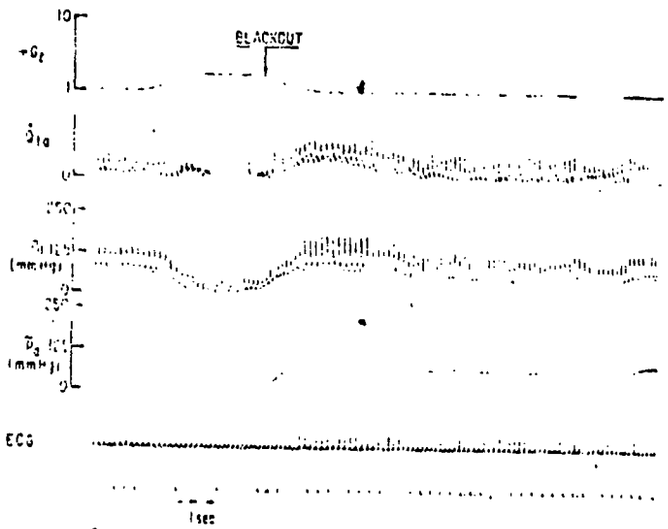


FIG. 3. Eye-level arterial pressure and blood flow responses during rapid onset-run (ROR, 1 G/s). Qta = nondirectional temporal artery blood flow velocity; Pa = eye-level arterial blood pressure; $\bar{P}_a$ = mean eye-level blood pressure.

SHEET 2 OF 2

TITLE:

G Tolerance and Protection with Anti G Suit Concepts.

REF.# 32

HG- 20

DATE:

LEAD AUTHOR:

Burton, R. R.

HUMANS - X
ANIMALS -

ABSTRACT

The effects of pressurizing various functional units of an experimental pneumatic-lever anti-G suit (PLS; frequently called a capstan suit) on a G_z tolerance and protection were determined at relaxed + G_z levels during +G_z for 60 s - termed high sustained G (HSG) Measured were +G_z tolerance and protection on nine male subjects using light loss criteria, increases in heart rate during HSG and subjective analysis. These data from the PLS were compared with similar findings obtained from the same persons wearing the USAF standard anti-G suits (CSU-12/p) with and without suit pressurization. Abdominal bladder inflation offered the highest increase in relaxed +G_z tolerance (0.7 G) whereas leg pressurization offered the greatest anti-G protection (heart rate criterion and subjective analysis) at HSG. Specifically regarding the PLS, it was found superior to the CSU-12/p at HSG regarding both +G_z protection and subject comfort.

RELEVANCE

G Stress & cardiovascular effect of G Suit usage.

SALIENT DATA

1. Abdominal pressurization has most effect on increasing G level endpoint but hardly any effect on heart rate.

2. Leg pressurization has most effect on heart rate reduction but only small effect on increasing G level endpoint.

3. Leg pressurization contributed to absense of pain and feeling of support. (GK - heart rate psychological effect caimed by feeling of support?)

4. Breakdown of G level Increase:
   a) wearing unpressurized suit = 0.3g
   b) leg pressurization = 0.2g
   c) abdominal pressurization = 0.7g
   Total = 1.2g

PHYSIOLOGICAL CATEGORY
- AUDITORY
- BIOMECHNL
- X CARDIOVSCL
- FORCE
- GENERAL
- LABYRINTH
- MAN.CNTRL
- X PROTECTIVE
- REVIEW
- RESPIRAT'N
- SIMULATION
- VISUAL
- OTHER

AUGMENTATION DEVICES
- HELMET
- STRAPS
- AURAL
- EXTREMITY
- X LBNP
- VISUAL
- RESPIRATORY
- LACRIMATION
- TEMPERATURE
- MASK

SHEET 1 OF 2

5. Authors postulate following equation for leg pressurization effect on heart rate:

   Heart rate (BPM) = 163 - (6)(leg pressure$_{psi}$)

6. Uses 100% loss of peripheral light & 60% of central light loss as an indicator of limit.

7. "The ROR (rapid Onset Rate) toleranced (Group mean) found for either anti-g suit w/o. Pressurization was the same 4.0 g's. This is similar to the 4.1 G's relaxed tolerance level reported by Parkhurst et al (11) in their HSG study where subjects were the SBS w/o pressurization. Both Parkhurst & Burton reported a .3 to .4G increase in ROR tolerance as a result of wearing either SBS or PLS anti-g suit w/o application of pressure. The effect of pressurizing both suits & specific portions of PLS upon the +Gz tolerance is seen in Table I.

Table I. RELAXED ROR AND GOR +Gz TOLERANCE (MEAN ± S.E.) FOR NINE MALES WEARING FITHER THE CSU-12/p(SBS) OR PNEUMATIC LEVER (PLS) ANTI-G SUITS WITH AND WITHOUT SUIT PRESSURIZATION. THE ANTI-G EFFECT FROM INFLATING ONLY THE LEG OR ABDOMINAL PORTION OF THE PLS IS ALSO COMPARED.

	Control No Pressure (NP) (Both Suit Types)	SBS*	PLS*	Abdominal Pressure	Leg Pressure
ROR	4.0	5.0**	4.9**	4.7**	4.2
Mean ± S.E.	0.29	0.30	0.31	0.30	0.36
GOR	5.0	5.9**	5.6**	5.4**	5.2
Mean ± S.E.	0.27	0.28	0.26	0.31	0.39

* Suits were pressurized (Note Text):
** Significantly different from NP control +Gz tolerance $p < 0.01$ using paired t-Testing
\+ PLS was used (note Text).

SHEET 2 OF 2

TITLE: Effect of Prolonged Bedrest & +Gz Acceleration Upon Peripheral Visual Response Time.

REF. # 106

HG- 21

DATE:

LEAD AUTHOR: Haines, R. F.

HUMANS - X
ANIMALS -

ABSTRACT

Cardiovascular deconditioning, dehydration, and other physiological changes which occur as a result of prolonged exposure to the zero -g space environment raise some questions about the applicability of much previous research which has shown that spacecraft reentry accelerations pose no appreciable physiological or performance problems for the astronauts. The present paper deals with whether or not peripheral visual response time changes during +Gz acceleration after 14 days of bedrest. Eighteen test lights, placed 10^{o} are apart along the horizontal meridian of the subject's field of view, were presented in a random sequence. The subject was instructed to press a button as soon as a light appeared. This testing occurred periodically during bedrest and continuously during centrifugation testing. The results indicated that: (1) mean response time was significantly longer (P 0.01) to stimuli imaged in the far periphery than to stimuli imaged closer to the line of sight during +Gz acceleration, (2) mean response time at each stimulus position tends to be longer at plateau g than during the pre-acceleration baseline period far that run by an amount which ranged from about 20 to 120 mscc, (3) mean response time tends to lengthen as g level is increased, and (4) under these testing conditions peripheral visual response time during +Gz acceleration within approximately 40 seconds of blackout does not provide a reliable indicater that blackout is going to occur. The bedrest response time data showed that the distribution of RTs across the horizontal retinal meridian remained remarkably constant within subjects from day to day during the bedrest and recovery periods. These findings are discussed in relation to previous studies and to the design and placement of aerospace vehicle cockpit instruments.

RELEVANCE

PHYSIOLOGICAL CATEGORY
- AUDITORY
- BIOMECHNL
- CARDIOVSCL
- FORCE
- GENERAL
- LABYRINTH
- MAN.CNTRL
- PROTECTIVE
- REVIEW
- RESPIRAT'N
- SIMULATION
- X VISUAL
- OTHER

AUGMENTATION DEVICES
- HELMET
- STRAPS
- AURAL
- EXTREMITY
- LBNP
- X VISUAL
- RESPIRATORY
- LACRIMATION
- TEMPERATURE
- MASK

SALIENT DATA

Detailed data on time delays to visual stimuli at various retinal locations as a function of S-level (We could simulate the long reaction time by reducing contrast or intensity appropriately.) Good review of earlier reaction time illustrative for +Gz.

SHEET 1 OF 2

AUTHOR Haines, R. F. REF # 106

Response time lags is not a good indicator to loss of peripheral vision.

SHEET 2 OF 2

TITLE:

Acceleration & Human Performance

REF.: 98

HG- 22

DATE:

AUTHOR: Grether, W. F.

HUMANS - X
ANIMALS -

ABSTRACT

Research on acceleration (G), such as experienced in aircraft and space vehicles is reviewed in terms of effects on human performance capabilities. Almost all such research has been conducted on human centrifuges with the inertial force vectors in the +Gx and -Gx direction for seated subjects, and the +Gz and -Gz directions for supine and prone subjects. Visual blackout has become the standard indicator of human tolerance to +Gz acceleration. Other functions, namely absolute thresholds, brightness, discrimination, visual acuity, and instrument reading all have been found to be impaired at G levels well below physiological tolerance limits, for +Gz, +Gx, and -Gx vectors. Motor capabilities, namely tracking, reaction time, reading, and manipulation also show impairment at relatively low G levels. Limited data on intellectual or central progress suggest that these are more resistant, but not immune, to effects of exposure to acceleration. Included in the review is discussion of probable mechanisms causing performance impairment.

PHYSIOLOGICAL CATEGORY
- X AUDITORY
- X BIOMECHNL
- X CARDIOVSCL
- X FORCE
- X GENERAL
- LABYRINTH
- X MAN.CNTRL
- PROTECTIVE
- REVIEW
- RESPIRAT'N
- SIMULATION
- VISUAL
- OTHER

RELEVANCE

Good ref., pertains primarily to the visual sense, tracking performance, reaction time, manual control.

AUGMENTATION DEVICES
- HELMET
- STRAPS
- X AURAL
- X EXTREMITY
- LBNP
- X VISUAL
- RESPIRATORY
- LACRIMATION
- TEMPERATURE
- MASK

SALIENT DATA

1. p 1159 - Brightness thresholds not affected by Gz when source brightness is in 0.2 Ft-L to 100 Ft-L range; is affected in the 0.03 Ft-L range & due to retinal hypoxia visual acuity affected up to 4 Gz & severe when brightness down at 0.01 Ft. L - acuity decrement mechanism not known.

2. p 1160 - "Hearing relatively immune to acceleration up to the point of unconsciousness" but reaction time increased (See Below).

3. P1161 - "very little research on manual capabilities during acceleration ... perhaps the effects seemed obvious" See Table IV.

SHEET 1 OF 3

AUTHOR	Grether, W. F.	REF # 98

4. P1164 - Primary mechanism for impairment of tracing seems to be direct mechanical disturbance of motor performance however blood supply loss also affects tracking.

5. P1163 - States acceleration feedback improves tracking.

6. P1160 - Decremation in instrument reading under low light levels particularly.

7. Reports "Scuba Mask" negative pressures to attempt to maintain intraocular blood pressure-may be able to use in reverse - Reighley, Clark, and Drury.

8. Rogge showed blackout theshold constant for .2 to 100 foot lamberts (Ft.L)(fairly high) "The study by White showed further that the effect of acceleration on absolute visual thresholds for the periphery can be reduced by providing the subject w/ anti-G protection." (Fig 1) "As long ago as 1946 Warrick & Lund tested the ability of pilots to read instrument dials during +Gz acc. using 1½ G as a control condition, they showed a significant decrement in dial reading ability at 3 G."

9. Further studies of dial reading as a funtion of +Gz by White & Riley & White, showed decrements dependent on luminance levels (fig. 4).

10. Hearing is relatively immune to increased acceleration but semicircular canals & otoliths cause visual illusions & erroneous judgements of motion.

AUTHOR Grether, W. F. REF # 98

TABLE II. SUMMARY OF DATA ON VISUAL FUNCTIONS AS AFFECTED BY ACCELERATION

Area	Tests	Acceleration Conditions	Major Findings
[illegible]	[illegible]	$+G_z$ up to 3.8 G	Up to 3.5 G no change. Increase of 3.8 to 4.8 G small but significant reduction
[illegible]	Reaction Potential, Simple Light Level [illegible] to [illegible] Lambert and [illegible] G	$+G_z$ up to level needed to [illegible] in Blackout	Blackout G level essentially independent of luminance of visual signal field
[illegible]	[illegible] and Visual Acuity Level [illegible]	$+G_z$ up to 4 G with and without anti-G suit	Increase of threshold luminance with increasing G level (See Fig. 1)
[illegible]	[illegible]	$+G_z$ up to 3 G	Some increase in threshold contrast
[illegible]	[illegible]	$+G_z$ up to 7 G	Greatest effect for $+G_z$ and low luminance
[illegible]	[illegible]	$+G_z$ up to 5 G with and without supplementary O_2	Increase in threshold contrast with increase G. Effect reduced by supplementary O_2 (See Fig. 2)
[illegible]	Visual Acuity	$+G_x$ up to 5 G $-G_x$ up to 5 G	Decrease in acuity with increase in G. Smaller effect for both $+G_x$ and $-G_x$ (See Fig. 3)
[illegible]	Visual Acuity, Luminance Range 0.01 to [illegible]	$+G_z$ up to 3 G	Decrease in acuity with increase in G. Greatest effect at low luminance levels
[illegible]	Visual Acuity	$+G_z$ up to 3 G	Decrement in acuity at 3 G
[illegible]	[illegible]	$G_z = 1, 2$ and 3 G	Increased reaction times at $+G_z$ no decrease in readout speed
Visual Tracking	Dual Tracking, Luminance Range 0.01 to 12 mL	$+G_z$ up to 4 G	Decreased tracking accuracy at 3 and 4 G. Greatest effect at low luminance
[illegible]	Dual Tracking, Luminance Range 0.001 to 12 mL	$+G_z$ up to 4 G	Decreased tracking accuracy at 3 G, and at 4 G. At lowest luminance levels [illegible] by [illegible]

TABLE V. SUMMARY OF DATA ON TRACKING AND FLIGHT CONTROL AS AFFECTED BY ACCELERATION

Area	Tests	Acceleration Conditions	Major Findings
[illegible]	2-D Compensatory Tracking	$+G_z$ at 2, 3 & 4 G	Small increase in tracking error with increased G. Less tracking error with side-arm controller as compared with center stick
[illegible]	[illegible]	$+G_z$ at 2.5 G, closed loop	Increased tracking error at 2.5 G, but flight coordination improved because of closed loop
[illegible]	[illegible]	$+G_z$ at 2, 3 & 4 G	Increased tracking error with increased G
[illegible]	[illegible]	$+G_z$ up to 15 G, $-G_z$ up to 7 G, $+G_x$ up to 7 G, closed loop	Generally little increase in tracking error with increased G except at G levels near physiological limit. Tracking decrement greater for some controller configurations
[illegible]	2-D Compensatory Tracking, 2 Axis Pursuit and Compensatory Tracking	$+G_z$ up to 14 G, G_x up to 10 G, $+G_x$ up to 9 G, closed loop	Small increase in tracking error with increased G for $+G_z$ and $-G_z$. Much greater decrement for $+G_x$ (See Fig. 7). Decrement greatest during Curvilinear G (See Fig. 8)
[illegible]	[illegible]	$+G_z$ up to 7 G, $-G_z$ & $-G_x$ up to 3.5 G, $+G_x$ up to 6 G, closed loop	Decrement in tracking efficiency as a consequence of increased G
[illegible]	[illegible]	$+G_z$ up to 16 G, with and without anti-G protection	Increase in tracking error with increased G. Anti-G protection had little effect on tracking error
[illegible]	[illegible]	G_z up to 3.8 G, with 61 in. & 12 in. centrifuge radii	Increase in tracking error with increased G. Error greater for smaller centrifuge radius
[illegible]	[illegible]	G_z up to 4 G	Increase in tracking error with increased G (See Fig. 9)
[illegible]	[illegible]	G_z up to 4 G_z in both centrifuge and Closed Capsule. Latter included TV-2 aircraft	Performance in aircraft generally better than on centrifuge under comparable conditions
[illegible]	[illegible]	$+G_z$ up to 4 G	Increased tracking error at 3 G

SHEET 3 OF 3

TITLE: Hand Eye Coordination in Altered Gravitational Fields.

REF. # 48

IIG- 23

DATE:

LEAD AUTHOR: Cohen, M. M.

HUMANS - X
ANIMALS -

ABSTRACT

Conflicting reports have appeared in the literature concerning the effects of exposure to increased G, upon human visual-motor coordination. In the current study, samples of hand-eye coordination were obtained while each of 8 subjects was exposed to accelerative forces of 1.0, 1.5, and 2.0 Gz in the Naval Air Development Center Human Centrifuge. Systematic changes in coordination were observed as a function of the Gz conditions employed. In the 2.0Gz environment, subjects initially reached below, and then above, a mirror viewed target. In the 1.5 Gz environment, subjects tended to reach above the target throughout the exposure session. In the 1.0 Gz environment (natural terrestrial conditions) there were no significant changes in coordination. The data suggest that the relationship between intended motor outputs and thier proprioceptive kinesthetic consequences provides adequate information for rapid behavioral compensation to altered accelerative forces. Further, vestibular and/or sensorytonic factors are implicated in bringing about changes in the apparent elevation of targets viewed under increased accelerative forces.

RELEVANCE

Extremity drive
Visual effects.

SALIENT DATA

1. Data consists primarily of measurement of arm extended pointing error under various G levels and repeated trials.

2. Subject first points low due to arm loading, then high due to "elevator effect". Author introduces this effect as a visual effect wherein objects appear (or are thought) to rise under increased G load.

PHYSIOLOGICAL CATEGORY
- AUDITORY
- X BIOMECHNL
- CARDIOVSCL
- FORCE
- GENERAL
- LABYRINTH
- MAN.CNTRL
- PROTECTIVE
- REVIEW
- RESPIRAT'N
- SIMULATION
- X VISUAL
- OTHER

AUGMENTATION DEVICES
- HELMET
- STRAPS
- AURAL
- X EXTREMITY
- LBNP
- X VISUAL
- RESPIRATORY
- LACRIMATION
- TEMPERATURE
- MASK

SHEET 1 OF 1

TITLE: Cardiac Rate Changes in Humans After Abrupt Deceleration

REF.# 212

HG 29

DATE:

LEAD AUTHOR: Rothstein, J. D.

HUMANS - X
ANIMALS -

ABSTRACT

Transient slowing of the cardiac rate has been observed after experimental abrupt deceleration (impact) when the deceleration inertial vector is directed craniad (-Gz). We have attempted to clarify the incidence and conditions of this response. Eighteen healthy male subjects (21-41 years) were exposed to -Gz and +Gz impact profiles to 10 G peak deceleration in paired experiments. Cardiac rate was monitored prior to and after impact by vectorcardiography. The data show that -Gz deceleration produces a statistically significant decrease in cardiac rate immediately after impact. An insignificant increase in cardiac rate occurred after Gz impact. It is suggested that the observed changes in cardiac rate are mediated through the pressoreceptors of the carotid sinus and aortic arch.

PHYSIOLOGICAL CATEGORY
- AUDITORY
- BIOMECHNL
- X CARDIOVSCL
- FORCE
- GENERAL
- LABYRINTH
- MAN.CNTRL
- PROTECTIVE
- REVIEW
- RESPIRAT'N
- SIMULATION
- VISUAL
- OTHER

RELEVANCE

CARDIOVASCULAR - Research applies mainly to impacts where the level is 10G with a rate of 650G/sec. These parameters are beyond the area of interest for this study.

AUGMENTATION DEVICES
- HELMET
- STRAPS
- AURAL
- EXTREMITY
- LBNP
- VISUAL
- RESPIRATORY
- LACRIMATION
- TEMPERATURE
- MASK

SALIENT DATA

SHEET 1 OF 1

TITLE: Positive-Pressure Breathing As A Protective Technique During +Gz Acceleration.

REF. # 222

HG- 3 3

DATE:

LEAD AUTHOR: Shubrooks, S. J.

HUMANS - X
ANIMALS -

ABSTRACT

Use of continuous positive-pressure breathing (PPB) as a means of increasing tolerance to positive (+Gz) acceleration was investigated in healthy subjects experienced in riding a human centrifuge. Five were studied during PPB (25-35 mm Hg.) and during an M-1 maneuver, both performed throughout 15-s rapid-onset +Gz exposures without muscular tensing; tolerance increased 0.3-1.5 G with PPB, equal to the M-1 in two subjects and greater than the M-1 by 0.3 to more than 0.5 G in three. Ten other subjects were studied during 30-s exposures with PPB increased to 40 mm Hg and generalized muscular straining added to PPB and the M-1; PPB increased tolerance by 0.7-2.2 G (mean 1.2 G), not significantly different from the M-1. Three highly trained subjects were studied during both maneuvers combined with anti-G suit inflation and muscular straining at +8.0 Gz for 45-60 s without limitation by visual symptoms. Measurement of eye-level systemic arterial pressure (Psa) demonstrated the effectiveness of PPB in maintaining an elevation of Psa during +Gz. PPB afforded reliable +Gz protection equivalent to that of the M-1 but with less fatigue and less inspiratory fall in Psa. Training, muscular tensing, and use of the suit were important in increasing effectiveness of PPB.

RELEVANCE

Visual, cardiovascular, protective devices.

SALIENT DATA

1. Author states that M1 maneuver aids in a higher threshold to +Gz by increasing the systemic arterial pressure primarily by a direct transmission of increased intra-thoracic pressure to the heart and great vessels.

2. Study demonstrates PPB to be approximately equivalent either with or without use of an anti G suit. Study shows PPB to be approximately equivalent to the M1 maneuver in increasing +Gz tolerance. However, less work is required for PPB.

PHYSIOLOGICAL CATEGORY
- AUDITORY
- BIOMECHNL
- CARDIOVSCL
- FORCE
- GENERAL
- LABYRINTH
- MAN.CNTRL
- PROTECTIVE
- REVIEW
- RESPIRAT'N
- SIMULATION
- VISUAL
- OTHER

AUGMENTATION DEVICES
- HELMET
- STRAPS
- AURAL
- EXTREMITY
- LBNP
- VISUAL
- RESPIRATORY
- LACRIMATION
- TEMPERATURE
- MASK

SHEET 1 OF 3

3. Data is presented comparing PPB/M1 eye level systemic arterial pressure.

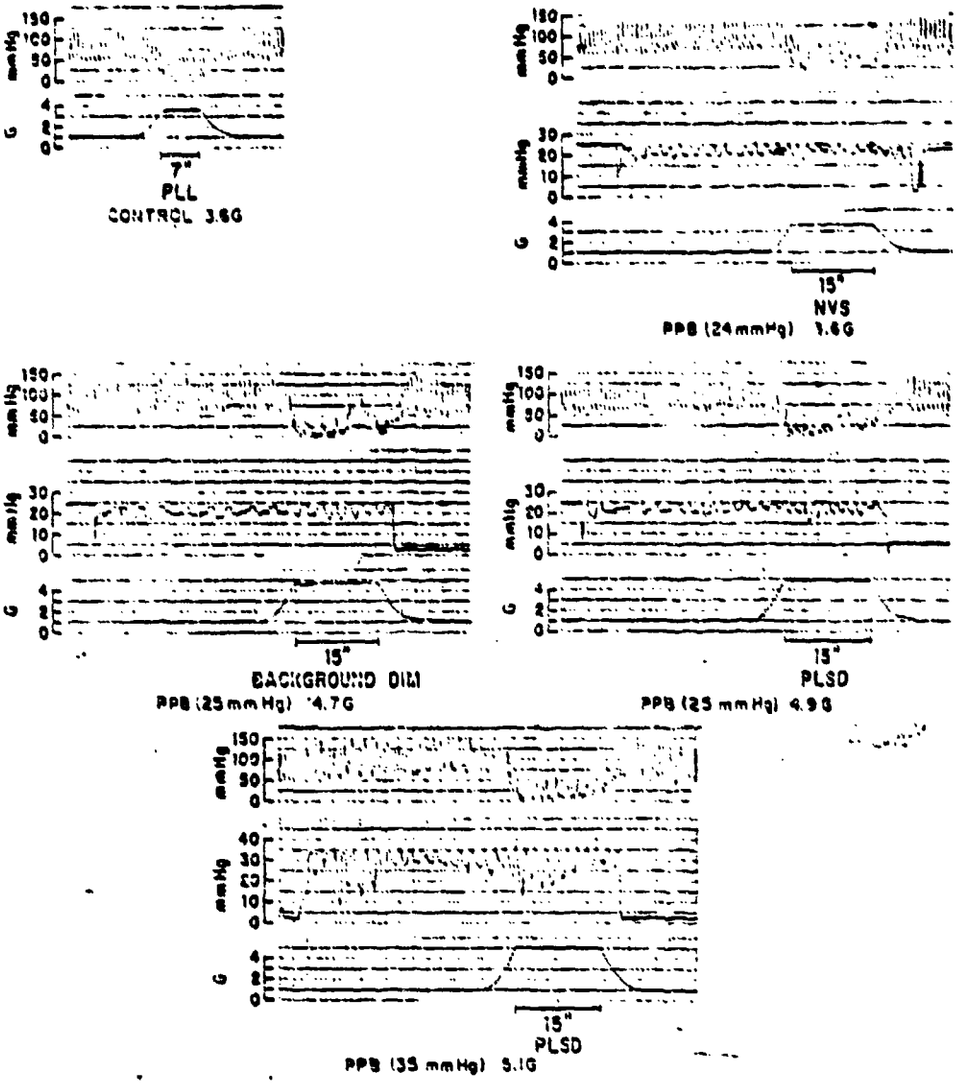


FIG. 1. Typical eye-level Psa response to $+G_z$ during 3.6-G control run and runs at progressively higher $+G_z$ levels using PPB. In each panel, upper tracing shows eye-level Psa and lower tracing indicates acceleration profile. Middle tracing for all PPB runs is breathing pressure (*subject A*).

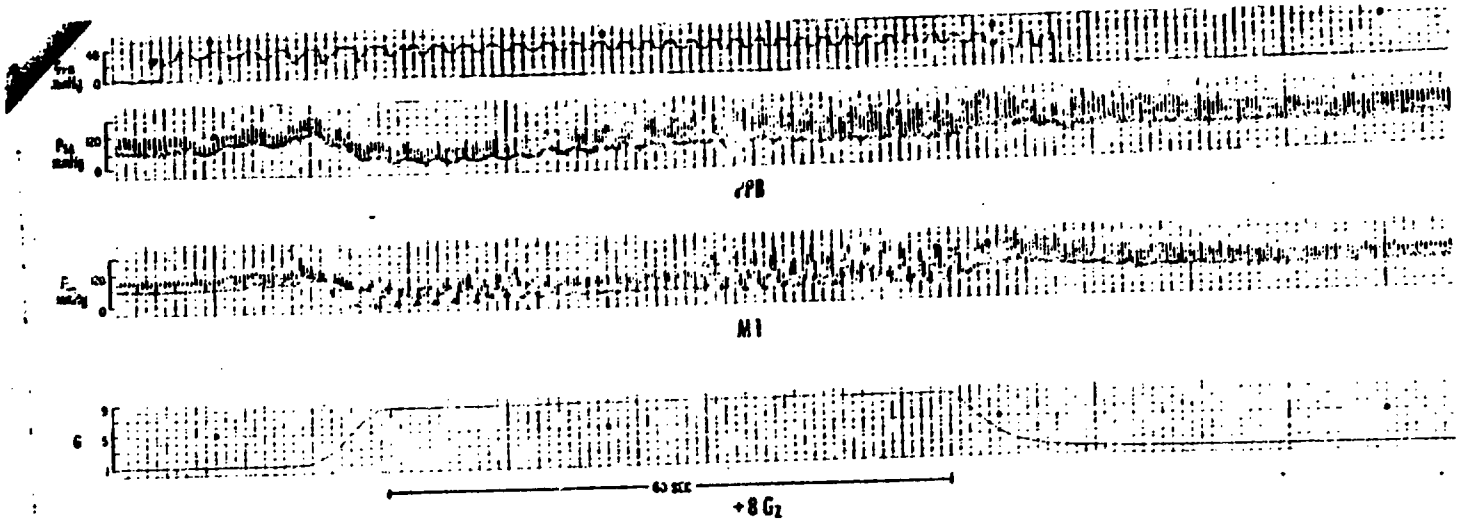


FIG. 2. Psa response during PPB and during the M-1 maneuver at +8.0 G_z for 60 s. (*subj P*). Acceleration profile, the same for both runs, is indicated in the lower tracing. Eye-level Psa for both maneuvers, performed 1 week apart, is shown along with breathing pressure (Peyn) for PPB (upper tracing).

TITLE: Effects of an Anti-G Suit on the Hemodynamic & Renal Responses to Positive (+Gz) Acceleration

REF.# 223

HG- 34

DATE:

LEAD AUTHOR: Shubrooks, S. J.

HUMANS - X
ANIMALS -

ABSTRACT

The effects of the currently used US Air Force (CSU-12/P) anti-G suit on renal function during positive radial acceleration (+Gz) were assessed in seven normal male subjects in balance on a 200 meq sodium diet. Following suit inflation in the seated position, +2.0 Gz for 30 min resulted in a decrease in the rate of sodium excretion ($U_{Na}V$) from 125 ± 19 to 60 ± 14 meq/min ($P < 0.01$) which persisted during a 25 min recovery period. Fractional excretion of sodium also decreased significantly during +Gz ($P < 0.01$). The magnitude of the antinatriuresis was indistinguishable from that observed during +Gz without suit inflation. In contrast to the antinatriuresis observed during centrifugation without suit, however, the antinatriuresis with suit was mediated primarily by an enhanced tabular reabsorbtion of sodium. Addition studies of suit inflation without Gz demonstrated an elevation of arterial pressure which was sustained during 5-10 min of observation. In contrast, an initial elevation in central venous pressure was followed by a rapid return toward base-line levels. The enhanced renal tubular reabsorption of sodium in the present study suggests that the anti-G suit probably is ineffective in redistributing blood volume.

RELEVANCE

Visual, protective devices, cardiovascular.

SALIENT DATA

1. Paper concentrates on the renal effects and therefore has limited applicability other than for static effects of G Suit on systemic pressure.

2. Data is presented illustrating the effects of the anti-G suit on CVP & mean systemic arterial pressure.

PHYSIOLOGICAL CATEGORY
- AUDITORY
- BIOMECHNL
- X CARDIOVSCL
- FORCE
- GENERAL
- LABYRINTH
- MAN.CNTRL
- X PROTECTIVE
- REVIEW
- RESPIRAT'N
- SIMULATION
- VISUAL
- OTHER

AUGMENTATION DEVICES
- HELMET
- STRAPS
- AURAL
- EXTREMITY
- LBNP
- X VISUAL
- RESPIRATORY
- LACRIMATION
- TEMPERATURE
- MASK

SHEET 1 OF 1

TITLE:
Changes in ECG Contour During Prolonged +Gz Acceleration.

REF. # 45

HG- 36

DATE:

LEAD AUTHOR:
Cohen, G. H.

HUMANS - X
ANIMALS -

ABSTRACT

One hundred and sixteen centrifuge runs were performed on the USAFSAM Human Centrifuge using a highly experienced subject panel of eighteen subjects ranging in ages from 21-40 (mean 26). The subjects were exposed to rapid onset profiles of 2.8, 3.1 +Gz (0.75 G/sec) with a 15 second plateau and gradual onset run (1 G/10 second) to a firm peripheral light loss. The subjects were monitored throughout with a simultaneously recording ECG system permitting the recording of leads I, II, III, AVR, AVL, and AVF or leads V_1-V_6.

Analysis of the tracings for heart rate, P, QRS and T wave contour revealed a pattern of P-wave peaking in II, III and AVF associated with T wave flattening or inversion in II, III, AVF and the precordial leads with changes in V_5-V_6 being seen most consistently.

Although the P wave changes returned to control configuration with return of the subject to 1 G, the T changes were most persistent and are felt to be similar to those seen during orthostasis in humans.

The time relation of the T wave changes to the G profiles used supports the contention that the ECG changes seen during +Gz acceleration are related to increased sympathetic tone rather than myocardial ischemia.

It appears that the ECG changes noted can be a useful parameter of the cardiovascular sympathetic response to +Gz acceleration.

PHYSIOLOGICAL CATEGORY
- AUDITORY
- BIOMECHNL
- XCARDIOVSCL
- FORCE
- GENERAL
- LABYRINTH
- MAN.CNTRL
- PROTECTIVE
- REVIEW
- RESPIRAT'N
- SIMULATION
- VISUAL
- OTHER

AUGMENTATION DEVICES
- HELMET
- STRAPS
- AUPAL
- EXTREMITY
- XLBNP
- VISUAL
- RESPIRATORY
- LACRIMATION
- TEMPERATURE
- MASK

RELEVANCE

Cardiovascular, LBNP

SALIENT DATA

Authors report alterations of the normal ECG as a result of +Gz stress. They report magnitude increase of the P wave, T wave flattening or inversion, no change in cardiac rhythm other than sinus tachycardia and no disturbance of intraventricular or artrioventricular conduction. These results have value to this study in they would indicate conditions which would be expected in monitoring a subject during LBNP exposure.

SHEET 1 OF 1

TITLE: Tolerance to Transverse (+Gx) & Headward (+Gz) Acceleration After Prolonged Bed Rest.

REF.# 174

HG- 37

DATE:

LEAD AUTHOR: Miller, P. B.

HUMANS - X
ANIMALS -

ABSTRACT

Tolerance to the transverse (+Gx) acceleration simulated Gemini re-entry profile was determined before and after weeks of absolute bed rest. Tolerance to headward (+Gz) acceleration was studied before and after 4 weeks of obsolute bed rest and 2 weeks of modified bed rest.

As judged by the degree of physical discomfort, the ability to respord to a central light, or the presence of electrocardiographic abnormalities, tolerance to +Gx was unaffected by 4 weeks of absolute bed rest. In each subject studied, heart rates during peak acceleration were higher after bed rest than before. As judged by the level of acceleration at which central vision was lost, no significant change in tolerance to headward (+Gz) acceleration of rapid onset was observed after 2 weeks of modified bed rest or after 4 weeks of absolute bed rest. After each type of bed rest, the majority of the subjects had decreased tolerance in headware (+Gz) acceleration of gradual onset, but the mean decrease was not statistically significant.

Mean heart rates at equivalent levels of +Gz were significantly higher after both periods of bed rests. The only arrhythmia of clinical importance notes the appearance of bursts of premature atrial contractions during G.O.R. -Gz in 1 subject after 2 weeks of bed rest.

RELEVANCE

Cardiovascular, LBNP
Work was directed toward manual orbiting Lob(MOL) program so it has only limited application to this study.

SALIENT DATA

Main value of this work is that it provides some thresnold data and heart rate data for ROR (lg/sec) and that it confirms some other work by different researchers on the effects of the reflex arteriolar constriction and reflex venotonstriction.

PHYSIOLOGICAL CATEGORY
- AUDITORY
- BIOMECHNL
- CARDIOVSCL
- FORCE
- GENERAL
- LABYRINTH
- MAN.CNTRL
- PROTECTIVE
- REVIEW
- RESPIRAT'N
- SIMULATION
- VISUAL
- OTHER

AUGMENTATION DEVICES
- HELMET
- STRAPS
- AURAL
- EXTREMITY
- X LBNP
- VISUAL
- RESPIRATORY
- LACRIMATION
- TEMPERATURE
- MASK

SHEET 1 OF 1

TITLE: Instrumentation for the Rhesus Monkey as a Cardiovascular Analog for Man during Air-Combat Maneuvering Acceleration.

REF.# 64

HG- 40

DATE:

LEAD AUTHOR: Erickson, H. H.

HUMANS - X
ANIMALS -

ABSTRACT

The development of high-performance, fighter-attack aircraft has created a need for new techniques and methods to study the effects of acceleration stress on the cardiovascular system. Instrumentation methods were developed in the rhesus monkey (Macaca Mulatta) in order to evaluate cardiovascular performance in a high-G, air-combat maneuvering environment. The results indicate that the rhesus monkey is a useful model in studying the effects of gravitoinertial forces encountered by man during repetitive and maneuvering acceleration. The model permits investigation of risk limits, damage mechanisms, fatigue of the cardiovascular system, and pathophysiologic responses to acceleration. Increasing the seat angle during acceleration provides protection to the cardiovascular system and results in improved eye-level blood pressure. Repeated exposure to sustained and maneuvering acceleration indicates that fatigue occurs and that cardiovascular compensation becomes inadequate.

RELEVANCE

Cardiovascular, Protective Devices, LBNP

SALIENT DATA

The Rhesus monkey is a suitable human analog, comparable acc tolerance.
The seat back angles used were 13^{o}, 30^{o}, 45^{o}, and 65^{o}.
Simulated ACM profiles were used. The exposure was terminated when mean eye level BP reached 0 mm Hg.
The point was approximately 4g.
There was little or no change in left ventricular pressure.
Decrease in left ventricular dp/dt, eye level arterial pressure, central venous pressure and cardiac output.
Exposure to the maneuvering profile resulted in significantly greater stress to the cardiovascular system than exposure to sustained "G" particularly at the smaller seat angles.

PHYSIOLOGICAL CATEGORY
- AUDITORY
- BIOMECHNL
- X CARDIOVSCL
- FORCE
- GENERAL
- LABYRINTH
- MAN.CNTRL
- X PROTECTIVE
- REVIEW
- RESPIRAT'N
- SIMULATION
- VISUAL
- OTHER

AUGMENTATION DEVICES
- HELMET
- STRAPS
- AURAL
- EXTREMITY
- X LBNP
- VISUAL
- RESPIRATORY
- LACRIMATION
- TEMPERATURE
- MASK

SHEET 1 of 1

TITLE: Mechanism of Head & Neck Response to -Gx Impact Acceleration: A Math Modeling Approach.

REF. # 74

HG- 41

DATE:

LEAD AUTHOR: Frisch, G. D.

HUMANS - X
ANIMALS -

ABSTRACT

Mathematical modeling has attained wider acceptance in recent years. In particular, the use of computer programs to simulate the dynamic response of a human in a crash situation has become an attractive alternative to full-scale experimental testing. This paper analyzes data on the dynamic response of the living human head and neck to -Gx impact acceleration, where the subject's head and neck in the midsagittal plane was monitored with inertial instrumentation and high-speed photography for confirmation. The Calspan "3D Computer Simulator of Motor Vehicle Crash Victims" was used to predict expected responses for the deceleration pulses employed. These estimates were compared to the fully instrumented human test runs. The standard 15-segment and 14-joint representation of the occupant was modified to include two sterno-clavicular joints, increasing the articulation in the upper torso. Analysis of the data indicated that muscular activity in the head and neck seemed to be evident and does influence motion of the head, even at relatively high (10-G peak, 530 G/s onset) acceleration levels. Simulation of muscular contraction, using a spring-damper arrangement, improved the results significantly. Additionally, possible limitations to head-to-neck motion such as ligament restrictions, were also modeled.

PHYSIOLOGICAL CATEGORY
- AUDITORY
- X BIOMECHNL
- CARDIOVSCL
- FORCE
- GENERAL
- LABYRINTH
- MAN.CNTRL
- PROTECTIVE
- REVIEW
- RESPIRAT'N
- SIMULATION
- VISUAL
- OTHER

AUGMENTATION DEVICES
- HELMET
- STRAPS
- AURAL
- X EXTREMITY
- LBNP
- VISUAL
- RESPIRATORY
- LACRIMATION
- TEMPERATURE
- MASK

RELEVANCE

Paper presents results of math model of head & neck response to impact loading in the negative X directon. The model does not have much application to this study.

SALIENT DATA

1. Maximum head and neck excursion angles.

SHEET 1 OF 1

TITLE: Transfer Functions For Arterial Oxygen Saturation During +Gz Stress

REF. # 84

HG- 42

DATE:

LEAD AUTHOR: Gillingham, K. K.

HUMANS - X
ANIMALS -

SALIENT DATA

RELEVANCE

ABSTRACT

None available at this time.

Visual, Respiratory

Authors present a transfer function which they claim correlates well with ACM profiles as well as steps. The transfer function is synthesized as an impulse response: Sa_{O_2} is in %.

$$Sa_{O_2} = 0,\ t < 1.17 \text{ sec}$$

$$= 100, 1.17 \leq t \leq 1.95 \text{ sec}$$

$$= 0,\ 1.95 < t < 4.69$$

$$= -19.5e^{-\left(\frac{t-4.69}{37.5}\right)},\ t \geq 4.69 \text{ sec}$$

This was based on a 6g impulse response.

PHYSIOLOGICAL CATEGORY
- AUDITORY
- BIOMECHNL
- XCARDIOVSCL
- FORCE
- GENERAL
- LABYRINTH
- MAN.CNTRL
- PROTECTIVE
- REVIEW
- XRESPIRAT'N
- SIMULATION
- XVISUAL
- OTHER

AUGMENTATION DEVICES
- HELMET
- STRAPS
- AURAL
- EXTREMITY
- LBNP
- XVISUAL
- XRESPIRATORY
- LACRIMATION
- TEMPERATURE
- MASK

SHEET 1 OF 1

TITLE: Physiologic Effects of Seatback Angles < 45° (From The Vertical) Relative to G.

REF.# 31

HG- 44

DATE:

LEAD AUTHOR: Burton, R. R.

HUMANS - X
ANIMALS -

ABSTRACT

Eight experimental subjects from the USAF School of Aerospace Medicine (SAM) and four YF-16/17 test pilots were exposed to a simulated aerial combat maneuver (SACM) which included a maximum G exposure of 6 s at 8 G. The following physiologic parameters were examined relative to seatback angles of 23°, 28°, and 40°: heart rate and rhythm; arterial oxygen saturation; performance; intrathoracic (isophageal) pressure; arterial pressure; and subject comfort, effort, and fatigue. Relaxed and straining high sustained G (HSG) tolerances (6 G for 60 s) were also determined using only SAM subjects. The advantages of the 40° seatback angle during the SACM included increased subject comfort, less fatigue and effort, greater pilot acceptance and a statistically significant reduction in the increased mean heart rate associated with G exposure. On the other hand, a statistically significant reduction in arterial oxygen saturation was obtained during the SACM at 40° compared with the 23° back angle. An increase in relaxed G tolerance was found with the 40° seatback angle - statistically significant only compared with the 28° seatback angle.

PHYSIOLOGICAL CATEGORY
- AUDITORY
- BIOMECHNL
- X CARDIOVSCL
- FORCE
- GENERAL
- LABYRINTH
- MAN.CNTRL
- X PROTECTIVE
- REVIEW
- X RESPIRAT'N
- SIMULATION
- X VISUAL
- OTHER

AUGMENTATION DEVICES
- HELMET
- STRAPS
- AURAL
- EXTREMITY
- X LBNP
- X VISUAL
- X RESPIRATORY
- LACRIMATION
- TEMPERATURE
- MASK

RELEVANCE

visual & LBNP, respiration

SALIENT DATA

1. Presents data for 23°, 28°, & 40° seat back angle: thresholds (ROR & GOR), mean heart rates, cardiac arrhythmia, O_2 saturation, performance systolic arterial pressure (after exposure).

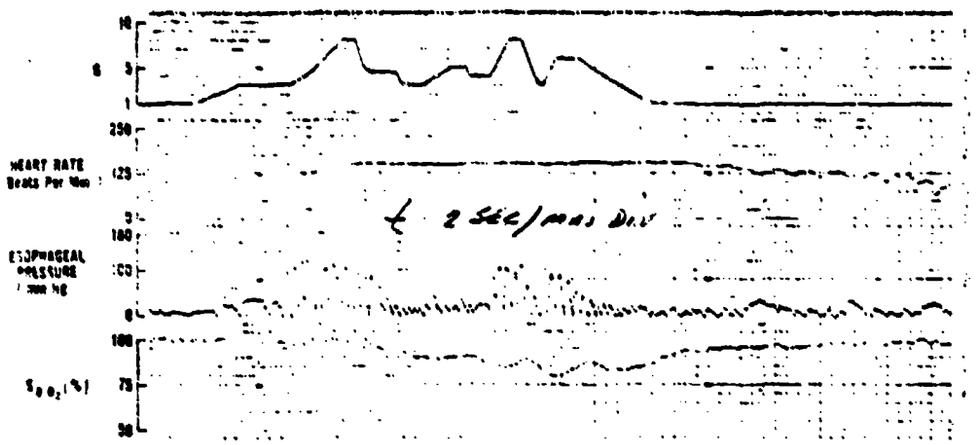
2. Simulated ACM maneuver developed by pilots & used herein for centrifuge profile. Represents F4E maneuvering as uprated to be applicable to F16 type A/C.

SHEET 1 OF 2

AUTHOR Burton, R. R.

REF # 31

PHYSIOLOGIC RESPONSES TO A SIMULATED AERIAL COMBAT MANEUVER



SHEET 2 OF 2

TITLE:

Mechanical Impedance of Supine Humans Under Sustained Acceleration

REF.# 248

HG- 45

DATE:

LEAD AUTHOR:

Vogt, L. H.

HUMANS - X
ANIMALS -

ABSTRACT

Measurements of the mechanical impedance of the supine human body were conducted to investigate the non-linearities of the body system. A hydraulically driven shake table was installed on a centrifuge. Transmitted force and the acceleration of the platform, on which the subjects were lying, were recorded in the frequency range of 2Hz-20Hz. Sinusoidal acceleration amplitude was held constant at 0.5g. The impedance and phase results show that sustained acceleration up to +5Gx stiffens the human body with increasing Gx and shifts the resonance frequency from 6Hz under normal gravity to 8Hz under +2Gx and further up to 11Hz, 13Hz and 15 Hz under +3Gx, +4Gx and +5Gx respectively.

PHYSIOLOGICAL CATEGORY

- AUDITORY
- X BIOMECHNL
- CARDIOVSCL
- FORCE
- GENERAL
- LABYRINTH
- MAN.CNTRL
- PROTECTIVE
- REVIEW
- RESPIRAT'N
- SIMULATION
- VISUAL
- OTHER

RELEVANCE

Head/helmet, extremeties

AUGMENTATION DEVICES

- X HELMET
- STRAPS
- AURAL
- X EXTREMITY
- LBNP
- VISUAL
- RESPIRATORY
- LACRIMATION
- TEMPERATURE
- MASK

SALIENT DATA

Overall, data herein is not directly useful to us. Authors state that their experimental data could be approximated by (simple system) a fixed class with 3 spring mass damper systems attached there to (two of the mass/spring/dampers directly coudled to each other). Authors state that masses located distant from the forcing function may be characterized (modelled) as decreasing "apparant mass" and decreasing damping (under fairly constant spring rate) overall Gx acceleration increases.

SHEET 1 OF 1

TITLE: Changes in Cardiac Rhythm During Sustained High Levels of Positive (+Gz) Acceleration.

REF.: 221

HG- 46

DATE:

LEAD AUTHOR: Shubrooks, S. J. (Jr.)

HUMANS -X
ANIMALS -

ABSTRACT

Electrocardiograms were recorded during 45-sec. exposures to +6.5 to +9.0 Gz of 14 human subjects on the USAF School of Aerospace Medicine human centrifuge. Maximum heart rate (HR) reached by each subject ranged from 155 to 205 beats/min. Four subjects developed a slowing of HR at 16 to 38 seconds into the run due to slowing of the sinus pacemaker, sometimes the escape of an A-V junctional or ventricular pacemaker. Similar escape rhythms also occurred during the sinus slowing the deceleration. Ventricular premature beats (VPB's) occurred frequently in 7 subjects, occasionally in 6, and not at all in one. When frequent, the number increased markedly in the latter part of the 45-sec. runs. These VPB's were frequently multiform and occasionally occurred in runs of 2 or 3 with a few runs of 4 to 7. In no case did any serious arrhythmias persist after deceleration, nor did G tolerance appear to be affected. The etiology and significance of these arrhythmias remain unclear.

PHYSIOLOGICAL CATEGORY
- AUDITORY
- BIOMECHNL
- X CARDIOVSCL
- FORCE
- GENERAL
- LABYRINTH
- MAN.CNTRL
- X PROTECTIVE
- REVIEW
- RESPIRATN
- SIMULATION
- VISUAL
- OTHER

AUGMENTATION DEVICES
- HELMET
- STRAPS
- AURAL
- EXTREMITY
- X LBNP
- VISUAL
- RESPIRATORY
- LACRIMATION
- TEMPERATURE
- MASK

RELEVANCE

Cardiovascular & LBNP, limited relevance to our study. The primary purpose of the work was to determine if at these high sustained levels of Gz, cardiac failure might be the limiting physiological factor rather than cerebral circulation.

SALIENT DATA

Data on heart rate for 14 subjects and ECG traces from selected subjects are presented. The discussion presented adds to the understanding of the cardiovascular effects of High G flight.

The author indicates that an observed increase in artena pressure during acceleration with repeated M1 maneuvers through baroreceptor reflexes can result in an increase in vagal activity sufficient to cause bradycardia and at times long periods of sinus arrest.

SHEET 1 OF 1

TITLE: Human Tolerance to High, Sustained +Gz Acceleration.

REF. #195

HG- 47

DATE:

LEAD AUTHOR: Parkhurst, M. J.

HUMANS -X
ANIMALS -

ABSTRACT

Levels of 6.5 to 9.0 G for a duration of 45 seconds were sustained by a goup of centrifuge subjects wearing standard personal protective clothing and using maximum voluntary M-1 maneuver. Of 14 subjects exposed at weekly intervals to progressively higher G levels above 6.5 G/45 sec, 9 tolerated 9 G/45 sec. without loss of victim. The amount of protection afforded the subjects at high-G levels was found to be dependent on (a) the type and amount of instruction in the performance of the M-1 straining maneuver (b) amount of experience and confidence in performing the M-1 maneuver and (c) overall physical endurance and muscular coordination of the subject. A marked increase in heart rate was observed during all runs with pre-acceleration heart rates ranging from 10½ bpm to 110 bpm. At peak G, the average heart rates ranged from 153 to 167 bpm. Changes in ECG patterns and cardiac arrhythmias were observed. This series of experiments indicates that man's ability to tolerate high, sustained G forces is greater than previously anticipated when using presently available protective techniques. The anti-G suit/M-1 combination during sustained exposures to 7.5 G to 9.0 G in a 45-sec. time frame is effective and essential for combat survival.

RELEVANCE

Relevant to LBNP, visual.

SALIENT DATA

1. Study presents data $6.5 \leq Gz \leq 9.0$ for 30 to 45 sec..

2. States human tolerance with anti-G Suit and M1 maneuver above 7.5 G/45 Sec. Varied from 7.5 - 9.0 (avg. 8.8 g)

3. Restates previously reported data: unprotected tolerance 3.5 - 4.0 G at 18/sec. (avg. 3.7g)

4. Heart rate data for $3.0 \leq Gz \leq 9.0$ pre/peak acceleration.

5. Some subjects had PLL and/or blackout at 7.0g for 10-20 sec.

PHYSIOLOGICAL CATEGORY
- AUDITORY
- BIOMECHNL
- X CARDIOVSCL
- FORCE
- GENERAL
- LABYRINTH
- MOT.CNTRL
- X PROTECTIVE
- REVIEW
- RESPIRAT'N
- SIMULATION
- X VISUAL
- OTHER

AUGMENTATION DEVICES
- HELMET
- STRAPS
- AURAL
- EXTREMITY
- X LBNP
- X VISUAL
- RESPIRATORY
- LACRIMATION
- TEMPERATURE
- MASK

SHEET 1 OF 2

6. States lack of std procedures produces varying results for thresholds.

	Howard	Cochran (lg/sec)	Gauer
PLL	4 g	4.1 g	3.0-3.5g
CLL	5 g	4.7 g	
UNC	5.5-6.0 g	5.4 g	4.5-5 g

7. Statement attributed to Lambert concerning applicability of centrifuge to A/C is questionable based on the fact that the MAYO centrifuge is an old machine.

TITLE: Bradycardia Induced by Negative Acceleration

REF. # 134

HG- 49

DATE:

LEAD AUTHOR: Kennealy, J. A.

HUMANS - X
ANIMALS -

ABSTRACT

Four volunteers were subjected to negative acceleration in a human centrifuge for the purpose of testing a standard lap belt. Three subjects developed a sinus bradycardia. The fourth developed a sinus arrest with a junctional rhythm at -2G. With return to +1 G, the sinus mechanism recovered with a prolonged P-R interval. Within 2 h, the P-R interval returned to normal. Negative acceleration maneuvers well within the capabilities of high-performance aircraft, can effect marked changes in the cardiac rhythm. This phenomenon appears to be vagally induced and is remarkably well tolerated.

RELEVANCE

Cardiovascular, LBNP/LBPP, visual

SALIENT DATA

None of the four centrifuge subjects lost consciousness or vision but all reported discomfort. Total exposure at negative Gz was 30-40 seconds. The onset rate was slow.

Data are presented illustrating some of the ECG results.

No other symptoms were reported by the authors.

PHYSIOLOGICAL CATEGORY
- AUDITORY
- BIOMECHNL
- XCARDIOVSCL
- FORCE
- GENERAL
- LABYRINTH
- MAN.CNTRL
- PROTECTIVE
- REVIEW
- RESPIRAT'N
- SIMULATION
- VISUAL
- OTHER

AUGMENTATION DEVICES
- HELMET
- STRAP
- AURAL
- EXTREMITY
- XLBNP
- XVISUAL
- RESPIRATORY
- LACRIMATION
- TEMPERATURE
- MASK

SHEET 1 OF 1

TITLE:

Comparison of the Incidence of Cardiac Arrhythmias during +Gx Acceleration, Treadmill Exercise and Tilt Table Testing.

REF.# 206

HG- 51

DATE:

LEAD AUTHOR:

Rogge, J. D.

HUMANS - X
ANIMALS -

ABSTRACT

The occurrence and significance of cardiac arrhythmias during acceleration have been discussed by several authors. Recently, a large group of men was referred to the USAF School of Aerospace Medicine for medical evaluation which included exposure to +Gz acceleration, treadmill exercise and tilt table testing. Because of the different hemodynamics during these procedures a comparison of the incidence of cardiac arrhythmias during these tests was felt to be of interest.

The electrocardiographic records of a total of 61 normal male subjects taken during evaluation on the human centrifuge, treadmill and tilt table were examined for arrhythmias.

There was significantly increased incidence of arrhythmias during +Gz acceleration compared with that during treadmill and tilt table test as well as a difference in predominant type of arrhythmias.

The contributions of cardiac chamber distention, sympathetic nervous system activity, circulating norepinephrine levels and respiratory pattern to the production of the arrhythmias are discussed.

PHYSIOLOGICAL CATEGORY

- AUDITORY
- BIOMECHNL
- CARDIOVSCL
- FORCE
- GENERAL
- LABYRINTH
- MAN.CNTRL
- PROTECTIVE
- REVIEW
- X RESPIRAT'N
- SIMULATION
- VISUAL
- OTHER

RELEVANCE

Cardiovascular, respiratory

AUGMENTATION DEVICES

- HELMET
- STRAPS
- AURAL
- EXTREMITY
- LBNP
- VISUAL
- XRES IRATORY
- LACRIMATION
- TEMPERATURE
- MASK

SALIENT DATA

Authors reported that during +Gx acceleration breathing becomes difficult because of the increased weight of the chest and partial occlusion of the posterior pharynx. The conscious efforts by the subjects to breath when added to the normal respiratory changes caused by +Gx acceleration may well have contributed to the arrhythmias during acceleration since deep breathing & hyperventilation as well as other respiratory maneuvers have been shown to precipitate arrhythmias. Three centrifuge runs were made at 5.5, 7.4, & 8 Gx.

SHEET 1 OF 1

TITLE:

Physiological Endpoints in Acceleration Research.

REF.# 42

HG- 52

DATE:

LEAD AUTHOR:

Coburn, K. R.

HUMANS - X
ANIMALS -

ABSTRACT

The problem of duplicating acceleration environments in different laboratories is a difficult one. No two human centrifuges have quite the same performance characteristics and the geometrics vary widely. Since the physiological response of man is in part dependent upon these characteristics several suggestions are put forth which could aid in establishing criteria which would enable closer duplication of a given acceleration environment. The location of anatomical structures with regard to geometric references is discussed. Within this context the commonly used physiological endpoints are briefly dealt with and relative advantages and disadvantages of each are mentioned. Certain aspects of the responsibility of the investigator are mentioned as are some aspects of experimentation in which the investigator may also be acting as one of his own subjects.

PHYSIOLOGICAL CATEGORY

- X AUDITORY
- BIOMECHNL
- X CARDIOVSCL
- FORCE
- X GENERAL
- LABYRINTH
- MAN.CNTRL
- PROTECTIVE
- REVIEW
- X RESPIRAT'N
- SIMULATION
- X VISUAL
- OTHER

RELEVANCE

Visual, auditory, respiration, general physiology

Good general info on acceleration research protocol.

AUGMENTATION DEVICES

- HELMET
- STRAPS
- X AURAL
- EXTREMITY
- LBNP
- X VISUAL
- X RESPIRATORY
- LACRIMATION
- TEMPERATURE
- MASK

SALIENT DATA

1. Author cautions reader on the interpretation of centrifuge data. Particularly interesting is the effect of radius of centrifuge.

2. The theory of endpoints is discussed. Visual, auditory, EEG & cardiorespiratory endpoints or lack thereof are discussed.

3. The classical endpoint is described as greyout and blackout. However variations of definitions among subjects are noted.

4. Author mentions use of a bulb thermistor for respiratory rate measurement.

SHEET 1 OF 1

TITLE:
Re-Evaluation of a Tilt-Back Seat as a Means of Increasing Acceleration Tolerance.

REF.# 28
HG- 55
DATE:

LEAD AUTHOR:
Burns, J. W.

HUMANS -X
ANIMALS -

ABSTRACT

Relaxed tolerance was determined on seven subjects exposed to rapid onset (RO; 1 G/s) and gradual onset (GO: 1 G/10 s) acceleration at seat back angles of 13°, 30°, 45°, 55°, 65°, and 75° from the vertical. There was no significant difference between relaxed tolerance at the control angle of 13° and tolerance at 30°. However, at 45° there was a significant 0.5 G increase in tolerance compared to control. Thereafter, tolerance continued to increase in an exponential manner to 8 G at 75°, an increase over control of 100%. As relaxed tolerance increased with increasing back angle, peak heart rate during acceleration significantly decreased. In addition, four subjects were instrumented with an esophageal balloon for the measurement of intrathoracic pressure, which was equated as work during the M-1 straining maneuver. The amount of thoracic pressure necessary to maintain a preselected visual field declined as the back angle was increased from 13° to 45° to 65° at the same acceleration level. The increase in relaxed tolerance along with the decrease in heart rate and the decrease in esophageal pressure at the greater back angles all demonstrate the acceleration protection provided by the tilt-back seat.

PHYSIOLOGICAL CATEGORY
- AUDITORY
- BIOMECHNL
- X CARDIOVSCL
- FORCE
- GENERAL
- LABYRINTH
- MAN.CNTRL
- X PROTECTIVE
- REVIEW
- RESPIRAT'N
- SIMULATION
- VISUAL
- OTHER

AUGMENTATION DEVICES
- HELMET
- STRAPS
- AURAL
- EXTREMITY
- X LBNP
- X VISUAL
- RESPIRATORY
- LACRIMATION
- TEMPERATURE
- MASK

RELEVANCE

Singularly relevant because it identifies a G stress resistivity sensitivity starting at 30° tilt back. F16 30° tilt back seat usage means large variations in AOA (Also a characteristic of this type A/C) become meaningful and should be accounted for within simulation.
Data applicable to cardiovascular area.

SALIENT DATA

1. 7 subjects wearing G suit and practicing M1 at various seat angles under constant G magnitudes.

2. See attached data sheet for plots.

3. Authors postulate following expression from data
   a) Acceleration tolerance = 180.3(X) - 2.1 where x = 1/n and n = retinal/aorta vertical distance in cm.
   b) Heart rate = 3.4(X) + 53 where X = vertical carotid sinus/aorta distance in cm.

SHEET 1 OF 3

AUTHOR Burns, J. W. REF # 28

4. Note also heart rate response to acceleration on attached data sheet.

5. 30^{0} tilt back affords little protection in itself-author suggest the reason is that retinal/aorta distance does not change much over first 17^{0} (29.7 cm@13^{0} and 29.6 cm @ 30^{0}).

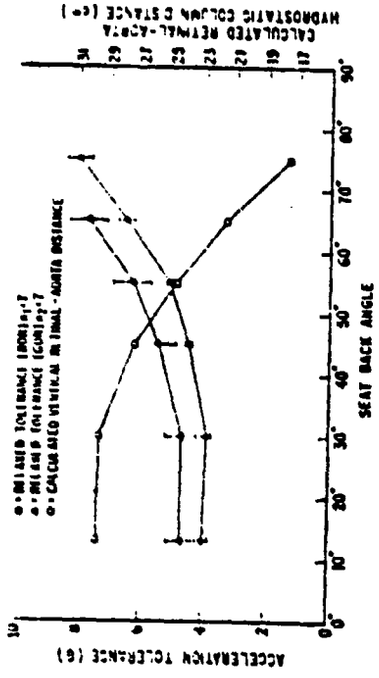


Fig. 1. Relationship between relaxed acceleration tolerance, calculated retinal-aorta hydrostatic column distance, and seat back angle. ROR = rapid onset rate of acceleration. GOR = gradual onset rate of acceleration. N_2 contains three subjects also included in N_1

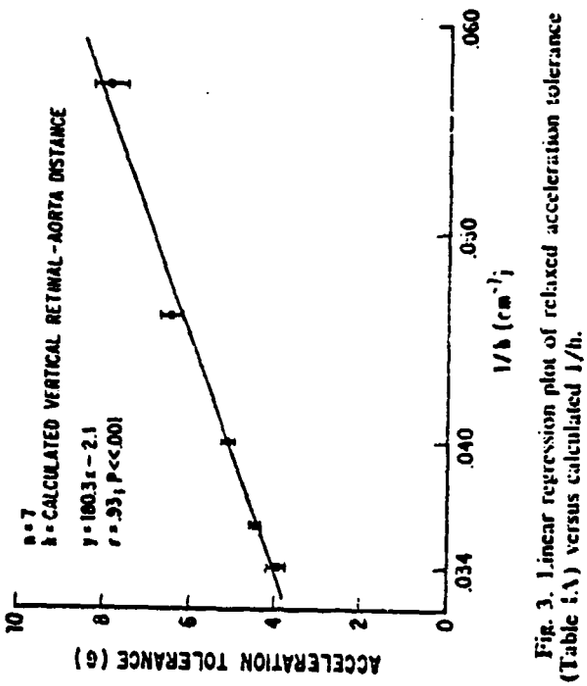


Fig. 3. Linear regression plot of relaxed acceleration tolerance (Table 1.1) versus calculated 1/h.

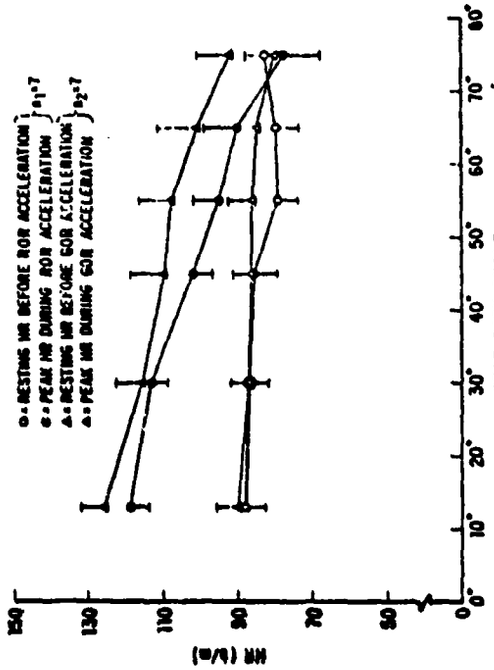


Fig. 2. Relationship between heart rate (HR) and seat back angle before and during rapid and gradual onset acceleration. N_2 = same as Fig. 1.

SHEET 2 OF 3

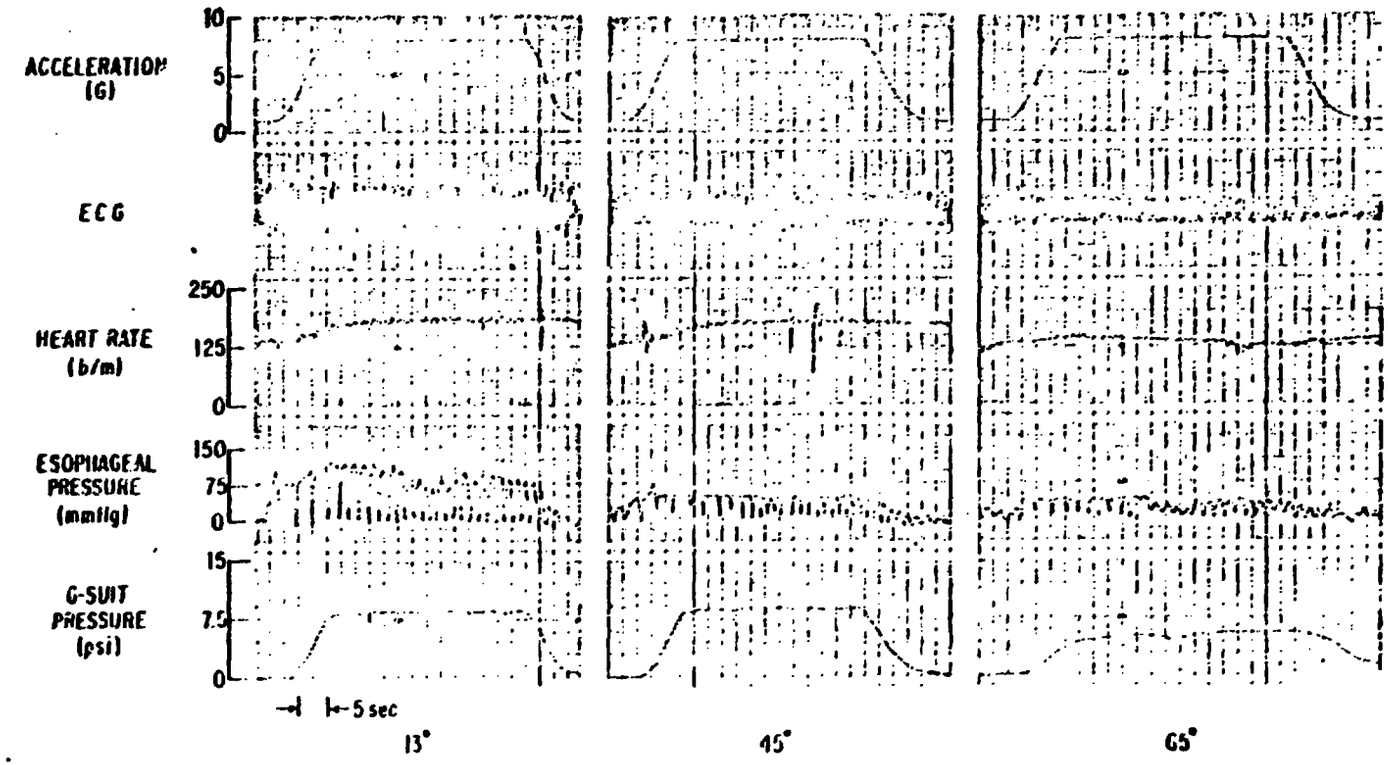


Fig. 4. Representative data from subject exposed to an 8 G acceleration profile at 13°, 45°, and 65°. G-suit pressure was manually adjusted to a lower level before the 65° run.

TITLE:
Head Movement Induced by Angular Oscillation of the Body in the Pitch and Roll Axis.

REF.: 202
HG- 57
DATE:

LEAD AUTHOR:
Barnes, G. R.

HUMANS -
ANIMALS -

ABSTRACT

The transmission of angular acceleration to the head of the human subject has been investigated during sinusoidal angular oscilation of the body in either pitch or roll about an axis through the upper lumbar vertebrae. The results indicated that angular acceleration of the skull was induced in all three axes of the head by both pitch and by roll motion. At frequencies below 1-2 Hz the head moved with the body, but in the frequency range 2-s Hz the amplitude of head acceleration was augmented indicating that oscilation about a center of rotation low in the body may induce large angular movements in this frequency range because of the linear component of acceleration delivered at the cervical vertebrae. At higher frequencies, the acceleration at the head was attenuated with an associated increase in phase lag, probably due to the absorption of input acceleration by the upper torso.

PHYSIOLOGICAL CATEGORY
- AUDITORY
- X BIOMECHNL
- CARDIOVSCL
- FORCE
- GENERAL
- LABYRINTH
- MAN.CNTRL
- PROTECTIVE
- REVIEW
- RESPIRAT'N
- X SIMULATION
- X VISUAL
- OTHER

AUGMENTATION DEVICES
- XHELMET
- STRAPS
- AURAL
- EXTREMITY
- LBNP
- XVISUAL
- RESPIRATORY
- LACRIMATION
- TEMPERATURE
- MASK

RELEVANCE

Helmet/head
Visual
Seat shaker systems

SALIENT DATA

1. "One of the more important problems associated with head and body motion is the ability to maintain visual fixation. During head movement, the vestibular system is stimulated and reflex compensatory eye movements are generated which enable the subject to fixate objects fixed in space; this reflex provides effective eye stabilization at frequencies up to 6-8 Hz (3) The present experiment suggests that motion of the head at higher frequencies may be present if the body is firmly harnessed, which would result in impairment of visual acuity. Conversely, in situations where the object to be fixated is also moving with the subject, the reflex eye movements are inappropriate and must be suppressed in order to maintain visual acuity. The results of a recent experiment (1) have indicated that suppression was grossly impaired at frequencies greater than about 1-2 Hz. The results of the present experiment indicate that the angular acceleration

transmission consequent upon either linear or angular acceleration of the body in the pitch and roll axes is maximal between 2 and 8 Hz. It is, therefore, to be expected that vision will be greatly impaired in this frequency range. The practical situation which corresponds to this experimental condition is that where the pilot of an aircraft attempts to fixate objects within the cockpit when both man and aircraft are being vibrated at the same frequency. In conditions of severe turbulence the predominant frequency band of aircraft vibration is likely to include the specific range of action of the vestibulo-ocular reflex. In such conditions, it has often been reported by pilots that the instruments appear to move and vision is impaired. The other area in which this point of particular interest is in the use of helmet mounted displays and target acquisition systems. For the effective use of such systems, it is necessary to eliminate eye movement relative to the skull. This is not possible if movement of the head induces the reflex eye movements which cannot be suppressed."

2. Frequency response data is presented for head motion in the three rotational degrees of freedom for stimulation of the body in pitch & roll. The stimulation was oscillatory foram 0.5 Hz - 20 Hz.

3. Paper points out that the body/head response is that of a second order system ($W \leq 9$ Hz)

4. Frequency and Laplace domain models are presented.

TITLE:

Heart Pathology Associated with Exposure to High Sustained +Gz.

REF.# 166

HG- 58

DATE:

LEAD AUTHOR:

Burton, R. R.

HUMANS - ANIMALS -

The pathology of +Gz acceleration was examined using unanesthetized adult miniature and immature "farm-type" swine, with and without anti-g suit inflation. Following single exposures of +8 or 9 Gz for 45 to 90 s - acceleration exposures that have been shown "tolerable" to man-swine were sacrificed and a detailed necropsy performed. Considering only the adult miniature swine, the endocardial area of the left ventricles showed evidence grossly of recent hemorrhage of varying severity involving both the wall and papilary muscles. The degree of location of the subendocardial hemorrhage were quantitated by grading the area of ventricle involved-1 (sight) to 4 (extensive). Of the 23 adult miniature pigs autopsied, the scores for papilary muscle hemorrhage, after one exposure to +9 Gz (45 to 90 s) ranged from a mean of 2.3 to 3.3 and the extent of ventricular wall involement was 2.5 to 3.3. Histologically, heart hemorrhage was limited to the subendocardial area, primarily involving the space between heart muscle and the endocardium and was particularly evident surrounding Parkiaje's fibers. Similar studies using immature farm-type swine (not miniature pigs) found these younger swine (4 to 5 months of age) to be less susceptible to such endocardial hemorrhage. Heart tissue recovery in these pigs following one exposure to +9 Gz for 45 s required approximately 14 [illegible]. It appears that this lesson is similar, although less severe, than heart muscle lesions associated with low blood volume (hemorrhagic shock) studies and may have similar physiologic bases. It was concluded that particular attention should be made of the endocardium of victims of high-performance aircraft accidents.

Not relevant to the Hi-G simulation problem.

Paper is mainly concerned with pathological effects of the high G environment on the heart.

PHYSIOLOGICAL CATEGORY
- AUDITORY
- BIOMECHNL
- XCARDIOVSCL
- FORCE
- GENERAL
- LABYRINTH
- MAN.CNTRL
- PROTECTIVE
- REVIEW
- RESPIRAT'N
- SIMULATION
- VISUAL
- OTHER

AUGMENTATION DEVICES
- HELMET
- STRAPS
- AURAL
- EXTREMITY
- LBNP
- VISUAL
- RESPIRATORY
- LACRIMATION
- TEMPERATURE
- MASK

SHEET 1 OF 1

ABSTRACT

RELEVANCE

SALIENT DATA

TITLE:

A Model Describing the Response of the Circulatory System to Acceleration Stress.

REF.# 96

HG-59

DATE:

LEAD AUTHOR:

Green, J. F.

HUMANS - X
ANIMALS -

ABSTRACT

A mathematical model of the circulatory system based on the principles of venous return is described and applied to the condition of acceleration stress. The model consists of two single compartments representing the pulmonary and systemic portions of the circulatory system. During periods of acceleration stress, the pressure in the systemic compartment, which is the upstream driving pressure for venous return, is decreased relative to the pressure at the right atrium due solely to hydrostatic effects. This decreased driving pressure causes a diminished venous return which is reflected in reduced cardiac output and arterial pressure without any changes in arterial resistance. Pressures at other points in the arterial tree, e.g. at eye-level, are related to the arterial pressure at the aortic root by hydrostatic effects.

These concepts are incorporated into equations which are used in an analog computer simulation, the results of which are shown both for a passive system and an active controlled system. The latter responds to changes in arterial pressure by altering the driving pressure for venous return by means of a change in systemic compliance. The results of this study are compared to experimental tracings obtained from dogs undergoing acceleration stress and discussed in relation to their implications for blood volume shifts and human responses.

PHYSIOLOGICAL CATEGORY
- AUDITORY
- BIOMECHNL
- CARDIOVSCL
- FORCE
- GENERAL
- LABYRINTH
- MAN.CNTRL
- PROTECTIVE
- REVIEW
- RESPIRAT'N
- SIMULATION
- VISUAL
- OTHER

AUGMENTATION DEVICES
- HELMET
- STRAPS
- AURAL
- EXTREMITY
- LBNP
- VISUAL
- RESPIRATORY
- LACRIMATION
- TEMPERATURE
- MASK

RELEVANCE

Cardiovascular, LBNP, visual

SALIENT DATA

Short duration accelerations produce initial drop in cardiac output with a concomitant drop in B.P. followe by recovery toward or above normal. Model assumes 1) rigid blood vessels 2) treats vascular system as pulmonary and systemic "compartments" with compliance parameters associated with each 3) arterial resistance, venous resistance and total compliance are represented by a single parameter the eye level blood pressure is modeled as

Pae = Pa - 0.736e ghe where Pa is the mean aortic root pressure. Model was verified using measured parameters in a dog as reported by Guyton(1963)

SHEET 1 OF 1

TITLE: Psychomotor & Physiologic changes during Acceleration.

REF.# 161

HG- 60

DATE:

LEAD AUTHOR: Little, V. Z.

HUMANS - X
ANIMALS -

ABSTRACT

Nine men were studied for physiologic and psychomotor changes during +5 Gz, +7 Gz, and +9 Gz. Each subject participated in three runs at one G level during a single session and underwent 3 such sessions, each at a different G level.
Acceleration stress resulted in a decrement of performance, with the degree of decrement dependent on the level of acceleration.
Heart rate also increased significantly as a function of the level of acceleration.
An increase in systolic blood pressure was dependent only on acceleration stress, without regard for the level of acceleration. From psychometer and physiologic data considered simultaneously, it appears that: (1) performance decrement resulted from specific factors rather than physiologic insult; (2) there was a heightened level of physiologic response to higher levels of acceleration; and (3) the physiologic responses were within tolerable limits, and clearly short of any objective medical or operational end-point.

PHYSIOLOGICAL CATEGORY
- AUDITORY
- X BIOMECHNL
- X CARDIOVSCL
- FORCE
- GENERAL
- LABYRINTH
- MAN.CNTRL
- PROTECTIVE
- REVIEW
- X RESPIRAT'N
- SIMULATION
- VISUAL
- OTHER

AUGMENTATION DEVICES
- HELMET
- STRAPS
- AURAL
- X EXTREMITY
- X LBNP
- X VISUAL
- X RESPIRATORY
- LACRIMATION
- TEMPERATURE
- MASK

RELEVANCE

1. Data presented from tests run on the SAM centrifuge at Gz = 5,7, & 9. Data on heart rate, systolic BP and heart arrhythmias. Also presented are mean scores for a psychomotor task at all three acceleration levels. The psychomotor data does not appear to be relevant to our study.

2. Relevant to underlying argument for High G augmentation devices (As mitagrated by Gx data rather than Gz data).

3. Relevant to cardiovascular effects, extremities, tidal respiration.

SALIENT DATA

1. The heart rate data means are:

	5g	7g	9g	
pre	80.4	86.1	89.0	B/mi
onset	88.4	93.2	97.6	
Peak	91.0	98.4	105.6	
Brake	96.0	101.5	110.8	

SHEET 1 OF 2

Post	87.1	90.2	96.6
Max	96.0	101.5	110.8
Peak Max	94.4	100.9	109.6

2. The period of peak acceleration was 90 sec "Respiration, which directly affects BP is one of the first physiological factors influenced by transverse acceleration". Performance was degraded by limb loading & stress.

3. Heart rate habituation occurred by runs 2 and 3, (?)

4. Authors relate a 10-15% degradation in tracking performance as a function of Gx ranging in 5-9 g region. Although this is along x axis and A/C g might not be this high the data forms some substantiation for attempting to recreate symptoms in simulation.

5. Authors report little degradation (further) as a function in time under acceleration and hypothesize limb loading fatigue is compensated by adaptation to g stress.

6. Heartbeat f of g level data given

7. "Respiration...is one of the first physiological factors influenced by transverse acceleration".

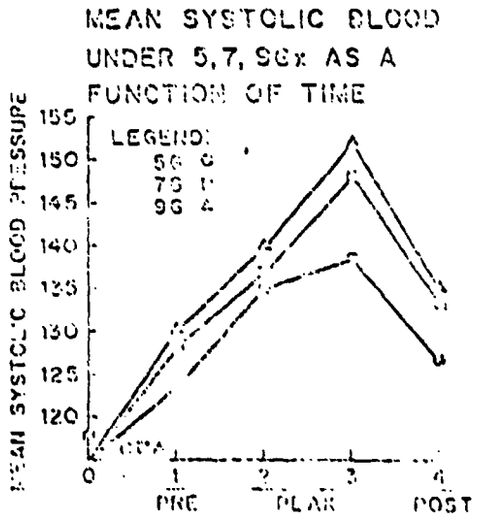


Fig. 6. Graphic summary of systolic blood pressure (mean of 15 second intervals, subjects pooled) for each of the three acceleration levels.

SHEET 2 OF 2

TITLE: Changes in Mesenteric Renal and Aortic Flows with $+G_x$ Acceleration

REF.# 236

HG- 61

DATE:

LEAD AUTHOR: Stone, H. L.

HUMANS -
X ANIMALS -

ABSTRACT

Previous studies in man and dogs have indicated that the splanchnic bed might contribute to the maintenance of arterial pressure during +Gx acceleration. Eight mongrel dogs were chronically instrumented with Doppler flow probes around the superior mesenteric (SMA) and renal arteries (RA) as well as the terminal aorta (TA). A solid-state pressure transducer was placed in the aorta distal to the flow probe. Using alpha-chloralose anesthesia following a 2-4 week recovery period, the animals were subjected to 120 s at levels of 5, 10 and 15 + Gx acceleration on a 7.6 m radius centrifuge. Roentgenograms and angiograms were taken in instrumented control animals during the study. Significant decreases in flow were found in the SMA of 69% and 37% at 10 and 15 + Gx, RA of 34% at 15 + Gx, while the TA only declined significantly at 15 + Gx. Angiograms indicate that there is a mechanical component to the reduction in flow in the abdomen in both instrumented and uninstrumented animals. The results indicate that both an active component and the mechanical component contribute to the maintenance of arterial pressure during +Gx, acceleration. A scheme is presented to explain the results from these and other studies.

PHYSIOLOGICAL CATEGORY
- AUDITORY
- BIOMECHNL
- X CARDIOVSCL
- FORCE
- GENERAL
- LABYRINTH
- MAN.CNTRL
- PROTECTIVE
- REVIEW
- X RESPIRAT'N
- SIMULATION
- VISUAL
- OTHER

AUGMENTATION DEVICES
- HELMET
- STRAPS
- AURAL
- EXTREMITY
- LBNP
- VISUAL
- X RESPIRATORY
- LACRIMATION
- TEMPERATURE
- MASK

RELEVANCE

. . . . . .

Cardiovascular, Respiration

SALIENT DATA

Heart rate decreased at 10 and 15Gx, at 5 Gx it remained constant. BP increased (aortic) at all three levels. There is an increase in peripheral vascular resistance. Authors state increases due to displacement of vessels have been observed. Also they postulate vasoconstriction due to the reflex increase in the nervous system.

Note the attached figure for schematic representation.

Also attached are sample data plots.

SHEET 1 OF 3

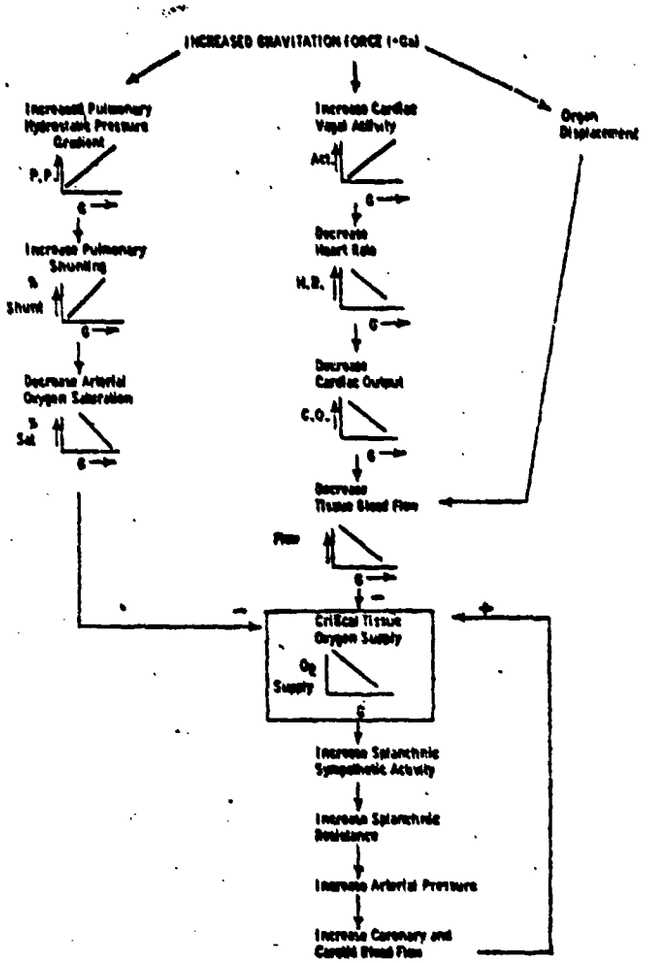


Fig. 8. Schematic representation of the known and possible effects of $+G_z$ acceleration.

SHEET 2 OF 3

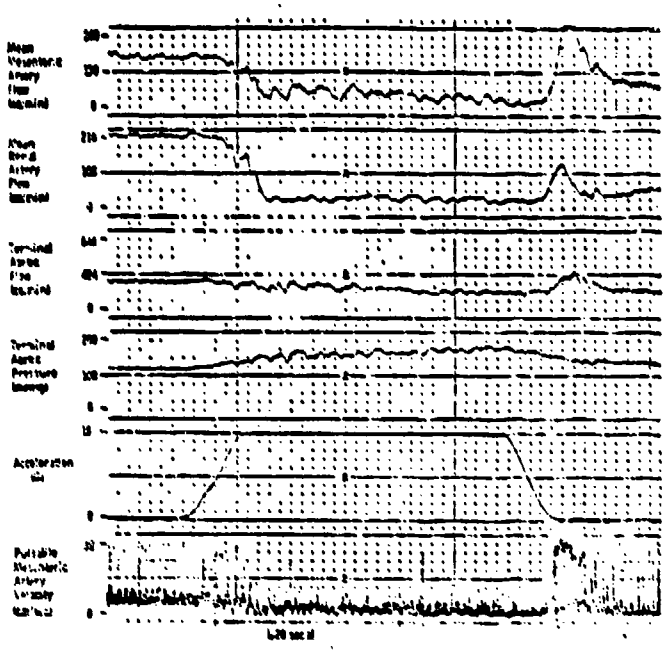


Fig. 1. Record of mean mesenteric, renal, and terminal aortic flows before and during exposure to 15 $+G_z$ for 2 min. Pulsatile mesenteric artery flow is shown at the bottom of the figure. The level of $+G_z$ acceleration is also given in the record.

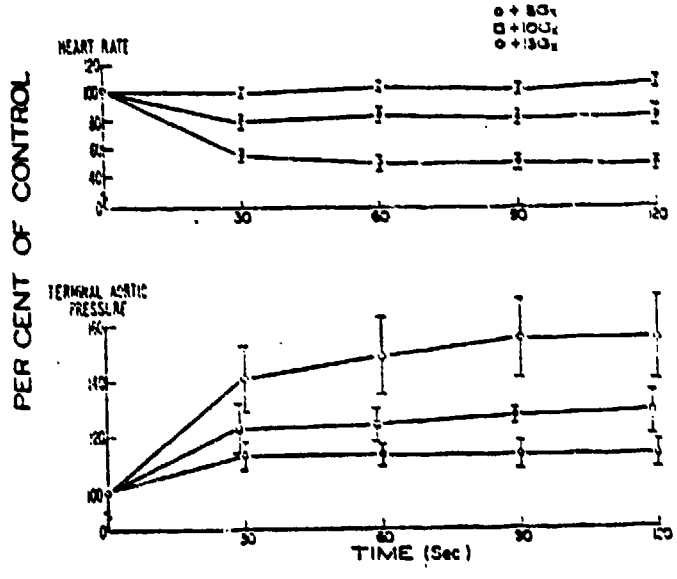


Fig. 2. Changes in heart rate and terminal aortic pressure as percent of control values at 30, 60, 90, and 120 s after reaching the peak acceleration levels listed. The bars through the points represent 1 S.E.M.

SHEET 3 OF 3

TITLE: Physiology of the Eye, Chapter 9-The Ocular Circulation.

REF.# 1

HG- 62

DATE:

LEAD AUTHOR: Adler, F. H.

HUMANS - X
ANIMALS -

ABSTRACT

No abstract is available at this time.

Good discussion of ocular circulation and intraocular pressure, and lacrimation.

RELEVANCE

1. Diagram-fig 93 (pg 307) & 98(pg 315) retinal & uveal circulation fig 99 (pg 316) fall in blood pressure.

2. "Under normal circumstances a pressure of 25mm Hg is required to overcome the force of gravity in order to raise blood from the heart to the head level, ie., a distance of 0.3M with a specific gravity of 4 (4g turn) the pressure required would be about 100 mm Hg. Assuming that the normal intraocular pressure is approximately 20 mm. Hg, it is evident that the blood flow will cease under these conditions. Blackout generally occurs with a force of 4G's after an exposure of 3 sec."

3. "Lacrimal fluid is a combination of the fluid secreted by the lacrimal gland and that secreted by mucus cells and an oily substance secreted by the meibomian glands."

4. The lacrimal gland is innervated by the lacrimal, the facial, and the cervical sympathetic nerves. The best evidence now indicates that the lacrimal nerve is not concerned in any way with secretory function but is purely the afferent pathway for the reflex arc.

5. Reflex lacrimation is easily produced by stimulation of the fifth and olfactory nerves. Any irritation of the endings of the fifth nerve, particularly those which supply the eye, result in tearing from strong odor, particularly that from onions.

SALIENT DATA

PHYSIOLOGICAL CATEGORY
- AUDITORY
- BIOMECHNL
- X CARDIOVSCL
- FORCE
- GENERAL
- LABYRINTH
- X MAN.CNTRL
- PROTECTIVE
- REVIEW
- X RESPIRAT'N
- X SIMULATION
- VISUAL
- OTHER

AUGMENTATION DEVICES
- HELMET
- STRAPS
- AURAL
- X EXTREMITY
- X LBNP
- VISUAL
- X RESPIRATORY
- LACRIMATION
- TEMPERATURE
- MASK

SHEET 1 OF 1

TITLE: Visual Field Contraction during G Stress at 13°; 45°; and 65° Seatback Angles.

REF. # 87

HC- 65

DATE:

LEAD AUTHOR: Gillingham, K. K.

HUMANS - X
ANIMALS -

ABSTRACT

In support of the High Acceleration Cockpit program, two groups of six experienced subjects, operating a high-resolution visual field limit tracker, were exposed to gradual-onset (0.067 G/s) G stress to a 7-G maximum on the USAFSAM human centrifuge. Data obtained from one group described the G-induced vertical visual field contraction, and that from the other described horizontal visual field contraction-as they occurred in relaxed subjects in seats 13°, 45°, and 65° seatback angles. Curves of peripheral vision remaining vs. G level indicated a statistically significant difference in tolerance provided by the 65° seat over that provided by the 13° and 45° seats in the 5- to 7-G range, and a significant difference in tolerance provided by the 45 and 65 seats over that provided by the 13° seat in the 4- to 5-G range. Two-dimensional reconstruction of the superior half of mean binocular vision remaining at the various levels of G stress showed complete visual loss near 5 G in the 13° seat, complete loss near 6 G in the 45° seat, and substantial peripheral vision remaining at 7 G in the 65° seat.

PHYSIOLOGICAL CATEGORY
- AUDITORY
- BIOMECHNL
- CARDIOVSCL
- FORCE
- GENERAL
- LABYRINTH
- MAN.CNTRL
- PROTECTIVE
- REVIEW
- RESPIRAT'N
- SIMULATION
- X VISUAL
- OTHER

AUGMENTATION DEVICES
- HELMET
- STRAPS
- AURAL
- EXTREMITY
- LBNP
- X VISUAL
- RESPIRATORY
- LACRIMATION
- TEMPERATURE
- MASK

RELEVANCE

Pertinant to complete visual area. Contains data showing time and Gz dependancy of visual field (peripheal) collapse for GOR runs-some strip chart recordings covering peripheral field collapse under ACM maneuvers containing ROR.

SALIENT DATA

1. Field determined by observation of white lights with brightness approximately 4-5 mili lamberts.
2. Flashing lights have lower threshold than steady lights. Under complete peripheral vision loss, indistinct flashing lights can sometimes be seen in peripheral area.
3. Visual field collapse appears to be more rapid along vertical FOV axis than along horizontal FOV axis.
4. 65° seat back angle obviously superior in retarding FOV collapse.

SHEET 1 OF 4

5. Although data is given in terms of "peripheral vision" it seems to include the "central FOV" as well.

6. The data acts much like a 2^{4r} order lag applied to a flip flop whose threshold is a specific G level:

Horizontal FOV	Threshold	Rise Time	Vertical FOV	Threshold	Rise Time
13^0 seat -	3 g	30 sec	13^0 seat -	2.5G	- 20 sec
45^0 seat	3.5 g	25 sec	45^0 seat	2.5G	- 30 sec
65^0 seat	5 g	N/A	65^0 seat	3 G	- 45 sec

This data based on GOR runs ~ .067 G/sec and although the thresholds seem to stay constant in moving to a ROR run the rise times reduce significantly under ROR - the same flip nature seems to exist in ROR.

7. The paper reports the relationship of peripheral vision remaining (field of view) vs G force for different seat back angles. See Fig 3, 4, and 7.

8. The study used no anti-G devices & the test subjects were relaxed (no M-1)
Also small dg/dt = .067 G/S

9. T-test were also computed to insure statictical significant of the information of each angle (fig 5 & 6).

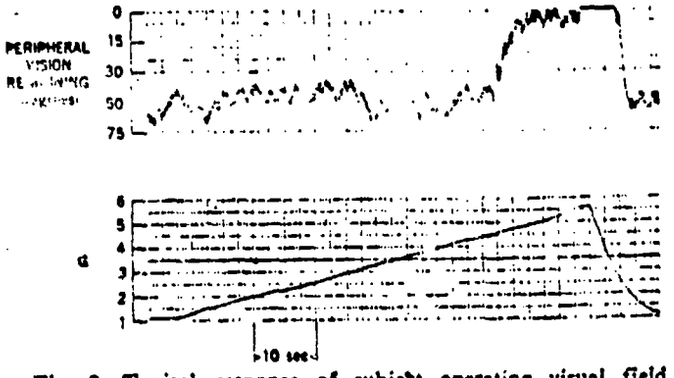


Fig. 2. Typical response of subject operating visual field limit tracker (upper vertical meridian; 45° seat).

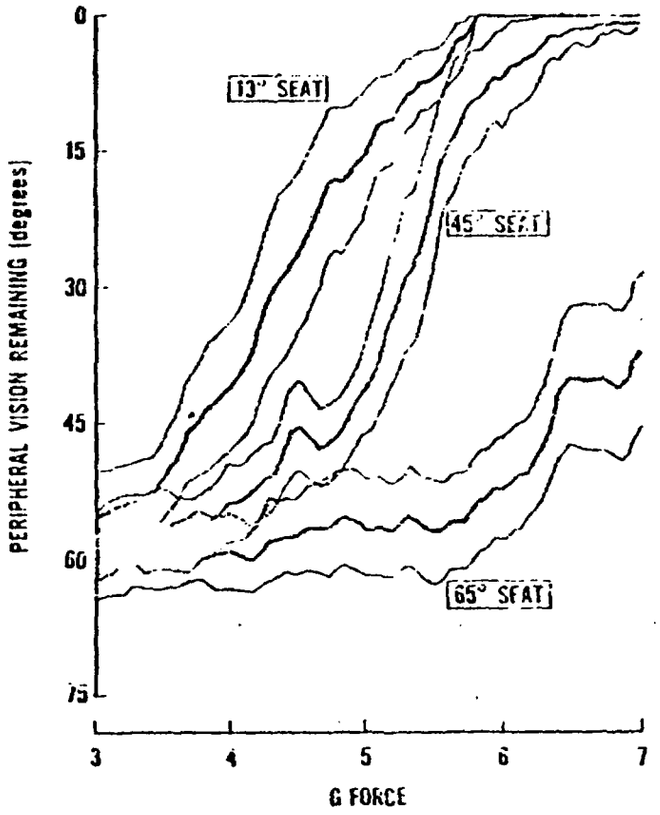


Fig. 3. Mean horizontal visual field remaining ± 1 S.E.M. (shaded) as a function of G level, during gradual-onset centrifuge runs of six relaxed, unprotected subjects at 13°, 45°, and 65° seatback angles.

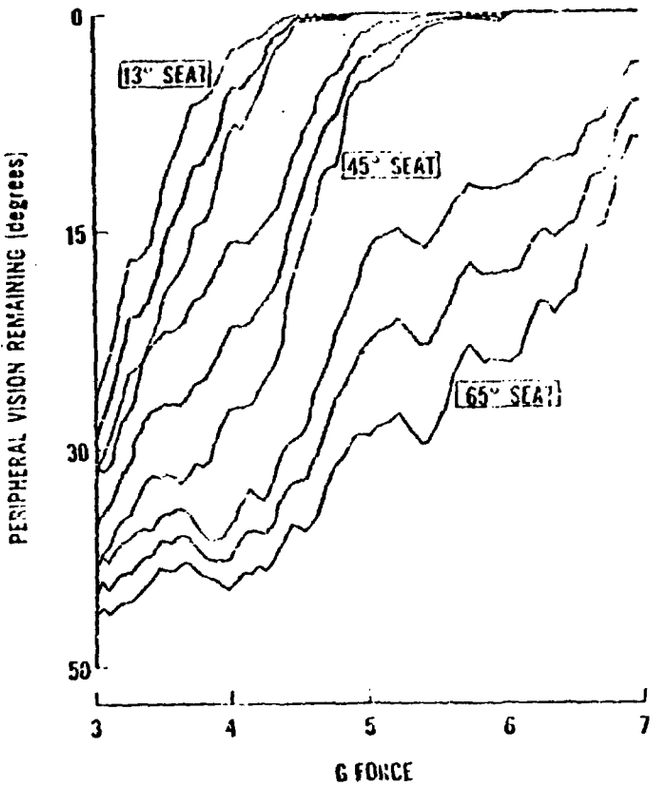


Fig. 4. Mean vertical visual field remaining as a function of G level, under conditions as in Fig. 3.

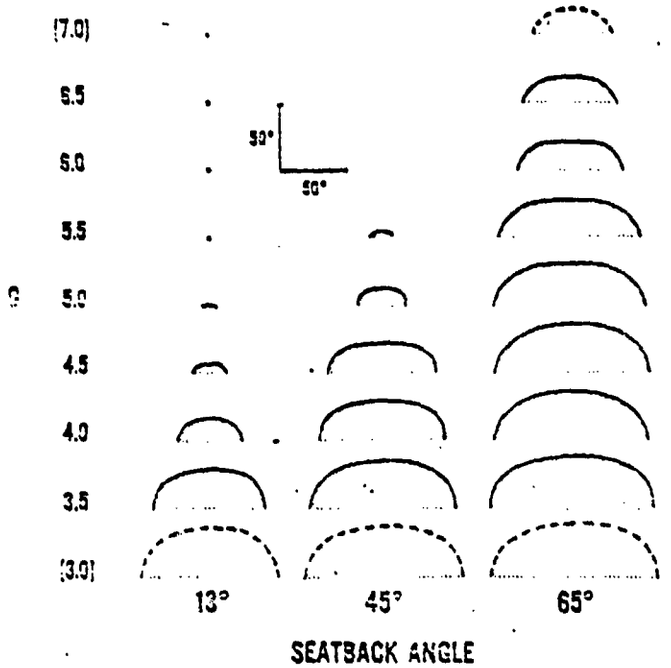
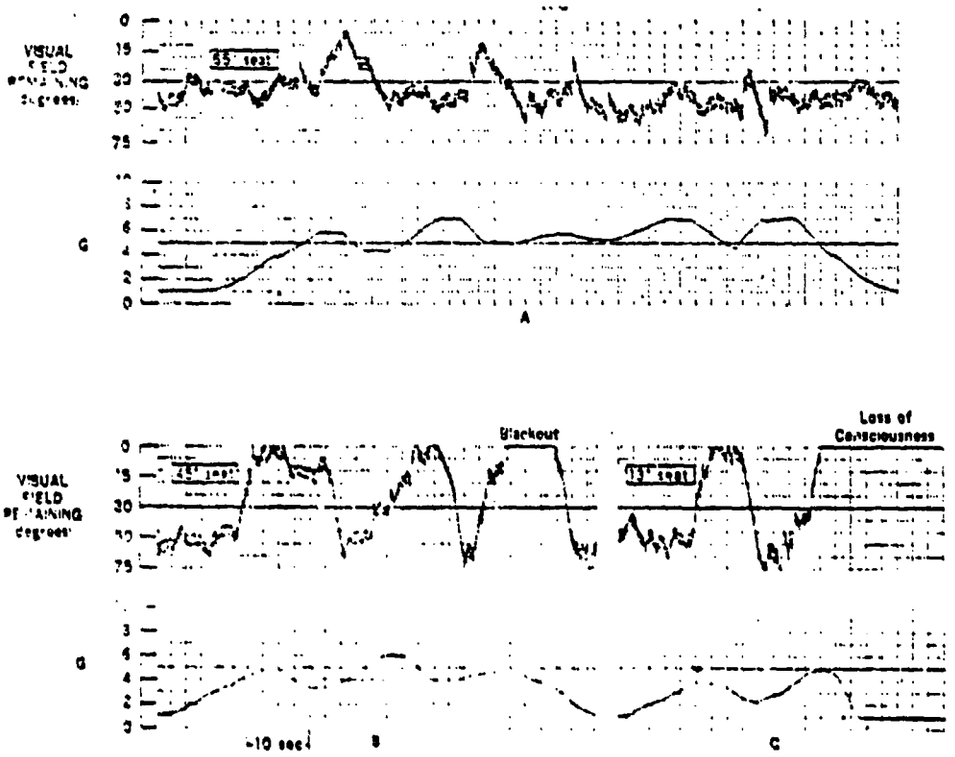


Fig. 7. Reconstructed upper halves of mean visual fields of relaxed subjects exposed to indicated G levels at 13°, 45°, and 65° seatback angles.

Fig. 8. Responses of subject G.M. operating visual field limit tracker in vertical mode during simulated ACM G stress at 65°, 45°, and 13° seatback angles. At 65°, subject tolerated 7-G peaks with little visual loss; at 45°, he blacked out after a 6-G peak; at 13°, he lost consciousness during a 5-G peak.



SHEET 4 OF 4

TITLE:

Experimental Blackout and the Visual System

REF. # 62

HG- 67

DATE:

LEAD AUTHOR:

Duane, T. D., Dr.

HUMANS - X
ANIMALS -

ABSTRACT

No abstract is available at this tim

---

1. A very complete collection of experimentation and interpretation into the blackout effect.
2. Visual System physiological section.
3. Visor system
4. Visual display dimming
5. Instrument dimming
5. Audition.
7. Lacrimation.

RELEVANCE

1. In blackout subject "sees blackness" (pg. 948).
2. Blackout refers to the total loss of vision to ambient light including that of an ophthalmoscope. (pg 950).
3. Unconciousness in 1.28 sec at 8-15 Gz. Unconciousness defined as failure to respond to auditory and visual stimulus. (pg 951)
4. In blackout subject still responds to auditory and tactile stimuli (pg 948)
5. Dimming, then complete loss of peripheral lights - retinal arteriolar blood became slightly darker and entire arteriolar tree began rhythmically opening and collapsing..but not serpentine type seen in aortic regurgitation..venous system unchanged. Then complete light loss (CLL)-arterioles noted to cease their pulsations and became completely exsanguinated.. veins remain unchanged. Then, within 1 second of removal of peak G-arterial tree began above type rhythmical pulsations with tremendous surge of blood into venous system and subsequent ballooning of venules lasting 2-3 beats. The arterioles stopped pulsing and were normal. Vison returns within 3 sec of G

SALIENT DATA

PHYSIOLOGICAL CATEGORY

- X AUDITORY
- BIOMECHNL
- X CARDIOVSCL
- FORCE
- GENERAL
- LABYRINTH
- MAN.CNTRL
- PROTECTIVE
- REVIEW
- RESPIRAT'N
- SIMULATION
- X VISUAL
- OTHER

AUGMENTATION DEVICES

- HELMET
- STRAPS
- X AURAL
- EXTREMITY
- LBNP
- X VISUAL
- RESPIRATORY
- X LACRIMATION
- TEMPERATURE
- MASK

SHEET 1 OF 2

removal.

6. Transverse acceleration +Gz (of 6-8 G) tear film appeared in upper temporal area and spread across cornea...ascribe to a pooling of the normal tears. (pg 953)

7. Developed successful plethysmographic goggle (pg 954)-no comment of X axis distortion in using the goggle.

8. Blackout occurs not due dysfunction of higner visual pathways (pg 956) (then solely in the retina?)

9. Retinal field asymetric about central disk with more area located temporally & no arterial compensation for this increased area nasal field of view (temporal retina) first to suffer vision loss. (pg 959) - 50% more area temporally.

10. Ophthalmodynamometry & +Gz acceleration produce exact same things. (pg 960)

11. Central acuity remains even with major constriction of peripheral FOV (pg 959)

TITLE: Visual Field Changes During Positive Acceleration

REF. #127

HG- 69

DATE:

LEAD AUTHOR: Jaeger, E. A.

HUMANS - X
ANIMALS -

ABSTRACT

The monocular pattern of visual field closure is the same whether due to ophthalmodynamometry, positive acceleration or a combination of both. It consists of an initial selective nasal field defect, which approaches a hemianopic character before marked temporal field loss begins. The last remaining visual field is not at fixation but is confined to an island located temporally between fixation and the blind spot. It is felt that this pattern is best explained by the anatomic arrangement of the retinal arteriolar system. plethysmographic goggle type ophthalmodynamometer is described which has been adapted to assist in visual field studies on the centrifuge.

---

visual

RELEVANCE

1. A comparison of the monocular pattern of visual field closure due to acceleration ophthalmodynamometry or a combination of both was made. The ophthalmodynamometry was effected with plethsmographic goggles. Plots are presented which illustrate the geometry of the closure.

2. It is int esting to note that the last remaining island of vision is not the fixation point but a point between the fixation point and the blind spot. Left eye plots are presented.

3. Lights were not used for this experiment but rather a large poster with the alphabet printed (letters 1.5 cm high & 1.5 cm apart).

SALIENT DATA

PHYSIOLOGICAL CATEGORY
- AUDITORY
- BIOMECHNL
- CARDIOVSCL
- FORCE
- GENERAL
- LABYRINTH
- MAN.CNTRL
- PROTECTIVE
- REVIEW
- RESPIRAT'N
- SIMULATION
- X VISUAL
- OTHER

AUGMENTATION DEVICES
- HELMET
- STRAPS
- AURAL
- EXTREMITY
- LBNP
- X VISUAL
- RESPIRATORY
- LACRIMATION
- TEMPERATURE
- MASK

SHEET 1 OF 1

TITLE: Applications of Liquid Crystals

REF. #166

HG- 73

DATE:

LEAD AUTHOR: Meier, G.

HUMANS - X
ANIMALS -

ABSTRACT

Not available at this time

. . . . . .

Varible Transmittance Visor

Textbook on Liquid Crystal Applications

(1) AC excitation preferred to DC for purposes of extending life time by preventing electrolytic action which reduces contrast. Nematic esters of seniff bases display 5000 hrs. life under A.C. and only 500 hours under D.C. (pg. 115, 123)

(2) Colorizers (pg. 125-132) seem to require polarizers and assurance of white light source. Both conditions might present constraints when used with simulator visual systems.

(3) Matrixing (pg. 133) can produce crosstalk, however the crosstalk can be suppressed (pg. 136) by a technique called "two frequency addressing" wherein one of the two frequencies employed has an amplitude greater than the drive voltage and frequency higher than that required for domain formation and this signal acts as a suppressor.

RELEVANCE

SALIENT DATA

PHYSIOLOGICAL CATEGORY
- AUDITORY
- BIOMECHNL
- CARDIOVSCL
- FORCE
- GENERAL
- LABYRINTH
- MAN.CNTRL
- PROTECTIVE
- REVIEW
- RESPIRAT'N
- SIMULATION
- XVISUAL
- OTHER

AUGMENTATION DEVICES
- HELMET
- STRAPS
- AURAL
- EXTREMITY
- LBNP
- XVISUAL
- RESPIRATORY
- LACRIMATION
- TEMPERATURE
- MASK

SHEET 1 OF 4

2.8.2.1. Matrix Array Using Two-frequency Addressing

It was found [102] that the formation of Williams domains [103] and the dynamic scattering caused by d.c. or low frequency a.c. voltages can be suppressed by a superimposed a.c. voltage with an amplitude greater than that of the d.c. voltage and a frequency above the cutoff frequency f_c for domain formation (Fig. 42). Thus if a voltage $U_1 + U_2$ is applied to a matrix row, where U_1 is a d.c. or low frequency a.c. voltage greater than the threshold voltage U_{th} and U_2 is an a.c. voltage of suitable amplitude and frequency, and a voltage $-U_1 + U_2$ is applied to a column, scattering is only observed in the fully selected cell, which does not see the

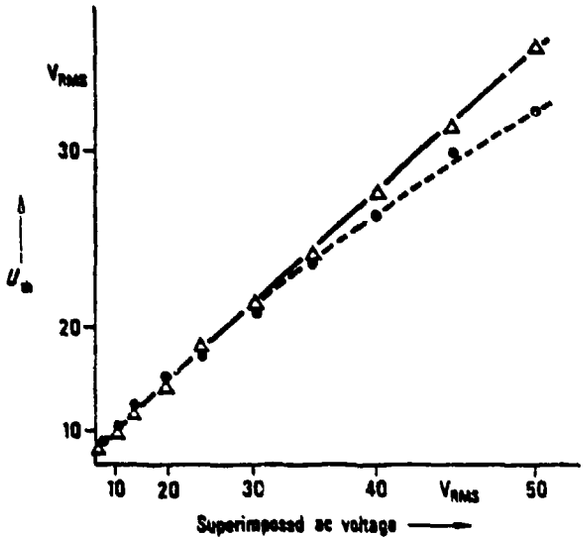


Figure 42. Dependence of the threshold voltage U_{th} for domain formation on the superimposed a.c. voltage (1.5 kHz), for d.c. (broken curve) and a.c. (50 Hz). (Quadratic scale for abscissa and ordinate). (After reference [102]).

suppressing signal and therefore scatters with an intensity corresponding to $2U_1$. A result obtained with a 3 × 7 matrix without crosstalking is shown in Fig. 43. In addition to the enhanced contrast, a turn-on time was observed at least three times faster than that under normal driving conditions. This means that in matrix-addressed liquid crystal light valve arrays, the number of rows can be increased by superimposing an a.c. electric field of sufficiently high frequency.

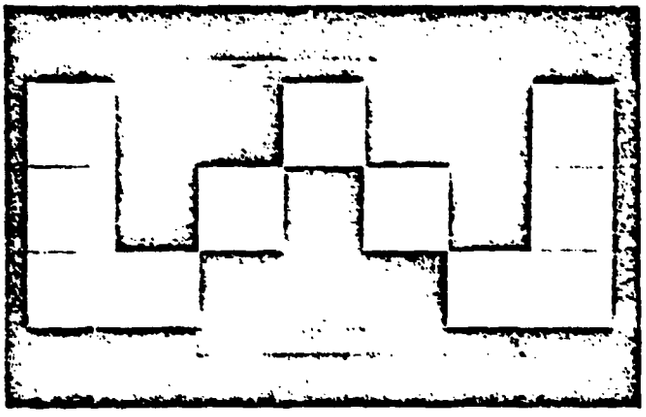


Figure 43 3 × 7 liquid crystal matrix array without crosstalking using two frequency-addressing (after reference [102]).

The matrix addressing scheme is shown in Fig. 44. The voltage across the selected cells X_1Y_2, X_3Y_2 and X_4Y_2 is $2U_1$. No voltage is applied to the unselected cells X_2Y_1 and X_2Y_3. The remaining cells shown in Fig. 44 are partially selected and subjected to a combined signal of U_1 and $2U_2$. The amplitude and frequency of U_2 are so chosen that the electrooptic effect caused by U_1 alone can be suppressed. The matrix is addressed column by column. After each scan the controller reverses the polarity of the applied d.c. voltages U_1 to avoid undesirable electrochemical reactions in the liquid crystal layer.

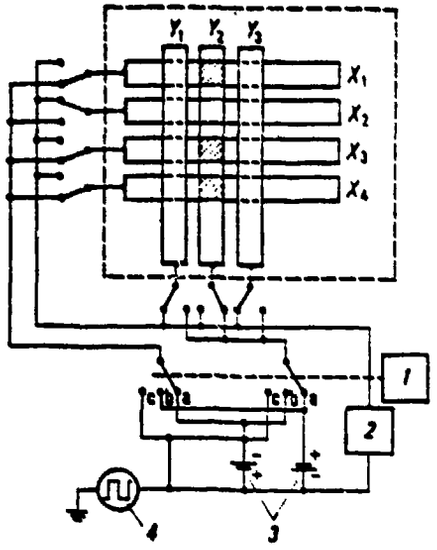


Figure 44. Matrix addressing scheme using two frequency addressing (after reference [102]).
X_{1-4} and Y_{1-3} Conductor path
1 Scan Controller
2 Phase shifter, $\Delta\gamma = 180°$
3 Batteries for voltage U_1
4 Oscillator for voltage U_2

102. Wild, P. J., Nehring, J.; Appl. Phys. Lett. 19, 335 (1971).

TITLE: Mechanical Impedance of the Sitting Human Under Sustained Acceleration

REF. # 247

HG- 75

DATE:

LEAD AUTHOR: Vogt, H. L.

HUMANS - X
ANIMALS -

ABSTRACT

Measurements of the mechanical impedance of the sitting human body under sustained acceleration were conducted to investigate the nonlinearity of the body system. A hydraulically driven shake table was installed on a centrifuge and the transmitted force and the acceleration of the platform, whereon the subjects were sitting, were recorded. The fundamental resonance of the body changes from 5 Hz to 7 Hz and 8 Hz under normal gravity (+1 Gz abs.), +2Gz and +3Gz respectively. The relative displacement of the effective body mass per oscillatory acceleration was reduced at resonance from 1.73 to 0.88 and 0.675 mm/g by these + Gz- loads. The static deflection of the human body follows the equation > = F/(34 +0.5F). The stiffness of the human body increases from 69 x 10^6 dyne/cm under normal gravity to 164 x 10 dyne/cm under +3 Gz, or generally: K=(34 + 0.5F) 10^6dyne/cm. Therefore a natural frequency of the human body of 3.5 Hz is resulting for zero gravity. This is in good agreement with previous measurements in supine position.

. . . . . .

RELEVANCE

Only very remotely relevant to head extremities

SALIENT DATA

1. A sustained acceleration stiffens the sitting human body in spinal direction and increases his fundamental natural frequency from 5 Hz to 7 Hz under +2 Gz and to 8 Hz under +3 Gz..
2. The second resonance at 10 Hz does not change significantly under sustained acceleration.
3. Though the changes of the third resonance at 15 Hz did not come out clearly it seems to go up to a higher frequency under +3 Gz.
4. In the very low frequency range the human body responds more and more as a pure mass, practically up to 5 Hz, under +3 Gz.
5. The effective mass of the basic subsystems does not change with increasing Gz-load.

PHYSIOLOGICAL CATEGORY
- AUDITORY
- X BIOMECHNL
- CARDIOVSCL
- FORCE
- GENERAL
- LABYRINTH
- MAN.CNTRL
- PROTECTIVE
- REVIEW
- RESPIRAT'N
- X SIMULATION
- VISUAL
- OTHER

AUGMENTATION DEVICES
- XHELMET
- XSTRAPS
- AURAL
- XEXTREMITY
- LBNP
- VISUAL
- RESPIRATORY
- LACRIMATION
- TEMPERATURE
- MASK

SHEET 1 OF 2

AUTHOR	Vogt, H. L.	REF # 247

6. The transmission factor decreases under + Gz-load in the low frequency range, especially for the 5 Hz resonance, but increases considerably in the frequency range above 6 Hz.

7. The damping coefficient of the erect sitting human remains unchanged at about 0.575 during + Gz.

8. Change in natural freq between sitting erect & sitting relaxed less than 1 hz Δ.

9. With increasing acceleration (sustained), vibration is felt less. Mass displacement is less (data & expression given).

TITLE: Pulsus Paradoxus: Effect of Gravity & Acceleration in its Production

REF.# 242

HG- 76

DATE:

LEAD AUTHOR: Urschel, C. W.

X HUMANS - ANIMALS -

ABSTRACT

Not available at this time

. . . . . .

RELEVANCE

Largely irrelevant to this study

SALIENT DATA

Pulsus Paradoxus (the alternate strengthening & weakening of each pulse beat) is caused by alternate increase and decrease in cardiac output with each respiration. Pulsus Paradoxus seems predominately due to phasic right ventricular output delayed by resistive and capacitive impedance of the lung.

PHYSIOLOGICAL CATEGORY
- AUDITORY
- BIOMECHNL
- X CARDIOVSCL
- FORCE
- GENERAL
- LABYRINTH
- MAN.CNTRL
- PROTECTIVE
- REVIEW
- X RESPIRAT'N
- SIMULATION
- VISUAL
- OTHER

AUGMENTATION DEVICES
- HELMET
- STRAPS
- AURAL
- EXTREMITY
- LBNP
- VISUAL
- X RESPIRATORY
- LACRIMATION
- TEMPERATURE
- MASK

SHEET 1 OF 1

TITLE: Effect of Sustained Muscular Contraction on Tolerance to + G_z Acceleration

REF. # 164

HG- 77

DATE:

LEAD AUTHOR: Lohrbauer, L. A.

HUMANS - X
ANIMALS -

ABSTRACT

The increase in +G, acceleration (the inertial force vector acting in a head-to-foot direction) tolerance afforded by static forearm muscular contraction (hardgrip) was evaluated and compared with that of the standard G suit. Acceleration tolerance was assessed in eight subjects in each of four conditions for both rapid onset (1.0 G/s and slow onset (0.1 G/s) acceleration profiles. The conditions were: 1) unprotected, 2) handgrip, 3) G suit, and 4) handgrip and G suit. The mean tolerance levels achieved for those four conditions for the rapid onset runs as defined by peripheral light loss were 3.6, 4.5, 4.8, and 5.4G, respectively. For the slow onset runs, the tolerance levels were 4.6, 5.6, 5.8 and 6.3G. Thus the handgrip and G-suit procedures each provided approximately 1 G of protection. Significantly, the effect of the two procedures combined proved to be additive. In the rapid on-set runs, the static contraction was begun 60-90s before the onset of acceleration and in the slow onset runs, the contraction was begun with the onset of acceleration. The protection provided by the static contraction is at least in part due to the increase in mean systemic blood pressure which accompanies any such contraction. This increase prolongs the time necessary for acceleration to result in a blood pressure below intraocular pressure, this latter being the time at which peripheral light loss occurs. Unlike during respiratory straining maneuvers, no increase in intrathoracic or intra-abdominal pressure occurred during handgrip exercise at 1G.

. . . . . .

RELEVANCE

Visual, LBNP, Protective Devices, Cardiovascular

SALIENT DATA

(1) Tolerance data is presented for both ROR (1g/sec) and GOR (0.1g/sec).

(2) Several protective devices were employed singly and in combination; Anti-G Suit, M1, Valsalva and straining (muscular). Effects of these devices were reported and compared.

(3) It should be noted that most of the data is presented as a continuum but are in reality a series of discrete measurements connected by straight line segments.

PHYSIOLOGICAL CATEGORY
- AUDITORY
- BIOMECHNL
- X CARDIOVSCL
- FORCE
- GENERAL
- LABYRINTH
- MAN.CNTRL
- X PROTECTIVE
- REVIEW
- RESPIRAT'N
- SIMULATION
- X VISUAL
- OTHER

AUGMENTATION DEVICES
- HELMET
- STRAPS
- AURAL
- EXTREMITY
- X LBNP
- X VISUAL
- RESPIRATORY
- LACRIMATION
- TEMPERATURE
- MASK

SHEET 1 OF 2

AUTHOR	Lonrbauer, L. A.	REF #164

4) The eye-level BP was recorded via a pressure transducer and a canulated radial artery held at eye level. (I submit that this may not accurately reflect eye level BP because the vascular dynamics differences are not considered).

SHEET 2 OF 2

TITLE: Effect of the Valsalva Maneuver on Tolerance to + Gz Acceleration

REF. # 224

HG-78

DATE:

LEAD AUTHOR: Shubrooks, S. J.

HUMANS - X
ANIMALS -

ABSTRACT

Systemic arterial pressure (Psa) response to the Valsalva maneuver and its effects on acceleration tolerance were studied in 10 healthy men during exposure to positive ($+G_z$) radial acceleration. For rapid onset (1 G/s) exposures of both 15s and 45s duration, large increases in $+G_z$ tolerance were found to occur during performance of a Valsalva maneuver accompanied by vigorous voluntary muscular tensing, either with or without use of an anti-G suit. This effect was seen with single prolonged (up to 15s) maneuvers as well as with repeated maneuvers. Systolic, diastolic, and pulse pressures were in all cases maintained at levels far greater than those which would have occurred during acceleration without the Valsalva; with repeated maneuvers Psa rose progressively, often to levels greater than control. These responses were shown to be equivalent to those accompanying the M-1 maneuver, the generally accepted means of increasing +G, tolerance. The increased intrathoracic pressure, whether produced by the Valsalva or the M-1, if combined with muscular tensing or use of an anti-G suit, resulted in an elevation of Psa and an increased tolerance even during sustained high $+G_z$ exposures.

. . . . . .

RELEVANCE

Cardiovascular response to Gz (eye level blood pressure and heart rate) with and without G Suits and using M-1 or Valsalva maneuver. Authors argue the case for acceptability of Valsalva maneuver.

SALIENT DATA

(1) Definitions:

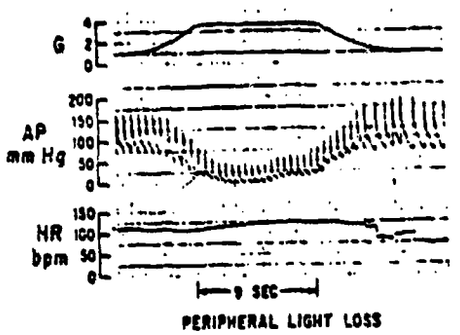
a) M1 Maneuver; repeated forceful exhalations against the partially closed glottis accompanied by vigorous tensing of the voluntary muculature, the exhalation being repeated every 4 or 5 seconds following rapid inhalations.

b) Valsalva Maneuver: maximally forceful exhalations against the completely closed glottis and is accompanied by tensing of the lower extremnity and abdominal musculature as is done during the M1 maneuver.

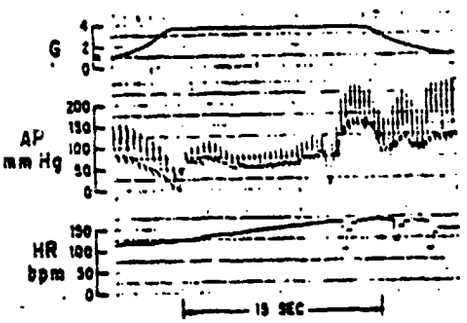
PHYSIOLOGICAL CATEGORY
- AUDITORY
- BIOMECHNL
- X CARDIOVSCL
- FORCE
- GENERAL
- LABYRINTH
- MAN.CNTRL
- X PROTECTIVE
- REVIEW
- RESPIRAT'N
- SIMULATION
- VISUAL
- OTHER

AUGMENTATION DEVICES
- HELMET
- STRAPS
- AURAL
- EXTREMITY
- X LBNP
- X VISUAL
- RESPIRATORY
- LACRIMATION
- TEMPERATURE
- MASK

SHEET 1 OF 4

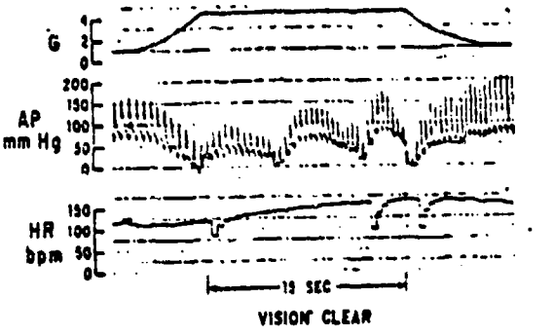


A. CONTROL 3.7 G

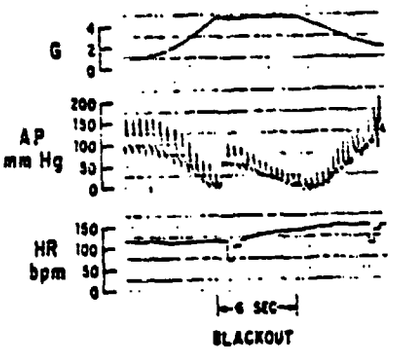


B. VALSALVA 3.7 G

FIG. 1. Arterial pressure (AP) and heart rate (HR) response to the Valsalva maneuver with voluntary muscular straining without use of the anti-G suit (*subj F*). All arterial pressures are referred to eye level. Inhalations between repeated Valsalva maneuvers in this and all other figures are indicated by the sudden drop in AP. Beat-by-beat HR was recorded from the ECG using a Brush Instruments cardiotachometer; occasional sharp drops in HR seen in this figure are artifacts occurring when baseline shift of the ECG prevented triggering of the cardiotachometer.

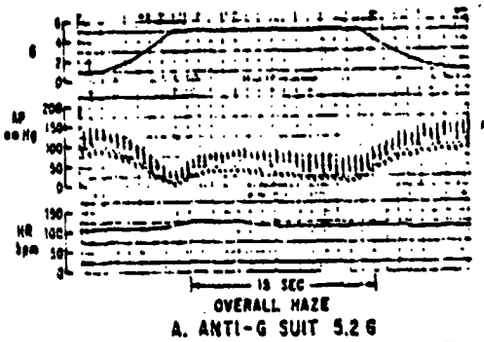


C. VALSALVA 4.5 G

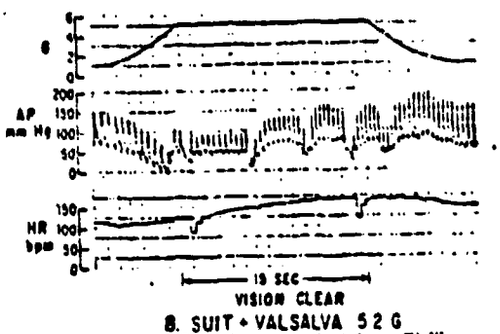


D. VALSALVA 4.9 G

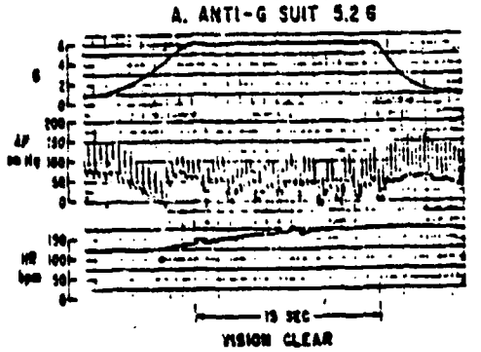
FIG. 2. Arterial pressure (AP) and heart rate (HR) response to the Valsalva maneuver with voluntary muscular straining and use of the anti-G suit (*subj F*). All arterial pressures are referred to eye level.



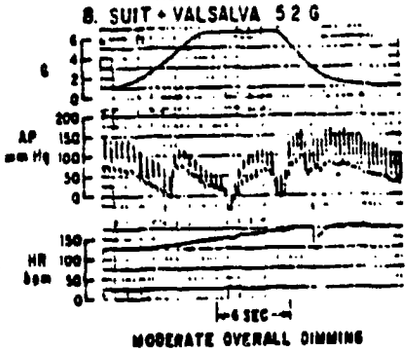
A. ANTI-G SUIT 5.2 G



B. SUIT + VALSALVA 5.2 G



C. SUIT + VALSALVA 6.2 G



D. SUIT + VALSALVA 6.7 G

SHEET 2 OF 4

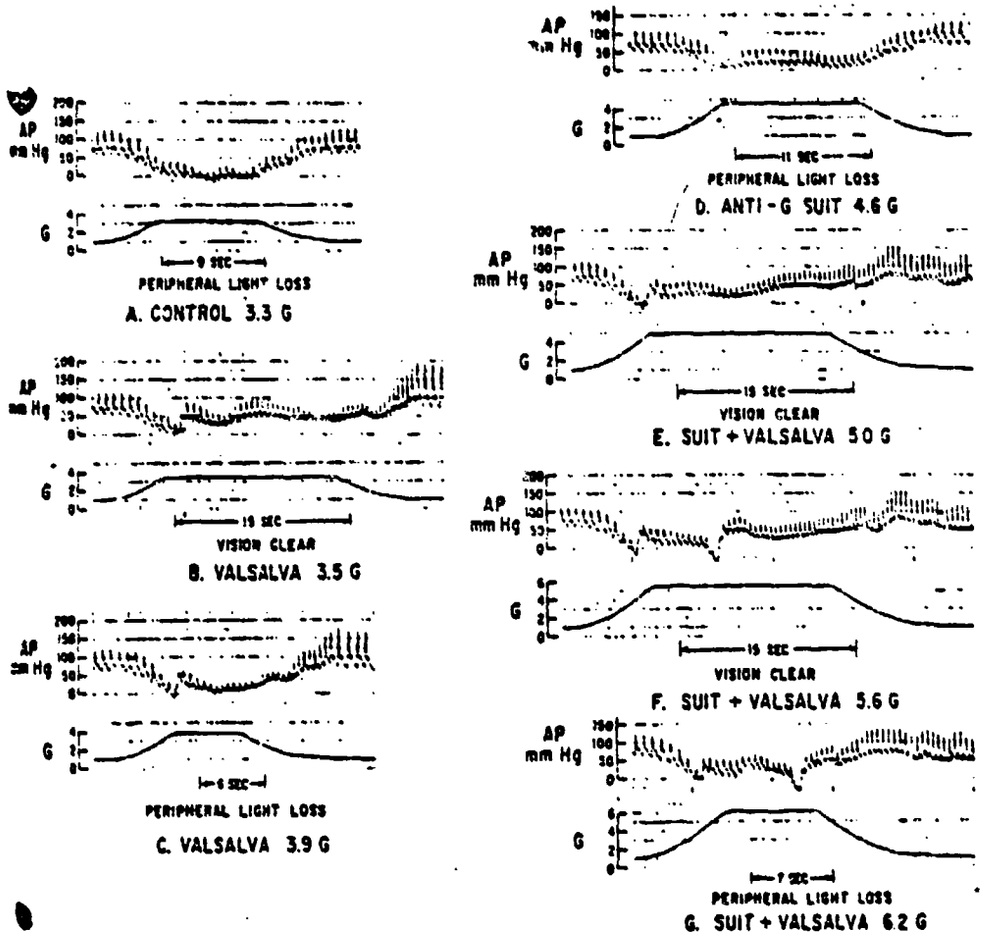


FIG. 3. Arterial pressure (AP) response to the Valsalva maneuver with voluntary muscular straining without and with use of the anti-G suit (*subj D*). All arterial pressures are referred to eye level.

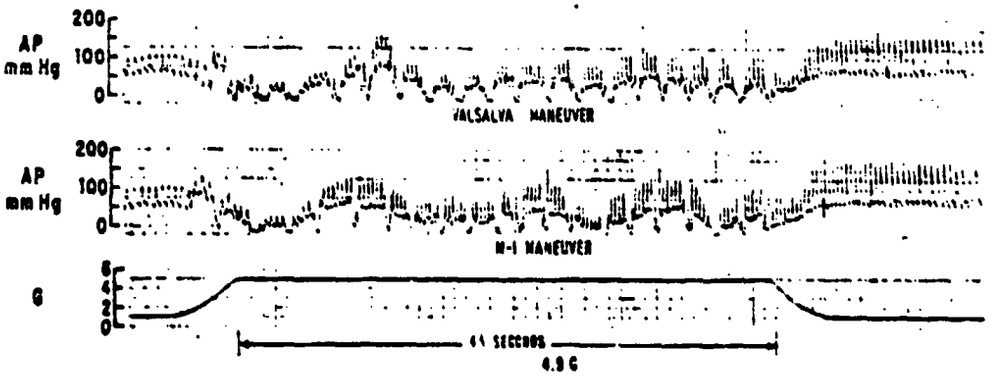


FIG. 4. Arterial pressure (AP) response to repeated Valsalva and M-1 maneuvers at +4.9 G_z for 45 s without use of an anti-G suit (*subj G*). Arterial pressures are referred to eye level.

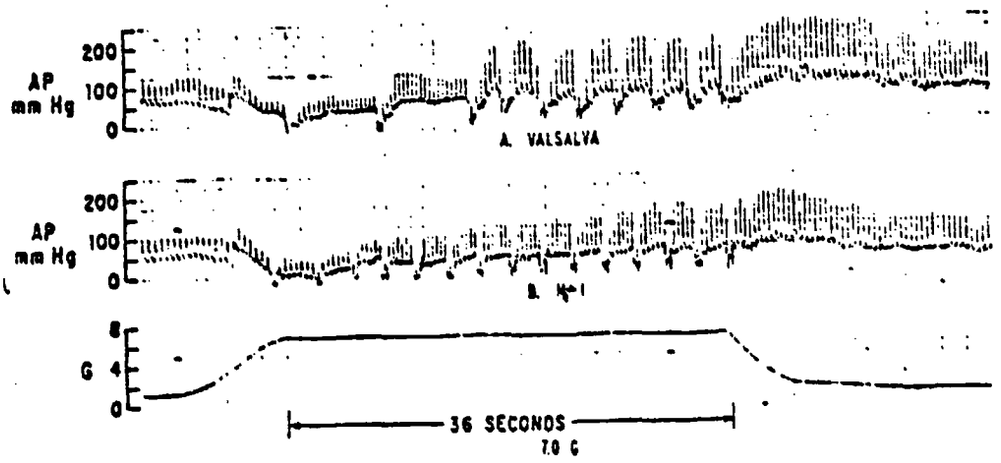


FIG. 5. Arterial pressure (AP) response to repeated Valsalva and M-1 maneuvers at +7.0 G_z for 45 s with use of an anti-G suit (*subj I*). Arterial pressures are referred to eye level.

TITLE: Systolic Time Intervals During +G_z Acceleration

REF. # 94

HG- 80

DATE:

LEAD AUTHOR: Graboys, T. B.

X HUMANS - ANIMALS -

ABSTRACT

Systolic time intervals (STI) were recorded in 8 healthy male volunteers before, during, and after 30-s exposures to +3 G, +5G, and +7G, acceleration. Heart rate (HR) increased at all +G, levels, as did the HR corrected QS interval, left ventricular ejection time (LVET), pre-ejection period (PDP) and PEP/LVET. These changes in STI were also proportional to the +G level. At the higher +G levels, PEP and PEP/LVET continued to increase early in the recovery period but HR and all STI returned to control after 60 s of recovery. Although physiological variables other than myocardial contractility, such as preload and afterload may influence STI during +G, the effects of +G, on stroke volume (SV) and cardiac output (CO) were estimated using previously described relationships between STI and invasively determined indices of cardiovascular function. In general, CO increased as SV decreased. During recovery, HR and CO fell and CO remained slightly below control levels, primarily because estimated SV remained low. This study demonstrates the feasibility of using STI to estimate noninvasively the transient changes in cardiovascular function during +G acceleration.

PHYSIOLOGICAL CATEGORY
- AUDITORY
- BIOMECHNL
- X CARDIOVSCL
- FORCE
- GENERAL
- LABYRINTH
- MAN.CNTRL
- X PROTECTIVE
- REVIEW
- RESPIRAT'N
- SIMULATION
- VISUAL
- OTHER

AUGMENTATION DEVICES
- HELMET
- STRAPS
- AURAL
- EXTREMITY
- LBNP
- VISUAL
- RESPIRATORY
- LACRIMATION
- TEMPERATURE
- MASK

RELEVANCE

. . . . . .

Cardiovascular, LBNP

Basic relevance is in the use of systolic time interval (STI) to estimate noninvasively the transient changes in cardiovascular function during LBNP.

SALIENT DATA

The authors state that +Gz acceleration induces acute changes in the cardiovascular system primarily through venous pooling, resulting in decreased ventricular filling, end diastolic volume, stroke volume and cardiac output. Bororeceptor mediated reflexes then cause an increase in total peripheral resistance, heart rate and mean arterial pressure, all of which are heightened by muscle tensing and the use of a modified Valsalva maneuver. They state correlation in changes in stroke volume and cardiac output estimated from STI during LBNP with invasive mesurements of cardiac function. Supporting data are presented.

SHEET 1 OF 1

TITLE:

Cardiovascular Function During Sustained $+G_z$ Stress

REF. #65

HG- 81

DATE:

LEAD AUTHOR: Erickson, H. H.

HUMANS -
X ANIMALS -

ABSTRACT

The development of aerospace systems capable of very high levels of positive (+Gz) stress, has created a need for a better understanding of the cardiovascular responses to acceleration. Using a canine model, the heart and cardiovascular system were instrumented to continuously measure coronary blood flow, cardiac output, left ventricular and aortic root pressure, and oxygen saturation in the aorta, coronary sinus, and right ventricle. The animals were exposed to acceleration profiles up to +6 Gz, 120 s at peak G; a seatback angle of 45^0 was simulated in some experiments. Radiopaque contrast medium was injected to visualize the left ventricular chamber, coronary vasculature, aorta, and branches of the aorta. The results suggest mechanisms responsible for arrhythmias which may occur, and subendocardial hemorrhage which has been reported in other animals.

PHYSIOLOGICAL CATEGORY
- AUDITORY
- BIOMECHNL
- X CARDIOVSCL
- FORCE
- GENERAL
- LABYRINTH
- MAN.CNTRL
- PROTECTIVE
- REVIEW
- X RESPIRAT'N
- SIMULATION
- VISUAL
- OTHER

RELEVANCE

Cardiovascular, LBNP, Visual, Respiratory

One of the few sources which illustrate heart level blood pressure during $+G_z$ exposure.

AUGMENTATION DEVICES
- HELMET
- STRAPS
- AURAL
- EXTREMITY
- LBNP
- VISUAL
- X RESPIRATORY
- LACRIMATION
- TEMPERATURE
- MASK

SALIENT DATA

DATA: Blood flow, Blood Pressure, O_2 Saturation and heart rate. Data shows an immediate decrease in arterial and left ventricular blood pressure, which subsequently increases towards the control level. For $\pm$ Gz < 2.0g the BP returns to control. For greater accelerations it does not reach control. Coronary blood flow and heart rate increased in response to the drop in BP. Also data is presented on the effects of 45^0 seat back angle.

SHEET 1 OF 1

TITLE: +Gz Protection Afforded by Standard and Preacceleration Inflations of the Bladder and Capstan Type G Suits

REF. # 34

HG- 82

DATE:

LEAD AUTHOR: Burton, R. R.

HUMANS - X
ANIMALS -

ABSTRACT

Positive (+G,) rapid onset acceleration tolerances were determined on eight male subjects: (a) Without a G-suit, (b) G-suit on, not inflated, and (c) G-suit on, inflated. Three types of suits were used on each subject: (a) standard bladder CSU-12/P; and (b) two types of capstan suits with (1) standard and (2) modified abdominal bladder. Two G-suit inflation procedures also were used in developing +Gz tolerances: (a) standard inflation, which began at 2.2G and continued at the rate of 1.5 psi/G (abdominal bladder) and 3 psi/G (capstan): and (b) preacceleration inflation (0, 5, or 10 sec) prior to acceleration onset, which involved suit pressures of 1 psi (abdominal bladder) and 12 psi (capstan), with suit inflation continuing immediately upon acceleration onset. Acceleration mean tolerances for the three suits tested using standard inflation, ranged from 4.5 to 4.7 (+Gz) - not satistically significantly different between suits using paired t-tests. Preacceleration inflations of 0.5, or 10 sec increased mean +Gz tolerances 0.4 to 0.6G above standard inflation methods - statistically significant (paired t-test) for all three suits tested. Procedural differences in preacceleration suit inflation were considered major reasons for finding an increase in +G, tolerance in this investigation as opposed to a decrease in acceleration tolerances previously reported in other preinflation studies.

. . . . . .

RELEVANCE

Gz Stress Resistance Increase as a Function of G Suit Usage

SALIENT DATA

(1) Authors Postulate the following relationships:

a) Gs = (1.2) (Gc) -0.41 - non inflated G suit

b) Gt = 0.78 + 1.19 Gc - inflated G suit
where Gc is subjects end point without a suit on.

These expressions pertain to standard inflation. Additional expressions are given for preinflation.

PHYSIOLOGICAL CATEGORY
- AUDITORY
- BIOMECHNL
- X CARDIOVSCL
- FORCE
- GENERAL
- LABYRINTH
- MAN.CNTRL
- X PROTECTIVE
- REVIEW
- RESPIRAT'N
- SIMULATION
- VISUAL
- OTHER

AUGMENTATION DEVICES
- HELMET
- STRAPS
- AURAL
- EXTREMITY
- XLBNP
- VISUAL
- RESPIRATORY
- LACRIMATION
- TEMPERATURE
- MASK

SHEET 1 OF 1

TITLE:

Positive (+Gz) Acceleration Tolerances of the Miniature Swine: Application as a Human Analog

REF. # 30

UG- 83

DATE:

LEAD AUTHOR: Burton, R. R.

X HUMANS -
X ANIMALS -

ABSTRACT

Positive (+Gz) rapid onset (1 G/sec.) acceleration tolerances were determined using conscious adult minature swine with chronically implanted intravascular polyethylene catheters. Peripheral light loss (PLL) and central light loss (CLL) tolerance criteria were estimated from direct arterial eye-level blood pressures of 50 torr and 20 torr, respectively. Acceleration PLL tolerances were 4.1 G and 5.7 G without and with an inflated G suit, respectively; CLL occurred at 4.9G and 6.6G and were similar to human +Gz tolerance data. The pig naturally exhibits a straining "M-1" maneuver that, like man, increases acceleration tolerances. Also like man, the pig exhibits a baroceptor-like response, 5 to 10 sec. post-acceleration onset, increasing +Gz tolerances approximately 1 G. Miniature swine appear to be generally acceptable as an analog for positive acceleration research on pathophysiologic limits for man.

. . . . . .

RELEVANCE

Cardiovascular, LBNP, Visual

Main relevance is in the potential use of miniature swine in place of human subjects for LBNP research.

SALIENT DATA

The author states that the anatomy and the physiology of the miniature swine, in many respects, are remarkably similar to man. He postulates that these similarities include Gz Tolerance.

- Eye/heart seat dimensions are presented and compare favorably.
- Minature swine performs tensing maneuvers during acceleration which produce arterial BP. Response not unlike that reported for man.
- Barorecptor reflexes are similar.

Comparison of tolerances is presented

Linear model for systolic pressure as a function of G presented.

PHYSIOLOGICAL CATEGORY
- AUDITORY
- BIOMECHNL
- X CARDIOVSCL
- FORCE
- GENERAL
- LABYRINTH
- MAN.CNTRL
- X PROTECTIVE
- REVIEW
- RESPIRAT'N
- SIMULATION
- VISUAL
- OTHER

AUGMENTATION DEVICES
- HELMET
- STRAPS
- AURAL
- EXTREMITY
- LBNP
- X VISUAL
- RESPIRATORY
- LACRIMATION
- TEMPERATURE
- MASK

SHEET 1 OF 1

TITLE: The Physiology of Negative Acceleration

REF. # 82

HG- 88

DATE:

LEAD AUTHOR: Gillies, J. A.

HUMANS - X
ANIMALS -

ABSTRACT

Not Available at this time

. . . . . .

General - Discussion of the Effects of -G

(1) Discussion of possible causes of red-out

"Red-out" or the red mist is a symptom analogous to blackout, but it is as inconsistent as all the other visual disturbance which have been recorded during negative acceleration. From the descriptions given by various subjects, the time-course of impairment of vision is similar to that seen during positive G. Indistinctness or blurring is followed by grey-out, in which there is a uniform loss of fine detail and contrast. At a later stage vision disappears entirely and it is in this phase that "red-out" sometimes appears in many subjects, however, the impairment of vision at the higher accelerations, and a few have remarked that bright objects seem to develop a halo, or surrounding ring of light.

RELEVANCE

SALIENT DATA

PHYSIOLOGICAL CATEGORY
- AUDITORY
- BIOMECHNL
- CARDIOVSCL
- FORCE
- GENERAL
- LABYRINTH
- MAN.CNTRL
- PROTECTIVE
- REVIEW
- RESPIRAT'N
- SIMULATION
- X VISUAL
- OTHER

AUGMENTATION DEVICES
- HELMET
- STRAPS
- AURAL
- EXTREMITY
- LBNP
- VISUAL
- RESPIRATORY
- LACRIMATION
- TEMPERATURE
- MASK

SHEET 1 OF 1

TITLE:

The Physiology of Positive Acceleration

REF.: 82

EG- 88

DATE:

LEAD AUTHOR: Gillies, J. A.

HUMANS - X
ANIMALS -

ABSTRACT

General Discussion of acceleration effects

Origine mechanism of black-out - "Andina...compared the effects of acceleration on vision with the impairment produced by appling pressure to the eyeballs w/ a tonometer " Andina found that complete loss of vision was proved when effective blood pressure in the central retinal artery was reduced to 21mm Hg - The normal intra-ocular tension being also about 21mm Hg. - then no blood flow into the eyes

Based on arterial distribution - increasing acceleration should by progressively cutting off the blood supply to the peripheral parts of the retina produce an almost concentric narrowing of the field of vision & because of no direct arterial supply to the fovea, visual acuity should degenerate well before perception of light is lost. (See Fig. 259, 260).

RELEVANCE

There appears to be a time lag between G onset and lose of acuity or blackout of a vascular origin - capillary vessels within the eye may hold blood pressure until main artery pressure fails providing about a 6 sec lag.

Note: threshold vs G Fig. 204

"The rate of application of acceleration (dg/dt) can have a profound effect on the determination of threshold."

SALIENT DATA

PHYSIOLOGICAL CATEGORY
- AUDITORY
- BIOMECHNL
- CARDIOVSCL
- FORCE
- GENERAL
- LABYRINTH
- MAN.CNTRL
- PROTECTIVE
- REVIEW
- RESPIRAT'N
- SIMULATION
- X VISUAL
- OTHER

AUGMENTATION DEVICES
- HELMET
- STRAPS
- AURAL
- EXTREMITY
- LBNP
- X VISUAL
- RESPIRATORY
- LACRIMATION
- TEMPERATURE
- MASK

SHEET 1 OF 1

TITLE:

Sustained Linear Acceleration

REF. # 194

HG- 89

DATE:

LEAD AUTHOR:

Fraser, T. M.

HUMANS - X
ANIMALS -

ABSTRACT

Not available at this time.

SALIENT DATA

Retinal & Visual Response

(1) There would appear to be a change in absolute threshold of vision under acceleration. "White showed that for a given stimulus intensity to be perceived as of equal intensity w/a probability of 50% under increased acceleration..." See ratios of increase Table 4-5. Foveal & peripheral thresholds as a function of acceleration are illustrated in Fig. 4-5 & 4-6.

(2) Visual Fields - at about 4.5 Gz, the field of view is narrowed to less than 46° Fig. 4.9 shows the effect of retinal position of a signal on perception of light signals under acceleration.

RELEVANCE

PHYSIOLOGICAL CATEGORY
- AUDITORY
- BIOMECHNL
- CARDIOVSCL
- FORCE
- GENERAL
- LABYRINTH
- MAN.CNTRL
- PROTECTIVE
- REVIEW
- RESPIRAT'N
- SIMULATION
- X VISUAL
- OTHER

AUGMENTATION DEVICES
- HELMET
- STRAPS
- AURAL
- EXTREMITY
- LBNP
- X VISUAL
- RESPIRATORY
- LACRIMATION
- TEMPERATURE
- MASK

SHEET 1 OF 1

TITLE:

Vision

REF.# 194

HG- 89

DATE:

LEAD AUTHOR:

Taylor

HUMANS - X
ANIMALS -

ABSTRACT

Not available at this time.

General Review of the Mechanics of the eye

RELEVANCE

1. Threshold - Some value of stimuli or interstimulus difference to which an observer responds with some selected probability (usually 50%). "Useful approximations can be made, for example, in the data for contrast discrimination & visual acuity, where doubling the value of threshold at P = 0.5 yields magnitudes where P is close to 1.0.

2. Good discription of color discrimination & contrast discrimination - particularly significant for the reduction of contrast in visual & instrument lighting during simulated Hi G's.

SALIENT DATA

PHYSIOLOGICAL CATEGORY

- AUDITORY
- BIOMECHNL
- CARDIOVSCL
- FORCE
- GENERAL
- LABYRINTH
- MAN.CNTRL
- PROTECTIVE
- REVIEW
- RESPIRAT'N
- SIMULATION
- X VISUAL
- OTHER

AUGMENTATION DEVICES

- HELMET
- STRAPS
- AURAL
- EXTREMITY
- LBNP
- X VISUAL
- RESPIRATORY
- LACRIMATION
- TEMPERATURE
- MASK

SHEET 1 OF 1

TITLE: Effects of Acceleration on Human Performance and Physiology With Special Reference to Transverse G

REF. # 160

HG-90

DATE: 6-68

LEAD AUTHOR: Little, V. Z.

HUMANS - X
ANIMALS -

ABSTRACT

RELEVANCE

SALIENT DATA

Review of physiological effect, tolerance and performance decrement to G_Z and especially G_X

---

1. Nice photographs of facial droop at G_Z levels from 1 to 7 g's.
2. Reduction in auditory reaction time but no evidence of change in audition itself (Pg. 7). Page 14 indicates response time and error increase in addition for 4.6 G_Z.
3. Target seen at 1 g must be twice as large to be seen at 7 g. (Pg. 7)
4. Upper limit of performance +13 G_X for 1 minute or +5 G_X for 5 minutes
5. Lacrimination at 6 → 12 G_X (Page 10)
6. Page 13 - interesting chart of $+G_X$ effects
7. Respiration (p. 5)- "chest pressure limits thoracic breathing".

PHYSIOLOGICAL CATEGORY
- X AUDITORY
- BIOMECHNL
- CARDIOVSCL
- FORCE
- GENERAL
- LABYRINTH
- MAN.CNTRL
- PROTECTIVE
- X REVIEW
- RESPIRAT'N
- SIMULATION
- X VISUAL
- OTHER

AUGMENTATION DEVICES
- HELMET
- STRAPS
- X AURAL
- EXTREMITY
- LBNP
- X VISUAL
- RESPIRATORY
- X LACRIMATION
- TEMPERATURE
- MASK

SHEET 1 OF 1

TITLE: Human Force Capabilities for Operating Aircraft Controls at 1,3 and 5 G_Z

REF.# 141

HG-91

DATE: 2/'75

LEAD AUTHOR: Kroemer, K. H. Eberhard

HUMANS - X
ANIMALS -

ABSTRACT

The maximum isometric forces adult male subjects could exert at eight locations of hand-operated aircraft controls were measured at 1, +3 and +5g_z. Forces were measured in two vertical and four to eight horizontal directions. Selected anthropometric dimensions were obtained on the subjects and compared with those from the 1967 USAF anthropometric survey of flying personnel. Summary statistics including the mean, standard deviation, coefficient of variation, symmetry, kurtosis, and selected percentiles, are presented for each of the 60 force exertion measures.

Extremity Loading

RELEVANCE

1. No real apparant effects outside of the Z axis (as expected). Except for push forward (force REDCTN under G_Z).
2. Within the Z axis, data given shows reduction in force capability up as a function of G_Z and a compatible increase in force down as a function of G_Z.
3. Data presented may give general G load force regime but specific values are highly dependent upon hand locations - seems as though the extremity force profile might better be generated based on two serial masses on an articulated arm.
4. Y force capability nearly unaffected.

SALIENT DATA

PHYSIOLOGICAL CATEGORY
- AUDITORY
- X BIOMECHNL
- CARDIOVSCL
- X FORCE
- GENERAL
- LABYRINTH
- X MAN.CNTRL
- PROTECTIVE
- REVIEW
- RESPIRAT'N
- SIMULATION
- VISUAL
- OTHER

AUGMENTATION DEVICES
- HELMET
- STRAPS
- AURAL
- X EXTREMITY
- LBNP
- VISUAL
- RESPIRATORY
- LACRIMATION
- TEMPERATURE
- MASK

SHEET 1 OF 1

TITLE:

Correlation of Eye Level Blood Flow Velocity and Blood Pressure during $+G_z$ Acceleration

REF. # 145

HG-92

DATE: 11/73

LEAD AUTHOR: Krutz, R. W.

HUMANS - X
ANIMALS -

ABSTRACT

Eye-level blood flow and blood pressure changes were correlated on the USADSAM human centrifuge during both rapid onset (ROR, 1 G/sec) and gardual onset runs (GOR, 0.1 G/sec). A transcutaneous Doppler ultrasonic flowmeter was used to monitor temporal artery blood flow ($\dot{Q}_{ta}$); direct blood pressure was obtained by cannulation of a radial artery and measured at eye level with a Statham P-37 miniature transducer. Eye-level mean blood pressure (P_a) decreased to 20 mm Hg and zero forward $\dot{Q}_{ta}$ occurred 6 sec (range 4-9 sec) prior to blackout in experienced centrifuge subjects during RORs. The same degree of correlation was not seen during GORs.

RELEVANCE

Shows correlation between physiological measures during $+G_z$ (blood flow and pressure at eye level) and sufficient blackout.

SALIENT DATA

1. Visual effects can probably be totally explained by retinal hypoxia. Anything that drops arterial flow to eye level will simulate the visual $+G_z$ effect.
2. The use of a transcutlaneous Doppler ultrasonic flowmeter appears viable for predicting the inception of blackout.
3. Data presented on eye level blood pressure during ROR & GOR to blackout ($\simeq 3G_z$)

PHYSIOLOGICAL CATEGORY
- AUDITORY
- BIOMECHNL
- X CARDIOVSCL
- FORCE
- GENERAL
- LABYRINTH
- MAN.CNTRL
- PROTECTIVE
- REVIEW
- RESPIRAT'N
- SIMULATION
- VISUAL
- OTHER

AUGMENTATION DEVICES
- HELMET
- STRAPS
- AURAL
- EXTREMITY
- LBNP
- X VISUAL
- RESPIRATORY
- LACRIMATION
- TEMPERATURE
- MASK

SHEET 1 OF 1

TITLE: Lacrimation in Normal Eyes

REF.# 56

HG- 94

DATE:

LEAD AUTHOR: Roetth, A, (Sr.)

HUMANS -X
ANIMALS -

ABSTRACT

Pertains to the flow of tears which may be useful in establishing high G lacrimation device.

RELEVANCE

SALIENT DATA

1. Three methods of inducing tears

   a. Stimulate the conjunctiva
   b. Irritate the nasal mucosa
   c. Look at the sun

2. Data pertains almost exclusively to amount of tears produced as a function of age group. Young produce upwards of 6 times the amount of old subjects (6 yrs. vs. 80 yrs.)

3. "Lacrimal Gland, except during weeping, does not secrete without external stimuli."

PHYSIOLOGICAL CATEGORY
- AUDITORY
- BIOMECHNL
- CARDIOVSCL
- FORCE
- GENERAL
- LABYRINTH
- MAN.CNTRL
- PROTECTIVE
- REVIEW
- RESPIRAT'N
- SIMULATION
- VISUAL
- X OTHER

AUGMENTATION DEVICES
- HELMET
- STRAPS
- AURAL
- EXTREMITY
- LBNP
- VISUAL
- RESPIRATORY
- X LACRIMATION
- TEMPERATURE
- MASK

SHEET 1 OF 1

TITLE: Body Temperature Measuring System

REF. # 130

HG-97

DATE: 1977

LEAD AUTHOR: Lem, J.D., Johnston, R.S., Dietlein, L.F. (ed.)

HUMANS - ANIMALS -

PHYSIOLOGICAL CATEGORY
- AUDITORY
- BIOMECHNL
- CARDIOVSCL
- FORCE
- X GENERAL
- LABYRINTH
- MAN.CNTRL
- PROTECTIVE
- REVIEW
- RESPIRAT'N
- SIMULATION
- VISUAL
- OTHER

AUGMENTATION DEVICES
- HELMET
- STRAPS
- AURAL
- EXTREMITY
- LBNP
- VISUAL
- RESPIRATORY
- LACRIMATION
- TEMPERATURE
- MASK

ABSTRACT

Describes devices used to measure body temperature of Skylab astronauts. Seems to be irrelevant because device employs oral probe which would be inconvenient in a simulator.

RELEVANCE

SALIENT DATA

1. Performance Requirements

   a. Range 308.15 to 313.71 K
   b. Accuracy $\pm$ 0.11 K
   c. Power $\pm$ 10 V dc @ 4 ma
   d. Response within 1.5% of final value within 40 sec.

SHEET 1 OF 1

TITLE: Automatic Blood Pressure Measuring System

REF. # 130

HG-97

DATE: 1977

LEAD AUTHOR: Nolte, R.

HUMANS -
ANIMALS -

ABSTRACT

Article describes the automatic blood pressure measuring device used on skylab. This provides some background for possible use in some mechanization requiring BP measuring device described as non-invasive.

RELEVANCE

1. The device uses the familiar clinical approach using a cuff. However the stethescope is replaced by a microphone, a gas pressure and valving replaces the squeeze bulb and a quantitative electronics circuit replaces the clinician for the sound amplitude and frequency comparison. This device could possibly be used in a simulator with minimal environmental fidelity impact.

SALIENT DATA

2. Glen Talcott of the Martin Marietta Corp., Denver, were the project engineers for this device.

PHYSIOLOGICAL CATEGORY
- AUDITORY
- BIOMECHNL
- X CARDIOVSCL
- FORCE
- GENERAL
- LABYRINTH
- MAN.CNTRL
- PROTECTIVE
- REVIEW
- RESPIRAT'N
- SIMULATION
- VISUAL
- OTHER

AUGMENTATION DEVICES
- HELMET
- STRAPS
- AURAL
- EXTREMITY
- X LBNP
- X VISUAL
- RESPIRATORY
- LACRIMATION
- TEMPERATURE
- MASK

SHEET 1 OF 1

TITLE:

Vectorcardiograph

REF. # 130

HG-97

DATE: 1977

LEAD AUTHOR: Lintott, J., Johnston, R.S., Dietlein, L.F. (ed.)

HUMANS - ANIMALS -

ABSTRACT

Report describes a device for obtaining vectorcardiograms of Skylab astronauts.

RELEVANCE

1. Devices includes signal conditioning equipment or interface box which provides electrostatic discharge protection, electroshock protection and a preamplifier; a system to determine subject's heart rate from the vectorcardiograph output with a range of 40 to 200 heart beats/minute.

SALIENT DATA

Bibliography: Lintott, J & Costello, M.J. Skylab Vectocardiograph: System Description & Inflight Operation. NASA TN D-7997. June 1975

PHYSIOLOGICAL CATEGORY
- AUDITORY
- BIOMECHNL
- X CARDIOVSCL
- FORCE
- GENERAL
- LABYRINTH
- MAN.CNTRL
- PROTECTIVE
- REVIEW
- RESPIRAT'N
- SIMULATION
- VISUAL
- OTHER

AUGMENTATION DEVICES
- HELMET
- STRAPS
- AURAL
- EXTREMITY
- X LBNP
- VISUAL
- X RESPIRATORY
- LACRIMATION
- TEMPERATURE
- MASK

SHEET 1 OF 1

TITLE:

Variable Transmittance Visor for Helmet Mounted Display

REF. # 58

HC-98

DATE: 10/'73

LEAD AUTHOR: Dobbins, J. P. Dr.

HUMANS -
ANIMALS -

ABSTRACT

Efficient operation of HMD's (helmet-mounted displays) requires the use of VTV's (variable-transmittance visors) to maintain constant visual contrast between projected images and their backgrounds. No VTV's responding controllably or reversibly with rapidity had been developed prior to this program. A high-priority military objective was to encourage the design and development of such VTV's. An unsolicited proposal to the USAF, based on a new concept, suggested the use of a liquid optronic medium in a sandwich-cell visor configuration with automatic control of variable transmittance. This was rewarded by Contract No. F33615-71-c-1938 from the Aerospace Med. Res. Lab. In a two-year program, VTV's were designed, fabricated, and tested, which in most major respects met the AF requirements. Three such units were installed in flight helmets and delivered to the customer as airborne feasibility demonstrators. These accommodated variations in external brightness over a range greater than 80:1. Automatic regulation was provided from light sensors, behind the visors, connected to closed-loop, electronic controllers using 28-vdc aircraft power. Controllers were packaged as pocket-size units with self-contained batteries for emergency operation. Most effort was directed toward solving critical problems involved in the selection, processing, and fabrication of materials suitable for this application. Among the many mathematical relationships, both optical and optronic, put to practical use in the VTV design were several derived by the writer and made available here for the first time in English.

RELEVANCE

Helmet visor high G effects. This document is final report covering the construction of 3 visors using liquid crystals to obtain variable transmittance.

SALIENT DATA

PHYSIOLOGICAL CATEGORY
- AUDITORY
- BIOMECHNL
- CARDIOVSCL
- FORCE
- GENERAL
- LABYRINTH
- MAN.CNTRL
- PROTECTIVE
- REVIEW
- RESPIRAT'N
- SIMULATION
- XVISUAL
- OTHER

AUGMENTATION DEVICES
- HELMET
- STRAPS
- AURAL
- EXTREMITY
- LBNP
- X VISUAL
- RESPIRATORY
- LACRIMATION
- TEMPERATURE
- MASK

SHEET 1 OF 2

AUTHOR Dobbins, Dr. J. P. REF # 58

1. Used methacrylate sheeting, bubble blown and omniguard coating to protect against the solvent characteristics of the liquid crystal - final findings suggest allyldigycol carbonate, casted, with no need for protective layer would have been better.

2. Used indium & tin oxide due to good reflectance (low) and uniform thickness characteristics. Sputter applied under slow rotation of visor shells and careful control of sputter chamber gas pressure & oxygen backfill (This controls amount of free metal deposited and consequently controls unwanted absorption)

3. End result contained variations in transmittance from one segment of visor to another. This unwanted condition arose due to inability to precisely control the geometry of visor shells and consequently the thickness of the liquid crystal layer.

SHEET 2 OF 2

TITLE: The Use of a Fixed Base Simulator as a Training Device for High Sustained or ACM (Air Combat Maneuvering) + G Stress

REF. # 154

HG-102

DATE: 4/'76

LEAD AUTHOR: Leverett, S. D. (Jr.)

HUMANS - ANIMALS -

ABSTRACT

O_2 Mask, Helmet

Report discusses an experiment wherein pilots were taught high G techniques to forestall physiological effects. Centrifuge was used as simulator. Not too much information for us here except this reference documents O_2 mask slippage and helmet compression (see pictures) Also F4E ACM profile presented (Recorded by Accelerometer).

PHYSIOLOGICAL CATEGORY
- AUDITORY
- X BIOMECHNL
- CARDIOVSCL
- FORCE
- GENERAL
- LABYRINTH
- MAN.CNTRL
- PROTECTIVE
- REVIEW
- RESPIRAT'N
- SIMULATION
- VISUAL
- X OTHER

AUGMENTATION DEVICES
- XHELMET
- STRAPS
- AURAL
- EXTREMITY
- LBNP
- VISUAL
- RESPIRATORY
- LACRIMATION
- TEMPERATURE
- X MASK

RELEVANCE

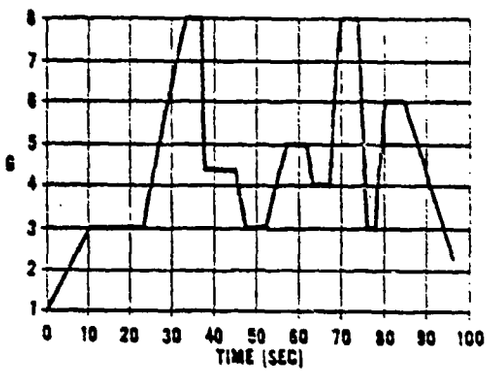


Figure 2. A reconstructed F4E, G versus time air combat maneuvering profile.

SALIENT DATA

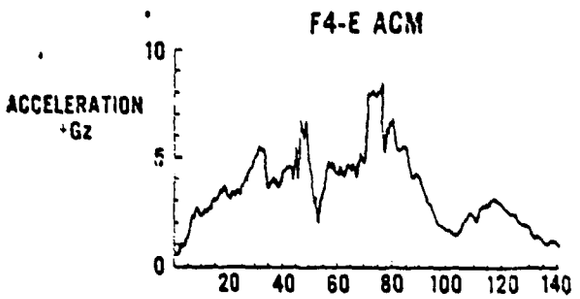


Figure 3. An accelerometer recorded G versus time air combat maneuvering profile taken from an engagement between two F4E's. A modification of ACM traces such as this was used in the training. The abscissa is time in seconds.

SHEET 1 OF 2

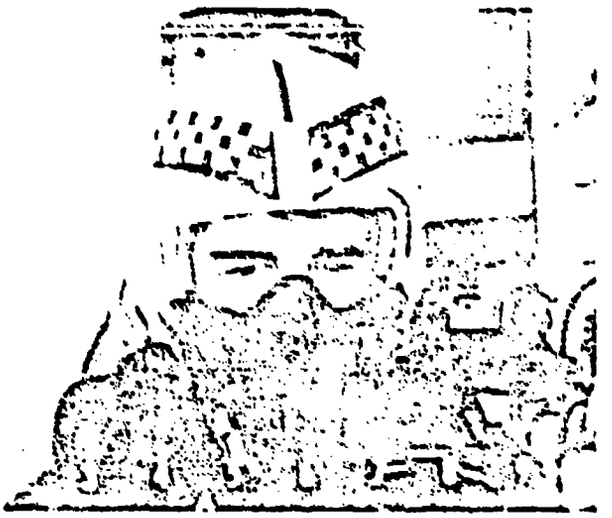


Figure 5a. Pilot's face at +4.5 G_z. Very slight facial distortion.

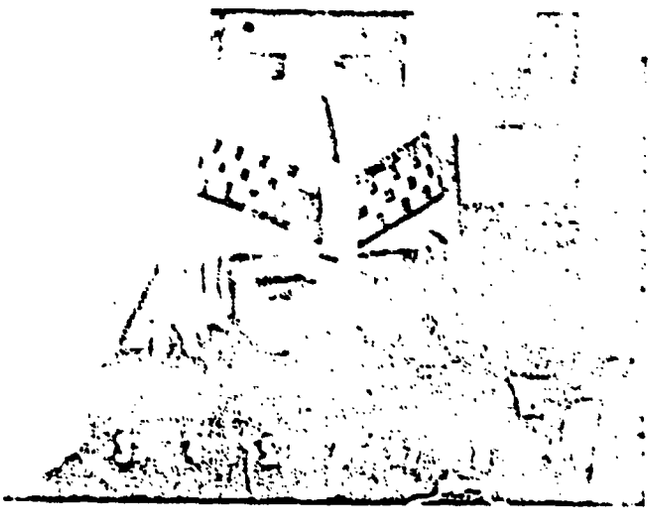


Figure 5b. Pilot's face at +7.5 G_z. Severe facial distortion and oxygen mask [illegible].

TITLE:

Description & Flight Tests of an Oculometer

REF. # 171

HG-103

DATE: 6/'77

LEAD AUTHOR: Middleton, D. B.

HUMANS - X
ANIMALS -

ABSTRACT

A remote-sensing oculometer has been successfully operated during flight tests with an NASA experimental Twin Otter aircraft at the Langley Research Center. Although the oculometer was designed primarily for the laboratory, it was able to tract the pilot's eye-point-of-regard (lookpoint) consistently and unobtrusively in the flight environment. The instantaneous position of the lookpoint was determined to within approximately 1°. Data were recorded on both analog and video tape. The video data consisted of continuous scenes of the aircraft's instrument display and a superimposed white dot (simulating the lookpoint) dwelling on an instrument or moving from instrument to instrument as the pilot monitored the display information during landing approaches.

PHYSIOLOGICAL CATEGORY
- AUDITORY
- BIOMECHNL
- CARDIOVSCL
- FORCE
- GENERAL
- LABYRINTH
- MAN.CNTRL
- PROTECTIVE
- REVIEW
- RESPIRAT'N
- SIMULATION
- X VISUAL
- OTHER

RELEVANCE

Report describes a remote oculometer and a flight test recording the instrument scan pattern of a Twin Otter pilot during an ILS approach. Relevant to the extent that it describes hardware function and application to determining a pilot's LOS.

AUGMENTATION DEVICES
- HELMET
- STRAPS
- AURAL
- EXTREMITY
- LBNP
- X VISUAL
- RESPIRATORY
- LACRIMATION
- TEMPERATURE
- MASK

SALIENT DATA

The test verified the device's capability to track the human eye during landing. It further verified the device will operate in a vibratory environment. The instantaneous position of the LOS was determined to within 1°.

Device was developed for Langley Research Center by the Honeywell Radiation Center of Lexington, Mass. Device contains eye movement to a 1 in^3 volume. A later version permits a 1 ft^3 volume for eye movement. Near IR is used for illumination and is reputed to be non-distracting. Head tracking not a problem because of fixed mirror ref.

SHEET 1 OF 1

TITLE:

Control of Tearing by Blocking the Nasal Ganglion

REF. # 213

BG- 104

DATE: 1930

LEAD AUTHOR: Ruskin, Suron L. (M.D.)

X HUMANS - ANIMALS -

ABSTRACT

Lacrimation

1. Anatomical development of nervous system controlling tearing
2. The only glands supplied by the nasal ganglion are the tear gland (lacrimal) and the mucus glands of the nasopharynx.
3. Lacrimal gland innervation is double - cranial automatic and sympathetic nerves.

RELEVANCE

PHYSIOLOGICAL CATEGORY
- AUDITORY
- BIOMECHNL
- CARDIOVSCL
- FORCE
- GENERAL
- LABYRINTH
- MAN.CNTRL
- PROTECTIVE
- REVIEW
- RESPIRAT'N
- SIMULATION
- VISUAL
- X OTHER

AUGMENTATION DEVICES
- HELMET
- STRAPS
- AURAL
- EXTREMITY
- LBNP
- VISUAL
- RESPIRATORY
- X LACRIMATION
- TEMPERATURE
- MASK

SALIENT DATA

SHEET 1 OF 1

TITLE:

The Lacrimation Reflex

REF.#181

HC- 105

DATE: 7/'44

LEAD AUTHOR: Mutch, J. R.

X HUMANS - ANIMALS -

ABSTRACT

Lacrimation

Primarily an anotomical development of the nervous system related to lacrimation with case history clinical evidence supporting a)reflex lacrimation as unilateral, b) 5th cranial nerve (opthalmic division) as the afferent pathway for reflex lacrimation c) 7th nerve is efferent pathway d) motor impulses travel on the greater superficial petrosal nerve.

Seems to reinforce other work covering the fact that tearing is caused emotionally, by irritation of the conjunctiva and/or cornea but I do not recognize this author's method for accounting for olfactory stimulus (other references (physiology of the eye) with olfactory stimulation as an input to the 5th cranial nerve).

Normally little of the normal secretion goes through the canaliculi (drain)- most evaporates.

Phenyl-bromo-accto-nitrite (teargas) administered to the cornea/conjunctiva stimulates pain and tears (p. 325)- 5th nerve input.

Sympathetic nerve probably not part of reflex or psychic lacrimation but may be part or normal secretion.

RELEVANCE

SALIENT DATA

PHYSIOLOGICAL CATEGORY
- AUDITORY
- BIOMECHNL
- CARDIOVSCL
- FORCE
- GENERAL
- LABYRINTH
- MAN.CNTRL
- PROTECTIVE
- REVIEW
- RESPIRAT'N
- SIMULATION
- VISUAL
- X OTHER

AUGMENTATION DEVICES
- HELMET
- STRAPS
- AURAL
- EXTREMITY
- LBNP
- VISUAL
- RESPIRATORY
- X LACRIMATION
- TEMPERATURE
- MASK

SHEET 1 OF 1

TITLE:

Design & Test of a full scale wearable Exoskeletal Structura

REF. #175

IG-106

DATE: 3/'64

LEAD AUTHOR:

Cornell Aeronautical Lab Contract

HUMANS X
ANIMALS

ABSTRACT

A final design of a nonpowered, wearable exoskeletal device is presented. The device follows all basi movements of the wearer except for the fingers, toes and neck. Two features of the exoskeleton are that each joint has adjustable stops that can be used to limit the range of motion, and each joint is instrumented to record its position continuously with time. The extroskeleton is adjustable for size so that it can be worn by 90 percent of the adult, male population. (The source of the antropological data used is presented in Reference 1.)

A test program is discussed that is used to draw conclusions concerning the feasibility of surrounding a person with an exoskeleton during the performance of work tasks. Experiments to determine experimentally the effect of limiting the allowable range of motion at given joints upon the ability of the subject to perform selected tasks are presented. Velocity and acceleration of exoskeletal joints during the performance of certain tasks are given.

PHYSIOLOGICAL CATEGORY

- AUDITORY
- X BIOMECHNL
- CARDIOVSCL
- FORCE
- GENERAL
- LABYRINTH
- MAN.CNTRL
- PROTECTIVE
- REVIEW
- RESPIRAT'N
- SIMULATION
- VISUAL
- OTHER

AUGMENTATION DEVICES

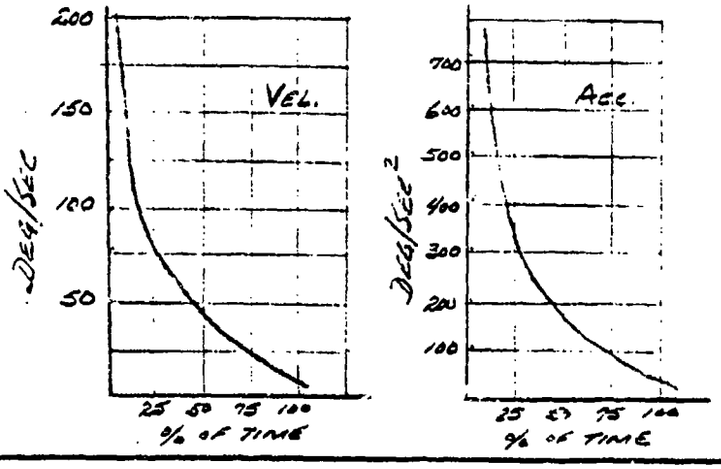
- HELMET
- STRAPS
- AURAL
- X EXTREMITY
- LBNP
- VISUAL
- RESPIRATORY
- LACRIMATION
- TEMPERATURE
- MASK

RELEVANCE

Extremity Drive

SALIENT DATA

Interesting data concerning position, velocity and acceleration of various human skeletal joints during certain motions (poorly defined). Most useful piece of information pertains to elbow joint (P. 62, 63) werein we can obtain the orderofmagnitude of elbow velocity position & acceleration.



SHEET 1 OF 4

AUTHOR Cornell Aeronautical Lab Contract REF # 175

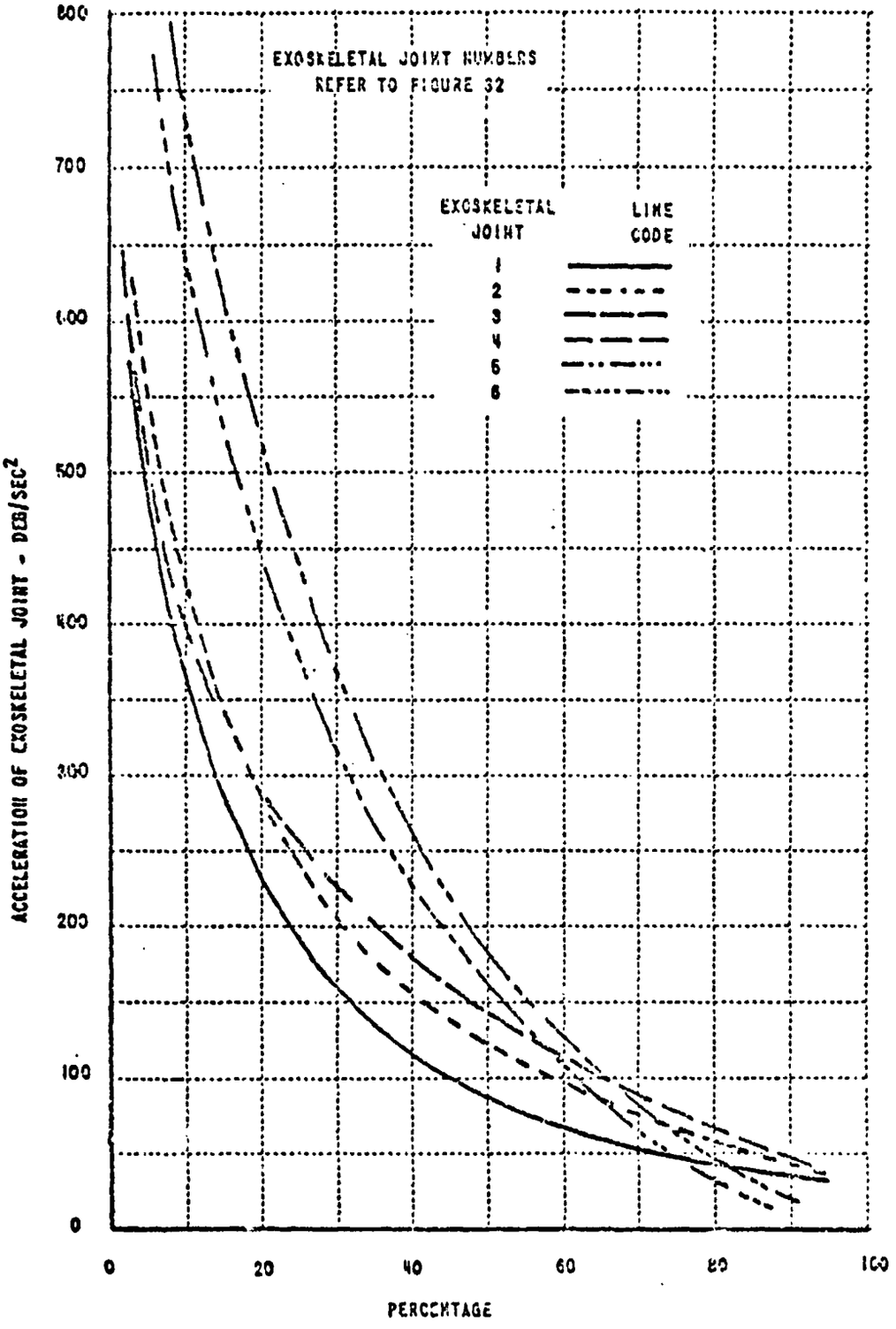


Figure 35

ACCELERATION OF EXOSKELETAL JOINTS DURING TYPICAL SHOULDER AND ARM MOVEMENTS

SHEET 2 OF 4

AUTHOR Cornell Aeronautical Lab Contract REF # 175

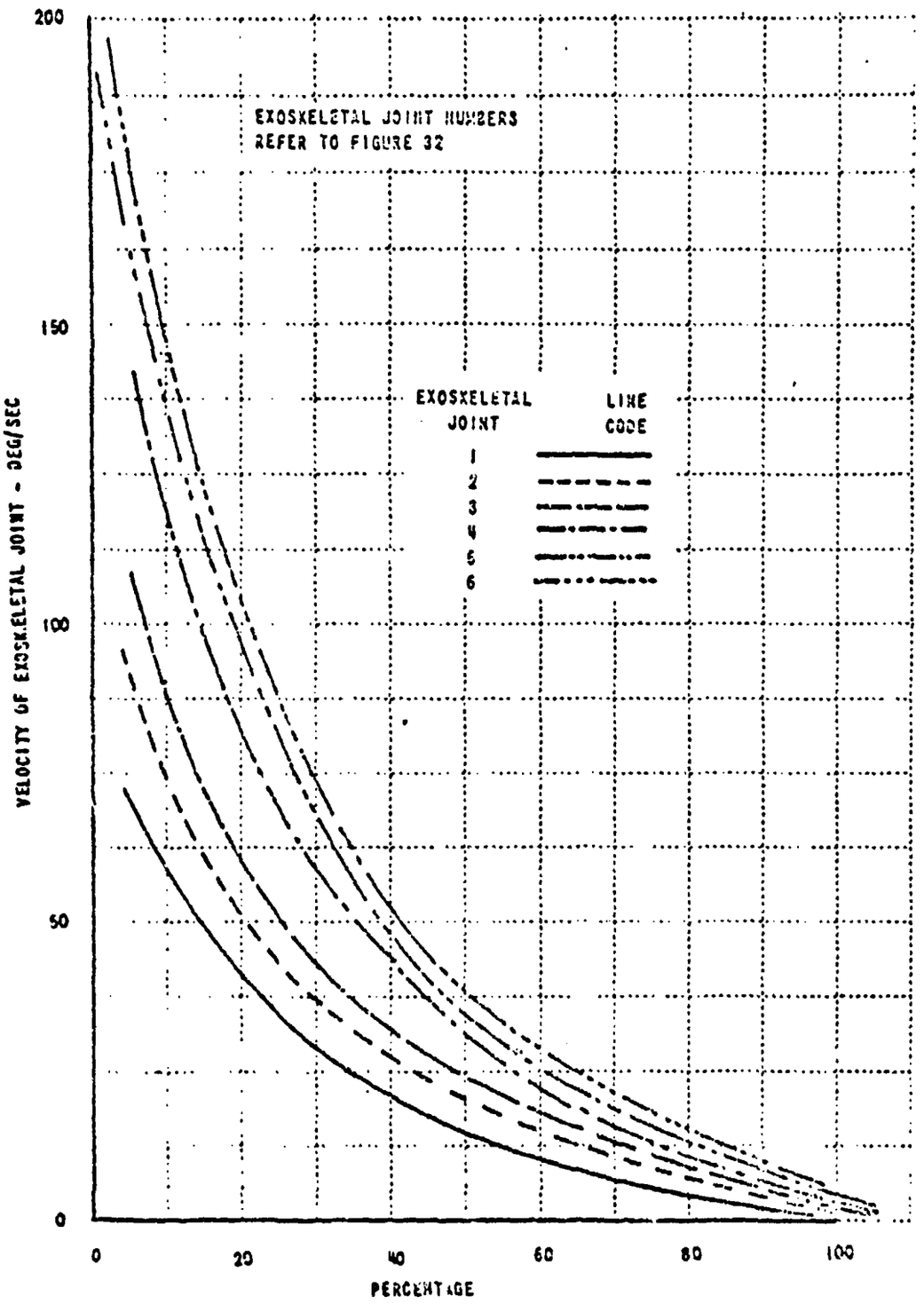


Figure 34
VELOCITY OF EXOSKELETAL JOINTS DURING TYPICAL SHOULDER AND ARM MOVEMENTS

SHEET 3 OF 4

AUTHOR Cornell Aeronautical Lab Contract REF # 175

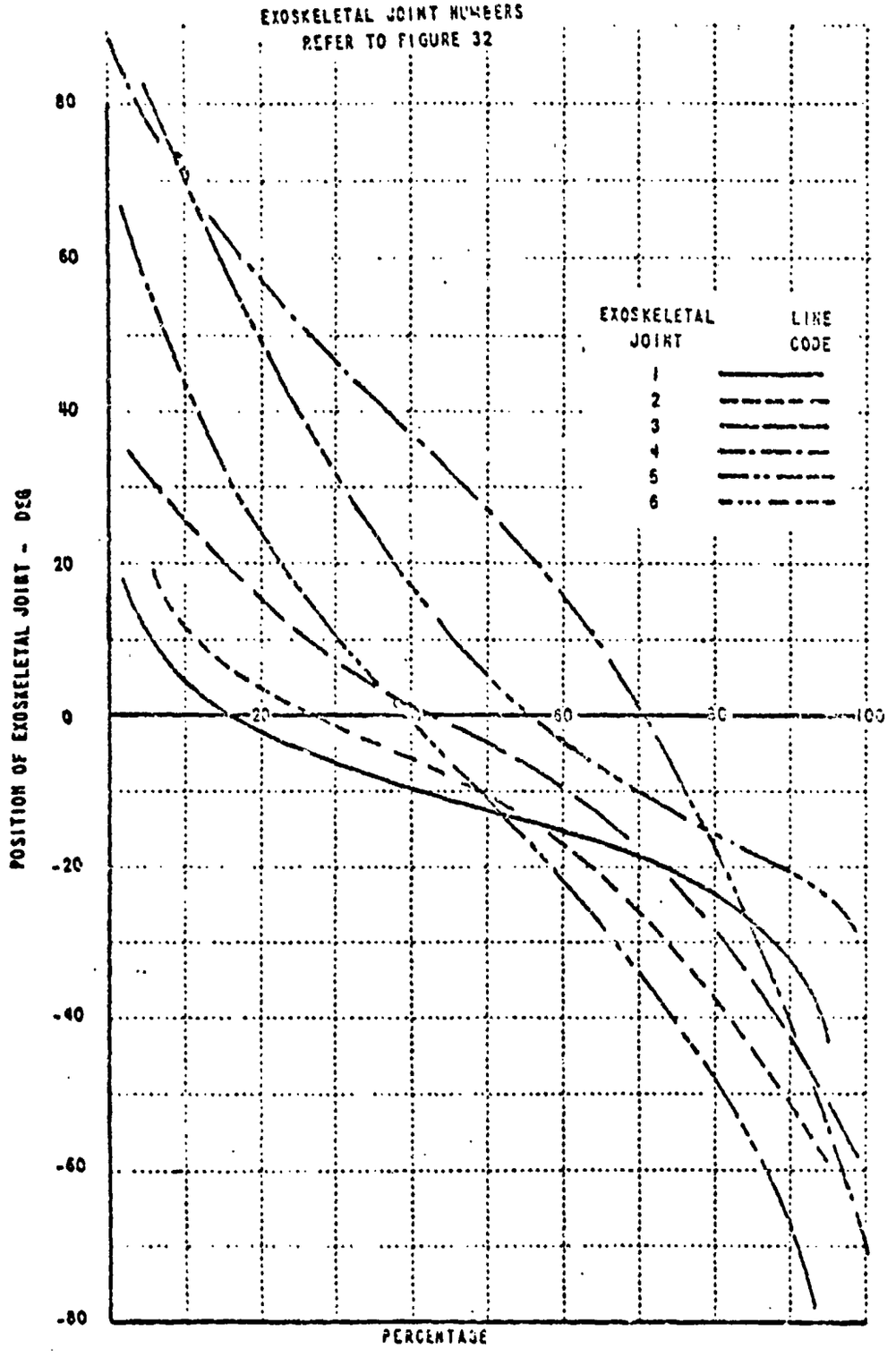


Figure 33
POSITION OF EXOSKELETAL JOINTS DURING TYPICAL SHOULDER AND ARM MOVEMENTS

SHEET 4 OF 4

TITLE:

A Technique for Photographing Human Retinal Circulation During Blackout on the USAFSAM Human Centrifuge

REF. # 136

HG-107

DATE: 3/'68

LEAD AUTHOR: Kirkland, V. E.

X HUMANS - ANIMALS -

ABSTRACT

To study the human retina on a moment-to-moment basis during the rapid sequence of events occurring before, during, and after a blackout episode on the human centrifuge requires a technique which will not harm the subject, yet will allow constant viewing. In a previous study an ophthalmoscope was used to study the retinal changes and then the subjective impressions of the investigator were recounted to a medical illustrator.

A method has now been developed using a modified Zeiss fundus camera which allows photographs to be taken of the retinal circulation every 0.6 second during the entire $+G_z$ maneuver at the subject's blackout level.

PHYSIOLOGICAL CATEGORY

- AUDITORY
- BIOMECHNL
- X CARDIOVSCL
- FORCE
- GENERAL
- LABYRINTH
- MAN.CNTRL
- PROTECTIVE
- REVIEW
- RESPIRAT'N
- SIMULATION
- VISUAL
- OTHER

RELEVANCE

1. Largely irrelevant to our needs.
2. Results of experiments using this device would however be useful.

AUGMENTATION DEVICES

- HELMET
- STRAPS
- AURAL
- EXTREMITY
- LBNP
- X VISUAL
- RESPIRATORY
- LACRIMATION
- TEMPERATURE
- MASK

SALIENT DATA

USAFM had developed a technique for photographing the human retinal circulation during blackout.

SHEET 1 OF 1

TITLE: The Normal Human EKG & Its Common Variations in Experimental Situations

REF. # 167

HG- 108

DATE: 6/'56

LEAD AUTHOR: McGuire, T. F.

X HUMANS - ANIMALS -

ABSTRACT

An attempt has been made to define as clearly as possible, within the limits of presently accepted knowledge, the boundaries of normal in electrocardiography. "Normal" having been defined, attention is turned to possible changes during experimental procedures. These changes include the following five basic modes or combinations thereof: positional effect, chemical effect, circulatory effect, nervous system effect, and temperature effect. Varying arrthythmias and conduction defects are discussed, as are cardiac chamber dilitation, cardiac strain, myocardial hypoxia, and various EKG artefacts.

RELEVANCE

Relevant to the interpretation of EKG traces.

SALIENT DATA

Report presents a technique for analyzing these traces. Describes each wave and interval. Also describes several abnormalities and their effect on the EKG. Main use is in understanding the vernacular presented in other works. Description presented below.

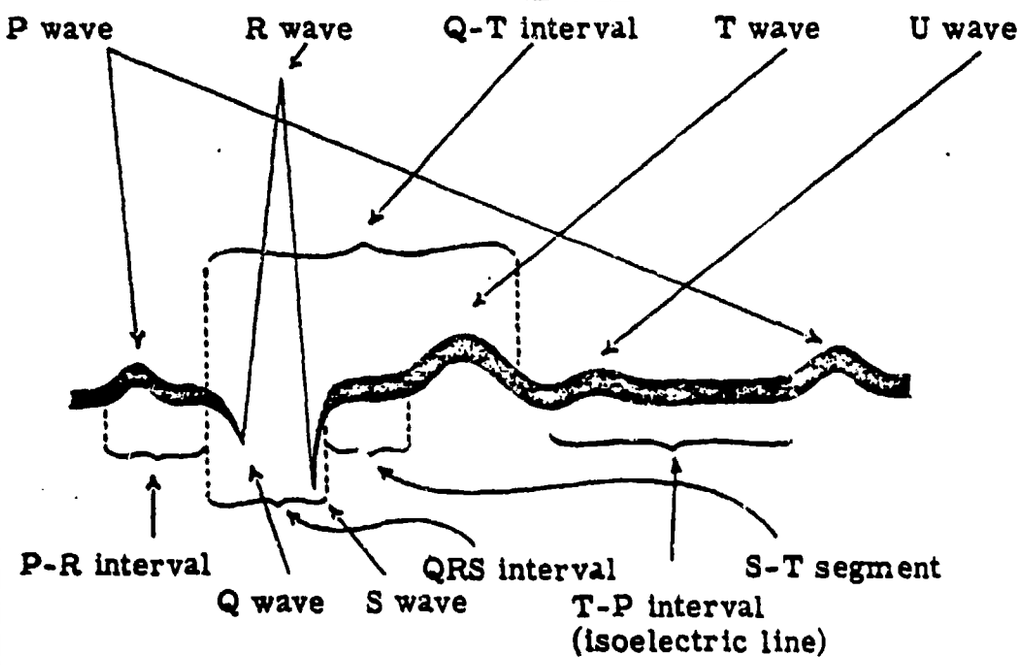


Figure 1. Normal EKG Complex

PHYSIOLOGICAL CATEGORY
- AUDITORY
- BIOMECHNL
- X CARDIOVSCL
- FORCE
- GENERAL
- LABYRINTH
- MAN.CNTRL
- PROTECTIVE
- REVIEW
- RESPIRAT'N
- SIMULATION
- VISUAL
- OTHER

AUGMENTATION DEVICES
- HELMET
- STRAPS
- AURAL
- EXTREMITY
- X LBNP
- VISUAL
- RESPIRATORY
- LACRIMATION
- TEMPERATURE
- MASK

SHEET 1 OF 1

TITLE: Protocol for Research Project "Feasibility of Using LBNP to Simulate Transient & Sustained Acceleration Forces"

REF.#118

HG-109

DATE: 3/8/76

LEAD AUTHOR: Howard, J. C.

X HUMANS - ANIMALS -

ABSTRACT

Relevant to LBNP. Memo outlines Howard's approach to a experiment to determine feasibility of rising LBNP to stimulate the vascular response of High G. A bibliography is also presented.

RELEVANCE

SALIENT DATA

1. He intended to use eight male subjects.

2. His associates for the project were to be Richard F. Haines, PHD and Ernest P. McCutcheon, M.D.

PHYSIOLOGICAL CATEGORY
- AUDITORY
- BIOMECHNL
- X CARDIOVSCL
- FORCE
- GENERAL
- LABYRINTH
- MAN.CNTRL
- PROTECTIVE
- REVIEW
- RESPIRAT'N
- SIMULATION
- VISUAL
- OTHER

AUGMENTATION DEVICES
- HELMET
- STRAPS
- AURAL
- EXTREMITY
- X LBNP
- VISUAL
- RESPIRATORY
- LACRIMATION
- TEMPERATURE
- MASK

SHEET 1 OF 1

TITLE: Precautions to Ensure the Safety of Subjects During LBNP Experimentation. (Memorandum)

REF. #119

HG-110

DATE:

LEAD AUTHOR: Howard, J.C.

X HUMANS - ANIMALS -

ABSTRACT

Relevant to LBNP. Memo by Howard to safety office at Ames.

RELEVANCE

SALIENT DATA

1. Memo contains stress analyses for the LBNP device. It also indicates a maximum pressure differential of 2 psi.
2. Also included is a system block diagram.

PHYSIOLOGICAL CATEGORY
- AUDITORY
- BIOMECHNL
- X CARDIOVSCL
- FORCE
- GENERAL
- LABYRINTH
- MAN.CNTRL
- PROTECTIVE
- REVIEW
- RESPIRAT'N
- SIMULATION
- VISUAL
- OTHER

AUGMENTATION DEVICES
- HELMET
- STRAPS
- AURAL
- EXTREMITY
- X LBNP
- VISUAL
- RESPIRATORY
- LACRIMATION
- TEMPERATURE
- MASK

SHEET 1 OF 1

TITLE:

Letter to G. J. Kron

REF. # 268

HG- 111

DATE: 2/9/78

LEAD AUTHOR:

Young, L. R.

X HUMANS - ANIMALS -

ABSTRACT

LBNP, Respiration, Visual

1. Larry suggests the use of reduced O_2 pressure in the breathing mixture to produce Hypoxia and thereby inducing the cardio-vascular effects desired by LBNP. He hypothesizes all the effects (visual etc.) may be induced in this manner.

2. He also discusses LBNP and enclosed the J. Howard documents (HG-109 & HG-110)

PHYSIOLOGICAL CATEGORY

- AUDITORY
- BIOMECHNL
- X CARDIOVSCL
- FORCE
- GENERAL
- LABYRINTH
- MAN.CNTRL
- PROTECTIVE
- REVIEW
- X RESPIRAT'N
- SIMULATION
- X VISUAL
- OTHER

AUGMENTATION DEVICES

- HELMET
- STRAPS
- AURAL
- EXTREMITY
- X LBNP
- X VISUAL
- X RESPIRATORY
- LACRIMATION
- TEMPERATURE
- MASK

RELEVANCE

SALIENT DATA

SHEET 1 OF 1

TITLE:

Sensory Motor Adaptation & After Effects of Exposure to Increased Gravitational Forces

REF.# 49

HG-121

DATE: 3/'70

LEAD AUTHOR:

Cohen, M. M.

X HUMANS - ANIMALS -

ABSTRACT

Eight subjects were exposed to accelerative forces of 2.0 G in the Navel Air Development Center human centrifuge facility. Samples of hand-eye coordination were examined both during and after exposure.

While exposed to the 2.0 G environment, subjects initially reached below, and then, above, a mirror-viewed target. When the accelerative forces were removed, transient after-effects were observed in which subjects reached still further above the target before they returned to baseline levels of accuracy. The after-effects resulted only when the subjects had an opportunity to make reaching movements while they were exposed to the increased accelerative forces. Where present, the after-effects were observed for both arms.

The data suggest that the relationship between intended motor outputs and their proprioceptive-kinasthetic consequences provides adequate information for rapid behavioral compensation and adaptation to altered accelerative forces. Further, vestibular and/or sensory-tonic factors are implicated in bringing about changes in the apparent elevation of targets viewed under increased accelerative forces.

PHYSIOLOGICAL CATEGORY

- AUDITORY
- X BIOMECHNL
- CARDIOVSCL
- X FORCE
- GENERAL
- LABYRINTH
- X MAN.CNTRL
- PROTECTIVE
- REVIEW
- RESPIRAT'N
- SIMULATION
- X VISUAL
- OTHER

RELEVANCE

Extremities

AUGMENTATION DEVICES

- HELMET
- STRAPS
- AURAL
- X EXTREMITY
- LBNP
- X VISUAL
- RESPIRATORY
- LACRIMATION
- TEMPERATURE
- MASK

SALIENT DATA

1. See abstract.
2. Elevator effect further described - Under +Gz objects appear higher than what they really are but this effect of this illusion do not become apparent until downstream in the acceleration profile and after some "neurological recalibration to increased arm weight has occurred.
3. After Gz there is recalibration process to the 1G state where 2 overreaches with not only the practiced area but the unpracticed arm (one left at rest during acceleration) as well indicating recalibration is central (neurological) rather than localized in the muscles.

SHEET 1 OF 1

TITLE: Analysis of Position Sense in Human Shoulder

REF. # 46

HG- 122

DATE:

LEAD AUTHOR: Cohen, L. A.

HUMANS - X
ANIMALS -

PHYSIOLOGICAL CATEGORY
- AUDITORY
- X BIOMECHNL
- CARDIOVSCL
- FORCE
- GENERAL
- LABYRINTH
- MAN.CNTRL
- PROTECTIVE
- REVIEW
- RESPIRAT'N
- SIMULATION
- VISUAL
- OTHER

AUGMENTATION DEVICES
- HELMET
- STRAPS
- AURAL
- X EXTREMITY
- LBNP
- VISUAL
- RESPIRATORY
- LACRIMATION
- TEMPERATURE
- MASK

ABSTRACT

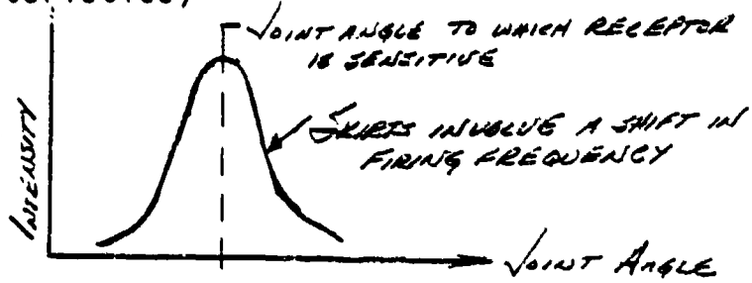
RELEVANCE

SALIENT DATA

1. Six subjects required to touch, with extended arm, eyes closed, a reference point and then lower arm and retouch the point from "memory". Reference points located in 4 concentric circles in front of subject. Error in reposition was x 1.5^0 which is considered to be the accuracy of the position sense of the shoulder.

2. Author also cites Goldscheider's finding of a movement sense threshold of the shoulder ~ 0.05 cm

3. Author also concludes that the understanding of a specific shoulder position is not provided by 1 receptor sensitive to that position but also the frequency of firing of various receptors. (joint receptors attributed the following fire characteristics)



SHEET 1 OF 1

TITLE: Effect of Gradual Onset +G_z Acceleration on Rate of Visual Field Collapse & Intraocular Pressure

REF. # 107

HG-124

DATE:

LEAD AUTHOR: Haines, R.F.

HUMANS - X
ANIMALS -

ABSTRACT

Visual, LBNP

PHYSIOLOGICAL CATEGORY
- AUDITORY
- BIOMECHNL
- X CARDIOVSCL
- FORCE
- GENERAL
- LABYRINTH
- MAN.CNTRL
- PROTECTIVE
- REVIEW
- RESPIRAT'N
- SIMULATION
- X VISUAL
- OTHER

AUGMENTATION DEVICES
- HELMET
- STRAPS
- AURAL
- EXTREMITY
- X LBNP
- X VISUAL
- RESPIRATORY
- LACRIMATION
- TEMPERATURE
- MASK

RELEVANCE

1. The rate of visual field collapse is presented for GOR of 0.5g 1 min. These data are largely irrelevant because of this. Authors reference a paper by Rositano et al which presents data for more rapid onset rates. The FOV collapse cited from that work is 1/6°/sec as compared to 0.279°/sec - 0.356°/sec results of authors work.

2. Interesting fact presented - Foveal light loss (blackout occurred before complete PLL during all eight test runs for five of the six subjects.

SALIENT DATA

SHEET 1 OF 1

TITLE: Effects of High G on Pilot Muscle Strength Available for Aircraft Control Operation

REF.# 140

HG- 128

DATE:

LEAD AUTHOR: Kroemer, K.H.E.

HUMANS - X
ANIMALS -

ABSTRACT

RELEVANCE

SALIENT DATA

Extremities

---

1. Specific data not legible. Text points out:

   a) Little formalized work in this area
   b) The obvious occurred in the centrifuge experiments:

   ia) $+G_z$ decreased available x axis force of limb

   iia) $+G_z$ increased available downward force

   iiia) $+G_z$ decreased available upward force (above 5g some subjects could not move limbs but others could contrary to prior belief).

PHYSIOLOGICAL CATEGORY
- AUDITORY
- X BIOMECHNL
- CARDIOVSCL
- FORCE
- GENERAL
- LABYRINTH
- MAN.CNTRL
- PROTECTIVE
- REVIEW
- RESPIRAT'N
- SIMULATION
- VISUAL
- OTHER

AUGMENTATION DEVICES
- HELMET
- STRAPS
- AURAL
- EXTREMITY
- LBNP
- VISUAL
- RESPIRATORY
- LACRIMATION
- TEMPERATURE
- MASK

SHEET 1 OF 1

TITLE: Testing Psychometer Performance During Sustained Acceleration

REF. [illegible]

PAGE 122

LEAD AUTHOR: Collyer, S. C.

HUMANS - X
ANIMALS -

ABSTRACT

Some material useful to our introduction. Survey covering visual light detection thresholds, contrast thresholds, lacrimation, visual acuity, tracking & piloting tasks, color shifts

---

Author notes in his conclusions:

1) Only a few studies (with disappointing results no less) which attempt to measure simultaneously G induced changes in behavioral and physiologic variables . Some researchers doubt the success of such physiologic-psychologic approaches in the near future.

2) Basic problem is the complexity in establishing the connection between behavioral integrity and integrity of the physiologic system.

3) Also notes that the physiologic indices have not been reliable or sensitive correlates to change in psychomotor efficiency-especially in complex tasks approximating operational conditions.

4) But stresses best hope of success involves study of acceleration induced hypoxia.

On fidelity of simulation: High fidelity implies good relevance to operational situation but is costly, has few test subjects, and produces difficulty in choosing an appropriate measure of performance decrement. Low fidelity (GK.-simpler?) avoids these problems.

On color shifts-few significant results found at low acceleration (less than 3G) levels.

On lacrimation:

1) Study by Creer et.al. incountered visual degradation above -14Gx due to excessive lacrimation.

2) Study by Smedal et.al. suggests blurring of vision under -Gx due to lacrimation & due above -6Gx to distortion of the placids disk reflection due to lacrimation.

RELEVANCE

SALIENT DATA

PHYSIOLOGICAL CATEGORY
- AUDITORY
- BIOMECHNL
- CARDIOVSCL
- FORCE
- X GENERAL
- LABYRINTH
- X MAN.CNTRL
- PROTECTIVE
- REVIEW
- RESPIRAT'N
- SIMULATION
- VISUAL
- X OTHER

AUGMENTATION DEVICES
- HELMET
- STRAPS
- AURAL
- EXTREMITY
- LBNP
- X VISUAL
- RESPIRATORY
- X LACRIMATION
- TEMPERATURE
- MASK

SHEET 1 OF 2

AUTHOR Collyer, S. C. REF # 50

Problems in using a piloting task as a performance measurement of G stress is the difficulty in determining the source of impairment (specific sensory or cognitive impairment?) p. 21.

Interesting point (P. 17): performance of subjects inexperienced in the G stress environment varies widely even though they were extensively trained under static conditions whereas performance degradation of experienced subjects was predictable.

Under G stress (P. 16) pilots tend to concentrate on most demanding single task (pitch control for instance) and ignore simpler tasks (yaw control) with consequent large error build up in the simpler tasks.

Recommendations, developed for the USAF School of Aerospace Medicine (SAM), concern a human psychomotor performance task which could be used to monitor, on a moment-to-moment basis, an operator's ability to perform satisfactorily during sustained acceleration stress. First, a survey was made of the literature on logic and behavior changes during acceleration. Next, an experimental program was planned and carried out, in which candidate tasks were evaluated under conditions of hypoxia and alcohol intoxication. Final recommendations were then made for: (a) a running memory task to measure a decrement in cognitive skills; and (b) an automated testing system, for installation on the SAM centrifuge, suitable not only for the recommended test but also for many other diversified tasks.

SHEET 2 OF 2

TITLE: Systems Analysis of Physiological Performance Related to Stresses such as those Experienced in High Performance Aircraft.

REF.# 250

HG- 137

DATE:

LEAD AUTHOR: Walters, R. F.

HUMANS - X
ANIMALS -

ABSTRACT

Cardiovascular, respiratory, LBNP .

. Author states that in an exercise environment, which would probably be the case in a simulator cockpit, the movement artifacts cause difficulty with most noninvasive blood pressure monitoring devices. U. C. Davis has therefore relied primarily on the use Doppler ultrasound & Korotkov sounds in a manual mode.

. Heart rate data is also subject to the effects of artifacts. The use of a NASA supplied R-wave detector has mitigated these considerably.

. A cardiorespiratory steady state model was limited to use in nonexercise mode. Gair & phase indicate a first order system with t = 6 min. The response to dynamic exercise is linear up to 70% of VO_2 max. As workload increases t increases . Stroke volume unimportant at work loads < 70% VO_2 max.

. The ventilatory response to exercise is influenced by the degree of proprioceptor activity in the working links.

RELEVANCE

A final summary of contract work performed during the five year period October 1, 1972 through September 30, 1976 is presented . Results of the contract include significant findings in information systems technology, physiology of exercise, and instrumentation associated with human subject experiments in human physical performance.

SALIENT DATA

PHYSIOLOGICAL CATEGORY
- AUDITORY
- BIOMECHNL
- X CARDIOVSCL
- FORCE
- GENERAL
- LABYRINTH
- MAN.CNTRL
- PROTECTIVE
- REVIEW
- X RESPIRAT'N
- SIMULATION
- VISUAL
- OTHER

AUGMENTATION DEVICES
- HELMET
- STRAPS
- AURAL
- EXTREMITY
- XLBNP
- VISUAL
- XRESPIRATORY
- LACRIMATION
- TEMPERATURE
- MASK

SHEET 1 OF 1

TITLE:

Environment Modification for Human Performance

REF.# 241

HG- 144

DATE:

LEAD AUTHOR: Trumbull, R.

HUMANS - X
ANIMALS -

ABSTRACT

No abstract available at this time.

Very general survey covering many other environmental inpacts other than acceleration.

PHYSIOLOGICAL CATEGORY
- AUDITORY
- BIOMECHNL
- CARDIOVSCL
- FORCE
- XGENERAL
- LABYRINTH
- MAN.CNTRL
- PROTECTIVE
- REVIEW
- RESPIRAT'N
- SIMULATION
- VISUAL
- OTHER

SALIENT DATA

RELEVANCE

1. Author references a study by Hendler where "as ambient, and skin temperature decreased, tactile sensitivity also decreased." Notes that a similiar symptom occurs at high temperatures.

AUGMENTATION DEVICES
- HELMET
- STRAPS
- AURAL
- EXTREMITY
- LBNP
- VISUAL
- RESPIRATORY
- LACRIMATION
- TEMPERATURE
- MASK

SHEET 1 OF 1

TITLE: Relation of Signal Light Intensity to Physiologic Endpoints During $+G_z$ Acceleration

REF.# 207

HG- 150

DATE:

LEAD AUTHOR: Rogge, J. D.

HUMANS - X
ANIMALS -

ABSTRACT

Results of previous studies suggest that lowering the luminance of the signal lights lowers the blackout and grayout level during $+G_z$ acceleration. In this study, variations in luminance of the central and peripheral signal lights in the range that is suitable for routine centrifuge operation failed to produce any detectable change in blackout or grayout levels. The visual phenomena described in the previous studies may have risen mainly from such local changes in the eye as changes in visual threshold, retinal metabolism, and visual acuity; whereas, blackout obtained with light intensities used in this study resulted from hemodynamic changes caused by $+G_z$ acceleration and possibly some local changes in the eye itself.

RELEVANCE

Cardiovascular, visual

SALIENT DATA

1. Data is presented relating luminance, G_z level and blackout & greyout. Four subjects were used. The centrifuge was programmed to provide a series of ROR rides (1 g/sec & 15 sec plateau) and GOR rides (.07 g/sec) until the endpoint was reached.

2. The results of these data analyses showed no trends toward higher or lower end points as a function of luminance. The variation between light settings is no greater than the variation among the control runs done at constant light setting.

3. These results differ from the results of previous studies. The authors speculate that this may be due to the fact that in previous work the luminance was close to the visual threshold & (luminances for these tests .01 $\leq$ periph $\leq$ 100 & 0.12 $\leq$ and $\leq$ 120 foot-lamberts). According to the authors, White (WADD 60-34) has shown that the visual threshold itself increases with increase in $+G_z$. Authors state that studies in which very bright light sources have been used have shown that there is still some visual capability left in blackout and perhaps even in unconsciousness.

PHYSIOLOGICAL CATEGORY
- AUDITORY
- BIOMECHNL
- X CARDIOVSCL
- FORCE
- GENERAL
- LABYRINTH
- MAN.CNTRL
- PROTECTIVE
- REVIEW
- RESPIRAT'N
- SIMULATION
- X VISUAL
- OTHER

AUGMENTATION DEVICES
- HELMET
- STRAPS
- AURAL
- EXTREMITY
- LBNP
- X VISUAL
- RESPIRATORY
- LACRIMATION
- TEMPERATURE
- MASK

SHEET 1 OF 1

TITLE:
Th^ Effect of Positive Acceleration (G) on the R ation Between Illumination and Dial Reading

REF. #258

HG- 152

DATE:

LEAD AUTHOR: White, W. S.

HUMANS - X
ANIMALS -

ABSTRACT

No abstract available at this time.

Visual dimming as a function of G for both visual scene and instruments.

RELEVANCE

1. Dial reading performance not affected by G above 42 f.l. illumination (1-4g region).

2. Dial reading performance definitely affected in the 0.1 - 1.0 fl. region. Cross plot of data given (for constant performance to find effective illumination vs G) yeilds well behaved plot - see attached sheet. This illumination attention factor should probably be washed out as illumination 42 f.L. from 1 f.L. If washed out however not sure what function to use for dimming as we enter blackout.

SALIENT DATA

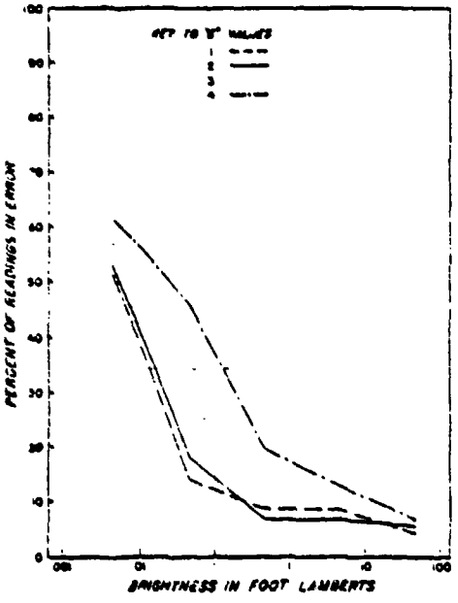


FIG. 2. Percentage of readings in error as a function of brightness level for each g value.

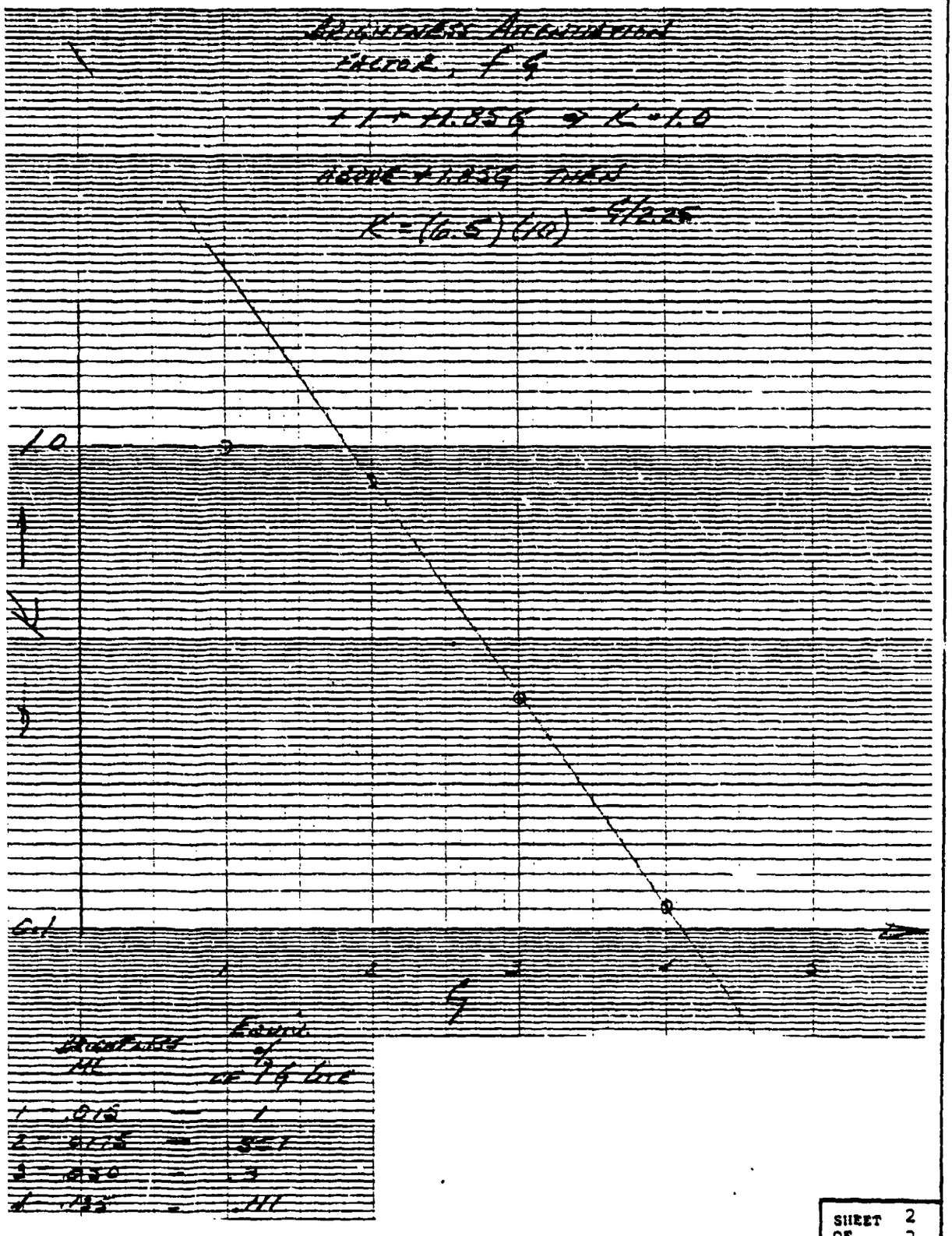
PHYSIOLOGICAL CATEGORY
- AUDITORY
- BIOMECHNL
- CARDIOVSCL
- FORCE
- GENERAL
- LABYRINTH
- MAN.CNTRL
- PROTECTIVE
- REVIEW
- RESPIRAT'N
- SIMULATION
- X VISUAL
- OTHER

AUGMENTATION DEVICES
- HELMET
- STRAPS
- AURAL
- EXTREMITY
- LBNP
- XVISUAL
- RESPIRATORY
- LACRIMATION
- TEMPERATURE
- MASK

SHEET 1 OF 2

AUTHOR White, W. S.

REF # 258



SHEET 2 OF 2

TITLE:

Acceleration Effects on the Ability to Activate Emergency Devices in F4 Aircraft

REF. # 69

HG- 156

DATE:

LEAD AUTHOR:

Fessenden, E.

HUMANS - X
ANIMALS -

ABSTRACT

Experiments have been performed and are described in this report which measure the influence of environment on the time it takes to reach an emergency control activation device and which measure the change of physical position at the time of activation due to the environmental forces. Data are reported for both loose and tight torso harness straps. Minus G_x and minus G_z are identified as the components of various likely emergency environments which cause pilots the greatest difficulties.

The contribution of combined individual anthropometric measures has been identified as having pronounced influence on the reach ability of certain control devices under specific environments. Improvements in existing seat harness systems and testing for future systems to be developed are recommended.

PHYSIOLOGICAL CATEGORY

- AUDITORY
- X BIOMECHNL
- X CARDIOVSCL
- FORCE
- GENERAL
- LABYRINTH
- MAN.CNTRL
- PROTECTIVE
- REVIEW
- RESPIRAT'N
- SIMULATION
- VISUAL
- OTHER

AUGMENTATION DEVICES

- X HELMET
- X STRAPS
- AURAL
- X EXTREMITY
- LBNP
- VISUAL
- RESPIRATORY
- LACRIMATION
- TEMPERATURE
- MASK

RELEVANCE

Shoulder straps, extremity movement, and helmet.

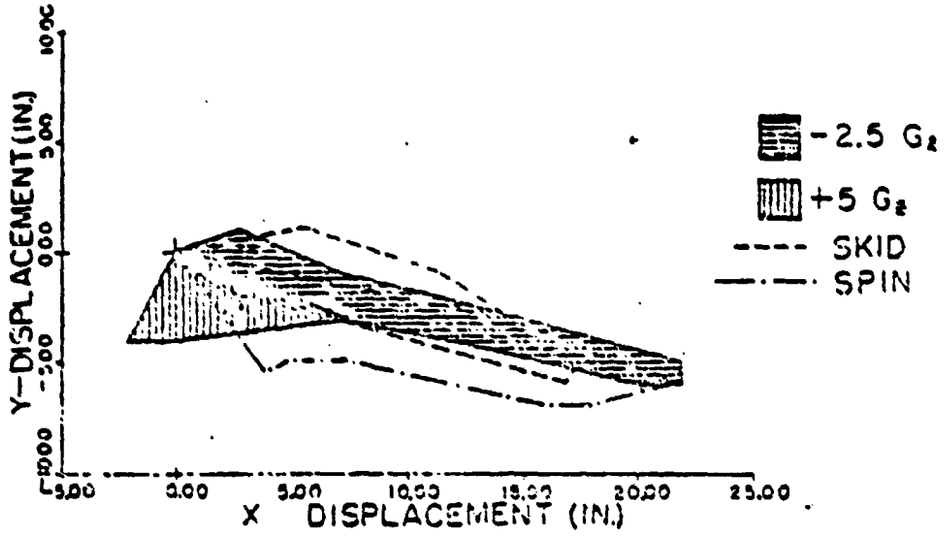
SALIENT DATA

1. Very little data of direct use to our needs. Most extremity movement deals with ability to reach a control and not accuracy in reaching the control under High G nor is force reduction data as a function of G presented in a form useful to us. Strap forces are not given.

2. There is considerable data given on the envelope of helmet and shoulder movement extent at various G levels in G_z and G_x.

AUTHOR Fessenden, E. REF # 69

HEAD POSITIONS



SHOULDER POSITIONS

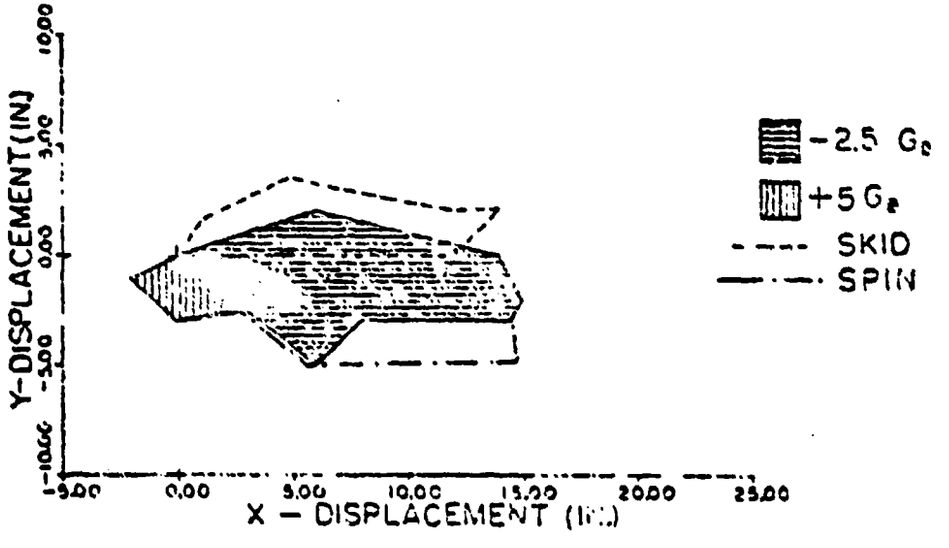


FIGURE 6 - Environmental Envelopes (Loose Straps).

SHEET 2 OF 2

TITLE: Human Musculoskeletal Tolerance Limits to Ejection and Related High Mechanical Stress Environments

REF.# 29

HG- 157

DATE:

LEAD AUTHOR: Burstein, A. H.

HUMANS - X
ANIMALS -

ABSTRACT

No abstract is available at this time.

Extremities - Joint stiffness.

No data that we could use.

RELEVANCE

SALIENT DATA

PHYSIOLOGICAL CATEGORY
- AUDITORY
- X BIOMECHNL
- CARDIOVSCL
- FORCE
- GENERAL
- LABYRINTH
- MAN.CNTRL
- PROTECTIVE
- REVIEW
- RESPIRAT'N
- SIMULATION
- VISUAL
- OTHER

AUGMENTATION DEVICES
- HELMET
- STRAPS
- AURAL
- X EXTREMITY
- LBNP
- VISUAL
- RESPIRATORY
- LACRIMATION
- TEMPERATURE
- MASK

SHEET 1 OF 1

TITLE:
Exploratory Investigation of the Man Amplifier Concept.

REF.: 40

HG- 158

DATE:

LEAD AUTHOR: Clark, D. C.

HUMANS - X
ANIMALS -

ABSTRACT

Preliminary investigations were conducted to ascertain and define some of the major problems and uncertainties requiring additional research before feasibility of the Man Amplifier concept can be evaluated. Study areas included carrying capability human factors from the standpoints of body kinematics and physical anthropology, structures and mechanical design, and servo system and power requirements. The dynamic response characteristics of an elbow-joint amplifier, as determined theoretically and experimentally, were compared. Comparison of position tracking tests performed both with and without power boost provided by the elbow-joint servo indicated that employment of power boost did not increase the tracking error above that exhibited by the unaided operation. It was concluded that: (1) duplication, in the Man Amplifier, of all the human joint motion capability is impractical; (2) experimentation is necessary to determine the essential joints, motion ranges, and dynamic responses; (3) the inability to connect the overturning moments will, in many instances, limit the load-handling capability; (4) conventional valve controlled hydraulic servos are unsuitable for the Man Amplifier, (5) particularly difficult problems will be encountered in the general areas of mechanical design, sensors, and servo-mechanisms. Some specific tasks that should be undertaken to assess engineering feasibility of the concept are outlined.

Extremities

RELEVANCE

1. Contains positional trace of maximum effort elbow flexion & extension.

2. Otherwise, not much data pertinant to our needs.

3. Note: Hydraulics ruled out because of power supply needed, not due to response etc.

SALIENT DATA

PHYSIOLOGICAL CATEGORY
- AUDITORY
- X BIOMECHNL
- CARDIOVSCL
- FORCE
- GENERAL
- LABYRINTH
- MAN.CNTRL
- PROTECTIVE
- REVIEW
- RESPIRAT'N
- SIMULATION
- VISUAL
- OTHER

AUGMENTATION DEVICES
- HELMET
- STRAPS
- AURAL
- X EXTREMITY
- LBNP
- VISUAL
- RESPIRATORY
- LACRIMATION
- TEMPERATURE
- MASK

SHEET 1 OF 2

AUTHOR Clark, D. C.

REF # 40

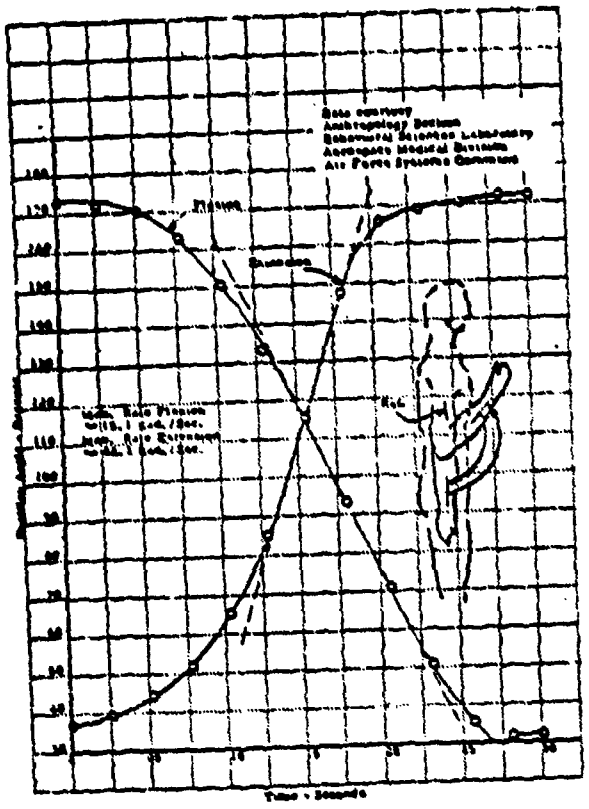


Figure 3 Maximum-Effort Flexion and Extension of Right Elbow

SHEET 2
OF 2

TITLE: Arterial Tonometry for the Atraumatic Measurement of Arterial Blood Pressure.

REF.# 230

HG- 159

DATE:

LEAD AUTHOR: Stein, P. D.

HUMANS - X
ANIMALS -

ABSTRACT

A new method of arterial tonometry was developed. This noninvasive technique is based on the principle that displacement of a mechanical force-sensing device located over a superficial artery can be made to be proportional to blood pressure (BP) within the artery. The particular advantage of the method is that instantaneous and transient variations of blood pressure can be observed and the configuration of wavenorms can be recorded. In normotensive patients, peak systolic or diastolic BP changes of 30% or less from control values correlated linearly with intra-arterial BP ($P < 0.001$). Increments of greater magnitude were indicated by prominent changes, but did not show this linear correlation. Absolute immobility of the extremity and transducer was required for satisfactory measurements. This constituted a practice problem. The method seems potentially suited for the atraumatic measurement of transient effects of drugs or physiological interventions, or for the continuous monitoring of arterial BP during surgery.

RELEVANCE

LBNP, visual, Indirect BP Measurement

SALIENT DATA

Authors investigate the use of a tonometer for measuring blood pressure in superficial arteries, non-invasively. The device is a force transducer placed over the vessel. It operates on the principle that the force measured is proportional to the pressure in the artery. This method provides good results in continuous fashion however the method is rendered unusable by the constraint that the limb containing the artery must be maintained immobile.

PHYSIOLOGICAL CATEGORY
- AUDITORY
- BIOMECHNL
- X CARDIOVSCL
- FORCE
- GENERAL
- LABYRINTH
- MAN.CNTRL
- PROTECTIVE
- REVIEW
- RESPIRAT'N
- SIMULATION
- X VISUAL
- OTHER

AUGMENTATION DEVICES
- HELMET
- STRAPS
- AURAL
- EXTREMITY
- X LBNP
- X VISUAL
- RESPIRATORY
- LACRIMATION
- TEMPERATURE
- MASK

SHEET 1 OF 2

AUTHOR Stein, P. D.

REF # 230

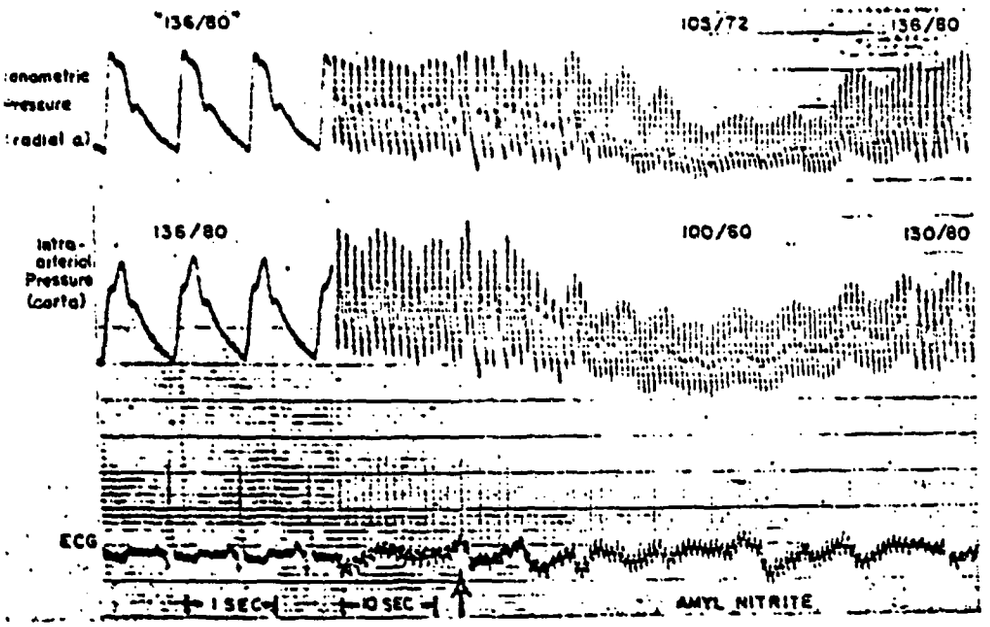


FIG. 1. Simultaneous tonometric pressure (*top*), aortic pressure (*middle*), and electrocardiogram (ECG, *bottom*). After amyl nitrite inhalation (arrow), tonometric and aortic systolic pressures showed similar decrements. Drop in tonometrically recorded diastolic pressure was somewhat less prominent.

SHEET 2 OF 2

TITLE:

Blood Pressure Measurement with Doppler Ultrasonic Flowmeter

REF. #132

HG-160

DATE:

LEAD AUTHOR:

Kazamias, T.M.

HUMANS - X
ANIMALS -

ABSTRACT

The frequency shift of sound scattered from blood moving within a superficial vessel has been shown to provide a reliable indication of blood flow velocity. This approach appears to be more sensitive than indirect sphygmomanometers utilizing Korotkoff sounds but hitherto it has not been directly validated. A transducer was applied to the skin over the radial artery and the Doppler signal was radiotelemetered and recorded together with pressure from a proximal cuff. The pressure at which arterial flow resumed during cuff deflation measured systolic pressure and the cuff pressure at which diastolic flow was sustained measured diastolic pressure. Brachial arterial pressure was measured through an indwelling arterial needle in the opposite arm. In 65 measurements in 12 subjects in whom arterial pressure was lowered from normal levels by amyl nitrite inhalation, the Valsalva maneuver, or partial occlusion of the brachial artery, the correlation coefficient was 0.991 for systolic pressure and 0.905 for diastolic pressure. The maximum error was 10 mm Hg in these studies. In five patients in clinical hypotension and shock, the Doppler ultrasonic flowmeter was shown to be superior to standard sphygmomanometry and to indicate accurately systolic pressure at values as low as 44 mm Hg. It is concluded that the Doppler method provides a sensitive and accurate noninvasive approach for the semicontinuous measurement of systemic arterial pressure.

RELEVANCE

Monitoring, non invasively, of blood pressure for LBNP & visual effects.

SALIENT DATA

1. Authors compare results using a transcutaneous Doppler ultrasonic flowmeter to results using an indwelling artinal needle connected to a pressure transducer. The output of the flowmeter is fed through signal processing equipment & a frequency analyzer.

PHYSIOLOGICAL CATEGORY
- AUDITORY
- BIOMECHNL
- X CARDIOVSCL
- FORCE
- GENERAL
- LABYRINTH
- MAN.CNTRL
- PROTECTIVE
- REVIEW
- RESPIRAT'N
- SIMULATION
- X VISUAL
- OTHER

AUGMENTATION DEVICES
- HELMET
- STRAPS
- AURAL
- EXTREMITY
- X LBNP
- X VISUAL
- RESPIRATORY
- LACRIMATION
- TEMPERATURE
- MASK

SHEET 1 OF 2

AUTHOR Kazamias, T. M. REF # 132

2. The results show significant correlation. The method, however, still requires a pressure cuff to record systolic & diastolic pressures. The only apparent advantage of this method over the syphymomanometer is that the frequency shift for velocity changes is more reliable than the Korotkoff sounds.

SHEET 2 OF 2

TITLE: Effect of Moderate Positive Acceleration (G) on Ability to Read Aircraft-Type Instrument Dials

REF.# 251

HG- 164

DATE:

LEAD AUTHOR: Warrick, M. J.

HUMANS -X
ANIMALS -

ABSTRACT

No abstract is available at this time.

Visual - Instruments

RELEVANCE

1. Very early work (centrifuge) to determine if there is progressive degradation in reading instruments at G levels lower than that crossing blackout. 3 G selected and findings were limited to simple answer yes 3 G produced increased error in reading instruments. No significant attempt made to explain why error increased from 18% @ 1.5 G to 24% @ 3 G.

2. Authors note at increased G the subject may experience a dimming of a bright light. Peripheal vision is lost (?-no definition of lost) and finally blackout occurs however subject is still conscious.

SALIENT DATA

PHYSIOLOGICAL CATEGORY
- AUDITORY
- BIOMECHNL
- CARDIOVSCL
- FORCE
- GENERAL
- LABYRINTH
- MAN.CNTRL
- PROTECTIVE
- REVIEW
- RESPIRAT'N
- SIMULATION
- X VISUAL
- OTHER

AUGMENTATION DEVICES
- HELMET
- STRAPS
- AURAL
- EXTREMITY
- LBNP
- X VISUAL
- RESPIRATORY
- LACRIMATION
- TEMPERATURE
- MASK

SHEET 1 OF 1

TITLE: Human Carotid Artery Wall Thickness, Diameter & Blood Flow by Non-Invasive Techniques

REF.# 190

HG- 166

DATE:

LEAD AUTHOR: Olson, Robert M.

HUMANS - X
ANIMALS -

SALIENT DATA

RELEVANCE

LBNP, visual indirect BP measurement

ABSTRACT

Olson, Robert M. Human carotid artery wall thickness diameter, blood flow by a noninvasive technique. J. Appl. Physiol. 37(6):955-1974-This paper presents a technique tested in vitro and dogs a.d used in humans to measure carotid artery wall thickness blood flow, and diameter continuously by piacing a transducer on the skin over the artery. The transducer consists of a pulse echo crystal used to locate the carotid artery and measure its diameter and wall thickness. It also has a pair of Doppler shift crystals used to measure the velocity of blood flow in the vessel In a typical case, the diastolic inside diamete the carotid artery was 8.C mm, diastolic wall thickness 600, systolic inside diameter 8.6 mm and pulsatile wall thinning 100mm. The peak blood flow varied inversely with pulse rate. Occlusion of one carotid resulted in an increase in diastolic but not systolic flow in the other.

Method combines the use of pulse echo for artery diameter measurement and aiming of the Doppler shift ultrasonic transducer which measures the blood flow & velocity and the arterial wall velocity. BP is not presently an output. While this method appears to be promising at present the appropriate signal processing and analysis hardware is not available. However, simple calibration on each subject premission may be sufficient. Somebody probably should continue to develop this technique.

PHYSIOLOGICAL CATEGORY
- AUDITORY
- BIOMECHNL
- X CARDIOVSCL
- FORCE
- GENERAL
- LABYRINTH
- MAN.CNTRL
- PROTECTIVE
- REVIEW
- RESPIRAT'N
- SIMULATION
- X VISUAL
- OTHER

AUGMENTATION DEVICES
- HELMET
- STRAPS
- AURAL
- EXTREMITY
- X LBNP
- X VISUAL
- RESPIRATORY
- LACRIMATION
- TEMPERATURE
- MASK

SHEET 1 OF 1

TITLE: Estimation of Retinal Blood Flow by Measurement of the Mean Circulation Time.

REF.# 27

HG- 170

DATE:

LEAD AUTHOR:
Bulpit, C. J.

HUMANS - X
ANIMALS -

ABSTRACT

A method is described for measuring the segmental mean circulatory time and estimating the segmental flow in the human retina. Serial retinal photographs were taken after intravenous fluorescein injection and the relative concentration of fluorscein in the superior temporal artery and vein calculated from measurements of the optical density of the vessel images. Arterial and venous time-concentration curves were constructed and the mean circulation time calculated. In normal subjects the mean circulation time in the superior temporal segment varied from 1.39 to 6.85 sec. This variation was largely explained by variations in the volume of the vascular bed which was taken to be relative to the sum of the square of arterial and venous diameters. Volume flow shows less than a two-fold variation in normal subjects, mean 55 ± SD 11 units/sec. Similar results for volume flow were found in hypertensive subjects although flow was more variable in these patients, mean 54 ± 18 units/sec. Some anaemic patients showed a marked increase in volume flow, and there was a significant relationship between packed cell volume and retinal volume flow ($R = 0.65$, $P = 0.01$).

RELEVANCE

Not relevant to this study

SALIENT DATA

Method requires extensive calibration of each subject and the injection of fluorescein dye. Further, a camera is required to photograph the retina.

PHYSIOLOGICAL CATEGORY
- AUDITORY
- BIOMECHNL
- X CARDIOVSCL
- FORCE
- GENERAL
- LABYRINTH
- MAN.CNTRL
- X PROTECTIVE
- REVIEW
- RESPIRAT'N
- SIMULATION
- VISUAL
- OTHER

AUGMENTATION DEVICES
- HELMET
- STRAPS
- AURAL
- EXTREMITY
- X LBNP
- X VISUAL
- RESPIRATORY
- LACRIMATION
- TEMPERATURE
- MASK

SHEET 1 OF 1

TITLE: Comparison of the Protective Value of an Anti-Blackout Suit on Subjects in an Airplane & on the Mayo Centrifuge.

REF. #150
HG-171
DATE:

LEAD AUTHOR: Lambert, E. H.

HUMANS - X
ANIMALS -

ABSTRACT

No abstract is available at this time.

Cardiovascular, LBNP, visual protective devices.

---

1. Data are presented on various levels of visual degradation as a function of acceleration, w/o an anti G-Suit, both in the Mayo centrifuge & in an airplane (Ra-24a). The data are both continuous & discrete. The author implies the accelerations have been transferred to the subjects head. This is important because of the short arm of the Mayo Centrifuge ($\simeq$13'). Some average values are:

	CLEAR	DIM	PLL	BO	
Control	2.7g	3.0g	3.3	3.8	CENTRIFUGE
Anti-G Suit	3.5	4.1	4.3	5.0	
Control	3.2	3.7	4.0	4.5	AIRPLANE
Anti-G Suit	4.5	4.9	5.0	5.5	

2. Also presented are data on ear pulse & ear opacity. The author concludes that there is no statistically significant differences in the effect of the anti-blackout suit between the airplane and centrifuge. The anti-G Suit used was G-4 (Z-1).

RELEVANCE

SALIENT DATA

PHYSIOLOGICAL CATEGORY
- AUDITORY
- BIOMECHNL
- X CARDIOVSCL
- FORCE
- GENERAL
- LABYRINTH
- MAN.CNTRL
- X PROTECTIVE
- REVIEW
- RESPIRAT'N
- SIMULATION
- X VISUAL
- OTHER

AUGMENTATION DEVICES
- HELMET
- STRAPS
- AURAL
- EXTREMITY
- X LBNP
- X VISUAL
- RESPIRATORY
- LACRIMATION
- TEMPERATURE
- MASK

SHEET 1 OF 1

TITLE: Prolonged Linear and Radial Accelerations Chapter 5 of Foundations of Space Biology and Medicine.

REF. # 244

HG-172

DATE:

LEAD AUTHOR: Vasil'yev, P. V., Kotovskaya, A. R.

HUMANS - X
ANIMALS -

ABSTRACT

Cardiovascular data
References to lacrimation
Vision effects
Bioelectric activity of myocardium reduces with G suit usage

RELEVANCE

1) Authors stress the importance of the aorta-retina angle of 15^0 (13^0-18^0).

2) Vision disruption (fogging loss of acuity) attributed to "abundant" lacrimation in -Gx and relate this indirectly to levels of -8Gx.

3) "No correlation has been found between increases in cardiac rhythm and tolerance to +Gx forces." Progressive bradycardial may occur at various heart rates degrading heart rate as a predictor of tolerance.

4) Vision disruption in +Gx is characterized by the authors to be "..grey veil, fog, whitish fog, looking through rain or fog.." note word 'through'.

5) Cardiovascular compensatory reactions have a time response of 8-12 sec. (GK-in contrast to the 5 sec stated in HG 191) and some recovery is experienced under continued acceleration, when such compensation occurs.

6) Authors state -Gx loss of acuity due to lacrimation and note Smedal et.al. tested for cornea deformation and found none.

SALIENT DATA

7) Re: light stimulus thresholds-central vision:
Threshold 2 times 1 Gz level at 3 Gz
Threshold 3.4 times 1 Gz level at 4 Gz.
Peripheral vision:
Threshold 1.5 times 1 G_z level at $2G_z$
Threshold 3 times 1 G_z level at $3G_z$
Threshold 4 times 1 G_z level at $4G_z$

8) Critical point of hypoxia application is at the sympathetic connections of the ganglionic and bipolar cells of the retina (GK-think later Duane may have altered this opinion).

9) Vision maintained only when blood pressure (retina) is above 22-23 mm Hg.

PHYSIOLOGICAL CATEGORY
- AUDITORY
- BIOMECHNL
- X CARDIOVSCL
- FORCE
- X GENERAL
- LABYRINTH
- MAN.CNTRL
- X PROTECTIVE
- REVIEW
- X RESPIRAT'N
- SIMULATION
- VISUAL
- OTHER

AUGMENTATION DEVICES
- HELMET
- STRAPS
- AURAL
- EXTREMITY
- X LBNP
- X VISUAL
- X RESPIRATORY
- X LACRIMATION
- TEMPERATURE
- MASK

SHEET 1 OF 1

TITLE: Lighting, Integral, Red, Aircraft Instrument, General Specification for; MIL-L-25467D and Lighting, Instrument, Integral, White General specification for; MIL-L-27160C.

REF. #172

HG-173

DATE:

LEAD AUTHOR: U. S. Government

HUMANS - X
ANIMALS -

ABSTRACT

No abstract is available at this time.

Data for cockpit instrument dimming due to visual effects.

RELEVANCE

SALIENT DATA

1. White light illumination (MIL-L-27160C)
   * 3.3.5 Brightness, When 4.50 +0.050V are applied to the lighting terminals, the light intensity and distribution shall be as follows·

   a. White areas: 1.00 ±0.50 foot,lambert.

   b. Gray area: 0.06 ±0.30 foot-lambert.

   c. Black areas: 0.05 ±0.03 foot-lambert when reflected light (wedg and ring lighting) is used and 0.04 ±0.02 foot-lambert for refracted light (back lighting).

   d. Pointer, lubber lines, command bars, miniature airplane symbols, diviation bards, and other similar reference marks: 1.20 ±0.50 foot-lambert.

   e. Red areas: 1.00 ±0.05 foot-lambert.

   The brightness of other colors and the selection of colors shall be governed by their relative brightness in daylight and shall be subject to the approval of the procuring activity. When no other guidance is available, the birghtness of these other colored areas shall be 1.00 ±0.05 foot-lambert.

2. Red light illumination (MIL-L-25467D)
   3.3.8 Brightness. When 5.00 ±0.10V or 115 ±2V, 400 ±20 Hz are applied to the lighting terminals, whichever is applicable, the light intensity and the light distribution of the lighting system shall be such that the brightness of the presentation shall conform to Table I. For any single display markings. In no case shall the brightness of the pointer and lubber line exceed 1.7 foot lamberts.

PHYSIOLOGICAL CATEGORY
- AUDITORY
- BIOMECHNL
- CARDIOVSCL
- FORCE
- GENERAL
- LABYRINTH
- MAN.CNTRL
- PROTECTIVE
- REVIEW
- RESPIRAT'N
- SIMULATION
- X VISUAL
- OTHER

AUGMENTATION DEVICES
- HELMET
- STRAPS
- AURAL
- EXTREMITY
- LBNP
- X VISUAL
- RESPIRATORY
- LACRIMATION
- TEMPERATURE
- MASK

SHEET 1 OF 2

TABLE I. Photometric Brightness

Daylight Color	Incandescent Lighting System Brightness (Foot-Lamberts)	Electroluminescent Lighting System Brightness (Foot-Lamberts)
White - (Markings)....	1.0 ± 0.5	0.5 ± 0.2
White - (Pointer and Lubber Lines)	1.2 ± 0.5	0.5 ± 0.2
Transilluminated		
Gray - (Background)....	0.6 ± 0.3	0.2 ± 0.1
Black -(Background)	0.04 ± 0.2	0.02 ± 0.01

TITLE: Head and Neck Mobility of Pilots Measured at the Eye.

REF.: 37

IIG- 174

DATE:

LEAD AUTHOR: Champion, M. C.

HUMANS - X
ANIMALS -

ABSTRACT

1. The mean harness tensions chose by pilots on initial strap-in were in most cases greater with winter than summer AEA.

   Mean initial tensions:

Leg straps	5-2 lb	Summer AEA
Shoulder straps	5-7 lb	
Leg Straps	7-6 lb	Winter AEA
Shoulder straps	8-3 lb	

2. During a run the mean tensions required to restrain the subject's back and shoulder movement were increased by 1½ to 2 lb more than the initial tensions.

RELEVANCE

A study of the head and neck mobility of nine selected pilot subjects has been made by measuring the movement envelope of the pilot's eye position as he cranes his head and neck up, down and side to side. During these movements the subjects looked forward at a target board through a sight aperture. The subjects were strapped into an ejection seat instrumented to monitor harness tension and were clothed in standard RAF summer and winter aircrew equipment assemblies. The effects of wearing a standard RAF Mark 2/3 flying helmet, and differences between movement with summer and winter flying clothing have been assessed.

SALIENT DATA

Shoulder harness tension given for initial comfortable strap in and then once retightened such that there is no appreciable movement of his 7th cervical vertebrae when head craned forward. Data may also be applicable to head/helmet motion.

PHYSIOLOGICAL CATEGORY
- AUDITORY
- X BIOMECHNL
- CARDIOVSCL
- X FORCE
- GENERAL
- LABYRINTH
- MAN.CNTRL
- PROTECTIVE
- REVIEW
- RESPIRAT'N
- SIMULATION
- X VISUAL
- OTHER

AUGMENTATION DEVICES
- HELMET
- STRAPS
- AURAL
- EXTREMITY
- LBNP
- X VISUAL
- RESPIRATORY
- LACRIMATION
- TEMPERATURE
- MASK

SHEET 1 OF 2

Subject	Tensions on Initial Strap-In (lb) Left Shoulder	Tensions on Initial Strap-In (lb) Right Shoulder	Tensions with Straps Readjusted (lb) Left Shoulder	Tensions with Straps Readjusted (lb) Right Shoulder	Mean Tensions at Start of Each Run (lb) Left Shoulder	Mean Tensions at Start of Each Run (lb) Right Shoulder	Clothing
1	5.3	4.2	3.6	5.9	5.0	6.1	
2	2.8	6.3	5.4	11.8	4.4	9.9	
3	14.0	9.0	16.0	10.5	14.3	10.0	
4	4.9	18.9	5.9	16.4	4.0	13.2	Summer
5	4.1	3.7	6.1	4.5	6.9	6.4	
6	3.5	3.7	2.3	2.3	2.4	5.4	
7	1.6	2.1	2.3	1.8	3.6	2.9	
8	12.5	13.0	16.5	23.0	15.1	19.8	
9	2.8	12.5	5.2	22.8	6.6	25.9	
Mean	5.7	8.1	7.1	10.9	6.9	11.1	
1	6.1	6.3	5.7	6.4	4.8	5.7	
2	6.6	13.5	4.4	9.8	5.4	10.4	
3	14.2	11.7			13.4	9.6	
4	2.4	11.5	2.3	10.4	2.9	9.8	Winter
5	8.2	13.4	12.4	9.3	6.7	8.7	
6	4.1	6.1			3.1	4.9	
7	4.2	1.1	8.0	4.1	5.5	2.3	
8	11.0	9.5	10.5	24.5	12.5	17.1	
9	5.0	14.4	9.1	21.2	7.4	23.1	
Mean	6.8	9.7	7.5	13.8	6.9	10.2	

AUTHOR Champion, M. C.

SHEET OF 2

REF. # 37

TITLE: General Performance Specification Lighting, Instrument, Integral White; Sepcification Nos 16ZF031 and 16ZF032.

REF.: 78

HG-175

DATE:

LEAD AUTHOR: General Dynamics

HUMANS - X
ANIMALS -

ABSTRACT

No abstract is available at this time.

Instrument Dimming

---

1. Pretty much the same data is included in MIL-L-24567D and MIL-L-27160C except additional areas covered: a) lamps other than MS24367-715 A515, MS90451-7152 or MS90452-7153 shall be illuminated to 0.1 ±0.05 foot lamberts @ 2.7 vdc. b) Knob markings illuminated to 0.8 foot lamberts .c) Yellow emergency markings illuminated to 0.35 ±0.15 foot lamberts.

RELEVANCE

PHYSIOLOGICAL CATEGORY
- AUDITORY
- BIOMECHNL
- CARDIOVSCL
- FORCE
- GENERAL
- LABYRINTH
- MAN.CNTRL
- PROTECTIVE
- REVIEW
- RESPIRAT'N
- SIMULATION
- X VISUAL
- OTHER

AUGMENTATION DEVICES
- HELMET
- STRAPS
- AURAL
- EXTREMITY
- LBNP
- X VISUAL
- RESPIRATORY
- LACRIMATION
- TEMPERATURE
- MASK

SALIENT DATA

SHEET 1 OF 1

TITLE: Comparison of the Effects of 70° Tilt & Several Levels of LBNP on Heart Rate & Blood Pressure in Man

REF. #180

HG-176

DATE:

LEAD AUTHOR: Musgrave, F.S.

HUMANS - X
ANIMALS -

ABSTRACT

The purpose of this investigation was to compare, with respect to heart rate and blood pressure, several levels of lower body negative pressure (LBNP) with a change in posture from the supine to the erect position. Five young male subjects were exposed, in separate experiments, to 15 minutes of tilt at 70° and LBNP at levels of 20, 40, and 60 mm Hg. The mean heart rates and blood pressures for the five subjects during a control period and after 5, 10 and 15 minutes respectively of tilt or LBNP, were: 70° tilt (75,129/79), (88, 119/77), (90, 118/77) and (90, 119/77); for LBNP at 20 mm Hg (74, 128/80), (76, 125/81), and (76, 125/81); for LBNP at 40 mm Hg (72, 129/79), (83, 121/83) and (82, 122/83); and for LBNP at 60 mm Hg (75,129/80), (92, 120/84); (94,116/82) and (98, 115/82). In terms of heart rate and blood pressure, a 70° tilt is closely approximated by LBNP at a level of 50 mm Hg. In a previous study, we determined that LBNP at the 40 mm Hg level produced redistributions of blood similar to those observed in assuming the upright posture. That a greater level of LBNP is needed to produce equivalent changes in heart rate and blood pressure is probably due to the elevation of the carotid and aortic barorecptors above the heart which occurs during a tilt but not during LBNP The subjects reported sensations of head-up tilt during the onset of LBNP and head-down tilt below the horizontal during the cessation of LBNP. Cardiovascular phenomena, such as large shifts in blood between thoracic reservoirs and the lower extremnities, may influence spatial orientation.

RELEVANCE

LBNP

SALIENT DATA

1. The orthostatic effects on heart rate and BP of a 70° tilt @1.0g is closely approximated by LBNP @ 50 mm Hg. Temporal data are presented for 20, 40 & 60 mm Hg LBNP & 70° tilt. The data are presented at 2 minute intervals which is too long to ascertain any time response information in the interval of interest (< 1.0 min.). Systolic & diastolic blood pressure and heart rate at various levels of LBNP are shown in the abstract above. Graphical data are presented in the paper.

PHYSIOLOGICAL CATEGORY
- AUDITORY
- BIOMECHNL
- X CARDIOVSCL
- FORCE
- GENERAL
- LABYRINTH
- MAN.CNTRL
- PROTECTIVE
- REVIEW
- RESPIRAT'N
- X SIMULATION
- X VISUAL
- OTHER

AUGMENTATION DEVICES
- HELMET
- STRAPS
- AURAL
- EXTREMITY
- XLBNP
- VISUAL
- RESPIRATORY
- LACRIMATION
- TEMPERATURE
- MASK

SHEET 1 OF 1

TITLE:

Improved Waist Seal Design for Use with LBNP Devices.

REF. # 261

HG- 177

DATE:

LEAD AUTHOR:

Wolthuis, R. A.

HUMANS - X
ANIMALS -

ABSTRACT

A new waist seal is described which permits placement of the seat at a descrete anatomical level, provides for adequate subject comfort, allows case of ingress and egress, and accommodates a wide range of subject waist sizes. Details of the design are provided through the use of appropriate photographs.

RELEVANCE

LBNP

SALIENT DATA

A description of an improved waist seal is presented. It is a relatively crude, inexpensive but apparently effective device. It is constructed from plywood, masonite and dental dam material (source given). While this device would not be appropriate in a simulator, laboratory use would be possible. This device would probably be effective as an interface between LBNP & UBPP or vice-versa.

PHYSIOLOGICAL CATEGORY

- AUDITORY
- BIOMECHNL
- CARDIOVSCL
- FORCE
- GENERAL
- LABYRINTH
- MAN.CNTRL
- PROTECTIVE
- REVIEW
- RESPIRAT'N
- X SIMULATION
- X VISUAL
- OTHER

AUGMENTATION DEVICES

- HELMET
- STRAPS
- AURAL
- EXTREMITY
- XLBNP
- VISUAL
- RESPIRATORY
- LACRIMATION
- TEMPERATURE
- MASK

SHEET 1 OF 4

TITLE: LBNP as an Assay Technique for Orthostatic Tolerance: I. The Individual Response to a Constant Level (-40 mm Hg) of LBNP

REF.# 262

HG-178

DATE:

LEAD AUTHOR: Wolthuis, R. A.

HUMANS - X
ANIMALS -

ABSTRACT

Seven male subjects each participated in six LBNP experiments. These experiments were separated by at least one week intervals and consisted of 15 minutes of -40 mm Hg LBNP. A trials by subject trend analysis was used to determine the presence or absence of change as a function of time for each measurement in each individual. Measurements showing a trend were chacacterized by slope and intercept; those not changing with time were averaged. The large, between individual variability of response in the present study indicated that -40 mm Hg. is not an optimal level for all subjects where LBNP is used as an orthostatic assay test; the level of reduced pressure used must be tailored to each individual response. In addition, the week to week response variability within each subject was substantial, indicating the difficulty in establishing a valid normal response by a fixed set of trials.

RELEVANCE

LBNP

SALIENT DATA

1. Experimenters used a plywood chamber with plywood & foam rubber waist seal. Devices had a 12.5 ft^3 volume BP measured every 30 seconds using an automatic blood pressure cuff pumping device & microphone. Leg volume, VCG & VBCG were monitored as well.

2. Data presented shows:

Heart rate change	+2.5 → 22.5 BPM
Systolic BP Change	-0.7 → -10.8 mm Hg
Diastolic BP Change	-2.3 → 2.6 mm Hg
Stroke Volume change	-3.8 → -32.9 ml
Calf Volume Change avg @ 15 min	+1.34% avg. @30sec, +2.16%

PHYSIOLOGICAL CATEGORY
- AUDITORY
- BIOMECHNL
- CARDIOVSCL
- FORCE
- GENERAL
- LABYRINTH
- MAN.CNTRL
- PROTECTIVE
- REVIEW
- RESPIRAT'N
- SIMULATION
- VISUAL
- OTHER

AUGMENTATION DEVICES
- HELMET
- STRAPS
- AURAL
- EXTREMITY
- LBNP
- VISUAL
- RESPIRATORY
- LACRIMATION
- TEMPERATURE
- MASK

SHEET 2 OF 4

TITLE: LBNP As An Assay Technique For Orthostatic Tolerance Part II. A Comparison of the Individual Response to Incremental vs Constant LBNP.

REF. # 263

HG- 179

DATE:

LEAD AUTHOR: Wolthuis, R. A.

HUMANS - X
ANIMALS -

ABSTRACT

Seven male subjects each participated in six incremental (-20-30-40 mm. Hg) and six constant level (-40 mm. Hg) LBNP experiments. The incremental and constant level LBNP experiments were performed in parts, with each pair separated by at least a one week interval. The physiologic data were analyzed by subject, measurement and experiment. The individual physiologic responses to -40 mm Hg within each of these two protocols were statistically similar indicating that the level of pressure rather than duration at pressure is the major determinant of individual response to this type of stress. The use of a slope-intercept and correlation coefficient provided a good data reduction scheme for characterizing the individual response to incremental LBNP. Finally, it is suggested that incremental LBNP offers a more flexible protocol where LBNP is used as a test for changing orthostatic tolerance.

RELEVANCE

LBNP

SALIENT DATA

1. Similar data & techniques to Part I data also presented vs time but not in the intervals of interest to us.

2. Slope (rate of change) information presented but biased by the long term effects.

PHYSIOLOGICAL CATEGORY
- AUDITORY
- BIOMECHNL
- CARDIOVSCL
- FORCE
- GENERAL
- LABYRINTH
- MAN.CNTRL
- PROTECTIVE
- REVIEW
- RESPIRAT'N
- X SIMULATION
- X VISUAL
- OTHER

AUGMENTATION DEVICES
- HELMET
- STRAPS
- AURAL
- EXTREMITY
- X LBNP
- VISUAL
- RESPIRATORY
- LACRIMATION
- TEMPERATURE
- MASK

SHEET 3 OF 4

TITLE: LBNP as an Assay Technique for Orthostatic Tolerance: III. A Comparison of the Individual Response to Incremental LNP vs Incremental LBNP

REF.# 264

HG-180

DATE:

LEAD AUTHOR: Wolthuis, R. A.

HUMANS - X
ANIMALS -

ABSTRACT

Four trained subjects each participated in several paired LBNP and Leg Negative Pressure (LNP) experiments. Negative pressure was applied in three five-minute incremental steps; pressure levels for LNP were -10 mm. Hg greater than the corresponding levels used for a given individual during LBNP. Individual calf volume changes during LNP were greater than those measured during LBNP. On the other hand, individual heart rate and stroke volume changes during LBNP always exceded those obtained during LNP. These findings suggest that the abdominal-pelvic region plays an important role in the response elicited by LBNP.

PHYSIOLOGICAL CATEGORY
- AUDITORY
- BIOMECHNL
- CARDIOVSCL
- FORCE
- GENERAL
- LABYRINTH
- MAN.CNTRL.
- PROTECTIVE
- REVIEW
- RESPIRAT'N
- X SIMULATION
- X VISUAL
- OTHER

RELEVANCE

LBNP

AUGMENTATION DEVICES
- HELMET
- STRAPS
- AURAL
- EXTREMITY
- X LBNP
- VISUAL
- RESPIRATORY
- LACRIMATION
- TEMPERATURE
- MASK

SALIENT DATA

1. The LBNP levels used were -30, -40, -50, -60, & -70 mm Hg. The results show more dramatic effects from LBNP than from LNP. As would be expected. Not much useful information for this study contained herein.

SHEET 4 OF 4

TITLE:
Physical Effects of Seated & Supine Exercise with & Without Subatmospheric Pressure Applied to the Lower Body.

REF.# 51
HG- 182
DATE:

LEAD AUTHOR:
Cooper, K. H.

HUMANS - X
ANIMALS -

ABSTRACT

Eight subjects were evaluated on a bicycle ergometer once a week for four weeks in both the upright and the supine position, with and without the addition of -30 mm. Hg lower body negative pressure. Upright ergometry without negative pressure was associated with the highest maximum oxygen consumption, whereas upright exercise with negative pressure and supine exercise with and without negative pressure were remarkably comparable. The cardiovascular response during submaximal upright exercise with negative pressure resembled that seen after physical deconditioning. This difference was not as apparent at maximum performance. These results indicate that in an earth environment the integration of LBNP with upright exercise provides an overload phenomenon that may be used to accelerate a cardiovascular conditioning response. In space, the mechanics of exercise might be facilitated, a good cardiovascular conditioning device could be provided, and a means of orthostatic stress testing would be available.

PHYSIOLOGICAL CATEGORY
- AUDITORY
- BIOMECHNL
- X CARDIOVSCL
- FORCE
- GENERAL
- LABYRINTH
- MAN.CNTRL
- PROTECTIVE
- REVIEW
- X RESPIRAT'N
- X SIMULATION
- X VISUAL
- OTHER

AUGMENTATION DEVICES
- HELMET
- STRAPS
- AURAL
- EXTREMITY
- LBNP
- VISUAL
- RESPIRATORY
- LACRIMATION
- TEMPERATURE
- MASK

RELEVANCE

LBNP

SALIENT DATA

1. Data presented: heart rate, minute ventilation, maximal O_2 consumption, and respiratory quotient. LBNP at -30 mm Hg. purpose was to compare exercise on ergometer with & without LBNP at supine & seated attitudes.

2. Not much useful data to us other than plot of heart rate over the first minute but points out at 0 & 1.0 min. Vacuum cleaner used for vacuum source. Device made by Lackhand Missile & Space Company Sunnyvale California.

SHEET 1 OF 1

TITLE: Cardiovascular Changes During Tilt & Leg Negative Pressure Tests.

REF.# 15

HG- 183

DATE:

LEAD AUTHOR: Bartok, S. J.

HUMANS - X
ANIMALS -

ABSTRACT

Eight students were studied before and following nine days of supervised bedrest using 15 minutes of 70° tilt, followed by 15 minutes of negative pressure up to 30 mm Hg applied to the left leg as the testing stresses for measuring cardiovascular change. Values recorded included heart rate, blood pressure and relative changes in leg volume using mercury in silastic strain gauges at the greatest calf circumference. The maximal increase in heart rate during tilt was approximately 40 percent higher at 0 and 2.5 hours post-bedrest than pre-bedrest. The diastolic pressure following bedrest tended to be higher pretilt and increased more during tilt, resulting in higher mean pressure and narrowed pulse pressures. The maximum leg volume after 15 minutes of tilt was unchanged following bedrest, but the slope of the initial change in leg volume with tilt was 50 percent lower at 0 and 2.5 hours post-bedrest than during pre-bedrest or later recovery periods. These filling curves were digitized and the filling pattern at 10 seconds, 30 seconds and 3 minutes was significantly ($P \leq .05$) lower at 0, 2.5 and 12 hours post-bedrest, than during pre-bedrest. At 3, 5 and 7 days post-bedrest, the filling curves were still significantly lower at 3 minutes after tilt, but were significantly higher at 5, 10 and 30 seconds after tilt. The four students who were exercised during bedrest showed greater changes in the filling curve than the four who did not exercise.
The negative pressure tests showed changes in heart rate and blood pressure similar to the tilt tests, but to a lesser degree. Leg volume increases were greater following bedrest.

RELEVANCE

LBNP

SALIENT DATA

1. Blood pressure was taken at 2 & 3 minute intervals but leg volume was monitored continuously. Data shows the effect of bedrest on leg volume changes due to the first three minutes of tilt. These data are only useful if the leg volume data can be related to B.P. and if tilt can be related to LNP. Relationships between tilt and LBNP have been previously made.

PHYSIOLOGICAL CATEGORY
- AUDITORY
- BIOMECHNL
- X CARDIOVSCL
- FORCE
- GENERAL
- LABYRINTH
- MAN.CNTRL
- PROTECTIVE
- REVIEW
- RESPIRAT'N
- X SIMULATION
- X VISUAL
- OTHER

AUGMENTATION DEVICES
- HELMET
- STRAPS
- AURAL
- EXTREMITY
- X LBNP
- VISUAL
- RESPIRATORY
- LACRIMATION
- TEMPERATURE
- MASK

SHEET 1 OF 1

TITLE: Effects of LBNP on Central Venous Pressure, Venous Tone & Heart Rate.

REF. # 218

HG- 184

DATE:

LEAD AUTHOR: Sears, W. J.

HUMANS - X
ANIMALS -

ABSTRACT

Fifteen healthy volunteers were exposed to graded lower body negative pressures of -40, -60, -80 cm H_2O for 4 minutes at each level. EKG and forearm plethysmographic traces were taken simultaneously. Central venous pressure and arterial cuff pressures were recorded in 4 cases. No change in venomotor tone was noted below -60 cm H_2O. Exposure to this pressure produced a mean decrease in central venous pressure of 7 cm H_2O. This effect was graded at pressures below -60 cm H_2O, flattening at higher levels. A mean pulse rate increase of 50% (range 18-80%) occurred in 24 runs at -60 cm H_2O. An increase in venous tone resulted from exposure to -80 cm H_2O and in one subject with pre-exposure to -80 cm H_2O and in one subject with pre-syncopal symptoms at -60 cm H_2O. The increased tone was associated with mean pulse rate increases of 60% (range 54-70%). Mean blood pressures remained at approximately control values. A brief rise in blood pressure and fall in heart rate followed exposure. (Supported in part by Los Angeles County Heart Assn., Grant #293-C1)

PHYSIOLOGICAL CATEGORY
- AUDITORY
- BIOMECHNL
- X CARDIOVSCL
- FORCE
- GENERAL
- LABYRINTH
- MAN.CNTRL
- PROTECTIVE
- REVIEW
- RESPIRAT'N
- SIMULATION
- VISUAL
- OTHER

AUGMENTATION DEVICES
- HELMET
- STRAPS
- AURAL
- EXTREMITY
- X LBNP
- VISUAL
- RESPIRATORY
- LACRIMATION
- TEMPERATURE
- MASK

RELEVANCE

LBNP

SALIENT DATA

1. Abstract only - no report

2. Note: That data is presented in cm H_2O rather than mm Hg.

$$0.0142 \frac{psi}{cm\ H_2O} \quad ; \quad 0.0193 \frac{psi}{mm\ Hg} \quad ; \quad 0.7358 \frac{mm\ Hg}{cm\ H_2O}$$

SHEET 1 OF 1

SALIENT DATA | RELEVANCE | ABSTRACT

TABLE 1. MEAN REACTION TIMES AND t-RATIOS BETWEEN REACTIONS TO LIGHT AND SOUND AT VARIOUS g-LEVELS
Number of Subjects - 16

G-Level	Light M	Light SD	Light SEm	Sound M	Sound SD	Sound SEm	
1	1.229	.107	.028	1.006	.134	.035	CUMMULATIVE TIME (sec) FOR 5 EVENTS
3	1.280	.125	.032	1.061	.123	.032	
5	1.327	.106	.027	1.131	.163	.042	

t-RATIOS

LIGHT			SOUND		
1 to 3	1 to 5	3 to 5	1 to 3	1 to 5	3 to 5
3.53	7.21	2.16*	4.08	4.52	3.71

*Significant at 5% level; all others significant beyond 1% level.

TITLE: A Study of Reaction Time to Light and Sound as Related to Increased Positive Radial Acceleration.

AUTHOR: Canfield, A. A.

DATE:

HUMANS - X
ANIMALS -

PHYSIOLOGICAL CATEGORY
X AUDITORY
BIONECHNL
CARDIOVSCL
FORCE
GENERAL
LABYRINTH
MAN.CNTRL
PROTECTIVE
REVIEW
RESPIRAT'N
SIMULATION
X VISUAL
OTHER

AUGMENTATION DEVICES
HELMET
STRAPS
X AURAL
EXTREMITY
LBNP
VISUAL
RESPIRATORY
LACRIMATION
TEMPERATURE
MASK

REF.# 36
HG- 189

SHEET 1 OF 5

AUTHOR Canfield, A. A. | REF # 36

Audition purportedly persists to unconsciousness however reaction time to auditory stimuli increases under High G.

---

1. 16 subjects wearing G Suits subjected to 1, 3 & 5 G-grayout and blackout not encountered reaction time tabulatized below for middle intensity light and sound stimuli (divide by 5 for reaction time per stimulius event).

2. "Reaction times to both sound and light were found to be significantly longer under conditions of increased positive radial acceleration" (centrifuge).

3. "...Reactions to sound are more rapid than those to light in the middle range of intensity..."

4. Authors tend to believe increased reaction time was not due to degradation of higher mental progress (previous studies of theirs show no such degradation up to 5 g) but rather increased g adversly affects the sensitivity of the sense organ such that the stimulus looses much of its effectivity and acts like a lower intensity stimulus with associated increased reaction time (normally encountered with lower level stimulus).

5. HG 133 pg. 23 contests this interpretation of results quite directly.

SHEET 2 OF 5

TITLE: The Influence of Positive G on Reaching Movements

REF.# 35

HG-190

DATE:

LEAD AUTHOR: Canfield, A. A.

HUMANS - X
ANIMALS -

ABSTRACT

Not available at this time

. . . . . .

RELEVANCE

Very useful document for extremity loading area. Does not pertain to force capability degradation under G load but rather the end result of arm ballistic movement under G load in terms of accuracy. Believe it forms good justification for our mechanization approach (dual torque motors).

SALIENT DATA

(1) Woods Et.Al. at Mayo Clinic shown that man cannot rise from his seat under 5G.

(2) Extremity loading under increased G "... introduces serious problems for the pilot when he attempts to reach for .... controls." (if not a cue, this condition, as a minimum, ought to affect mission performance and control mode).

(3) 48 S's, 47 using right hand, reach 19" for target areas (as on attached data sheet) under 1,3, and 5G conditions - quadrant, accuracy, speed of movement, response latency measured. No grayout or blackout.

(4) Subjects use ballistic, not moving fixation, movement. Each subject makes 4 trials to each target at each G level. No mention of G suit.

(5) Attached data sheet shows error and propensity to hit a given quadrant not position in the quadrant, as G varies. As G level increases the responses tend to move to the nearer and lower quadrants".

(6) Accuracy degrades as G level increases and authors attribute this to "inadequacy of the normal kinesthetic cues under increased G conditions".

(7) Movement time increases with G and is attributed to "Failure of S's to throw the arm with sufficient force to compensate for its increased weight." (GK-Tends to substantiate usefulness of under arm torque motor tether).

(8) Reaction time increases and is attributed to "increased cogitation period" as subjects considered mediation changes necessary to preserve accuracy.

PHYSIOLOGICAL CATEGORY
- AUDITORY
- X BIOMECHNL
- CARDIOVSCL
- X FORCE
- GENERAL
- LABYRINTH
- X MAN.CNTRL
- PROTECTIVE
- REVIEW
- RESPIRAT'N
- SIMULATION
- X VISUAL
- OTHER

AUGMENTATION DEVICES
- HELMET
- STRAPS
- AURAL
- X EXTREMITY
- LBNP
- X VISUAL
- RESPIRATORY
- LACRIMATION
- TEMPERATURE
- MASK

SHEET 3 OF 5

(9) Directional error most interesting:

a) "Experimental error" - under increased G, S's first response often quite low and on returning to 1G response was high - this surprised the subject. "The first movement at 1g was frequently made in response to the patten of kinethetic cues that had been used for moving the arm under the previous atypical weight conditions."

b) Movement to nearer and lower quadrants explained as

i) "Negative Inertia Error" as termed by Brown Et.al. and reflects arm to the intended termination point (GK-A longitudinal force "restriction" due to vertical acceleration-more justification for under arm tether)

ii) "Error of Downward Tendency" strike low under increased acceleration (GK-elbow joint torquer for this)

These two offset one another with target in down position with negative inertia error predominant.

(10) No mention of elevator effect

Table 2

Means, Standard Deviations, and Standard Error of the Means of the Circular Error Scores*

No. of subjects = 48

	g Level					
	1 g		3 g		5 g	
Target Position	M	S.D.	M	S.D.	M	S.D.
Up	4.74	1.73	8.38	3.63	9.67	3.84
Down	4.61	2.23	5.84	2.88	6.91	3.72
Left	5.73	2.61	6.97	2.84	9.66	4.57
Right	4.33	1.90	7.15	2.97	7.79	3.82

* All values presented in this table are given in tenths of inches. Each of the 48 scores from which these values were computed represented the average error score of four responses made at the g level and target position indicated.

Table 3

Means, Standard Deviations, and Standard Error of the Means of the Movement Times*

No. of subjects = 48

	g Level					
	1 g		3 g		5 g	
Target Position	M	S.D.	M	S.D.	M	S.D.
Up	1.35	.295	1.50	.484	2.20	.620
Down	1.31	.337	1.27	.378	1.31	.406
Left	1.33	.306	1.38	.438	1.59	.505
Right	1.28	.323	1.23	.339	1.35	.397

* All values are given in seconds. Each of the 48 scores from which these values were computed represented the total time taken for four response movements at the g level and target position indicated.

	1 g			3 g			5 g		
UP	48	73	121	20	41	61	25	23	48
	33	38	71	36	95	131	49	95	144
	81	111	192	56	136	192	74	118	192
DOWN	26	63	89	42	38	80	60	47	107
	26	77	103	54	58	112	48	37	85
	52	140		96	96		108	84	
LEFT	92	45	127	45	29	74	24	35	59
	31	34	65	56	62	118	52	81	133
	123	79		101	91		76	116	
RIGHT	38	68	106	58	45	103	37	24	61
	43	43	86	52	37	89	74	57	131
	81	111		110	82		111	81	

FIG. 1. Frequency of responses in the various target quadrants by target position and g level.

TITLE: G Effect on the Pilot During Aerobatics

REF. 176

HG-191

DATE:

LEAD AUTHOR: Moher, S. K.

HUMANS - X
ANIMALS -

ABSTRACT

Sport, precision, and competive aerobatics , and especially air show and demonstration flying are enjoying a rebirth of interest exceeding that of the 1930's. Improved aerobatic airplanes and power plants are in the hands of more civilian pilots than ever before. These aircraft enable the pilot to easily initiate maneuvers which exceed human tolerances, yet not over stress the aircraft. Military aircraft reached this point in World War II and the G-suit was perfected to protect the pilot. The military groups still use the G-suit but this equipment is impractical for most civil aerobatic activities. This paper provides information on (1) the nature of aerobatic G forces, (2) human physiology in relation to G forces, (3) human tolerances to various levels and times of exposure to G forces, and (4) means by which tolerance to G forces may be increased in terms of (a) the general physical condition and (b) the time during the maneuver when the G forces are imposed.

. . . . . .

RELEVANCE

Cardiovascular terminology. Review of the effects a student pilot might encounter during standard aerobatic work.

SALIENT DATA

(1) Author states a 5 second system response time to change the blood pressure from one +Gz level to another.

(2) Blood pressure contrdled by heart rate and constriction or dilation of arteries. Stretch receptors, baroreceptors or pressorecptors, monitor the arteriac pressure and play a feedback role to this control loop called "Marey's Law"

(3) Blood pools in the veins because the veins have thinner walls than the arteries and tend to distend easier. Stretch receptors in great neck veins monitor distention under "Bainbridge Effect" and signal for faster heart rate to reduce neck vein engorgement.

(4) Author states some redout (eyelid) experiences referenced in the literature. Lists -2 Gz for 5 sec produces onset of -Gz symptoms in student pilots and maximum experimental exposures of -4.5G for 5 seconds.

PHYSIOLOGICAL CATEGORY
- AUDITORY
- BIOMECHNL
- X CARDIOVSCL
- FORCE
- GENERAL
- LABYRINTH
- MAN.CNTRL
- PROTECTIVE
- X REVIEW
- RESPIRAT'N
- SIMULATION
- VISUAL
- OTHER

AUGMENTATION DEVICES
- HELMET
- STRAPS
- AURAL
- EXTREMITY
- X LBNP
- VISUAL
- RESPIRATORY
- LACRIMATION
- TEMPERATURE
- MASK

SHEET 1 OF 1

TITLE: Cardiovascular Responses of Men & Women to Lower Body Negative Pressure.

REF. # 177

HG- 194

DATE:

LEAD AUTHOR: Montgomer, L. D., et al

HUMANS - X
ANIMALS -

ABSTRACT

Changes in blood flow and blood redistribution were measured by impedance plethysmography in the pelvic and leg regions of six male and four female subjects during three 5-min exposures to -20, -40, and -60 mm Hg lower body negative pressure (LBNP). Female subjects demonstrated significantly higher mean heart rate and lower leg blood flow indices than the male subjects during the recumbent control periods. Men had slightly higher mean resting systolic and diastolic blood pressures and higher mean control pelvic blood flow indices. Women demonstrated significantly less blood pooling in the legs and slightly less in the pelvic region than men. All of the 18 tests with male subjects at -60 mm Hg were completed without initial signs of syncope, while only two of the tests with women were completed successfully without the subject exhibiting presyncopal conditions. The results of this study indicate that impedance plethysmography can be used to measure segmental cardiocascular responses during LBNP and that females may be less tolerant to -60 mm Hg. LBNP than males.

RELEVANCE

LBNP, cardiovascular

SALIENT DATA

Authors present data at four levels of LBNP (0, -20, -40, -60 mm Hg) for men & women. The data includes leg & pelvic blood volumes, pulse pressure, heart rate, systolic & diastolic BP, and lower body volume. The BP was measured every minute with a Roche arteriosonde automatic ultrasonic BP monitor. Therefore the short interval dynamics is unknown. It is interesting to note that the diastolic pressure (males) is consistent with the results reported by Wolthuis et al (Hg 127). That result is that there is not a consistent decrease in diastolic BP with an increase in LBNP. For women however there is the expected decrease with the corresponding increase in LBNP. The authors use impedance plethysmography to measure blood flow & pooling. They report satisfactory results and minimum subject instrument interface.

PHYSIOLOGICAL CATEGORY
- AUDITORY
- BIOMECHNL
- X CARDIOVSCL
- FORCE
- GENERAL
- LABYRINTH
- MAN.CNTRL
- PROTECTIVE
- REVIEW
- RESPIRAT'N
- SIMULATION
- VISUAL
- OTHER

AUGMENTATION DEVICES
- HELMET
- STRAPS
- AURAL
- EXTREMITY
- X LBNP
- VISUAL
- RESPIRATORY
- LACRIMATION
- TEMPERATURE
- MASK

SHEET 1 OF 1

TITLE: Venous Pressure in the Head Under Negative Acceleration

REF.# 2

HG- 195

DATE:

LEAD AUTHOR: Shaw, R. S.

HUMANS - X
ANIMALS -

ABSTRACT

Not available at this time

Cardiovascular, visual, protective devices

Venous pressure in the heads of human subjects varied linearly with acceleration level comparable to a hydrostatic column extending from the heart to head. At -3Gz venous pressure in the frontal vein ranged 80-110 mm Hg. Use of the Muller maneuver (inspiration against a closed glottis) causes a decrease in intrathoracic pressure and a marked relief of discomfort. It provides considerable alleviation of symptoms up to -3Gz by decreasing venous pressure. 45° or 60° backward tilt provides no significant protection against negative acceleration.

RELEVANCE

SALIENT DATA

PHYSIOLOGICAL CATEGORY
- AUDITORY
- BIOMECHNL
- X CARDIOVSCL
- FORCE
- GENERAL
- LABYRINTH
- MAN.CNTRL
- X PROTECTIVE
- REVIEW
- RESPIRAT'N
- SIMULATION
- VISUAL
- OTHER

AUGMENTATION DEVICES
- HELMET
- STRAPS
- AURAL
- EXTREMITY
- LBNP
- XVISUAL
- RESPIRATORY
- LACRIMATION
- TEMPERATURE
- MASK

SHEET 1 OF 1

TITLE: The Effect of High Acceleration Forces upon Certain Psysiological Factors of Human Subjects Placed in a Modified Supine Pcsition.

REF.# 229

HG- 202

DATE:

LEAD AUTHOR: Stauffer, F. R.

HUMANS X
ANIMALS -

ABSTRACT

Not available at this time.

Extremity cardiovascular, visual, respiratory, protective devic s.

The seat in the centrifuge was pivoted such that the acceleration resultant vector created a force on the subject in a chest to back direction. This was done to evaluate this approach as a protective device. The results though should be applicable to the +Gx problem. However there appears to be several artifacts which limits the applicability of these results in the aforementioned manner.

PHYSIOLOGICAL CATEGORY
- AUDITORY
- BIOMECHNL
- CARDIOVSCL
- FORCE
- GENERAL
- LABYRINTH
- MAN.CNTRL
- PROTECTIVE
- REVIEW
- RESPIRAT'N
- SIMULATION
- VISUAL
- OTHER

AUGMENTATION DEVICES
- HELMET
- STRAPS
- AURAL
- EXTREMITY
- LBNP
- VISUAL
- RESPIRATORY
- LACRIMATION
- TEMPERATURE
- MASK

RELEVANCE

SALIENT DATA

SHEET 1 OF 1

TITLE: Correlation of Eye Level Blood Flow Velocity & Peripheral Light Loss During +G_z Stress

REF. # 209

HG- 205

DATE:

LEAD AUTHOR: Rositano, S. A.

X HUMANS - ANIMALS -

ABSTRACT

Not available at this time

. . . . . .

RELEVANCE

Cardiovascular, Visual, LBNP

SALIENT DATA

Purpose of paper was to determine if eye level blood flow velocity could serve as a predictor of impending visual degradation during + Gz stress. Data were taken for ROR, GOR & G on G runs. 50% CLL was the endpoint. Retrograde flow precedes visual effects by 5 seconds. Mean eye level arterial pressure at zero flow was 25 $\pm$ 5 mm Hg for all subjects.

G on G - Temporal flow velocity provided consistent objective indication of impending visual degradation. Diastolic retrograde flow preceded onset of visual change by 3 to 5 sec for all subjects. Negative mean or flow cessation preceded peak visual degradation by up to 10 seconds for all subjects.

PHYSIOLOGICAL CATEGORY
- AUDITORY
- BIOMECHNL
- X CARDIOVSCL
- FORCE
- GENERAL
- LABYRINTH
- MAN.CNTRL
- PROTECTIVE
- REVIEW
- RESPIRAT'N
- SIMULATION
- X VISUAL
- OTHER

AUGMENTATION DEVICES
- HELMET
- STRAPS
- AURAL
- EXTREMITY
- LBNP
- X VISUAL
- RESPIRATORY
- LACRIMATION
- TEMPERATURE
- MASK

SHEET 1 OF 2

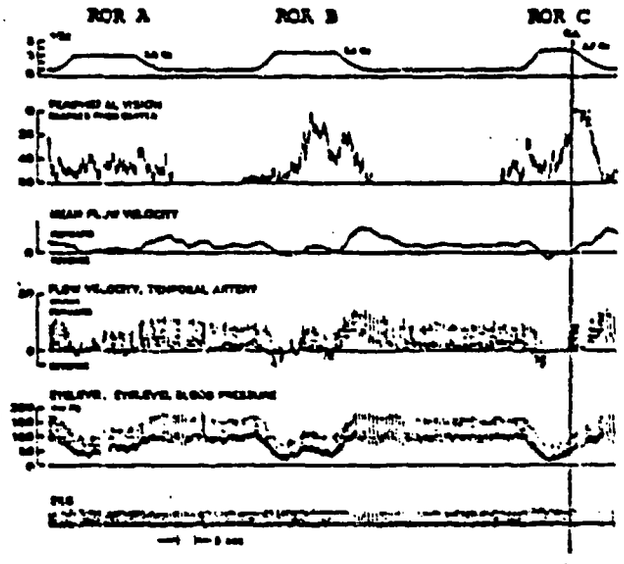


Figure 2

Response To Rapid Onset Acceleration

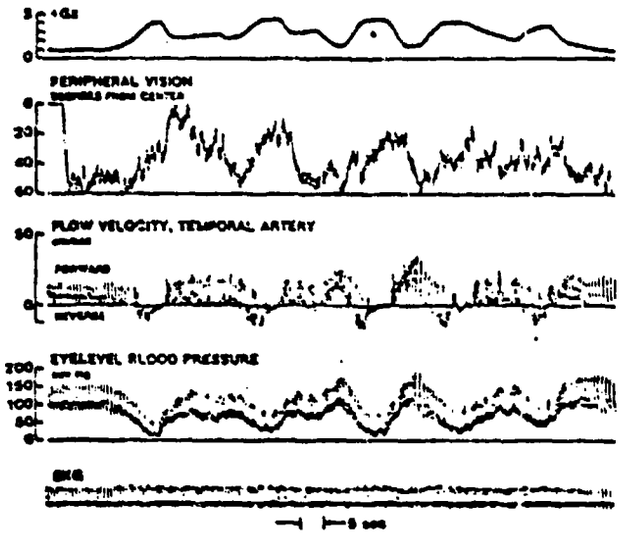


Figure 4

Response To "G on G" Acceleration Profiles

TITLE: Effects of Acceleration on Pilot Performance

REF.# 111

HG- 211

DATE:

LEAD AUTHOR: Chambers, R. M.

HUMANS -
ANIMALS -

ABSTRACT

Not available at this time

. . . . . .

Authors find significant differences in pilot control between static and dynamic simulations.

Data on contrast thresholds as a function G lacrimation noted.

RELEVANCE

(1) +6 to +12Gx may be some tearing & difficulty in keeping eyes open. For -Gx some pain may be experienced, small petechire may occur on lower eyelids (pg. 7)

(2) At +7Gx target must be twice as large as unaccelerated state conditions to be seen. White observes that at 4Gz light must be 3 times as bright as 1G to be seen. (Pg. 8).

(3) In a spacecraft orientation acceleration study performance of pilot was altered in dynamic simulations as opposed to static: Under dynamic -

a) Pilot unaware of some of their control inputs (p44).

b) Acceleration disrupted timing and precision of control inputs - inputs become less discrete and much higher frequency of occurance. (55)

c) Control response variability increases under dynamic conditions.

SALIENT DATA

PHYSIOLOGICAL CATEGORY
- AUDITORY
- BIOMECHNL
- X CARDIOVSCL
- FORCE
- X GENERAL
- LABYRINTH
- X MAN.CNTRL
- PROTECTIVE
- REVIEW
- X RESPIRAT'N
- X SIMULATION
- X VISUAL
- OTHER

AUGMENTATION DEVICES
- HELMET
- STRAPS
- AURAL
- EXTREMITY
- LBNP
- XVISUAL
- XRESPIRATORY
- XLACRIMATION
- TEMPERATURE
- MASK

SHEET 1 OF 3

AUTHOR Chambers, R. M.

REF # 111

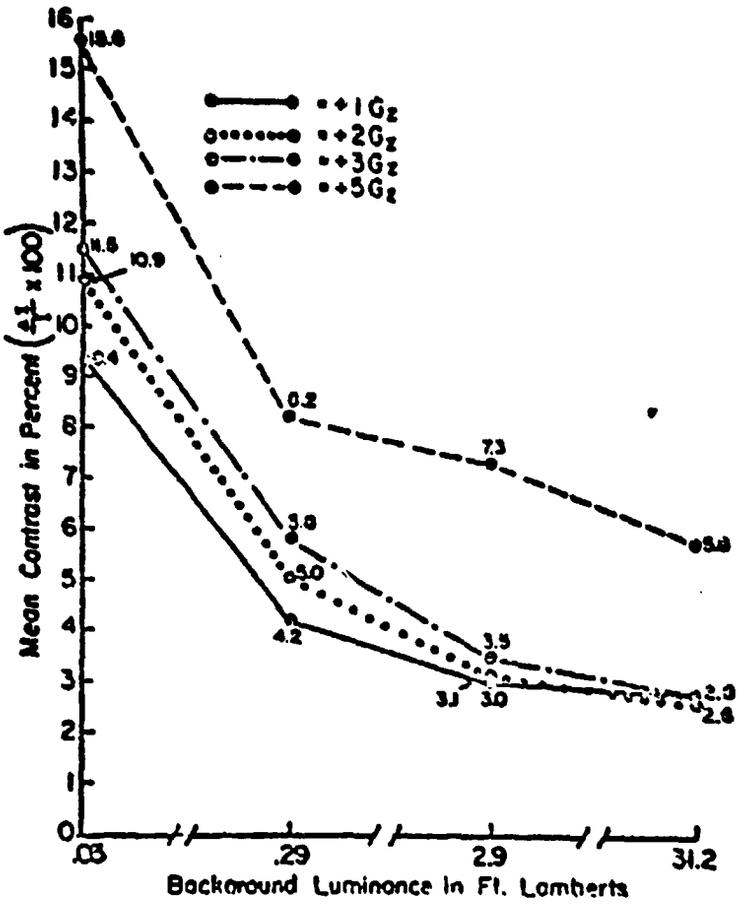


Figure 8. Results of experiment showing the relationship between brightness discrimination threshold and background luminance for each of four levels of positive acceleration.

SHEET 2 OF 3

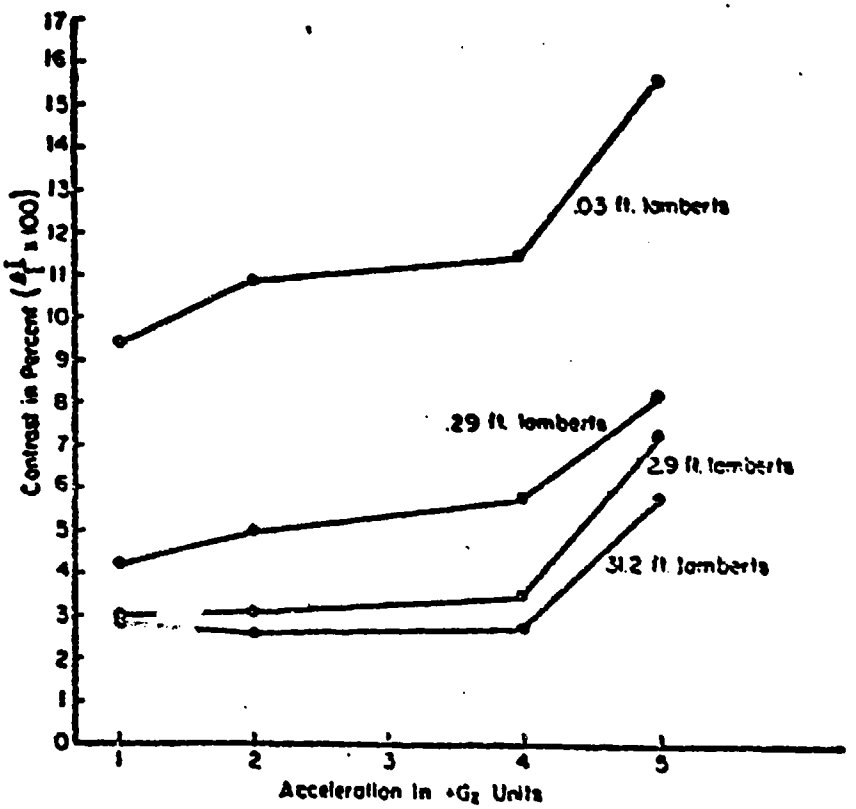


Figure 10. Effects of Positive acceleration (+G_z) on brightness discrimination thresholds for perceiving an achromatic circular target against each of four background luminances.

TITLE: Syncope Induced by Application of Negative Pressure to the Lower Body & its Effect on Lung CO Diffusing Capacity.

REF.# 220

HG- 219

DATE:

LEAD AUTHOR: Shaw, D. B.

HUMANS - X
ANIMALS -

ABSTRACT

Application of negative pressure of -70 cmH_2O to the lower half of the body in nine healthy human volunteers induced progressive changes in all subjects, which appeared to be typical of vasovagal syncope. The subjects withstood the strain for 7 to 17 min; atmospheric pressure was restored in time to prevent loss of consciousness in most individuals. Heart rate rose steadily to maxima between 110-140/min, then fell precipituously to normal or sub-normal levels one or two min before fainting. In all subjects the pulmonary diffusing capacity for carbon monoxide (D_{CO}) fell by 12.5 per cent on the average during the first six min of negative pressure, then rose toward control levels in 5 of the 7 subjects who had tolerated the strain thus far; it was within normal limits in all subjects 8 min after removal of the strain. The circumference of the upper arm fell progressively until the pressure was restored. One experiment using radioactive Xenon (133Xe) indicated that there was an increase in the perfussion gradient down the lung during the negative pressure phase. The application of reduced pressure to the lower body should provide a safe, rapid method for studying individual resistance to vasovagal syncope and possibly to the strain of positive acceleration.

RELEVANCE

LBNP - Main thrust is to carbon monoxide diffusion during LBNP.

SALIENT DATA

The application of -70 cm H2O produced, in some subjects, presyncopal, and in one subject, syncopal episodes. Although the syncoped occurred after 13 minutes of exposure.

An interesting reaction was reported;"every subject noted heaviness or straining sensation in the injuinal region from the onset of negative pressure This was accompanied by a feeling of fullness in the legs and thighs and of being forced into the seat which was likened by a trained pilot to that experienced when pulling an aircraft out of a dove.

PHYSIOLOGICAL CATEGORY
- AUDITORY
- BIOMECHNL
- X CARDIOVSCL
- FORCE
- GENERAL
- LABYRINTH
- MAN.CNTRL
- PROTECTIVE
- REVIEW
- X RESPIRAT'N
- SIMULATION
- VISUAL
- OTHER

AUGMENTATION DEVICES
- HELMET
- STRAPS
- AURAL
- EXTREMITY
- X LBNP
- VISUAL
- X RESPIRATORY
- LACRIMATION
- TEMPERATURE
- MASK

SHEET 1 OF 1

TITLE: The Elevator Illusion: Apparent Motion of a Visual Target During Vertical Acceleration

REF. # 185

HG- 223

DATE:

LEAD AUTHOR: Niven, J. I.

HUMANS - X
ANIMALS -

ABSTRACT

Not available at this time

. . . . . .

RELEVANCE

Pertains to High G Visual effects and control of limbs during reaching maneuvers under high G

SALIENT DATA

(1) Subjects with normal vestibular labyrinthine functions (5) and three with a dysfunction of the labyrinthine were exposed to ± Gz in elevators (not centrifuge)

a) Normal subjects tend to see real target rise briefly under +Gz and settle under - Gz.

b) Abnormal subjects see no such movement.

c) Visual afterimages in normal subjects tend to fall under +Gz and rise under -Gz.

d) No clear cut rise or fall (but some movement) of visual after images in abnormal subjects.

e) Normal subjects eyes tend to rotate down briefly under +Gz and up under -Gz. This is not observed in abnormal subjects.

f) Authors conclude that elevator effect is a part of the oculogravic illusion and otolithic in origin.

(2) Since the otolith is pitched up slightly an increase in Gz would be perceived the same as a pitch up of the body/head. This is the predominant oculogravic illusion. During the change in Gz or the change in perceived pitch, the eye in attempting to stay on target, is probably reflexly pitched downward giving appearance of upward moving field of view. Refixation would likely occur within 200 m.s. after achieving steady state acceleration level. (This would then seem to be only a transient portion of the oculogravic illusion).

PHYSIOLOGICAL CATEGORY
- AUDITORY
- BIOMECHNL
- CARDIOVSCL
- FORCE
- GENERAL
- X LABYRINTH
- MAN.CNTRL
- PROTECTIVE
- REVIEW
- RESPIRAT'N
- SIMULATION
- X VISUAL
- OTHER

AUGMENTATION DEVICES
- HELMET
- STRAPS
- AURAL
- X EXTREMITY
- LBNP
- X VISUAL
- RESPIRATORY
- LACRIMATION
- TEMPERATURE
- MASK

SHEET 1 OF 1

TITLE: Electrmygraphic Signals of the Spinal Musculature During +Gz Impact Acceleration

REF.: 239

HG- 226

DATE:

LEAD AUTHOR: Tennyson, S.A.

HUMANS - X
ANIMALS -

ABSTRACT

Not available at this time

Head neck muscle } Delay Times
Extremity muscle }
Primary work on dogs but some data on humans.

---

1. Electromyographic delay in spinal musculature of dogs found to be approximately 30ms(21ms-58ms)
2. Authors present compartive information on humans:

   a. Neural delay in arm = 60 - 80 ms per hammond.
   b. Neural delay in arm = 90 - 140 ms per soechting
   c. Neural delay in neck =54 - 92 ms per foust

a, b, c above include duration of spindle activity up to time of α efferent arriving at muscle

   d. Actual muscle tension peak follows behind peak electromyographic signal by 80 ms. Per Hannan and Inman studies.

RELEVANCE

SALIENT DATA

PHYSIOLOGICAL CATEGORY
- AUDITORY
- X BIOMECHNL
- CARDIOVSCL
- X FORCE
- GENERAL
- LABYRINTH
- MAN.CNTRL
- PROTECTIVE
- REVIEW
- RESPIRAT'N
- SIMULATION
- VISUAL
- OTHER

AUGMENTATION DEVICES
- X HELMET
- STRAPS
- AURAL
- X EXTREMITY
- LBNP
- VISUAL
- RESPIRATORY
- LACRIMATION
- TEMPERATURE
- MASK

SHEET 1 or 1

TITLE: Human Response to Sustained Acceleration

REF.# 71

HG- 229

DATE:

LEAD AUTHOR: Fraser, T. M.

X HUMANS - X ANIMALS -

ABSTRACT

Not available at this time

. X

General Reviw Report

Relevant to many areas

Major emphasis is on cardiovascular & pulmonary. Especially good pulmonary section. Not much visual. Extensive annotated bibliography.

RELEVANCE

X PHYSIOLOGICAL CATEGORY
- AUDITORY
- BIOMECHNL
- CARDIOVSCL
- FORCE
- GENERAL
- LABYRINTH
- MAN.CNTRL
- PROTECTIVE
- REVIEW
- RESPIRAT'N
- SIMULATION
- VISUAL
- OTHER

AUGMENTATION DEVICES
- HELMET
- STRAPS
- AURAL
- EXTREMITY
- LBNP
- X VISUAL
- X RESPIRATORY
- LACRIMATION
- TEMPERATURE
- MASK

SALIENT DATA

SHEET 1 OF 1

TITLE: The Components of the Korotkoff Sounds

REF.# 205

HG- 238

DATE:

LEAD AUTHOR: Rodbard, S

HUMANS - X
ANIMALS -

ABSTRACT

Not available at this time

. . . . . .

Non-invasive blood pressure monitoring

(1) The authors contend that much more than systolic and diastolic blood pressure may be inferred from analysis of the Korotkoff sounds. They describe the meaning they attribute to the changes in sound. The only application here may be to the development of a Korotkoff sounds signal processor. Their summary includes the following.

a) An opening top generated as the rising intra-arterial pressure overcomes the obstructive force of the compression produced by the cuff; b) a rumble generated by flow through the partially opened, vibrating arterial wall; (c) a closing bruit produced during the arterial downstroke as intra-arterial pressure falls below the cuff pressure; and d) breakers which occur prior to the opening top when the arterial upstroke is steep, e) silences represent laminar flow through a fully opened vessel, or absence of flow.

RELEVANCE

SALIENT DATA

PHYSIOLOGICAL CATEGORY
- AUDITORY
- BIOMECHNL
- X CARDIOVSCL
- FORCE
- GENERAL
- LABYRINTH
- MAN.CNTRL
- PROTECTIVE
- REVIEW
- RESPIRAT'N
- SIMULATION
- X VISUAL
- OTHER

AUGMENTATION DEVICES
- HELMET
- STRAPS
- AURAL
- EXTREMITY
- X LBNP
- X VISUAL
- RESPIRATORY
- LACRIMATION
- TEMPERATURE
- MASK

SHEET 1 OF 1

TITLE: Critique of Indirect Diastolic End Point

REF. 165

HG- 239

DATE:

LEAD AUTHOR: London, S. B., London, R. E.

HUMANS -X
ANIMALS -

ABSTRACT

Not available at this time

. . . . . .

Non-invasive blood pressure monitoring

(1) The authors attempt to resolve the controversy over whether the so called "last sound" or "muffing" is the correct end point for diastolic index. The first sound of Korotkoff is accepted as the index or of systolic pressure. Three methods were employed to conduct this study a) the usual clinical method of listening to first, muffle and last sound, b) electronic recording of the Korothkoff sounds and cuff pressures c) intra-arterial pressure recording.

Their conclusion was that the "last sound" occurs 4 to 10 min Hg above the intra-arterial diastolic end point and is a clinically accurate and reliable index of diastolic pressure.

(2) Note: Extensive references accompany this article.

RELEVANCE

SALIENT DATA

PHYSIOLOGICAL CATEGORY
- AUDITORY
- BIOMECHNL
- X CARDIOVSCL
- FORCE
- GENERAL
- LABYRINTH
- MAN.CNTRL
- PROTECTIVE
- REVIEW
- RESPIRAT'N
- SIMULATION
- X VISUAL
- OTHER

AUGMENTATION DEVICES
- HELMET
- STRAPS
- AURAL
- EXTREMITY
- X LBNP
- X VISUAL
- RESPIRATORY
- LACRIMATION
- TEMPERATURE
- MASK

SHEET 1 OF 1

TITLE: New Criteria in Indirect Blood Pressure Recording

REF.# 245

HG- 240

DATE:

LEAD AUTHOR: Verghese, C. A.

HUMANS - X
ANIMALS -

ABSTRACT

Not available at this time

. . . . . .

RELEVANCE

Non-invasive blood pressure monitoring

SALIENT DATA

(1) Authors claim that auscultatory methods based on variations of K sounds are not acceptable in most stress environments. They suggest employing an occlusion cuff pressure of which is recorded along with the brachial artery pulse which is recorded in their embodiement via a crystal. Systolic and diastolic pressures are obtained by observing the amplitude variations of the pulses. They report a mean difference between their method and the std. sphymomanometer of +2.7 mm Hg Systolic & -0.8mm Hg diastolic among 50 subjects. Note Ref 3 below which uses the ear opacity method.

(2) Note: References

1) Bramvell, J. C. & Hickson, S.K. The relation of pulse form to sound production in arteries. Parts I & II Heart 13:109, 129, 1926.

2) Malcolm, J. E. Blood pressure sounds and their meaning, William Heinemann Medical Books London Vol 20.

3) Wood, E. H. Oximetry. Medical Physics Vol. III Year Book Publishers Inc. Chicago pp440-413 1960

4) Masterpaolo, J. A. et al Validity of phonoarterio-graphic blood pressure during rest and exercise. J Appl. Physiology 19:1219, 1964

PHYSIOLOGICAL CATEGORY
- AUDITORY
- BIOMECHNL
- X CARDIOVSCL
- FORCE
- GENERAL
- LABYRINTH
- MAN.CNTRL
- PROTECTIVE
- REVIEW
- RESPIRAT'N
- SIMULATION
- X VISUAL
- OTHER

AUGMENTATION DEVICES
- HELMET
- STRAPS
- AURAL
- EXTREMITY
- X LBNP
- X VISUAL
- RESPIRATORY
- LACRIMATION
- TEMPERATURE
- MASK

SHEET 1 OF 1

TITLE: Artifact Suppression in Indirect Blood Pressure Measurements

REF.# 152

HG- 241

DATE:

LEAD AUTHOR: Lagerwerff, J. M.

HUMANS - X
ANIMALS -

ABSTRACT

Not available at this time

. . . . . .

Non-Invasive Blood Pressure Monitoring

(1) Indirect BP measurements usually results in grossly inaccurate values due to the fact that most arm and body movements generate such broad noise and pressure spectra that the signal processing electronics is unable to interpret which signals are true arterial pulse wave phenomena. The authors use ECG output as input, along with Korotkoff sounds and pressure Xducer readings, to their signal processing circuit. The use of the ECG allows prediction of the corresponding K sound. Thereby the circuit only processes signals that have a corresponding ECG indication.

(2) Results presented seemed to indicate device is usable. However calibration may be a problem in the opinion of the authors.

RELEVANCE

SALIENT DATA

PHYSIOLOGICAL CATEGORY
- AUDITORY
- BIOMECHNL
- X CARDIOVSCL
- FORCE
- GENERAL
- LABYRINTH
- MAN.CNTRL
- PROTECTIVE
- REVIEW
- RESPIRAT'N
- SIMULATION
- X VISUAL
- OTHER

AUGMENTATION DEVICES
- HELMET
- STRAPS
- AURAL
- EXTREMITY
- X LBNP
- X VISUAL
- RESPIRATORY
- LACRIMATION
- TEMPERATURE
- MASK

SHEET 1 OF 1

TITLE: An Automatic Device for Recording Blood Pressure

REF.# 68

HG- 242

DATE:

LEAD AUTHOR: Fernandez, H.

HUMANS - X
ANIMALS -

ABSTRACT

Not available at this time

. . . . . .

Non-Invasive Blood Pressure Monitoring

(1) Devices measures digital or brachial blood pressure depending on the placement of the cuff which contains the sound microphone.

(2) Method inflates cuff automatically then deflates based on Korotkoff Sounds. (See diagrams on Sheet 2)

(3) A system for the automatic indirect measurement of B.P. has been designed. The system makes possible the determination of digital or brachial blood pressure by use of an automatically inflated cuff and a system for detecting Korotkoff Sounds.

RELEVANCE

PHYSIOLOGICAL CATEGORY
- AUDITORY
- BIOMECHNL
- X CARDIOVSCL
- FORCE
- GENERAL
- LABYRINTH
- MAN.CNTRL
- PROTECTIVE
- REVIEW
- RESPIRAT'N
- SIMULATION
- X VISUAL
- OTHER

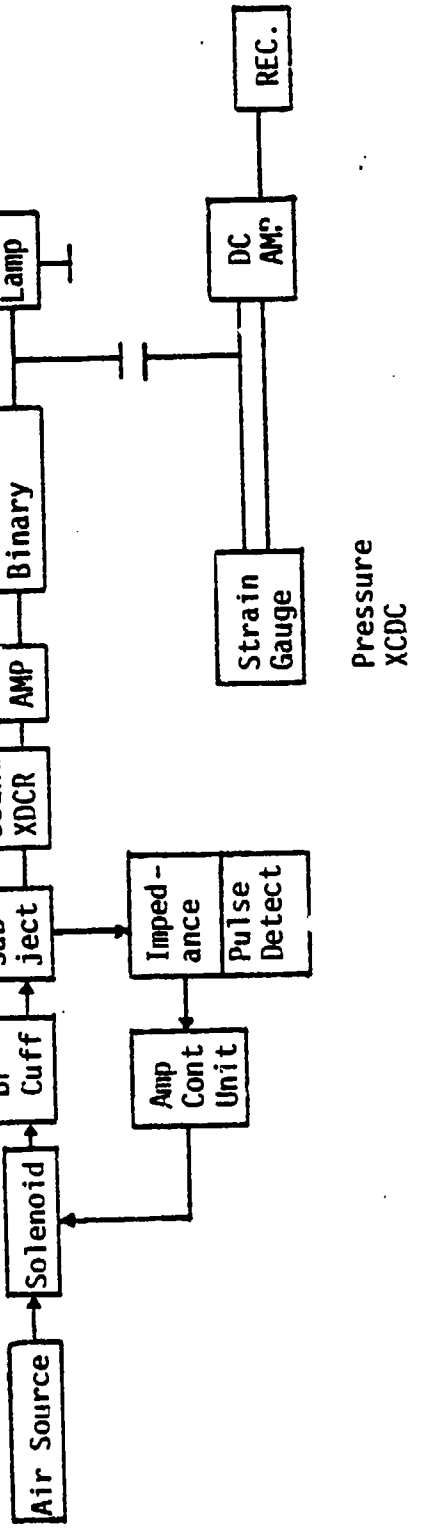
AUGMENTATION DEVICES
- HELMET
- STRAPS
- AURAL
- EXTREMITY
- XLBNP
- XVISUAL
- RESPIRATORY
- LACRIMATION
- TEMPERATURE
- MASK

SALIENT DATA

SHEET 1 OF 2

AUTHOR Frenandez, H.

REF # 68



SHEET 2 OF 2

TITLE: Evaluation of Performance of Selected Devices for Measuring Blood Pressure

REF.# 147

HG- 243

DATE:

LEAD AUTHOR: Labarthe, D. R.

HUMANS - X
ANIMALS -

ABSTRACT

Not available at this time

. . . . . .

RELEVANCE

Non-invasive monitoring of Blood Pressure

1) The results of evaluating 5 devices is presented: Arteriosonde 1216, Boston Automatic Recorder, Physiometrics USM-105, Seurs 1080, Ramdon Zero Hawksley and Baumanometer 0300, V-lock.

2) In the author's opinion none of the tested devices performed adequately for substitution, in the program, for the standard mercury sphygmomanometer.

3) Quantitative data resulting from the evaluation is present.

4) Descriptions (brief) are given for each device.

5) Address for reprints Darwin R. Labarthe M.D. coordinating Center, Hypertension Detection & Fol.ow-Up Program School of Public Health, University of Texas, Health Science Center, Room 1114, Prudential Building, 1100 Holcombe Blvd. Houston TX. 77025

SALIENT DATA

PHYSIOLOGICAL CATEGORY

- AUDITORY
- BIOMECHNL
- X CARDIOVSCL
- FORCE
- GENERAL
- LABYRINTH
- MAN.CNTRL
- PROTECTIVE
- REVIEW
- RESPIRAT N
- SIMULATION
- X VISUAL
- OTHER

AUGMENTATION DEVICES

- HELMET
- STRAPS
- AURAL
- EXTREMITY
- X LBNP
- X VISUAL
- RESPIRATORY
- LACRIMATION
- TEMPERATURE
- MASK

SHEET 1 OF 1

TITLE: Non-invasive Methods for Assessing Left Ventricular Performance in Man

REF. # 256

HG- 244

DATE:

LEAD AUTHOR: Weissler, A. M.

HUMANS - X
ANIMALS -

ABSTRACT

Not available at this time

. . . . . .

Non-invasive monitoring of cardiac performance

(1) The techniques presented permit estimation of

(a) Left Ventricular diameter & volume (b) Left V muscle mass (c) Left V wall motion (d) L.V. outflow dyanmics & (e) Time sequence of L.V. cycle.

(2) Techniques presented are Echocardiogram & Scintiphotography for (a) Apex cardiograms, (b) Kinetocardiograms Radarkymongraphy, and Cihocardiogram for (c) Ballistocardiogram & Impedance Plethysmogram for (d) EKG & Phonocardiogram for systolic intervals.

(3) None seem particularly applicable to the continuous monitoring, quantitatively in the simulator environment.

RELEVANCE

SALIENT DATA

PHYSIOLOGICAL CATEGORY
- AUDITORY
- BIOMECHNL
- X CARDIOVSCL
- FORCE
- GENERAL
- LABYRINTH
- MAN.CNTRL
- PROTECTIVE
- REVIEW
- RESPIRAT'N
- SIMULATION
- X VISUAL
- OTHER

AUGMENTATION DEVICES
- HELMET
- STRAPS
- AURAL
- EXTREMITY
- X LBNP
- X VISUAL
- RESPIRATORY
- LACRIMATION
- TEMPERATURE
- MASK

SHEET 1 OF 1

TITLE: The Effects of Gravity and Acceleration on the Lung.

REF.# 90

HG- 246

DATE:

LEAD AUTHOR: Glaister, D. H.

HUMANS - X
ANIMALS -

ABSTRACT

The most comprehensive review to date on acceleration effects on respiration, tying in both operational data and underlying animal tests and theory. Lays the basis for Gz and Gx effects, with special emphasis on lung mechanics and the varying distribution of ventilation and of perfusion with G. Considerable quantitative data relevant to respiratory high g augmentation devices.

Especially strong in pictures and analysis of lung perfusion under ventilation, building on Glaister's personal research. Also introduces and justifies the 4 compartment model of lung perfusion; by West, and deals with V/Q regional distribution with G. Many of the illustrations are used or adapted for our report.

RELEVANCE

Table of Contents:
Accel. and the centrifuge
Ventilation and the mechanics of breathing
Distribution of ventilation
The effects of acceleration on ventilation distribution
The effect of acceleration on the cardiovascular system
Regional distribution of blood flow
Effects of acceleration on the distribution of pulmonary blood flow
Acceleration atelectasis
Ventilation-perfusion ratio inequality and gas exchange
The effect of acceleration on gas exchange, arterial oxygen saturation and alveolar shunting
Summary and conclusions.

SALIENT DATA

PHYSIOLOGICAL CATEGORY
- AUDITORY
- BIOMECHNL
- CARDIOVSCL
- FORCE
- GENERAL
- LABYRINTH
- MAN.CNTRL
- PROTECTIVE
- REVIEW
- X RESPIRAT'N
- SIMULATION
- VISUAL
- OTHER

AUGMENTATION DEVICES
- HELMET
- STRAPS
- AURAL
- EXTREMITY
- LBNP
- VISUAL
- XRESPIRATORY
- LACRIMATION
- TEMPERATURE
- XMASK

SHEET 1 OF 1

TITLE: Ein Oneumatisches Ophthalmomodynamometer Fur Den Laborgebrauch

REF.# 19

HG- 247

DATE:

LEAD AUTHOR: Behrendt, T.

HUMANS X
ANIMALS -

ABSTRACT

Ophthalmodynamometry- device for simulating visual grayout and blackout effects of G by raising the intraocular pressure through goggles over the eyes

The earlier goggles used by Jaeger, Duane and their associates, although producing the desired retinal arterial occulusion, were uncomfortable, difficult to fit, and experienced high leak rates at the higher pressures needed to produce blackout. This paper presents a vastly improved design of the goggles which overcomes these problems yet retains simplicity. By constructing the goggle with a soft and flexible wall which bends under against the skin. to form a seal, they get a good seal which improves as the pressure builds up, in the manner of a tube-less tire. For pressure below 50 mm Hg they required the use of double faced tape to maintain the seal. The self sealing was best at pressures between 80 and 150 mm Hg. Pressure drop due to leaks was under 1 mm Hg per minute. The glasses required about 30 min to fit, and were worn without discomfort for 1 hour.

RELEVANCE

A pneumatic ophthalmodynamometer for the use in the laboratory.

SALIENT DATA

An improved construction of spectacle is presented which permits a pneumatic ophthalmodynamometry. The basic principle of the developed device and the efficiency of function are explained. Details of the construction and first results are described which show that the previously encountered difficulties can be overcome.

PHYSIOLOGICAL CATEGORY
- AUDITORY
- BIOMECHNL
- CARDIOVSCL
- FORCE
- GENERAL
- LABYRINTH
- MAN.CNTRL
- PROTECTIVE
- REVIEW
- RESPIRAT'N
- SIMULATION
- X VISUAL
- OTHER

AUGMENTATION DEVICES
- HELMET
- STRAPS
- AURAL
- EXTREMITY
- LBNP
- XVISUAL
- RESPIRATORY
- LACRIMATION
- TEMPERATURE
- X MASK

SHEET 1 OF 1

TITLE: The Ophthalmic Artery Pulsensor

REF.# 240

HG- 248

DATE:

LEAD AUTHOR: Thorner, M.

HUMANS - X
ANIMALS -

SALIENT DATA

RELEVANCE

ABSTRACT

none

Plethysmographic goggles. This is a non-technical description of a device developed and apparently commercially available to measure systolic pressured in, for example, the ophthalmic artery, by watching it become occluded as external pressure is raised in a rigid cup over the eye.

No technical details on the device or its use. The discussion following the paper, concerning the clinical relevance of such measure and their history is quite interesting.

PHYSIOLOGICAL CATEGORY
- AUDITORY
- BIOMECHNL
- CARDIOVSCL
- FORCE
- GENERAL
- LABYRINTH
- MAN.CNTRL
- PROTECTIVE
- REVIEW
- RESPIRAT'N
- SIMULATION
- VISUAL
- OTHER

AUGMENTATION DEVICES
- HELMET
- STRAPS
- AURAL
- EXTREMITY
- LBNP
- VISUAL
- RESPIRATORY
- LACRIMATION
- TEMPERATURE
- MASK

SHEET 1 OF 1

TITLE: Intraocular Pressure and Ophthalmodynamometry

REF.# 91

HG- 249

DATE:

LEAD AUTHOR: Goldstein, J.A.

HUMANS - X
ANIMALS -

SALIENT DATA

None

RELEVANCE

Use of pressure goggles

ABSTRACT

Authors studied the relationship between intraocular pressure (Pi) as measured with applanation tonometry, and the systolic and diastolic pressures in the retinal circulation as measured by ophthalmodynamometry. They found that especially the diastolic was strongly influenced by p_i.

For application of the pressure goggles to High G cuing, therefore, one must be aware of the pilot's P_i, or at least of his range, in order to establish the correct values of goggle pressure to correspond to grayout and blackout.

PHYSIOLOGICAL CATEGORY
- AUDITORY
- BIOMECHNL
- CARDIOVSCL
- FORCE
- GENERAL
- LABYRINTH
- MAN.CNTRL
- PROTECTIVE
- REVIEW
- RESPIRAT'N
- SIMULATION
- VISUAL
- OTHER

AUGMENTATION DEVICES
- HELMET
- STRAPS
- AURAL
- EXTREMITY
- LBNP
- VISUAL
- RESPIRATORY
- LACRIMATION
- TEMPERATURE
- MASK

SHEET 1 OF 1

TITLE: The Effects of Hyperbaric Oxygenation on Retinal Arterial Occlusion.

REF. # 5

HG- 250

DATE:

LEAD AUTHOR: Anderson, B.

HUMANS - X
ANIMALS -

SALIENT DATA

None

ABSTRACT

Ophthalmodynamometry. Interaction of raised Pi and breathing 100% O_2

RELEVANCE

Primarily a clinical investigation paper, exploring the effectiveness of breathing 100% 03 at normal pressure and at elevated pressure and improving the visual fields of patients with retinal arterial occlusive disease. Results are generally discouraging. However for our pruposes we find the following interesting statement which relates 02 effects duing Gz and during increased Pi.

"The inhalation of 100% oxygen at high atmospheric pressures is associated with a great increase in oxygen carrying capacity of the blood and produces a significant prolongation of visual function after occlusion of the retinal circulation by ophthalmodynamometric pressure on the eye."

PHYSIOLOGICAL CATEGORY
- AUDITORY
- BIOMECHNL
- CARDIOVSCL
- FORCE
- GENERAL
- LABYRINTH
- MAN.CNTRL
- PROTECTIVE
- REVIEW
- RESPIRAT'N
- SIMULATION
- VISUAL
- OTHER

AUGMENTATION DEVICES
- HELMET
- STRAPS
- AURAL
- EXTREMITY
- LBNP
- VISUAL
- RESPIRATORY
- LACRIMATION
- TEMPERATURE
- MASK

SHEET 1 OF 1

TITLE:

Experimental Blackout and The Visual System

REF.# 63

HG- 252

DATE:

LEAD AUTHOR:

Duane, T. D.

HUMANS - X
ANIMALS -

ABSTRACT

A somewhat longer version of the excellent summary which appeared later in Aerospace Med. (HG67).

RELEVANCE

SALIENT DATA

PHYSIOLOGICAL CATEGORY
- AUDITORY
- BIOMECHNL
- CARDIOVSC'
- FORCE
- GENERAL
- LABYRINTH
- MAN.CNTRL
- PROTECTIVE
- REVIEW
- RESPIRAT'N
- SIMULATION
- VISUAL
- OTHER

AUGMENTATION DEVICES
- HELMET
- STRAPS
- AURAL
- EXTREMITY
- LBNP
- VISUAL
- RESPIRATORY
- LACRIMATION
- TEMPERATURE
- MASK

SHEET 1 OF 1

TITLE:

The Phylogeny of Muscular Control Configurations

REF. # 114

HG- 256

DATE:

LEAD AUTHOR:

Houk, J. C.

HUMANS - X
ANIMALS -

ABSTRACT

This report presents the theoretical constructs for the various models of muscular control in resisting external loads, and is directly applicable to an understanding of the problem involved in artifically loading the limb during high g cuing.

Reviews the physiological literature only in as much detail as is necessary to motivate the discussion of the different control engineer rather than for the physiologist. Presents, motivates and criticizes the models for spindle and tendon organ innervation, and the system's aspects. Review open loop control, alpha control, gamma control, alpha-gamma linkage (or co-activation), and introduces the concepts of a beta system having zero sensitivity of main system parameter changes. He emphasizes the role of force feedback, both for reducing muscle stiffness and in minimizing the dependence on variations in the characteristics of extrafusal muscle.

RELEVANCE

SALIENT DATA

PHYSIOLOGICAL CATEGORY

- AUDITORY
- BIOMECHNL
- CARDIOVSCL
- FORCE
- GENERAL
- LABYRINTH
- MAN.CNTRL
- PROTECTIVE
- REVIEW
- RESPIRAT'N
- SIMULATION
- VISUAL
- OTHER

AUGMENTATION DEVICES

- HELMET
- STRAPS
- AURAL
- EXTREMITY
- LBNP
- VISUAL
- RESPIRATORY
- LACRIMATION
- TEMPERATURE
- MASK

SHEET 1 OF 1

TITLE:
An Evaluation of Length and Force Feedback to Soleus Muscles of Decerebrate cats

REF.# 115
HG- 257
DATE:

LEAD AUTHOR:
Houk, J. C.

HUMANS - X
ANIMALS -

ABSTRACT

This article treats the basic spindle and tendon organ sensors in the regulation of limb position in response to external loads, and is directly applicable to the case of extremity loading for a High G cue.

Dealing with the decerebrate cat, in which only lower level control is involved, the authors try to determine how the gain of stiffness of the limb resistance to stretch is affected by length feedback from spindles and by force feedback (which tends to reduce stiffness) from the Golgi tendon organs. Force feedback loop gains of the order of 0.2 and 0.8 were measured, with half of this attributable to tendon organ pathways. Length feedback stiffen muscle strech reflex by about 5 times. Gains of both spindle and tendon loops are nonlinear, increasing with the square root of operating force. Force Feedback may compensate for the inherent muscle nonlinearity over its operating range. Data analyzed and presented in simple control theory terms.

RELEVANCE

SALIENT DATA

PHYSIOLOGICAL CATEGORY
- AUDITORY
- BIOMECHNL
- CARDIOVSCL
- FORCE
- GENERAL
- LABYRINTH
- MAN.CNTRL
- PROTECTIVE
- REVIEW
- RESPIRAT'N
- SIMULATION
- VISUAL
- OTHER

AUGMENTATION DEVICES
- HELMET
- STRAPS
- AURAL
- EXTREMITY
- LBNP
- VISUAL
- RESPIRATORY
- LACRIMATION
- TEMPERATURE
- MASK

SHEET 1 OF 1

TITLE:

Regulatory Actions of the Human Stretch Reflex.

REF.# 52

HG- 258

DATE:

HUMANS - X
ANIMALS -

LEAD AUTHOR:

Crago, P. E.

SALIENT DATA

RELEVANCE

ABSTRACT

The closest basic experimental work oh human to situation of extremity control in high g. Examines the importance of instructions to the subject and the length regulation portion of the stretch reflex in resisting sudden and unexpected variations in external load, much as would be the case for some of the high g maneuvers.

Instructions to resist of not resist a limb displacement can modify the stretch reflex. They argue that the stretch reflex gain are not modulated by a gain servo act in as frequently suggested, but rather is a triggered reaction based upon instruction. The stretch reflex may compensate for variations in muscle properties, maintaining stiffness, but does participate in joint position control. Rather, errors in limb position are corrected by the super position of triggered reactions, not a continuous servo.

PHYSIOLOGICAL CATEGORY
- AUDITORY
- BIOMECHNL
- CARDIOVSCL
- FORCE
- GENERAL
- LABYRINTH
- MAN.CNTRL
- PROTECTIVE
- REVIEW
- RESPIRAT'N
- SIMULATION
- VISUAL
- OTHER

AUGMENTATION DEVICES
- HELMET
- STRAPS
- AURAL
- EXTREMITY
- LBNP
- VISUAL
- RESPIRATORY
- LACRIMATION
- TEMFERATURE
- MASK

SHEET 1 OF 1